VOLUME 65
NUMBER 8 / NUMÉRO 8
AUGUST / AOÛT
2008

An NRC Research Press
JOURNAL
Une REVUE des
Presses scientifiques du CNRC

Canadian Journal of
FISHERIES AND AQUATIC SCIENCES
cjfas.nrc.ca

Journal canadien des
SCIENCES HALIEUTIQUES ET AQUATIQUES
jcsha.cnrc.ca

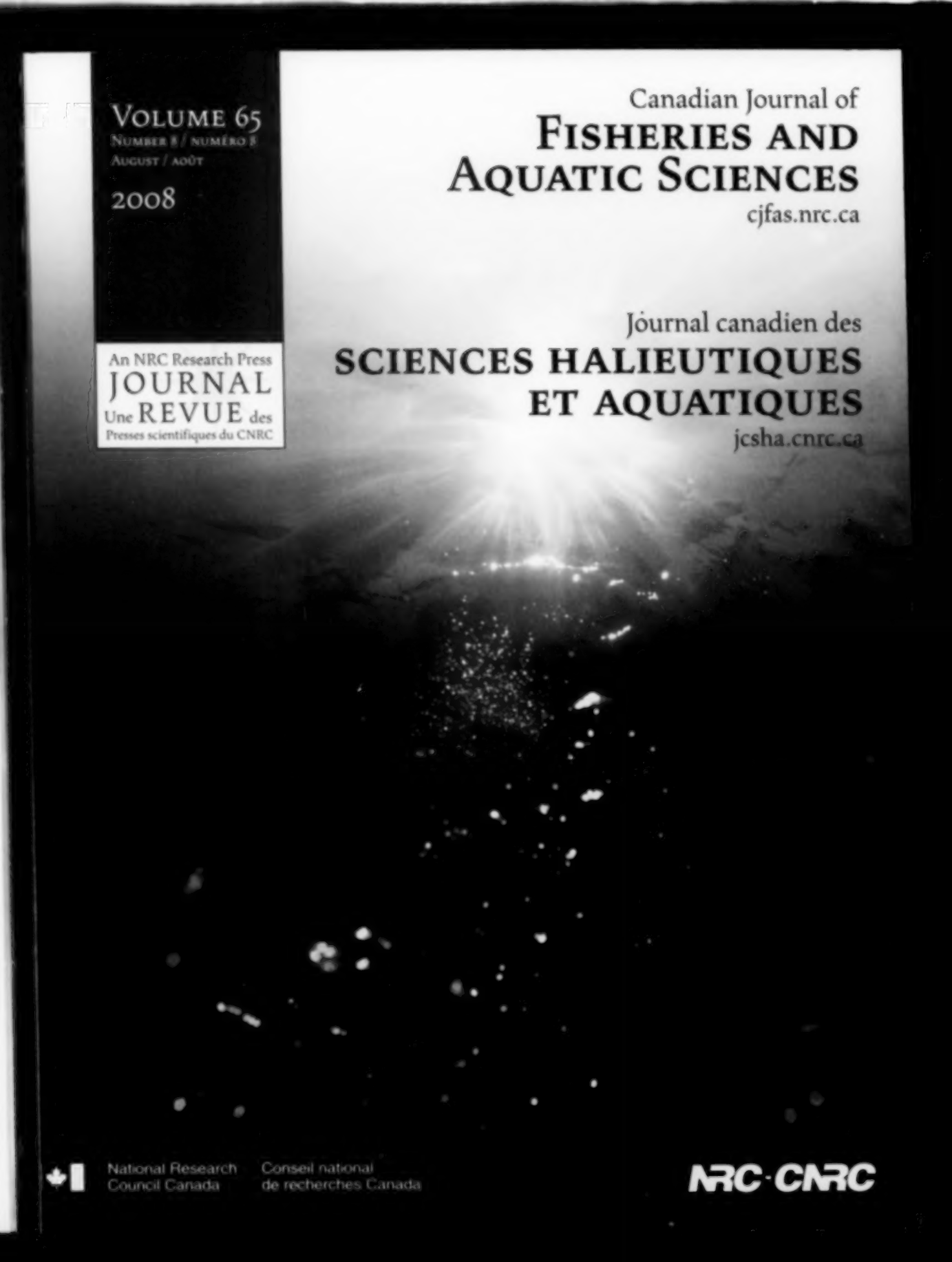

National Research Council Canada
Conseil national de recherches Canada
NRC·CNRC

ISSN 0706-652X / CJFSDX 65(8) 1523–1796 (2008)

The *Canadian Journal of Fisheries and Aquatic Sciences*, previously published as *Contributions to Canadian Biology* 1901–1925, *Contributions to Canadian Biology and Fisheries* 1926–1934, *Journal of the Biological Board of Canada* 1934–1937, and *Journal of the Fisheries Research Board of Canada* 1938–1979, is issued monthly to form annual volumes of 12 numbers plus supplements.

Editorial policy. The Journal publishes original research articles, perspectives (syntheses, critiques, reevaluations), discussions (comment and reply), and rapid communications. Manuscripts may concern cells, organisms, populations, communities, ecosystems, or processes that affect aquatic systems. They may cover a range of disciplines including biology and ecology of marine and freshwater organisms, limnology, oceanography, physiology, toxicology, genetics, economics, disease, and management. Preference will be given to manuscripts that emphasize understanding of observed phenomena and interpretation of experimental results. The Journal encourages papers that lead from clearly stated purpose or rationale and from testable hypotheses, concepts, or questions to identifiable conclusions or syntheses. Such papers may amplify, modify, question, or redirect accumulated knowledge embodied in contemporary perceptions of a particular state of aquatic sciences. The Journal discourages papers that are essentially descriptive, except in emerging disciplines; have only site-specific or local applications (a certain year, place, taxon, chemical compound, etc.); only confirm previously established principles; or apply standard techniques without breaking new methodological ground.

Manuscripts for publication should be submitted to the Editorial Office via NRC Research Press' online submission and peer review system (**OSPREY**) at http://pubs.nrc-cnrc.gc.ca/cjfas/osprey. Alternatively, manuscripts may be submitted to the Editor, *Canadian Journal of Fisheries and Aquatic Sciences*, Department of Ecology and Evolutionary Biology, University of Toronto, Toronto, ON M5S 3G5, Canada (416-946-0609; fax: 866-523-4174 (Canada and United States) or 416-946-0509; e-mail: cjfas@utoronto.ca).

Submissions in either English or French are acceptable. The information must be original, that is, not copyrighted, published, or submitted elsewhere except in abstract form or unless by written consent of the Editor.

Correspondence concerning accepted manuscripts and corrected proofs should be sent to NRC Research Press, National Research Council of Canada, Ottawa, ON K1A 0R6, Canada (fax: 613-952-7656; e-mail: pubs@nrc-cnrc.gc.ca).

Instructions to Authors are published once a year in the first issue of each volume. Copies are available from NRC Research Press or at cjfas.nrc.ca. The **Publishing Policy** of NRC Research Press is available at pubs.nrc-cnrc.gc.ca.

The *Canadian Journal of Fisheries and Aquatic Sciences*, ISSN 0706-652X, is published monthly, 12 times per year, by NRC Research Press, c/o USACAN Media Dist. Srv. Corp. at 26 Power Dam Way, Suite S1-S3, Plattsburgh, NY 12901, USA. Periodicals postage paid at Plattsburgh, NY. POSTMASTER: Send address changes to *Canadian Journal of Fisheries and Aquatic Sciences*, c/o NRC, P.O. Box 2888, Plattsburgh, NY 12901, USA.

Publié sans interruption depuis 1901, le *Journal canadien des sciences halieutiques et aquatiques* a paru sous plusieurs titres : *Contributions to Canadian Biology* 1901–1925, *Contributions to Canadian Biology and Fisheries* 1926–1934, *Journal of the Biological Board of Canada* 1934–1937, et *Journal of the Fisheries Research Board of Canada* 1938–1979. Le Journal paraît tous les mois, formant ainsi un volume de 12 numéros, et offre en plus jusqu'à deux suppléments par année.

Politique éditoriale. On publie, dans le Journal, des articles rendant compte de recherche originale, des perspectives (synthèses, critiques et réévaluations), des discussions (commentaires et réponses) et des communications rapides. Les documents peuvent porter sur les cellules, organismes, populations, communautés, écosystèmes ou processus qui affectent les systèmes aquatiques. Ils peuvent relever de divers domaines y compris la biologie et l'écologie des organismes marins et d'eau douce, la limnologie, l'océanographie, la physiologie, la toxicologie, la génétique, l'économie, la pathologie et la gestion. On accorde la préséance aux articles qui contribuent à la compréhension de phénomènes observés et à l'interprétation de résultats expérimentaux. On invite les auteurs à soumettre des articles ayant des objectifs précis ou relevant d'hypothèses, de concepts ou de questions vérifiables et se terminant par de solides conclusions ou d'utiles synthèses. Ces articles enrichissent, changent, mettent en question ou réorientent les connaissances acquises sur divers aspects des sciences aquatiques. On décourage toutefois la soumission d'articles simplement descriptifs (à moins qu'il ne s'agisse de nouvelles disciplines), d'application très limitée (applicables à une seule année, une seule région ou un seul taxon, portant sur un unique composé chimique, etc.); d'articles qui ne font que reprendre les principes énoncés dans des articles précédents; et d'articles rendant compte de l'application de normes sans gain de méthodologie.

Les auteurs sont invités à soumettre leur manuscrit au Bureau de la rédaction par le truchement du Système de soumission et d'examen en direct des articles (**OSPREY**) des Presses scientifique du CNRC à http://pubs.nrc-cnrc.gc.ca/jcsha/osprey. Sinon, ils peuvent transmettre leur manuscrit par la poste au rédacteur en chef, *Journal canadien des sciences halieutiques et aquatiques*, Département d'écologie et de biologie évolutive, Université de Toronto, Toronto, ON M5S 3G5, Canada (416-946-0609; télécopieur : 866-523-4174 (Canada et États-Unis) ou 416-946-0509; courriel : cjfas@utoronto.ca).

Les contributions peuvent être en anglais ou en français. Elles doivent être originales, c.-à.-d. qu'elles ne doivent pas avoir fait l'objet d'un copyright, avoir été publiées ou soumises ailleurs, sauf sous forme abrégée ou avec le consentement du rédacteur en chef.

La correspondance ayant trait aux manuscrits acceptés et les **épreuves corrigés** doivent être envoyées aux Presses scientifiques du CNRC, Conseil national de recherches du Canada, Ottawa, ON K1A 0R6, Canada (télécopieur : 613-952-7656; courriel : pubs@nrc-cnrc.gc.ca).

Les **Recommandations aux auteurs** sont publiées une fois par année dans le premier numéro de chaque volume. Des copies sont disponibles auprès du Bureau de la rédaction aux Presses scientifiques du CNRC ou au jcsha.cnrc.ca. La **Politique éditoriale** est disponible auprès des Presses scientifiques du CNRC ou au pubs.nrc-cnrc.gc.ca.

This Journal is indexed or abstracted in / Cette revue est signalée ou résumée dans

ABSEARCH; Applied Science and Technology Index and Abstracts; Aquatic Sciences and Fisheries Abstracts; Biological Abstracts; Biological and Agricultural Abstracts; CAB Abstracts; Chemical Abstracts; Current Contents; Elsevier BIOBASE; Environmental Abstracts; ETDE Energy Database; General Science Index and Abstracts; GEOBASE; GeoRef; Life Sciences Collection; Meteorological and Geoastrophysical Abstracts; Oceanic Abstracts; PASCAL Database; Science Citation Index.

Volume 65, Number 8, August 2008

Canadian Journal of Fisheries and Aquatic Sciences

Published by the National Research Council of Canada

Volume 65, numéro 8, août 2008

Journal canadien des sciences halieutiques et aquatiques

Publié par le Conseil national de recherches du Canada

Editor / Rédacteur en chef **Don Jackson**

Vice-editor / Sous-rédacteur en chef

Rolf Vinebrooke, *University of Alberta*

Assistant to the Editors / Adjointe au rédacteur en chef **Holly Foster**

Associate Editors / Comité de rédaction

D. Boisclair, *Université de Montréal*
M.J. Bradford, *DFO/MPO and Simon Fraser University*
D. Brickman, *DFO/MPO, Dartmouth*
S.E. Campana, *DFO/MPO, Dartmouth*
X. Chen, *Shanghai Fisheries University, Shanghai, China*
Y. Chen, *University of Maine, Orono, Maine*
B. Gillanders, *University of Adelaide, Australia*
J.W.A. Grant, *Concordia University*
M.M. Hansen, *Danish Institute for Fisheries Research, Silkeborg, Denmark*
R. Hilborn, *University of Washington*
J.M. Jech, *NFSC/NOAA, Woods Hole, Mass.*
B. Jonsson, *Norwegian Institute for Nature Research, Oslo, Norway*
K.A. Kidd, *University of New Brunswick*
C. Kraft, *Cornell University, N.Y.*
D.L. MacLatchy, *University of New Brunswick, Saint John*
P. Magnan, *Université du Québec à Trois Rivières*
C.T. Marshall, *University of Aberdeen*
J. Post, *University of Calgary*
Y.T. Prairie, *Université du Québec à Montréal*
T.J. Quinn II, *University of Alaska–Fairbanks, Juneau, Alaska*
C.W. Ramcharan, *Laurentian University*
J.S. Richardson, *The University of British Columbia*
K. Rose, *Louisiana State University, Baton Rouge, La.*
B. Sainte-Marie, *DFO/MPO, Mont-Joli*
R.E.H. Smith, *University of Waterloo*
S.J. Smith, *DFO/MPO, Dartmouth*
W.G. Sprules, *University of Toronto at Mississauga*
E.B. Taylor, *The University of British Columbia*
M. Trudel, *DFO/MPO, Pacific Biological Station, Nanaimo*
A. Vasemägi, *University of Turku, Turku, Finland*
C.J. Walters, *The University of British Columbia*
G. Weyhenmeyer, *Swedish University of Agricultural Sciences, Uppsala, Sweden*

NRC Research Press / Presses scientifiques du CNRC

Fax / Télécopieur : 613-952-7656; e-mail / courriel : pubs@nrc-cnrc.gc.ca; URL / URL : pubs.nrc-cnrc.gc.ca

Editor-in-Chief / Directeur de la publication **Bruce P. Dancik**
Deputy Editor-in-Chief / Sous-directeur de la publication **Donald S. Mavinic**
Publisher / Éditeur **Cameron D. Macdonald**

Business Manager / Gestionnaire des affaires commerciales **Mike Boroczki**
Advertising and Reprints / Annonces publicitaires et tirés à part **Roxanne Landriault** (613-990-2254)
Subscriptions / Abonnements **Eileen Evans-Nantais** (613-990-7873), **André Séguin** (613-993-9084)

Manager, Journals Program / Gestionnaire du Programme des revues **Carolyn Brown**
Managing Editor / Gestionnaire de la rédaction **Cecily M. Pearson** (613-993-9099)
Scientific Publishing Editors / Réviseurs de publications scientifiques **Jennifer McColl, Thad Costigan**
Editorial Publication Technicians / Techniciens à la publication éditoriale **Diana Leck, Luc Julien**
Editorial Applications Training and Support Officers / Agentes de formation et de soutien à l'éditique **Sue Lantos, Mary Seligy**

Production Manager / Gestionnaire de la production **Brad Stoppa**
Production Application Support Technician / Technicienne au soutien de la production **Judy Hum**
Desktop Publishing Technician / Technicienne en éditique **Lisette Séguin**
Graphics Technician / Technicien en graphisme **Dario Ferrara**
Web Technician / Technicien Web **Dennis Cafferty**

The National Research Council of Canada accepts no responsibility for statements or opinions expressed by a contributor. Acceptance of an advertisement, announcement, or other material does not imply endorsement by either the Journal's Editor or the National Research Council.

© National Research Council of Canada 2008. All rights reserved.

No part of this publication may be reproduced, stored, or transmitted in any form or by any means, without the written permission of the publisher, except as stated below.

The National Research Council of Canada grants permission to individuals to make single copies of articles for personal use. Any person may reproduce short excerpts from articles in the journal for any purpose that respects the moral rights of authors, provided that the source is fully acknowledged. As a courtesy, the consent of authors of such material should be obtained directly from the author.

Authorization to reproduce items for other than personal use, as stated above, is granted by the National Research Council of Canada provided that the copyright fee of $10.00 per copy is paid directly to Access Copyright, The Canadian Copyright Licensing Agency, One Yonge Street, Suite 800, Toronto, ON M5E 1E5, Canada.

The above permission does not extend to other kinds of copying, such as copying for general distribution, for advertising, or promotional purposes, for creating new collective works, or for resale. For such copying, arrangements must be made with the publisher, National Research Council of Canada, Ottawa, ON K1A 0R6, Canada.

Subscription information

The *Canadian Journal of Fisheries and Aquatic Sciences* (ISSN 0706-652X) is published monthly by the National Research Council of Canada. The 2008 annual subscription rates (second class postage) for Canada are $1145CAN institutional and $350CAN personal, for US & foreign $1145US institutional and $350US personal. For air mail add $150US to foreign rate. Canadian customers please include GST (business no. 12149 1807 RT 0275). Subscriptions are entered for the calendar year. Remittances should be made payable to the Receiver General for Canada, credit NRC. Price for regular single issues: institutional, $110.00; personal, $35.00. Supplements will be priced separately. Special rates apply to members of Canadian scientific and engineering societies if they subscribe through their respective societies.

Issues of the *Canadian Journal of Fisheries and Aquatic Sciences* are available on the Web. Pricing information can be found at pubs.nrc-cnrc.gc.ca.

There are no refunds on cancelled subscriptions once delivery has begun. Claims for missing issues should be made within four months (North America) or six months (outside North America) following the date of publication. The publisher expects to supply missing issues only when losses have occurred in transit and when the reserve stock will permit. For change of address and subscription enquiries: Subscription Office, NRC Research Press, National Research Council of Canada, Ottawa, ON K1A 0R6, Canada; tel.: 613-993-9084; fax: 613-952-7656; e-mail: pubs@nrc-cnrc.gc.ca.

Microform backfiles are available from UMI, P.O. Box 1346, Ann Arbor, MI 48106-1346, USA, and Micromedia Ltd., 20 Victoria St., Toronto, ON M5C 2N8, Canada.

Le Conseil national de recherches du Canada ne se tient en aucune façon responsable des opinions exprimées par un collaborateur ou des déclarations que pourrait faire ce dernier. La publication d'annonces publicitaires, d'avis et autres n'implique pas l'endossement de leur contenu par le rédacteur en chef de la Revue ou le Conseil national de recherches du Canada.

© Conseil national de recherches du Canada 2008. Tous droits réservés.

Il est interdit de reproduire, de sauvegarder ou de transmettre quelque partie de la présente publication dans quelque format ou de quelque façon sans le consentement écrit de l'éditeur, à l'exception des conditions suivantes.

Le Conseil national de recherches du Canada accorde aux particuliers le droit de faire des copies individuelles pour leur usage personnel. Toute personne peut reproduire de courts extraits des articles de la Revue pour autant que les droits moraux de l'auteur soient respectés et que la mention de provenance soit clairement indiquée. Il est de convenance de demander le consentement de l'auteur avant de faire mention de son travail.

On obtiendra l'autorisation de reproduire des articles à d'autres fins que l'usage personnel (tel qu'on l'a décrit ci-dessus) auprès du Conseil national de recherches du Canada pour autant que des redevances de droits d'auteurs de 10,00 $/copie soient versées au Access Copyright, The Canadian Copyright Licensing Agency, 1, rue Yonge, bureau 800, Toronto, ON M5E 1E5, Canada.

La permission ci-dessus ne s'applique pas à la reproduction à grande échelle, telle que la reproduction aux fins de distribution générale, publicitaire ou promotionnelle, de compilation de nouveaux ouvrages collectifs ou de revente. Dans de tels cas, il faudra ratifier une entente particulière avec l'éditeur, le Conseil national de recherches du Canada, Ottawa, ON K1A 0R6, Canada.

Renseignements sur l'abonnement

Journal canadien des sciences halieutiques et aquatiques (ISSN 0706-652X) est une publication mensuelle du Conseil national de recherches du Canada. Le prix de l'abonnement annuel en 2008 au Canada (courrier de deuxième classe) est de 1145 $CAN pour les organismes et de 350 $CAN pour les particuliers. À l'étranger (y compris les É.-U.), le prix de l'abonnement est de 1145 $US pour les organismes et de 350 $US pour les particuliers. L'expédition par avion exige des frais de 150 $US en sus du prix d'abonnement à l'étranger. Les clients du Canada doivent ajouter la TPS (numéro d'entreprise 12149 1807 RT 0275). Les abonnements sont pour l'année civile. Tout paiement doit être adressé au Receveur général du Canada, crédit du CNRC. Le prix par numéro est de 110,00 $ pour les organismes et de 35,00 $ pour les particuliers. Le prix des hors-série varie. Les membres des sociétés canadiennes de sciences et de génie bénéficient de taux préférentiels en s'abonnant via leurs sociétés respectives.

Les numéros de *Journal canadien des sciences halieutiques et aquatiques* sont accessibles sur le Web. On trouvera des renseignements sur les tarifs à pubs.nrc-cnrc.gc.ca.

Aucun remboursement ne sera accordé ni aucune annulation acceptée une fois que les livraisons auront commencé. Les réclamations de numéros manquants devront être soumises dans les quatre mois (Amérique du Nord) ou dans les six mois (à l'extérieur de l'Amérique du Nord) suivant la date de publication. L'éditeur ne fournira de numéros manquants que si le document a été perdu pendant l'expédition et que si le stock le permet. Adressez tout changement d'adresse ou toute question quant à l'abonnement au : Bureau des abonnements, Presses scientifiques du CNRC, Conseil national de recherches Canada, Ottawa, ON K1A 0R6, Canada; téléphone : 613-993-9084; télécopieur : 613-952-7656; courriel : pubs@nrc-cnrc.gc.ca.

On peut obtenir les fichiers rétrospectifs sur **microforme** auprès de UMI, P.O. Box 1346, Ann Arbor, MI 48106-1346, É.-U., et auprès de Micromedia Ltée, 20, rue Victoria, Toronto, ON M5C 2N8, Canada.

RAPID COMMUNICATION / COMMUNICATION RAPIDE

A validated description of age and growth of western Atlantic bluefin tuna (*Thunnus thynnus*)

John D. Neilson and Steven E. Campana

Abstract: Current stock assessments of western Atlantic bluefin tuna (*Thunnus thynnus*) use age-structured population analyses, but the age assignment in the population model is made using an age–length relationship derived from mark and recapture studies largely completed during the 1970s. In our study, the deposition of bomb radiocarbon was used as a dated mark to validate age inferences of bluefin tuna and to compare the validated ages with those predicted from the age–length relationship. The results support the view that the age–length relationship currently in use for the assessment overestimates growth rate and the ultimate size of the fish. These findings have implications for the estimation of stock productivity and may negatively impact the rebuilding schedules established by fisheries managers.

Résumé : Les évaluations courantes des stocks de thons rouges (*Thunnus thynnus*) dans l'Atlantique ouest sont basées sur des analyses de populations structurées en fonction de l'âge, mais l'attribution des âges dans le modèle démographique se fait à partir de relations âge–longueur obtenues lors d'études de marquage et de recapture réalisées en grande partie dans les années 1970. Dans notre étude, nous utilisons les dépôts de radiocarbone provenant des essais nucléaires comme repères de date connue pour valider les estimations de l'âge chez les thons rouges et pour comparer ces âges validés à ceux prédits à partir des relations âge–longueur. Nos résultats appuient le point de vue qui veut que la relation âge–longueur en usage courant pour l'évaluation des stocks surestime le taux de croissance et la taille finale des poissons. Ces observations ont des conséquences sur l'estimation de la productivité des stocks et peuvent avoir un impact négatif sur les calendriers de reconstruction établis par les gestionnaires des pêches.

[Traduit par la Rédaction]

Introduction

Atlantic bluefin tuna (*Thunnus thynnus*) are among the largest, most widely-ranging, and highly-valued members of the marine fish fauna. The responsible regional fisheries management agency (International Commission for the Conservation of Atlantic Tunas (ICCAT)) considers that there are two management units in the Atlantic (western Atlantic and Eastern Atlantic – Mediterranean). However, both Atlantic populations of bluefin tuna are considered to be severely overfished (Fromentin and Powers 2005), and there are growing concerns about their future, as indicated by the recent identification of the stock as a candidate species for special conservation measures by COSEWIC (Committee on the Status of Endangered Wildlife in Canada, www.cosewic.gc.ca/eng/sct3/sct3_1_e.cfm#4).

While direct age determination from hard parts such as otoliths have been attempted (i.e., Hurley and Iles 1983), such information has not been used in stock assessments because of the absence of validation that annulus counts corresponded with age. In the absence of direct estimates from hard parts, ages in the western Atlantic stock are currently assigned by empirical length modal separation for ages 1–3, then through application of a length–age relationship (ICCAT 2003). The growth model that informs the slicing is that of Turner and Restrepo (1994), who used mark and recapture information to provide estimates of L_∞ and K, following the von Bertalanffy growth equation, and modal analyses to provide an estimate of t_0.

However, the information used by Turner and Restrepo (1994) is now somewhat dated (about 89% of the available records included recaptures made before 1979; Turner et al. 1991), and there is a possibility that growth patterns observed in the past may no longer reflect the contemporary situation. More importantly, the data set used by Turner and Restrepo, while consisting of a large number of observations (N = 908), had relatively few (N = 11) observations of fish 250 cm or larger. The relatively few observations of larger fish may have impacted the estimation of L_∞. The impact of potential errors in age assignment for older fish could include errors in calculations of critical stock parameters, such as age at maturity and natural mortality.

We employed the bomb radiocarbon method to evaluate the accuracy of age interpretations from otoliths, a method considered to be one of the most accurate means available

Received 1 May 2008. Accepted 19 June 2008. Published on the NRC Research Press Web site at cjfas.nrc.ca on 27 June 2008. J20545

J.D. Neilson.[1] Fisheries and Oceans Canada, Biological Station, 531 Brandy Cove Road, St. Andrews, NB E5B 2L9, Canada.
S.E. Campana. Fisheries and Oceans Canada, Bedford Institute of Oceanography, Dartmouth, NS B2Y 4A2, Canada.

[1]Corresponding author (e-mail: neilsonj@mar.dfo-mpo.gc.ca).

 doi:10.1139/F08-127 © 2008 NRC Canada

to obtain such validation (Baker and Wilson 2001). In brief, this method uses the observation that bomb-derived radiocarbon from nuclear testing conducted during the late 1950s resulted in elevated ^{14}C in the bony parts formed in marine organisms at the time. This deposition forms a dated reference that can be used to validate inferences of age (Campana 2001). Using ages validated with the radiocarbon method, we provide a description of the growth of bluefin tuna and contrast this with the model that has been used previously.

Materials and methods

Bluefin tuna sagittal otoliths were collected from archived material stored at the St. Andrews Biological Station, Fisheries and Oceans Canada (St. Andrews, New Brunswick). Material selected for the study is listed in Supplemental Table S1[2]. Otoliths were only collected from the western Atlantic management unit and were generally collected during the 1970s and 1980s, with two exceptions. Samples were selected from that time period to include otoliths that were likely formed during the period of increasing radiocarbon and to be comparable with the material available to Turner and Restrepo (1994). The material was stored dry in coin envelopes, and details of the sampled fish were available from an electronic database. Consistent with the approach of Turner and Restrepo (1994), we report fish length as fork length. To do this, it was necessary to convert curved fork length (CFL) to fork length (FL) using the conversion factor used by the ICCAT (FL = 0.955 × CFL) for the majority of the samples.

Otoliths to be aged were first embedded in a slow-drying hard epoxy (Araldite epoxy GY502 and hardener HY956 in a 5:1 weight ratio). Otolith cores for bomb radiocarbon age validation were isolated from three adjacent transverse sections of the sagittae: a 1.2 mm central section through the core intended for micromilling and ~450 µm thick sections on either side for age determination. All sections were prepared with a single cut using multiple blades separated by spacers on an Isomet low-speed diamond-bladed saw. Sections were lightly polished to improve visibility of the growth sequence and then digitally photographed at 1280 × 1024 pixel resolution while under a binocular microscope at 16×–40× magnification using reflected light. Age interpretation was based on digitally-enhanced images, and counts were made along the longer of the two arms of the sectioned sagittae (Fig. 1*a*). The ages provided by the second author are referred to here as those from the "primary age reader" and are those used in the radiocarbon calibration and the von Bertalanffy growth curve. The electronic images were also supplied to two experts familiar with age determination using otoliths of bluefin tuna along with information on length at capture, who supplied independent estimates of ages. Those readers are referred to here as "secondary age readers". These additional age estimates provide an indication of the expected consistency of age interpretations possible with this species.

Otolith cores representing the first 2–3 years of life were isolated as solid pieces encompassing the innermost otolith annuli from the central thick section and one or both adjacent sections with a Merchantek computer-controlled micromilling machine using 300 µm diameter steel cutting bits and burrs. Although major error in isolating the otolith core is unlikely, any such error could only reduce the apparent age of the fish by incorporating more recently formed material. Thus the radiocarbon method assigns a minimum age to the fish.

Cores from both sections were sometimes required to

Fig. 1. (*a*) Polished transverse section of a sagittal otolith from sample No. 1536, aged as 31 years old. The specimen was photographed using reflected light, and the digital image was modified to enhance contrast. Black dots were added by the primary age reader to identify presumed annuli, and the otolith core sampled for radiocarbon analyses is also highlighted. The white scale bar is 0.5 mm in length. (*b*) $\Delta^{14}C$ in otolith cores of bluefin tuna (*Thunnus thynnus*) versus year of formation inferred from counts of presumed annuli. The $\Delta^{14}C$ chronology of the cores (■) was similar to that of a reference carbonate chronology (line smoothed with a LOESS curve), with the crucial feature being the period of rapid increase.

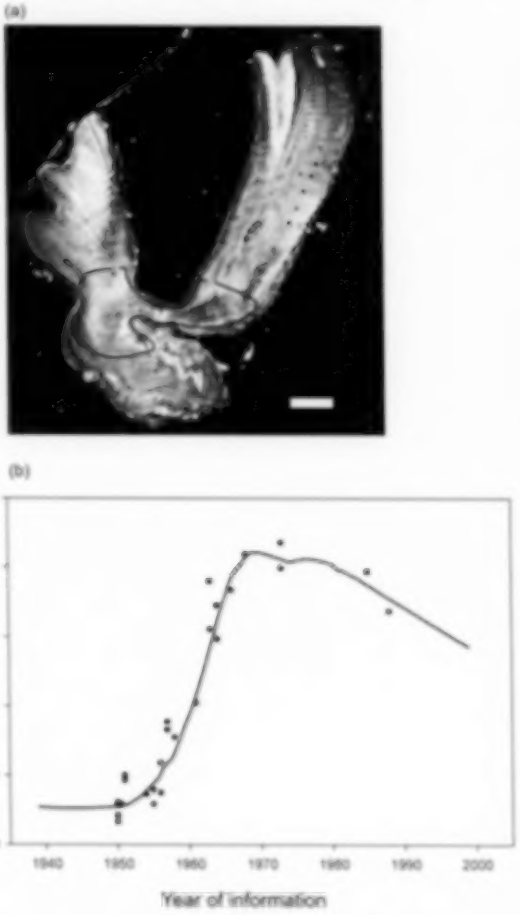

[2] Supplementary data for this article are available on the journal Web site (cjfas.nrc.ca) or may be purchased from the Depository of Unpublished Data, Document Delivery, CISTI, National Research Council Canada, Building M-55, 1200 Montreal Road, Ottawa, ON K1A 0R6, Canada. DUD 3778. For more information on obtaining material refer to cisti-icist.nrc-cnrc.gc.ca/cms/unpub_e.html.

© 2008 NRC Canada

Fig. 2. (*a*) Paired comparisons of ages of the primary age reader with the two secondary age readers and the predicted ages from the Turner and Restrepo (1994) growth model. (*b*) Predicted relationship between length and age, from Turner and Restrepo (1994), shown as the gray line. The parameters of the von Bertalanffy fit to the Turner and Restrepo model were L_∞ = 382 cm, t_0 = –0.707, and K = 0.079. The estimated ages obtained by the primary age reader are shown (◆), and the fit to those data is shown by the black line, with the parameters L_∞ = 289 cm, t_0 = –0.06, and K = 0.116.

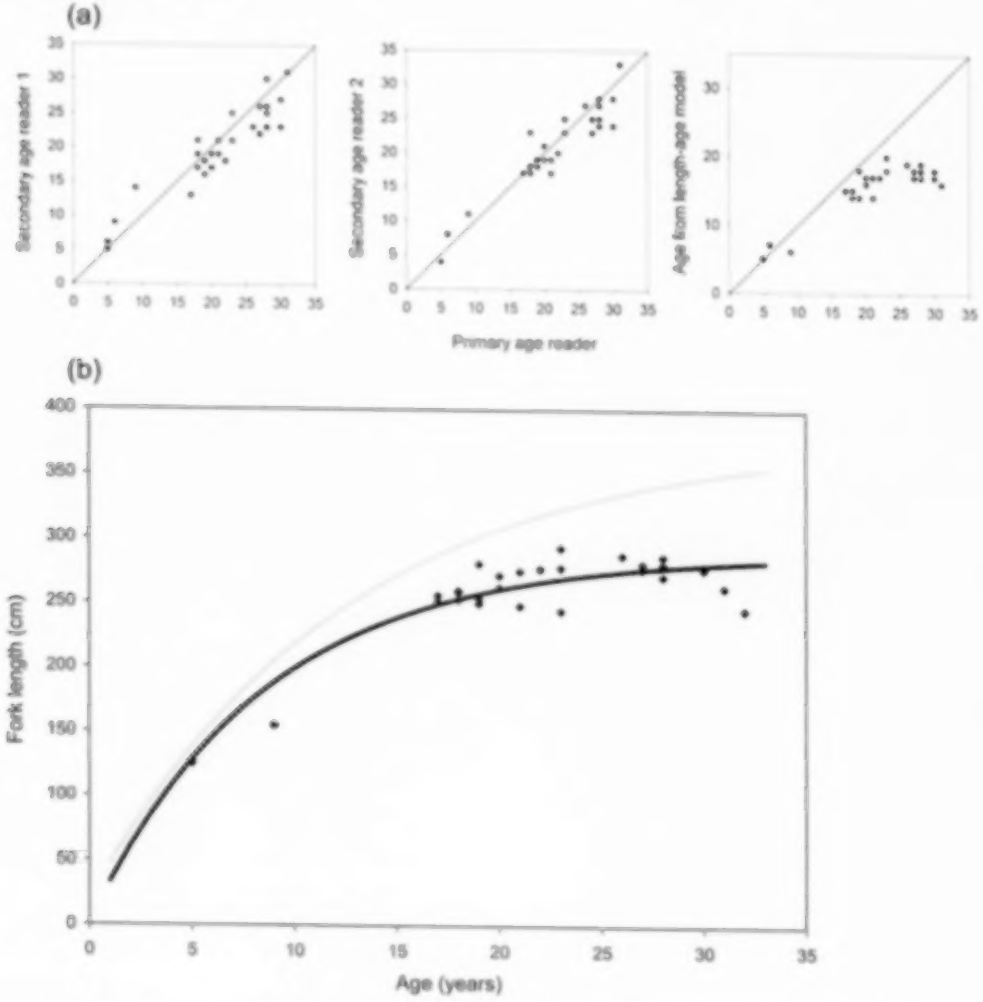

Table 1. Parameters of the von Bertalanffy growth equation, fitted using age interpretations from the three age readers or from the primary age reader only.

	L_∞		K		t_0		CV	
	Mean	SD	Mean	SD	Mean	SD	Length error	Age error
All readers	304.0	15.2	0.098	0.021	–0.15	1.03	0.06	0.12
Primary reader only	289.0	16.9	0.116	0.040	–0.06	1.56	0.10	

Note: CV, coefficient of variation; SD, standard deviation.

bring the sample weight up to the minimum of 3 mg necessary for radiocarbon assay. The date of sample formation was calculated as the year of fish collection minus the number of increments between the otolith edge and the midpoint of the growth increments extracted in the core. After sonification in Super Q water and drying, the sample was weighed to the nearest 0.1 mg in preparation for ^{14}C assay with accelerator mass spectrometry (AMS). AMS assays also provided $\delta^{13}C$ (‰) values, which were used to correct for isotopic fractionation effects and provide information on the source of the carbon. Radiocarbon values were subsequently reported as $\Delta^{14}C$, which is the per mil (‰) deviation of the

© 2008 NRC Canada

sample from the radiocarbon concentration of 19th-century wood, corrected for sample decay prior to 1950 according to methods outlined by Stuiver and Polach (1977). The mean standard deviation of the individual radiocarbon assays was about 5‰.

To assign dates of core deposition for the bluefin tuna otoliths, we compared the tuna $\Delta^{14}C$ data to a $\Delta^{14}C$ chronology based on known-age material (a reference chronology) for the northwest Atlantic derived from known-age fish otoliths formed between 1949 and 2000 (Campana et al. 2008). The $\Delta^{14}C$ chronology of fish otoliths in the Northwest Atlantic parallels that of North Atlantic corals and bivalves (Campana 1997), so it is a good proxy for the $\Delta^{14}C$ dissolved inorganic carbon history of the tuna environment assuming that the tuna spent at least part of their first 2–3 years of life in the upper 200 m of the water column.

Estimation of the parameters of the von Bertalanffy growth equation were made using nonlinear estimation approaches, described in Cope and Punt (2007). Those authors have also developed random effects methods that allow for multiple age readings from the same fish and thereby provide estimates of ageing error.

Results and discussion

An example of a transverse section is shown, demonstrating the periodic banding that we assumed to represent annuli (Fig. 1*a*). Based on our experience, these annuli were relatively straightforward to identify and count compared with other species.

The results of the radiocarbon assays are shown, in comparison with the reference chronology for the Northwest Atlantic (Fig. 1*b*). The distribution of the radiocarbon results appears consistent with the reference chronology, implying that the age determinations of the primary age reader are accurate. Consistent age underestimation or overestimation would have been clearly evident as a shift of the entire fitted curve to the left or the right of the reference chronology. Campana (2001) has indicated that the expected precision of ages validated with the bomb radiocarbon approach is 1–3 years.

There was, however, a slight but not significant (paired *t* test, $p > 0.01$) tendency for the secondary age readers to underage relative to the primary reader (Fig. 2*a*), but those differences were small in relation to the predicted values from age–length model of Turner and Restrepo (1994). Age underestimation from the Turner and Restrepo (1994) model was evident at ages greater than 7 years, but was most acute at ages exceeding 18 years.

Although the sample size is small and the collection generally skewed towards larger fish, we fitted the available data to a von Bertalanffy growth equation using a standard nonlinear fit (Table 1). Using the ages obtained by all three age readers, we also fitted the growth equation using the random effects method described by Cope and Punt (2007).

The von Bertalanffy curve for the primary reader is plotted along with the Turner and Restrepo (1994) fit currently used in the assessment (Fig. 2*b*). On the basis of the validated age determinations, it appears that the older analysis has overestimated L_∞ and the growth rate, despite the fact that the bluefin tuna samples used in our analysis were contemporaneous with those used in the Turner and Restrepo (1994) analysis. As noted by Restrepo et al. (2007), the estimation of the von Bertalanffy growth parameters may be influenced by the size and age ranges included in the analyses, and the differences between our results and those of Turner and Restrepo (1994) are probably related to this, at least in part. Our results present an estimate of L_∞ that is more comparable with those of Hurley and Iles (1983) (L_∞ of 278 and 266 cm for males and females, respectively). Hurley and Iles (1983) also raised the issue of frequency of formation of apparent annuli as a possible source of error. Our results provide evidence that the structures considered to be annuli are indeed formed annually.

The coefficient of variation for the multiple ages is also relatively low (0.12) compared with most of the values reported by Cope and Punt (2007) for other taxa, suggesting that the secondary age readers were able to obtain ages that were reasonably consistent when compared with the primary reader.

While our results provide a more realistic estimate of L_∞ than was available previously, more work is required to refine the estimate of t_0, as relatively few small fish are included here. Furthermore, the applicability of our description of bluefin growth to the current situation remains unknown, as our samples were necessarily taken from older collections to ensure that the ages included in the validation included the period of rapidly increasing radiocarbon. However, our results, which include electronically annotated images of the material used in this study, form a valuable reference set for future age and growth studies of bluefin tuna. The validation results completed here, along with the observations that the periodic structures of bluefin tuna are readily observed and consistently counted, provide a basis for routine age determinations in the future.

Acknowledgements

This work was supported by the International Fisheries and Oceans Governance and Strategic Science Funds of Fisheries and Oceans Canada and the Bluefin Year Program of ICCAT. Persephone Megalafonou and Naomi Clear provided expert interpretations of the bluefin otoliths used in this study. Warren Joyce and Jamie Joudrey provided imaging and micromilling expertise. We thank Jason Cope (University of Washington) for assistance with the software used for the estimation of the von Bertalanffy growth equation presented here and Enrique Rodriguez-Marin for his helpful review of an earlier version of this paper.

References

Baker, M.S., and Wilson, C.A. 2001. Use of bomb radiocarbon to validate otolith section ages of red snapper *Lutjanus campechanus* from the northern Gulf of Mexico. Limnol. Oceanogr. **46**: 1819–1824.

Campana, S.E. 1997. Use of radiocarbon from nuclear fallout as a dated marker in the otoliths of haddock, *Melanogrammus aeglefinus*. Mar. Ecol. Prog. Ser. **150**: 49–56. doi:10.3354/meps150049.

Campana, S.E. 2001. Accuracy, precision and quality control in age determination, including a review of the use and abuse of age validation methods. J. Fish Biol. **59**: 197–242. doi:10.1111/j.1095-8649.2001.tb00127.x.

© 2008 NRC Canada

Campana, S.E., Casselman, J.M., and Jones, C.M. 2008. Bomb radiocarbon chronologies in the Arctic, with implications for the age validation of lake trout (*Salvelinus namaycush*) and other Arctic species. Can. J. Fish. Aquat. Sci. **65**: 733–743. doi:10.1139/F08-012.

Cope, J.M., and Punt, A.E. 2007. Admitting ageing error when fitting growth curves: an example using the von Bertalanffy growth function with random effects. Can. J. Fish. Aquat. Sci. **64**: 205–218. doi:10.1139/F06-179.

Fromentin, J.-M., and Powers, J.E. 2005. Atlantic bluefin tuna: population dynamics, ecology, fisheries and management. Fish Fish. **6**: 281–306.

Hurley, P.C.F., and Iles, T.D. 1983. Age and growth estimation of Atlantic bluefin tuna *Thunnus thynnus* using otoliths. NOAA–NMFS Tech. Rep. 8. pp. 71–75.

ICCAT. 2003. Report of the 2002 bluefin tuna stock assessment session. Col. Vol. Sci. Pap. ICCAT, **55**: 710–937.

Restrepo, V.R., Rodriguez-Marin, E., and Rodriguez-Cabello, C. 2007. Are the growth curves currently used for Atlantic bluefin tuna statistically different? Col. Vol. Sci. Pap. ICCAT, **60**: 1014–1026.

Stuiver, M., and Polach, H.A. 1977. Reporting of C-14 data. Radiocarbon, **19**: 355–363.

Turner, S.C., and Restrepo, V.R. 1994. A review of the growth rate of west Atlantic bluefin tuna, *Thunnus thynnus*, estimated from marked and recaptured fish. Col. Vol. Sci. Pap. ICCAT, **42**: 170–172.

Turner, S.C., Restrepo, V.R., and Eklund, A.M. 1991. A review of the growth rate of Atlantic bluefin tuna, *Thunnus thynnus*. Col. Vol. Sci. Pap. ICCAT, **35**: 271–293.

© 2008 NRC Canada

RAPID COMMUNICATION / COMMUNICATION RAPIDE

Copepod production drives recruitment in a marine fish

Martin Castonguay, Stéphane Plourde, Dominique Robert, Jeffrey A. Runge, and Louis Fortier

Abstract: Predicting fluctuations in recruitment of commercial marine fish remains the Holy Grail of fisheries science. In previous studies, we identified statistical relationships linking Atlantic mackerel (*Scomber scombrus*) recruitment to regional climate, zooplankton biomass, and the production of copepod nauplii over a decade (1982–1991) that included the exceptionally strong year class of 1982. Here we tested the validity of these relationships by adding a second decade (1992–2003) of observations that includes another exceptional year class in 1999. We provide the first field-based evidence linking availability of plankton prey in the sea to early growth of larval fish and to year-class strength in a commercially exploited marine fish. Recruitment is shown to strongly depend on production of the copepod nauplii species that contribute to the diet of mackerel larvae. Both strong year classes were characterized by exceptionally high availability of these specific prey. We suggest that mackerel recruitment can be anticipated 3 years in advance based on prey availability during the first weeks of planktonic life and predict a strong year class for fish hatched in 2006.

Résumé : La prédiction des fluctuations de recrutement des poissons marins d'importance commerciale demeure le Saint Graal des sciences halieutiques. Au cours d'études précédentes, nous avons identifié des relations statistiques reliant le recrutement du maquereau bleu (*Scomber scombrus*) au climat régional, à la biomasse du zooplancton ainsi qu'à la production en nauplii de copépodes durant une décennie (1982–1991) qui incluait la classe d'âge exceptionnelle de 1982. Ici nous testons la validité de ces relations en ajoutant une deuxième décennie (1992–2003) d'observations qui incluent une autre classe d'âge exceptionnelle en 1999. Nous présentons les premières preuves basées sur des données de terrain qu'il existe un lien entre la disponibilité des proies planctoniques en mer, la croissance des jeunes larves et la force des classes d'âge chez une espèce de poisson marin exploitée commercialement. Nous démontrons que le recrutement dépend fortement de la production en nauplii des espèces de copépodes qui contribuent à l'alimentation des larves de maquereau. Les deux fortes classes d'âge ont été caractérisées par une disponibilité exceptionnelle de ces proies spécifiques. Nous suggérons que le recrutement du maquereau peut être anticipé 3 ans à l'avance selon la disponibilité des proies durant les premières semaines de vie planctonique et prédisons une forte classe d'âge pour les poissons nés en 2006.

Hjort's (1914) seminal hypothesis that the abundance of fish cohorts (i.e., year classes) is determined during early larval life in the plankton still prevails (Houde 2002; Platt et al. 2003). Availability of adequate prey in the weeks after hatching is considered necessary for a strong year class to emerge (e.g., Cushing 1990). However, empirical evidence of the role of prey availability in driving fluctuations in year-class strength has remained elusive (Leggett and Deblois 1994). Most studies that attempted to link recruitment to environmental conditions focused on abiotic factors, such as temperature or salinity (Myers 1998; Beaugrand et al. 2003). Statistical links between prey availability and recruitment success (Cushing 1990; Runge et al. 1999; Beaugrand et al. 2003) remain few and often fail when retested with longer time series (Myers 1998). The impacts of feeding conditions in the plankton on recruitment are particularly difficult to elucidate owing to (*i*) an often low spatial and temporal sampling resolution; (*ii*) imprecision in the identification of the actual prey of the larvae; and (*iii*) relatively little contrast between the weakest and strongest year classes in some fish stocks or species. Atlantic mackerel (*Scomber scombrus*) represents an ideal model to study the effect of

Received 4 April 2008. Accepted 13 June 2008. Published on the NRC Research Press Web site at cjfas.nrc.ca on 27 June 2008. J20494

M. Castonguay[1] and S. Plourde. Institut Maurice-Lamontagne, Ministère des Pêches et des Océans, 850 Route de la Mer, C.P. 1000, Mont-Joli, QC G5H 3Z4, Canada.
D. Robert and L. Fortier. QC-Océan, Département de Biologie, Université Laval, 1045 avenue de la Médecine, Québec, QC G1K 7P4, Canada.
J.A. Runge. School of Marine Sciences, University of Maine, Gulf of Maine Research Institute, 350 Commercial Street, Portland, ME 04101, USA.

[1]Corresponding author (e-mail: martin.castonguay@dfo-mpo.gc.ca).

 doi:10.1139/F08-126 © 2008 NRC Canada

Fig. 1. Environmental relationships and recruitment for 1982–1991 (left column) and 1982–2003 (right column): regressions of zooplankton (Zoo) biomass >1000 µm (g dry weight (DW) $\cdot m^{-2}$) (*a*, *b*) and of mackerel recruitment index (MACREC; i.e., percentage of age-3 fish in Canadian catch-at-age) (*c*, *d*) versus an index of climate variability (RIVSUM; i.e., January–May freshwater discharge from St. Lawrence River into Gulf). Lower panels (*e*, *f*) show regressions of MACREC against zooplankton biomass >1000 µm. Blue circles represent 1982–1991 data, while red ones show 1992–2003 data (1995 and 1997 missing); 1982 and 1999 are highlighted. Coefficient of determination (r^2), level of significance (*p*), and sample size (*n*) are reported.

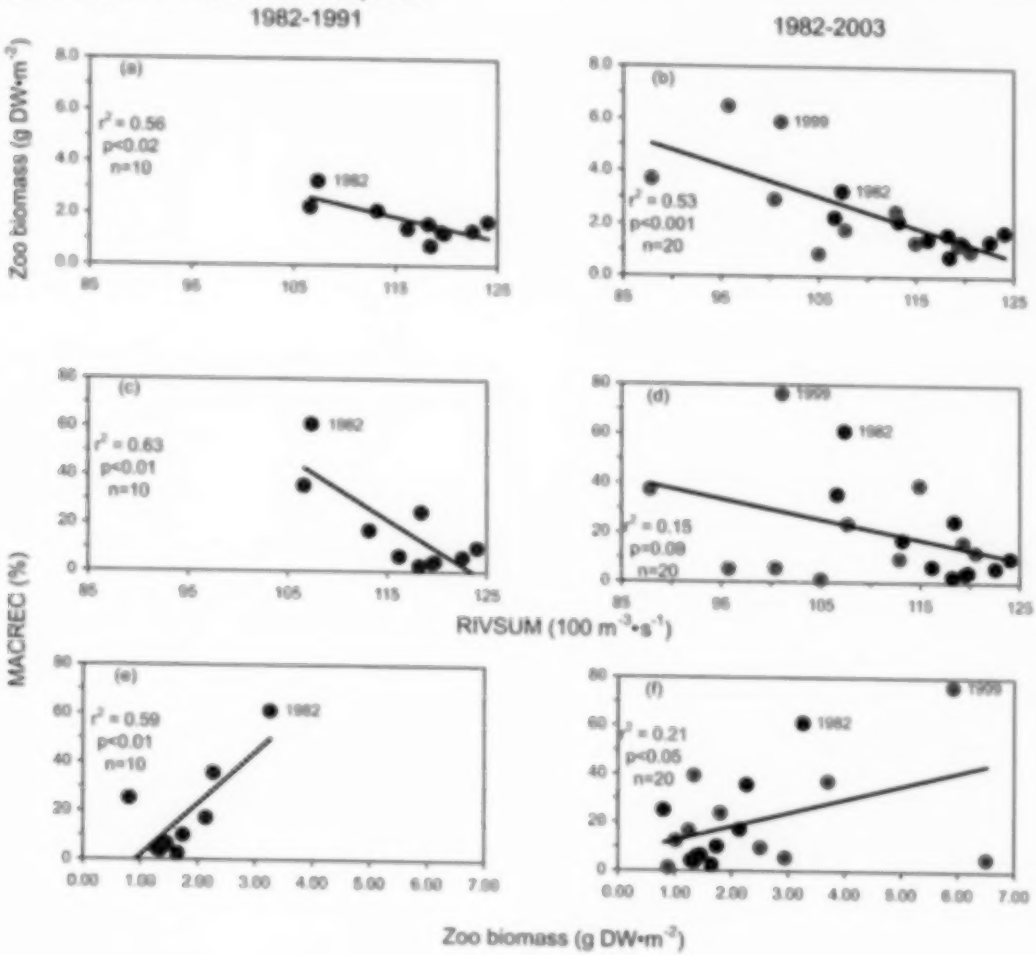

prey availability during larval life on recruitment because it exhibits high interannual variability in year-class strength and completes spawning over a short time interval (<1 month) in a well-defined area (southern Gulf of St. Lawrence), facilitating sampling of the larvae and their prey (e.g., Grégoire 2000).

Since 1982, Atlantic mackerel reproductive biomass in Canada has been estimated annually (except 1994 and 1997) by measuring egg abundance on the main spawning site during peak spawning in late June (Grégoire 2000). A bongo net (61 cm diameter) fitted with 333 µm mesh and flow meters is deployed at 65 stations over a fixed grid covering the southern Gulf of St. Lawrence. Double-oblique tows are conducted between 0 and 50 m to sample fish eggs and larvae and zooplankton. Zooplankton biomass is measured for the size fractions <1000 µm (mainly small copepods) and >1000 µm (mainly late copepodites of *Calanus* spp.). The relationships between recruitment success and zooplankton biomass for 1982–1991, the mackerel recruitment index MACREC, and details of methods are presented in Runge et al. (1999). Data on zooplankton stage abundance and egg production are from Ringuette et al. (2002) for 1982, 1985, 1987, and 1990 and from new analyses for 1988, 1993, 1996, 1999, 2000, and 2003. Years were selected to span the two decades evenly while including the strong year classes of 1982 and 1999.

The exceptionally strong mackerel recruitment of 1982 occurred during a year of atypical abiotic and biotic conditions in the southern Gulf of St. Lawrence. Winter–spring freshwater discharge from the St. Lawrence River into the Gulf, an index of climate variability in eastern Canada termed RIVSUM, was particularly low, while the biomass

© 2008 NRC Canada

Fig. 2. (*a*) Daily egg production rates for the copepods *Calanus finmarchicus* (red), *Pseudocalanus* spp. (blue), and *Temora longicornis* (yellow) in the southern Gulf of St. Lawrence for selected years. Rates were calculated as the product of mean female abundance and specific egg production rates to obtain an estimate of prey production (Ringuette et al. 2002). (*b*) Regression of mackerel recruitment (MACREC) as a function of copepod egg production as presented in (*a*). Blue circles: 1982–1991; red circles: 1992–2003. Years of exceptional recruitment in 1982 and 1999 are highlighted. Coefficient of determination (r^2), level of significance (p), and sample size (n) are reported.

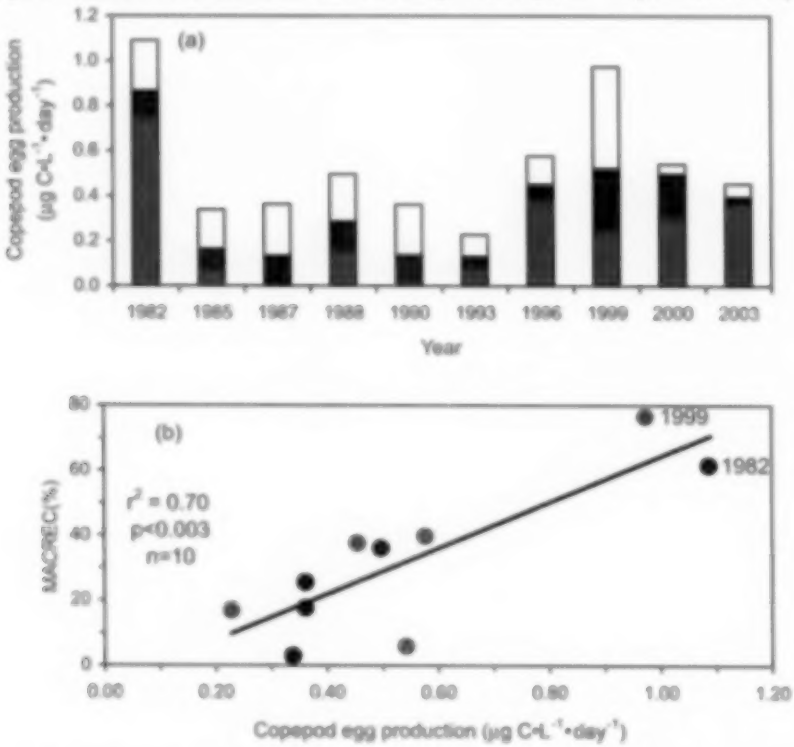

of large (>1000 µm) zooplankton was the highest of the decade (Runge et al. 1999). The latter was considered a proxy of the abundance of *Calanus finmarchicus* females, with the underlying assumption that the abundance of eggs and nauplii of this species dictate larval mackerel survival (Runge et al. 1999). The abundance of *C. finmarchicus* females in 1982 was the greatest of the 1982–1991 period, and stomach contents of mackerel larvae during that year were significantly heavier largely because of a greater ingestion of *C. finmarchicus* nauplii (Ringuette et al. 2002).

The following decade of data (1992–2003) included a second year of exceptional mackerel recruitment in 1999. As in the strong year class of 1982, low RIVSUM and high zooplankton biomass prevailed in the southern Gulf of St. Lawrence in 1999. Despite these similarities between the 2 years of extreme recruitment, only two of the three relationships linking year-class strength to climate and zooplankton identified by Runge et al. (1999) for the decade 1982–1991 remained significant with the addition of new data for 1992–2003 (Fig. 1). The relationship between recruitment strength and RIVSUM became nonsignificant (Fig. 1*d*), while the once strong relationship between recruitment and zooplankton biomass >1000 µm weakened, explaining only 21% of the variance of the expanded data set (Fig. 1*f*). Statistical relationships linking recruitment to broad indices of the environment such as temperature, salinity, or total zooplankton biomass often subside when retested with longer time series (Myers 1998).

In this study, the weakening of the recruitment – zooplankton biomass relationship is likely attributable to changes in the relative abundance of large copepods between the two decades. When comparing the 1982–1991 and 1992–2003 periods in the southern Gulf, the average contribution of the large arctic calanoid *Calanus hyperboreus* to zooplankton biomass almost doubled, from 39% to 73%. *Calanus hyperboreus* typically reproduces from mid-December to March in the Gulf of St. Lawrence and therefore does not contribute to the production of nauplius prey during the period of mackerel larval growth in summer (Plourde et al. 2003). Hence interdecadal shifts in the relative abundance of this large copepod will seriously bias total zooplankton biomass as a proxy for the availability of nauplius prey to mackerel larvae.

The above emphasises the importance of focusing on the actual zooplankton prey of larvae in trying to link recruitment variability to fluctuations in ecosystem productivity. In the Gulf of St. Lawrence, mackerel larvae prey selectively on the nauplii of the copepods *C. finmarchicus*, *Pseudocalanus* spp., and *Temora longicornis* (Ringuette et al. 2002; Robert et al. 2008), the availability of which is approximated by the number of eggs spawned by females (Fig. 2*a*). A strong linear relationship linked year-class

© 2008 NRC Canada

strength to the combined egg production of the three species (Fig. 2*b*). The exceptional recruitment of 1982 and 1999 corresponded to the highest egg production, ~1 μg C·L^{-1}·day^{-1}, by the three preferred copepods. Further validation in other mackerel spawning regions and for other pelagic species should be carried out to test the generality of relationships between copepod production and pelagic fish recruitment.

High prey availability is assumed to promote early survival and recruitment through the optimization of food intake and growth during larval life in the plankton (Cushing 1990). In the southern Gulf of St. Lawrence, feeding success and recent growth of young mackerel larvae increased hyperbolically as a function of the density of their preferred nauplius prey (D. Robert, M. Castonguay, and L. Fortier, unpublished data). Optimal feeding and growth were achieved above a threshold concentration of preferred nauplius prey of ~1 μg C·L^{-1}. Taken altogether, these results provide the first field-based evidence linking the availability of actual plankton prey to early growth and, ultimately, to year-class strength in a commercially exploited fish.

The zooplankton biomass >1000 μm remained negatively related to RIVSUM with the addition of the new decade of data (Fig. 1*b*), indicating that environmental conditions in winter–spring would still play a key role in the control of overall biological production in the region. Even though processes behind this relationship remain equivocal (Runge et al. 1999), recent research conducted with a 3-dimensional (3D)-coupled biophysical model of *C. finmarchicus* in the Gulf of St. Lawrence suggests that advection from the upstream northwest areas through the Gaspé Current is the most likely source of *Calanus* for the southern Gulf of St. Lawrence. Simulations showed that the Gaspé Current splits into two main branches, carrying surface-dwelling development stages either offshore north of the region along the deep Laurentian Channel towards the Magdalen Islands or inshore in the western part of the region. How these two circulation pathways would react to variations in environmental forcing (RIVSUM) remains unknown. However, the opposite relationships between recruitment and RIVSUM once observed in the region for American lobster (*Homarus americanus*) (positive) and Atlantic mackerel (negative) suggest that these two branches of the Gaspé Current could react differently to environmental forcing, leading to region-specific conditions favourable to recruitment (F. Saucier, Institut des sciences de la mer de Rimouski, Université du Québec à Rimouski, 310 Allée des Ursulines, Rimouski, QC G5L 3A1, Canada, personal communication, 2008; and J. Chassé, Gulf Fisheries Centre, Fisheries and Oceans Canada, Moncton, NB E1C 9B6, Canada, personal communication, 2008).

Our results provide support for a strong dependence of year-class strength on food production during the larval stage, as postulated by prevailing hypotheses on recruitment determination in marine fish (Hjort 1914; Cushing 1990). In contrast with many previous studies, including ours, this dependence was revealed by estimating the in situ production of the actual prey species selected by the young fish (rather than bulk zooplankton standing biomass). On the basis of the measured high production of copepod eggs (>1 μg C·L^{-1}; S. Plourde, unpublished data), larval food conditions were in place for exceptional mackerel recruitment in 2006.

Acknowledgements

We thank Pierre Joly and Jean-Louis Beaulieu for help with sample processing and data management and François Grégoire for providing the mackerel recruitment index. The efforts of Alain Gagné and numerous people who collected and analysed zooplankton samples are acknowledged. Laure Devine, Patrick Ouellet, Bernard Sainte-Marie, and two anonymous referees provided comments on an earlier version. This study was supported by Fisheries and Oceans Canada and Québec-Océan at Université Laval. J.R. acknowledges National Science Foundation (NSF) award OCE-0733907 to the US GLOBEC Northwest Atlantic/Georges Bank program.

References

Beaugrand, G., Brander, K.M., Allstair Lindley, J., Souissi, S., and Reid, P.C. 2003. Plankton effect on cod recruitment in the North Sea. Nature (London), **426**: 661–664. doi:10.1038/nature02164. PMID:14668864.

Cushing, D.H. 1990. Plankton production and year-class strength in fish populations: an update of the match/mismatch hypothesis. Adv. Mar. Biol. **26**: 249–294.

Grégoire, F. 2000. The Atlantic mackerel (*Scomber scombrus*) of NAFO Subareas 2 to 6. Can. Stock Assess. Sec. Res. Doc. 2000/021.

Hjort, J. 1914. Fluctuations in the great fisheries of northern Europe viewed in light of biological research. Rapp. P.-V. Reun. Cons. Int. Explor. Mer, **20**: 1–228.

Houde, E.D. 2002. Mortality. *In* Fishery science: the unique contributions of early life stages. *Edited by* L.A. Fuiman and R.G. Werner. Blackwell Publishers, Malden, Mass., USA. pp. 64–87.

Leggett, W.C., and Deblois, E. 1994. Recruitment in marine fishes: Is it regulated by starvation and predation in the egg and larval stages? Neth. J. Sea Res. **32**: 119–134. doi:10.1016/0077-7579(94)90036-1.

Myers, R.A. 1998. When do environment–recruitment correlations work? Rev. Fish Biol. Fish. **8**: 285–305. doi:10.1023/A:1008828730759.

Platt, T., Fuentes-Yaco, C., and Frank, K.T. 2003. Spring algal bloom and larval fish survival. Nature (London), **423**: 398–399. doi:10.1038/423398b. PMID:12761538.

Plourde, S., Joly, P., Runge, J.A., Dodson, J., and Zakardjian, B. 2003. Life cycle of *Calanus hyperboreus* in the lower St. Lawrence Estuary and its relationship to local environmental conditions. Mar. Ecol. Prog. Ser. **255**: 219–233. doi:10.3354/meps255219.

Ringuette, M., Castonguay, M., Runge, J.A., and Grégoire, F. 2002. Atlantic mackerel (*Scomber scombrus*) recruitment fluctuations in relation to copepod production and juvenile growth. Can. J. Fish. Aquat. Sci. **59**: 646–656. doi:10.1139/f02-039.

Robert, D., Castonguay, M., and Fortier, L. 2008. Effects of intra- and inter-annual variability in prey field on the feeding selectivity of larval Atlantic mackerel (*Scomber scombrus*). J. Plankton Res. **30**: 673–688. doi:10.1093/plankt/fbn030.

Runge, J.A., Castonguay, M., de Lafontaine, Y., Ringuette, M., and Beaulieu, J.-L. 1999. Covariation in climate, zooplankton biomass and mackerel recruitment in the southern Gulf of St. Lawrence. Fish. Oceanogr. **8**: 139–149. doi:10.1046/j.1365-2419.1999.00095.x.

© 2008 NRC Canada

River flow controls ecological processes and invertebrate assemblages in subsurface flowpaths of an ephemeral river reach

Thibault Datry and Scott T. Larned

Abstract: We present the first measurements of solutes, invertebrates, and microbial activity in the semi-perched hyporheic, parafluvial, and riparian flowpaths of an ephemeral river channel. Dissolved organic carbon (DOC), nitrogen (DON), and phosphorus (DOP) concentrations decreased as water from an adjacent river mainstem moved through the flowpaths. DOC, DON, and DOP processing rates decreased with increasing mainstem flow and increased with parafluvial zone length. These patterns suggest that the surface water zones of perched river systems are organic nutrient sources to subsurface flowpaths and that parafluvial zones of these systems are strong sinks for organic matter. No longitudinal changes were detected in NO_3^- concentrations, and relationships between NO_3^- processing and hydrological variables were not significant. NO_3^- concentrations were uniformly high, and microbial activity and DOC and dissolved reactive phosphorus (DRP) concentrations were low, suggesting that biological NO_3^- removal was carbon- or phosphorus-limited. Invertebrate assemblages also varied between subsurface zones: density and taxon richness in the hyporheic and parafluvial zones were higher than in the riparian zone, and evenness was higher in the riparian zone than in the hyporheic or parafluvial zones. Distinct invertebrate assemblages in riparian zones may reflect greater hydrologic stability compared with hyporheic and parafluvial zones.

Résumé : Nous présentons les premières mesures des solutés, des invertébrés et de l'activité microbienne dans les voies de passage hyporhéiques semi-perchées, parafluviales et riveraines du chenal d'une rivière éphémère. Les concentrations de carbone organique (DOC), d'azote (DON) et de phosphore (DOP) dissous diminuent à mesure que l'eau provenant du cours principal d'une rivière adjacente traverse les diverses voies de passage. Les taux de transformation de DOC, DON et DOP décroissent lorsque le débit augmente dans le cours principal et s'accroissent en fonction de la longueur de la zone parafluviale. Ces patrons laissent croire que les zones d'eau superficielle des systèmes de rivières perchés servent de source de nutriments organiques pour les voies de passage souterraines et que les zones parafluviales de ces systèmes sont d'importants pièges de matière organique. Nous ne détectons aucun changement longitudinal des concentrations de NO_3^- et il n'y a pas de relation significative entre la transformation de NO_3^- et les variables hydrologiques. Les concentrations de NO_3^- sont uniformément élevées, alors que l'activité microbienne et les concentrations de DOC et de phosphore réactif dissous (DRP) sont faibles; ces observations indiquent que le retrait biologique de NO_3^- est limité par le carbone ou par le phosphore. Les peuplements d'invertébrés varient aussi d'une zone souterraine à une autre: la densité et la richesse en taxons sont plus élevées dans les zones hyporhéiques et parafluviales que dans la zone riveraine et l'équitabilité est plus grande dans la zone riveraine que dans les zones hyporhéiques et parafluviales. Les peuplements particuliers d'invertébrés dans les zones riveraines peuvent être le reflet d'une plus grande stabilité hydrologique par comparaison aux zones hyporhéiques et parafluviales.

[Traduit par la Rédaction]

Introduction

Hydrologic variability is one of the most important determinants of community structure and biogeochemical processes in river–floodplain systems. In early evaluations of hydrologic variability, the focus was on low-frequency, large-magnitude floods and droughts (e.g., Junk et al. 1989; Townsend 1989; Yount and Niemi 1990). More recently, consideration of hydrologic variability has expanded to include flow fluctuations that remain below bankfull (Tockner et al. 2000). These high-frequency "flow pulses" drive surficial expansion–contraction cycles in many alluvial rivers (Stanley et al. 1997; Malard et al. 2000; Poole et al. 2002). In turn, expansion and contraction of wetted surface

Received 21 August 2007. Accepted 27 March 2008. Published on the NRC Research Press Web site at cjfas.nrc.ca on 4 July 2008. J20144

T. Datry.[1,2] Biologie des Ecosystèmes Aquatiques, CEMAGREF, Groupement de Lyon, 3 bis quai Chauveau, F-69336 Lyon Cedex 09, France.
S.T. Larned. National Institute of Water and Atmospheric Research, P.O. Box 8602, Christchurch, New Zealand.

[1]Corresponding author (e-mail: thibault.datry@cemagref.fr).
[2]Present address: National Institute of Water and Atmospheric Research, P.O. Box 8602, Christchurch, New Zealand.

 doi:10.1139/F08-075 © 2008 NRC Canada

area increases habitat heterogeneity and taxonomic diversity and influences nutrient cycling (Van der Nat et al. 2003; Malard et al. 2006; Tockner et al. 2006).

The same river flow fluctuations that drive surficial expansion–contraction cycles appear to drive expansion–contraction cycles in the sediments beneath and adjacent to alluvial channels. Empirical relationships between river flow and the dimensions of subsurface flowpaths have been reported for stream reaches with saturated connections to aquifers (e.g., Wondzell and Swanson 1996*a*; Morrice et al. 1997; Wroblicky et al. 1998). In these cases, subsurface flowpath size was inversely related to surface flow, because groundwater inflow increased directly with stream discharge and reduced surface water outflow. Unlike the preceding examples, subsurface flowpaths associated with ephemeral rivers are "perched", or separated from regional aquifers by layers of unsaturated sediment (Malard et al. 2000, 2002). It is likely that subsurface flowpaths extending from ephemeral rivers expand with increasing surface flow rather than contract, because the hydraulic gradients imposed by groundwater are very small (Malard et al. 2002).

River flow fluctuations affect the composition and arrangement of subsurface flowpaths, as well as flowpath dimensions. Three classes of subsurface flowpath are distinguished on the basis of hydrologic exchange: hyporheic, parafluvial, and riparian (Boulton et al. 1998; Dahm et al. 1998; Fisher et al. 1998). Hyporheic flowpaths lie beneath submerged channels and are characterized by vertical surface–subsurface exchange along their lengths. Parafluvial flowpaths are located within emergent bars, terraces, and periodically flooded side branches, and surface–subsurface exchange only occurs where the flowpath meets the surface water zone (e.g., along stream banks and bar margins). Riparian or floodplain flowpaths lie within terraces and hillslopes distal to parafluvial zones and have no direct exchange with surface water. The classes and relative sizes of flowpaths that occur along subsurface gradients can change over surface-water expansion and contraction cycles. Parafluvial and riparian zones can become hyporheic zones during expansion phases, when gravel bars and riparian areas are submerged, and hyporheic zones can become parafluvial during contraction phases (Boulton et al. 1992; Dahm et al. 1998; Del Rosario and Resh 2000). Parafluvial and riparian zones are composed of both saturated and unsaturated sediments, and the proportion of saturated sediment varies with flow and (or) groundwater level (Dahm et al. 1998).

Rates of biogeochemical processes, microbial activity, and invertebrate assemblage structure in subsurface flowpaths can vary in response to surface flow fluctuations (Valett et al. 1997; Wondzell and Swanson 1996*b*; Dole-Olivier et al. 1997). Comparisons of ecological processes and biodiversity in hyporheic, parafluvial, and riparian flowpaths are rare, but there is some evidence that these flowpaths have distinct chemical and invertebrate compositions (Stanley and Boulton 1995; Lewis et al. 2006). Based on the preceding observations, we predicted that surface flow fluctuations in ephemeral rivers would affect subsurface ecosystems by altering the sizes of subsurface flowpaths. Specifically, we predicted that the size or predominance of parafluvial flowpaths relative to hyporheic flowpaths would influence ecological processes and biodiversity, because reduced surface–subsurface exchange and slow advection in parafluvial flowpaths create steep longitudinal gradients in chemical reactants and organic matter (Boulton and Stanley 1995; Lewis et al. 2006).

In this study, we examined dissolved carbon (C), nitrogen (N), and phosphorus (P) dynamics, microbial activity, and invertebrate assemblages along a subsurface gradient in a perched ephemeral river channel in New Zealand. We compared ecological processes and invertebrate assemblages in hyporheic, parafluvial, and riparian zones. We then quantified the effects of surface flow on parafluvial flowpath length and the effects of surface flow and parafluvial flowpath length on dissolved C, N, P, microbial activity, and invertebrate assemblages.

Materials and methods

Study site

The study was carried out in the Selwyn River, on the east coast of New Zealand's South Island (Fig. 1). The Selwyn River flows east through the foothills of the Southern Alps across the alluvial Canterbury Plains to Lake Ellesmere on the Pacific coast. For the first 38 km of its course across the plains, downward seepage through the bed (transmission loss) causes flow in the Selwyn to decrease with distance downstream, except at points of tributary inflow (Larned et al. 2008). Aerial photographs indicate that the river changed course between 1999 and 2001 and abandoned a 450 m long arcuate reach, which we selected for our study site (Fig. 1). This reach (hereafter, referred to as the "ephemeral channel") is separated at its head and tail from the current mainstem by marginal gravel bars.

Surface flow in the Selwyn is unregulated and varies in response to runoff and groundwater levels. A flow recorder was installed in the mainstem 25 m upstream of the ephemeral channel in February 2005. During our March 2005 – November 2006 study, mean daily average flow at this site was 2.1 $m^3 \cdot s^{-1}$ (range 0 to 28 $m^3 \cdot s^{-1}$). At flows over ~3 $m^3 \cdot s^{-1}$, the bar separating the mainstem from the head of the ephemeral channel overtops and surface flow commences in the ephemeral channel. At lower flows, subsurface flow in the ephemeral channel is fed from the mainstem by seepage through the bar.

Bed material in the ephemeral channel is heterogeneous and consists of gravels, cobbles, and small boulders, with occasional well-sorted gravel sheets and scour pools with fine depositional material. Vegetation in the ephemeral channel bed is predominately annual grasses and herbs. The true right bank is bordered by a low terrace and an excised island that is vegetated with annual grasses and perennial shrubs. The true left bank is bordered by a higher terrace, 1–2 m above the ephemeral channel elevation, and vegetated with annual grasses, perennial shrubs, and trees. We refer to the terraces as the riparian zone and to flowpaths within the terraces and above the regional water table as riparian flowpaths.

The section of the Selwyn mainstem adjacent to the ephemeral channel loses water to groundwater at an average rate of 0.5 $m^3 \cdot s^{-1} \cdot km^{-1}$ (Larned et al. 2008). The elevation of the regional groundwater table near the study site is 190–205 m above sea lavel (a.s.l.) or 10–25 m below ground sur-

© 2008 NRC Canada

Fig. 1. Location of the ephemeral channel and layout of piezometers and wells: (*a*) location of the Selwyn River on the South Island of New Zealand (left) and location of the study area in the ephemeral section of the Selwyn River; (*b*) distribution of piezometers along the ephemeral channel thalweg and sampling wells on the riparian terrace.

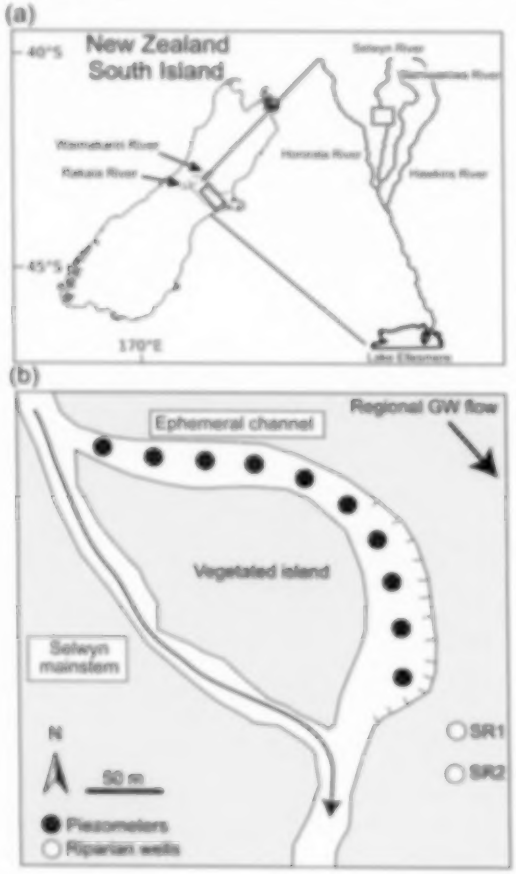

face. Rapid losses to groundwater and the position of the mainstem above the regional water table indicate that the river and saturated subsurface flowpaths extending from the river, including the study site, are "perched". Hereafter, we use the term "semi-perched" rather than perched, because the mainstem channel and subsurface flowpaths are underlain by a patchwork of high- and low-permeability sediments and the latter impede but do not prevent downward seepage (Smakhtin 2001; Osman and Bruen 2002; Shentsis and Rosenthal 2003).

Sampling design

Ten clusters of piezometers (open polyvinyl chloride (PVC) tubes, 20 mm diameter) were installed at 20 to 30 m intervals along the ephemeral channel thalweg. The first and last clusters were located 30 and 288 m downstream from the ephemeral channel head, respectively. Each cluster consisted of three piezometers, which sampled sediment depths of 30, 60, and 80 cm. Only the 60 and 80 cm piezometers were sampled for the present study, as the 30 cm piezometers did not reach saturated sediments on all occasions. Two 100 mm diameter sampling wells, designated SR1 and SR2, were installed in the riparian terrace 30 m (SR1) and 35 m (SR2) from the ephemeral channel. Well depth and screen length were 6.8 m and 6.0 m, respectively, for SR1 and 9.6 m and 9.0 m, respectively, for SR2. Screens were stainless steel with 4 mm slots. The locations of each piezometer and well were georeferenced with a global positioning system (Trimble 5700 RTK; Trimble Navigation Ltd., Sunnyvale, Calif.), with 2 cm horizontal and vertical resolution.

Riparian water levels and temperatures were continuously recorded in SR1 at 15 min intervals with a Solinst 3001 logger (Solinst Canada, Georgetown, Ontario, Canada). Water temperature was recorded in SR2 at 15 min intervals with a temperature logger (Stowaway Tidbit; Onset Computer, Bourne, Mass.). Surface and parafluvial water temperatures were recorded every 30 min for 5 months (26 February – 20 June 2005) with iButton loggers (Maxim Integrated Products, Sunnyvale, Calif.). The surface water iButton was anchored to the mainstem bed near the top of the ephemeral channel, and the parafluvial iButton was located in a piezometer at the downstream end of the ephemeral channel at a sediment depth of 80 cm. The iButtons remained immersed throughout the recording period.

Field procedures

Porewater, invertebrate, and sediment samples were collected from the piezometers on nine dates from March 2005 to November 2006. During this period, river flow at the recorder ranged from 0.7 to 12.9 $m^3 \cdot s^{-1}$. On each sampling date, the lengths of the hyporheic (wetted surface) and parafluvial (dry on surface) zones were measured along the channel thalweg, and each piezometer was classified as hyporheic or parafluvial. Because of the fixed length of the ephemeral channel transect (288 m), lengths of the hyporheic and parafluvial zones were inversely proportional. On sampling dates when flow in the mainstem was less than ~3 $m^3 \cdot s^{-1}$, there was no surface water in the ephemeral channel and no hyporheic zone; at flows over 15 $m^3 \cdot s^{-1}$ (not sampled), the ephemeral channel flowed for its entire length, and there was no parafluvial zone. Historic flow records indicate that the riparian terrace in the study area has not been inundated in at least 40 years.

On each sampling date, water surface elevation was measured in the piezometers with a water level sensor (Waterra WS-1; Solinst Canada, Georgetown, Ontario, Canada). Samples were then collected from the piezometers with a hand-operated bilge pump at a rate of ~6 $L \cdot min^{-1}$. The following procedure was used to collect subsurface water, invertebrates, and sediment; the aim of this procedure was to collect multiple aliquots from each piezometer, while retaining the invertebrates in each aliquot. The first 500 mL aliquot was filtered through a 63 µm mesh sieve. This aliquot served to rinse the pump hoses and flask, and the sieve retained invertebrates. A 2 L aliquot was then filtered through the same sieve, and the filtrate was used to triple-rinse and fill a 1 L acid-washed polyethylene bottle for nutrient analyses. Another 2 L aliquot was filtered through the sieve, and the filtrate was used to triple-rinse and fill a plastic bucket for water temperature, pH, and electrical conductivity meas-

© 2008 NRC Canada

urements, using a TPS meter (TPS WP 81; Enviroequip, Melbourne, Australia) and a pH electrode (Ionode IJ44; Ionode Pty. Ltd., Tennyson QLD 4105, Australia). A final 1.5 L aliquot was collected while agitating the pump hose to dislodge sediment at the base of the piezometer. The invertebrates in this aliquot were elutriated onto the 63 µm sieve, and the sediment remaining in the pump flask was transferred to an acid-washed polyethylene bottle for particulate organic matter (POM) and microbial analyses. Invertebrates were preserved in 95% isopropyl alcohol. The polyethylene bottles used for nutrient analyses were leached with deionized water for several weeks before each sampling date.

Water samples were collected from the riparian wells using a surface suction pump (pumping rate 10 L·min^{-1}) and a double packer that fixed the sampling depth at 50 cm below the water surface (Datry et al. 2005). A 50 L sample was filtered though a 63 µm mesh sieve to collect invertebrates, which were preserved in 95% alcohol. The filtrate was used for dissolved nutrient samples and water temperature, pH, and electrical conductivity measurements, as described above. A final 5 to 15 L aliquot was collected while shaking the pump hose to dislodge and withdraw sediment below the screen depth for POM and microbial analyses.

Surface water samples were collected from the mainstem 1 m from the head of the ephemeral channel by filling 1 L acid-washed, triple-sample-rinsed polyethylene bottles under the water surface. Electrical conductivity, water temperature, and pH were measured at the same site.

Laboratory procedures

Water samples for nutrient analysis were filtered (Whatman GF/F) within 3 h of collection and analyzed or frozen for subsequent analysis within 72 h of collection. Ammonium-N (NH_4^+), nitrate-N + nitrite-N, and dissolved reactive phosphorus (DRP) concentrations were determined using a flow-injection analyzer (QuikChem 8000; Lachat Instruments, Milwaukee, Wisconsin). Nitrite-N concentrations were <1% of nitrate-N concentrations, and nitrate-N + nitrite-N is hereafter referred to as NO_3^-. Detection limits for DRP, NH_4^+, and NO_3^- were 1 µg·L^{-1}. Total dissolved N (TDN) and P (TDP) concentrations were determined using the QuikChem 8000 after persulfate digestion (detection limits 10 µg·L^{-1} for TDN, 1 µg·L^{-1} for TDP). Dissolved organic N (DON) and P (DOP) concentrations were calculated as TDN ($NO_3^- + NH_4^+$), and TDP–DRP, respectively. Dissolved organic carbon concentrations (DOC) were determined in acidified samples by catalytic oxidation and infrared carbon dioxide detection using a LiquiTOC-2 analyzer (Elementar, Hanau, Germany) with a detection limit of 0.2 mg·L^{-1}. POM samples were weighed wet, dried at 60 °C to constant mass, ashed for 4 h at 400 °C, and reweighed. POM was determined from differences in dry and ash-free dry mass (AFDM).

Hydrolysis of fluorescein diacetate (FDA) by nonspecific esterases was used as an assay for total enzyme activity. Esterase activity in sediment samples was measured using the procedures of Fontvieille et al. (1992), with some modifications. Three 1 g subsamples were transferred from each sediment sample to ashed glass vials containing 3 mL phosphate buffer (pH 7.6) and 0.1 mL FDA solution (FDA in 60% acetone, 2 g·L^{-1}). Vials were incubated at 20 °C in darkness for 60–90 min, and the reactions were stopped with 3 mL $HgCl_2$ (400 mg·L^{-1}), followed by freezing. The supernatant in each vial was filtered through a 0.45 µm acetate filter, and absorbance was measured at 490 nm with a spectrophotometer (UV-2550; Shimadzu Corp., Columbia, Maryland) and then converted to µmoles of fluorescein. The fluorescein detection limit using this technique is ~0.1 µmol·L^{-1}. Sediment aliquots were dried at 60 °C to constant mass, and esterase activity rates were expressed as µmoles of FDA per hour per gram of sediment DM.

Invertebrates were enumerated and identified to the lowest taxonomic level possible. Taxonomic resolution varied among groups and developmental stages. Insects, gastropods, amphipods, and isopods were identified to family, genus, or species; mites, nematodes, flatworms, and tardigrades were identified to phylum; and other taxa were identified to class or family.

Data analyses

Subsurface water flow along the ephemeral channel was characterized using mainstem river flow, piezometer and well water levels, and water temperature data from February–June 2005. Temperature and flow data were converted to hourly averages. Temperature is a near-conservative tracer in highly permeable sediments, and we used a cross-correlation between surface flows and riparian well temperatures to estimate average subsurface water residence time in the ephemeral channel (Malard et al. 2001; Constantz et al. 2002). The cross-correlation corresponded to the correlation of the time series of surface water flow with the time series of riparian water temperature, shifted by a fixed number of hourly observations (lags). A second cross-correlation was used to estimate the lag time between surface flow and riparian well levels. In both analyses, correlation coefficients were calculated for 150 lags in 1 h intervals (1–75 h positive and 1–75 h negative).

Differences in water chemistry, esterase activity, and invertebrate density, taxon richness, Pielou evenness (J'), and percent insect taxa in the hyporheic, parafluvial, and riparian flowpaths were compared using one-way analyses of variance (ANOVAs) and pairwise Scheffé tests. The surface water zone was included in the comparisons of water chemistry. Dates were pooled for the ANOVAs. Because of differences in piezometer and well numbers and shifting numbers of hyporheic and parafluvial piezometers, the ANOVAs were unbalanced; sample sizes were 9 for the surface water zone, 27 for the hyporheic zone, 34 for the parafluvial zone, and 12 for the riparian zone. All invertebrate samples were normalized by volume. Nutrient concentrations and invertebrate densities were $\log_{10}(x + 1)$-transformed prior to statistical analysis to reduce variance heterogeneity. The significance level for all statistical analyses was 0.05.

Nutrient processing along the subsurface gradient (the net effect of retention, transformation, and production) was estimated from differences in concentrations between the surface water zone and the downstream-most piezometer. Regressions were used to quantify relationships between nutrient processing and two explanatory variables, river flow and length of the parafluvial zone. River flow data were daily means at the recorder. Relationships between nutrient processing and parafluvial zone length were used to

© 2008 NRC Canada

Fig. 2. (*a*) A 2005 times series of mainstem river flow (thick line) and water level (thin line) in the riparian zone well SR1; (*b*) 2005 times series of river surface (thin line), parafluvial (thick line), and riparian water (broken line) temperatures.

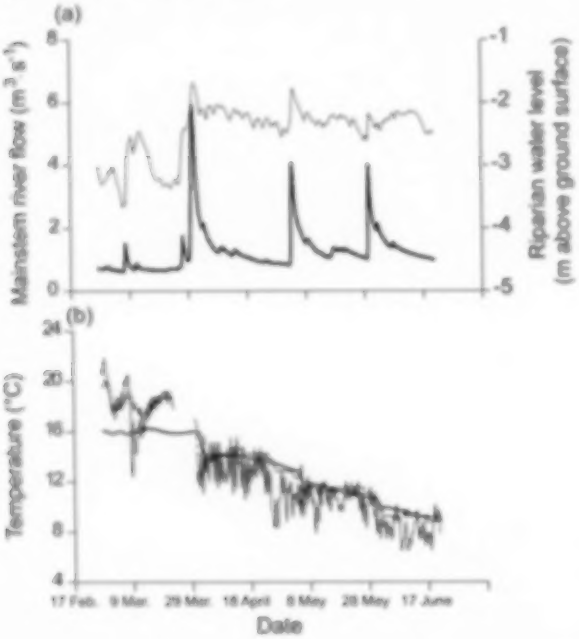
(a)
Mainstem river flow (m³ s⁻¹)
Riparian water level (m above ground surface)
(b)
Temperature (°C)
17 Feb. 9 Mar. 29 Mar. 18 April 8 May 28 May 17 June
Date

evaluate the prediction that ecological processes are influenced by the size and predominance of parafluvial flowpaths.

Differences in invertebrate assemblages among the subsurface flowpaths were assessed using a correspondence analysis (CA) with log-transformed invertebrate densities. The CA was carried out, and graphics were prepared using the ADE-4 software package for R (Thioulouse et al. 1997).

Results

River flow and subsurface flowpaths

Surface flow pulses in the Selwyn River mainstem were followed by peaks in riparian water levels (Fig. 2*a*); the highest correlation (r = 0.65) between surface flow and riparian water level was at a 10.2 h time lag. Flow pulses in the mainstem also caused sequential changes in water temperature in the surface, parafluvial, and riparian zones (Fig. 2*b*).

A long-term record of hyporheic water temperatures was not included because hyporheic flowpaths did not persist for more than 10 consecutive days during the study. Short-term water temperature fluctuations caused by surface flow pulses were superimposed on a progressive decline in water temperature from summer (February) to winter (June) (Fig. 2*b*). Time lags between water temperature in the surface and subsurface zones increased from the parafluvial to the riparian zones, and the magnitude of temperature changes following flow pulses decreased in the same order. These patterns indicate unidirectional water flow from the surface

Fig. 3. Water surface elevations (metres above sea level, m a.s.l.) on nine sampling dates along the ephemeral channel. On one date, the water surface was below the depth of all piezometers and water surface elevations were recorded only in the riparian zone wells (solid diamonds).

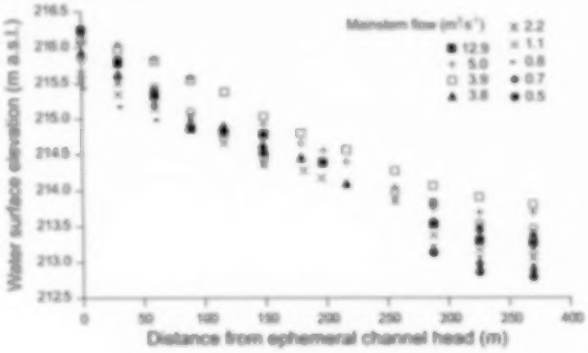

zone down the subsurface gradient. The cross-correlation indicated that the river flow – riparian water temperature relationship was strongest at a lag time of 39 h (r = 0.35), which gives an average subsurface water velocity in the 380 m long flowpath of 7.8 m·h^{-1}. The difference in lag times between the surface flow – water level relationship and the surface flow – riparian water temperature relationship indicates that the former is primarily a response to pressure wave propagation and the latter is primarily a response to advection of water from the mainstem to the riparian terrace.

The water surface within the ephemeral channel bed sloped downward from the channel head to the riparian zone. The average slope was 1% and was not strongly affected by variation in surface flow (Fig. 3). The length of the parafluvial zone decreased with increasing surface flow in the mainstem; the good fit of a negative exponential model was due, in part, to a small number of topographic high points in the ephemeral channel that remained dry at high flow levels (Fig. 4). At the lowest flow level measured, there was no surface water in the ephemeral channel and the entire subsurface zone was parafluvial (Fig. 4). The riparian zone was not inundated during the study. The average water level in all piezometers and wells was highly correlated with surface discharge in the mainstem (r = 0.98, n = 12).

Differences in chemistry and invertebrates among subsurface zones

Differences in DOC, DON, NH_4^+, and DOP concentrations, pH, and water temperature in the surface, hyporheic, parafluvial, and riparian zones were significant. No significant differences among zones were detected in NO_3^- concentrations or electrical conductivity (Table 1; Fig. 5). There were several statistically significant pairwise differences among the zones: DOC, DON, and DOP concentrations were higher in the hyporheic zone than in the parafluvial and riparian zones; DRP concentrations were higher in the hyporheic zone than in the parafluvial zone; NH_4^+ concentrations were higher in surface water than in the riparian zone (Fig. 5).

POM concentrations were similar in all subsurface zones

© 2008 NRC Canada

Fig. 4. Parafluvial zone length in the ephemeral channel versus mainstem flow level. Line corresponds to negative exponential regression.

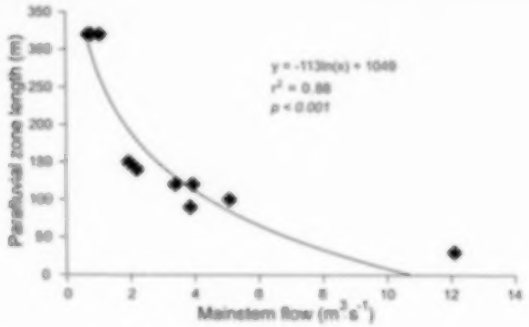

and ranged from 0.8% to 2.1% dry mass (Fig. 5). No significant differences among zones were detected in esterase activity, but within-zone variability was high, as indicated by large coefficients of variation (CVs) for each zone, ranging from 0.48 to 0.53.

Invertebrate taxon richness, density, evenness, and percent insect taxa differed significantly among the subsurface zones (Table 1). Pairwise comparisons indicated that invertebrate density and taxon richness were significantly higher in the hyporheic and parafluvial zones than in the riparian zone (Fig. 5). Evenness was higher in the riparian zone than in the hyporheic or parafluvial zones, and percent insect taxa was higher in the hyporheic zone than in parafluvial or riparian zones (Fig. 5).

The CA indicated that invertebrate assemblages varied among the three subsurface flowpaths, with the parafluvial assemblage intermediate in structure between the hyporheic and riparian assemblages (Fig. 6*a*). The first two axes of the CA explained 40% of the variance in the invertebrate data set. Insect taxa (e.g., *Deleatidium* spp. and dipteran larvae) characterized the hyporheic flowpath. Trichoptera, including those with high affinities for subsurface habitats (e.g., *Olinga* sp.), and Oligochaeta characterized the parafluvial flowpath. Crustaceans, including groundwater syncarids (Harpacticoida, Cyclopoida, and Bathynellidae), characterized the riparian flowpath (Fig. 6*b*).

Effects of surface flow

Surface water DOC, DON, and DOP concentrations near the head of the ephemeral channel increased with surface flow in the mainstem; surface water DIN and DRP concentrations did not vary systematically with surface flow (Fig. 7). Nutrient processing was regressed on surface flow to assess the effects of flow on nutrient retention or transformation in the subsurface system. DOC, DON, and DOP processing decreased with increasing surface flow; each relationship was characterized by a negative exponential function (Fig. 7).

At flows of <2.0–2.5 $m^3 \cdot s^{-1}$ in the mainstem, DOC and DON processing was positive but became negative (i.e., shifted from net consumption to production) at higher flows. DOP processing was positive over the ranges of surface flows, but approached zero at flows >6 $m^3 \cdot s^{-1}$. Linear and curvilinear regressions of processing on flow were not significant for DIN or DRP. Regressions of nutrient processing on parafluvial length were significant and positive for DOC, DON, and DOP, indicating that retention or remineralisation increased as the parafluvial zone occupied a greater proportion of the channel (Fig. 8). Regressions of DIN and DRP processing, esterase activity, and invertebrate assemblage properties on parafluvial zone length were not significant.

Table 1. Comparisons of chemical, physical, and biological variables in surface and subsurface flowpaths.

Variables	*F*	*p* value	Pairwise comparisons
Temperature	2.797	*0.009*	R > H
Electrical conductivity	1.000	0.321	—
pH	10.695	*<0.001*	R > H
DOC	8.709	*0.004*	H > P, R
DON	7.201	*0.009*	H > P, R
NO_3^-	0.517	0.471	—
NH_4^+	10.803	*0.004*	S > R
DOP	7.211	*0.009*	H > P, R
DRP	0.859	0.357	—
FDA	0.064	0.801	—
Taxon richness	3.991	*0.021*	H, P > R
Density	23.347	*<0.001*	H, P > R
Evenness	3.759	*0.029*	R > H, P
Percent insect taxa	6.275	*0.003*	H > P, R

Note: S, surface; H, hyporheic; P, parafluvial; R, riparian. Results from pairwise Scheffé tests are shown for those variables with significant ($p < 0.05$, in italics) among-flowpath differences. FDA hydrolysis, POM, and invertebrate variables were not measured in the surface water zone.

Invertebrate density, taxon richness, and percent insect taxa in the hyporheic zone varied widely with surface flow but were less variable in the parafluvial and riparian zones (Fig. 9). In all zones, taxon richness, density, and percent insect taxa were relatively low at the highest flow levels, but no monotonic trends were detectable. Taxon richness appeared to reach a maximum at intermediate flows, but a parabolic function fit to the aggregated data from all zones did not explain a significant proportion of the variation among flow levels.

Discussion

River flow and subsurface flowpaths

The subsurface flowpaths that we studied correspond in part to the "perched hyporheic zone" described by Malard et al. (2002). As noted previously, subsurface flowpaths in losing stream reaches are more accurately termed "semi-perched" when they are underlain by low-permeability sediments (Smakhtin 2001; Osman and Bruen 2002; Ruehl et al. 2006). We propose an expansion of the semi-perched hyporheic zone concept to include parafluvial and riparian zones when low-permeability layers are continuous across these zones. Previous studies of semi-perched flowpaths have focused largely on recharge of deep aquifers, not on the saturated sediments at or near the surface (e.g., Shentsis and Rosenthal 2003). Consequently, hyporheic ecologists have expressed uncertainty about the existence of semi-perched subsurface flowpaths (Harvey and Wagner 2000; Malard et al. 2002). As the free water surfaces in these

© 2008 NRC Canada

Fig. 5. Box plots of electrical conductivity (Cond.), water temperature (Temp.), pH, particulate organic matter (POM), esterase activity (as FDA hydrolysis), nutrient concentrations, and invertebrate variables in surface (S), hyporheic (H), parafluvial (P), and riparian (R) zones. Boxes show first and third quartiles, bold horizontal lines are medians, vertical bars bracket 5%–95% of the range, dots are values outside of the 5%–95% range. FDA hydrolysis, POM, and invertebrate variables were not measured in surface water.

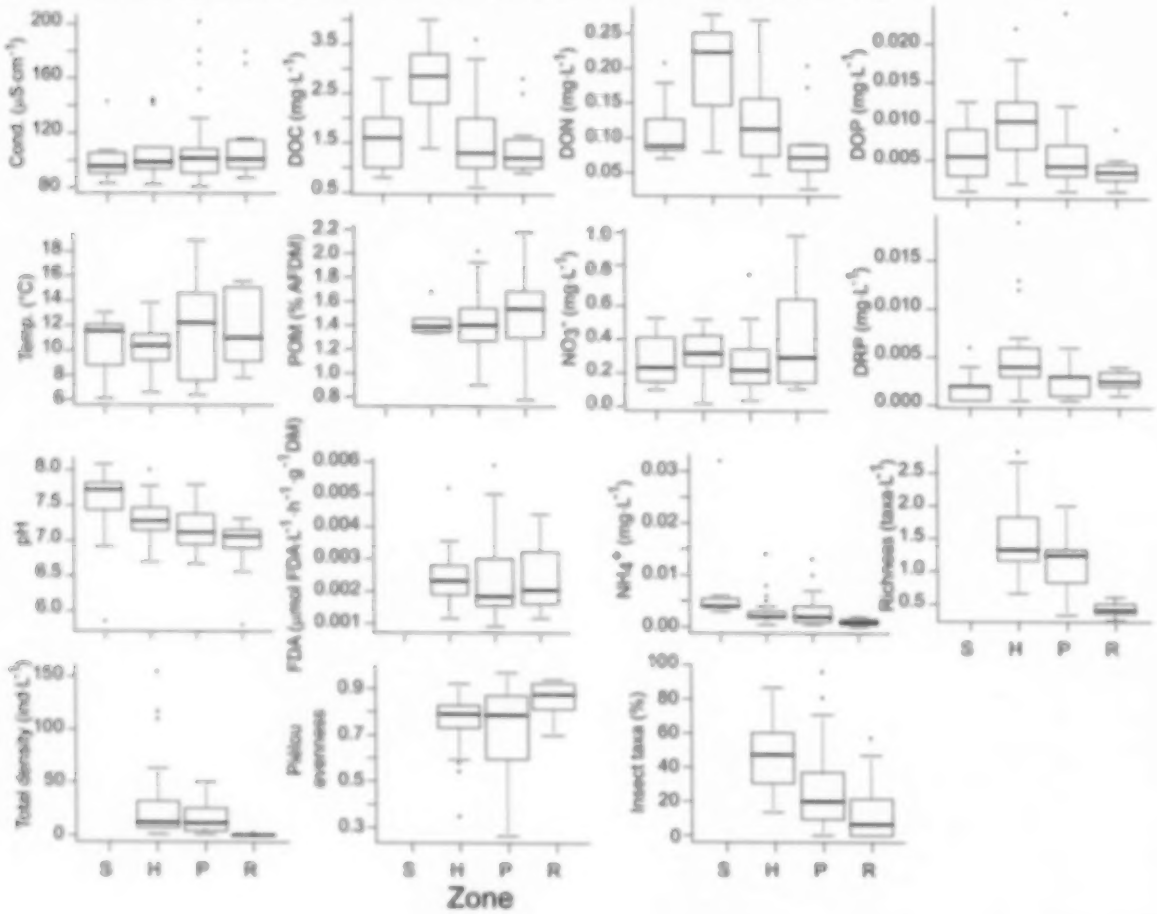

flowpaths are easily observed, the uncertainty appears to be whether they are hydraulically connected to regional groundwater aquifers or separated from groundwater by unsaturated sediments. Our measurements were limited to depths to the free water surface along the ephemeral channel; the thickness of the saturated zone was not determined and the presence of an underlying unsaturated zone was not confirmed. However, circumstantial evidence suggests that saturated flowpaths in the area, both surface and subsurface, are semi-perched. The mainstem reach adjacent to our study site is perennial, but loses water very rapidly, ~0.5 $m^3 \cdot s^{-1} \cdot km^{-1}$ (Larned et al. 2008). Long-term groundwater level data are available from a 27 m deep monitoring well <2 km from the study site (http://www.ecan.govt.nz/Our+Environment/Water/Groundwater). During our study, the median daily average groundwater level in this well was 18.6 m below ground surface (range 11.5–24.6 m, $n = 104$ measurement days). The maximum depth that we measured to the free water surface in the ephemeral channel and riparian terrace was <2 m below ground. These observations suggest that the monitoring well penetrates an aquifer below the semi-perched flowpath that extends from the Selwyn River. The presence of an extensive unsaturated (vadose) zone above the uppermost regional aquifer in the study area is confirmed by well logs and near-surface stratigraphy (Brown and Wilson 1988; Brooks 1998).

Seepage losses cause longitudinal flow depletion in saturated subsurface flowpaths, and at some distance from the river wetted front, downward seepage exceeds longitudinal flow rates and the saturated subsurface flowpath ends. This process is identical to transmission loss of surface flow, and the same variables that govern transmission losses also govern losses in subsurface flowpaths: porosity and depth of unsaturated sediment below the flow path and matrix potential (Keppel and Renard 1962; Reid and Frostick 1997). Lengths of subsurface flowpaths strongly influence the degree of nutrient and organic matter processing (Fisher et al. 1998; see below for further discussion). We have not measured the lateral extent of subsurface flow from the Selwyn River or developed a relationship between lateral extent and surface flow. However, the positive relationship that we

© 2008 NRC Canada

Fig. 6. Correspondence analysis (PCA) of invertebrate data, using log(*x* + 1)-transformed densities. (*a*) Ordination diagram of sites. Individual points are sampling dates within zones; lines connect each point to one of the zone centroids. (*b*) Ordination diagram of invertebrate taxa.

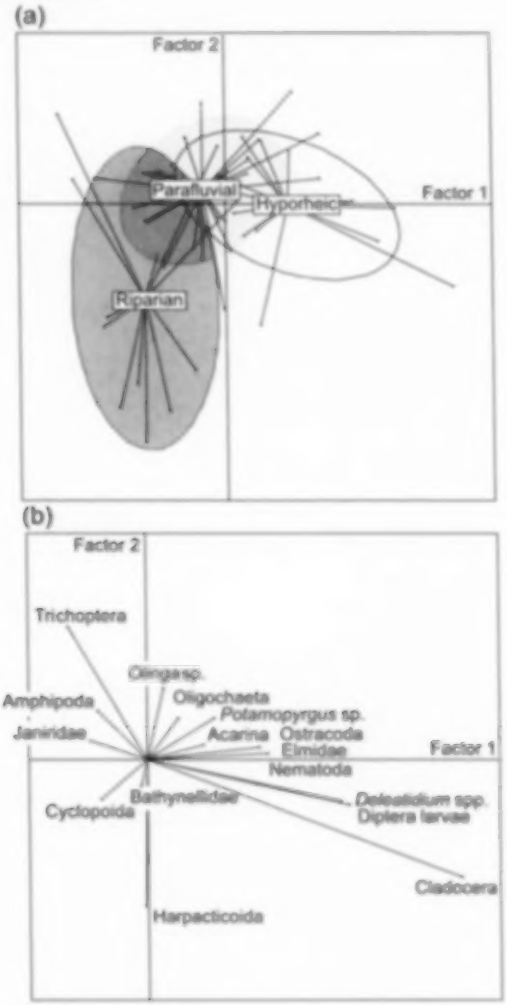

Fig. 7. (*a*) Dissolved organic carbon (DOC), (*b*) dissolved organic nitrogen (DON), and (*c*) dissolved organic phosphorus (DOP) processing in the ephemeral channel versus mainstem surface flow (solid diamonds), and surface water DOC, DON, and DOP concentrations versus mainstem surface flow (open triangles). Solid lines, significant regressions for processing rates; broken lines, significant regressions for surface water concentrations.

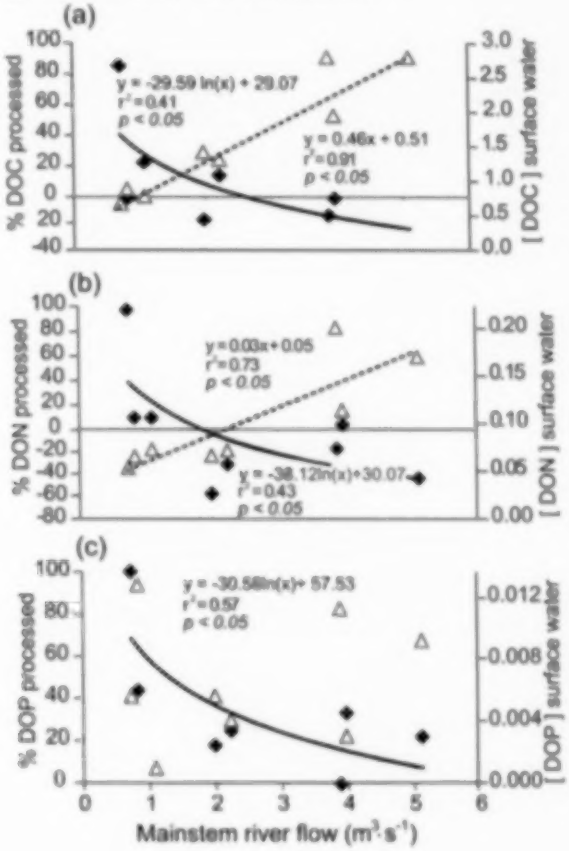

observed between water level in the ephemeral channel and mainstem flow indicates that at least one dimension of flowpath size increases with surface flow. We predict that surface flow also controls the lateral extent of subsurface flow. Data from the ephemeral Fuirosos stream in Spain support this prediction (Butturini et al. 2003; Vásquez et al. 2007). In the Fuirosos, low groundwater levels result in lateral transport of stream water up to 10 m into the riparian zone during summer and autumn floods. Further infiltration may be impeded by hillslope groundwater or low hydraulic conductivity. In the Selwyn River and in other semi-perched rivers on alluvial floodplains, coarse sediments and the absence of hill-slope constraint suggest that the lateral subsurface flow will be far greater than in the Fuirosos or other hill-constrained rivers. Extensive lateral flow in alluvial floodplains is further favored by high hydraulic conductivity along paleochannels and, as in the present study, abandoned braids (Poole et al. 2002).

Chemical and microbial activity in subsurface flowpaths

The majority of studies of dissolved nutrients in subsurface flowpaths have focused on gaining stream reaches, with subsurface flow directed from hillslopes into stream channels (Mulholland 1992; Triska et al. 1993; Ohrui and Mitchell 1998). In these settings, upland forests and agricultural lands are source areas for nutrients, and DIN, DON, DRP, and DOC typically decline sequentially from riparian zones, to hyporheic and (or) parafluvial zones, to surface zones. In some cases, rapid decomposition and remineralisation and differences in redox state result in peak concentrations in parafluvial or hyporheic zones rather than in riparian zones (Triska et al. 1993). Even when denitrification or immobilization removes large proportions of nutrients in these flow paths, they are hydrologic sources to

© 2008 NRC Canada

Fig. 8. (*a*) Dissolved organic carbon (DOC), (*b*) dissolved organic nitrogen (DON), and (*c*) dissolved organic phosphorus (DOP) processing in the ephemeral channel versus parafluvial zone length.

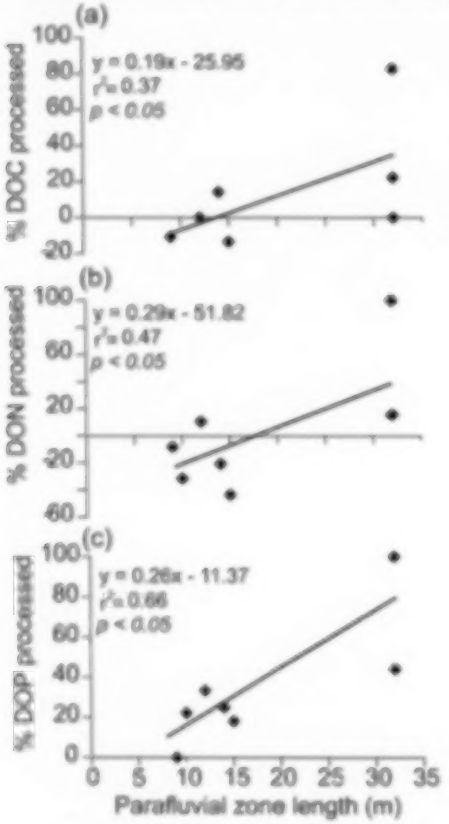

streams, and surface zones tend to have lowest concentrations.

In contrast, dissolved nutrient concentrations (particularly organic forms) in losing, semi-perched systems may decrease from the surface zone to the riparian zone. This pattern holds for DOC, DON, and DOP in the present study and DOC in the Fuirosos (Vásquez et al. 2007). Although our study was limited to a single reach, the relationships that we report should be widely applicable in semi-perched systems. Comparable patterns have been reported for parafluvial gravel bars that receive little or no groundwater input; DOC and DON concentrations decreased with distance down these flowpaths, and NO_3 and DRP concentrations increased, except in cases of very high hydraulic conductivity (Holmes et al. 1998; Sobczak and Findlay 2002; Schade et al. 2002). These observations suggest that well-oxygenated parafluvial zones can be strong sinks for dissolved organic matter (DOM), given sufficient hydrologic residence times. We found no previous reports of DOP processing in subsurface flowpaths.

In semi-perched subsurface flowpaths lacking groundwater input, longitudinal changes in solute concentrations are due to tributary and diffuse inputs (e.g., soil leaching; Bechtold et al. 2003), biogeochemical processes within the streambed, and exchange with surface water in hyporheic zones. The ephemeral channel that we studied lacks tributaries, and we assume that diffuse inputs were minor as there was little organic soil or riparian vegetation. Higher DOC, DON, and DOP concentrations in the hyporheic zone compared with the surface, parafluvial, and riparian zones indicate rapid POM processing and (or) efficient retention and mineralization of DOM in the hyporheic zone. Because there were no detectable differences in POM concentrations among subsurface zones, we cannot attribute differences in DOC, DON, and DOP to differences in POM pools or POM turnover. A simpler explanation is that the DOM supplied from the surface zone is removed from the subsurface flowpath within the hyporheic zone by adsorption to biofilms and fine sediment and by microbial mineralization (McDowell 1985; Wondzell and Swanson 1996*b*; Baker et al. 1999).

Fig. 9. (*a*) Invertebrate taxonomic richness, (*b*) density, and (*c*) percent insect in subsurface flowpaths versus mainstem river flow. Hyporheic, open squares; parafluvial, solid triangles; riparian, solid circles. Values are means ± 1 standard deviation.

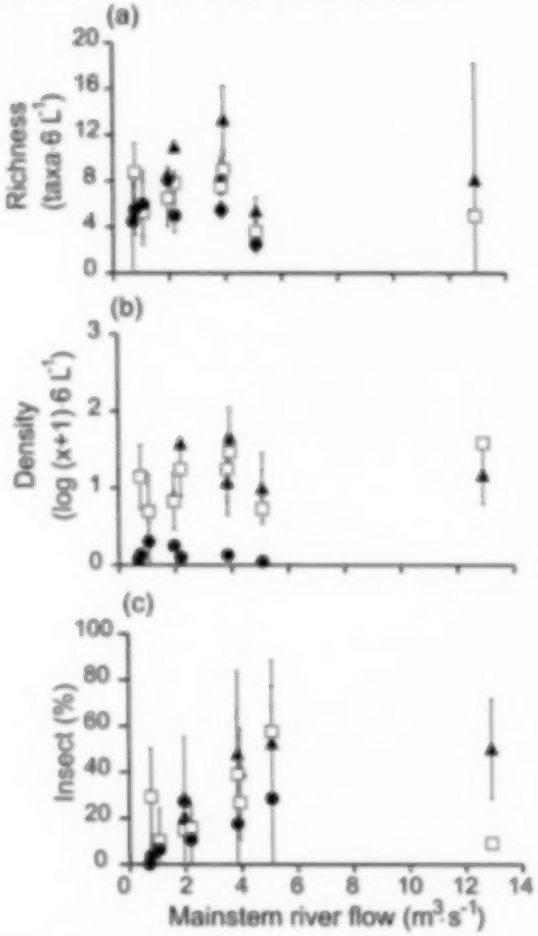

In contrast to the dissolved organic nutrients, no longitudinal gradients were evident for NO_3^- and there was no

© 2008 NRC Canada

detectable effect of parafluvial zone length or surface water flow on NO_3^- or DRP processing. NO_3^- was present at relatively high concentrations (~0.3 mg·L^{-1}), and its near-conservative transport was unexpected. Two general explanations have been proposed for cases in which longitudinal changes in dissolved nutrients are undetectable. First, when hydraulic conductivity is high, residence times may be too short for effective reactant–biofilm interactions (Bencala 2000). Second, biogeochemical reactions may be limited by the availability of reactants (Hedin et al. 1998; Baker et al. 1999; McClain et al. 2003). These explanations are not mutually exclusive. The high flow rates that we measured in the subsurface flowpath (~8 m·h^{-1}) support the argument for low residence times, and low concentrations of DOC, NH_4^+, and DRP and low FDA rates throughout the flowpath suggest that microbial NO_3^- removal was limited by one or more reactants. In other subsurface flowpaths characterized by high NO_3^- and low DOC concentrations, NO_3^- removal was shown to be DOC-limited (Hill et al. 2000; Sobczak et al. 2003).

Significantly lower DOC concentrations in the parafluvial and riparian zones compared with the hyporheic zone upstream suggests that DOC is rapidly drawn down to ~1 mg·L^{-1}, concentrations that may limit bacterial activity in stream sediments (Baker et al. 2000). The concentrations that we report are for total DOC, and bioavailable DOC (BDOC) concentrations will be even lower (Volk et al. 1997). Assuming that the BDOC fraction comprises ≤50% of total DOC (Kaplan and Newbold 1995; Marmonier et al. 1995), the concentrations that we observed were well below reported thresholds for microbial limitation.

DRP concentrations were low in each subsurface flowpath zone (average concentration <0.005 mg·L^{-1}), raising the possibility that NO_3^- removal or other microbial processes were DRP-limited rather than DOC-limited (Miettinen et al. 1997; Stallcup et al. 2006). However, DOC–DRP ratios in the subsurface zones (range of average ratios among zones 34:1–89:1) were below the Redfield ratio (106:1), making it unlikely that DRP was limiting. DRP appeared to be removed between the hyporheic and parafluvial zones, but we cannot distinguish microbial DRP assimilation from abiotic adsorption (Hendricks and White 2000). Experimental DOC and DRP additions will be required to unequivocally establish nutrient limitation of microbial NO_3^- removal.

Microbial activity in the subsurface flow path, as measured by FDA hydrolysis, was very low. Our measurements ranged from 0.001 to 0.006 μmol FDA·h^{-1}·(g sediment DM)$^{-1}$; this range is 1–4 orders of magnitude lower than measurements made using the same procedure in other fluvial sediments (Marmonier et al. 1995; Battin 2000; Claret and Boulton 2003). Subsurface microbial activity and FDA hydrolysis, in particular, have been directly related to POM concentrations (Claret et al. 2001; Claret and Boulton 2003) and inversely related to interstitial flow rates (Battin 2000). As the ephemeral channel was characterized by both low POM concentration and high flow rates, low levels of microbial activity are expected. Low microbial activity and the lack of clear differences among subsurface zones provide further circumstantial support for the contention that NO_3^- removal in the ephemeral channel is limited by microbial processes.

Invertebrates in subsurface flowpaths

We predicted that subsurface invertebrate assemblages would vary along subsurface flowpaths in response to variation in food availability and connectivity with surface water. Although there were significant differences in invertebrate variables among subsurface zones, food availability (as indicated by POM concentration) does not appear to be a primary influence. Invertebrate assemblages in the hyporheic and parafluvial zones were generally similar, with higher density and diversity and lower evenness than in the riparian zone. In contrast, the largest differences in physicochemical variables were between the hyporheic and parafluvial zones. This spatial shift may correspond to the different rates at which invertebrates and solutes respond to immersion and emersion. Shifts between immersed (hyporheic) and emersed (parafluvial) conditions lead to rapid physicochemical changes owing to the onset and cessation of vertical exchange between surface and subsurface water. Invertebrate assemblages are somewhat buffered from these shifts by vertical mobility in some taxa and tolerance to desiccation in others (Del Rosario and Resh 2000; Larned et al. 2007). Riparian zone assemblages occupy more stable environments in terms of immersion and emersion, and the distinct composition of riparian assemblages may reflect lower tolerance to stress.

Taxon richness appeared to reach a maximum at intermediate surface flows, resulting in a hump-shaped curve over the range of flows that we observed (0.7–12.9 m^3·s^{-1}). Corresponding conditions in the ephemeral channel ranged from complete emersion to near-complete immersion (i.e., >90% of channel immersed). No samples were collected while the channel was completely immersed, but floods caused complete immersion several times during the study, and some sampling dates coincided with flood recessions. We suggest that decreasing diversity at high and low flow levels reflects environmental harshness at both ends of the hydrological spectrum. Low flows are associated with low POM input, elevated water temperatures, and reduced dissolved oxygen concentrations in subsurface flowpaths. High flows are associated with substrate movement, sediment deposition, and possibly clogging of pore space. Both sets of conditions eliminate sensitive taxa in subsurface environments (Boulton and Stanley 1995; Olsen and Townsend 2005). Our observations of subsurface invertebrates sampled at both ends of the hydrological spectrum are consistent with a model proposed by Fritz and Dodds (2005) that links invertebrate diversity to hydrological harshness. In this model, harshness increases with increasing intermittence and increasing flood frequency. Fritz and Dodds (2005) tested the model using benthic invertebrates in intermittent streams and reported decreased diversity with increasing harshness and no effects of harshness on invertebrate density or Pielou evenness. In the present study, very low flows and high flows also resulted in reduced diversity, with no detectable effects on density or Pielou evenness.

Acknowledgements

We thank S. Bernard, J. Bind, C. Mohlmann, and M. Scarsbrook for assistance with fieldwork, P. Lambert and G. Fenwick for assistance with invertebrate identification, and the NIWA Water Quality Laboratory for nutrient

© 2008 NRC Canada

analyses. For advice and critique, we thank C.N. Dahm, F. Malard, A. Packman, and two anonymous reviewers. This project was funded through the New Zealand Foundation for Research, Science and Technology (Water Allocation Programme, contract No. C01X0308) and CEMAGREF.

References

Baker, M.A., Valett, H.M., and Dahm, C.N. 1999. Acetate retention and metabolism in the hyporheic zone of a mountain stream. Limnol. Oceanogr. **44**: 1530–1539.

Baker, M.A., Valett, H.M., and Dahm, C.N. 2000. Organic carbon supply and metabolism in a shallow groundwater ecosystem. Ecology, **81**: 3133–3148.

Battin, T.J. 2000. Hydrodynamics is a major determinant of streambed biofilm activity: from the sediment to the reach scale. Limnol. Oceanogr. **45**: 1308–1319.

Bechtold, J.S., Edwards, R.T., and Naiman, R.J. 2003. Biotic versus hydrologic control over seasonal nitrate leaching in a floodplain forest. Biogeochemistry, **63**: 53–72. doi:10.1023/A:1023350127042.

Bencala, K.E. 2000. Hyporheic zone hydrological processes. Hydrol. Process. **14**: 2797–2798. doi:10.1002/1099-1085(20001030)14:15<2797::AID-HYP402>3.0.CO;2-6.

Boulton, A.J., and Stanley, E.H. 1995. Hyporheic processes during flooding and drying in a Sonoran Desert stream. II. Faunal dynamics. Arch. Hydrobiol. **134**: 27–52.

Boulton, A.J., Valett, H.M., and Fisher, S.G. 1992. Spatial distribution and taxonomic composition of the hyporheos of several Sonoran Desert streams. Arch. Hydrobiol. **125**: 37–61.

Boulton, A.J., Fisher, S., Marmonier, P., Stanley, E.H., and Valett, H.M. 1998. The functional significance of the hyporheic zone in streams and rivers. Annu. Rev. Ecol. Syst. **29**: 59–81. doi:10.1146/annurev.ecolsys.29.1.59.

Brooks, T. 1998. Groundwater resources near Te Pirita, Central Plains. Canterbury Region Council Report No. U98/42, Christchurch, New Zealand.

Brown, L.V., and Wilson, D.D. 1988. Stratigraphy of the late Quaternary deposits of the northern Canterbury Plains, New Zealand. N.Z. J. Geol. Geophys. **31**: 305–335.

Butturini, A., Bernal, S., Nin, E., Hellin, C., Rivero, L., Sabater, S., and Sabater, F. 2003. Influences of stream groundwater hydrology on nitrate concentration in unsaturated riparian area bounded by an intermittent Mediterranean stream. Water Resour. Res. **39**: 1110. doi:10.1029/2001WR001260.

Claret, C., and Boulton, A.J. 2003. Diel variation in surface and subsurface microbial activity along a gradient of drying in an Australian sand-bed stream. Freshw. Biol. **48**: 1739–1755. doi:10.1046/j.1365-2427.2003.01120.x.

Claret, C., Boulton, A.J., Dole-Olivier, M.-J., and Marmonier, P. 2001. Functional processes versus state variables: interstitial organic matter pathways in floodplain habitats. Can. J. Fish. Aquat. Sci. **58**: 1594–1602. doi:10.1139/cjfas-58-8-1594.

Constantz, J., Stewart, A.E., Niswanger, R., and Sarma, L. 2002. Analysis of temperature profiles for investigating stream losses beneath ephemeral channels. Water Resour. Res. **38**: 1316–1328. doi:10.1029/2001WR001221.

Dahm, C.N., Grimm, N.B., Marmonier, P., Valett, H.M., and Vervier, P. 1998. Nutrient dynamics at the interface between surface waters and groundwaters. Freshw. Biol. **40**: 427–451. doi:10.1046/j.1365-2427.1998.00367.x.

Datry, T., Malard, F., and Gibert, J. 2005. Response of invertebrate assemblages to increased groundwater recharge rates in a phreatic aquifer. J. North Am. Benthol. Soc. **24**: 461–477.

Del Rosario, R.B., and Resh, V.H. 2000. Invertebrates in intermittent and perennial streams: is the hyporheic zone a refuge from drying? J. North Am. Benthol. Soc. **19**: 680–696.

Dole-Olivier, M.J., Marmonier, P., and Beffy, J.L. 1997. Response of invertebrates to lotic disturbance: is the hyporheic zone a patchy refugium? Freshw. Biol. **37**: 257–276. doi:10.1046/j.1365-2427.1997.00140.x.

Fisher, S., Grimm, N.B., Martí, E., Holmes, R.N., and Jones, J.B. 1998. Material spiraling in stream corridors: a telescoping ecosystem model. Ecosystems (N.Y. Print), **1**: 19–34. doi:10.1007/s100219900003.

Fontvieille, D.A., Outaguerouine, A., and Thevenot, D.R. 1992. Fluorescein diacetate hydrolysis as a measure of microbial activity in aquatic systems: application to activated sludges. Environ. Technol. **13**: 531–540.

Fritz, K.B., and Dodds, W.K. 2005. Harshness: characterisation of intermittent stream habitat over space and time. Mar. Freshw. Res. **56**: 13–23. doi:10.1071/MF04244.

Harvey, J.W., and Wagner, B.J. 2000. Quantifying hydrologic interactions between streams and their subsurface hyporheic zones. *In* Streams and ground waters. *Edited by* J.B. Jones and P.J. Mulholland. Academic Press, San Diego, California. pp. 4–44.

Hedin, L.O., von Fischer, J.C., Ostrom, N.E., Kennedy, B.P., Brow, M.G., and Robertson, G.P. 1998. Thermodynamic constraints on nitrogen transformations and other biogeochemical processes at soil–stream interfaces. Ecology, **79**: 684–703.

Hendricks, S.P., and White, D.S. 2000. Stream and groundwater influences on phosphorus biogeochemistry. *In* Streams and ground waters. *Edited by* J.B. Jones and P.J. Mulholland. Academic Press, San Diego, California. pp. 221–235.

Hill, A.R., Devito, K.J., Campagnolo, S., and Sanmugadas, K. 2000. Subsurface denitrification in a forest riparian zone: interactions between hydrology and supplies of nitrate and organic carbon. Biogeochemistry, **51**: 193–223. doi:10.1023/A:1006476514038.

Holmes, R.M., Fisher, S.G., Grimm, N.B., and Harper, B.J. 1998. The impact of flash floods on microbial distribution and biogeochemistry in the parafluvial zone of a desert stream. Freshw. Biol. **40**: 641–654. doi:10.1046/j.1365-2427.1998.00362.x.

Junk, W.J., Bayley, P.B., and Sparks, R.E. 1989. The flood-pulse concept in river–floodplain systems. Can. Spec. Publ. Fish. Aquat. Sci. No. 106. pp. 110–127.

Keppel, R.V., and Renard, K.G. 1962. Transmission losses in ephemeral stream beds. J. Hydraul. Div. ASCE, **88**: 59–68.

Kaplan, L.A., and Newbold, J.D. 1995. Measurement of streamwater biodegradable dissolved organic carbon with a plug-flow bioreactor. Water Res. **29**: 2696–2706. doi:10.1016/0043-1354(95)00135-8.

Larned, S.T., Datry, T., and Robinson, C.T. 2007. Invertebrate and microbial responses to inundation in an ephemeral river: effects of preceding dry periods. Aquat. Sci. **69**: 554–567. doi:10.1007/s00027-007-0930-1.

Larned, S.T., Hicks, D.M., Schmidt, J., Davey, A.J.H., Dey, K., Scarsbrook, M., Arscott, D.B., and Woods, R.A. 2008. The Selwyn River of New Zealand: a benchmark system for alluvial river plain rivers. River Res. Appl. **24**: 1–21. doi:10.1002/rra.1054.

Lewis, D.B., Schade, J.D., Huth, A.K., and Grimm, N.B. 2006. The spatial structure of variability in a semi-arid, fluvial ecosystem. Ecosystems (N.Y. Print), **9**: 386–397. doi:10.1007/s10021-005-0161-z.

Malard, F., Ward, J.V., and Robinson, C.T. 2000. An expanded view of the hyporheic zone. Verh. Int. Ver. Theor. Angew. Limnol. **27**: 431–437.

© 2008 NRC Canada

Malard, F., Mangin, A., Uehlinger, U., and Ward, J.V. 2001. Thermal heterogeneity in the hyporheic zone of a glacial floodplain. Can. J. Fish. Aquat. Sci. **58**: 1319–1335. doi:10.1139/cjfas-58-7-1319.

Malard, F., Tockner, K., Dole-Olivier, M.-J., and Ward, J.V. 2002. A landscape perspective of surface–subsurface hydrological exchanges in river corridors. Freshw. Biol. **47**: 621–640. doi:10.1046/j.1365-2427.2002.00906.x.

Malard, F., Uehlinger, U., Zah, R., and Tockner, K. 2006. Flood-pulse and riverscape dynamics in a braided glacial river. Ecology, **87**: 704–716. doi:10.1890/04-0889. PMID:16602300.

Marmonier, P., Fontvieille, D., Gibert, J., and Vanek, V. 1995. Distribution of dissolved organic carbon and bacteria at the interface between the Rhône River and its alluvial aquifer. J. North Am. Benthol. Soc. **14**: 382–392. doi:10.2307/1467204.

McClain, M., Boyer, E.W., Dent, C.L., Gergel, S.E., Grimm, N.B., Groffman, P.M., Hart, S.C., Harvey, J.W., Johnston, C.A., Mayorga, E., McDowell, W.H., and Pinay, G. 2003. Biogeochemical hot spots and hot moments at the interface of terrestrial and aquatic ecosystems. Ecosystems (N.Y. Print), **6**: 301–312. doi:10.1007/s10021-003-0161-9.

McDowell, W.H. 1985. Kinetics and mechanisms of dissolved organic carbon retention in a headwater stream. Biogeochemistry, **1**: 329–352. doi:10.1007/BF02187376.

Miettinen, I.T., Vartiainen, T., and Miettinen, P.J. 1997. Phosphorus and bacterial growth in drinking water. Appl. Environ. Microbiol. **63**: 3242–3245. PMID:9251211.

Morrice, J.A., Valett, H.M., Campana, M.E., and Dahm, C.N. 1997. Alluvial characteristics, groundwater–surface water exchange and hydrological retention in headwater streams. Hydrol. Process. **11**: 253–267. doi:10.1002/(SICI)1099-1085(19970315)11:3<253::AID-HYP439>3.0.CO;2-J.

Mulholland, P.J. 1992. Regulation of nutrient concentrations in a temperate forest stream: roles of upland, riparian and instream processes. Limnol. Oceanogr. **37**: 1512–1526.

Ohrui, K., and Mitchell, M.J. 1998. Spatial patterns of soil nitrate in Japanese forested watersheds: importance of the near-stream zone as a source of nitrate in stream water. Hydrol. Process. **12**: 1433–1445. doi:10.1002/(SICI)1099-1085(199807)12:9<1433::AID-HYP646>3.0.CO;2-N.

Olsen, D.A., and Townsend, C.R. 2005. Flood effects on invertebrates, sediments and particulate organic matter in the hyporheic zone of a gravel-bed stream. Freshw. Biol. **50**: 839–853. doi:10.1111/j.1365-2427.2005.01365.x.

Osman, Y.Z., and Bruen, M.P. 2002. Modelling stream–aquifer seepage in an alluvial aquifer: an improved losing-stream package for MODFLOW. J. Hydrol. **264**: 69–86. doi:10.1016/S0022-1694(02)00067-7.

Poole, G.C., Stanford, J.A., Frissell, C.A., and Running, S.W. 2002. Three-dimensional mapping of geomorphic controls on floodplain hydrology and connectivity from aerial photos. Geomorphology, **48**: 329–347. doi:10.1016/S0169-555X(02)00078-8.

Reid, I., and Frostick, L.E. 1997. Channel form, flows and sediments in deserts. *In* Arid zone geomorphology. 2nd ed. *Edited by* D.S.G. Thomas. Wiley, Chichester, UK. pp. 205–229.

Ruchi, C., Fisher, A.T., Hatch, C., Los Huertos, M., Stemler, G., and Shennan, C. 2006. Differential gauging and tracer tests resolve seepage fluxes in a strongly-losing stream. J. Hydrol. **330**: 235–248. doi:10.1016/j.jhydrol.2006.03.025.

Schade, J.D., Marti, E., Welter, J.R., Fisher, S.G., and Grimm, N.B. 2002. Sources of nitrogen to the riparian zone of a desert stream: implications for riparian vegetation and nitrogen retention. Ecosystems (N.Y. Print), **5**: 68–79. doi:10.1007/s10021-001-0056-6.

Shentsis, I., and Rosenthal, E. 2003. Recharge of aquifers by flood events in an arid region. Hydrol. Process. **17**: 695–712. doi:10.1002/hyp.1160.

Smakhtin, V.U. 2001. Low flow hydrology: a review. J. Hydrol. **240**: 147–186. doi:10.1016/S0022-1694(00)00340-1.

Sobczak, W.V., and Findlay, S. 2002. Variation in bioavailability of dissolved organic carbon along stream hyporheic flowpaths. Ecology, **83**: 3194–3209.

Sobczak, W.V., Findlay, S., and Dye, S. 2003. Relationship between DOC bioavailability and nitrate removal in an upland stream: an experimental approach. Biogeochemistry, **62**: 309–327. doi:10.1023/A:1021192631423.

Stallcup, L.A., Ardon, M., and Pringle, C.M. 2006. Does nitrogen become limiting under high-P conditions in detritus-based tropical streams? Freshw. Biol. **51**: 1515–1526. doi:10.1111/j.1365-2427.2006.01588.x.

Stanley, E.H., and Boulton, A.J. 1995. Hyporheic processes during flooding and drying in a Sonoran Desert stream. I. Hydrologic and chemical dynamics. Arch. Hydrobiol. **134**: 1–26.

Stanley, E.H., Fisher, S.G., and Grimm, N.B. 1997. Ecosystem expansion and contraction in streams. Bioscience, **47**: 427–435. doi:10.2307/1313058.

Thioulouse, J., Chessel, D., Dolédec, S., and Olivier, J.-M. 1997. ADE-4: a multivariate analysis and graphical display software. Stat. Comput. **7**: 75–83. doi:10.1023/A:1018513530268.

Tockner, K., Malard, F., and Ward, J.V. 2000. An extension of the flood pulse concept. Hydrol. Process. **14**: 2861–2883. doi:10.1002/1099-1085(200011/12)14:16/17<2861::AID-HYP124>3.0.CO;2-F.

Tockner, K., Paetzold, A., Karaus, U., Claret, C., and Zettel, J. 2006. Ecology of braided rivers. *In* Braided Rivers — IAS Special Publication. *Edited by* G.H. Sambrook Smith, J.L. Best, C.S. Bristow, and G. Petts. Blackwell Publishing, London, UK. pp. 332–352.

Townsend, C.R. 1989. The patch dynamics concept of stream community ecology. J. North Am. Benthol. Soc. **8**: 36–50. doi:10.2307/1467400.

Triska, F.J., Duff, J.H., and Avanzino, R.J. 1993. The role of water exchange between a stream channel and its hyporheic zone in nitrogen cycling at the terrestrial–aquatic interface. Hydrobiologia, **251**: 167–184. doi:10.1007/BF00007177.

Valett, H.M., Dahm, C.N., Campana, M.E., Morrice, J.A., Baker, M.A., and Fellows, C.S. 1997. Hydrologic influences on groundwater–surface water ecotones: heterogeneity in nutrient composition and retention. J. North Am. Benthol. Soc. **16**: 239–247. doi:10.2307/1468254.

Van der Nat, D., Tockner, K., Edwards, P.J., Ward, J.V., and Gurnell, A.M. 2003. Habitat change in braided flood plains (Tagliamento, NE-Italy). Freshw. Biol. **48**: 1799–1812. doi:10.1046/j.1365-2427.2003.01126.x.

Vásquez, E., Romani, A.M., Sabater, F., and Butturini, A. 2007. Effects of the dry–wet hydrological shift on dissolved organic carbon dynamics and fate across stream–riparian interface in a Mediterranean catchment. Ecosystems (N.Y. Print), **10**: 239–251. doi:10.1007/s10021-007-9016-0.

Volk, C.J., Volk, C.B., and Kaplan, L.A. 1997. Chemical composition of biodegradable organic matter in streamwater. Limnol. Oceanogr. **42**: 39–44.

Wondzell, S.M., and Swanson, F.J. 1996*a*. Seasonal and storm dynamics of the hyporheic zone of a 4th-order mountain stream. I. Hydrologic processes. J. North Am. Benthol. Soc. **15**: 3–19. doi:10.2307/1467429.

Wondzell, S.M., and Swanson, F.J. 1996*b*. Seasonal and storm dynamics of the hyporheic zone of a 4th-order mountain stream. II. Nitrogen cycling. J. North Am. Benthol. Soc. **15**: 20–34. doi:10.2307/1467430.

© 2008 NRC Canada

Wroblicky, G.J., Campana, M.E., Valett, H.M., and Dahm, C.N. 1998. Seasonal variation in surface–subsurface water exchange and lateral hyporheic area of two stream-aquifer systems. Water Resour. Res. **34**: 317–328.

Yount, J.D., and Niemi, G.J. 1990. Recovery of lotic communities and ecosystems from disturbance: a narrative review of case studies. Environ. Manag. **14**: 547–569. doi:10.1007/BF02394709.

© 2008 NRC Canada

The effects of abiotic factors and intraspecific versus interspecific competition on the diel activity patterns of Atlantic salmon (*Salmo salar*) fry

Simon Blanchet, Géraldine Loot, Louis Bernatchez, and Julian J. Dodson

Abstract: We conducted semi-natural experiments to measure the relative contribution of various environmental factors and intraspecific and interspecific competition with an exotic invader on the daytime and crepuscular activity levels of Atlantic salmon (*Salmo salar*) fry. We demonstrated that interspecific competition with the exotic rainbow trout (*Oncorhynchus mykiss*) significantly increases the daytime activity of Atlantic salmon. The effect of intraspecific competition on the daytime activity of salmon was half that of interspecific competition. This indicates that the effect of rainbow trout was a combination of increasing density and the identity of the competitor. We also demonstrated that the effect of rainbow trout was probably the result of territorial interference between species. Moreover, we showed that water temperature simultaneously played an important role in explaining daytime activity of Atlantic salmon. During twilight, we observed no effect of competition on salmon activity, but environmental cues other than temperature (e.g., invertebrate drift, cloud cover) became significant predictors of activity. Feeding and growth rates of Atlantic salmon were not affected by the different levels of competition. Nevertheless, the exotic species may have a major impact by exposing the native species to increased risks of daytime predation.

Résumé : Nous avons mené des expériences en milieu semi-naturel pour mesurer les contributions relatives de divers facteurs du milieu, de la compétition intraspécifique et de la compétition interspécifique avec un envahisseur exotique sur les niveaux d'activité durant le jour et le demi-jour chez des alevins de saumons atlantiques (*Salmo salar*). Nous démontrons que la compétition interspécifique avec la truite arc-en-ciel (*Oncorhynchus mykiss*) exotique augmente significativement l'activité diurne de saumon atlantique. L'effet de la compétition intraspécifique sur l'activité diurne du saumon est la moitié de celui de la compétition interspécifique. Cela indique que l'effet de la truite arc-en-ciel est dû à une combinaison d'une densité accrue et de l'identité du compétiteur. Nous démontrons aussi que l'effet de la truite arc-en-ciel est probablement le résultat d'une interférence territoriale entre les espèces. De plus, nous montrons qu'au même moment la température de l'eau permet d'expliquer une partie importante de l'activité diurne chez le saumon atlantique. Au demi-jour, nous n'observons aucun effet de la compétition sur l'activité des saumons, mais des signaux du milieu autres que la température (par ex., la dérive des invertébrés, la couverture de nuages) deviennent des variables prédictives significatives de l'activité. Les taux d'alimentation et de croissance du saumon atlantique ne sont pas affectés par les différents niveaux de compétition. Les espèces exotiques peuvent néanmoins avoir un impact important en exposant les espèces indigènes à des risques accrus de prédation durant la journée.

[Traduit par la Rédaction]

Introduction

Within a complex and dynamic environment, individual activity patterns may vary at both spatial and temporal scales (Reebs 2002; Kronfeld-Schor and Dayan 2003) to optimize the trade-off between growth and survival (Kotler et al. 1994; Biro et al. 2003; but see Railsback and Harvey 2002). For most animals, the temporal partitioning of resource acquisition seems to be largely shaped by predation risk (Flecker 1992; Kronfeld-Schor and Dayan 2003; Fraser et al. 2004). Indeed, during daytime, food is generally easier to detect but the risk of being eaten by a predator is higher (Fraser and Metcalfe 1997; Metcalfe et al. 1999; Kronfeld-Schor and Dayan 2003). However, competition has also been demonstrated to influence daily activity patterns (for a review, see Kronfeld-Schor and Dayan 2003). For instance, at the intraspecific level, Alänära et al. (2001) demonstrated in the laboratory that dominant individual brown trout (*Salmo trutta*) fed mainly at the most beneficial times of dusk and in the early part of the night; whereas subordinate fish fed at other times.

In the same way, the effect of interspecific competition on diel activity has been demonstrated (e.g., desert rodents; Ziv et al. 1993; Wasserberg et al. 2006) and has been proposed

Received 4 July 2007. Accepted 2 April 2008. Published on the NRC Research Press Web site at cjfas.nrc.ca on 4 July 2008. J20080

S. Blanchet,[1] **L. Bernatchez, and J.J. Dodson.**[2] CIRSA and QC-Océan, Département de biologie, Pavillon Vachon, Université Laval, Ste Foy, QC G1K 7P4, Canada.
G. Loot. Laboratoire Evolution et Diversité Biologique, UMR 5174, CNRS — Université Paul Sabatier, 118 route de Narbonne, F-31062 Toulouse Cedex 4, France.

[1]Corresponding author (e-mail: blanchet@cict.fr).
[2]Corresponding author (e-mail: julian.dodson@bio.ulaval.ca).

 doi:10.1139/F08-079 © 2008 NRC Canada

as an important mechanism influencing population dynamics and species coexistence (Kronfeld-Schor and Dayan 2003). In fish, only Harwood et al. (2001) has provided evidence that the competitive interactions between two species (brown trout and Atlantic salmon, *Salmo salar*) modified individual diel activity patterns. However, in most of the studies designed to evaluate the effect of interspecific competition, authors used simple additive designs that do not allow the measurement of the strength of interspecific competition relative to intraspecific competition (Connell 1983; Fausch 1998). Therefore, to gain insight into the effect of interspecific competition on the temporal activity of fish, the use of a more adequate design (i.e., combined additive and substitutive design; Fausch 1998) is needed to discriminate between the confounding effects of increasing density and the identity of competitors.

In addition, several interacting ecological forces (including both biotic and abiotic factors) may also influence individual foraging decisions. Indeed, Hansen and Closs (2005) compared daily activity patterns within the hierarchy of an endemic New Zealand fish (the giant kokopu, *Galaxias argenteus*) under different food supply conditions. Under normal food densities, dominant fish were mainly nocturnal; whereas subdominants were diurnal. In contrast, when food density was artificially limited, dominant fish increased diurnal activity while simultaneously reducing the overall activity of subdominants.

Understanding the influence of interspecific competition on diel activity patterns may be particularly relevant in the context of invasion biology. Analysis of competition between indigenous and exotic species has been considered in a spatial context (e.g., Mills et al. 2004; Morita et al. 2004; Blanchet et al. 2007*a*), but the effect of exotic species on the diel activity patterns of native species has rarely been investigated.

Thus, the main objective of the present study was to assess the relative influence of intra- versus inter-specific competition with an exotic invader, food availability, and selected abiotic factors in shaping the diel activity patterns of a native species. We also aimed to verify whether changes in the patterns of diel activity of the native species might alter its subsequent growth performance.

To address these issues, we used the salmonid model system, native Atlantic salmon (*Salmo salar*) – invasive rainbow trout (*Oncorhynchus mykiss*). Worldwide stocks of Atlantic salmon are declining, and in this context, interaction with exotic species may represent an additional risk to such weakened populations (Fausch 1998). Juvenile Atlantic salmon are territorial sit-and-wait predators living in streams and feeding on invertebrate drift (Klemetsen et al. 2003). Feeding activity generally exposes the fish to predators, and salmon are thus confronted with the competing demands of gaining energy and sheltering under a refuge for protection from predators. Several natural observations (e.g., Gries et al. 1997; Johnston et al. 2004; Breau et al. 2007) and laboratory experiments (e.g., Fraser et al. 1993; Metcalfe et al. 1999; Alanärä et al. 2001) have shown that fish daily activity patterns varied according to season and (or) water temperature. In many rivers of the eastern coast of North America, Atlantic salmon now coexists with the exotic rainbow trout (Crawford and Muir 2008). In sympatry, juveniles of both species occupy similar macro- and micro-habitats and are likely to compete for resources (Hearn and Kynard 1986; Blanchet et al. 2007*b*), but the effect of rainbow trout on the diel activity of Atlantic salmon has never been investigated.

To study the influence of competition and selected environmental variables (invertebrate drift, water temperature, cloud cover, moon phase, water depth, and water velocity) on the diel activity patterns of the native Atlantic salmon, we placed juvenile salmon in field enclosures (outdoor channels) subjected to natural environmental fluctuations and to three competitive conditions: low intraspecific competition, high intraspecific competition, and interspecific competition with the rainbow trout. We first compared the effect of intraspecific competition versus interspecific competition on the diel activity of Atlantic salmon. Then, we assessed the relative contribution of competition and other ecological forces on daytime and crepuscular activity separately to verify whether biotic and abiotic factors acted synergistically in shaping individual activity patterns. Finally, we compared the growth rate and behaviour (feeding rate and aggression rate) of Atlantic salmon among the different competitive treatments to evaluate the fitness consequences of potential change in diel activity patterns.

Materials and methods

Sampling sites

During the summers of 2005 and 2006, young-of-the-year (YOY) Atlantic salmon and rainbow trout were sampled by electrofishing in the Malbaie River (Québec, Canada; 47°67′N, 70°16′W). A self-sustaining population of rainbow trout coexists with Atlantic salmon in the lower 9 km of the river. Atlantic salmon were sampled in locations where rainbow trout are not present (i.e., above a human-controlled fish ladder) to avoid the effects of previous encounters between the two species. Atlantic salmon fry emerged from their nests earlier than rainbow trout fry and consequently maintained a size advantage until the end of their first summer of life (i.e., end of August; S. Blanchet, G. Loot, and J.J. Dodson, unpublished data). In our experiments, we selected juvenile salmon and trout of similar size to avoid confounding the effects of size and species identity (Connell 1983; see Table 1 for the size range of each species). Fish were maintained in several holding tanks (0.30 × 0.30 × 0.60 m) placed in the river for 10–15 days before the experiments began.

Experimental design

The same experiment was carried out in the summers of 2005 and 2006 to test for the temporal consistency of the results. The experiments were done in flow-through stream channels installed along the bank of the river. Experiments started on 1 August and lasted 24 days and 28 days for 2005 and 2006, respectively. Channels were constructed of 20 mm thick plywood, but their dimensions varied between years (Table 1). In 2005, they were 4.8 m long × 0.6 m wide × 0.6 m deep, and six Plexiglas windows (0.30 m × 0.30 m) were disposed along one side of each channel to allow direct underwater observations. Both the upstream and downstream ends of each channel were covered with

© 2008 NRC Canada

Table 1. Characteristics of the two semi-natural experiments carried out in 2005 and 2006 designed to assess the effects of competition and selected abiotic factors on the diel activity of Atlantic salmon (*Salmo salar*).

	Experiments	
	2005	2006
Channel characteristics		
Channel length (m)	4.80	2.00
Water depth (cm)	11 (7–19)	17 (9–24)
Water velocity ($cm \cdot s^{-1}$)	8.34 (6.32–12.41)	17.56 (9.34–28.82)
Screen mesh size (mm)	3.00	4.50
Biological material characteristics		
Length, Atlantic salmon (mm)	42.27 (38–49)	42.76 (35–56)
Weight, Atlantic salmon (g)	0.73 (0.48–0.96)	0.74 (0.37–1.61)
Length, rainbow trout (mm)	41.65 (34–47)	41.93 (37–46)
Weight, rainbow trout (g)	0.69 (0.52–1.01)	0.70 (0.51–0.98)
Total density ($individuals \cdot m^{-2}$)	3.13, 6.26	3.33, 6.66
Environmental characteristics		
Daytime water temperature (°C)	18.5 (15.8–22.0)	18.0 (14.5–20.0)
Crepuscular water temperature (°C)	18.0 (15.0–22.0)	17.0 (14.0–19.0)
Cloud cover (%)	52 (0–100)	43 (0–100)
Discharge ($m^3 \cdot s^{-1}$)	8.92 (7.31–11.48)	12.29 (8.43–18.58)
Daytime food availability*	0.73 (0.42–1.22)	1.68 (0.8–2.48)
Crepuscular food availability*	5.62 (1.83–12.45)	13.65 (2.18–35.07)

Note: Values are expressed as the mean with the range given in parentheses.

*Daytime and crepuscular food availability was expressed as number of invertebrates per minute drifting in a net.

3 mm mesh plastic screen to allow natural drift of invertebrates and prevent fish from escaping. To increase the statistical power, more channels of smaller size were used in 2006. They were 2 m long × 0.6 m wide × 0.6 m deep, and there were three Plexiglas windows (0.30 m × 0.30 m). Moreover, to ensure that the flow was as natural as possible, the mesh size of the plastic screen was increased to 4.5 mm (see Table 1). Each year, the screens were gently brushed twice a day to prevent the mesh from clogging and to limit sedimentation. The top of each channel was covered with transparent nylon monofilament (10 cm × 10 cm mesh size) to prevent predation from birds (i.e., gulls). The bottom of the channels was covered with river substratum (mainly sand, gravel, pebbles, and cobbles) to mimic the natural habitat of juvenile Atlantic salmon and rainbow trout and to allow rapid colonization of invertebrates. Water depth and water velocity were repeatedly measured in each channel. Water depth was measured at a single fixed point (directly downstream of the upstream plastic screen) in each channel (the water depth of each channel was homogeneous along its length). Water velocity was evaluated as the time needed for an inert object (a 8 cm^3 piece of wood) to cover the distance of a channel. Water depth and water velocity in the channels varied according to daily discharge and years. In 2005, depth was 11 cm on average and velocity was 8.34 $cm \cdot s^{-1}$ on average, whereas in 2006, both depth (17 cm on average) and velocity (17.56 $cm \cdot s^{-1}$ on average) were higher (Table 1). Depth and water velocity values were in the range used by Atlantic salmon and rainbow trout in the Malbaie River (Blanchet et al. 2007*b*).

Experiments consisted of three competitive treatments (combined substitutive and additive design; Connell 1983); each was replicated three times in 2005 ($n = 9$ channels) and four times in 2006 ($n = 12$ channels). In the low intraspecific competition treatment, salmon were maintained at a density of 3 $fish \cdot m^{-2}$. In the high intraspecific competition treatment, salmon density was doubled to 6 $fish \cdot m^{-2}$. Finally, in the interspecific competition treatment, equal numbers of salmon and trout were maintained in sympatry for a total density of 6 $fish \cdot m^{-2}$. A density of 3 salmon or trout $fry \cdot m^{-2}$ is commonly observed in Malbaie River (S. Blanchet, G. Loot, and J.J. Dodson, unpublished data), whereas a density of 6 $fish \cdot m^{-2}$ is observed in highly productive areas of the Malbaie River (S. Blanchet, G. Loot, and J.J. Dodson, unpublished data). A density of 6 $fish \cdot m^{-2}$ is high enough to expect interference competition, but below the maximum predicted density of 15 $fish \cdot m^{-2}$ (Grant and Kramer 1990) for fish as small as 45 mm. Space competition and aggressive interference in Atlantic salmon have already been observed at a density of 6 $fish \cdot m^{-2}$ (Blanchet et al. 2006).

The length and weight of fish used in the experiments are detailed in Table 1. The size and the weight of both Atlantic salmon and rainbow trout did not differ between years (one-way analyses of variance, ANOVAs, $p > 0.05$). Moreover, there was no difference between the size and weight of Atlantic salmon and rainbow trout used within a year (one-way ANOVAs, $p > 0.05$). In each channel, Atlantic salmon were individually marked using Visible Implant Elastomer tags (VIE; Northwest Marine Technology, Shaw Island, Washington) to evaluate and compare growth rate of salmon among treatments.

The activity observations were conducted once every 3 days, and between two and four channels per treatment were observed during each observation (i.e., 6 to 12 channels per observation). Daytime observations were performed in the morning (0900 to 1100). Activity was quantified by

© 2008 NRC Canada

observing fish through the Plexiglas windows from the downstream to the upstream end of the channel. Each window was scanned for a 5 min period (i.e., 30 and 15 min per channel in 2005 and 2006, respectively), and the total number of active fish observed was counted. A fish was considered as active when it was observed out of the substrate for at least 30 s over the 5 min observation and when it was facing into the current, propped up on its pectoral fins. Salmon that briefly left its refuge to chase a competitor or to catch a drifting prey was not counted as active. In addition, we recorded the number and direction of aggression acts (chases, nips, and displays) and feeding events initiated by each species. Crepuscular observations were conducted during the early part of the night (2030 to 2230, a foraging period considered as being profitable for salmonids; Alanärä et al. (2001)). In Malbaie River, the time of sunset was 2017 on 1 August and 1927 on 30 August, and the nautical twilight was 2138 on 1 August and 2037 on 30 August. Thus, our crepuscular observations took place mainly during twilight. At this time, the light intensity was inferior to 0.01 lx (S. Blanchet and G. Loot, personal observation). Fish were detected, identified, and counted by briefly scanning the water surface from the downstream to the upstream end of the channels using a flashlight with a red filter to avoid disturbing the fish (Harwood et al. 2001; Reebs 2002). To ensure species identification (based on body shape, patterns of body pigmentation, and swimming behaviour of each species), counts were repeated twice by two different observers (S. Blanchet and G. Loot), and the mean of these two observations was used to quantify the number of active fish during twilight. The visibility was, however, too low to quantify rates of aggression and feeding.

To account for possible effects of fish size on growth rate, the mass-specific growth rate (Ω) (Ostrovsky 1995; Flodmark et al. 2006) was calculated for each individual using the following formula:

$$(1) \qquad \Omega = \frac{M_t^b - M_0^b}{b \cdot t}$$

where M_t and M_0 are body mass (g) at the end and start of the experiment, respectively; b is the allometric mass exponent for the relation between specific growth rate and body mass, estimated at 0.31 for Atlantic salmon (Elliott and Hurley 1997), and t is the experimental period.

For each observation, selected environmental variables were measured according to previous studies on the foraging activity of Atlantic salmon (five for daytime observations and six for crepuscular observations). First, before behavioral observations, water temperature was recorded (±0.5 °C), as it has been shown to influence diel activity patterns of Atlantic salmon (e.g., Johnston et al. 2004). The percentage of cloud cover (±5%) was also visually estimated as a surrogate of light intensity (see Girard et al. 2003). In addition, during the crepuscular observations, we evaluated the percentage of moon visible (based on calendar estimation) (see Imre and Boisclair 2005). Secondly, after behavioral observations, water depth (±1 cm) and water velocity (±1 cm·s^{-1}) were measured to evaluate hydraulic variation in the habitat. Finally, during the behavioral observations, invertebrate drift (as a measure of food supply) was quantified at a fixed sampling point within the study section. Drift was sampled during a 30–60 min period during each activity observation using a drift net (mesh size 250 µm). We assumed that the quantity of invertebrates drifting at this sampling point was representative of the quantity of food available in each channel for a given observation session. This assumption seems realistic for two reasons. First, in 2005, two nets separated by a 200 m long transect were simultaneously used to estimate invertebrate drift. The correlation between the numbers of invertebrates drifting at the two sampling sites was strong and highly significant ($r = 0.83$, $n = 22$, $p < 0.001$). Secondly, in 2006, we found that the quantity of food drifting in seven channels monitored individually was relatively homogeneous within an observation period. The variance in invertebrate drift was two times higher between sampling periods than between channels within a sampling period (the coefficients of variation were 59.01% and 33.58%, respectively; S. Blanchet, G. Loot, and J.J. Dodson, unpublished data). These two observations indicated that the drift of invertebrate was relatively spatially homogeneous and that sampling the invertebrate at single sampling site was representative of what was drifting in each channel. The mouth of the drift net was covered with 3 and 4.5 mm mesh plastic screen in 2005 and 2006, respectively, to insure that the drift net filtered the same size range of drift that was filtered at the entrance to the experimental channels in the two years. Given the gape size of Atlantic salmon and rainbow trout, all the invertebrates (mainly chironomid larvae) sampled in the drift net were potential prey for the fish. Invertebrates were preserved in 95% alcohol and counted under a binocular microscope. Food supply in each channel was expressed as the number of invertebrates caught at the fixed station per minute and per cubic metre per second by multiplying the number of invertebrates caught per minute in the drift net by the flow rate (width × depth × water velocity) of each channel.

Statistical analyses

Diel activity

Atlantic salmon activity was expressed as the number of fish active in a channel divided by the number of salmon present in this channel at the end of the experiment (mortality was low but occurred in some channels (mean = 0.24 individuals·channel^{-1}) and was unrelated to the treatments). The proportion of active salmon was arcsin-transformed (Zar 1999) in all subsequent analyses to meet the assumptions of normality and homoscedasticity.

We first assessed the influence of year of the experiments (2005 or 2006), period of observation (daytime or twilight), and competitive treatments on the proportion of active salmon. In this analysis, the mean of each channel, for daytime and crepuscular observations, was used as the replicate unit. We used mixed linear models, which are a generalization of standard linear models; the generalization permits the data to exhibit dependency (Pinheiro and Bates 2000). Because the proportion of active fish observed during the day in a channel may be dependent on the proportion of fish active during twilight (repeated measures), channel was integrated as the random factor to deal with this potential temporal dependency (Pinheiro and Bates 2000). Year of the experi-

© 2008 NRC Canada

Table 2. Results of mixed-linear models used to evaluate the effect of the year of experiment (2005 or 2006), period of observation (daytime vs. crepuscular), and competitive treatment (low intraspecific, high intraspecific, and interspecific competition) and the resulting interactions on the proportion of active Atlantic salmon (*Salmo salar*).

Source of variation	df	*F* value	*P* value
Year of experiment	1,19	3.76	0.067
Period of observation	1,12	124.49	**<0.001**
Competitive treatment	2,12	2.12	0.163
Year × period	1,12	13.19	**0.003**
Year × treatment	2,12	0.07	0.925
Period × treatment	2,12	4.64	**0.032**
Year × period × treatment	2,12	0.14	0.871

Note: Significant effects ($p < 0.05$) are indicated in bold. df, degrees of freedom.

ments, period of observation, and competitive treatments were the fixed factors. Multiple comparisons were performed using contrast tests.

Secondly, we assessed the relative contribution of biotic (competitive treatments, expressed as a categorical factor) and abiotic variables (environmental factors, expressed as continuous factors). Recently, several statistical tools have been developed to evaluate the relative importance of each predictor in multiple linear regressions, particularly in the case of collinear predictors (for a review, see Grömping 2007). However, to our knowledge, no tool has been specifically published for models integrating both fixed and random factors (i.e., mixed models; U. Grömping, Department II — Mathematics, Physics and Chemistry, TFH Berlin, University of Applied Sciences, Berlin, Germany, personal communication). Here, to deal with mixed models, we used a simple technique developed online within the R project (R Development Core Team 2005). We calculated the contribution of a given predictor by comparing the percentage of variance explained by the fixed factors of a full model (i.e., all predictors included) with the variance explained by the fixed factors of the same model without the predictor of interest. The difference of variance explained between the two models gives the relative contribution of the given predictor. Because statistical interactions are difficult to test (and to interpret) with such an approach (Grömping 2007) and because environmental differences occurred between the two years of experiments (for a summary, see Table 1), 2005 and 2006 were analyzed separately. For each year, two full models were constructed: one for daytime and one for crepuscular observations. In this descriptive analysis, we used each observation as a replicate unit. The full model included competitive treatments and the five or six environmental variables (i.e., invertebrates drift, water temperature, cloud cover, water depth, water velocity, and moon phase for crepuscular observations) as fixed factors. Period of observation nested within channel was the random factor (Pinheiro and Bates 2000). The variance explained by the fixed portion of this model was compared with the variance explained by the fixed portion of simplified models that each included all but the predictor of interest. This relative contribution (or effect size) of each predictor was expressed as the percentage of the total variance explained by each variable itself.

Fig. 1. Mean proportion (± standard error, SE) of Atlantic salmon (*Salmo salar*) active during daytime (open bars) and twilight (solid bars) when maintained at low intraspecific density (3 fish·m^{-2}) and high intraspecific density (6 fish·m^{-2}), and with rainbow trout (*Oncorhynchus mykiss*), respectively (3 + 3 fish·m^{-2}) for (*a*) 2005 and (*b*) 2006. Significantly different values ($p < 0.05$, contrasts tests) are identified with different letters.

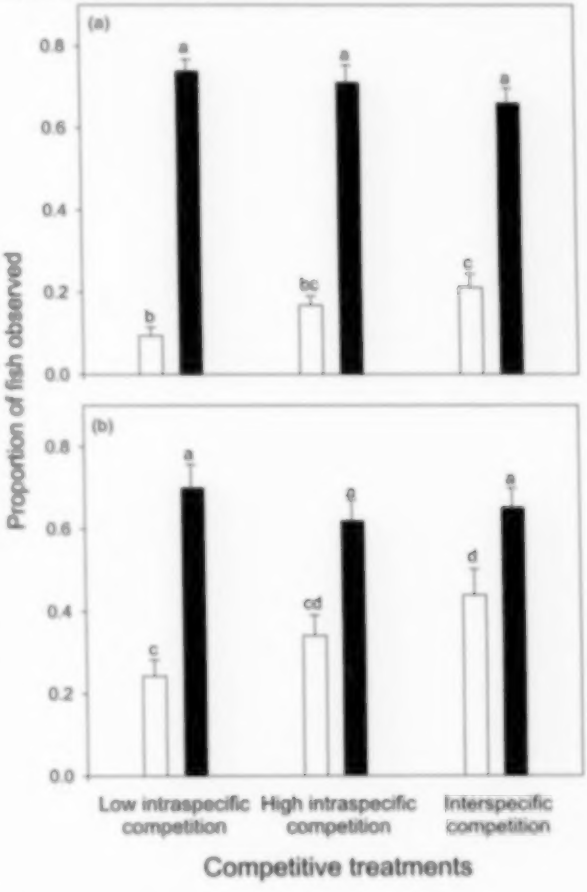

Growth and behaviour

Growth rate of Atlantic salmon was compared among competitive treatments and years using a two-way ANOVA. Aggression rate and feeding rate ($\log(x+1)$-transformed) were tested across treatments and species using two-way ANOVAs (years and competitive treatments as main factors). In the latter analyses, the mean in each channel was used as the replicate unit. SNK tests (Zar 1999) were used for subsequent multiple comparisons analyses.

All statistical analyses were performed using R (version 2.2.1; R Development Core Team 2005).

Results

Diel activity

On average, there were no significant differences between the proportion of active Atlantic salmon observed in 2005 and 2006 (Table 2). We found that Atlantic salmon were

© 2008 NRC Canada

Fig. 2. The percentage of the total explained variance of the predictor variables from a mixed linear model explaining the activity of Atlantic salmon (*Salmo salar*), computed separately for daytime (open bars) and twilight (solid bars) in (*a* and *c*) 2005 and (*b* and *d*) 2006. The signs indicate the slope (+, positive slope; –, negative slope) for the relationship between each predictor and the proportion of active salmon.

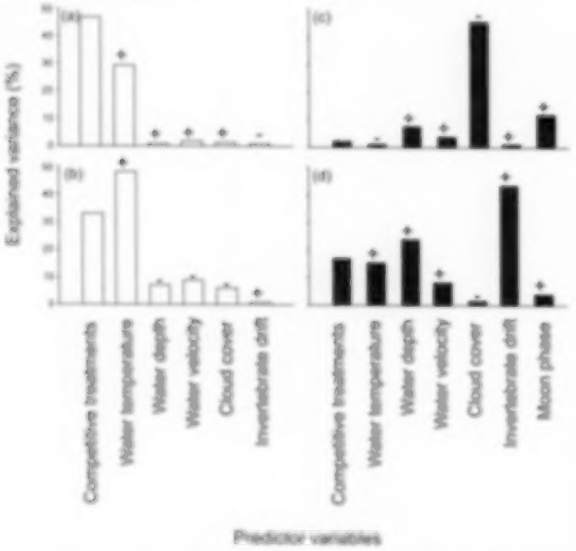

significantly more active during twilight (Fig. 1; Table 2). However, we detected a significant interaction between the year of experiment and the period of observation, indicating that the daytime activity of salmon was higher in 2006 than in 2005 (Table 2; Fig. 1). We found a significant interaction between periods of observation and competitive treatment (Table 2). Indeed, the proportion of salmon active during daytime was significantly higher when salmon occurred with rainbow trout than when salmon occurred at a low density (contrast test, both years pooled, $p = 0.01$; Fig. 1). During the day, there was no difference between either the low and high intraspecific treatments (contrast test, both years pooled, $p = 0.09$; Fig. 1) or between the high intraspecific and interspecific treatments (contrast test, both years pooled, $p = 0.21$; Fig. 1). In contrast, during twilight, competitive treatments did not affect the proportion of active salmon (Fig. 1). The nonsignificant three-term interaction indicated that these patterns were identical in 2005 and 2006 (see Fig. 1).

For comparison, the percentage of rainbow trout active was 59% ± 0.26% (standard deviation, SD) during the day compared with 68% ± 0.23% during twilight (paired *t* test, $t = 0.73$, $p = 0.45$).

Relative contributions of environmental variables

During daytime, the relative importance of the various environmental variables was generally consistent in 2005 and 2006, with competitive treatment and water temperature each contributing to 30%–45% of the total variance (Figs. 2*a* and 2*b*). Water temperature positively affected the proportion of fish observed during the day (Figs. 2*a* and 2*b*).

Fig. 3. Mass-specific growth rate (mean ± standard error, SE) calculated for Atlantic salmon (*Salmo salar*) in two years (2005, solid bars; 2006, shaded bars) for the three treatments: low intraspecific competition (3 fish·m^{-2}), high intraspecific competition (6 fish·m^{-2}), and interspecific competition (3 + 3 fish·m^{-2}).

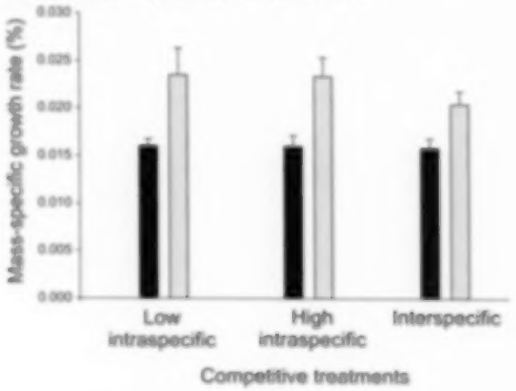

During twilight, the relative importance of variables differed between years (Figs. 2*c* and 2*d*). In 2005, the percentage of cloud cover alone contributed to ~45% of the total variance (Fig. 2*c*). Greater cloud cover reduced the crepuscular activity of salmon (Fig. 2*c*), and the other predictors contributed relatively little to the total variance (<16% each). In 2006, invertebrate drift was positively related to activity during twilight, explaining about 40% of the variation in activity (Fig. 2*d*). Greater invertebrate drift increased the crepuscular activity of salmon (Fig. 2*d*). During both years, water depth in each channel was a relatively good predictor of activity (Figs. 2*c* and 2*d*), with greater water depth being associated with a higher proportion of salmon active during twilight (Figs. 2*c* and 2*d*). In contrast to daytime activity, we detected no strong effects of competitive treatment or water temperature in explaining crepuscular activity in either 2005 or 2006 (Figs. 2*a*–2*d*).

Growth and behaviour

Growth rate of Atlantic salmon was higher in 2006 than in 2005 (year effect, ANOVA, $F_{[1,15]} = 18.03$, $p = 0.001$; Fig. 3), but in both years, competitive treatments did not affect growth rate of salmon (competitive treatment effect, ANOVA, $F_{[2,15]} = 0.48$, $p = 0.63$; interaction term, ANOVA, $F_{[2,15]} = 0.37$, $p = 0.69$; Fig. 3). At the end of the experiment, the weight of the Atlantic salmon was increased by a factor of 1.35 in 2005 (all treatments pooled) and by a factor of 1.78 in 2006 (all treatments pooled).

Feeding rate did not differ between years (year effect, ANOVA, $F_{[1,20]} = 0.34$, $p = 0.57$; Fig. 4*a*), and trends were similar between years (interaction term, ANOVA, $F_{[3,20]} = 0.19$, $p = 0.89$; Fig. 4*a*). In 2005 and 2006, rainbow trout fed at a rate significantly higher than Atlantic salmon (competitive treatment and species effects, ANOVA, $F_{[3,20]} = 4.49$, $p = 0.01$; SNK tests, $p < 0.05$ for all comparisons; Fig. 4*a*), but the feeding rate of salmon did not differ between competitive treatments (SNK tests, $p > 0.05$ for all comparisons; Fig. 4*a*).

Aggression rate did not differ between years (year effect,

© 2008 NRC Canada

Fig. 4. (*a*) Mean (± standard error, SE) feeding rate (log(*x* + 1)) per fish per 5 min observation and (*b*) mean aggression rate (log(*x* + 1)) per fish per 5 min observation calculated for Atlantic salmon (*Salmo salar*, "Salmon") and rainbow trout (*Oncorhynchus mykiss*, "Trout") in two years (2005, solid bars; 2006, shaded bars) for the three treatments: low intraspecific competition (3 fish·m^{-2}), high intraspecific competition (6 fish·m^{-2}), and interspecific competition (3 + 3 fish·m^{-2}). Nonsignificant differences between species and (or) treatments are indicated (n.s.).

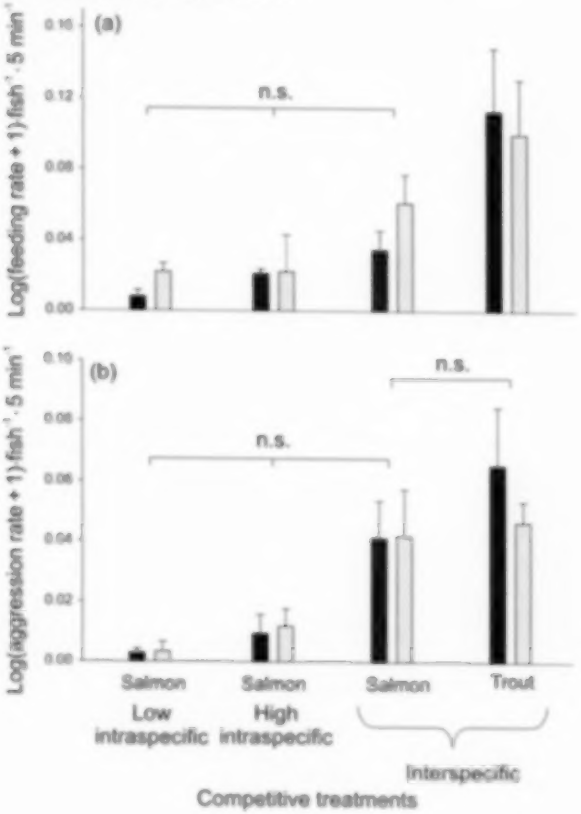

ANOVA, $F_{[1,20]} = 0.73$, $p = 0.40$; Fig. 4*b*), and trends were similar in both years (interaction term, ANOVA, $F_{[3,20]} = 0.91$, $p = 0.45$; Fig. 4*b*). The aggression rate of rainbow trout was higher than that of Atlantic salmon (competitive treatment and species effects, ANOVA, $F_{[3,20]} = 4.27$, $p = 0.02$; SNK tests, $p < 0.05$ for all comparisons; Fig. 4*b*). Moreover, the aggression rate of Atlantic salmon tended to be greater when maintained with rainbow trout than when in allopatry (salmon with rainbow trout compared with salmon in low intraspecific density, SNK test, $p = 0.08$; salmon with rainbow trout compared with salmon in high intraspecific density, SNK test, $p = 0.08$; Fig. 4*b*). Rainbow trout and Atlantic salmon displayed a similar rate of aggression when they were in sympatry (SNK test, $p = 0.53$; Fig. 4*b*). A finer analysis of the sympatric situation that integrated the direction of each aggressive act revealed that Atlantic salmon and rainbow trout directed a similar amount of aggression toward heterospecifics and toward conspecifics (paired *t* tests, $t = -0.68$, $p = 0.51$ for Atlantic salmon and $t = 0.28$, $p = 0.78$ for rainbow trout).

Discussion

Because our experimental design differed slightly between 2005 and 2006, it was difficult to disentangle the factors explaining some differences that we observed between years. For instance, larger screen mesh, greater depth and water velocity, and higher discharge could explain why invertebrate drift was higher in 2006 and therefore why daytime activity and growth rate of Atlantic salmon were also higher (for a study on the effects of changing screen mesh size in outdoor channels, see Dahl and Greenberg 1999). Nevertheless, some trends were consistent in both years, which will be the focus of our discussion.

Our study confirmed previous field observations reporting that Atlantic salmon fry were predominantly active during twilight at high summer temperatures (Gries et al. 1997; Johnston et al. 2004; but see Breau et al. 2007). More interestingly, we highlighted the importance of interspecific competition on diel activity patterns. Neither intraspecific nor interspecific competition influenced the crepuscular activity of Atlantic salmon. However, during the day, interspecific competition had a significant effect on the activity of Atlantic salmon fry. The effect of doubling the density of Atlantic salmon was half the effect of interspecific competition at the same total density. Moreover, we found no significant differences between the low and high intraspecific treatments and the high intra- and inter-specific treatments. These observations indicated that the effect of competition with rainbow trout was probably mediated by both the effect of increasing density and the identity of the competitors (Connell 1983; Blanchet et al. 2007*b*). The temporal partitioning (sensu stricto) of Atlantic salmon was not strongly affected by rainbow trout, as salmon remained mainly crepuscular, even in the presence of interspecific competitor. However, because fish increased their risk of predation when they are active during the day (Martel and Dill 1995; Fraser et al. 2004), Atlantic salmon used a more risky tactic when maintained in sympatry with rainbow trout than when maintained at a low intraspecific density.

Rainbow trout are generally considered to be more aggressive than Atlantic salmon (Volpe et al. 2001). Territorial interference competition imposed by trout may thus force salmon to leave their refuge during the day. Indeed, when in sympatry with rainbow trout, Atlantic salmon tended to be more aggressive than when in allopatry, and they directed half of their aggression toward rainbow trout and received the same amount of aggression from trout. Moreover, rainbow trout were highly active during both the day and twilight. Therefore, we propose that rainbow trout (which cruise more than Atlantic salmon; Volpe et al. 2001) frequently penetrated Atlantic salmon territories, resulting in greater daytime activity associated with territory defence in the presence of rainbow trout. During twilight, the effect of competition was lower, probably because aggressive interactions have been shown to be less frequent at this time or during low light intensity (Fraser et al. 1993; Blanchet et al. 2007*c*). Alternatively, Atlantic salmon may be more active

© 2008 NRC Canada

during the day to compensate for strong exploitative competition imposed by rainbow trout.

In addition, we found that the growth rate of Atlantic salmon was not influenced by the presence of competitors, at least at the densities we studied. It is possible that even if the feeding rate of Atlantic salmon was constant across treatments, they maintained their growth rate by being active during a longer period of time during the day, thereby increasing feeding opportunities and compensating for the energy spent when in the presence of the rainbow trout. The weak effect of competition on the growth rate of Atlantic salmon suggested that the tactic adopted by the Atlantic salmon when in sympatry with the rainbow trout was not energetically costly but may nevertheless increase the probability of encountering predators. Such "growth compensation" is consistent with recent studies emphasizing the fact that animals adjust their behaviour in a manner to follow a maximal growth trajectory, even if they expose themselves to a higher predation risk (Biro et al. 2003; Imre et al. 2005).

We demonstrated that during the day, water temperature was another important factor to consider in explaining activity of Atlantic salmon. This positive effect of water temperature on the daytime activity pattern of Atlantic salmon was consistent with the results of previous studies (e.g., Gries et al. 1997; Johnston et al. 2004; Breau et al. 2007). During twilight, the effect of water temperature was weak relative to the effects of other environmental cues (invertebrate drift, cloud cover), at least within the range of temperatures found in this study. Fraser et al. (1993) also demonstrated in laboratory experiments that nocturnal foraging rate was independent of water temperature. By shifting from the use of thermal cues to other environmental cues during twilight, Atlantic salmon may acquire more accurate information about whether or not to be active. For instance, during twilight, the information provided by the level of light intensity (i.e., cloud cover and moon phase) is considered to be of high quality for use in predicting predation risk (Fraser et al. 1993) and food intake (Fraser and Metcalfe 1997). This result suggests that the sensitivity of Atlantic salmon to environmental cues might vary over a 24 h cycle, perhaps to maximize the ratio between energy gain and the risk of being detected by a predator.

To summarize, we demonstrated that interspecific competition acted as an important factor in shaping the daytime activity of Atlantic salmon. Moreover, we demonstrated that this effect was the result of both the competitor's identity and the effect of increasing density. The effect of interspecific competition was strongest during the day and was probably the result of territorial interference between species. During twilight, no effect of competition was detected and the influence of the other environmental factors was different from the patterns observed during the day. Overall, these results suggest interplay between biotic and abiotic factors in determining fish activity (Reebs 2002; Kronfeld-Schor and Dayan 2003). Moreover, these results suggest that fish were highly plastic at the daily time scale in their responses to biotic and abiotic changes, probably to maximize the ratio between net energy gain and the risk of being eaten by predators.

The effect of competition imposed by rainbow trout did not seem to influence the growth rate of Atlantic salmon. However, by increasing activity during the day, Atlantic salmon increase the probability of being detected by a predator (Martel and Dill 1995), and in that context, the exotic species may indirectly alter the fitness of the native species by reducing survival probability. As such, our results illustrate how plasticity for foraging activity can occur along a temporal axis and how it may play a pivotal role in the outcome of interactions between native and exotic species.

Acknowledgments

We sincerely thank J.F. Bourque, V. Duclos, T. Garneau, and A. Richard for help in the field. Three anonymous referees provided comments on an early version of the manuscript. We also thank S. Reebs and J.W.A. Grant for their fruitful comments on the manuscript. This research was financially supported by a Natural Sciences and Engineering Research Council of Canada grant (strategic program) to J.J.D. and L.B. The experiments conducted comply with current Canadian laws.

References

Alanärä, A., Burns, M.D., and Metcalfe, N.B. 2001. Intraspecific resource partitioning in brown trout: the temporal distribution of foraging is determined by social rank. J. Anim. Ecol. **70**: 980–986. doi:10.1046/j.0021-8790.2001.00550.x.

Biro, P.A., Post, J.R., and Parkinson, E.A. 2003. From individuals to populations: prey fish risk-taking mediates mortality in whole-system experiments. Ecology, **84**: 2419–2431. doi:10.1890/02-0416.

Blanchet, S., Dodson, J.J., and Bresse, S. 2006. Influence of habitat structure and fish density on Atlantic salmon *Salmo salar* L. territorial behaviour. J. Fish Biol. **68**: 951–957. doi:10.1111/j.0022-1112.2006.00970.x.

Blanchet, S., Loot, G., Grenouillet, G., and Brosse, S. 2007*a*. Competitive interactions between native and exotic salmonids: a combined field and laboratory demonstration. Ecol. Freshw. Fish, **16**: 133–143.

Blanchet, S., Loot, G., Bernatchez, L., and Dodson, J.J. 2007*b*. The disruption of dominance hierarchies by a non-native species: an individual-based analysis. Oecologia (Berl.), **152**: 569–581. doi:10.1007/s00442-007-0668-4.

Blanchet, S., Bernatchez, L., and Dodson, J.J. 2007*c*. Behavioural and growth responses of a territorial fish (Atlantic salmon, *Salmo salar* L.) to multiple predatory cues. Ethology, **113**: 1061–1072. doi:10.1111/j.1439-0310.2007.01410.x.

Breau, C., Weir, L.K., and Grant, J.W.A. 2007. Individual variability in activity patterns of juvenile Atlantic salmon (*Salmo salar*) in Catamaran Brook, New Brunswick. Can. J. Fish. Aquat. Sci. **64**: 486–494. doi:10.1139/F07-026.

Connell, J.H. 1983. On the prevalence and relative importance of interspecific competition: evidence from field experiments. Am. Nat. **122**: 661–696. doi:10.1086/284165.

Crawford, S., and Muir, A. 2008. Global introductions of salmon and trout in the genus *Oncorhynchus*: 1870–2007. Rev. Fish Biol. Fish. **18**: 313–344. doi:10.1007/s11160-007-9079-1.

Dahl, J., and Greenberg, L. 1999. Effects of prey dispersal on predator–prey interactions in streams. Freshw. Biol. **41**: 771–780. doi:10.1046/j.1365-2427.1999.00422.x.

Elliott, J.M., and Hurley, M.A. 1997. A functional model for maximum growth of Atlantic Salmon parr, *Salmo salar*, from two populations in northwest England. Funct. Ecol. **11**: 592–603. doi:10.1046/j.1365-2435.1997.00130.x.

© 2008 NRC Canada

Fausch, K.D. 1998. Interspecific competition and juvenile Atlantic salmon (*Salmo salar*): on testing effects and evaluating the evidence across scales. Can. J. Fish. Aquat. Sci. **55**(Suppl. 1): 218–231. doi:10.1139/cjfas-55-S1-218.

Flecker, A.S. 1992. Fish predation and the evolution of invertebrate drift periodicity: evidence from neotropical streams. Ecology, **73**: 438–448. doi:10.2307/1940751.

Flodmark, L.E.W., Forseth, T., L'Abee-Lund, J.H., and Vollestad, L.A. 2006. Behaviour and growth of juvenile brown trout exposed to fluctuating flow. Ecol. Freshw. Fish, **15**: 57–65. doi:10.1111/j.1600-0633.2006.00127.x.

Fraser, N.H.C., and Metcalfe, N.B. 1997. The costs of becoming nocturnal: feeding efficiency in relation to light intensity in juvenile Atlantic salmon. Funct. Ecol. **11**: 385–391. doi:10.1046/j.1365-2435.1997.00098.x.

Fraser, N.H.C., Metcalfe, N.B., and Thorpe, J.E. 1993. Temperature-dependent switch between diurnal and nocturnal foraging in salmon. Proc. R. Soc. Lond. B Biol. Sci. **252**: 135–139. doi:10.1098/rspb.1993.0057.

Fraser, D.F., Gilliam, J.F., Akkara, J.T., Albanese, B.W., and Snider, S.B. 2004. Night feeding by guppies under predator release: effects on growth and daytime courtship. Ecology, **85**: 312–319. doi:10.1890/03-3023.

Girard, P., Boisclair, D., and Leclerc, M. 2003. The effect of cloud cover on the development of habitat quality indices for juvenile Atlantic salmon (*Salmo salar*). Can. J. Fish. Aquat. Sci. **60**: 1386–1397. doi:10.1139/f03-118.

Grant, J.W.A., and Kramer, D.L. 1990. Territory size as a predictor of the upper limit to population density of juvenile salmonids in streams. Can. J. Fish. Aquat. Sci. **47**: 205–212.

Gries, G., Whalen, K.G., Juanes, F., and Parrish, D.L. 1997. Nocturnal activity of juvenile Atlantic salmon (*Salmo salar*) in late summer: evidence of diel activity partitioning. Can. J. Fish. Aquat. Sci. **54**: 1408–1413. doi:10.1139/cjfas-54-6-1408.

Grömping, U. 2007. Estimators of relative importance in linear regression based on variance decomposition. Am. Stat. **61**: 139–147. doi:10.1198/000313007X188252.

Hansen, E.A., and Closs, G.P. 2005. Diel activity and home range size in relation to food supply in a drift-feeding stream fish. Behav. Ecol. **16**: 640–648. doi:10.1093/beheco/ari036.

Harwood, A.J., Metcalfe, N.B., Armstrong, J.D., and Griffiths, S.W. 2001. Spatial and temporal effects of interspecific competition between Atlantic salmon (*Salmo salar*) and brown trout (*Salmo trutta*) in winter. Can. J. Fish. Aquat. Sci. **58**: 1133–1140. doi:10.1139/cjfas-58-6-1133.

Hearn, W.E., and Kynard, B.E. 1986. Habitat utilization and behavioral interaction of juvenile Atlantic salmon (*Salmo salar*) and rainbow trout (*Salmo gairdneri*) in tributaries of the White River of Vermont. Can. J. Fish. Aquat. Sci. **43**: 1988–1998.

Imre, I., and Boisclair, D. 2005. Moon phase and nocturnal density of Atlantic salmon parr in the Sainte-Marguerite River, Quebec. J. Fish Biol. **66**: 198–207. doi:10.1111/j.0022-1112.2005.00592.x.

Imre, I., Grant, J.W.A., and Cunjak, R.A. 2005. Density-dependent growth of young-of-the-year Atlantic salmon *Salmo salar* in Catamaran Brook, New Brunswick. J. Anim. Ecol. **74**: 508–516.

Johnston, P., Bergeron, N.E., and Dodson, J.J. 2004. Diel activity patterns of juvenile Atlantic salmon in rivers with summer water temperature near the temperature-dependent suppression of diurnal activity. J. Fish Biol. **65**: 1305–1318. doi:10.1111/j.0022-1112.2004.00532.x.

Klemetsen, A., Amundsen, P.A., Dempson, J.B., Jonsson, B., Jonsson, N., and Mortensen, E. 2003. Atlantic salmon *Salmo salar* L., brown trout *Salmo trutta* L., and Arctic charr *Salvelinus alpinus* (L.): a review of aspects of their life histories. Ecol. Freshw. Fish, **12**: 1–59. doi:10.1034/j.1600-0633.2003.00010.x.

Kotler, B.P., Ayal, Y., and Subach, A. 1994. Effects of predatory risk and resource renewal on the timing of foraging activity in a Gerbil community. Oecologia (Berl.), **100**: 391–396. doi:10.1007/BF00317860.

Kronfeld-Schor, N., and Dayan, T. 2003. Partitioning of time as an ecological resource. Annu. Rev. Ecol. Evol. Syst. **34**: 153–181. doi:10.1146/annurev.ecolsys.34.011802.132435.

Martel, G., and Dill, L.M. 1995. Influence of movement by coho salmon (*Oncorhynchus kisutch*) parr on their detection by common mergansers (*Mergus merganser*). Ethology, **99**: 139–149.

Metcalfe, N.B., Fraser, N.H.C., and Burns, M.D. 1999. Food availability and the nocturnal vs. diurnal foraging trade-off in juvenile salmon. J. Anim. Ecol. **68**: 371–381. doi:10.1046/j.1365-2656.1999.00289.x.

Mills, M.D., Rader, R.B., and Belk, M.C. 2004. Complex interactions between native and invasive fish: the simultaneous effects of multiple negative interactions. Oecologia (Berl.), **141**: 713–721. doi:10.1007/s00442-004-1695-z.

Morita, K., Tsuboi, J.-I., and Matsuda, H. 2004. The impact of exotic trout on native charr in a Japanese stream. J. Appl. Ecol. **41**: 962–972. doi:10.1111/j.0021-8901.2004.00927.x.

Ostrovsky, I. 1995. The parabolic pattern of animal growth — determination of equation parameters and their temperature dependencies. Freshw. Biol. **33**: 357–371. doi:10.1111/j.1365-2427.1995.tb00398.x.

Pinheiro, J.C., and Bates, D.M. 2000. Mixed-effects models in S and S-PLUS. Springer-Verlag, New York.

Railsback, S.F., and Harvey, B.C. 2002. Analysis of habitat-selection rules using an individual-based model. Ecology, **83**: 1817–1830.

R Development Core Team. 2005. R: a language and environment for statistical computing. R Foundation for Statistical Computing, Vienna, Austria. ISBN 3-900051-07-0, URL http://www.R-project.org.

Reebs, S.G. 2002. Plasticity of diel and circadian activity rhythms in fishes. Rev. Fish Biol. Fish. **12**: 349–371. doi:10.1023/A:1025371804611.

Volpe, J.P., Anholt, B.R., and Glickman, B.W. 2001. Competition among juvenile Atlantic salmon (*Salmo salar*) and steelhead (*Oncorhynchus mykiss*): relevance to invasion in British Columbia. Can. J. Fish. Aquat. Sci. **58**: 197–207. doi:10.1139/cjfas-58-1-197.

Wasserberg, G., Kotler, B.P., and Abramsky, Z. 2006. The role of site, habitat, seasonality and competition in determining the nightly activity patterns of psammophilic gerbils in a centrifugally organized community. Oikos, **112**: 573–579. doi:10.1111/j.0030-1299.2006.14302.x.

Zar, J.H. 1999. Biostatistical analysis. Prentice Hall International, Upper Saddle River, New Jersey.

Ziv, Y., Abramsky, Z., Kotler, B.P., and Subach, A. 1993. Interference competition and temporal and habitat partitioning in two gerbil species. Oikos, **66**: 237–246. doi:10.2307/3544810.

© 2008 NRC Canada

Have atmospheric emissions from the Athabasca Oil Sands impacted lakes in northeastern Alberta, Canada?

Roderick R.O. Hazewinkel, Alexander P. Wolfe, Sergi Pla, Chris Curtis, and Kris Hadley

Abstract: The rate of bitumen extraction in northeastern Alberta, Canada, is outpacing the state of ecological understanding of the region, so that the extent of potential disturbances caused by atmospheric deposition remains largely unknown. Atmospheric SO_2 emissions from the Fort McMurray region of Alberta ($\sim$300 t·day^{-1}) constitute $\sim$5% of the Canadian total. Combined with an estimated NO_x production of $\sim$300 t·day^{-1}, these emissions have the potential to acidify surface waters. Diatom assemblages in dated sediment cores from eight acid-sensitive lakes were analyzed to assess the effects of acidifying emissions on boreal lake ecosystems. There is no evidence that these lakes have become acidified. Instead, many of the lakes show characteristic changes towards greater productivity and occasionally greater alkalinity. The absence of evidence for acidification does not imply that emissions from the Oil Sands are environmentally benign, but rather suggests that the biogeochemistry of these lakes differs fundamentally from well-studied acidified counterparts in northern Europe and eastern North America. Complex interactions involving in-lake alkalinity production, internal nutrient loading, and climate change appear to be driving these lakes towards the new ecological states reported.

Résumé : Le taux d'extraction du bitume dans le nord-est de l'Alberta est en train de surpasser l'état de notre compréhension de l'écologie de la région, au point où l'importance des perturbations potentielles causées par les précipitations atmosphériques reste en grande partie inconnue. Les émissions de SO_2 atmosphérique dans la région de Fort McMurray de l'Alberta ($\sim$300 t·jour^{-1}) représentent $\sim$5 % du total canadien. Combinées à une production estimée de $\sim$300 t·jour^{-1} de NO_x, ces émissions peuvent potentiellement acidifier les eaux de surface. Nous avons analysé les peuplements de diatomées dans des carottes de sédiments de date connue provenant de huit lacs vulnérables à l'acidité afin d'évaluer les effets de ces émissions acidifiantes sur les écosystèmes des lacs boréaux. Il n'y a pas d'indication d'acidification de ces lacs. Au contraire, plusieurs des lacs affichent des changements caractéristiques d'une évolution vers une plus grande productivité et, à l'occasion, une alcalinité accrue. L'absence de signes d'acidification n'implique pas que les émissions provenant des sables bitumineux soient sans effet sur l'environnement, mais elle indique plutôt que la biogéochimie de ces lacs diffère de celle des lacs acidifiés similaires bien connus du nord de l'Europe et de l'est de l'Amérique du Nord. Des interactions complexes impliquant la production d'alcalinité dans le lac même, la charge interne de nutriments et le changement climatique semblent être en train de conduire ces lacs vers les nouveaux états écologiques que nous avons décrits.

[Traduit par la Rédaction]

Introduction

Activities directly related to extraction and processing of the Athabasca Oil Sands bitumen resource in northeastern Alberta currently generate an estimated 204 t·day^{-1} SO_2 and 312 t·day^{-1} NO_x in atmospheric emissions (Deer Creek Energy Ltd. 2006). The Canadian Government's National Pollutant Release Inventory (NPRI 2006) provides far higher estimates of 291 t·day^{-1} SO_2 at 2006 production levels for the Deer Creek air emissions study area, but lower estimates of NO_x emissions (73 t·day^{-1} NO_2), reflecting the exclusion of mine vehicles from emissions reporting requirements. The available emissions inventory for the Fort McMurray region

Received 15 April 2007. Accepted 12 March 2008. Published on the NRC Research Press Web site at cjfas.nrc.ca on 5 July 2008. J19947

R.R.O. Hazewinkel[1] and A.P. Wolfe.[2] Department of Earth and Atmospheric Sciences, University of Alberta, Edmonton, AB T6G 2E3, Canada.
S. Pla[3] and C. Curtis. Environmental Change Research Centre, University College London, Gower Street, London, WC1E 6BT, United Kingdom.
K. Hadley. Paleoecological Environmental Assessment and Research Lab (PEARL), Department of Biology, Queen's University, Kingston, ON K7L 3N6, Canada.

[1]Present address: Alberta Environment, 4999-98 Avenue, Edmonton, AB T6B 2X3, Canada.
[2]Corresponding author (e-mail: awolfe@ualberta.ca).
[3]Present address: Centre de Estudis Avançats de Blanes (CEAB–CSIC), Limnology Group, C/ Acces Cala St Francesc, 14, Blanes, 17300 Girona, Spain.

 doi:10.1139/F08-074 © 2008 NRC Canada

(Fig. 1; Golder Associates Inc. 2002; NPRI 2006) shows that current SO_2 emissions are comparable with those produced early in the commercial development of the oil sands following initial commercial-scale mine development by Great Canadian Oil Sands (now Suncor Energy, Inc.) in 1967. Commencement of production by Syncrude Canada, Ltd. in 1978 effectively doubled total SO_2 emissions. Installation of flue gas desulphurisation technology by Suncor Energy, Ltd. in 1996 resulted in a reduction in SO_2 emissions to current levels. NO_x emissions have increased gradually since the inception of commercial-scale bitumen extraction and have risen dramatically since electrically operated mining equipment has been replaced with diesel-fueled equipment. Because emissions from the mobile mining fleet are not reported in the NPRI, NO_x emissions reported by the NPRI are far lower than actual NO_x emissions. The acidification potential of these emissions, sustained near current levels for more than 40 years, is undeniable. Industry estimates further suggest that an area of 13 000 km^2 receives in excess of 0.17 kequiv. $H^+ \cdot ha^{-1} \cdot year^{-1}$ (Deer Creek Energy Ltd. 2006), although efforts to validate these estimates have only recently been initiated. As well, local meteorological data may not provide an accurate indication of pollutant transport, as local wind patterns reflect the channelling influence of the Clearwater and Athabasca river valleys (AMEC Earth and Environmental 2007). The actual extent of the area affected by acid deposition from the Oil Sands thus remains an open question. Nonetheless, estimates of acid deposition conducted by industry exceed critical loads derived from the steady state water chemistry model (Henriksen and Brakke 1988) for a number of lakes in northeastern Alberta (RAMP 2005*a*). These critical load estimates were calculated for an alkalinity threshold of 3.75 $mg \cdot L^{-1}$ $CaCO_3$, derived from regressions between pH and alkalinity, and a threshold lake water pH of 6. As well, assessments of an extensive suite of Alberta lakes place those located in northeastern Alberta at the greatest risk of acidification (Hesslein 1979; Erickson 1987; Saffran and Trew 1996). While preliminary investigations suggest that alkalinity in a small number of lakes in the immediate vicinity of Oil Sands operations is declining (R. Hazewinkel, unpublished data), there is thus far no indication that these effects are geographically widespread or related to acid deposition. However, sustained monitoring of the most acid-sensitive lakes in the region has only been conducted since 1999 (RAMP 2005*a*), with sporadic prior measurements. In this limited historical context, it is impossible to conduct suitable trend analyses to determine the onset and extent of acidification. Because they are based on current alkalinity measurements, critical load estimates rely on the unverified assumption that surface-water alkalinities have remained constant.

An extensive body of research from eastern North America and northern Europe has established strong linkages among acid deposition, lake acidification, and reorganization of lake ecosystems (Schindler 1988; Battarbee and Renberg 1990; Charles and Smol 1990). Paleolimnology has played a central role in these studies, permitting establishment of baseline lake water pH and the range of natural (before heavy industrial) variability. In the absence of suitable long-term monitoring records, paleolimnology offers a robust means of evaluating the effects of acid deposition on aquatic ecosystems (Smol 2002). In these investigations, down-core sedimentary diatom assemblages, coupled to training sets that explicitly relate modern water chemistry to extant communities, have been proven to be invaluable techniques for inferring pH trends (Smol et al. 1986; Birks et al. 1990; Battarbee et al. 2001). In the present paper, we examine recent (after ~1750 AD) trends in diatom assemblages and lake water pH from eight northeastern Alberta lakes.

Fig. 1. Inventory of SO_2 and NO_x (as NO_2) emissions from industrial sources in the Fort McMurray area. Emissions from Golder Associates Inc. (2002) are calculated from available predictions relative to historic levels of production. Emissions from the National Pollutant Release Inventory (NPRI 2006) are reported by industry under the applicable regulatory agreements. Emissions reported to the NPRI do not include NO_x emissions generated by the mobile mining fleet. As these account for the majority of NO_x emissions, the NPRI NO_x figures can be understood to under-represent actual NO_x emissions.

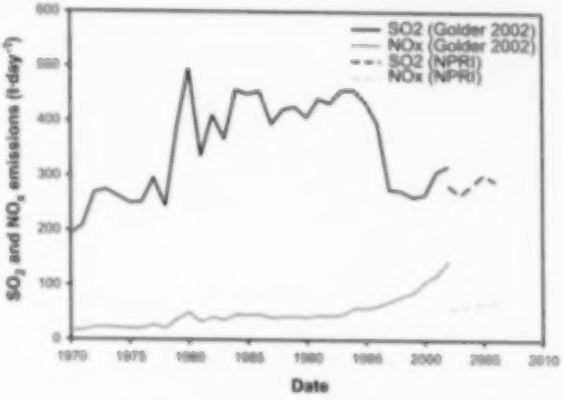

Materials and methods

Study sites

The majority of Alberta lakes are underlain by calcareous tills that confer carbonate buffering of atmospherically derived acids. However, surveys in northeastern Alberta have identified a number of lakes of moderate to high acid sensitivity (i.e., having alkalinities <20 and <10 $mg \cdot L^{-1}$ $CaCO_3$, respectively) (Hesslein 1979; Erickson 1987; Saffran and Trew 1996). These criteria, adapted from those established for the early characterization of acid-sensitive lakes in eastern Canada (Altschuller and McBean 1979; NRCC 1981), are based on the position of the lake relative to the point of inflection of the sigmoid pH–alkalinity curve (e.g., Camarero and Catalan 1998). The lakes identified in these surveys are located in four distinct physiographic regions (Fig. 2), but share certain geological and hydrological characteristics that confer greater acid sensitivity. The Birch and Stony uplands are underlain by dark grey and silty pyritic Cretaceous shales draped by fine loamy to clayey ground moraine. The Caribou Mountains are underlain by non-calcareous Cretaceous shales and coarse glacial drift and, like the Birch and Stony uplands, contain extensive peatlands interspersed with dense mixed wood forest. The northeastern corner of the province is underlain by the Archaean

© 2008 NRC Canada

crystalline lithologies of the Canadian Shield, with open canopy mixed wood forest and lowland peatlands. The Muskeg uplands are characterized by late Cretaceous non-calcareous shales, sandstones, and siltstones and by a vast expanse of muskeg with sparse open-canopy forest (Turchenek and Lindsay 1982). The heightened acid sensitivity of all of these regions is due in part to low concentrations of base cations in groundwater (Ozoray et al. 1980), their relatively high position within the watershed, altered groundwater flow in the presence of discontinuous permafrost (Ozoray et al. 1980), and the influence of peatlands (Vitt et al. 1996).

The names and locations of the eight study lakes are presented in Table 1. Site selection reflects the regional distribution of acid-sensitive lakes along a 550 km transect extending north and south from the acidifying emission source (Fig. 2). With the exception of Touchwood Lake and S1, these lakes are moderately (<20 mg·L^{-1} $CaCO_3$) to highly (<10 mg·L^{-1} $CaCO_3$) acid sensitive (Table 1). Their alkalinities fall within the 10th percentile of lakes contained within a larger regional data set (mean alkalinity 120 mg·L^{-1} $CaCO_3$, median alkalinity 100 mg·L^{-1} $CaCO_3$, n = 450), indicating that they are more likely to be affected by acid deposition. Whereas a number of the more acid-sensitive lakes are located east of the emission sources, these are predominantly thermokarst lakes with maximum depths of approximately 1.5 m and were thought to be unsuited to high-resolution paleoecological study because of the possibility of sediment resuspension. The majority of the study lakes are moderately productive. Two of the study lakes (NE-4 and BM-1) are eutrophic (total phosphorus (TP) > 35 μg·L^{-1}) and produce cyanobacterial blooms, whereas only one (S-1) is oligotrophic (TP < 10 μg·L^{-1}). The potential for substantial internal P loading likely exists throughout the region (Burley et al. 2001) and is one of the causes for their relatively elevated TP concentrations. With the exception of Touchwood Lake, access to the lakes is limited by their distance from roads and populated areas and by peatlands, which are impassable during the ice-free season. Touchwood Lake, the southern-most site, is within the Lakeland Provincial Recreation area and is protected from intense catchment disturbances. Human impacts within the catchments of all of the lakes are therefore minimal. Namur Lake (BM-2), the largest lake investigated, supports a fly-in fishing lodge and a modest winter fishery. There is also a small subsistence fishery on Legend Lake (BM-1). Touchwood Lake is subject to intense angling pressure and has experienced several game-fish collapses over the last century.

Fig. 2. Locations of the study lakes in northeastern Alberta, Canada.

Sediment coring and chronology

Sediment cores were collected in 2003 and 2004 from the central region of each lake with a modified Kajak–Brinkhurst gravity corer (Glew 1989). The cores were extruded (Glew 1988) immediately upon retrieval and sectioned in 0.25 cm increments from the surface to 10 cm, 0.50 cm increments from 10 to 20 cm, and 1.00 cm increments thereafter, with the exception of the cores from Touchwood Lake and SM-7, which were sectioned in 0.50 cm increments from the surface to 20 cm and in 1.00 cm increments thereafter. Samples were frozen upon return from the field and freeze-dried for further analysis and archiving. Core chronologies were established from sediment ^{210}Pb activities measured by α-spectrometry, to which the constant rate of supply (CRS) model was applied (Appleby and Oldfield 1978). Sediment deposition rates varied substantially among the study lakes, with the unsupported ^{210}Pb inventory contained in the upper 10 cm (NE-4) to 30 cm

© 2008 NRC Canada

Table 1. Selected limnological characteristics of the study lakes, including estimated acid loads and critical loads.

Lake code (name)	Latitude (°N)	Longitude (°W)	Elevation (m asl)	Area (ha)	Depth (m)	TN (mg·L^{-1})	TP (mg·L^{-1})	DOC (mg·L^{-1})	pH	Alkalinity (mg·L^{-1} as $CaCO_3$)	PAI (keq·m^{-2}·a^{-1}·year^{-1})*	Critical load (keq·m^{-2}·a^{-1}·year^{-1})†
BM-1 (Legend)	57.41	112.93	789	1685	9.1	523.44	37.58	9.21	6.82	7.24	0.135	0.099
BM-2 (Namur)	57.44	112.62	724	4322	31.3	351.83	20.47	8.91	7.22	19.19	0.126	0.226
BM-9 (Dusan)	57.71	112.39	747	348	10.7	576.62	17.95	14.15	6.82	7.16	0.117	0.065
S-2 (Fletcher)	59.12	110.82	287	103	12.9	785.20	13.43	20.02	7.06	18.21	NA	0.341
S-1 (Wenkes)	59.72	110.01	340	340	27.4	507.26	5.22	11.45	7.22	21.36	NA	0.114
NE-4	57.96	110.38	356	116	1.2	1632.50	41.97	15.40	6.85	8.47	0.104	0.144
SM-7	55.68	111.83	670	148	3.0	1237.71	31.50	16.62	6.63	5.40	0.117	0.057
Touchwood	54.83	111.40	632	2900	40.0	767.14	18.40	11.17	8.31	143.33	0.131	NA

Note: Metres above sea level, m asl; total nitrogen, TN; total phosphorus, TP; dissolved organic carbon, DOC.
*Potential acid input (PAI) from Alberta Sands Energy Inc. (2005).
†RAMP 2005*b*.

(Touchwood) of cores. However, there are no substantial reversals in the unsupported ^{210}Pb inventories, suggesting that sedimentation rates have remained relatively constant (Fig. 3). Where appropriate, basal CRS sediment accumulation rates have been extrapolated to yield approximate ages for sediments below unsupported ^{210}Pb levels.

Diatom analysis

For diatom analysis, 100–200 mg of freeze-dried sediment was heated to 70 °C in 30% H_2O_2, then centrifuged (1000*g*), rinsed, and diluted to 10 mL. 200 µL aliquots were then diluted in deionized water (to 5–10 mL) and mounted on cover slips, air dried, and mounted permanently onto slides with Naphrax medium. Diatoms were enumerated from full transects at 1000× under oil immersion. A minimum of 400 valves were identified and counted per sample, using standard freshwater floras (Krammer and Lange-Bertalot 1986–1991), as well as regional iconographs addressing diatoms from low-alkalinity (Camburn and Charles 2000; Fallu et al. 2000) and northern Alberta (Moser et al. 2004) lakes. Results are presented as relative frequencies of taxa that comprise >5% of the diatom sum in any one assemblage (Fig. 4).

Numerical methods

Diatom stratigraphic data were synthesized using principal components analysis (PCA), a linear, indirect ordination method. Exploratory ordination using detrended correspondence analysis revealed short gradient lengths in the diatom data from each lake (i.e., <1.5 standard deviation units), thus justifying the choice of linear approaches such as PCA in reducing the dimensionality of the data (ter Braak and Prentice 1988). For each lake, PCA was conducted on relative frequencies of all diatom taxa >1% in any one sample, using CANOCO ver. 4.5 (ter Braak and Šmilauer 2002). Comparisons of results using untransformed, square-root-transformed, and log(1 + *x*)-transformed diatom relative frequencies were undertaken. Analyses using untransformed data produced unacceptably high λ_1/λ_2 ratios, indicating a disproportionate influence of dominant taxa. Log-transformation best satisfied the assumption of normality based on analysis of normal probability plots, and consistently produced the highest eigenvalues on the first two PCA axes. For this reason, we report only PCA results using this strategy. Sample scores from the first principal component are plotted stratigraphically to represent variation along the dominant mode of variability among downcore diatom assemblages (Fig. 5).

Paleolimnological inferences of lake water pH were obtained by applying a 45-lake diatom–pH training set based on sites from within the Regional Aquatics Monitoring Program (RAMP 2005*a*, 2005*b*) sampling network (Pla and Curtis 2006), to which Touchwood Lake was added (Appendix A, Table A1). With the exception of the Caribou Mountain sites, which are located in the uplands west of Lake Athabasca, the sites included in the training set are located within the area depicted in Fig. 2. First axis detrended correspondence analysis (λ_1 = 0.459) scores of samples in the training set are strongly correlated with pH (r^2 = 0.76), indicating that pH is an important determinant of diatom community composition (Pla et al. 2006). The inference

© 2008 NRC Canada

Fig. 3. Sediment ^{210}Pb activities and constant rate of supply (CRS) age models for the study lakes.

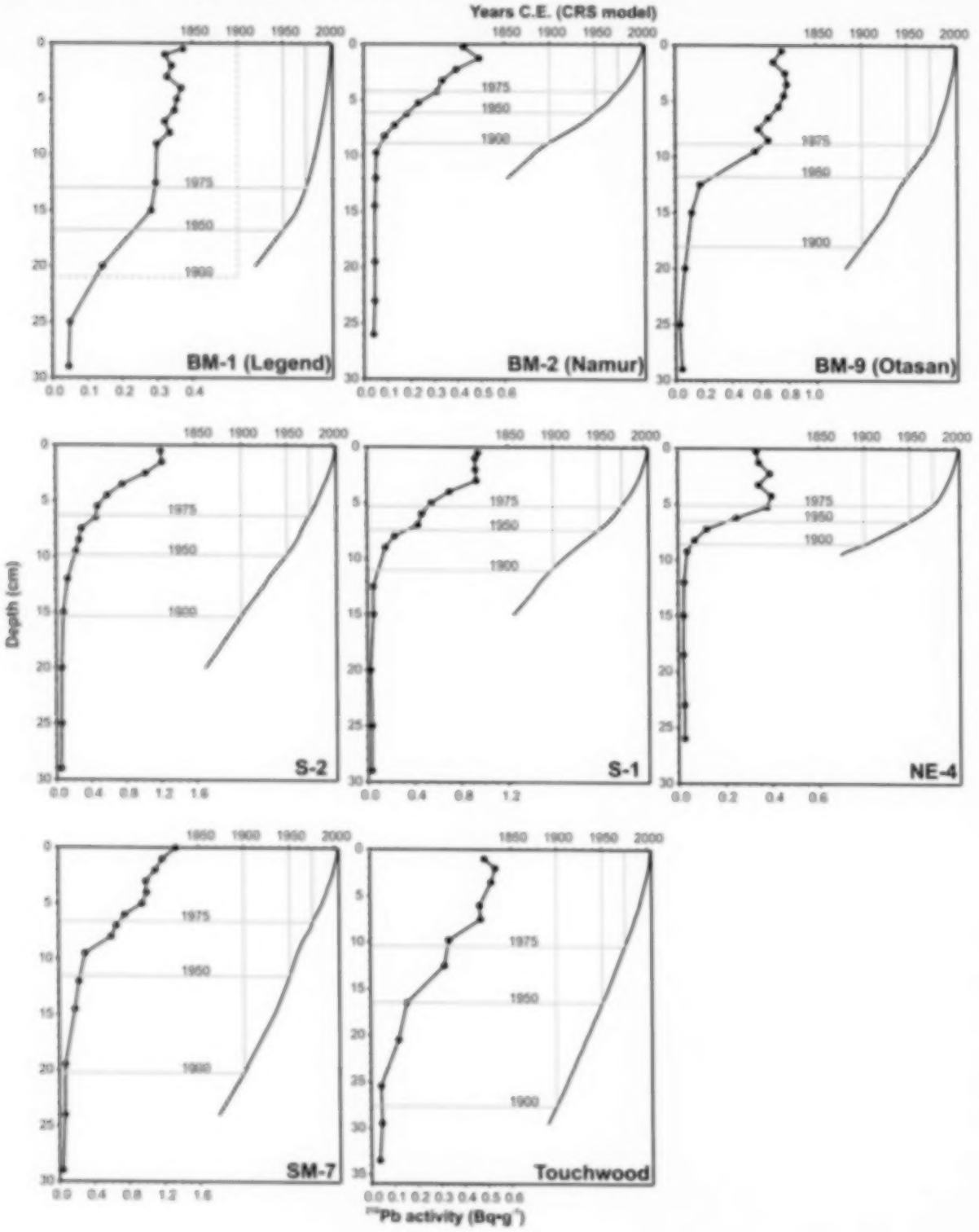

© 2008 NRC Canada

Fig. 4. Diatom stratigraphies from the study lakes. Only dominant taxa (>5% in any one sample) are shown. Grey horizontal lines are the years 1950 and 1900 according to constant rate of supply (CRS) ^{210}Pb age–depth models. Photomicrographs and taxonomic authorities are presented by Hazewinkel (2006).

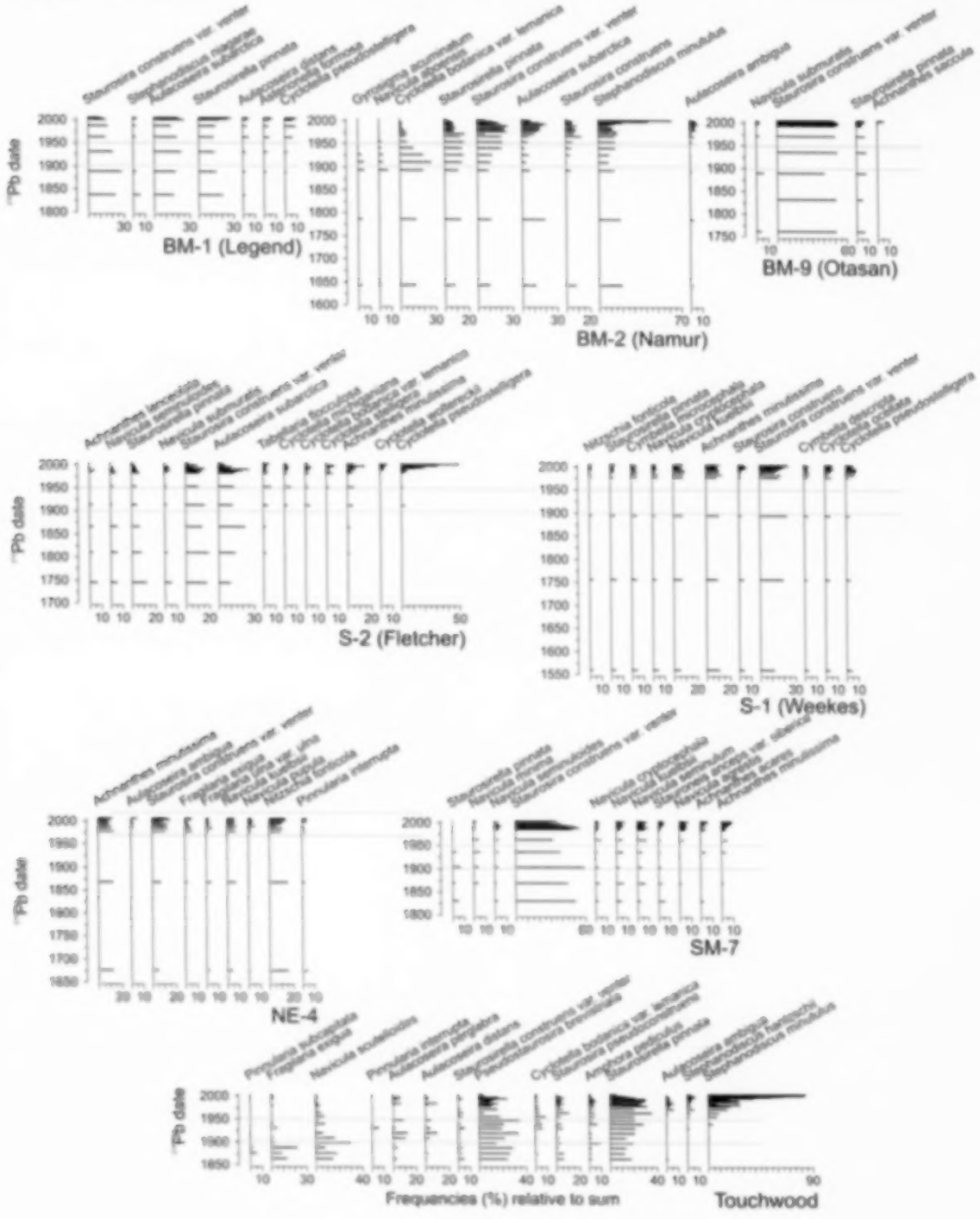

© 2008 NRC Canada

Fig. 5. Stratigraphies of diatom-inferred pH (DIpH) and of the first axis of principal component analysis (PCA) obtained from assemblage relative frequencies, both expressed against time. Dates in grey font are extrapolated. Horizontal bars express the standard error of pH estimates. Measured lake water pH and standard deviations are shown above each DIpH reconstruction, with numbers of measurements indicated.

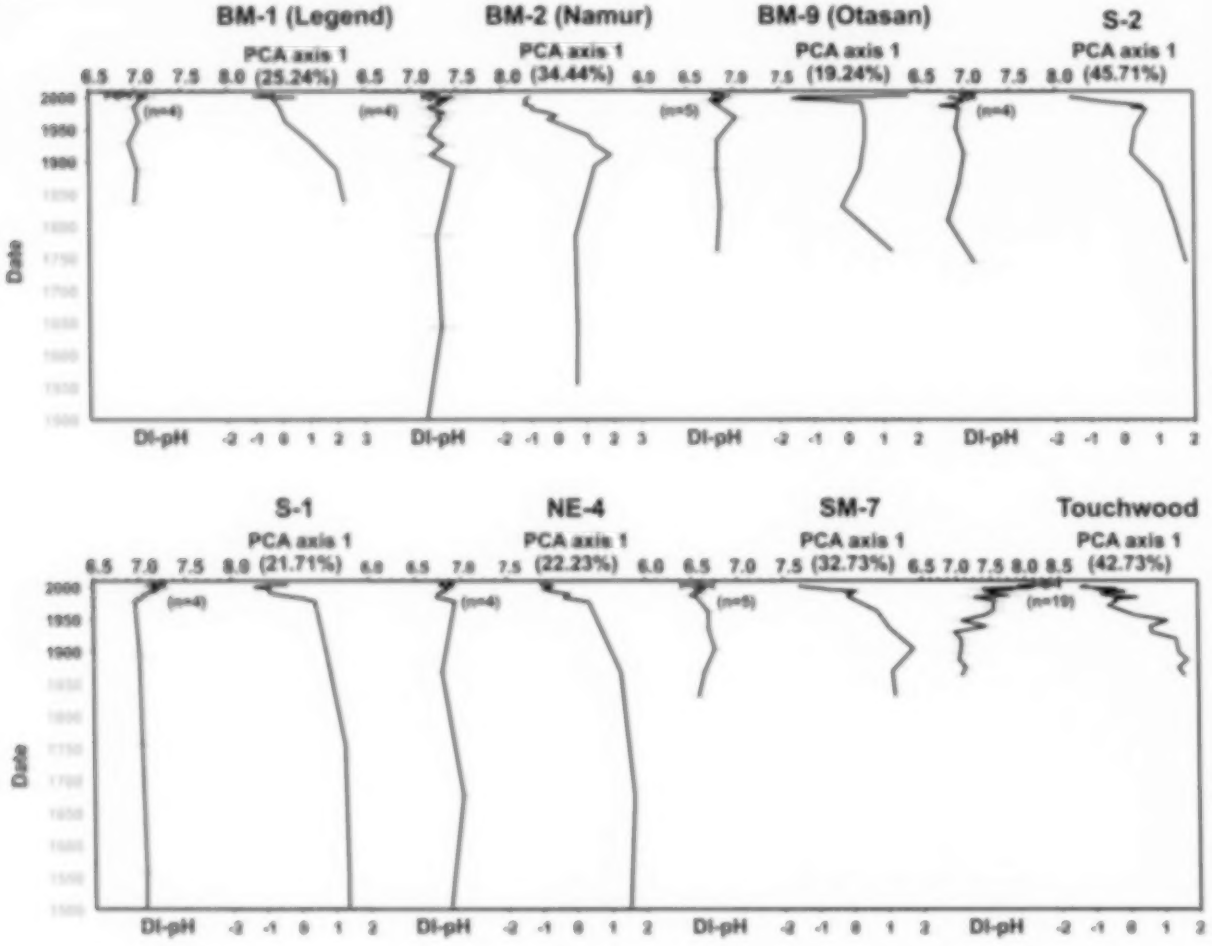

model is based on weighted-averaging partial-least-squares (WA-PLS) regression and calibration, with two components retained (ter Braak and Juggins 1993). The WA-PLS model minimized bootstrap root mean squared error of prediction ($RMSEP_{boot}$ = 0.38 pH units) and bias and maximized the regression coefficient of bootstrap pH estimates versus observed pH (r^2 = 0.84; Fig. 6*a*). Performance of the inference model is also assessed by comparison of surface sediment diatom-inferred pH (DIpH) and measurements from the study lakes (Fig. 5) and by favourable comparisons of DIpH profiles with those generated using other inference models (Camburn and Charles 2000; Philibert et al. 2003). The plot of residuals shows a slight but systematic bias in the model predictions, as indicated by a maximum bias of 0.65 pH units (Fig. 6*b*). This indicates that the model tends to overpredict the pH of acid lakes and underpredict in alkaline lakes by a maximum of 0.65 units according to the bootstrap validation. The approximate range for optimal prediction is between pH 6.0 and 7.5; presently, only Touchwood Lake lies outside of this range.

Results

Diatom stratigraphy

A total of 280 diatom taxa were identified during the course of the study (Hazewinkel 2006). Diatom assemblage composition varies substantially among lakes (Fig. 4), reflecting a broad range of limnological characteristics. Prior to ~1950, diatoms in S-2 (Fletcher) and BM-1 (Legend) were dominated by small colonial Fragilariaceae (*Staurosirella pinnata* and *Staurosira construens* var. *venter*) and *Aulacoseira subarctica*. BM-9 (Otasan) and SM-7 were also dominated by small Fragilariaceae, to the extent that they frequently comprise >50% of assemblages. Sediments from NE-4 and S-1 (Weekes) were not dominated by any one species, but contained combinations involving *Achnanthes min-*

© 2008 NRC Canada

Fig. 6. Performance of the bootstrapped weighted-averaging partial-least-squares (WA-PLS) diatom–pH training set (two components, 45 lakes). Diatom-inferred versus measured lake water pH confirm the predictive power of the model (*a*), while the plot of residuals indicates slight biases at the high and low end of the pH gradient (*b*). $RMSEP_{boot}$, bootstrap root mean squared error of prediction.

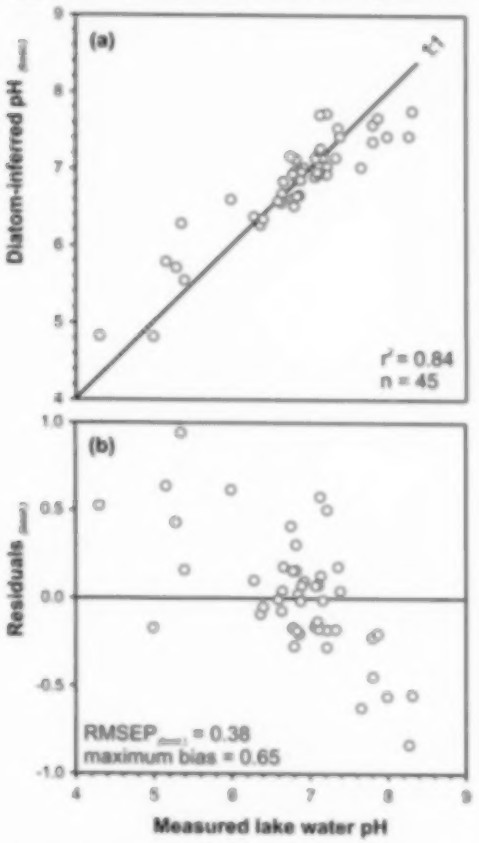

utissima, *Navicula kuelbsii*, *Nitzschia fonticola*, and *Staurosira construens* var. *venter*, in addition to *Cyclotella ocellata* and *Cymbella descripta* in Lake S-1.

Of the above six lakes, the most pronounced stratigraphic change occurred in S-2 (Fletcher), with an abrupt increase in *Cyclotella pseudostelligera* from trace abundances before ~1985 to 50% in surface sediments. Other taxa, notably *Staurosira construens* var. *venter* and *Aulacoseira subarctica*, show concomitant declines. In BM-1 (Legend), changes are more subtle and expressed over a slightly longer period than in S-2 (Fletcher). *Asterionella formosa* and *Cyclotella pseudostelligera* show modest increases accompanied by loss of *Staurosira construens* var. *venter* beginning ~1950. The remaining three lakes (BM-9, S-1, and NE-4) show less stratigraphic change.

Changes in the diatom stratigraphies of BM-2 (Namur) and Touchwood Lake predate those observed in other study lakes by about 50 years. Prior to ~1900, diatom assemblages in BM-2 (Namur) were typical of a deep, moderately productive alkaline system, being composed of more or less equivalent abundances of small Fragilariaceae (*Staurosirella pinnata* and *Staurosira construens* var. *venter*), *Cyclotella bodanica* var. *lemanica*, *Aulacoseira subarctica*, and *Stephanodiscus minutulus*. Touchwood Lake was dominated by Fragilariaceae (*Staurosira exiguiformis* and *Pseudostaurosira brevistriata*) and *Navicula scutelloides*. Progressive changes in these two lakes began around 1900. A decline of *Cyclotella bodanica* var. *lemanica* in BM-2 (Namur) was concomitant to increases of *Staurosira construens* var. *venter* and *Aulacoseira subarctica*, followed by sudden declines ~1990, as the abundance of *Stephanodiscus minutulus* rose markedly from 15% to 62% (Fig. 4). The stratigraphic changes in Touchwood Lake are similar to those in BM-2 (Namur). *Staurosira exiguiformis* and *Navicula scutelloides* declined from 20%–30% around 1900 to near-absence. *Pseudostaurosira brevistriata* and *Staurosirella pinnata* remain abundant (20%–30%) until ~1990, after which they decline to less than 6% in surface sediments. These declines occur at the expense of *Stephanodiscus minutulus*, which first appeared ~1930 prior to ascending in abundance to 84% in surface sediments (Fig. 4).

With the sole exception of BM-9 (Otasan), all of the study lakes show coherent, directional shifts in the structure of diatom assemblages as indicated by the first axis PCA sample scores (Fig. 5). These shifts are asynchronous and reflect varied ecological responses to indeterminate environmental factors. The magnitude of these shifts is indicated by the percentage of cumulative variance explained by the axis. Although the first PCA axis in NE-4 and S-1 (Weekes) is short, the directionality of change suggests a coherent community shift. Changes along the first PCA axis are greater among the remaining lakes (BM-1, BM-2, S-2, SM-7, and Touchwood) as indicated by the longer gradient lengths.

Lake water pH reconstructions

Surface-sediment DIpH values lie within one standard deviation of the measured pH values of BM-9 (Otasan), NE-4, SM-7, and Touchwood lakes (Fig. 5). The diatom model underpredicts mean pH by 0.18 in S-2 (Fletcher) and 0.10 in S-1 (Weekes) and overpredicts observed pH by 0.23 in BM-1 (Legend) and 0.26 in BM-2 (Namur). Some discrepancy between inferred and measured pH may arise from a collection bias of the measured data, which were obtained late August through October and thus reflect late-season pH only.

There is no indication that any of the lakes is becoming acidified. Although inferred pH in BM-1 (Legend), S-2 (Fletcher), S-1 (Weekes), and SM-7 trend downward slightly, the values are within natural variability. DIpH from Touchwood Lake rose from 7 to >8 during the 20th century, concomitant with the rise of *Stephanodiscus minutulus*. Although BM-2 (Namur) experienced a similar increase of *Stephanodiscus minutulus*, DIpH values do not increase in this core. However, S-1 (Weekes) also produced a record of increasing DIpH. Concordance between DIpH values and sample scores on the primary axis of PCA provides an index of the importance of pH as a driver of diatom community structure (Wolfe 2002). DIpH and the PCA axis 1 trends track each other well in Touchwood and S-1 (Weekes) lakes, implying that pH is the dominant ecological gradient. In the case of BM-2 (Namur), SM-7, and S-2 (Fletcher), major proportions of the floristic variability captured by PCA

© 2008 NRC Canada

axis 1 are unrelated to pH. Given the mesotrophic to eutrophic character of several taxa that have increased in recent decades (e.g., *Stephanodiscus* spp.), it would appear that assemblage changes are more closely linked to increasing lake production rather than to acidification. In lakes lacking *Stephanodiscus*, such as L-109 (Fletcher) and L-25 (Legend), it is another centric planktonic genus, *Cyclotella*, which has increased. Several studies have associated increased planktonic diatom production with climate warming and prolonged ice-free seasons (Rühland et al. 2003; Smol et al. 2005).

Discussion

Diatom communities in the majority of the study lakes have undergone substantial and unidirectional changes during the past century. The magnitude of these changes is expressed by the strength of the first PCA axis, which varies from 19.2% in BM-9 (Otasan) to 45.7% in S-2 (Fletcher). Floristic shifts are most pronounced in S-2 (Fletcher), BM-2 (Namur), and Touchwood lakes, all of which have moderate to high alkalinities. Conversely, BM-9 (Otasan), NE-4, and S-1 have undergone relatively little change, despite having more acid-sensitive water chemistries. Furthermore, there appears to be no relationship between lake location and the magnitude of floristic change. Although the diatoms from BM-2 (Namur) undergo a dramatic shift beginning ~1900, the flora from BM-9 (Otasan), 30 km away, remains relatively unchanged, despite having a greater acid sensitivity. A similar contrast exists between S-2 (Fletcher), which has changed substantially over the past 20 years, and NE-4, which has not. Perhaps the greatest similarity among the lakes, therefore, is the absence of an acidification signal. Indeed, the scarcity of acidophilic and dystrophic genera (e.g., *Eunotia*, *Frustulia*, *Pinnularia*, and *Brachysira* spp.) throughout the study is noteworthy and surprising, especially given the frequently high dissolved organic carbon concentrations recorded. The paleolimnological evidence is entirely consistent with surface water chemistry data, which show no recent temporal trends in pH or alkalinity in the study lakes (Saffran and Trew 1996; RAMP 2005*a*, 2005*b*). The evident mismatch between the chronology of acidifying emissions associated with bitumen processing and inferred or measured pH change could reflect mediation of ecological response by catchment factors. Acid buffering properties of catchment soils have been shown to delay a direct ecological response to acid deposition following the initial exceedence of the critical acid load (Davis 1987). Notwithstanding the apparent intransigence of surface water pH relative to current acid loads, the chronology of the stratigraphic changes, although somewhat variable between sites, is broadly consistent with increasing anthropogenic pressures in the region. Therefore, relationships to atmospheric emission from the Oil Sands may involve an indirect response to acid deposition. We explore several explanations for the observations, none of which are mutually exclusive.

Climate change

The northern Canadian prairies and the boreal transition zone have warmed by 2–4 °C over the past century, substantially more than the global average, and precipitation has decreased by as much as 20% (Schindler and Donahue 2006). Warming has profound, but increasingly understood, effects on a range of physical (Jankowski et al. 2006), biogeochemical (Schindler et al. 1996), and biological (Smol et al. 2005) limnological processes. Warming induces earlier onset and increasing stability of lake thermal stratification (DeStasio et al. 1996). This favours planktonic algae that follow the thermocline, including planktonic diatoms such as *Stephanodiscus minutulus* (Bradbury 1988). Longer ice-free seasons provide longer growing seasons for most algae, enhancing overall lake primary production. Higher peak epilimnetic temperatures, usually coupled to internal or external nutrient loading, produce cyanobacterial blooms that in turn augment oxygen demand. Greater hypolimnetic residence times, which accompany drought, enhance the importance of in-lake biogeochemical processes, allowing more time for both the removal of SO_4^{2-} by dissimilatory microbial reduction, as well as the mineralization of calcium and its subsequent diffusion from sediments (Schindler et al. 1986). The extent and duration of hypolimnetic and surface-sediment anoxia, which is ultimately under climatic control, thus controls geochemical processes in dimictic or polymictic lakes. Furthermore, factors such as lake morphometry and groundwater inflow may interact to produce asynchronous and variable responses between even nearby lakes. For example, Touchwood Lake, which is the deepest and only lake in the study known to stratify strongly every summer, produces the greatest diatom-inferred alkalinization trend. The diatom that marks this trend (*Stephanodiscus minutulus*) is also strongly associated with nutrient enrichment (Bradbury 1988; Reavie and Smol 2001). Although alkalinity may be generated by altered dissolved inorganic carbon dynamics due to increased overall lake primary production, we also infer that P concentrations in lakes now dominated by *Stephanodiscus* have increased in recent decades. Similar observations have been made from a lake to the northeast of Wood Buffalo National Park, where the changes have been ascribed directly to the effects of 20th century climate warming (Moser et al. 2002). From our perspective nearer to the Oil Sands, the importance of in-lake processes resides in the fact that they potentially operate in intimate association with atmospheric deposition of nitrogen and sulphur.

In-lake alkalinity and internal P loading

The stimulation of in-lake microbial alkalinity pumps in response to modest inputs of strong acid anions has been well established (Schindler 1985; Rudd et al. 1990). Peatlands may also contribute to biological neutralization of SO_4^{2-} and concomitant assimilation of NO_3^- (Bayley et al. 1987), a relevant factor for most of the catchments considered here. Shallow and moderately productive Alberta lakes also have characteristics conducive to strong internal P loading. One accepted model for shallow lakes (Caraco et al. 1992; Søndergaard et al. 2003) is that Fe^{3+} is reductively scavenged preferentially by SO_4^{2-}, curtailing the accumulation in sediments of iron phosphates such as vivianite ($Fe(PO_4)_2$) and strengite ($FePO_4$). When the supply of free Fe^{3+} is limited, sediments diffuse PO_4^{3-} to the water column where it is rapidly exploited, particularly if other key nutrients (N and, for diatoms, Si) are not limiting. If the

© 2008 NRC Canada

importance of these processes is confirmed within northeastern Alberta, increased industrial SO_2 deposition may be inducing transients of increased P loading that will endure until sediment and groundwater alkalinities are overwhelmed.

Unsuspected roles for acid deposition?

The possibility that atmospheric deposition, coupled to climate change, are inducing the observed changes in Alberta lakes remains to be systematically investigated from a geochemical standpoint. However, such an interpretation conforms to the results of the present study. N deposition is already a known vector for increased peatland production in Alberta (Vitt et al. 2003), at levels ($\sim$3 kg N·ha^{-1}·year^{-1}) that have been shown to elicit diatom responses in other areas and in the absence of attendant acidification (Wolfe et al. 2003; Saros et al. 2005). For the southern portion of our study area, N deposition likely occurs at much higher rates, given estimates of 15.8 and 22.1 kg N·ha^{-1}·year^{-1} for Elk Island and Grasslands National Parks, respectively (Köchy and Wilson 2001). The relevance of atmospheric N subsidies is the potential alleviation of N limitation at times when supply of P is enhanced by internal microbial generation associated with accelerated SO_4^{2-} cycling and insufficient reducible Fe. These processes raise algal production while mitigating — for now — the undeniable acidification potential of industrial emissions from the Oil Sands. Lakes that lack evidence of enhanced internal P loading (i.e., absence of *Stephanodiscus* increases) likely contain sufficient Fe to effectively bind PO_4^{3-}, but nonetheless experience ecological shifts as climate change favours genera such as *Cyclotella*. RAMP data from two of the lakes in the Birch Mountains, BM-1 (Legend) and BM-2 (Namur), both of which have experienced marked recent changes in diatom community structure, have high surface-water SO_4^{2-} values (3.41 and 7.62 μg·L^{-1}, respectively) yet the lowest N:P ratios of any of the lakes in this study. The mechanisms linking the biogeochemical cycles of S, P, and Fe need to be evaluated systematically in the course of future studies, with particular attention to the sensitivity of biogeochemical processes towards limnological parameters linked to climate, namely stratification, water residence times, hypolimnetic anoxia, and primary production.

Although the results of this study are somewhat surprising, they signify neither that northeastern Alberta is unimpacted by atmospheric pollution nor that N and S emissions from the Oil Sands are environmentally sustainable. Rather, the results highlight how incomplete the current knowledge base is and how complex the interactive biogeochemical processes involved are likely to be. The observation that lakes in the study area have not acidified does not imply that their acid sensitivities have been systematically overstated, but rather that the potency of in-lake alkalinization and internal nutrient generation have not been adequately assessed. We emphasize that the results presented here do not apply to lakes more immediately proximal (i.e., <50 km) to the expanding Oil Sands footprint. An additional consideration is that the airshed for dispersion of pollution plumes may be grossly underestimated, resulting in relatively low SO_2 and NO_x fluxes to the study lakes. Additional investigations, particularly across the downwind Canadian Shield terrains of northern Saskatchewan, Manitoba, and the southern Northwest Territories, will be necessary to investigate this possibility. Paleolimnology, coupled to ancillary techniques such as dendrochemistry (Savard et al. 2002), should be combined to disentangle the effects of climate change from those of atmospheric deposition in this vast region. Finally, even in the absence of acidification trends, the majority of investigated lakes are nonetheless on trajectories of rapid ecological change. The character of these changes is not incompatible with industrial atmospheric inputs, because lake biogeochemical processes may buffer acidity while augmenting nutrient (P and N) availability, within the overarching context of a warming climate.

Acknowledgements

Research was funded by the Cumulative Environmental Management Association (CEMA) and the Natural Sciences and Engineering Research Council of Canada (NSERC). Cores were dated at Mycore Scientific Ltd., under the direction of R.J. Cornett. We thank W. Donahue, D. Froese, P. McEachern, and R. Vinebrooke for assistance at various stages of the study.

References

Albian Sands Energy Inc. 2005. Muskeg River Mine Expansion Project: summary of EIA and SEIA. Prepared for Shell Canada. Albian Sands Energy Inc., Fort McMurray, Alta.

Altschuller, A.P., and McBean, G.A. 1979. The LRTAP problem in North America: a preliminary overview. A report to the United States – Canada research consultation group on the long-range transport of air pollutants. USA State Department, Washington, D.C., and Canada Department of External Affairs, Ottawa, Ont.

AMEC Earth and Environmental. 2007. Air quality assessment of the Algar SAGD project. Prepared for Great Divide Oil Corporation. AMEC Earth and Environmental, Calgary, Alta.

Appleby, P.G., and Oldfield, F. 1978. The calculation of lead-210 dates assuming a constant rate of supply of unsupported ^{210}Pb to the sediment. CATENA, **5**: 1–8. doi:10.1016/S0341-8162(78)80002-2.

Battarbee, R.W., and Renberg, I. 1990. The surface water acidification project (SWAP) palaeolimnology programme. Philos. Trans. R. Soc. Lond. Ser. B Biol. Sci. **327**: 227–232. doi:10.1098/rstb.1990.0056.

Battarbee, R.W., Jones, V.J., Flower, R.J., Cameron, N.G., Bennion, H.B., Carvalho, L., and Juggins, S. 2001. Diatoms. *In* Tracking environmental change using lake sediments. Vol. 3. Terrestrial, algal, and siliceous indicators. *Edited by* J.P. Smol and H.J.B. Birks. Kluwer, Dordrecht, The Netherlands. pp. 155–202.

Bayley, S.E., Vitt, D.H., Newbury, R.W., Beatty, K.G., Behr, R., and Miller, C. 1987. Experimental acidification of a *Sphagnum*-dominated peatland: first year results. Can. J. Fish. Aquat. Sci. **44**(Suppl. 1): 194–205. doi:10.1139/f87-295.

Birks, H.J.B., Line, J.M., Juggins, S., Stevenson, A.C., and ter Braak, C.J.F. 1990. Diatoms and pH reconstruction. Philos. Trans. R. Soc. Lond. Ser. B Biol. Sci. **327**: 263–278. doi:10.1098/rstb.1990.0062.

Bradbury, J.P. 1988. A climate-limnologic model of diatom succession for paleolimnological interpretation of varved sediments at Elk Lake, Minnesota. J. Paleolimnol. **1**: 115–131. doi:10.1007/BF00196068.

Burley, K.L., Prepas, E.E., and Chambers, P.A. 2001. Phosphorus release from sediments from hardwater eutrophic lakes: the ef-

© 2008 NRC Canada

fects of redox-sensitive and -insensitive chemical treatments. Freshw. Biol. **46**: 1061–1074. doi:10.1046/j.1365-2427.2001.00789.x.

Camarero, L., and Catalan, J. 1998. A simple model of regional acidification for high mountain lakes: application to the Pyrenean Lakes (north-east Spain). Water Res. **32**: 1126–1136. doi:10.1016/S0043-1354(97)00291-1.

Camburn, K.E., and Charles, D.F. 2000. Diatoms of low alkalinity lakes in the northeastern United States. The Academy of Natural Sciences of Philadelphia, Philadelphia, Penn. Spec. Publ. 18.

Caraco, N.F., Cole, J.J., and Likens, G.E. 1992. Sulfate control of phosphorus availability in lakes: a test and re-evaluation of Hasler and Einsele's model. Hydrobiologia, **253**: 275–280. doi:10.1007/BF00050748.

Charles, D.F., and Smol, J.P. 1990. The PIRLA II project: regional assessment of lake acidification trends. Verh. Int. Ver. Theor. Angew. Limnol. **24**: 474–480.

Davis, R.B. 1987. Paleolimnological diatom studies of acidification of lakes by acid rain: an application of quaternary science. Quaternary Science Reviews, **6**: 147–163.

Deer Creek Energy Ltd. 2006. Joslyn North Mine Project: integrated application to Alberta Environment and the Alberta Energy and Utilities Board. Prepared for Total E&P Canada Limited, Calgary. Available through the Alberta Government Library, Edmonton, Alta.

DeStasio, B.T., Hill, J.M., Kleinhans, N.P., Nibbelink, N.P., and Magnuson, J.J. 1996. Potential effects of global climate change on small north temperate lakes: physics, fish, and plankton. Limnol. Oceanogr. **41**: 1136–1149.

Erickson, P.K. 1987. An assessment of the potential sensitivity of Alberta lakes to acidic deposition. Water Quality Control Branch, Alberta Environment, Edmonton. Available through the Alberta Government Library, Edmonton, Alta.

Fallu, M.-A., Allaire, N., and Pienitz, R. 2000. Freshwater diatoms from northern Quebec and Labrador (Canada). J. Cramer, Berlin, Germany.

Glew, J.R. 1988. A portable extruding device for close interval sectioning of unconsolidated core samples. J. Paleolimnol. **1**: 235–239. doi:10.1007/BF00177769.

Glew, J.R. 1989. A new trigger mechanism for sediment samplers. J. Paleolimnol. **2**: 241–243. doi:10.1007/BF00195474.

Golder Associates Inc. 2002. Evaluation of historic and future acid deposition effects on soils in the Athabasca oil sands region (draft). Prepared for the NO_x-SO_x Management Working Group of the Cumulative Environmental Management Association (CEMA), Fort McMurray. Available through the Cumulative Environmental Management Association (CEMA), Fort McMurray, Alta.

Hazewinkel, R.R.O. 2006. A paleolimnological assessment of environmental change in eight northeastern Alberta lakes. M.Sc. thesis, Department of Earth and Atmospheric Sciences, University of Alberta, Edmonton, Alta.

Henriksen, A.J., and Brakke, D.F. 1988. Sulphate deposition to surface waters: estimating critical loads for Norway and the eastern United States. Environ. Sci. Technol. **22**: 8–14. doi:10.1021/es00166a001.

Hesslein, R.H. 1979. Lake acidification potential in the Alberta Oil Sands Environmental Research Program study area. Prepared for Alberta Oil Sands Environmental Research Program, Edmonton. Available through the Alberta Government Library, Edmonton, Alta.

Jankowski, T., Livingstone, D.M., Buhrer, H., Forster, R., and Niederhauser, P. 2006. Consequences of the 2003 European heat wave for lake temperature profiles, thermal stability, and hypolimnetic oxygen depletion: implications for a warmer world. Limnol. Oceanogr. **51**: 815–819.

Kichy, M., and Wilson, S.D. 2001. Nitrogen deposition and forest expansion in the northern Great Plains. J. Ecol. **89**: 807–817. doi:10.1046/j.0022-0477.2001.00600.x.

Krammer, K., and Lange-Bertalot, H. 1986–1991. Bacillariophyceae. *In* Susswasserflora Von Mitteleuropa 2/1-4. *Edited by* H. Ettl, H. Gerloff, H. Heynig, and D. Mollenhauer. Gustav Fischer, Stuttgart, Germany.

Moser, K.A., Smol, J.P., MacDonald, G.M., and Larsen, C.P.S. 2002. 19th century eutrophication of a remote boreal lake: a consequence of climate warming? J. Paleolimnol. **28**: 269–281. doi:10.1023/A:1021635024757.

Moser, K., Smol, J.P., and MacDonald, G.M. 2004. The ecology and distribution of diatoms in Wood Buffalo National Park, Northern Alberta and the Northwest Territories, Canada. The Academy of the Natural Sciences of Philadelphia, Philadelphia, Penn.

NPRI. 2006. National Pollutant Release Inventory, Environment Canada [online]. Available from www.ec.gc.ca/pdb/npri/npri_home_e.cfm [accessed 24 February 2008; updated 13 March 2008].

NRCC. 1981. Acidification in the Canadian aquatic environment: scientific criteria for assessing the effects of acidic deposition on aquatic ecosystems. National Research Council of Canada, Ottawa, Ont. Publ. 18475.

Ozoray, G., Hackbarth, D., and Lytviak, A.T. 1980. Hydrogeology of the Bitumount-Namur Lake area, Alberta. Available through the Alberta Government Library, Edmonton, Alta. Res. Coun. Alberta Earth Sci. Rep. 78-6.

Philibert, A., Prairie, Y.T., Campbell, I., and Laird, L. 2003. Effects of late Holocene wildfires on diatom assemblages in Christina Lake, Alberta, Canada. Can. J. For. Res. **33**: 2405–2415. doi:10.1139/x03-165.

Pla, S., and Curtis, C.J. 2006. Lake sediment core top sample analysis. Prepared for the Cumulative Environmental Management Association (CEMA) NO_x–SO_x Management Working Group. Available through the Cumulative Environmental Management Association (CEMA), Fort McMurray, Alta.

Pla, S., Curtis, C.J., and Simpson, G. 2006. Lake sediment core bottom sample analysis and assessment of diatom change. Prepared for the Cumulative Environmental Management Association (CEMA) NO_x–SO_x Management Working Group. Available through the Cumulative Environmental Management Association (CEMA), Fort McMurray, Alta.

Reavie, E.D., and Smol, J.P. 2001. Diatom–environmental relationships in 64 alkaline southwestern Ontario (Canada) lakes: a diatom-based model for water quality reconstructions. J. Paleolimnol. **25**: 25–42. doi:10.1023/A:1008123613298.

RAMP. 2005*a*. Regional Aquatics Monitoring Program (RAMP) 2004 technical report. Section 3: 2004 RAMP monitoring program. Prepared for the RAMP Steering Committee, Edmonton. Available through the Alberta Government Library, Edmonton, Alta. Also available from www.ramp-alberta.org/.

RAMP. 2005*b*. Regional Aquatics Monitoring Program (RAMP) 2004 technical report. Section 6: regional-level assessment of 2004 results. Prepared for the RAMP Steering Committee, Edmonton. Available through the Alberta Government Library, Edmonton, Alta. Also available from www.ramp-alberta.org/.

Rudd, J.W.M., Kelly, C.A., Schindler, D.W., and Turner, M.A. 1990. A comparison of the acidification efficiencies of nitric and sulphuric acids by two whole-lake addition experiments. Limnol. Oceanogr. **35**: 663–679.

Rühland, K., Priesnitz, A., and Smol, J.P. 2003. Paleolimnologi-

© 2008 NRC Canada

cal evidence from diatoms for recent environmental changes in 50 lakes across Canadian arctic treeline. Arct. Antarct. Alp. Res. **35**: 110–123. doi:10.1657/1523-0430(2003)035[0110:PEFDFR]2.0.CO;2.

Saffran, K.A., and Trew, D.O. 1996. Sensitivity of Alberta lakes to acidifying deposition: an update of sensitivity maps with emphasis on 109 northern lakes. Alberta Environmental Protection, Edmonton. Available through the Alberta Government Library, Edmonton, Alta.

Saros, J.E., Michel, T.J., Interlandi, S., and Wolfe, A.P. 2005. Resource requirements of *Asterionella formosa* and *Fragilaria crotonensis* in oligotrophic alpine lakes: implications for recent phytoplankton community reorganizations. Can. J. Fish. Aquat. Sci. **62**: 1681–1689. doi:10.1139/f05-077.

Savard, M.M., Bégin, C., and Parent, M. 2002. Are industrial SO_2 emissions reducing CO_2 uptake by the boreal forest? Geology, **30**: 403–406. doi:10.1130/0091-7613(2002)030<0403:AISERC>2.0.CO;2.

Schindler, D.W. 1985. The coupling of elemental cycles by organisms: evidence from whole-lake chemical perturbations. *In* Chemical processes in lakes. *Edited by* W. Stumm. Wiley, New York. pp. 225–250.

Schindler, D.W. 1988. Effects of acid rain on freshwater ecosystems. Science (Washington, D.C.), **239**: 149–157. doi:10.1126/science.239.4836.149. PMID:17732976.

Schindler, D.W., and Donahue, W.F. 2006. An impending water crisis in Canada's western prairie provinces. Proc. Natl. Acad. Sci. U.S.A. **103**: 7210–7216. doi:10.1073/pnas.0601568103. PMID:16606829.

Schindler, D.W., Turner, M.A., Stainton, M.P., and Linsey, G.A. 1986. Natural sources of acid neutralizing capacity in low alkalinity lakes of the Precambrian Shield. Science (Washington, D.C.), **232**: 844–847. doi:10.1126/science.232.4752.844. PMID:17755965.

Schindler, D.W., Curtis, P.J., Parker, B.R., and Stainton, M.P. 1996. Consequences of climate warming and lake acidification for UV-B penetration in North American boreal lakes. Nature (London), **379**: 705–708. doi:10.1038/379705a0.

Smol, J.P. 2002. Pollution of lakes and rivers: a paleoenvironmental perspective. Oxford University Press, New York.

Smol, J.P., Battarbee, R.W., Davis, R.B., and Merilainen, J. 1986. Diatoms and lake acidity: reconstructing pH from siliceous algal remains in lake sediments. W. Junk, Dordrecht, The Netherlands.

Smol, J.P., Wolfe, A.P., Birks, H.J.B., Douglas, M.S.V., Jones, V.J., Korhola, A., Pienitz, R., Rühland, K., Sorvari, S., Antoniades, D., Brooks, S.J., Fallu, M.-A., Hughes, M., Keatley, B.E., Laing, T.E., Michelutti, N., Nazarova, L., Nyman, M., Paterson, A.M., Perren, B.B., Quinlan, R., Rautio, M., Saulnier-Talbot, É., Siitonen, S., Solovieva, N., and Weckström, J. 2005. Climate-driven regime shifts in the biological communities of arctic lakes. Proc. Natl. Acad. Sci. U.S.A. **102**: 4397–4402. doi:10.1073/pnas.0500245102.

Søndergaard, M., Jensen, J.P., and Jeppesen, E. 2003. Role of sediment and internal loading of phosphorous in shallow lakes. Hydrobiologia, **506/509**: 135–145. doi:10.1023/B:HYDR.0000008611.12704.dd.

ter Braak, C.J.F., and Juggins, S. 1993. Weighted averaging partial least squares regression (WA-PLS): an improved method for reconstructing environmental variables from species assemblages. Hydrobiologia, **269/270**: 485–502. doi:10.1007/BF00028046.

ter Braak, C.J.F., and Prentice, I.C. 1988. A theory of gradient analysis. Adv. Ecol. Res. **18**: 271–317.

ter Braak, C.J.F., and Šmilauer, P. 2002. CANOCO: software for canonical community ordination (version 4.5). Microcomputer Power, Ithaca, N.Y.

Turchenek, L.W., and Lindsay, J.D. 1982. Soils inventory of the Alberta Oils Sands Environmental Research Program study area. Prepared for Alberta Oil Sands Environmental Research Program, Edmonton. Available through the Alberta Government Library, Edmonton, Alta.

Vitt, D.H., Halsey, L.A., Thormann, M.N., and Martin, T. 1996. Peatland inventory of Alberta. Phase I. Overview of peatland resources in the natural regions and subregions of the province. Prepared for the Alberta Peat Task Force, Sustainable Forest Management Network, Edmonton. Available through the Alberta Government Library, Edmonton, Alta.

Vitt, D.H., Weider, K., Halsey, L.A., and Turetsky, M. 2003. Response of *Sphagnum fuscum* to nitrogen deposition: a case study of ombrogenous peatlands in Alberta, Canada. Bryologist, **106**: 235–245. doi:10.1639/0007-2745(2003)106[0235:ROSFTN]2.0.CO;2.

Wolfe, A.P. 2002. Climate modulates the acidity of arctic lakes on millennial timescales. Geology, **30**: 215–218. doi:10.1130/0091-7613(2002)030<0215:CMTAOA>2.0.CO;2.

Wolfe, A.P., Van Gorp, A.C., and Baron, J.S. 2003. Recent ecological and biogeochemical changes in alpine lakes of Rocky Mountain National Park (Colorado, U.S.A.). Geobiology, **1**: 153–168. doi:10.1046/j.1472-4669.2003.00012.x.

Appendix A

Table A1 appears on the following pages.

© 2008 NRC Canada

Table A1. Selected limnological parameters for the 45 lakes used in developing the diatom–pH training set.

Region and lake code	Latitude (°N)	Longitude (°W)	Area (ha)	Depth (m)	TN ($mg \cdot L^{-1}$)	TP ($mg \cdot L^{-1}$)	DOC ($mg \cdot L^{-1}$)	SO_4 ($mg \cdot L^{-1}$)	Conductivity ($\mu S \cdot cm^{-1}$)	pH	TDS ($mg \cdot L^{-1}$)	Chlorophyll *a* ($\mu g \cdot L^{-1}$)	Alkalinity ($mg \cdot L^{-1}$ as $CaCO_3$)
Stony Mountains													
SM1	55.76	110.75	237.00	1.83	1.42	24.65	24.52	0.26	53.85	7.20	84.25	5.75	21.69
SM2	55.79	111.82	197.00	1.22	1.50	35.90	25.55	0.47	32.60	6.80	107.25	10.93	9.82
SM7	55.68	111.83	148.00	3.00	1.45	33.47	16.25	1.70	25.23	6.63	41.27	14.71	5.40
SM10	56.26	111.26	138.00	1.20	1.36	64.17	21.59	5.59	15.60	5.02	49.37	8.01	0.29
Birch Mountains													
BM1	57.41	112.93	1685.00	9.10	0.44	35.90	9.21	2.92	29.03	6.80	34.20	8.37	7.24
BM2	57.44	112.62	4322.00	31.30	0.31	21.57	8.35	7.39	63.20	7.20	36.57	7.44	19.19
BM3	57.65	112.62	91.00	2.70	1.54	91.53	20.05	8.27	59.07	7.06	72.20	24.60	14.47
BM4	57.69	112.74	431.00	1.30	2.15	157.20	20.93	9.69	54.37	6.82	86.40	32.55	10.39
BM5	57.76	112.60	261.00	1.40	2.19	106.10	21.94	13.69	59.00	6.58	81.00	10.16	6.48
BM6	57.86	112.97	130.00	1.90	1.09	99.97	28.32	1.09	19.97	5.29	68.40	4.26	1.07
BM7	58.06	112.28	65.00	1.10	1.81	55.20	16.71	0.45	18.17	4.31	42.20	23.69	0.00
BM8	57.77	112.40	120.00	1.80	1.74	229.03	25.30	9.46	53.97	6.88	77.67	39.25	10.06
BM9	57.71	112.39	348.00	10.70	0.62	17.53	13.43	1.06	25.47	6.81	39.83	11.24	7.16
BM10	57.31	112.39	37.50	0.80	3.65	233.20	46.88	6.56	113.55	7.80	144.35	89.73	47.44
BM11	57.69	111.91	3.13	4.40	0.87	46.10	15.90	1.01	25.10	6.70	32.25	19.78	7.35
Northeast of Fort McMurray													
NE1	57.15	110.85	62.05	2.10	0.61	18.07	25.87	0.67	22.13	5.96	57.50	7.83	3.55
NE2	57.09	110.75	371.43	1.70	0.58	21.77	31.18	0.60	28.03	6.38	84.60	5.39	7.41
NE3	57.05	110.60	56.00	2.00	0.89	32.60	23.58	0.93	48.17	7.13	68.90	13.99	20.01
NE4	57.96	110.38	116.00	1.20	2.07	42.73	14.14	0.92	27.30	6.83	51.77	42.17	8.47
NE5	56.89	110.90	22.00	1.70	2.17	38.90	51.76	0.39	59.67	7.18	133.43	23.08	23.90
NE6	57.27	110.90	28.12	1.75	0.72	64.10	16.92	0.76	60.15	7.10	59.25	18.33	26.35
NE7	57.15	110.86	9.37	2.50	0.65	15.10	31.39	0.53	23.15	5.28	65.50	2.70	2.54
NE8	57.23	110.74	14.60	1.00	0.66	20.75	28.21	0.19	25.10	6.39	53.00	3.89	6.84
NE9	56.77	110.90	315.00	1.83	1.82	40.05	28.27	0.28	157.35	8.26	138.25	13.72	79.58
NE10	56.64	110.20	419.00	1.50	1.97	47.35	25.19	0.35	154.65	8.67	110.75	5.53	76.28
NE11	57.29	111.23	575.00	2.00	1.39	23.00	23.53	3.09	163.80	7.94	146.00	9.72	78.00
West of Fort McMurray													
WF1	56.35	113.18	320.00	1.30	7.02	221.63	50.90	0.52	42.43	6.91	127.93	173.68	14.95
WF2	56.25	113.14	76.00	1.80	1.73	96.20	20.71	1.47	35.15	6.70	41.75	12.34	8.34
WF3	55.91	112.86	216.00	2.00	1.45	63.43	32.30	1.74	24.90	5.48	71.50	20.81	2.17
WF4	57.15	111.98	3.25	0.80	2.48	69.55	50.48	11.41	118.65	7.41	165.25	14.89	41.08
WF5	56.80	111.92	20.55	0.80	1.65	27.35	33.01	0.82	79.00	7.42	92.00	7.79	33.94
WF6	56.81	111.72	16.23	1.50	1.15	27.50	31.96	0.50	43.50	6.84	85.50	8.81	14.26
WF7	56.78	111.79	8.25	0.90	1.47	25.50	33.89	1.64	81.50	7.39	109.75	5.61	34.63
WF8	56.77	111.95	202.00	1.52	1.40	31.20	22.62	0.51	93.40	7.80	76.75	6.89	43.28

© 2008 NRC Canada

Table A1 (*concluded*).

Region and lake code	Latitude (°N)	Longitude (°W)	Area (ha)	Depth (m)	TN ($mg \cdot L^{-1}$)	TP ($mg \cdot L^{-1}$)	DOC ($mg \cdot L^{-1}$)	SO_4 ($mg \cdot L^{-1}$)	Conductivity ($\mu S \cdot cm^{-1}$)	pH	TDS ($mg \cdot L^{-1}$)	Chlorophyll *a* ($\mu g \cdot L^{-1}$)	Alkalinity ($mg \cdot L^{-1}$ as $CaCO_3$)
Caribou Mountains													
CM1	58.77	115.43	160.00	8.50	0.68	43.20	22.62	2.88	52.27	7.15	66.97	5.59	18.09
CM2	59.13	115.13	940.00	6.00	1.05	26.33	12.34	2.05	30.20	6.86	35.50	5.52	8.37
CM3	59.20	115.46	230.00	3.50	1.86	83.43	21.89	3.73	41.03	6.87	61.87	12.00	11.15
CM4	59.31	115.33	310.00	11.50	1.12	32.50	22.84	1.02	30.97	6.83	53.33	3.47	9.46
CM5	59.24	114.52	80.00	1.80	1.28	43.03	19.21	1.19	20.13	6.22	37.33	13.94	3.03
Canadian Shield													
S1	59.72	110.01	340.00	27.40	0.53	5.30	9.27	0.95	60.67	7.20	40.33	2.49	21.36
S2	59.12	110.82	103.00	12.90	0.97	13.07	18.83	0.53	52.00	7.08	57.17	3.22	18.21
S3	59.20	110.69	54.79	13.10	1.04	8.20	18.60	0.51	43.90	7.08	49.83	3.77	13.81
S4	59.17	110.56	142.00	9.14	0.69	15.97	13.84	1.12	54.43	7.22	44.50	5.87	20.78
S5	59.12	110.69	70.21	1.80	1.57	38.47	20.19	0.60	34.23	6.88	55.00	23.09	10.10
Eastern Alberta Plains													
Touchwood	54.83	111.40	2900.00	40.00	0.70	16.95	10.80	7.86	273.67	7.69	147.00	3.58	143.33

Note: TN, total nitrogen; TP, total phosphorus; DOC, dissolved organic carbon; TDS, total dissolved solids.

© 2008 NRC Canada

Combining turbine blade-strike and life cycle models to assess mitigation strategies for fish passing dams

John W. Ferguson, Gene R. Ploskey, Kjell Leonardsson, Richard W. Zabel, and Hans Lundqvist

Abstract: The combined model produced a tool for evaluating effects on fish populations from passage through hydropower turbines at dams. Mean blade-strike mortality was higher for adult Atlantic salmon (*Salmo salar*) and sea-run brown trout (*Salmo trutta*) (25.2%–45.3%) than for juveniles (5.3%–9.7%). Based on life cycle modeling, salmon populations in two Swedish rivers responded differently to strategies for mitigating mortality caused by fish striking turbine blades. Although population growth rates increased up to 3% and were relatively similar for both rivers, the relative increase in the number of female salmon escaping above a dam annually after 20 years when both juveniles and adults were protected was greater in the River Piteälven (68%) than in the River Vindelälven (46%) and was approximately four times greater in the River Piteälven (38% vs. 10%) when only adults were protected. These population responses were not predicted by estimates of mortality through turbines. They showed the model could be used to evaluate strategies to conserve fish populations affected by dams located in fish migratory corridors and how postspawn adults contributed to population productivity.

Résumé : Le modèle combiné fournit un outil pour évaluer les effets sur les populations de poissons du passage à travers les turbines hydroélectriques dans un barrage. La mortalité moyenne due aux coups de pales est plus élevée chez les saumons atlantiques (*Salmo salar*) et les truites de mer (*Salmo trutta*) adultes (25,2–45,3 %) que chez les juvéniles (5,3–9,7 %). D'après une modélisation du cycle biologique, les populations de saumons dans deux rivières suédoises réagissent différemment aux stratégies de mitigation de la mortalité causée par les pales des turbines qui frappent les poissons. Bien que les taux de croissance des populations aient augmenté jusqu'à 3 % et aient été relativement semblables dans les deux rivières, l'accroissement relatif du nombre de saumons femelles à s'échapper annuellement en amont d'un barrage après 20 ans, lorsque les juvéniles et les femelles ont été protégés, a été plus importante dans la rivière Piteälven (68 %) que dans la Vindelälven (46 %); lorsque seuls les adultes ont été protégés, elle était quatre fois plus importante dans la Piteälven (38 % par rapport à 10 %). Ces réactions des populations ne pouvaient être prédites à partir des estimations de la mortalité durant le passage dans les turbines. Elles indiquent que le modèle peut servir à évaluer les stratégies pour protéger les poissons affectés par barrages construits dans les corridors de migration des poissons; il peut aussi évaluer comment les adultes après la fraye contribuent à la productivité de la population.

[Traduit par la Rédaction]

Introduction

Many diadromous and resident fishes migrate within riverine habitats or between freshwater and marine habitats where human alterations of the migratory corridors are often so pronounced that they become integral parts of a species' life cycle. Accordingly, to fully understand the effects of these alterations, we must consider their impacts in the context of overall population viability. In iteroparous fish, life cycle repercussions from alterations to migratory corridors may be especially important, as these individuals can make repeated spawning migrations. For example, Fleming (1998) reviewed the reproductive characteristics of the subfamily Salmonidae and reported that mean rates of repeat breeding ranged as high as 65% for resident and 41% for anadromous populations.

Received 4 June 2007. Accepted 30 January 2008. Published on the NRC Research Press Web site at cjfas.nrc.ca on 5 July 2008. J20034

J.W. Ferguson.[1] Fish Ecology Division, Northwest Fisheries Science Center, National Marine Fisheries Service, 2725 Montlake Boulevard East, Seattle, WA 98112-2097, USA; Department of Wildlife, Fish, and Environmental Studies, Swedish University of Agricultural Sciences (SLU), 901 83 Umeå, Sweden.
G.R. Ploskey. Battelle-Pacific Northwest National Laboratory, P.O. Box 999, Richland, WA 99352, USA.
K. Leonardsson and H. Lundqvist. Department of Wildlife, Fish, and Environmental Studies, Swedish University of Agricultural Sciences (SLU), 901 83 Umeå, Sweden.
R.W. Zabel. Fish Ecology Division, Northwest Fisheries Science Center, National Marine Fisheries Service, 2725 Montlake Boulevard East, Seattle, WA 98112-2097, USA.

[1]Corresponding author (e-mail: john.w.ferguson@noaa.gov).

 doi:10.1139/F08-078 © 2008 NRC Canada

Many of the 45 000 dams throughout the world that exceed 15 m in height (World Commission on Dams 2000) are located in fish migratory corridors and present obstacles to fishes that require movement to complete a life cycle (e.g., Winter and Van Densen 2001; Zigler et al. 2004). In addition, mortality from passing turbines and other passage routes at dams can be substantial enough to cause downward trends in migrating fish populations (National Research Council 1996; Parrish et al. 1998).

Mark–recapture methods are commonly used to develop empirical estimates of mortality from passage through turbines and other passage routes at dams (e.g., Muir et al. 2001; Scruton et al. 2002). Alternatively, mathematical models have been developed to estimate the probability that a fish will contact rotating turbine machinery during passage through a power station. While these models have the potential for broad application to a variety of species and locations, their use has been limited and mainly reported in gray literature (e.g., Montén 1985; Franke et al. 1997; Pavlov et al. 2002). Further validation with empirical estimates of mortality is needed to expand their utility.

Both mark–recapture and blade-strike estimates of fish survival through turbines at dams lack the means to connect the estimated mortality to the overall fish population and its productivity. However, models of an animal's entire life cycle are becoming increasingly available and are used to explore how populations respond to anthropogenic factors and environmental variability and to develop conservation strategies for populations at risk (e.g., Caswell 2001; Zabel et al. 2006; Battin et al. 2007).

In this paper, we develop a new tool for analyzing the effects of dams on fish populations by combining blade-strike and life cycle models. It goes beyond generating simple point estimates of mortality based on the outcomes of individual fish and incorporates any effects from dam passage on the unit of interest to fishery managers, the entire population and its productivity. It is simple enough to have broad applicability to many situations where dams have impacted riverine ecosystems, including those where basic information on fish populations is available, but specific information on fish survival past dams is lacking or is difficult or expensive to obtain. We provide a basic structure and approach that could be modified to answer more complicated questions, such as the relative effects of various mitigation strategies on a population. We applied the approach to two economically important populations of Atlantic salmon (*Salmo salar*) in Sweden because information was available for model parameterization. However, many salmonid populations have been impacted by dams (e.g., McClure et al. 2003; Williams et al. 2005), and development of this analytical tool will assist in identifying actions needed to maintain the viability of at-risk populations.

Specifically, we modeled Atlantic salmon and sea-run brown trout (*Salmo trutta*; hereafter referred to as sea trout) populations in the River Vindelälven and River Piteälven in northern Sweden (Fig. 1). Atlantic salmon and sea trout populations in both study rivers are generally depressed given the size of these rivers and amount of available habitat, having been impacted by human activities affecting freshwater habitats such as damming, dredging, pollution, and siltation of rivers (International Council for the Exploration of the Sea 2007).

We chose to study salmon and sea trout in these rivers because downstream-migrating fish in each river pass a single dam and power station containing either Kaplan or Francis turbines, the most common turbines placed in fish migratory corridors throughout the world. Also, these populations represent some of the few remaining populations of wild salmon and sea trout in the Baltic region, and information is needed to develop effective mitigation strategies and improve their status.

Materials and methods

General approach

Combining turbine blade-strike and life cycle models required three basic steps. First, we developed models of fish mortality caused by turbine blade-strike, as blade-strike is considered the primary mechanism of mortality when fish pass through turbines (Eicher Associates Inc. 1987; Turnpenny et al. 2000; Čada 2001), although shear has also been shown to produce at least 15% of the injuries to fish from passage through Kaplan turbines (Mathur et al. 2000). We then estimated the mortality of juvenile (smolt) and adult (kelt) salmon and sea trout passing dams in both rivers. Second, the mortality rates from turbine blade-strike were entered into salmon life cycle models that incorporated age-specific survival rates, fecundity, and life history variability in age of reproduction and repeated spawning. Third, we used the life cycle models to predict the responses of salmon populations in each river to hypothetical scenarios designed to eliminate any mortality from turbine blade-strike: (*i*) protect juveniles, (*ii*) protect adults, and (*iii*) protect both juvenile and adult age classes. Results of the scenarios were then compared with results from a base case that included effects from turbine blade-strike mortality, and differences represented the effects of the mortality on the populations and were expressed as absolute and relative changes in population growth rate (λ) and increased annual adult female salmon escapement over the dam in each river after 20 years.

Study sites and population status

The River Piteälven in northern Sweden enters the Baltic Sea just below the Arctic Circle at 65°14′N (Fig. 1). The river is approximately 450 km long and has an annual mean flow of 150 $m^3 \cdot s^{-1}$. The Sikfors Power Station is located 40 km upstream from the river mouth and has a total discharge capacity of 270 $m^3 \cdot s^{-1}$ through two identical Kaplan (propeller) turbines, which operate at 19 m of head and produce 40 MW of power (Fig. 2). Trashracks located upstream from the turbines have 13 cm wide openings. Turbine discharge returns to the river through a 0.6 km long outlet tunnel. The river is free flowing (undammed) upstream of the power station.

Since a new fish ladder was installed at the Sikfors Power Station in 1992, annual counts of adult Atlantic salmon migrating over the dam have averaged 598 fish (range 27–1628); since 1995, when changes to Baltic Sea fishing regulations reduced the number of fish caught and increased escapement, annual counts have averaged 734 fish (Interna-

© 2008 NRC Canada

Fig. 1. Area map of the Baltic region showing the location of the Rivers Umeälven, Vindelälven, and Piteälven and the Stornorrfors and Sikfors power stations in Sweden.

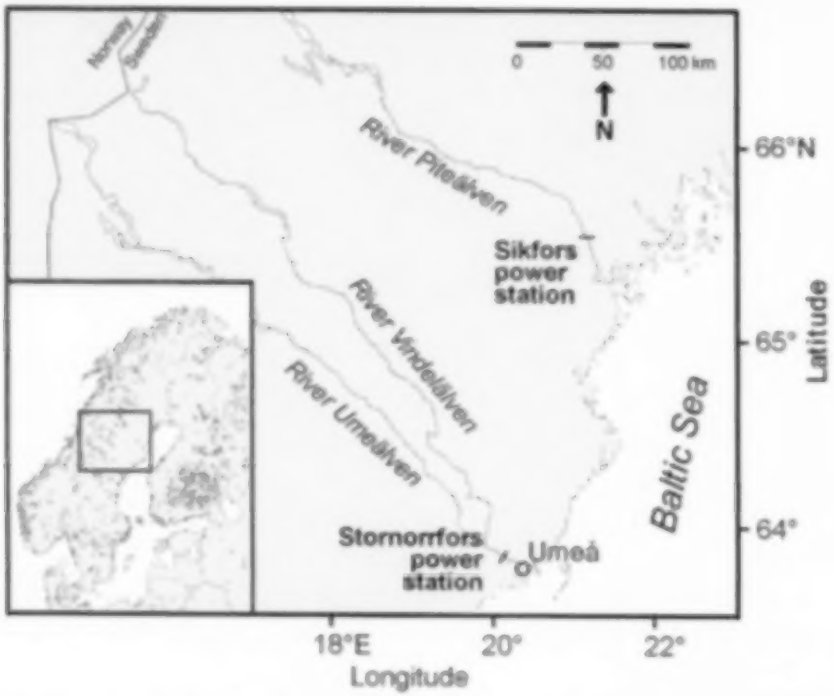

Fig. 2. Drawings showing the basic differences between Francis and Kaplan (propeller) turbine runner designs (redrawn from Eicher Associates Inc. 1987). Francis turbines typically have from 15 to 17 blades that are fixed in position and attached in a manner that forms a wheel. Kaplan turbines typically have from 4 to 6 blades attached to a hub, and the blades can be adjusted vertically to optimize unit efficiency throughout a wide range of turbine water discharge volumes.

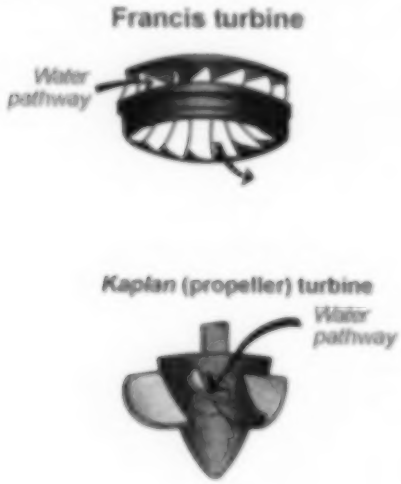

tional Council for the Exploration of the Sea 2007). Annual counts of sea trout passing the ladder have ranged from 100 to 350 fish over the past 10 years (S. Stridsman, Swedish National Board of Fisheries, Luleå, Sweden, personal communication).

The River Umeälven enters the Baltic Sea south of the River Piteälven near the city of Umeå (Fig. 1). This river is also approximately 450 km long and has an annual mean flow of 430 $m^3 \cdot s^{-1}$. The Stornorrfors Power Station is located 32 km upstream from the river mouth; it is the largest hydroelectric facility in Sweden and produces 600 MW of power through four Francis turbines that operate at 75 m of head and have a discharge capacity of 950 $m^3 \cdot s^{-1}$ (Fig. 2). Trashracks located upstream from the turbines have 10 cm wide opening, and discharge from the turbines returns to the river through a 4.0 km long outlet tunnel. Upstream from the power station, the River Umeälven has been heavily developed into a series of dams and reservoirs and is impassable to migrating fish. However, the 450 km long, unregulated River Vindelälven starts in Lapland near the Norwegian border and enters the Umeälven River just upstream from the Stornorrfors Power Station and contains the habitat available to wild salmon and trout in the Umeälven basin (Fig. 1).

Since 1974, annual counts of adult Atlantic salmon migrating over the Norrfors Dam that directs flow to the Stornorrfors Power Station have averaged 1618 fish (range 227–6052), and annual counts of sea trout have averaged 36 fish (range 6–139); since 1995, annual counts of salmon have averaged 2587 (International Council for the Exploration of the Sea 2007).

© 2008 NRC Canada

Turbine blade-strike modeling

Von Raben (1957) first developed the general forms of blade-strike models for both Kaplan and Francis turbines. The models are based on the probability that a fish of a given length and traveling at a certain velocity will pass through openings between turbine blades as the turbine runner rotates and the blades sweep through the water flow pathway. We chose to use the turbine blade-strike model formulations as expressed by Bell (1991) simply because we were familiar with them and they were designed for juvenile salmon; however, other formulations are available and are virtually identical (e.g., Montén 1985; Franke et al. 1997). The probability of turbine blade-strike varies with fish length and thus species and age class and also turbine characteristics such as geometry of the water passageway, flow rates, turbine type (e.g., Kaplan or Francis), and project operations (Eicher Associates Inc. 1987; Čada 2001; Skalski et al. 2002). Therefore, we incorporated these variables into the model formulations (Appendices A and B).

Existing blade-strike model studies have primarily focused on juvenile life stages (e.g., Pavlov et al. 2002; Ploskey and Carlson 2004). However, we also incorporated adults into the model analyses, since iteroparity is an important life history strategy and component of overall population productivity in many diadromous species. For example, repeat spawning is common in female steelhead (i.e., sea-run rainbow trout, *Oncorhynchus mykiss*) (Evans et al. 2004), and Atlantic salmon individuals can spawn multiple times (Ducharme 1969; Quinn 2005) and may constitute a large percentage of the spawning population. Fleming (1998) reported that repeat spawners averaged 11% (range 0.7%–42.5%) based on a review of Atlantic salmon breeding systems across the species' range.

Closer to our study rivers, Niemelä et al. (2006) reviewed catch data from 1975 to 2004 and reported that repeat spawners comprised 7% of the catch mass (t) of Atlantic salmon in the River Teno in northern Scandinavia. They also reported the proportion has increased in recent years and was 30% in 2004 and that repeat spawners accounted for 16%–35% of multi-sea-winter fish in 2001–2004. Calles (2005) observed that >50% of the adult brown trout outfitted with radio transmitters were observed as kelts moving downstream past power plants following tagging in the River Emån in southern Sweden. Data from the Ricklean River, located between the two rivers we studied, indicated that 62% of the adult salmon tagged in 1962 were caught as kelts in a smolt trap operated part of the following spring (unpublished data collected by L. Osterdahl, 1962–1966, available from K. Leonardsson). Thus, the percentage of postspawn salmonid adults that move downstream past power stations can be high. Passage of this life stage through turbines may result in substantial mortality to individual fish, ranging from 22% to 57% (Wagner and Ingram 1973; Liscom et al. 1985).

To construct the models, length–frequency data on wild juvenile Atlantic salmon and sea trout were obtained from a smolt trap on the River Säravån, which is also located between the study rivers (Lundqvist et al. 2006) (Table 1). Length–frequency data for adult salmon from the River Vindelälven were obtained from Rivinoja (2005). Length–frequency data for adult sea trout were developed from measurements of 179 fish that passed a ladder located near the Stornorrfors Power Station from 2001 through 2005 (P. Rivinoja, Swedish University of Agricultural Sciences, Department of Wildlife, Fish and Environmental Studies, SE-901 83 Umeå, Sweden, personal communication). Adult fish in the River Piteälven were assumed to have the same length–frequency distributions as fish in the River Vindelälven, because both rivers are within the same genetic management unit for this stock (International Council for the Exploration of the Sea 2005). We assumed that kelts in both rivers did not grow after spawning and thus had the same length–frequency distributions as upstream-migrating adults. Hereafter, we refer to adults migrating downstream as kelts and fish in the Baltic Sea or those migrating upstream as adults.

Table 1. Biological input parameters used in blade-strike modeling.

Parameter	Mean length (cm)	Range (cm)
Smolts		
Atlantic salmon	14.8	12.6–17.0
Sea trout	17.5	13.7–21.3
Kelts		
Atlantic salmon	78.4	39.0–116.0
Sea trout	64.0	47.2–80.9

Note: Range was defined as 2 standard deviations in fish length above and below mean length for Atlantic salmon (*Salmo salar*) smolts and sea trout (*Salmo trutta*) smolts and kelts. For Atlantic salmon kelts, the range in fish length was the same as that reported by Rivinoja (2005) from 2651 adults tagged from 1995 to 2005.

Several assumptions regarding fish length were made to incorporate this variable into the turbine blade-strike models. For salmon smolts, sea trout smolts, and sea trout kelts, we developed a range in fish lengths that was 2 standard deviations above and below mean fish length. For salmon kelts, where standard deviations for length data were not available, we assumed that lengths of 1-sea-winter (SW) kelts were at the low end of the range, lengths of 2- and 3-SW kelts were at the mean, and lengths of 4-SW kelts were at the high end of the range of lengths reported by Rivinoja (2005) (Table 1).

To estimate age-dependent mortality of downstream-migrating salmon smolts needed in life cycle modeling, we assumed that age-2 salmon smolts were 1 standard deviation below mean smolt length, and age-3 smolts were 1 standard deviation above mean smolt length. These fish lengths were input into the turbine blade-strike models to estimate mortality for each age class, and the results were used as input parameters to the life cycle models, as discussed below.

Turbine geometry data were obtained from power station owners for two turbine operations: maximum load and maximum efficiency (Table 2). Maximum load is the operation that results in the highest power output, regardless of the volume of water flow through the turbine. Maximum efficiency is the point of operation where the maximum output of power is produced per unit of water flow through the turbine. At the Sikfors Power Station, maximum load is the normal mode of operation during the fish migration

© 2008 NRC Canada

Table 2. Engineering input parameters used in blade-strike modeling of four Francis turbines at the Stornorrfors Power Station on the River Umeälven (labelled Units I to IV) and two identical Kaplan turbines at the Sikfors Power Station on the River Piteälven.

	Stornorrfors (Francis turbine)		Sikfors (Kaplan turbine)	
Parameter	Maximum load	Maximum efficiency	Maximum load	Maximum efficiency
No. of turbine blades	Unit I: 15 Units II–IV: 16	Unit I: 15 Units II–IV: 16	4	4
Blade rotational speed ($r \cdot min^{-1}$)	Units I–III: 125 Unit IV: 115	Units I–III: 125 Unit IV: 115	166.7	166.7
Overall turbine blades and hub (runner) diameter (m)	Units I–III: 4.33 Unit IV: 4.75	Units I–III: 4.33 Unit IV: 4.75	3.95	3.95
Radius of hub (distance from the centerline of the shaft to the outer edge of the hub where the blades attach (m)	NA	NA	1.625	1.625
Height of the wicket gates (m)	Units I–III: 1.56 Unit IV: 1.73	Units I–III: 1.56 Unit IV: 1.73	1.635	1.635
Angle of the wicket gate opening (°)	NA	NA	60	47.35
Radius of an imaginary vertical cylinder from the centerline of the shaft to the downstream tips of all wicket gates (m)	NA	NA	3.95	3.95
Turbine discharge ($m^3 \cdot s^{-1}$)	Units I–III: 200 Unit IV: 275	Units I–III: 170 Unit IV: 215	125	77

season. We modeled this as the primary operation and maximum efficiency as an alternative operation at this power station based on the hypothesis that fish survival and hydraulic efficiency of turbine units are positively correlated (Ferguson et al. 2005). At the Stornorrfors Power Station, maximum efficiency is the normal mode of operation during the fish migration season. Here, we compared this operation with one based on maximum load, a typical operation at many power stations.

Kaplan turbines

The physical and biological data for fish passing the Sikfors Power Station were entered into a spreadsheet to estimate the probability of blade-strike (P) based on the following formula:

$$(1) \qquad P = \left(\frac{n \cdot N}{60}\right)\left(\frac{l \cdot \cos\theta}{V_{axial}}\right)$$

where l is fish length (m), V_{axial} is the axial water velocity at the turbine blades, θ is the angle of the fish relative to the blade, n is the number of blades, and N is the rotation rate of the blades in revolutions per minute (Fig. 3; Appendix A).

Francis turbines

A similar spreadsheet was developed to estimate P for fish passing the Stornorrfors Power Station:

$$(2) \qquad P = \left(\frac{n \cdot N}{60}\right)\left(\frac{l \cdot \sin\alpha}{V_r}\right)$$

where V_r is the radial velocity of water at the entrance to the turbine runner, or "wheel" as it is commonly called in Francis turbines, and α is the flow angle between the absolute water velocity and the tangent to the runner (Fig. 4; Appendix B).

Common assumptions and adjustments used for both types of turbines

The water flow pathway in a turbine is an enclosed, dark, high-velocity environment that is extremely difficult to sample. Some research has focused on evaluating imaging systems to monitor fish during passage through turbines (Moursund and Carlson 2004). However, we were not aware of any studies that provide data on the orientation and behavior of fish as they approach and pass turbine blades, including whether data changed with fish size, species, turbine operational parameters, season, and river conditions. Therefore, similar to other model studies, we simply assumed that fish were oriented parallel to the incoming water flow fields as they approached turbine blades.

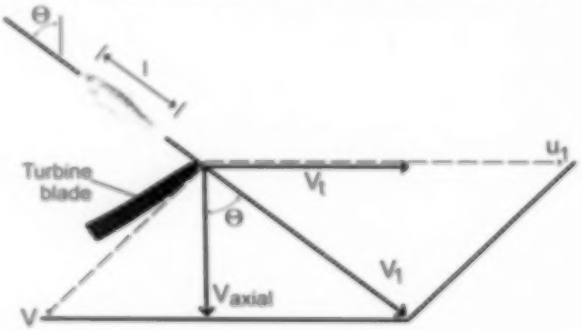

Fig. 3. Schematic of the angular geometry used in turbine blade-strike models of a fish passing the leading edge of a Kaplan turbine blade (shaded area) used in turbine blade-strike modeling. The probability of a fish striking a blade is calculated as the length of the fish relative to the distance the fish would travel in the time required for one blade to be replaced by the next adjacent blade as it rotates around the axis of the turbine. The position of Kaplan turbine blades can be adjusted upwards (vertically) under different operations to align the leading edge of the blade with the incoming flow angle (θ), or the angle between the axial and absolute water velocity vectors. In this schematic, l is the length of the fish, V_t is the tangential water velocity, V_1 is the absolute water velocity, and u_1 is the velocity of the rotating blade (adapted from Bell 1991).

However, not all strike events result in mortality (Turn-

© 2008 NRC Canada

Fig. 4. Schematic of the angular geometry used in turbine blade-strike models of a fish passing the leading edge of a Francis turbine blade (shaded area) used in turbine blade-strike modeling. The probability of a fish striking a blade is calculated as the length of the fish relative to the distance the fish would travel in the time required for one blade to be replaced by the next adjacent blade as it rotates around the axis of the turbine. The positions of Francis turbine blades are fixed and cannot be adjusted to the flow angle α, or the angle between the tangential and absolute water velocity vectors. In this schematic, V_t is the tangential velocity of water flow at the runner entrance, V_r is the radial velocity of water flow at the runner entrance, V_1 is the absolute water velocity, V is the water velocity relative to the velocity of the rotating blade, u_1 is the velocity of the rotating blade, β is the angle of the turbine blade, and l is the length of the fish (adapted from Bell 1991).

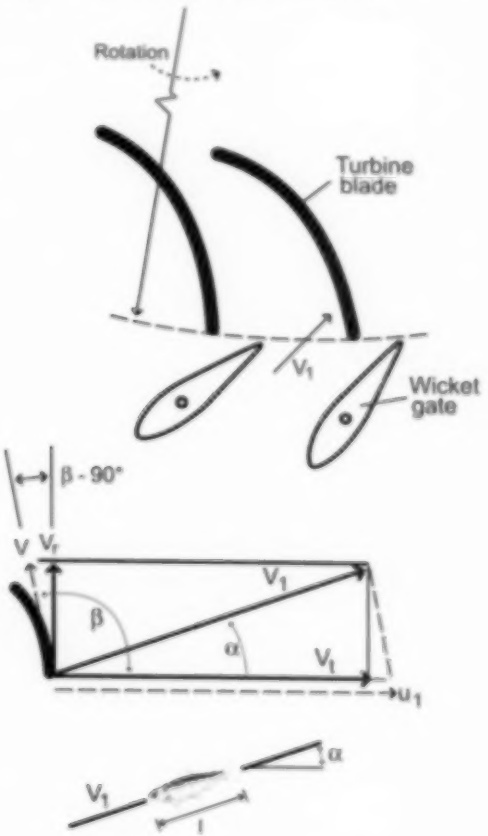

penny et al. 2000; Ploskey and Carlson 2004). Therefore, we adjusted P to estimate the actual probability of mortality (M) from a strike event, thereby incorporating variability in fish orientation and behavior into the model formulation to the extent practicable. For juvenile fish, we used a regression equation from Turnpenny et al. (2000):

$$M = P(0.1533 \cdot \log_{10} l + 0.0125) \quad (3)$$

where l is fish length (cm). For kelts we used Turnpenny's (1998) formula for fish weighing greater than 200 g:

$$M = P \cdot 0.47 \quad (4)$$

Estimated blade-strike mortality was then converted into survival (S) for input into life cycle models using the following formula:

$$S = 1 - M \quad (5)$$

Life cycle modeling

Age-structured, Leslie matrix models were used to estimate the responses of wild Atlantic salmon populations to strategies that mitigated mortality assigned to turbine passage:

$$\boldsymbol{n}(t+1) = \mathbf{A}(t) \cdot \boldsymbol{n}(t) \quad (6)$$

where the vector $\boldsymbol{n}(t)$ represents the number of individuals at the end of time step t at each age, and $\mathbf{A}(t)$ is a 9×9 population projection matrix that varies at each time step (Caswell 2001). The matrix $\mathbf{A}(t)$ was constructed using PopTools software (www.cse.csiro.au/poptools/) and was based on the life history characteristics of salmon in the Rivers Vindelälven and Piteälven. Each element of the matrix, aij, represents the transition of i-year-olds (columns) to j-year-olds (rows) during the yearly time step. The fertility of the population was captured in the top row of the matrix (smolt age 1), whereas the survival of each age class was captured by the off-diagonal cells (Table 3). Iteroparity was incorporated into the matrices by assuming that 40% of the adults that migrated to the spawning grounds did actually overwinter, resmolt, and migrate downstream the following spring (Table 3; row Kelt 1).

Parameters used in the matrix formulations ranged from a simple survival rate such as S2, which is the probability of 1-year-old parr surviving in the river through a second year, to more complex parameters based on variable life history patterns. For example, b2-Mu-D2-DS2 would estimate the proportion of 2-SW adults that migrated upstream to spawn, successfully passed a dam, and resmolted the year following spawning, as well as their subsequent survival through a dam while migrating downstream as kelts (Table 4).

Turbine blade-strike model outputs were incorporated into matrix parameters Sm2St (survival of age-2 smolts during their downstream migration through dam or turbines), Sm3St (survival of age-3 smolts during their downstream migration through dam or turbines), and DS1–DS4 (the proportion of 1-, 2-, 3- and 4-SW fish that migrated downstream after spawning; Table 4).

Results of studies conducted from 1995 to 2005 indicated that only 30% of adults migrating upstream in the River Umeälven successfully passed a fish ladder located near the Stornorrfors Power Station and entered the River Vindelälven based on a total of 2651 adult Atlantic salmon tagged with radio, passive integrated transponder (PIT), or Carlin tags (Rivinoja 2005). Therefore, we assumed that 30% of the adults migrating upstream passed the dam, and the remaining 70% migrated downstream to the sea, re-entered the population of adults at this location (Table 3; row Kelt 2), and later returned to the river in the same proportions as the adult population at sea. We assumed that 100% of upstream-migrating adults passed the Sikfors Power Station

© 2008 NRC Canada

Table 3. Life cycle matrix model formulation for Atlantic salmon (*Salmo salar*) in the River Vindelälven.

	Time (t = 0)									
	Smolt age			Ocean age						
Time (t + 1)	1	2	3	1	2	3	4	Kelt 1	Kelt 2
Smolt age									
1	0	0	0	b1·F1·S1·Mu	b2·F2·S1·Mu	b3·F3·S1·Mu	F4·S1·Mu	0	F4·S1·Mu
2	S2	0	0	0	0	0	0	0	0
3	0	(1 – Sm2)S3	0	0	0	0	0	0	0
Ocean age									
1	0	Sm2·Sm2S·Sm2Su·S01	Sm3S·Sm3Su·S01	0	0	0	0	0	0
2	0	0	0	(1 – b1)S02	0	0	0	0	0
3	0	0	0	0	(1 – b2)S03	0	0	0	0
4	0	0	0	0	0	(1 – b3)S04	0	0	0
Kelt 1	0	0	0	b1·Mu·D·1DS1	b2·Mu·D·2DS2	b3·Mu·D3·DS3	b4·Mu·D·4DS4	0	0
Kelt 2	0	0	0	b1(1 – Mu)S0k	b2(1 – Mu)S0k	b3(1 – Mu)S0k	(1 – Mu)S0k	S0k	0

Note: The same formulation was used for salmon in the River Pitealven, with the exception that most cells in row Kelt 2 were zero, except for cells in columns Kelt 1 and Kelt 2, which were S0k. Refer to Table 4 for parameter descriptions.

dam and entered the spawning population. Since no empirical information was available on adult passage at this dam, the assumption was based on our judgment that the existing fish ladder at the dam was relatively well designed based on visual observations of hydraulic conditions and the location of the ladder at the site and results of sensitivity analyses, discussed below.

Density-dependent factors were not considered to be limiting salmon populations in either river during the 20-year projection period based on evidence that the abundance of wild Atlantic salmon in northern Baltic Sea rivers is controlled primarily by Baltic Sea fisheries (Romakkaniemi et al. 2003) and that parr densities were well below the available carrying capacity of the River Piteälven habitat in 2005 (International Council for the Exploration of the Sea 2005). We assumed that demographic rates for the populations remained constant during the projection period, and 40% of the 2-year-old parr smolted and migrated downstream each year based on data from Lundqvist et al. (2006).

All smolts were assigned to turbine passage at the two power stations. Rivinoja (2005) reported that 100% of radio-tagged salmon smolts passed the Stornorrfors Power Station in 2003, when spill averaged 10% of powerhouse flow during the smolt outmigration period (20 May – 20 June) and was near the 10-year average of 11% spill. Rivinoja (2005) also observed that 85% of the radio-tagged salmon and sea trout smolts (n = 40) passed the Sikfors Power Station in 2003 when spill through deep gates averaged 19% of river flow and that none of the 60 salmon smolts that were radio-tagged in 2004 passed through the spillway during 4% spill through surface-oriented outlets. Over the past 10 years, spill volume has averaged 46% of total river flow at this dam during the smolt migration period; however, no passage behavior data are available under these conditions.

Passage of downstream-migrating kelts was assigned to turbines at the two dams. Östergren (2006) estimated that all 16 radio-tagged sea trout in the River Vindelälven that survived over the winter and migrated downstream in 2005 passed through the Stornorrfors Power Station and none through the spillway at Norrfors Dam. He also reported that 12 radio-tagged sea trout kelts migrated downstream in the River Piteälven in 2004 and that 25% of these died while passing the Sikfors Power Station, but provided no additional information as to whether the remaining nine fish passed through the power station or spillway.

State vectors needed to project the population matrices forward in time were developed from estimated smolt production levels for each river in 2005 (International Council for the Exploration of the Sea 2005) and from adult counts at ladders located near both power stations from 1995 to 2004, a period chosen to incorporate the recent changes to Baltic Sea fishery regulations (Table 5). A projection period of 20 years was selected to allow gains in population productivity to be expressed over several salmon generations.

The age-class structure of adult salmon populations in both rivers used in the vectors was estimated from length–frequency data collected from fish sampled in an adult trap located in a fish ladder near the Stornorrfors Power Station during this same time period (1995–2004) (n = 9057; P. Rivinoja, Swedish University of Agricultural Sciences,

© 2008 NRC Canada

Table 4. Life cycle matrix model input parameter values for Atlantic salmon (*Salmo salar*) in the Rivers Vindelälven and Piteälven under typical turbine operations.

Parameter	Description	Matrix value	
		Vindelälven	Piteälven
S1	Survival from egg to 1-year-old parr	0.1	0.075
S2	Parr survival in river through second year	0.4	0.4
Sm2	Propensity to smolt at age 2	0.286	0.286
Sm2S	Survival of age 2 smolts during downstream migration	0.95	0.9
Sm2St	Survival of age 2 smolts during downstream migration through dam or turbines	0.945 or 1.0	0.953 or 1.0
S3	Parr survival in river through third year	0.6	0.6
SmS3	Survival of age 3 smolts during downstream migration	0.95	0.95
Sm3St	Survival of age 3 smolts during downstream migration through dam or turbines	0.918 or 1.0	0.942 or 1.0
S01	Survival through first year in Baltic Sea	0.15	0.1
S02	Survival through second year in Baltic Sea	0.4	0.4
S03	Survival through third year in Baltic Sea	0.2	0.15
S04	Survival through fourth year in Baltic Sea	0.2	0.1
SOk	Kelt survival in nearshore coastal Gulf of Bothnia	0.8	0.7
Mu	Survival (passage success) during upstream migration in river	0.3	1.0
b1	Propensity of adults in ocean to return to river and breed as a grisle (1 sea winter (SW))	0.01	0.01
b2	Propensity of adults in ocean to return to river and breed (2 SW)	0.2	0.2
b3	Propensity of adults in ocean to return to river and breed (3 SW)	0.8	0.8
b4	Propensity of adults in ocean to return to river and breed (4 SW)	0.5	0.5
F1	Fertility (fecundity) of 1-SW adults	1260	1200
F2	Fertility (fecundity) of 2-SW adults	2640	2400
F3	Fertility (fecundity) of 3-SW adults	5220	4800
F4	Fertility (fecundity) of 4-SW adults	9600	8800
Fk	Fertility (weighted fecundity) of 3-SW (0.8) and 4-SW (0.2) fish that go to sea as kelts and stay in coastal Gulf waters for 1 year	6096	5600
D1	Proportion of 1-SW fish that migrate downstream after spawning	0.4	0.4
DS1	Survival of 1-SW kelts migrating downstream; river survival is assumed to be 1.0 so this reflects turbine mortality; Vindelälven estimates are for Stornorrfors Power Station unit IV under the maximum efficiency operation; survival was assumed to be 1.0 under Alternatives 1–3	0.65 or 1.0	0.73 or 1.0
D2	Proportion of 2-SW fish that migrate downstream after spawning	0.4	0.4
DS2	Survival of 2-SW kelts migrating downstream; river survival is assumed to be 1.0 so this reflects turbine mortality; Vindelälven estimates are for Stornorrfors Power Station unit IV under the maximum efficiency operation; survival was assumed to be 1.0 under Alternatives 1–3	0.60 or 1.0	0.70 or 1.0
D3	Proportion of 3-SW fish that migrate downstream after spawning	0.4	0.4
DS3	Survival of 3-SW kelts migrating downstream; river survival is assumed to be 1.0 so this reflects turbine mortality; Vindelälven estimates are for Stornorrfors Power Station unit IV under the maximum efficiency operation; survival was assumed to be 1.0 under Alternatives 1–3	0.60 or 1.0	0.70 or 1.0
D4	Proportion of 4-SW fish that migrate downstream after spawning	0.4	0.4
DS4	Survival of 4-SW kelts migrating downstream; river survival is assumed to be 1.0 so this reflects turbine mortality; Vindelälven estimates are for Stornorrfors Power Station unit IV under the maximum efficiency operation; survival was assumed to be 1.0 under Alternatives 1–3	0.41 or 1.0	0.54 or 1.0

Note: The range of values shown for parameters Sm2St, Sm3St, and DS1–DS4 reflect the range of input values for the base cases or Alternatives 1–3. Base cases reflect current conditions; Alternative 1 assumed that smolt survival was 100%; Alternative 2 assumed that kelt survival was 100%; Alternative 3 assumed that smolt and kelt survival was 100%. Unit IV was the unit with the largest discharge in the life cycle model.

Department of Wildlife, Fish and Environmental Studies, SE-901 83 Umeå, Sweden, personal communication). The proportion of the female salmon population in each class was estimated by assigning each fish to a 1-, 2-, 3-, or 4-SW age class based on its weight, where the respective weights for each age class were <3, 3.5–7, 7.5–9, and >9.5 kg. All other matrix input parameters were developed using data from International Council for the Exploration of the Sea (2005).

Once the matrices were projected forward, each parameter was adjusted ±10% from its base value while holding all other parameters constant, and the most influential parameters were adjusted so the 20-year projections fit the following criteria from ladder counts of salmon during the 1995–2004 period: (*i*) annual population growth rate (λ) represented as the dominant eigenvalue (Caswell 2001); (*ii*) adult age-class composition; and (*iii*) the average annual count of adult female salmon escaping above the dam. Annual population growth rates were calculated as

© 2008 NRC Canada

Table 5. State vectors used to project Atlantic salmon (*Salmo salar*) population size in the Rivers Vindelälven and Piteälven forward 20 years.

	Population size (N)	
Age class	Piteälven	Vindelälven
1-year-old	17 500	162 000
2-year-old	5 800	60 625
3-year-old	3 500	48 500
Females		
1 sea winter	18	74
2 sea winters	156	617
3 sea winters	32	124
4 sea winters	23	91
Kelt, first year fresh water	0	0
Kelt, second year at sea	70	86

Note: Values for 1- to 3-year-old fish were based on International Council for the Exploration of the Sea (2005). Data for adults was based on fish counts in ladders at dams in each river.

$$\lambda = \exp(\mu) \tag{7}$$

where μ is the arithmetic mean of $\log(N_{t+1}/N_t)$ or

$$\bar{\mu} = \frac{1}{q}\sum_{t=0}^{q-1} \log\left(\frac{N_{t+1}}{N_t}\right) \tag{8}$$

where N_t is the number of female salmon escaping above the dam in each river each year (Morris and Doak 2002). Calculated population growth rates were 1.115 for the River Vindelälven and 1.109 for the River Piteälven. The resulting matrices were considered the base case for each river because they reflected current conditions.

Three alternatives were then modeled to evaluate how salmon populations in both rivers would potentially respond if fish passing the power stations experienced no mortality and passed via non-turbine routes. In Alternative 1, we assumed that smolt survival was 100%; in Alternative 2, we assumed that kelt survival was 100%; and in Alternative 3, we assumed that smolt and kelt survival was 100%. These assumptions were optimistic but were based on discussions with local fishery managers regarding the potential installation of bypass systems at both study dams and their expected locations relative to hydraulic conditions at the sites. They were also based on studies that showed a high percentage (86%–100%) of downstream-migrating juvenile Atlantic salmon and steelhead can be guided away from power stations and into passage facilities (e.g., Ruggles et al. 1993; Simmons 2000) and evidence that fish survival through properly designed bypass facilities can approach 100% (Muir et al. 2001).

Population-level responses to turbine operations were not evaluated because differences in turbine blade-strike mortalities between maximum load and maximum efficiency operations were minimal for both types of turbines. Similarly, since results of turbine blade-strike modeling were similar among all four Francis turbines at the Stornorrfors Power Station, we used results for the unit with the largest discharge (IV) in the life cycle model, since presumably most fish would pass the power station through this unit.

The combined model approach and predictions were deterministic. This was primarily because we lacked information on fish orientation and horizontal and vertical distribution within turbines needed to make stochastic blade-strike predictions, and stochastic life cycle modeling would have required available and accurate information on each input parameter. Also, we felt strongly at this stage of model development that the adult count data was the best information available for developing the base cases for each river and that a count-based approach comported well with the type of data available in many other situations. Finally, we did not conduct life cycle model studies of sea trout populations in either river because of a lack of demographic information, their highly variable life history patterns (Jonsson 1985), and the extremely low escapement levels over the dams studied.

Sensitivity analyses

We conducted sensitivity analyses to evaluate the relative importance of parameters on combined model results. Similar to Zabel et al. (2006), we first assigned ranges and distributions to each parameter and then sampled from these distributions simultaneously to produce 10 000 Monte Carlo simulations for the base case scenarios using @RISK software (Palisades Corporation, Ithaca, New York, USA). For each run, we kept track of the parameter set used and the resulting population growth rate (λ) and number of females migrating over the dam. We regressed number of females versus the parameter values for each run; since the output metrics were highly correlated, we reported results for the number of females, as this metric is more intuitive than λ. We determined the importance of each parameter by calculating the standardized regression coefficient (coefficient divided by its standard error) associated with the parameter (Cross and Beissinger 2001). In addition, the sign of the standardized regression coefficients determines the direction of the relationship between number of females and the parameter. Because blade-strike model parameters were likely independent from the life cycle model parameters, we conducted separate sensitivity analyses for each submodel for ease of interpretation. Parameter ranges were based on empirical data described herein and were assigned a normal or uniform distribution (Table 6).

Smolt and kelt passage efficiency and survival through non-turbine dam passage routes were captured by the sensitivity analyses. For example, if 90% of the age-2 smolts are guided into a future bypass system installed at Sikfors Dam and 90% survive, their survival past the dam decreases from 0.953 (Sm2St, Table 4) to 0.905 and is within the 0.75 to 0.95 range in smolt passage mortality modeled in the sensitivity analyses.

In addition to these general sensitivity studies, we evaluated the specific assumption that 100% of the smolts passed through the Sikfors Power Station by assuming that 85% passed through the turbines and the remaining 15% passed through the spillway with survival rate of 0.98 (Muir et al. 2001) and then rerunning the combined model.

Results

Turbine blade-strike modeling

Estimated mean probabilities of mortality from blade-

© 2008 NRC Canada

Table 6. Sensitivity analyses input parameters, ranges, and distribution for the Rivers Vindelälven and Piteälven.

Input parameter	Vindelälven: range (distribution)	Piteälven: range (distribution)
Smolt length (m)		
Age-2	0.127–0.148 (normal)	0.127–0.148 (normal)
Age-3	0.148–0.170 (normal)	0.148–0.170 (normal)
Kelt length (m)		
1-SW	0.390–0.784 (normal)	0.390–0.784 (normal)
2-SW	0.587–0.972 (normal)	0.587–0.972 (normal)
3-SW	0.587–0.972 (normal)	0.587–0.972 (normal)
4-SW	0.784–1.160 (normal)	0.784–1.160 (normal)
Radius along the turbine blade where fish were assumed to have passed (m)	NA	0.813–1.975 (uniform)
Turbine passage mortality (%)		
Smolt	0.05–0.25 (uniform)	0.05–0.25 (uniform)
Kelt	0.20–0.70 (normal)	0.10–0.40 (uniform)
Percent repeat spawners (%)	0.10–0.60 (uniform)	0.10–0.60 (uniform)
Adult dam passage rate (%)[a]	0.00–0.47 (normal; skewed; mean 0.30)	0.65–1.00 (normal; skewed; mean 0.95)

Note: Age-2 and age-3 smolt lengths, lengths of 1-, 2-, 3-, and 4-SW kelts migrating downstream, and the radius along the Kaplan blade where smolts or kelts were assumed to pass (River Piteälven only) tested the sensitivity of these blade-strike model input parameters to the combined model outputs. Smolt and kelt turbine passage mortality, percent repeat spawners, and percentage of adults converting over the dam tested the sensitivity of these life cycle model input parameters to combined model outputs.

[a]The range in passage rates of adults over Norrfors Dam that entered the River Vindelälven was reported by Rivinoja (2005); the range in passage rates of adults over Sikfors Dam that entered the River Piteälven was assumed.

Table 7. Results of blade-strike modeling presented as the mean estimated mortality (*M*, in percent) fish experienced during passage through Kaplan and Francis turbines under two operations.

	Kaplan turbine		Francis turbine	
Fish species and age class	Maximum efficiency	Maximum load[a]	Maximum efficiency[a,b]	Maximum load[b]
Smolts				
Salmon	7.7 (6.2–9.3)	5.3 (4.2–6.4)	6.8 (5.5–8.2)	6.7 (5.4–8.1)
Trout	9.7 (7.0–12.6)	6.6 (4.8–8.6)	8.5 (6.1–11.1)	8.4 (6.0–10.9)
Kelts				
Salmon	45.3 (39.9–67.0)	30.9 (27.2–45.7)	39.8 (35.1–58.9)	39.3 (34.6–58.1)
Trout	37.0 (27.3–46.7)	25.2 (18.6–31.8)	32.5 (24.0–41.1)	32.1 (23.7–40.6)

Note: Values in parentheses are a range in estimated mortality developed by adjusting fish lengths. For Atlantic salmon (*Salmo salar*) smolts and sea trout (*Salmo trutta*) smolts and kelts, ranges were based on fish lengths that were 2 standard deviations below and above mean length. For Atlantic salmon kelts, the range represents the low and high range in lengths of 2651 adult salmon tagged from 1995 to 2005 (Rivinoja 2005).

[a]Current operation of turbines during the period fish are migrating downstream and passing the power station.

[b]Francis turbine results are shown for the largest turbine unit at the Stornorrfors Power Station (Unit IV).

strike (*M*) ranged from 25.2% to 45.3% for kelts and from 5.3% to 9.7% for smolts (Table 7). Based on a qualitative assessment of whether the reported ranges in estimated mortalities overlapped, the results indicated that (*i*) kelt mortality was substantially higher than smolt mortality for both species when passing both types of turbines (Francis and Kaplan); (*ii*) there were no differences in estimated mortality between Francis and Kaplan turbines for smolts or adults of either species; and (*iii*) the alternative turbine operations modeled had no effect on salmon and sea trout smolt and kelt mortality, although mean values of *M* were lower under the maximum load operation than under the maximum efficiency operation, especially for the Kaplan turbines.

Life cycle modeling

For salmon in the River Vindelälven, results from the combined mitigation strategies (Alternative 3) produced the highest increases in population growth rate (1.8%) and female escapement (45.8%). Mitigation strategies that addressed smolt mortality (Alternative 1) also produced substantial increases in population growth rate (1.3%) and number of females escaping over the dam (33.2%) near the Stornorrfors Power Station. In contrast, Alternative 2, which protected only kelts, produced minor increases in growth rate (0.5%) and escapement (9.7%) (Table 8). For salmon in the River Piteälven, all three alternatives produced substantial increases in population growth rate that ranged from

© 2008 NRC Canada

1.0% to 2.8%, and increases in the number of females escaping over Sikfors Dam ranged from 23.1% to 68.4% (Table 9).

Sensitivity analyses

Results of blade-strike model input parameter analyses were generally similar between both rivers, where the number of female salmon produced was most associated with the lengths of 2-SW and 3-SW kelts. However, for fish passing the Kaplan turbines in the River Piteälven, the passage location of 2-SW kelts, age-3 smolts, and 3-SW kelts also explained approximately 14% of the total variation in results. In contrast, results of life cycle model input parameters analyses demonstrated that the importance of some parameters varied considerably between the two rivers. In the River Vindelälven, population responses were primarily sensitive to the adult dam passage rate, whereas responses in the River Piteälven were associated with a number of dam passage factors, including adult dam passage rate, 2-SW and 3-SW kelt repeat spawn rate, and the passage mortality of age-2 and age-3 smolts (Figs. 5, 6).

When 85% of the smolts were assumed to have passed through the Sikfors Power Station, the relative increase in the number of female salmon was 20.5% under Alternative 1 and was similar to the combined model results when 100% were assumed to have passed through the power station (23.1%, Table 9).

Discussion

Blade-strike models

Results of blade-strike modeling indicated there were large differences in estimated mortality between fish age classes, as expected, since fish length is a component of the strike formulation and the differences in mean lengths among age classes was large. Mean probability of blade-strike mortality for Atlantic salmon and sea trout kelts was approximately four–six times higher than that for juveniles.

One surprising result was that the estimated mortality of salmon and sea trout smolts and kelts was similar between both types of turbines. Francis turbines are typically used at locations involving higher project head, which results in higher water velocities through the passageways, and Francis turbines have more blades (15–17) than Kaplan turbines (4–6). As a result of these factors, mortality rates for fish passing Francis turbines are usually higher than that for Kaplan turbines (Eicher Associates Inc. 1987). The lack of any differences in estimated mortality between the two types of turbines in our study likely resulted from the high rotation speed of Kaplan turbines at the Sikfors Power Station, which increased the probability of blade strike; these turbines rotate at 167 r·min^{-1}, which results in 11 blades per second passing a stationary point in the turbine. By way of comparison, the Kaplan turbines located at Columbia River dams and studied by Ploskey and Carlson (2004) rotate at just 75 r·min^{-1}.

We found no significant differences in estimated mortality between the two turbine operations tested. However, mean values of M were lower under the maximum load, especially for the Kaplan turbines. This finding is similar to results from other studies where survival was highest at discharges beyond the peak (maximum) efficiency operation (Mathur et al. 2000; Skalski et al. 2002). Because water flow volume and velocity are reduced under the maximum efficiency operation but the turbine blades rotate at a fixed speed, this operation resulted in increased strike probability. This resulted partly from the model formulation and suggests that empirical studies may be better suited than blade-strike models when evaluating turbine operations.

Turbine blade-strike model results for juvenile salmon and sea trout passing the Stornorrfors Power Station corresponded well with the available empirical estimates of mortality. Montén (1985) released hatchery Atlantic salmon (n = 32 000; mean length 152 mm) marked with Carlin tags in 1967 at various locations above, within, and below the power station. He recaptured these fish as adults in fisheries through 1971 and estimated that the mortality of test fish passing through the turbine only (not including the outlet tunnel) was 8%. This level was similar to our estimated mortalities of 6.8% for salmon smolts and 8.5% for sea trout smolts based on blade-strike modeling under the (typical) maximum efficiency operation and suggests that blade-strike is the primary mechanism of mortality to juvenile salmon passing these turbines.

However, Montén (1985) also estimated that smolt mortality through the entire Stornorrfors Power Station (turbine and 4 km long outlet tunnel) was 25%, although he acknowledged problems with releases of test fish at the turbine outlet tunnel but did not elaborate on these concerns. Eicher Associates Inc. (1987) related the mortality of juvenile salmonids through Francis turbines and project head using data from 22 survival studies conducted on Pacific salmon (*Oncorhynchus* spp.). By interpolating from their figure 5-1, we estimated that fish mortality would be 28% through a Francis turbines operating at 75 m of head, which would be equivalent to the head at the Stornorrfors Power Station. This is similar to Montén's (1985) estimate of 25% mortality and suggests that the blade-strike model may have substantially underestimated mortality at this power station or that mortality mechanisms such as shear within the runner environment or mortality caused by passage through the turbine outlet tunnel may be major components of overall mortality, as these were not captured by the blade-strike model. Additional field studies will be required to identify any effects to fish from passage through turbine outlet tunnels and resolve the discrepancy between the empirical and model estimates of mortality at this power station.

For juvenile fish passing the Sikfors Power Station, turbine blade-strike model estimates were substantially lower than empirical estimates of mortality. Rivinoja (2005) estimated that mean mortality of radio-tagged hatchery Atlantic salmon and sea trout smolts (n = 90; mean length 212 mm) was 19.2% for fish that passed through the turbine, a 0.6 km long outlet tunnel, and 4 km of river downstream from the power station. The mean length of these fish was similar to that of the upper range of sea trout smolts that we modeled, where estimated mortality from blade-strike was 8.6% under the (typical) maximum load operation. However, direct comparisons between model and empirical estimates were again confounded because the empirical estimates also included potential effects on fish from (*i*) non-strike causes of mortality such as shear, (*ii*) passage through the 0.6 km long outlet

© 2008 NRC Canada

Table 8. Results of combined blade-strike and life cycle modeling of turbine passage mitigation strategies for Atlantic salmon (*Salmo salar*) in the River Vindelälven that pass Francis turbines at the Stornorrfors Power Station on the River Umeälven.

Treatment	Population growth rate (λ)	Relative increase in λ compared with the base case	No. of female salmon from all age classes migrating over the Norrfors Dam on the River Umeälven	Relative increase in the no. of female salmon passing the Norrfors Dam compared with the base case
Base case – existing condition	1.0921 (1.0897–1.0953)[a]	NA	905 (862–966)[a]	NA
Alternative 1: smolt survival through turbines = 1.0	1.1066	1.3%	1205	33.2%
Alternative 2: kelt survival through turbines = 1.0	1.0975	0.5%	993	9.7%
Alternative 3: smolt and kelt survival through turbines = 1.0	1.1120	1.8%	1319	45.8%

Note: Results are for Unit IV, the largest of four turbine units. We did not model other turbine units or operations because results from blade-strike modeling suggested the differences among units and operations were minor (Table 6).

[a]Base case values in parentheses are estimated λ and number of female salmon escaping over the dam based on a range of estimated blade-strike mortalities developed by adjusting fish lengths (Table 6).

Table 9. Results of combined blade-strike and life cycle modeling of turbine passage mitigation strategies for Atlantic salmon (*Salmo salar*) passing Kaplan turbines at the Sikfors Power Station on the River Piteälven.

Treatment	Population growth rate (λ)	Relative increase in λ compared with the base case	No. of female salmon from all age classes migrating over the Sikfors Dam on the River Piteälven	Relative increase in the no. of female salmon passing the Sikfors Dam compared with the base case
Base case – existing condition	1.0606 (1.0585–1.0630)[a]	NA	234 (225–245)[a]	NA
Alternative 1: smolt survival through turbines = 1.0	1.0714	1.0%	288	23.1%
Alternative 2: kelt survival through turbines = 1.0	1.0795	1.8%	323	38.0%
Alternative 3: smolt and kelt survival through turbines = 1.0	1.0902	2.8%	394	68.4%

Note: We did not model different turbine operations because results from blade-strike modeling suggested the differences were minor based on overlapping confidence intervals (Table 6).

[a]Base case values in parentheses are estimated λ and number of female salmon escaping over the dam based on a range of estimated blade-strike mortalities developed by adjusting fish lengths (Table 6).

© 2008 NRC Canada

Fig. 5. Tornado diagrams of standardized regression coefficients (coefficient divided by its standard error) from sensitivity analyses of the relative importance these parameters have on the estimated the number of female salmon produced in the River Piteälven: (*a*) results for blade-strike model parameters; (*b*) results for life cycle model parameters.

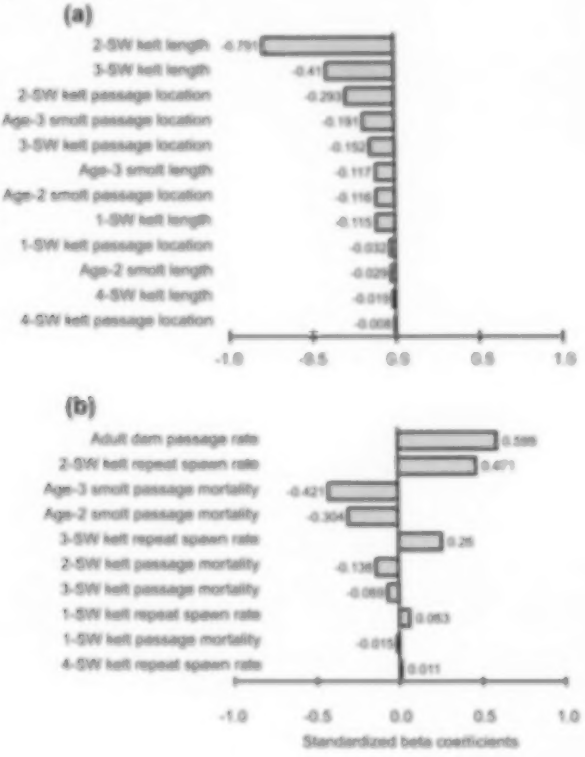

Fig. 6. Tornado diagrams of standardized regression coefficients (coefficient divided by its standard error) from sensitivity analyses of the relative importance these parameters have on the estimated the number of female salmon produced in the River Vindelälven: (*a*) results for blade-strike model parameters; (*b*) results for life cycle model parameters.

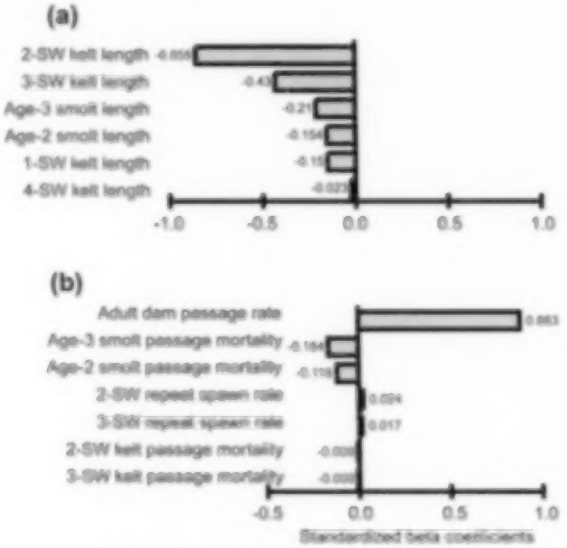

tunnel, and (*iii*) mortality that occurred in the river environment below the power station from having passed through the station.

Empirical data on the survival of kelts through turbines is very limited and is generally represented by extremely small sample sizes, as was the case in the rivers studied here. Östergren (2006) estimated that 11 of 16 radio-tagged sea trout that migrated downstream in the River Vindelälven in 2005 were lost during passage through the Stornorrfors Power Station, including one trout that was detected and found dead on the turbine intake trashracks. This estimated mortality of 69% was higher than mean blade-strike mortality of 32.5% under the maximum efficiency operation. Östergren (2006) also estimated that 3 of 12 (25%) radio-tagged sea trout kelts in the River Piteälven died during passage through the Sikfors Power Station in 2004. This estimated mortality rate was nearly identical to the mean blade-strike mortality of 25.2% from the blade-strike model under the maximum load operation. All three of the sea trout mortalities were associated with passage through the turbines, and none were found dead on the trashracks.

Because our approach was exploratory in nature and limited to qualitative assessments, we were relatively satisfied with the blade-strike model results. Although we introduced some variance into the results by modeling mortality for fish of different lengths, additional studies using stochastic techniques that incorporate information on the variability in fish orientation and distribution relative to the turbine blades under applicable turbine operations would be required to quantitatively assess differences in model outputs among study groups. However, the methods described here were developed specifically for this type of data-poor situation. Overall, the results indicated that blade-strike modeling could be used to make inferences regarding the relative level of mortality among alternatives when differences in mortality among fish groups are large. Also, Deng et al. (2007) compared results from deterministic (and stochastic) blade-strike models and found that strike probabilities were comparable with results of prototype-scale, well-replicated survival studies at two Columbia River dams equipped with Kaplan turbines.

Combining turbine blade-strike and life cycle models

Combining turbine blade-strike and life cycle models produced a simple method for assessing how salmon populations in different rivers responded to hypothetical strategies for mitigating fish mortality attributed to passing turbines at power stations. As expected, hypothetical measures that eliminated mortality to juvenile and adult salmon from passage through turbines increased population growth rates and the number of females escaping above each dam in both rivers. However, the utility of the combined model approach is best demonstrated by the salmon kelt data. For this life history stage, estimated survival through turbines at dams in different rivers was similar based on blade-strike model results. Use of this information alone would suggest that

© 2008 NRC Canada

actions to improve kelt survival past dams would result in similar benefits to the salmon populations in both rivers. However, the two salmon populations responded differently to reductions in kelt mortality during dam passage; the River Piteälven population increased 38% in response to Alternative 2, while the River Vindelälven population increased only 10%.

This differential response may have resulted from the River Piteälven salmon population starting at a much lower initial level of abundance. Alternatively, it may have resulted from only 30% of the adults passing the fish ladder near the Stornorrfors Power Station and entering the River Vindelälven. Resolution of this passage issue would undoubtedly affect the response of salmon in the River Vindelälven to the mitigation strategies modeled here.

When we relate these findings to existing population productivity, we note that the estimated production in 2005 in the River Piteälven was 19 700 smolts from an average of 157 females that escaped over the dam each year in 2000 and 2001, although the production capacity has been estimated at 46 000 smolts (95% probability interval: 32 000 to 67 000; International Council for the Exploration of the Sea 2005). In our study, protecting both smolts and kelts from turbine-induced mortality resulted in 160 additional female salmon escaping over the dam annually after 20 years, and this additional escapement would approximately double the estimated production of smolts observed in 2005 and achieve 86% of the estimated production capacity of the available habitat. It would also exceed the interim management goal of increasing wild salmon production in Baltic rivers to 50% of their capacity (International Council for the Exploration of the Sea 2005). Estimated smolt production in the River Vindelälven was 97 000 smolts in 2005, from an average of 776 females that escaped over the dam each year in 2000 and 2001, and the production capacity has been estimated at 83 000 smolts (95% probability interval: 32 000 to 1 960 000; International Council for the Exploration of the Sea 2005). Mitigation strategies that protected both smolts and kelts from turbine-induced mortality in this river resulted in 414 additional female salmon escaping over the dam annually after 20 years.

If the most probable estimate of production capacity along with the estimated smolt production levels for 2005 are accurate, our findings indicate that actions taken to protect salmon migrating downstream in the River Piteälven may produce a proportionately greater response from the existing population and available habitat than would similar actions in the River Vindelälven. However, the extremely wide probability interval associated with the estimated production capacity of habitat in the River Vindelälven suggests there is high uncertainty associated with the estimate. If the amount of available habitat is actually toward the higher end of the probability interval and the proportion of adults passing over the dam and into the River Vindelälven is increased from its current level (30%), the proportionate response of salmon in both rivers to actions taken to protect downstream migrants may be similar. Clearly, there is more capacity to produce smolts in the River Vindelälven than in the River Piteälven, but additional density-dependent model studies would be required to elucidate these issues further.

Only small improvements in survival appeared achievable through alternative turbine operations based on blade-strike model results, which suggests that changing operations alone would not greatly improve the productivity of salmon and sea trout populations in the rivers studied. Additional measures will be required to reduce the proportion of juveniles and kelts passing through turbines to reach stock conservation goals, such as installing surface-oriented guidance devices (Scruton et al. 2002) or outlets through spillways or powerhouses (Johnson et al. 2005).

The bulk of the available information on fish passage survival through dam turbines is based on empirical studies that used mark–recapture techniques including radio and acoustic telemetry and the detection or recapture of PIT- or balloon-tagged fish. These estimates are often for specific fish species, age classes, turbine types, and operations. They offer a rich source of data that could be used instead of blade-strike estimates as input parameters to life cycle models based on the approach discussed here. For example, if the estimated mortality of age-2 and age-3 salmon smolts passing through the Sikfors Power Station was 19% (Rivinoja 2005), the relative increase in the number of female salmon passing Sikfors Dam under Alternatives 1 and 3 would be 122.2% and 200.9%, respectively, which was substantially larger than was reported. Thus, empirical and model estimates of mortality could be used as a sensitivity analysis to help to identify critical uncertainties and prioritize future field research.

While we incorporated variance into the base cases by assuming different fish lengths and rerunning the blade-strike models, this variance could not be incorporated into the alternatives tested because these scenarios simply assumed that mortality from blade-strike was eliminated. Incorporating environmental and demographic stochasticity into future model applications would allow differences among treatments to be tested statistically and aid the interpretation of results. For example, incorporating density dependence into the life cycle models would expand their utility and allow dam passage mitigation strategies to be compared with other mitigation measures, such as changes to habitat, hatchery production, and harvest rates (Scheuerell et al. 2006).

Fishery managers often want to know whether populations at low abundance levels are at risk from environmental stochasticity, which may be exacerbated by mortality caused by passage through turbines and other dam passage routes. Analyses of whether mitigation strategies for turbine passage mortality reduce the probability that a population will reach a quasi-extinction threshold or shrink to a specified fraction of its current size could be added to future analyses using the model combination described here (Caswell 2001; Morris and Doak 2002).

Our analyses incorporated the potential impacts to fish population productivity from mortality that occurs to downstream-migrating kelts passing turbines at dams. However, upstream-migrating adults of both semelparous and iteroparous fish species in large river systems can overshoot (stray) past their natal river as part of normal, adaptive behaviors (Quinn 2005). In regulated rivers, these fish must pass dams as they move downstream to find their natal river (Boggs et al. 2004), and incorporating the potential impact this mortal-

© 2008 NRC Canada

ity has on population productivity may be warranted in large, regulated river systems with multiple dams.

Atlantic salmon stocks can disply considerable variability in life history strategies. For example, Niemelä et al. (2006) reported that adult salmon in the River Teno located between Finland and Norway displayed a total of 96 age–group combinations (smolts, 2–8 years; adults, 1–5 SW), and repeat spawners displayed 68 of these combinations. This life history diversity can have important effects on population viability (McElhany et al. 2000) by spreading the risk of encountering a catastrophic event across age classes and perhaps space and time. The modeling approach outlined here did not evaluate the potential effects of mortality to kelts during passage through turbines on salmon population viability, as this would require additional types of model studies. However, given the results reported in this paper, where protecting kelts from passage mortality resulted in substantial increases in salmon population productivity, these types of analyses appear warranted.

Sensitivity analyses

The variability in the number of female salmon produced in the River Vindelälven after 20 years is dependent almost exclusively on the passage rate of adults over Norrfors Dam, whereas the number produced in the River Piteälven is influenced by five parameters, including adult dam passage rate, 2- and 3-SW kelt repeat spawn rate, and age-2 and age-3 smolt passage mortality at the dam. This suggests that salmon populations in the two rivers were differentially affected by the dam located in each migratory corridor, which comports with the combined model results. Since 70% of the adults in the River Vindelälven are not able to spawn and enter kelt age classes, the productivity of this population is currently influenced primarily by dam passage mitigation strategies that protected smolts (Alternatives 1 and 3). In contrast, the productivity of the salmon population in the River Piteälven is benefitting from higher adult dam passage rates (65%–100%) and the kelts from these adults. Thus, this population responded positively to mitigation strategies that protected 2- and 3-SW kelts (Alternatives 2 and 3). Interestingly, although the 2- and 3-SW adult age classes are responsible for most of the productivity of the salmon populations in both rivers (based on life cycle model results not reported), the 2- and 3-SW kelts produced from these adults in the River Vindelälven have almost no effect of the variability in the number of female salmon returning to spawn after 20 years. This type of information is also useful in assessing future studies to reduce uncertainty in influential parameters.

Combined model approach

The combined model approach takes an important step in analyzing some of the effects on fish from dams placed in migratory corridors by evaluating impacts at the population level and can be used to inform the relative effects among fish populations, rivers, and dams from passage through turbines. It offers a basic approach that can be applied to situations where fish passage behavior and survival past dams are unknown, but basic demographic information for populations of interest is available and used to prioritize future research and mitigation efforts. It can also be modified further to address more complex questions of resource managers about population-level responses.

When applied to Atlantic salmon populations in two rivers in northern Sweden, the two populations responded differently to strategies for mitigating mortality caused by fish striking turbine blades and in ways not predicted by estimates of passage mortality through turbines alone. The results pointed out the benefits from protecting kelts in addition to juveniles because of their contribution to population productivity. This suggests a need to rethink the current emphasis placed on protecting only juveniles from dam passage mortality and consider the benefits of protecting kelts as well. Applying the combined model approach described in this paper to other situations can help conserve fish populations affected by the many dams installed in migratory corridors throughout the world.

Acknowledgements

We thank Johan Östergren from the Swedish University of Agricultural Sciences (SLU) for providing Fig. 1; Peter Rivinoja (SLU) for providing the adult count and length–frequency data; and Penni Mahon and James Peacock of NOAA Fisheries for providing considerable help in developing Figs. 1–6. The manuscript was considerably improved as a result of thoughtful review comments by Thomas Carlson, Doug Dey, Correigh Greene, John G. Williams, and three anonymous referees.

References

Battin, J., Wiley, M.W., Ruckelshaus, M.H., Palmer, R.N., Korb, E., Bartz, K.K., and Imaki, H. 2007. Projected impacts of future climate change on salmon habitat restoration actions in a Puget Sound river. Proc. Natl. Acad. Sci. U.S.A. **104**: 6720–6725. doi:10.1073/pnas.0701685104. PMID:17412830.

Bell, M. 1991. Revised compendium on the success of passage of small fish through turbines. Report to US Army Corps of Engineers, Portland, Oreg.

Boggs, C., Keefer, M., Peery, C., Bjornn, T., and Stuehrenberg, L. 2004. Fallback, reascension, and adjusted fishway escapement estimates for adult Chinook salmon and steelhead at Columbia and Snake River dams. Trans. Am. Fish. Soc. **133**: 932–949. doi:10.1577/T03-133.1.

Čada, G. 2001. The development of advanced hydroelectric turbines to improve fish passage survival. Fisheries, **26**: 14–23.

Calles, O. 2005. Re-establishment of connectivity for fish populations in regulated rivers. Ph.D. thesis, Division of Environmental Sciences, Karlstad University, Karlstad, Sweden. ISSN: 1403-8099; ISBN 91-7063-028-3. Available from www.vattenkraftmiljo.nu/Dokument/Greenberg_2.pdf [accessed 31 October 2007].

Caswell, H. 2001. Matrix population models. Sinauer Associates, Inc., Sunderland, Mass.

Cross, P., and Beissinger, S. 2001. Using logistic regression to analyze the sensitivity of PVA models: a comparison of methods based on African wild dogs. Conserv. Biol. **15**: 1335–1346. doi:10.1046/j.1523-1739.2001.00031.x.

Deng, Z., Carlson, T., Ploskey, G., Richmond, M., and Dauble, D. 2007. Evaluation of blade-strike models for estimating the biological performance of Kaplan turbines. Ecol. Model. **208**: 165–176. doi:10.1016/j.ecolmodel.2007.05.019.

Ducharme, L. 1969. Atlantic salmon returning for their fifth and

© 2008 NRC Canada

sixth consecutive spawning trips. J. Fish. Res. Board Can. **26**: 1661–1664.

Eicher Associates Inc. 1987. Turbine-related fish mortality: review and evaluation of studies. Rep. EPRI-AP-5480 to Electric Power Research Institute, Palo Alto, Calif.

Evans, A., Beaty, R., Fitzpatrick, M., and Collis, K. 2004. Identification and enumeration of steelhead kelts at a Snake River hydroelectric dam. Trans. Am. Fish. Soc. **133**: 1089–1099. doi:10.1577/T03-121.1.

Ferguson, J., Matthews, G., McComas, R.L., Absolon, R., Brege, D., Gessel, M., and Gilbreath, L. 2005. Passage of adult and juvenile salmonids through federal Columbia River power system dams. US Department of Commerce, Washington, D.C. NOAA Tech. Memo. NMFS-NWFSC-64. Available from www.nwfsc.noaa.gov/assets/25/6048_04222005_105920_fishpassagetm64final.pdf [accessed 31 October 2007].

Fleming, I.A. 1998. Pattern and variability in the breeding system of Atlantic salmon (*Salmo salar*), with comparisons to other salmonids. Can. J. Fish. Aquat. Sci. **55**(Suppl. 1): 59–76. doi:10.1139/cjfas-55-S1-59.

Franke, G., Webb, D., Fisher, R., Jr., Mathur, D., Hopping, P., March, P., Headrick, M., Laczo, I., Ventikos, Y., and Sotiropoulos, F. 1997. Development of environmentally advanced hydropower turbine system design concepts. Voith Hydro, Inc., Rep. No. 2677-0141 to US Department of Energy, Idaho Falls, Id. Contract DE-AC07-96ID13382.

International Council for the Exploration of the Sea. 2005. Report of the Baltic Salmon and Trout Assessment Working Group (WGBAST), 5–14 April 2005, Helsinki, Finland. ICES CM 2005 / ACFM:18.

International Council for the Exploration of the Sea. 2007. Report of the Baltic Salmon and Trout Assessment Working Group (WGBAST), 11–20 April 2007, Vilnius, Lithuania. ICES CM 2007 / ACFM:12.

Johnson, G., Anglea, S., Adams, N., and Wik, T. 2005. Evaluation of a prototype surface flow bypass for juvenile salmon and steelhead at the powerhouse of Lower Granite Dam, Snake River, Washington, 1996–2000. N. Am. J. Fish. Manag. **25**: 138–151. doi:10.1577/M04-024.1.

Jonsson, B. 1985. Life history patterns of freshwater resident and sea-run migrant brown trout in Norway. Trans. Am. Fish. Soc. **114**: 182–194. doi:10.1577/1548-8659(1985)114<182:LHPOFR>2.0.CO;2.

Liscom, K., Stuehrenberg, L., and Ossiander, F. 1985. Radiotracking studies of adult Chinook salmon and steelhead to determine the effect of "zero" river flow during water storage at Little Goose Dam on the lower Snake River. Report to Bonneville Power Administration, Contract DE-AI79-81BP27780. Available from Northwest Fisheries Science Center, Fish Ecology Division, Seattle, Wash.

Lundqvist, H., Öhlund, G., Karlsson, L., Larsson, S., Carlsson, U., Alanärä, A., Kiessling, A., Eriksson, L., Leonardsson, K., Östergren, J., and Nilsson, J. 2006. Salmon and sea trout migration in Sävarån 2005: study to determine Sävarån as a potential index river for Swedish forest rivers. Report to ICES Baltic Salmon and Trout Assessment Working Group, Work. Pap. No. 11. Swedish University of Agricultural Sciences, Department of Aquaculture, Umeå, Sweden. Rep. No. 50. Available from www.vfm.slu.se/ [accessed 31 October 2007].

Mathur, D., Heisey, P., Skalski, J., and Kenney, D. 2000. Salmonid smolt survival relative to turbine efficiency and entrainment depth in hydroelectric power generation. Journal of the American Water Resources Association, **36**: 737–747. doi:10.1111/j.1752-1688.2000.tb04302.x.

McClure, M., Holmes, E., Sanderson, B., and Jordan, C. 2003. A large-scale, multispecies status assessment: anadromous salmonids in the Columbia River basin. Ecol. Appl. **13**: 964–989. doi:10.1890/1051-0761(2003)13[964:ALMSAA]2.0.CO;2.

McElhany, P., Ruckelshaus, M., Ford, M., Wainwright, T., and Bjorkstedt, E. 2000. Viable salmonid populations and the recovery of evolutionarily significant units. NOAA Tech. Memo. NMFS-NWFSC-42. Available from www.nwfsc.noaa.gov/assets/25/5561_06162004_143739_tm42.pdf [accessed 10 May 2007].

Montén, E. 1985. Fish and turbines: fish injuries during passage through power station turbines. Vattenfall AB, Stockholm, Sweden.

Morris, W., and Doak, D. 2002. Quantitative conservation biology: theory and practice of population viability analysis. Sinauer Associates, Inc., Sunderland, Mass.

Moursund, R.A., and Carlson, T.J. 2004. Turbine imaging technology assessment. Pacific Northwest National Laboratory, Rep. No. PNNL-14759 to US Department of Energy, Contract DE-AC05-76RL01830, Richland, Wash. Available from www.pnl.gov/main/publications/external/technical_reports/PNNL-14759.pdf [accessed 8 May 2007].

Muir, W., Smith, S., Williams, J., and Sandford, B. 2001. Survival of juvenile salmonids passing through bypass systems, turbines, and spillways with and without flow deflectors at Snake River dams. N. Am. J. Fish. Manag. **21**: 135–146. doi:10.1577/1548-8675(2001)021<0135:SOJSPT>2.0.CO;2.

National Research Council. 1996. Upstream: salmon and society in the Pacific Northwest. National Academy Press, Washington, D.C.

Niemelä, E., Erkinaro, J., Julkunen, M., Hassinen, E., Länsman, M., and Brørs, S. 2006. Temporal variation in abundance, return rate and life histories of previously spawned Atlantic salmon in a large subarctic river. J. Fish Biol. **68**: 1222–1240. doi:10.1111/j.0022-1112.2006.001012.x.

Östergren, J. 2006. Migration and genetic structure of *Salmo salar* and *Salmo trutta* in northern Swedish rivers. Ph.D. thesis, Swedish University of Agricultural Sciences, Department of Aquaculture, Umeå, Sweden. Available from diss-epsilon.slu.se/archive/00001290/01/Paper-0-JO-Kappan.pdf [accessed 31 October 2007].

Parrish, D., Behnke, R., Gephard, S., McCormick, S., and Reeves, G. 1998. Why aren't there more Atlantic salmon (*Salmo salar*)? Can. J. Fish. Aquat. Sci. **55**(Suppl. 1): 281–287. doi:10.1139/cjfas-55-S1-281.

Pavlov, D., Lupandin, A., and Kostin, V. 2002. Downstream migration of fish through dams of hydroelectric power plants. [In Russian. English translation by T. Albert and *Edited by* G.F. Čada. Oak Ridge National Laboratory, Oak Ridge, Tenn. Rep. ORNL/TR-02/02.]

Ploskey, G., and Carlson, T. 2004. Comparison of blade-strike modeling results with empirical data. Battelle Pacific Northwest National Laboratory Rep. No. PNNL-14603 to US Army Corps of Engineers, Portland, Oreg. Available from www.pnl.gov/main/publications/external/technical_reports/PNNL-14603.pdf [accessed 6 November 2007].

Quinn, T.P. 2005. The behavior and ecology of pacific salmon and trout. University of Washington Press, Seattle, Wash.

Rivinoja, P. 2005. Migration problems of Atlantic salmon (*Salmo salar* L.) in flow regulated rivers. Ph.D. thesis, Swedish University of Agricultural Sciences, Department of Aquaculture, Umeå, Sweden. Available from diss-epsilon.slu.se/archive/00000987/01/PAPER_0_FINAL_in_Thesis_e-version.pdf [accessed 31 October 2007].

© 2008 NRC Canada

Romakkaniemi, A., Perä, I., Karlsson, L., Jutila, E., Carlsson, U., and Pakarinen, T. 2003. Development of wild Atlantic salmon stocks in the rivers of the northern Baltic Sea in response to management measures. ICES J. Mar. Sci. **60**: 329–342. doi:10.1016/S1054-3139(03)00020-1.

Ruggles, C., Robinson, D., and Stira, R. 1993. The use of floating louvers for guiding Atlantic salmon (*Salmo salar*) smolts from hydroelectric turbine intakes. Can. Tech. Rep. Fish. Aquat. Sci. No. 1905. pp. 87–94.

Scheuerell, M., Hilborn, R., Ruckelshaus, M., Bartz, K., Lagueux, K., Haas, A., and Rawson, K. 2006. The Shiraz model: a tool for incorporating fish-habitat relationships in conservation planning. Can. J. Fish. Aquat. Sci. **63**: 1596–1607. doi:10.1139/F06-056.

Scruton, D., McKinley, R., Kouwen, N., Eddy, W., and Booth, R. 2002. Use of telemetry and hydraulic modeling to evaluate and improve fish guidance efficiency at a louver and bypass system for downstream-migrating Atlantic salmon (*Salmo salar*) smolts and kelts. Hydrobiologia, **483**: 83–94. doi:10.1023/A:1021350722359.

Simmons, R. 2000. Effectiveness of a fish bypass with an angled bar rack at passing Atlantic salmon and steelhead trout smolts at the Lower Saranac Hydroelectric Project. *In* Advances in fish passage technology: engineering design and biological evaluation. *Edited by* M. Odeh. American Fisheries Society, Bioengineering Section, Bethesda, Md. pp. 95–102.

Skalski, J., Mathur, D., and Heisey, P. 2002. Effects of turbine operating efficiency on smolt passage survival. N. Am. J. Fish. Manag. **22**: 1193–1200. doi:10.1577/1548-8675(2002)022<1193:EOTOEO>2.0.CO;2.

Turnpenny, A. 1998. Mechanisms of fish damage in low-head turbines: an experimental appraisal. *In* Fish migration and fish bypasses. *Edited by* M. Jungwirth, S. Schmutz, and S. Weiss. Fishing News Books, Blackwell Science Ltd., Oxford, UK. pp. 300–314.

Turnpenny, A., Clough, S., Hanson, K., Ramsay, R., and McEwan, D. 2000. Risk assessment for fish passage through small, low-head turbines. Final Report. Energy Technical Support Unit, Harwell, UK.

Von Raben, K. 1957. Regarding the problem of mutilations of fishes by hydraulic turbines. Originally published in Die Wasserwirtschaft, **4**: 97–100. [In German; English translation: Fish. Res. Board Can. Translation Series No. 448, 1964.]

Wagner, E., and Ingram, P. 1973. Evaluation of fish facilities and passage at Foster and Green Peter Dams on the South Santiam River drainage in Oregon. Rep. No. DACW57-68-C-0013 by the Fish Commission of Oregon to US Army Corps of Engineers, Portland, Oreg.

Williams, J., Smith, S., Zabel, R., Muir, W., Scheuerell, M., Sandford, B., Marsh, D., McNatt, R., and Achord, S. 2005. Effects of the federal Columbia River power system on salmonid populations. NOAA Tech. Memo. NMFS-NWFSC-63. Available from www.nwfsc.noaa.gov/assets/25/6061_04142005_152601_effectstechmemo63final.pdf [accessed 31 October 2007].

Winter, H.V., and Van Densen, W.L. 2001. Assessing the opportunities for upstream migration of non-salmonid fishes in the weir regulated River Vecht. Fish. Manag. Ecol. **8**: 513–532. doi:10.1046/j.1365-2400.2001.00271.x.

World Commission on Dams. 2000. Dams and development: and new framework for decision-making. Earthscan Publications, London, England.

Zabel, R., Scheuerell, M., McClure, M., and Williams, J. 2006. The interplay between climate variability and density dependence in the population viability of Chinook salmon. Conserv. Biol. **20**: 190–200. doi:10.1111/j.1523-1739.2005.00300.x. PMID: 16909672.

Zigler, S., Dewey, M., Knights, B., Runstrom, A., and Steingraeber, M. 2004. Hydrologic and hydraulic factors affecting passage of paddlefish through dams in the upper Mississippi River. Trans. Am. Fish. Soc. **133**: 160–172. doi:10.1577/T02-161.

Appendix A. Kaplan turbine blade-strike model formulation

Using a spreadsheet, we proceeded sequentially from eqs. A1 through A10 to estimate the probability of blade-strike (P) in eq. 1. All spreadsheet entries were in metres unless noted otherwise. A schematic of the angular geometry used in turbine blade-strike model formulation is provided in Fig. 3. We first calculated the axial velocity of water at the turbine blades (V_{axial}):

$$\text{(A1)} \qquad V_{axial} = \frac{Q}{A_{blade}}$$

where Q is turbine discharge ($m^3 \cdot s^{-1}$) and A_{blade} is the area swept by the blades, which was calculated as

$$\text{(A2)} \qquad A_{blade} = \pi\left(D^2 - H^2\right)$$

where D is the radius of the blades at their tip, and H is the radius of the blades at their base (i.e., the radius of the runner hub where the blades are attached).

To estimate θ, a series of calculations were required that begin at the wicket gate and end at the turbine blades. The law of constant angular momentum was used to calculate the absolute water (and fish) velocity at the blades (V_1) from calculations of water passing through the wicket gates. First, we calculated the axial velocity of the water at the wicket gates ($V_{axialwg}$):

$$\text{(A3)} \qquad V_{axialwg} = \frac{Q}{A_{wg}}$$

where A_{wg} is the surface area the water passes through at the wicket gates. We defined A_{wg} as an imaginary vertical cylinder that extended from the center of the turbine shaft outward and touched the downstream tips of all wicket gates. The rotating element of a Kaplan turbine is called a runner. The runner consists of a hub with blades attached to it, and the blades are shaped so that pressure differences across the blades impose lift forces, which cause the runner to rotate. We used the radius of the runner as an estimate of the radius of the imaginary cylinder:

$$\text{(A4)} \qquad A_{wg} = 2\pi \cdot R_{wg} \cdot H_{wg}$$

where R_{wg} is the radius of the vertical imaginary cylinder, and H_{wg} is the height of the wicket gate. Next, we calculated the tangential water velocity at the wicket gate (V_{twg}):

$$\text{(A5)} \qquad V_{twg} = \frac{V_{axialwg}}{\tan(\mathrm{WGA})}$$

where WGA is the wicket gate angle ( ). We then calculated the tangential velocity at the runner entrance (V_1), which was proportional to V_{twg} at the wicket gate multiplied by

© 2008 NRC Canada

the ratio of the radial distance from the center of the runner at two respective elevations:

$$V_t = \frac{V_{wg} \cdot R_{wg}}{r} \quad \text{(A6)}$$

where r is the radius of a circle extending to the midpoint along the blade, the point at which we assumed fish passed the blade. Next, we estimated the angle (°) between the tangential and absolute velocity vectors (α) as

$$\alpha = \sin^{-1}\left(\frac{V_{axial}}{V_1}\right) \quad \text{(A7)}$$

where $\sin^{-1}$ is the arcsine (inverse sine) of V_{axial} divided by the V_1 at the runner, where V_1 is defined as

$$V_1 = (V_{axial}^2 + V_t^2)^{0.5} \quad \text{(A8)}$$

We then defined the angle (°) between the axial and absolute water velocity vectors (θ) as

$$\theta = 90^\circ - \alpha \quad \text{(A9)}$$

Next, we calculated the length of water (WL) passing between two turbine blades as

$$\text{WL} = \frac{V_{axial}}{\left(\frac{\cos\theta \cdot N \cdot \pi}{60}\right)} \quad \text{(A10)}$$

Finally, we calculated P as fish length (l) divided by WL (eq. 1):

$$P = \left(\frac{n \cdot N}{60}\right)\left(\frac{l \cdot \cos\theta}{V_{axial}}\right) \quad \text{(A11)}$$

Appendix B. Francis turbine blade-strike model formulation

Using a spreadsheet, we proceeded sequentially from eqs. B1 through B6 to estimate the probability of blade-strike (P) in eq. 2. All spreadsheet entries were in metres unless noted otherwise. A schematic of the angular geometry used in turbine blade-strike model formulation is provided in Fig. 4. We first calculated the area of the turbine flow passageway inlet:

$$A = \pi \cdot H_{wg} \cdot R_{wheel} \quad \text{(B1)}$$

where R_{wheel} is the diameter of the wheel (or runner as it is commonly referred to), and H_{wg} is the height of the wicket gate. Next, we calculated the radial velocity of water flow at the runner entrance (V_r):

$$V_r = \frac{Q}{A} \quad \text{(B2)}$$

where Q is turbine discharge ($m^3 \cdot s^{-1}$). We then calculated the velocity of the rotating blades (u_1):

$$u_1 = \left(\frac{2\pi \cdot N}{60}\right)\left(\frac{R_{wheel}}{2}\right) \quad \text{(B3)}$$

where N is the rotation speed of the blades in revolutions per minute. This was followed by a calculation of the tangential velocity of water flow at the runner entrance (V_t):

$$V_t = u_1 - (V_r \cdot \tan 10^\circ) \quad \text{(B4)}$$

where tan 10° is the tangent to the runner. Since blade angle (β), or the angle between the velocity components v and u, must be established to determine tan 10°, but is typically unknown, we assumed β was 100° based on Bell (1991), which produced a tangent of 10°. Next, we calculated the absolute velocity of water flow at the runner (V_1):

$$V_1 = \sqrt{(V_t^2 + V_t^2)} \quad \text{(B5)}$$

We then calculated sin α, where α is the flow angle between V_1 and tan 10°:

$$\sin\alpha = \frac{V_t}{V_1} \quad \text{(B6)}$$

Finally, we calculated P with this information as follows, where n is the number of blades and l is fish length (eq. 2):

$$P = \left(\frac{n \cdot N}{60}\right)\left(\frac{l \cdot \sin\alpha}{V_t}\right) \quad \text{(B7)}$$

Reference

Bell, M. 1991. Revised compendium on the success of passage of small fish through turbines. Report to US Army Corps of Engineers, Portland, Oreg.

© 2008 NRC Canada

Parameterizing age-structured models from a fisheries management perspective

Steven J.D. Martell, William E. Pine III, and Carl J. Walters

Abstract: Age-structured models are widely used in fisheries stock assessments and contain two very important parameters that determine the rate and amount of harvest that can be safely taken: the compensation rate in juvenile survival (α) and the unfished biomass (B_0). These two parameters are often confounded. It is common for relative abundance indices to lack contrast, and the use of informative priors, or fixing at least one of these parameters, is necessary to develop management advice. Providing management advice proceeds by transforming estimates of biological variables such as B_0 and α into management variables such as the maximum sustainable yield (C^*) and the fishing mortality rate that would achieve this yield (F^*). There is no analytical solution for the transformation of B_0, α to C^*, or F^* for age-structured models with commonly used stock–recruitment functions and therefore must be done numerically. The opposite transition, however, does have an analytical solution for both the Beverton–Holt and Ricker recruitment models with partial selectivities for all age classes. Use of these analytical solutions allows for age-structured assessment models to be directly parameterized in terms of the management variables C^* and F^*. The effects of informative priors on C^* and F^* on the results of the assessment model are completely transparent to management.

Résumé : Les modèles structurés en fonction de l'âge, qui sont couramment utilisés dans l'évaluation des stocks en pêches commerciales, contiennent deux variables très importantes qui déterminent le taux et l'importance de la récolte qui peut être réalisée sans danger, soit le taux de compensation dans la survie des jeunes (α) et la biomasse non exploitée (B_0). Ces deux variables sont souvent confondues. Il arrive fréquemment que les coefficients d'abondance relative ne fassent pas la distinction et il est nécessaire, afin d'obtenir des avis de gestion, d'utiliser des informations a priori ou de corriger au moins une de ces variables. Pour fournir des avis des gestion, il faut transformer les estimations des variables biologiques, telles que B_0 et α, en variables de gestion, telles que le rendement soutenu maximal (C^*) et le taux de mortalité dû à la pêche qui produit ce rendement (F^*). Il n'existe pas de solution analytique pour la transformation de B_0, α en C^*, ou F^* dans les modèles structurés en fonction de l'âge avec les fonctions de stock–recrutement en usage courant et il est ainsi nécessaire de le faire numériquement. La transformation inverse, cependant, possède une solution analytique, tant pour le modèle de recrutement Beverton–Holt que pour celui de Ricker, avec des sélectivités partielles pour toutes les classes d'âge. L'utilisation de ces solutions analytiques permet d'obtenir directement les variables de gestion C^* et F^* pour les modèles d'évaluation structurés en fonction de l'âge. Les effets des informations a priori au sujet de C^* et F^* sur les résultats du modèle d'évaluation sont complètement transparents dans une perspective de gestion.

[Traduit par la Rédaction]

Introduction

The overarching objectives of a fisheries stock assessment are threefold: (*i*) to estimate key population parameters that determine the population scale and productivity (e.g., unfished biomass, B_0, and the Goodyear compensation ratio (Goodyear 1980), here defined as α, or the relative improvement in juvenile survival rate as the spawning stock biomass approaches zero); (*ii*) to estimate the current state of the population relative to a predefined reference point (usually B_0); and (*iii*) to provide short-term projections of the population state subject to alternative harvest policies or the application of a predefined harvest rule (i.e., management advice). The stock assessment process has evolved to also characterize the uncertainty in the management advice primarily through the use of Bayesian approaches (Punt and Hilborn 1997). It is obvious (but sometimes forgotten) that the process of proceeding through steps *i*–*iii* and ultimately providing sound management advice based on this process is conditional on the information in the available data. In steps *i* and *ii*, population dynamics models are often fitted to time series data on relative abundance (i.e., catch-per-unit-effort (CPUE) indices), and the ability to discern between a large, unproductive stock and a small, productive stock requires sufficient contrast in the abundance index (see Hilborn and Walters 1992). Step *iii* involves a transformation of population parameters calculated in the previous steps (e.g., B_0 and the intrinsic rate of growth) into management parameters (e.g., target fishing rate (F^*) and maximum sustainable yield (MSY) (C^*)) and short-term projections of abundance.

Ricker (1975) first demonstrated that there was no analytical solution to transform population parameters to manage-

Received 24 March 2007. Accepted 10 October 2007. Published on the NRC Research Press Web site at cjfas.nrc.ca on 8 July 2008.
J19905

S.J.D. Martell[1] and C.J. Walters. Fisheries Centre, The University of British Columbia, 2202 Main Mall, Vancouver, BC V6T 1Z4, Canada.
W.E. Pine III. Department of Fisheries and Aquatic Sciences, University of Florida, 7922 NW 71st Street, Gainesville, FL 32653, USA.

[1]Corresponding author (e-mail: s.martell@fisheries.ubc.ca).

 doi:10.1139/F08-055 © 2008 NRC Canada

ment parameters for relatively simple nonlinear models (e.g., Ricker stock–recruitment model). Schnute and Kronlund (1996) demonstrated that the opposite transition was possible, and later, Schnute and Richards (1998) extended this approach to age-structured models. The approach of Schnute and Richards (1998) assumed knife-edge recruitment and discrete mortality and, based on these assumptions, demonstrated that this inverse approach improved the statistical properties of characterizing uncertainty. This improvement in assessing uncertainty enhances communication between assessment scientist and resource managers because the parameters being evaluated by the assessment process are directly relevant to policy. Despite these statistical and communicative advantages, to our knowledge there has been no application of this approach in stock assessments.

A common situation in stock assessments is that the relative abundance data lack sufficient contrast that permit the joint estimation of productivity and population-scale parameters. Many of the data sets available to conduct stock assessments consists of one-way trips (persistent decline or increase in relative abundance) or no long-term trend information in relative abundance indices. In such circumstances, a common practice is to use prior information on productivity parameters or derive independent estimates for the constant that relates relative abundance to absolute abundance, or both. The reality of such a practice is that the policy parameter(s), such as the C^{∞} or the F^{∞} that achieves C^{∞}, or both, are defined prior to fitting the models to time series data. There actually is some information about C^{∞} in one-way trip data sets. Consider the simple Schaefer production model where MSY is defined as $C^{\infty} = rK/4$, where r is the intrinsic rate of growth and K is the carrying capacity. For one-way trip data sets, it is well known that r and K are not estimable (Hilborn and Walters 1992), but C^{∞} may be well determined, as r and K are inversely correlated, and the estimate for C^{∞} would be relatively stable as r and K trade off. However, if the relative abundance data show no trend over time, it becomes absolutely necessary to develop informative priors for population-scale parameters.

The principal difference between the simpler Schaefer model and the more complex age-structured model is that the relationship between productivity and F^{∞} or bewteen B_{∞} and C^{∞} is not so transparent in complex, age-structured models. As such, the use of informative priors, or fixed values for scaling parameters, or stock productivity ultimately defines harvest policy in cases where relative abundance data are not informative about these key population parameters. A more transparent approach to this problem is to adopt the management-oriented approach, as first suggested by Schnute and Kronlund (1996), and parameterize age-structured models in terms of F^{∞} and C^{∞} directly. Under this parameterization, the sensitivity of policy parameters to prior distributions or fixed values is completely transparent in the decision-making process.

The main objective of this paper is to change the standard question of how likely are the B_{∞} and κ parameters given the data to how likely are the C^{∞} and F^{∞} hypotheses given the data? Parameters such as B_{∞} and κ ultimately define the harvest policies, yet it is easy to loose sight of this notion when the assessment model contains hundreds of additional parameters to explain, for example, variability in recruitment, temporal changes in selectivity, catchability, and variability in growth. Using fixed values for these key population parameters can be easily overlooked when reviewers are forced to consider model sensitivity with respect to hundreds of nuisance parameters. Using fixed values for κ is equivalent to assuming fixed values for F^{∞} (assuming some constant selectivity), and using fixed values for B_{∞} or parameters that define the overall population scale is equivalent to assuming the overall population scale a priori.

In this paper, we derive analytical relationships between the policy parameters C^{∞} and F^{∞} and parameters that describe the instantaneous dynamics of an age-structured population. The method also allows for partial selectivity of specific age classes, including dome-shaped selectivity curves. We adopt a similar notation of Schnute and Kronlund (1996) and Schnute and Richards (1998) for comparison. All of the models presented here assume that fishing mortality and natural mortality occur simultaneously through the use of the Baranov catch equation. First, we first review the classical numerical transitions between $(B_{\infty}, \kappa) \Rightarrow (C^{\infty}, F^{\infty})$ in a full age-structure model with Beverton–Holt-type recruitment. Second, we parameterize a full age-structured model using (C^{∞}, F^{∞}) as leading parameters and derive (B_{∞}, κ) from (C^{∞}, F^{∞}) conditional on vulnerability and life-history parameters. We then derive the analytical solution for the $(C^{\infty}, F^{\infty}) \Rightarrow (B_{\infty}, \kappa)$ transition using the Ricker model. Finally, we apply the approach developed here to the Pacfic hake (*Merluccius productus*) data using the Beverton–Holt recruitment model and compare the uncertainty in parameter estimates with that of Helser and Martell (2007).

Age-structured model (B_{∞}, κ)

To derive (C^{∞}, F^{∞}) from the unknown parameter vector $\boldsymbol{\Theta}$ and independently derived life-history parameters Φ (defined in Table 1) in an age-structured population dynamics model, we first consider the steady-state conditions for a given fishing mortality rate F_x in an age-structured model (Table 1). In this paper, we assume that life-history parameters Φ are known; however, it is also possible to jointly estimate these parameters if necessary data are available. Note that the sequence of equations laid out in each of the tables describes the model structure and is also intended to represent the order of operations or pseudocode in which to implement the model in a given computer language. Source code for implementations in AD Model Builder (Otter Research Ltd., Sidney, British Columbia) and R (R Development Core Team 2006) are available from the first author upon request.

For the model represented in Table 1, we assume that growth (eqs. T1.4 and T1.5) is independent of density, vulnerability-at-age (eq. T1.6) is represented by a logistic curve, and fecundity-at-age (eq. T1.7) is proportional to body weight times the probability of being sexually mature at a given age. Assuming steady-state conditions, the lifetime reproductive output per individual recruit in an unfished population (unfished eggs per recruit) is simply the product of survivorship (eq. T1.8) and the mean fecundity-at-age; the sum of these products is the unfished eggs per recruit (eq. T1.10). These are also known as incidence functions, after Botsford and Wickham (1979) (see also Botsford

© 2008 NRC Canada

Table 1. Steady-state, age-structured model assuming unequal vulnerability-at-age, age-specific natural mortality, age-specific fecundity, and Beverton–Holt-type recruitment.

Eq. No.	Model definitions
Parameters	
T1.1	$\Theta = (B_0, \kappa, M_a, \tilde{a}, \tilde{\gamma})$
T1.2	$B_0 > 0;\ \kappa > 1;\ M_a > 0$
T1.3	$\phi = (l_0, k, t_0, a, b, \hat{a}, \gamma)$
Age schedule information	
T1.4	$l_a = l_0\ \{1 - \exp[-k(a - t_0)]\}$
T1.5	$w_a = a(l_a)^b$
T1.6	$v_a = \{1 + \exp[-(\hat{a} - a)/\gamma]\}^{-1}$
T1.7	$f_a = w_a\{1 + \exp[-(\hat{a} - a)/\gamma]\}^{-1}$
Survivorship	
T1.8	$\ell_a = \begin{cases} 1, & a = 1 \\ \ell_{a-1}\exp(-M_{a-1}), & a > 1 \end{cases}$
T1.9	$\tilde{\ell}_a = \begin{cases} 1, & a = 1 \\ \tilde{\ell}_{a-1}\exp(-M_{a-1} - F_e v_{a-1}), & a > 1 \end{cases}$
Incidence functions	
T1.10	$\phi_E = \sum_{a=1}^{\infty} \ell_a f_a \qquad \phi_e = \sum_{a=1}^{\infty} \tilde{\ell}_a f_a$
T1.11	$\phi_B = \sum_{a=1}^{\infty} \ell_a w_a v_a \qquad \phi_b = \sum_{a=1}^{\infty} \tilde{\ell}_a w_a v_a$
T1.12	$\phi_y = \sum_{a=1}^{\infty} \frac{\tilde{\ell}_a w_a v_a}{M_a + F_e v_a}[1 - \exp(-M_a - F_e v_a)]$
Steady-state conditions	
T1.13	$R_e = B_e/\phi_B$
T1.14	$R_e = R_o\frac{\kappa - \phi_E/\phi_e}{\kappa - 1}$
T1.15	$C_e = F_e R_e \phi_y$

Note: To implement the Ricker type recruitment, substitute eq. T1.13 with eq. 6.

1981; Walters and Martell 2004), and we reserve the prefix ϕ to represent per-recruit incidence functions and use upper- and lower-case subscripts to denote unfished and fished conditions, respectively. The biomass per recruit is given by eq. T1.11, and eq. T1.11 subscript b is the yield per-recruit incidence function where both natural mortality and fishing mortality are assumed to occur simultaneously (note that $F_e\phi_y$ represents the yield per recruit). The unfished equilibrium age-1 recruits is given by eq. T1.12. In eq. T1.13, we assume that recruitment follows a Beverton–Holt-type relationship of the form

$$(1)\qquad R_e = \frac{s_o E_e}{1 + \beta E_e} = \frac{s_o R_e \phi_e}{1 + \beta R_e \phi_e}$$

where s_o is the maximum survival rate from egg E to age-1 recruit R, which can also be represented as $s_o = \kappa/\phi_E$. β is the density-dependent term defined as $\beta = (\kappa - 1)/(R_o\phi_E)$ in the unfished state. Substituting these expressions for s_o and β into eq. 1 yields

$$R_e = \frac{\kappa R_e \phi_e R_o}{R_o\phi_E + R_e\phi_e\kappa - R_e\phi_e}$$

and solving for R_e gives eq. T1.13. The overall yield C_e for a steady-state fishing mortality rate F_e is given by eq. T1.14.

Fig. 1. (*a*) Equilibrium yield, (*b*) recruits, (*c*) biomass, and (*d*) spawner per recruit (ϕ_e/ϕ_E) versus instantaneous fishing mortality (F_e) for two different values of the recruitment compensation ratio (κ = 12, solid lines; κ = 4, broken lines). Vertical lines in each panel correspond to F°; horizontal lines correspond to various reference points that would achieve C°.

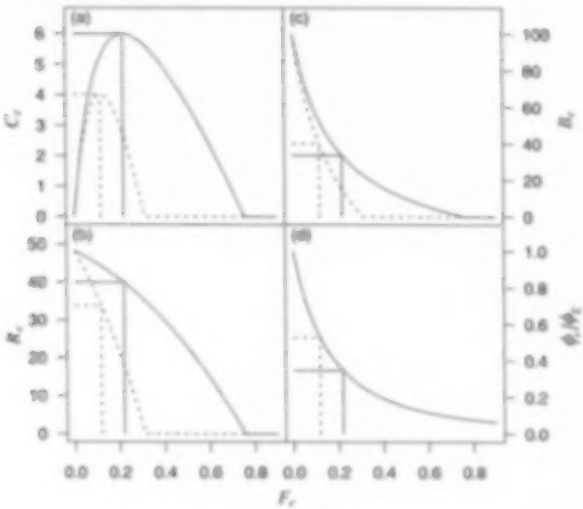

There are two commonly used parameterizations of stock–recruitment models in use today. One is the so-called steepness parameterization, where steepness (h) is defined as the ratio of recruits produced at 20% of the unfished spawning stock biomass and the unfished spawning stock biomass (Mace and Doonan 1988). For the Beverton–Holt model, the values of h range between 0.2 and 1; for the Ricker model, values of h are >0.2. The second parameterization uses κ, which is defined as the relative improvement in survival from egg to recruit as the spawning stock biomass tends towards zero (Goodyear 1980). For both the Ricker and Beverton–Holt models, values of κ must be >1. There are simple analytical transformations to go from $\kappa \Leftrightarrow h$, and we derive these in Appendix B.

$(B_o, \kappa) \Rightarrow (C^{\circ}, F^{\circ})$ transition

To determine (C°, F°) from (B_o, κ) and associated life-history parameters (eq. T1.3), the simplest approach is to plot C_e versus F_e and find the F_e value that maximizes C_e (e.g., Fig. 1). Furthermore, additional equilibrium values for recruitment (eq. T1.13), biomass ($B_e = R_e\phi_b$), or the ratio of spawners per recruit (SPR = ϕ_e/ϕ_E) versus F_e can be calculated and used to determine the ratios of fished states to unfished states that approximate a C° fishing policy (Figs. 1*b*, 1*c*, 1*d*, respectively).

The exercise of plotting equilibrium yield versus fishing mortality rates to determine the optimal values for (C°, F°) is rarely performed in annual stock assessments. Instead, simple reference points such as B_{20} or SPR_{35} are used to approximate C° and F°. It is often assumed that these reference points are insensitive to the estimates of recruitment compensation. While SPR is a strict function of life-history

© 2008 NRC Canada

Table 2. Partial derivatives, based on components in Table 1, required for the numerical calculation of F^* and C^* using eq. 3.

Eq. No.	Partial derivatives
Mortality and survival	
T2.1	$Z_a = M_a + F_c v_a$
T2.2	$S_a = 1 - \exp(-Z_a)$
Survivorship	
T2.3	$\frac{\partial \bar{N}_a}{\partial F_c} = \begin{cases} 0, & a = 1 \\ \exp(-Z_{a-1})\left(\frac{\partial \bar{N}_{a-1}}{\partial F_c} - \bar{i}_{a-1} v_{a-1}{}^{c-1}\right), & a > 1 \end{cases}$
Incidence functions	
T2.4	$\frac{\partial \phi_E}{\partial F_c} = \sum_{a=1}^{\infty} f_a \frac{\partial \bar{N}_a}{\partial F_c}$
T2.5	$\frac{\partial \phi_q}{\partial F_c} = \sum_{a=1}^{\infty} \frac{w_a v_a S_a}{Z_a} \frac{\partial \bar{N}_a}{\partial F_c} + \frac{\bar{i}_a w_a v_a^2}{Z_a}\left[\exp(-Z_a) - \frac{S_a}{Z_a}\right]$
Recruitment	
T2.6	$\frac{\partial R_c}{\partial F_c} = \frac{R_o}{\kappa - 1} \frac{\phi_E}{\phi_c^2} \frac{\partial \phi_c}{\partial F_c}$

parameters (independent of κ), the SPR level associated with MSY is sensitive to values of κ (Fig. 1*d*). As κ decreases, the corresponding SPR level that maximizes long-term yield increases. The SPR reference point is also sensitive to the age at first capture relative to the age at first maturity (Beddington and Kirkwood 2005).

It can be computationally difficult to evaluate the uncertainty in (C^*, F^*) because there is no analytical solution for the (B_o, κ) $\Rightarrow$ (C^*, F^*) transition. In cases where the uncertainty in (C^*, F^*) must be addressed, exact values for (C^*, F^*) can be obtained using numerical approaches (e.g., Newton–Raphson method). The optimal fishing mortality rate (F^*) corresponds to the zero derivative of eq. T1.14. This value can then be substituted back into eqs. T1.9, T1.10, T1.12, T1.14, and T1.15 to obtain C^*. Using the chain rule, the derivative of eq. T1.15 is given by

$$(2) \qquad \frac{\partial C_c}{\partial F_c} = R_c \phi_q + F_c \phi_q \frac{\partial R_c}{\partial F_c} + F_c R_c \frac{\partial \phi_q}{\partial F_c}$$

Using the Newton–Raphson method, F^* can be obtained numerically using

$$(3) \qquad F_{c+1} = F_c - \frac{R_c \phi_q + F_c \phi_q \frac{\partial R_c}{\partial F_c} + F_c R_c \frac{\partial \phi_q}{\partial F_c}}{\phi_q \frac{\partial R_c}{\partial F_c} + R_c \frac{\partial \phi_q}{\partial F_c}}$$

Analytical solutions for the partial derivatives in eqs. 2 and 3 are given in Table 2. Note that the use of eq. 3 requires an initial estimate of F_c and then an iterative approach must be used such that F_{c+1} converges to F_c. Equation 3 converges fairly quickly (approximately 10 to 15 iterations) and can be used to efficiently compute values of F^* and C^* from posterior samples of $\boldsymbol{\Theta}$.

Age-structured model (C^*, F^*)

In this section, our aim is to parameterize a full age-structured model in terms of (C^*, F^*), where C^* is roughly proportional to population scale (B_o), and F^* is a function of productivity (κ). In other words, rather than searching over values of B_o and κ when fitting models to time series data and then determining values of C^* and F^* after fitting, we parameterize the models directly in terms of C^* and F^* and then derive the values of B_o and κ that would be necessary to support (C^*, F^*) hypotheses, conditional on life-history parameters (Φ) and other model parameters in the vector $\boldsymbol{\Theta}$.

Assuming the same model structure outlined in Table 1, the first step in the (C^*, F^*) $\Rightarrow$ (B_o, κ) transition is to differentiate eq. T1.14 with respect to F_c, set the resulting equation equal to zero, and solve for κ. The end result of this transformation is given by the following (see Appendix A1 for derivation):

$$(4) \qquad \kappa = \frac{\phi_E}{\phi_c} - \frac{F^* \phi_q \frac{\phi_E}{\phi_c^2} \frac{\partial \phi_c}{\partial F_c}}{\phi_q + F^* \frac{\partial \phi_q}{\partial F_c}}$$

where the analytical solutions for the partial derivatives are specified in Table 2. To derive B_o from (C^*, F^*, κ), use

$$(5) \qquad B_o = \frac{C^* \phi_E (\kappa - 1)}{F^* \phi_q (\kappa - \phi_E / \phi_c)}$$

where ϕ_c and ϕ_q are evaluated at F^*. The results from eqs. 4 and 5 can then be substituted back into eq. T1.1 to be used in a standard age-structured model that is parameterized using B_o and κ as leading parameters.

There is constraint in the (C^*, F^*) $\Rightarrow$ (B_o, κ) transition in cases where the selectivity schedules are high for younger animals or growth overfishing. In such cases, F^* is independent of κ and much lower than the F that would maximize the yield per recruit. As the age at first capture decreases, the maximum sustainable fishing mortality rate decreases and recruitment compensation approaches infinity (for more details, see Forrest et al. 2008). In such cases, estimates of κ in eq. 4 will be negative; therefore, it is necessary to constrain κ to be greater than 1.0 when using nonlinear search procedures to estimate C^* and F^*.

Ricker formulation

To implement a Ricker-type stock–recruitment model of the form

$$R_c = s_o R_c \phi_c \exp(-\beta R_c \phi_c)$$

which can be rewritten in terms of R_o and κ as

$$(6) \qquad R_c = R_o \left[\frac{\ln(\kappa) - \ln(\phi_E / \phi_c)}{\ln(\kappa)}\right]$$

substitute eq. 6 into eq. T1.14 and proceed by differentiating this expression with respect to F_c, setting the resulting derivative equal to zero, and solving the expression for κ. For

© 2008 NRC Canada

Table 3. Combined United States and Canadian landings (C_t; in 1000 tonnes) and relative abundance indices (I_t) from a fisheries-independent acoustic survey for Pacific hake (*Merluccius productus*) in the northeastern Pacific.

Year	C_t	I_t
1966	137.700	
1967	214.375	
1968	122.180	
1969	180.131	
1970	234.584	
1971	154.612	
1972	117.546	
1973	162.639	
1974	211.259	
1975	221.360	
1976	237.521	
1977	132.693	1.915
1978	103.639	
1979	137.115	
1980	89.936	2.115
1981	139.121	
1982	107.734	
1983	113.924	1.647
1984	138.441	
1985	110.401	
1986	210.617	2.857
1987	234.147	
1988	248.804	
1989	305.916	1.238
1990	259.792	
1991	307.258	
1992	296.910	2.169
1993	199.435	
1994	361.529	
1995	249.770	1.385
1996	306.075	
1997	325.215	
1998	320.619	1.185
1999	311.855	
2000	230.820	
2001	235.962	0.737
2002	182.911	
2003	205.582	1.840
2004	334.672	
2005	349.571	1.265
2006	347.270	

the Ricker model, the recruitment compensation parameter κ can then be expressed as a function of F° using

$$(7)\qquad \kappa = \frac{\phi_E}{\phi_r}\exp\left[-\frac{F^{\circ}\phi_q\frac{\partial\phi_r}{\partial F_r^{\circ}}}{\phi_q\phi_r + F^{\circ}\left(\phi_r\frac{\partial\phi_E}{\partial F_r^{\circ}} - \phi_q\frac{\partial\phi_r}{\partial F_r^{\circ}}\right)}\right]$$

Note to carry out the necessary algebra to derive eq. 7, the partial derivative of eq. 6 with respect to F° must be substituted for eq. T2.6 in Table 2 (see Appendix A); otherwise, all other partial derivatives defined in Table 2 are the same. Note also that ϕ_r and ϕ_q in eq. 7 are evaluated at F°.

Fig. 2. Combined proportions-at-age in the United States and Canadian commercial fisheries for Pacific hake (*Merluccius productus*). The solid line represents the mean age of the landed catch, and each circle is proportional to the proportion-at-age landed in a given year. The vertical broken line indicates the year that age composition data were available from the Canadian fishery.

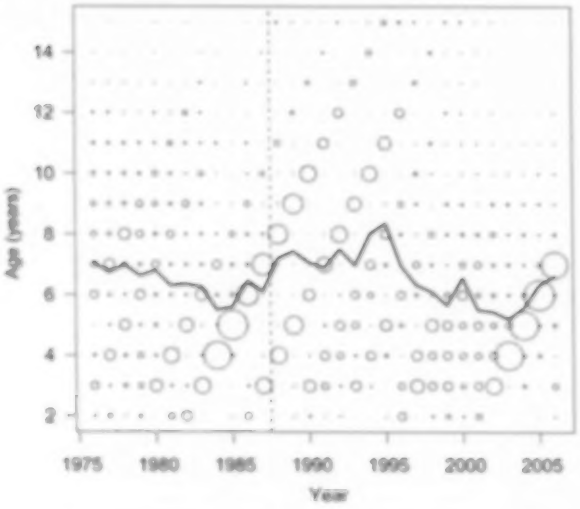

The unfished equilibrium biomass given (C°, F°, κ) is given by

$$(8)\qquad B_{\circ} = -\frac{\ln(\kappa)\phi_R\phi_r C^{\circ}}{\ln\left(\frac{\phi_E}{\kappa\phi_r}\right)\phi_q\phi_E F^{\circ}}$$

where ϕ_r and ϕ_q are evaluated at F°.

Application to the Pacific hake stock

The Pacific hake (hereafter, hake) stock assessment is not atypical of many other assessments for groundfish species on the west coast of North America. Many of the groundfish species are assessed using age-structured models. Hake in this region undergo seasonal migrations, moving northward in the summer months into Canadian waters and moving southward in the winter months to spawn off the coast of Baja California and southern California. Hake are harvested by both United States (US) and Canadian (CAN) fishing fleets, and the composition of the CAN landings tends to contain larger and older individuals. The official stock assessment for hake assumes a single unit stock, but treats US and CAN fisheries separately to capture the interannual variation in migration of hake along the west coast of North America (Helser et al. 2006).

For the purposes of demonstration, we have greatly simplified the data and age-structured model in this application in comparison with the annual assessment that is conducted each year using Stock Synthesis II (Helser et al. 2006). A summary of the historical removals by US and CAN fisheries combined, as well as relative abundance indices for hake, are provided (Table 3). Aggregate age composition in-

© 2008 NRC Canada

Table 4. Statistical catch-at-age model using the Baranov catch equation and C^o and F^o as leading parameters.

Eq. No.	Model definitions
Data	
T4.1	$C_t = C_t^{US} + C_t^{CAN}$
T4.2	$I_t, A_{t,a}, l_a, w_a, f_a$
Parameters	
T4.3	$\Theta = (C^o, F^o, M_a, \bar{a}, \bar{\gamma}, \{\omega_t\}_{t=1}^{T-1}, \rho, \vartheta^2)$
T4.4	$\sigma^2 = \rho\vartheta^2, \quad \tau^2 = (1-\rho)\vartheta^2$
T4.5	$\vartheta^2 = \sigma^2 + \tau^2, \quad \rho = \frac{\sigma^2}{\sigma^2+\tau^2}$
Unobserved states	
T4.6	$\mathbf{N}_{t,a}, B_t, E_t, F_t$
Initial states ($t = 1$)	
T4.7	$v_a = \{1+\exp[-(\bar{a}-a)/\bar{\gamma}]\}^{-1}$
T4.8	$\mathbf{N}_{1,a} = \frac{B_o}{\Omega_B}\exp(-M)^{(a-1)}$
State dynamics ($t > 1$)	
T4.9	$E_t = \sum_a \mathbf{N}_{t,a} f_a$
T4.10	$Z_{a,t} = M_a + F_t v_a$
T4.11	$\hat{C}_t = \sum_a \frac{\mathbf{N}_{t,a} w_a F_t v_a [1-\exp(-Z_{t,a})]}{Z_{t,a}}$
T4.12	$F_{t+1} = F_t - \frac{\hat{C}_t - C_t}{\hat{C}_t'}$
T4.13	$\mathbf{N}_{t,a} = \begin{cases} \frac{\kappa_a E_{t-1}}{1+\beta E_{t-1}}\exp(\omega_t - 0.5\tau^2), & a = 1 \\ N_{t-1,a-1}\exp(-Z_{t-1,a-1}), & a > 1 \end{cases}$
T4.14	$B_t = \sum_a \mathbf{N}_{t,a} w_a v_a$
Residuals and predicted observations	
T4.15	$\varepsilon_t = \ln\left(\frac{I_t}{B_t}\right) - \frac{1}{n}\sum_{t=1}^{n}\ln\left(\frac{I_t}{B_t}\right)$
T4.16	$\hat{A}_{t,a} = \frac{\mathbf{N}_{t,a}\frac{F_t v_a}{Z_{t,a}}[1-\exp(-Z_{t,a})]}{\sum_a \mathbf{N}_{t,a}\frac{F_t v_a}{Z_{t,a}}[1-\exp(-Z_{t,a})]}$

formation from the US and CAN fisheries are summarized in the form of bubble plots (Fig. 2). Age composition information from the CAN fishery are only available back to 1988. To construct the aggregated age composition matrix, we used a weighted average of the proportions-at-age landed in each fishery, where the weights are the proportion of the catch landed in each zone. Between 1984 and 1995, the catches were dominated by the 1980 and 1984 year classes, and in recent years, the 1999 year class has been dominant (Fig. 2). These exceptionally strong year classes have made it difficult to determine the underlying stock–recruitment relationship for hake.

Helser et al. (2006) noted that there is insufficient contrast in the relative abundance indices (I_t) that allow for the joint estimation of B_o, κ (or steepness as defined in Helser et al. 2006), and the scaling parameter q that relates the survey abundance to absolute abundance. To proceed with the stock assessment and provide management advice, κ and q have been fixed and only B_o is assumed unknown and estimated from the data. By fixing values of κ and q, the true uncertainty in B_o is underestimated and uncertainty surrounding subsequent management advice (e.g., estimates of MSY) is also underestimated.

Table 5. Assumed life-history parameters for Pacific hake (*Merluccius productus*).

Parameter	Value
Growth	
l_∞	55
k	0.25
t_o	–0.25
L* or *W	
a	6.54×10^{-6}
b	2.987
Maturity	
$\bar{a}$	2.65
$\bar{\gamma}$	0.05

Note: Length (L) is measured in centimetres; weight (W) is measured in in kilograms.

The relative abundance indices for hake (I_t) are derived from fisheries-independent acoustic surveys that have been conducted every 2–3 years since 1977. Unfortunately, there is little informative contrast in this abundance index, and a few of the survey points have been heavily downweighted in the official stock assessment because of known problems with the historical surveys. In particular, the 1986 survey has been heavily discounted because of substantive differences in biomass estimates based on presurvey and postsurvey calibrations of the acoustic gear. Including the 1986 survey improves the overall contrast in the data series. In Helser and Martell (2007), each survey year is assigned a specific coefficient of variation (CV is set to 0.29 for surveys after 1992 and 0.5 for surveys prior to 1992). In this assessment, we treat all of the relative abundance indices with equal weight and estimate the CV in the surveys.

Age-structured model

The system of equations used in this age-structured model are provided in Table 4. The data consist of combined observed catches eq. T4.1, relative to abundance indices (I_t) assumed to be proportional to the vulnerable biomass seen by the commercial fisheries. Commercial landings and relative abundance indices between 1966 and 2006 are provided (Table 3). Observations on the age proportions landed in both the US and CAN fishery are denoted as $A_{t,a}$ in T4.2. Information on length-at-age, weight-at-age, and fecundity-at-age can be obtained from eqs. T1.4, T1.5, and T1.7, respectively, using the assumed life-history parameters specified in Table 5.

© 2008 NRC Canada

Table 6. Likelihoods and priors used in the statistical estimation of $\boldsymbol{\Theta}$ from Table 4.

Eq. No.	Likelihoods and priors
Negative log-likelihoods	
T6.1	$\ell(\boldsymbol{\Theta})_1 = \sum_{t=1}^{T-1}\left[\ln(\tau) + \frac{\omega_t^2}{2\tau^2}\right]$
T6.2	$\ell(\boldsymbol{\Theta})_2 = \sum_{t\in\mathbf{I}}\left[\ln(\sigma) + \frac{\varepsilon_t^2}{2\sigma^2}\right]$
T6.3	$\ell(\boldsymbol{\Theta})_3 = \sum_{t\in\mathbf{I}_{ca}}\sum_{a=2}^{A}\left(\ln(\zeta) + \ln\left\{\exp\left[\frac{-(P_{t,a})^2}{2\zeta^2}\right]\right\} + 0.01\right)$ where $\zeta = \sqrt{\hat{A}_{t,a}(1-\hat{A}_{t,a})} + 0.1/A]a$ and $P_{t,a} = (A_{t,a} - \hat{A}_{t,a})$
T6.4	$\ell(\boldsymbol{\Theta}) = \sum_{i=1}^{3}\ell_i$
Prior distributions	
T6.5	$p(C^*) \sim \text{lognormal}(\mu = -0.8787, \sigma = 0.3960)$
T6.6	$p(F^*) \sim \text{lognormal}(\mu = -1.378, \sigma = 0.4697)$
T6.7	$p(M) \sim \text{lognormal}(\mu = -1.585, \sigma = 0.2435)$
T6.8	$p(\bar{a}) \sim U(0, 14)$
T6.9	$p(\bar{\gamma}) \sim U(0, 2)$
T6.10	$p(\rho) \sim \text{beta}(\alpha = 1.648, \beta = 10.1306)$
T6.11	$p(\vartheta^2) \sim \text{inverse gamma}(\alpha = 10.829, \beta = 13.368)$
Constraints	
T6.12	$\kappa > 1.0$
Posterior distribution	
T6.13	$P(\boldsymbol{\Theta}) \propto \exp[-\ell(\boldsymbol{\Theta})]p(C^*)p(F^*)p(M)p(\rho)p(\vartheta^2)$

Estimated parameters denoted as $\boldsymbol{\Theta}$ (eq. T4.3) include the C^* and F^* that achieves C^*. Here, we assume that the instantaneous natural mortality rate M is constant and age independent. Parameters for the vulnerability-at-age function are defined as the age and standard-deviation-at-age in which 50% of the fish are vulnerable to harvest ($\bar{a}$, $\bar{\gamma}$, respectively). Lognormal deviations from the mean stock–recruitment relationship are represented by ω_t. We assume that the total error ϑ is unknown and use variance-partitioning methods (see Schnute and Kronlund 2002; Deriso et al. 2007) to partition the observation and process errors using the ratio defined in eqs. T4.4 and T4.5. Note that the total variance in this mixed error model is estimable (Deriso et al. 2007), but the components of observation and process errors are not separable.

The unobserved states consists of a matrix of numbers-at-age ($\mathbf{N}_{t,a}$), biomass that is vulnerable to harvest (B_t), annual egg production (E_t), and the instantaneous fishing mortality rate (F_t). The model is initialized by first calculating the vulnerabilities-at-age eq. T4.7, then computing κ and B_o using eqs. 4 and 5, respectively, for the Beverton–Holt model (or eqs. 7 and 8, respectively, for the Ricker model), then using eq. T4.8 to initialize the numbers-at-age in the population for $t = 1$ (note that $t = 1$ implies 1966 as the starting year).

In each year, state variables are updated using eqs. T4.9–T4.14. Note that the model is conditioned on the observed catch (C_t), and the analytical value of the instantaneous fishing mortality rate (F_t) is computed using Newton's method. The algorithm is initialized by setting $F_{t_1} = C_t/B_t$, then using Newton's method to update $F_{t_{i+1}}$ until the difference between the predicted catch and observed catch is minimal. The derivative of the catch equation ($\hat{C}'_t$) is given by

$$\hat{C}'_t = \sum_a \frac{N_a w_a v_a[1 - \exp(-M - F_t v_a)]}{M + F_t v_a} - \frac{N_a w_a F_t v_a^2[1 - \exp(-M - F_t v_a)]}{(M + F_t v_a)^2} + \frac{N_a w_a F_t v_a^2 \exp(-M - F_t v_a)}{M + F_t v_a}$$

This algorithm converges rather quickly (5–7 iterations); however, we allow for a maximum of 30 iterations to occur and assess whether convergence was achieved by comparing the predicted and observed catches.

The final step in the age-structured model is computing the residuals between the relative abundance indices and the predicted catch-at-age proportions to be used in the negative log-likelihoods during parameter estimation or numerical integration of the posterior distribution. Here, we assume that the observation errors in the relative abundance index are lognormally distributed and are proportional to the vulnerable biomass defined by eq. T4.14. The residuals for the relative abundance indices are given by eq. T4.15, where the conditional maximum likelihood estimate for the scale parameter

© 2008 NRC Canada

Fig. 3. Three alternative prior densities for $F^{\%}$. The lower 10th percentile is equal to $0.6M = 0.132$ for all three models, and the 90th percentiles correspond to $2M$, $1.6M$, and $1.2M$ for runs A (solid line), B (broken line), and C (dotted line), respectively.

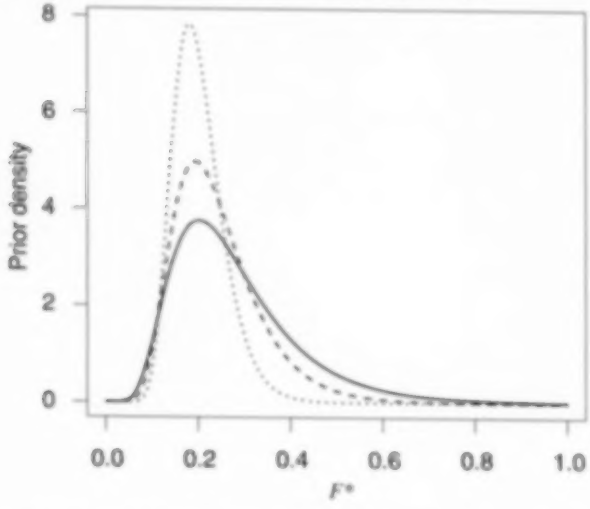

(ln(q)) is used (see Walters and Ludwig 1994). The predicted proportions-at-age for each year is the ratio of catch in numbers-at-age divided by the total catch in numbers (eq. T4.16).

Likelihoods and prior distributions

Parameter estimation was carried out using AD Model Builder (Otter Research Ltd., Sydney, British Columbia). Recruitment deviations (ω_t) were assumed to be lognormally distributed, with an unknown variance to be estimated from the data, and the negative log-likelihood of the recruitment deviations is given by eq. T6.1. The ω_t parameters represent the process error component in this model. Observation errors in the relative abundance index (I_t) were also assumed to be lognormally distributed with an unknown and assumed constant variance. The negative log-likelihood of the acoustic survey is given by eq. T6.2 (Table 6).

Hake are a schooling species, and individuals in each school are nearly uniform in size. Therefore, it was necessary to down-weight the age composition information because age composition samples are likely to be biased owing to the tendency for the fishery to target specific age–size classes (Fournier and Archibald 1982). We use a robust normal approximation to the mulitnomial likelihood (see Fournier et al. 1990 for details) for the proportion-at-age data, with an effective sample size of $n = 50$ in eq. T6.3 for all years of available catch-at-age data. The effective sample size for the age composition data was determined through an iterative process whereby a comparison between the root mean squared error for ω_t and ε_t was compared with the estimates of τ and σ. The sample size was then adjusted such that the root mean squared errors were approximately equal to the standard deviations in the observation errors and process errors.

Informative, lognormal prior distributions were used for $C^{\%}$, $F^{\%}$, and M where the log means and log standard deviations are defined by eqs. T6.5–T6.7 (Table 6). To derive the means and standard deviations for the lognormal prior distribution, we choose arbitrary 10th and 90th percentiles for each parameter and fit a lognormal distribution to these values. Since 1966, the combined landings for the US and CAN fisheries has averaged 216 867 t, and since 1996, it has averaged 286 427 t. Recent estimates of $C^{\%}$ from Helser et al. (2006) are 639 900 t with a 95th confidence interval of (582 000 – 690 000 t). The prior for $C^{\%}$ was constructed by setting the 10th and 90th percentiles equal to [0.25, 0.69], representing 250 000 and 690 000 t, respectively. The prior for $F^{\%}$ was constructed assuming [0.138, 0.46] for the 10th and 90th percentiles, which is roughly $0.6M$ to $2M$ for hake (assuming $M = 0.23$). Bounded uniform prior distributions were assumed for the selectivity parameters eqs. T6.8 and T6.9. The prior distribution for M was constructed assuming [0.15, 0.28] as the 10th and 90th percentiles.

To examine the influence of the assumed prior distribution for $F^{\%}$ on estimates of $C^{\%}$ and all other model parameters, we also explored two additional prior distributions for $F^{\%}$ (Fig. 3). For the two subsequent runs, we assume the lower 10th percentile for $F^{\%}$ was equal to $0.6M$ and reduced the 90th percentiles to $1.6M$ and $1.2M$, respectively. We denote these are runs A–C, representing three alternative prior distributions where the 90th percentiles for $F^{\%}$ range from $2M$ to $1.2M$.

For the variance parameters ρ and ϑ^2, the beta and inverse gamma distributions were used as priors. The beta distribution and inverse gamma distribution are the conjugate prior distributions for binomial distributions and normal variances, respectively (Gelman et al. 1995). In the Helser and Martell (2007) assessment, variances for error terms were assumed to be known and fixed at 0.29 for the observation error CV and 1.13 for the process error CV. This corresponds to a ratio of 0.2 for observation error to total error (or $\rho = 0.2$ under the eq. T4.5 definition). In deriving the α and β parameters in eq. T6.10 for this assessment, we assume a rather wide distribution for the ρ with a mode equal to 0.0663 and 0.275 for the 90th percentile. The assumed total variance ϑ^2 from Helser et al. (2006) was equal to 1.36 ($\sigma_R = 1.131$, and the CV for the acoustic surveys was assumed at 0.29 for recent years). To derive α and β in eq. T6.11, we assumed an expected value for $\vartheta = 1.36$, and the CV in this estimate was assumed at 0.1.

There are certain combinations of $C^{\%}$ and $F^{\%}$ along with selectivity parameters that lead to severe growth overfishing. Under growth-overfishing conditions, estimates of κ become negative; therefore, it was necessary to constrain κ to be greater than 1 (eq. T6.12). If estimates of $\kappa < 1.01$, a large penalty that was proportional to the difference was added to the objective function such that the objective function remained differentiable with respect to $F^{\%}$.

Marginal posterior distributions for model parameters were constructed by sampling (eq. T6.13) using a Metropolis–Hastings algorithm. The Metorpolis–Hastings algorithm is a Markov chain Monte Carlo (MCMC) method for a randomly walking through parameter (Gelman et al. 1995). A marginal posterior distribution for each parameter or derived variable was constructed from 4000 systematic samples of the joint posterior distribution taken from an MCMC chain of length 500 000, where the first 100 000 iterations were discarded to allow for convergence. Conver-

© 2008 NRC Canada

Fig. 4. Gaussian kernel densities of marginal posterior distributions (black lines) and prior distributions (shaded lines) for (*a*–*g*) model parameters and (*h* and *i*) two derived quantities (B_0 and steepness *h*) from model runs A (solid line), B (broken line), and C (dotted line). Posterior densities are based on 4000 systematic samples from a Markov chain Monte Carlo (MCMC) chain of length 500 000, where the first 100 000 are discarded to allow for convergence.

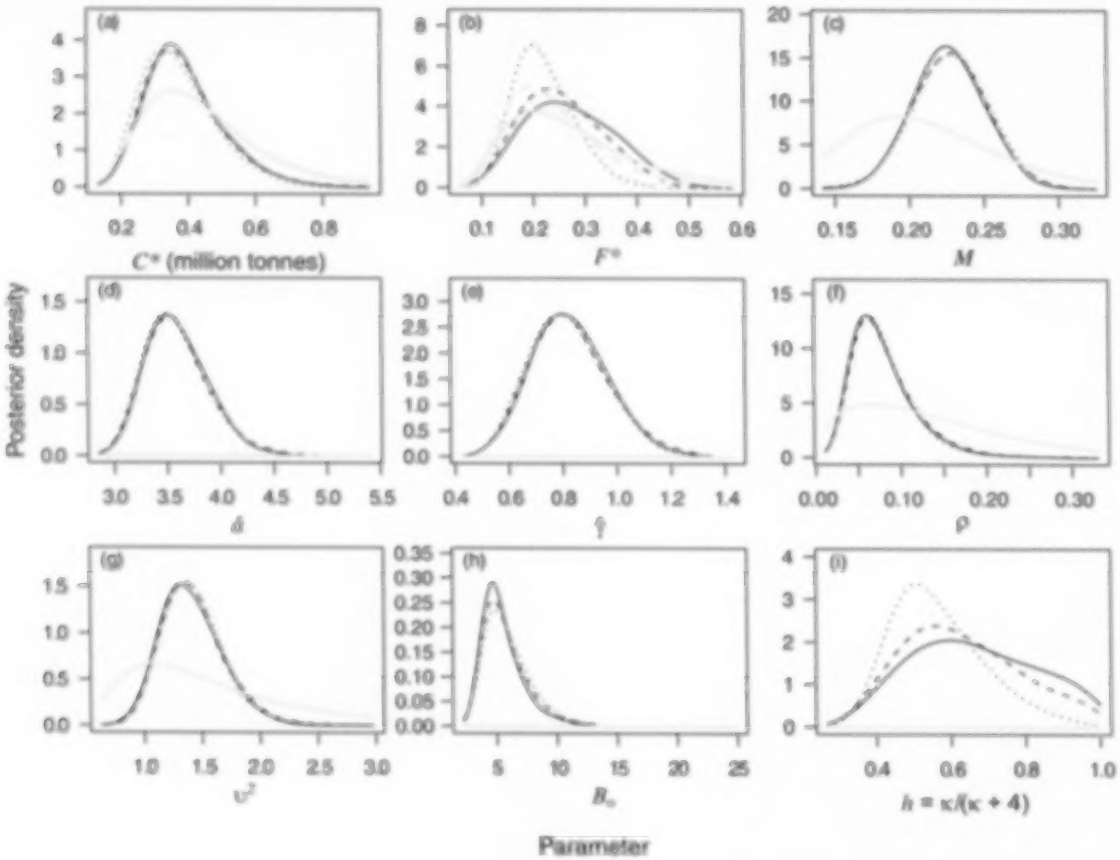

gence was assessed using the diagnostic tools provided in the coda package in R (R Development Core Team 2006).

Results

The marginal posterior distributions for all model parameters with the exception of the annual recruitment deviations ω_t for each of the three alternative prior densities assumed for F° are illustrated (Fig. 4). In addition, the marginal posterior distributions for the derived quantities B_0 (Fig. 4*h*) and steepness *h* (Fig. 4*i*) are also presented for comparison with the results in Helser and Martell (2007). Among the three alternative prior densities for F°, there is very little influence on the overall posterior density for C° or *M*, which are two key parameters that describe the underlying production relationship. Similar distributions were also obtained for selectivity parameters ($\bar{a}$, $\hat{\gamma}$) and the variance parameters (ρ, ϑ^2) among the three alternative prior densities for F°. The resulting estimates of the selectivity parameters are insensitive to the assumed prior density on F° ($\bar{a}$ and $\hat{\gamma}$ are largely determined by the age composition information and are positively correlated with *M* (Table 7)).

The marginal posterior distribution for C° is influenced by the assumed prior density for C° (Fig. 4*a*); we conducted additional runs with a uninformative prior distribution for C° and note here that the marginal posterior distribution has a slightly larger CV and the mode was slightly less than that shown in Fig. 4*a*. More importantly, however, is that C° was fairly insensitive to alternative prior distributions on κ, and there is only a very weak positive correlation between C° and F° (Table 7).

The prior densities for F° strongly influence the marginal posterior densities for F° (Fig. 4*b*); this reflects the absence of information in the relative abundance index to discern between a large unproductive stock and a small productive stock. Moreover, the resulting estimates of recruitment compensation (κ) or steepness (*h*) reflect a wide range of uncertainty (Fig. 4*i*), and the modes of all three distributions are considerably less than the assumed value of $h = 0.75$ in Helser and Martell (2007). Recall that steepness is derived from estimates of F°, life-history parameters, and the vulnerability schedule. Runs A and B assume a fairly wide prior density for F°, and high values of F° imply high values of *h*. However, this is conditional on the age at first capture or the estimated selectivity parameters in the model. As

© 2008 NRC Canada

Table 7. Correlations among estimated model parameters for model runs A–C.

	C°	F°	M	$\hat{a}$	$\hat{\gamma}$	ρ	ϑ^2
Run A							
C°	1						
F°	0.281	1					
M	0.507	–0.091	1				
$\hat{a}$	–0.107	0.139	0.411	1			
$\hat{\gamma}$	–0.155	0.119	0.261	0.888	1		
ρ	–0.084	0.001	–0.021	0.058	0.054	1	
ϑ^2	0.13	–0.047	0.121	0.069	0.066	–0.117	1
Run B							
C°	1						
F°	0.235	1					
M	0.51	–0.148	1				
$\hat{a}$	–0.081	0.162	0.436	1			
$\hat{\gamma}$	–0.146	0.15	0.283	0.895	1		
ρ	–0.096	0.022	–0.045	0.081	0.084	1	
ϑ^2	0.122	–0.045	0.103	0.03	0.03	–0.13	1
Run C							
C°	1						
F°	0.158	1					
M	0.525	–0.19	1				
$\hat{a}$	–0.138	0.064	0.425	1			
$\hat{\gamma}$	–0.193	0.077	0.263	0.884	1		
ρ	–0.069	0.025	–0.01	0.078	0.069	1	
ϑ^2	0.128	–0.065	0.106	0.019	0.024	–0.142	1

the selectivity curve shifts towards younger age classes, the resulting estimate of M decreases (i.e., making the stock less productive and larger in scale; see correlations in Table 7), and the standard deviation in selectivity ($\hat{\gamma}$) also decreases (i.e., selectivity becomes more knife-edge). In run C, the relative probability of high values of h decrease dramatically. Again, this is an artifact of the joint effects of selectivity and natural mortality; had the fishery targeted smaller fish, the posterior density for h would shift upwards.

Age composition data are informative about total mortality rates, size selectivity parameters, and relative abundance of each cohort. In this assessment, we assumed that the selectivity curve is an asymptotic function, and this assumption permits the joint estimation of natural mortality and selectivity. There was some positive correlation between M and C° and strong positive correlation between the selectivity parameters $\hat{a}$ and $\hat{\gamma}$ (Table 7). The mean of the marginal posterior distribution for M is roughly equal to the expected value of its corresponding prior distribution. Thus, the specified prior for M can influence the overall scale of the population when survey information lacks sufficient contrast to resolve the underlying production function.

Progressively increasing the amount of information in the prior density for F° decreases the confounding between F° and C° (Table 7) and slightly increases the confounding between C° and M. The three alternative prior densities for F° that we chose for this example have different expected values (0.25, 0.22, and 0.19 for runs A–C, respectively), and the modes of the marginal posterior distributions for F° are roughly equal to the expected values of the prior densities. The resulting 20% posterior density region for F° also decreases as the prior information increases; however, the ranges of uncertainty for C° do not decrease in a substantial manner for runs A–C (Fig. 5*a*). Transition to B_∞ and h show a progressively shrinking joint posterior density as the prior information on F° increases; however, the uncertainty in B_∞ is comparable for all three prior densities of F°. We also tried decreasing the amount of prior information on C° and found that the uncertainty for B_∞ and C° increases slightly, but the shift in the resulting posterior distributions are downward (i.e., lower values for C° and B_∞ were more likely). Similar results were also obtained when we progressively increased information in the prior density for M. The overall effect of fixing M is to increase the possible confounding between B_∞ and κ, creating more of a defined ridge in the joint posterior distribution.

The ability to estimate parameters that specify the observation error variance and process error variance owes to having both age composition information and relative abundance indices. The marginal posterior distributions for ρ and ϑ are largely determined by the assumed weight assigned to the effective sample size in eq. T6.3 in addition to the specified prior distributions. Decreasing the effective sample size for the age composition data shifts the marginal distributions for ϑ and ρ upwards, increasing the total errors. There was very little correlation between the variance parameters and all other model parameters (Table 7). As the effective sample size is reduced in eq. T6.3, the variance parameters are more influenced by the specified prior distributions, in particular the ratio between observation errors and process errors (ρ).

Helser and Martell (2007) make very different assump-

© 2008 NRC Canada

Fig. 5. Contour plots of the highest 20% and 90% posterior density regions of (*a*) (C^{∞}, F^{∞}) and (*b*) (B_0, *h*) for the three alternative prior densities for F^{∞} (run A, solid line; run B, broken line; run C, dotted line). Contours were constructed from 4000 systematic samples from the Markov chain Monte Carlo (MCMC) chain of length 500 000, where the first 100 000 were discarded for burn-in.

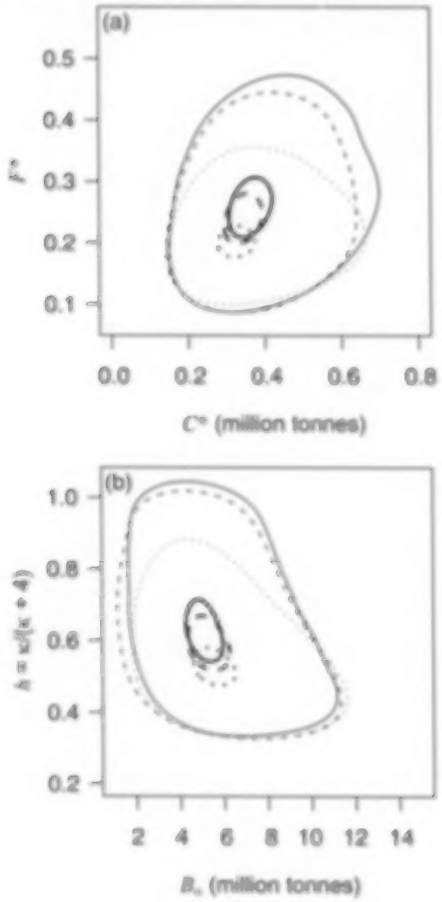

tions about the age composition data and the form of the selectivity parameters; therefore, the results of this study are not directly comparable. However, the number of estimated model parameters in Helser and Martell (2007) is nearly double the number of estimated parameters in this study; yet, estimates of uncertainty are very precise in Helser and Martell (2007) by comparison (Table 8). The high precision owes to assuming fixed values for steepness and the scaling parameter for the acoustic survey, as well as fixed values for the variance parameters. Estimates of unfished spawning stock biomass and the spawning stock biomass at MSY are not that different between the two models; however, the uncertainty in these estimates are significantly larger in this study (Table 8). Estimates of the current depletion state are much more conservative in this study owing to lower estimates of the initial unfished states. Furthermore, mean body weights in the hake populations have declined considerably since the late 1970s, and this model assumes constant growth. The most significant difference between the two models is in the estimates of MSY (or C^{∞}). Estimates of MSY from Helser and Martell (2007) are 536 600 t and in this study are 387 254 t (Table 8). This difference is due in part to the much lower estimates of B_0 than what was estimated in Helser and Martell (2007). Estimates of F^{∞} are slightly lower in this study because of lower estimates of steepness than what was assumed in Helser and Martell (2007).

Discussion

The main motivation for this paper is to change the question from how likely are B_0 and κ given the data to how likely are estimates of C^{∞} and F^{∞} given the data. We have demonstrated that the reverse transformation of management parameters to population parameters has an analytical solution for an age-structured model with age-specific selectivities and instantaneous mortality rates. This creates both a statistical advantage through reduced confounding (as demonstrated by Schnute and Kronlund 1996) as well as opportunities to develop informative priors for management parameter directly for cases in which relative abundance information lacks sufficient contrast to resolve the B_0, κ trade-off. It also allows for direct comparison of how likely current catches are relative to alternative hypotheses about MSY. We feel that this parameterization of age-structure models will greatly enhance communication with fisheries managers and industry partners.

In the traditional forward-projecting, age-structured stock assessment model, it is necessary to estimate two key population parameters (B_0 and κ) to develop management parameters (C^{∞} and F^{∞}) that are used in harvest control rules (e.g., the 40:10 harvest control rule). To reliably estimate κ, it is necessary to observe the recruitment response at low spawner abundance. Generating such observations may be undesirable because this would call for deliberate overfishing of the stock, and additional statistical problems such as time-series bias (Myers and Barrowman 1995) or measurement error (Walters and Ludwig 1981; Rivot et al. 2001) may not guarantee that such a deliberate overfishing experiment would yield the correct answer. However, there are alternative approaches to estimating F^{∞} for iteroparous species that are independent of knowing the underlying stock–recruitment relationship (e.g., Beverton and Holt 1957; Walters and Martell 2002; Beddington and Kirkwood 2005). Based on growth information, size-selectivity, and estimates of natural mortality, reasonable estimates of F^{∞} can be obtained from simple yield-per-recruit analysis. These alternative methods for estimating the fishing mortality that maximizes yield per recruit do not require observations over a wide range of stock sizes; however, these methods are sensitive to changes in growth, natural mortality, or selectivity over time. The main point is that reasonable priors can be developed for F^{∞} from simple life-history information (growth and natural mortality) and basic information on the age at first capture; whereas developing reasonable priors for the slope of the stock–recruitment curve may be much more difficult.

The current practice of estimating B_0 and κ by fitting models to uninformative time-series data can lead to mis-

© 2008 NRC Canada

Table 8. Comparison of reference points and current states for Pacific hake (*Merluccius productus*) with estimates obtained from Helser and Martell (2007) and this study.

	Helser and Martell (2007)		This study	
Quantity	Estimate	95% CI	Median	95% CI
Unfished spawning stock biomass (1×10^6 t)	3.567	3.112–4.023	3.145	1.829–6.593
Unfished total biomass (1×10^6 t)	8.702	NA	6.678	3.853–14.154
Unfished 3+ biomass (1×10^6 t)	7.321	NA	6.291	3.659–12.188
Spawning stock biomass at MSY (1×10^6 t)	0.986	0.773–1.203	1.23	0.667–2.768
Spawning stock biomass in 2006 (1×10^6 t)	1.241	0.906–1.576	2.18	0.843–6.028
Spawning stock depletion in 2006 (%)	34.8	27.7–41.9	69.20	33.3–128.49
Instantaneous fishing rate at MSY ($F^{\%}$)	0.282	NA	0.241	0.129–0.415
MSY ($C^{\%}$) (t)	536 600	468 853 – 595 015	387 254	217 146 – 736 138

Note: MSY, maximum sustainable yield.

guided discussions about developing informative priors for unobserved quantities (e.g., scaling parameters for acoustic surveys or selectivity parameter for dome-shaped selectivity curves). Currently, most stock assessment models that are used for guiding decision makers undergo a review process, either through an internal panel (e.g., Stock Assessment Review (STAR) Panel) or an external review. During this review process, members of the stock assessment teams are usually required to perform a series of additional analysis such that members of the review panel can further understand the sensitivity of management outcomes to alternative assumptions about model structure or the data. Presumably these requests are carried out to determine robustness of the management advice; however, often these requests are carried out because of concerns with the present management advice. In cases where it is absolutely clear that the abundance indices are not informative about the underlying stock production function, we recommend that the discussion begins with an honest admission of a reasonable long-term average yield that first meets conservation objectives and second satisfies the economic constraints of industry and then proceeds to ask how likely are the data given these objectives and constraints. The outcome of such a process can go in two possible directions: (*i*) both the conservation objectives and economic constraints are within the same domain and yield recommendations are straightforward; or (*ii*) economic constraints are beyond the conservation objectives and industry must adapt to lower yield options through cost reduction or enhancing product value. The latter scenario would provide clear incentives for industry partners to develop more efficient solutions that are compatible with management objectives.

The hake data is a great example of the challenges that stock assessment scientists and decision makers must face when a fisheries-independent survey lacks information to reliably estimate the productivity and population scale. To cope with these data challenges, typical responses have included fixing parameters (such as the steepness parameter) or using informative prior distributions based on the results of meta-analysis of similar species. Indeed, the work of Myers et al. (1999) has greatly improved our understanding of recruitment compensation and has been a valuable resource for developing informative priors. However, recruitment compensation defines the rate at which we can safely harvest a population; it does not define the absolute amount that can be safely removed. The absolute amount that can be safely removed is defined by the population scale, usually defined as the unfished spawning stock biomass. Unfished states are very rarely observed in fisheries, and this quantity must be estimated from time-series data that are often suspect, missing, or even that are estimated from other independent statistical models (e.g., see Maunder 2001). Furthermore, there are very few stock assessments that have a relative abundance index for the entire history of the fishery. If, however, the model is parameterized in a management-oriented approach, then information from historical removals can be used to develop informative priors for population scale. Even one-way trip data contain information on overall scale; in this case, B_o and κ are negatively confounded and the resulting estimates of $C^{\%}$ are fairly well determined over a wide range of likely B_o and κ values. The overarching message here is that it is difficult to determine if one-way trip data come from a large unproductive stock or a small productive stock; in either case, estimates of $C^{\%}$ are roughly the same. Thus, it seems much more intuitive to derive overall population-scale parameters from $C^{\%}$ and $F^{\%}$.

One of the more important difference between the assessment of hake presented here and that of Helser and Martell (2007) is that this assessment assumes an asymptotic selectivity curve. In Helser and Martell (2007), dome-shaped selectivity curves are assumed for both the US and CAN fisheries and also for the acoustic survey. This feature of the assessment model adds 12 additional unknown parameters to be estimated from the data, as well as assumes that there is some fraction of the older age classes that will never enter the fishery or be seen by the survey. These older or cryptic fish are still maintained in the calculations of spawning stock biomass and probably account for the differences between the two estimates of unfished spawning stock biomass in Table 8. The concern, at least with the hake stock, is that spawning stock biomass can be artificially created by assuming more of a dome in the selectivity function. Alternatively, biased estimates of the M can also have the same affect. Although the assessment for hake presented in this stock assessment does not assume a dome-shaped selectivity curve, we do admit a wide range of uncertainty in M rather than assuming a fixed value. We also note here that using a fixed value for M results in a much stronger correlation between B_o and κ; this results in much less uncertainty in the estimate of $C^{\%}$.

© 2008 NRC Canada

In comparison with Helser and Martell (2007), there is a much wider range of uncertainty for all model parameters in this assessment of hake. The interpretation of our approach for developing prior distributions could be considered naïve, and indeed it is. Our purpose here was to demonstrate that these data for hake are completely uninformative about the overall population-scale and recruitment compensation. When management requires an estimate of absolute abundance to apply harvest control rule, it is absolutely necessary to incorporate prior information on scaling parameters such as q or B_0 itself. When it is absolutely necessary to fix scaling parameters or use informative priors, the process should properly reflect the uncertainty (or at minimum some uncertainty) such that the risk of management options can be properly quantified.

An alternative to the management-oriented approach that we present here would be to develop informative priors for B_0 and κ directly and then proceed with model fitting and deriving reference points C^* and F^* required for decision making. However, it is not absolutely clear how priors on B_0 and κ would affect estimates of C^* and F^* because of structural assumptions in the model (e.g., the form of the stock–recruitment relationship), confounding with additional nuisance parameters, and assumed variance ration. For example, if the variance in process errors (ω_t in our example) is sufficiently large, then the shape of the stock–recruitment function is completely determined by the prior information, which ultimately defines C^* and F^*. In contrast, if the variance of the process errors is sufficiently small, then the shape of the stock–recruitment relationship is more influenced by the available data and the associated observation errors. Seeing the effect of the informative priors on estimates of C^* and F^* is confounded with nuisance parameters and the assumed variance ratio. Seeing the effect of informative priors on C^* and F^*, however, is much more transparent. Rivot et al. (2001) warn against using management-oriented approaches for parameterizing stock assessment models because they change the structural assumptions of the model. This is also true for the age-structured model presented here, and we also carry the same warning. In particular, the change in the structural assumptions does not permit growth overfishing as a viable long-term sustainable option. In cases where there has been strong growth-overfishing, estimates of κ are likely to be infinitely large, leading to optimistic management advice.

Acknowledgements

We thank Pierre Kleiber, Robert Ahrens, and Olaf Jensen for useful discussions about formulating the models in terms of management parameters. We also appreciate the discussions and data provided by Thomas Helser and Ian Stewart of the Northwest Fisheries Science Center, National Marine Fisheries Service, NOAA, for the Pacific hake case study. We also thank Jon Schnute and Alan Sinclair of Fisheries and Oceans Canada, Josh Korman, Ana Parma, and an anonymous reviewer for constructive comments on earlier versions of this manuscript. This work was financially supported by a grant to J.F. Kitchell from the Biological Oceanography Program of the National Science Foundation and a grant to S.J.D. Martell from the NOAA, Chesapeake Bay Office.

References

Beddington, J.R., and Kirkwood, G.P. 2005. The estimation of potential yield and stock status using life-history parameters. Philos. Trans. R. Soc. B Biol. Sci. **360**: 163–170. doi:10.1098/rstb.2004.1582.

Beverton, R., and Holt, S. 1957. On the dynamics of exploited fish populations. Chapman and Hall, London.

Botsford, L. 1981. Optimal fishery policy for size-specific density-dependent population models. J. Math. Biol. **12**: 265–293. doi:10.1007/BF00276917.

Botsford, L.W., and Wickham, D.E. 1979. Population cycles caused by inter-age, density-dependent mortality in young fish and crustaceans. *In* Proceedings of the 13th European Marine Biology Symposium: Cyclic Phenomena in Marine Plants and Animals. *Edited by* E. Naybr and R. Hartnoll. Permagon, New York. pp. 73–82.

Deriso, R.B., Maunder, M.N., and Skalski, J.R. 2007. Variance estimation in integrated assessment models and its importance for hypothesis testing. Can. J. Fish. Aquat. Sci. **64**: 187–197. doi:10.1139/F06-178.

Forrest, R.E., Martell, S.J.D., Melnychuk, M.C., and Walters, C.J. 2008. An age-structured model with leading management parameters, incorporating age-specific selectivity and maturity. Can. J. Fish. Aquat. Sci. **65**: 286–296. doi:10.1139/F07-156.

Fournier, D., and Archibald, C. 1982. A general theory for analyzing catch at age data. Can. J. Fish. Aquat. Sci. **39**: 1195–1207. doi:10.1139/f82-157.

Fournier, D.A., Sibert, J.R., Majkowski, J., and Hampton, J. 1990. MULTIFAN a likelihood-based method for estimating growth parameters and age composition from multiple length frequency data sets illustrated using data for southern bluefin tuna (*Thunnus maccoyii*). Can. J. Fish. Aquat. Sci. **47**: 301–317. doi:10.1139/f90-032.

Gelman, A., Carlin, J., Stern, H., and Rubin, D. 1995. Bayesian data analysis. Chapman and Hall, New York.

Goodyear, C.P. 1980. Compensation in fish populations. *In* Biological monitoring of fish. *Edited by* C. Hocutt and C.J. Stauffer. Lexington Books, D.C. Heath Co., Lexington, Mass.

Helser, T.E., and Martell, S.J.D. 2007. Stock assessment of Pacific hake (whiting) in U.S. and Canadian waters in 2007. Northwest Fisheries Science Center, National Marine Fisheries, National Oceanic and Atmospheric Administration, East Seattle, Wash., USA. Tech. Rep.

Helser, T.E., Stewart, I.J., Fleischer, G.W., and Martell, S.J.D. 2006. Stock assessment of Pacific Hake (whiting) in U.S. and Canadian waters in 2006. Northwest Fisheries Science Center, National Marine Fisheries, National Oceanic and Atmospheric Administration, East Seattle, Wash., USA. Tech. Rep.

Hilborn, R., and Walters, C.J. 1992. Quantitative fisheries stock assessment: choice, dynamics and uncertainty. Chapman and Hall, New York.

Mace, P., and Dooman, I. 1988. A generalized bioeconomic simulation model for fish dynamics. New Zealand Fishery Assessment Research Document No. 88/4, Wellington, New Zealand.

Maunder, M. 2001. A general framework for integrating the standardization of catch per unit of effort into stock assessment models. Can. J. Fish. Aquat. Sci. **58**: 795–803. doi:10.1139/cjfas-58-4-795.

Myers, R.A., and Barrowman, N.J. 1995. Time series bias in the estimation of density-dependent mortality in stock–recruitment models. Can. J. Fish. Aquat. Sci. **52**: 223–232. doi:10.1139/f95-022.

Myers, R.A., Bowen, K.G., and Barrowman, N.J. 1999. Maximum

© 2008 NRC Canada

reproductive rate of fish at low population sizes. Can. J. Fish. Aquat. Sci. **56**: 2404–2419. doi:10.1139/cjfas-56-12-2404.

Punt, A.E., and Hilborn, R. 1997. Fisheries stock assessment and decision analysis: the Bayesian approach. Rev. Fish Biol. Fish. **7**: 35–63. doi:10.1023/A:1018419207494.

R Development Core Team. 2006. R: a language and environment for statistical computing. R Foundation for Statistical Computing, Vienna, Austria. ISBN 3-900051-07-0.

Ricker, W.E. 1975. Computation and interpretation of biological statistics of fish populations. Bull. Fish. Res. Board Can. No. 191.

Rivot, E., Prevost, E., and Parent, E. 2001. How robust are Bayesian posterior inferences based on a Ricker model with regards to measurement errors and prior assumptions about parameters? Can. J. Fish. Aquat. Sci. **58**: 2284–2297. doi:10.1139/cjfas-58-11-2284.

Schnute, J.T., and Kronlund, A.R. 1996. A management oriented approach to stock–recruitment analysis. Can. J. Fish. Aquat. Sci. **53**: 1281–1293. doi:10.1139/cjfas-53-6-1281.

Schnute, J.T., and Kronlund, A.R. 2002. Estimating salmon stock–recruitment relationships from catch and escapement data. Can. J. Fish. Aquat. Sci. **59**: 433–449. doi:10.1139/f02-016.

Schnute, J.T., and Richards, L.J. 1998. Analytical models for fishery reference points. Can. J. Fish. Aquat. Sci. **55**: 515–528. doi:10.1139/cjfas-55-2-515.

Walters, C., and Ludwig, D. 1981. Effects of measurement errors on the assessment of stock–recruitment relationships. Can. J. Fish. Aquat. Sci. **38**: 704–710. doi:10.1139/f81-093.

Walters, C., and Ludwig, D. 1994. Calculation of Bayes posterior probability distributions for key population parameters. Can. J. Fish. Aquat. Sci. **51**: 713–722. doi:10.1139/f94-071.

Walters, C., and Martell, S.J.D. 2002. Stock assessment needs for sustainable fisheries management. Bull. Mar. Sci. **70**: 629–638.

Walters, C., and Martell, S.J.D. 2004. Fisheries ecology and management. Princeton University Press, Princeton, N.J.

Appendix A. Relationship between recruitment compensation (κ) and steepness (h)

Steepness is defined as the ratio of the resulting recruitment between unfished conditions and when egg production is reduced to 20% of its unfished state.

$$h = \frac{f(0.2\phi_E)}{f(\phi_E)}$$

Beverton–Holt model

To derive h from κ, first begin by substituting the Beverton–Holt model for $f(E)$ in the expression above and simplify:

$$\text{(A1)} \quad \begin{aligned} h &= \frac{\left(\frac{0.2aE}{1+0.2bE}\right)}{\left(\frac{aE}{1+bE}\right)} \\ &= \frac{0.2(1+bE)}{1+0.2bE} \end{aligned}$$

Next, substitute $b = (\kappa - 1)/E$ into eq. A1:

$$\text{(A2)} \quad h = \frac{0.2\kappa}{0.8+0.2\kappa} = \frac{\kappa}{4+\kappa}$$

The reverse transformation is given by

$$\text{(A3)} \quad \kappa = \frac{4h}{1-h}$$

Ricker model

Substitute the Ricker model into the definition of h and simplify:

$$\text{(A4)} \quad \begin{aligned} h &= \frac{0.2aE\exp(-0.2bE)}{aE\exp(-bE)} \\ &= \frac{0.2\exp(-0.2bE)}{\exp(-bE)} \\ &= 0.2\exp(0.8bE) \end{aligned}$$

Next, substitute $b = \ln(\kappa)/E$ for b in eq. A4 and simplify:

$$\text{(A5)} \quad \begin{aligned} h &= 0.2\exp[0.8\ln(\kappa)] \\ &= 0.2\kappa^{4/5} \end{aligned}$$

and the reverse transformation is given by

$$\text{(A6)} \quad \kappa = (5h)^{5/4}$$

Appendix B. Parameter derivations

Beverton–Holt model

The derivation of eq. 4 starts with substituting eqs. T1.13 and T2.6 into eq. 2:

$$\text{(B1)} \quad \frac{\partial C_e}{\partial F_e} = R_e\phi_q\frac{\kappa-\phi_E/\phi_e}{\kappa-1} + F_e\phi_q\frac{R_o}{\kappa-1}\frac{\phi_E}{\phi_e^2}\frac{\partial\phi_e}{\partial F_e} + F_eR_o\frac{\kappa-\phi_E/\phi_e}{\kappa-1}\frac{\partial\phi_q}{\partial F_e}$$

© 2008 NRC Canada

Setting eq. B1 equal to 0 and solving for κ yields

$$\begin{aligned} 0 &= \left(\kappa - \frac{\phi_E}{\phi_e}\right)\phi_q + F_e\phi_q\frac{\phi_E}{\phi_e^2}\frac{\partial\phi_e}{\partial F_e} + F_e\left(\kappa - \frac{\phi_E}{\phi_e}\right)\frac{\partial\phi_q}{\partial F_e} \\ -F_e\phi_q\frac{\phi_E}{\phi_e^2}\frac{\partial\phi_e}{\partial F_e} &= \left(\kappa - \frac{\phi_E}{\phi_e}\right)\left(\phi_q + F_e\frac{\partial\phi_q}{\partial F_e}\right) \\ \kappa &= \frac{\phi_E}{\phi} - \frac{F_e\phi_q\frac{\phi_E}{\phi_e^2}\frac{\partial\phi_e}{\partial F_e}}{\phi_q + F_e\frac{\partial\phi_q}{\partial F_e}} \end{aligned}$$

To prove eq. 5, start with

(B2) $$B_e = R_e\phi_E$$

Then solve eq. T1.13 for R_e and substitute the result into eq. B2:

(B3) $$B_e = \frac{R_e(\kappa - 1)}{\kappa - \phi_E/\phi_e}\phi_E$$

and solve eq. T1.14 for R_e and substitute this expression into eq. B3, which is equivalent to eq. 5 when $C_e = C^*$ and $F_e = F^*$.

Ricker model

As with eq. 5, the derivation of eq. 7 starts by substituting eq. 6 and its corresponding partial derivative with respect to F_e into eq. 2, setting this expression equal to zero, and solving for κ. The partial derivative of eq. 6 with respect to F_e is

(B4) $$\frac{\partial R_e}{\partial F_e} = R_e\phi_E\left[1 + \ln\left(\frac{\phi_E}{\kappa\phi_e}\right)\right]\phi_e^{-2}[\ln(\kappa)]^{-1}\frac{\partial\phi_e}{\partial F_e}$$

Let $H = \ln\left(\frac{\phi_E}{\kappa\phi_e}\right)$ and substitute eqs. B4 and B6 into eq. 2, set the expression equal to zero, and solve for κ:

$$\begin{aligned} 0 &= -\frac{HR_e\phi_E\phi_q}{\ln(\kappa)\phi_e} + \frac{F_e\phi_qR_e\phi_E(1+H)}{\phi_e^2\ln(\kappa)}\frac{\partial\phi_e}{\partial F_e} - \frac{HR_e\phi_eF_e}{\ln(\kappa)\phi_e}\frac{\partial\phi_q}{\partial F_e} \\ 0 &= -H\phi_q + \frac{F_e\phi_q(1+H)}{\phi_e}\frac{\partial\phi_e}{\partial F_e} - HF_e\frac{\partial\phi_q}{\partial F_e} \\ \frac{F\phi_q(1+H)}{\phi_e}\frac{\partial\phi_e}{\partial F_e} &= H\phi_q + HF_e\frac{\partial\phi_q}{\partial F_e} \end{aligned}$$

(B5)
$$\begin{aligned} H &= \ln\left(\frac{\phi_E}{\kappa\phi_e}\right) = \frac{F_e\phi_q\frac{\partial\phi_e}{\partial F_e}}{\phi_q\phi_e + F_e\phi_e\frac{\partial\phi_q}{\partial F_e} - F_e\phi_q\frac{\partial\phi_e}{\partial F_e}} \\ \kappa &= \frac{\phi_E}{\phi_e}\exp\left(-\frac{F_e\phi_q\frac{\partial\phi_e}{\partial F_e}}{\phi_q\phi_e + F_e\phi_e\frac{\partial\phi_q}{\partial F_e} - F_e\phi_q\frac{\partial\phi_e}{\partial F_e}}\right) \end{aligned}$$

© 2008 NRC Canada

Experimental policies for rebuilding depleted stocks

Steven J.D. Martell and Carl J. Walters

Abstract: Experimental policies for rebuilding stocks through reduction in fishing mortality rate can be classified by severity of the reduction and duration of application of the reduced rate before moving to a long-term fishing rate goal. For stocks ranging from highly productive shrimp (Penaeidae) in the Gulf of Mexico to longer-lived, less productive Atlantic yellowfin (*Thunnus albacares*) tuna, we show that highest expected long-term fishery values are likely to come from relatively harsh experiments (F reduced to lowest value likely to be optimum for the long term) for which there is a commitment to maintain the experimental fishing mortality rate for several generations. Shorter experiments and less severe reductions in fishing rate lead to high probabilities of poor choices for postexperimental fishing rate, while much longer experiments do not produce substantially more information yet forego opportunities for higher harvests.

Résumé : Les politiques expérimentales pour restaurer les stocks par la réduction des taux de mortalité dus à la pêche peuvent être classés selon la sévérité de la réduction et la durée du maintien du taux réduit avant l'établissement d'un objectif de taux de pêche à long terme. Dans les cas de stocks allant de crevettes (Penaeidae) à forte productivité du golfe du Mexique à des albacores à nageoires jaunes (*Thunnus albacares*) de l'Atlantique à cycle plus long, mais à productivité moins grande, nous démontrons que les plus grands avantages à long terme attendus pour la pêche sont plus susceptibles de venir d'expériences relativement brutales (un F réduit à sa valeur la plus basse est vraisemblablement l'optimum pour le long terme) dans lesquelles il existe une volonté de maintenir le taux de mortalité expérimentale due à la pêche pendant plusieurs générations. Des expériences plus courtes et des réductions moins sévères du taux de pêche résultent en de fortes probabilités de faire de mauvais choix concernant le taux de pêche après la période expérimentale; d'autre part, des expériences beaucoup plus longues ne produisent pas substantiellement plus d'information, tout en laissant échapper des occasions de faire des récoltes plus importantes.

[Traduit par la Rédaction]

Introduction

There have been widespread calls for reduction in fishing effort to rebuild overfished stocks and eventually produce higher long-term catches (see case studies in Caddy and Agnew 2004). In the USA, the Sustainable Fisheries Act was supposed to end overfishing, yet overfishing continues a decade later. Fishing industries have been both pessimistic and optimistic about policy changes intended to reduce overfishing. In some cases, industries (e.g., Canadian Sablefish Association) have borne the costs of fisheries-independent surveys and stock status assessments to ensure sustainable use. In other cases, industries have deliberately violated conservation measures in protest of policy changes. Some stocks (e.g., coho salmon (*Oncorhynchus kisutch*) in southern British Columbia and the 2J3KL Atlantic cod (*Gadus morhua*) stock off Newfoundland) have not recovered as expected following severe fishery reductions. Causes of such prediction failures range from incorrect assessments of stock status in the first place to loss of productive capability due to habitat alteration, loss of stock structure, bycatch, and continued targeted fishing (e.g., Shelton et al. 2006).

Many of the fisheries management schemes in place today use what we refer to as output controls (Walters and Martell 2004, chapter 4). That is, annual harvest polices each year are set using some form of quota (e.g., total allowable catch, allowable biological catch, etc.), as opposed to input controls (i.e., effort limits or fishing days). One requirement of using output controls is an estimate of harvestable biomass, which is usually based on the output of a population dynamics model to forecast abundance in the near future. Parameters for these models are usually estimated by fitting models to time series data, and often these data are uninformative (i.e., lack sufficient contrast in relative abundance indices to determine the underlying production function or stock–recruitment relationship). Experimental policies can be designed to deliberately provide contrast in relative abundance indices such that stock assessment models can discern between small, productive stocks and large, unproductive stocks. But how severe and how long should such an experiment have to run before certainty in model parameters is established? This is the overarching question we focus on in this paper.

Stock rebuilding situations are ones where there is a strong dual effect of control (Walters 1986) (i.e., where harvest rate policy choices have a strong effect on both short-term harvest values and on creating informative variation in stock size needed for estimation of the best long-term harvest strategy). While it is possible in principle to estimate

Received 5 May 2007. Accepted 8 November 2007. Published on the NRC Research Press Web site at cjfas.nrc.ca on 8 July 2008.
J19985

S.J.D. Martell[1] and C.J. Walters. Fisheries Centre, The University of British Columbia, 2204 Main Mall, Vancouver, BC V6T 1Z4, Canada.

[1]Corresponding author (e-mail: s.martell@fisheries.ubc.ca).

 doi:10.1139/F08-061 © 2008 NRC Canada

an optimum strategy for responding to new information as it becomes available, with responses representing a balance between the needs to obtain short-term values and also better information, the required optimization procedures are practically impossible to implement. Walters and Green (1997) suggested a relatively simple way to avoid the complex optimization calculations by treating future management as occurring in two time phases: an experimental phase, where harvest is set at an experimental rate for some fixed period, then a long-term management phase, where the results of the experimental phase are put into practice without expectation of further learning about the optimum stock size. Based on previous optimization studies of adaptive management policies (reviewed in Walters 1986), Walters and Green (1997) recommend evaluating only relatively harsh, rapid experimental changes, rather than gradual or incremental change, since gradual changes slow the adaptive learning process and lead to confounding of experimental responses with trends in other factors. Examination of possible future values under such two-phase policies can give useful insights about how to manage in the short term (e.g., whether or not to initiate an experimental effort reduction), even when it is admitted that the experimental plan is not likely to be followed exactly into the future.

Uncertainty about response to reduced fishing effort implies that stock rebuilding policies need to be treated as adaptive management experiments, with clear recognition of relatively high probabilities of failure. The key issue then becomes what experimental design to follow (i.e., how much to reduce fishing effort and for how long before deciding whether or not to continue the policy or adopt a simpler, nonexperimental policy). In this paper, we build on the approach suggested by Walters and Green (1997) for comparing experimental policy choices. We also develop a protocol for screening experimental design choices, and the protocol is tested on two case studies: shrimp (Penaeidae) fisheries off the west coast of Florida and yellowfin tuna (*Thunnus albacares*) in the Atlantic ocean.

Estimating expected values of experimental policies

The basic approach that we recommend is to develop a procedure for assigning an expected long-term value to each member of a set of experimental policy options, where each policy option is defined by two measures: severity of fishing mortality (F_{exp}) reduction and duration (t_x) over which that reduced F_{exp} is to be maintained before moving to a long-term F estimated from the results of the experimental period. The expected value calculation for any experimental option involves three basic steps (Walters and Green 1997): (*i*) identify a range of alternative hypotheses about population response to F_{exp} reduction; (*ii*) estimate the probability distribution for the fishing mortality rate that achieves the maximum sustainable yield (F_{MSY}) at the end of any experimental period under each hypothesis; and (*iii*) calculate the expected performance of the policy option over the set of alternative hypotheses. For the purposes of this paper, we assume that it is possible to implement the experimental F_{exp} policy, and catch is the measured response variable. In reality, it may be necessary to use biomass indices or catch rates as the response variable because of uncertainty in implementing F_{exp} policies. The following subsections outline each of the three steps defined above.

Identify a range of alternative hypotheses

A range of alternative hypotheses refers to hypotheses about stock productivity, a quantity that is of great interest to management to achieve harvest objectives (i.e., F_{MSY} is determined by stock productivity; see Appendix A). At this stage of planning the experiment, the issue is not to determine F_{MSY} per se, but to identify a range of plausible estimates of F_{MSY} in which to quantify the value of conducting an experiment.

Consider situations where the current catch is

$$C_{now} = F_{now}B_{now}$$

and where we can define a clear set of progressively more optimistic hypotheses about future choices (F_i) that would result in biomass (B_i) and catch (C_i) projections into the future. It does not really matter what specific model we use to calculate the expected B_i, C_i projections for each hypothesis about stock productivity (e.g., we might prefer to project forward in time with a detailed size- or age-structured model with stock–recruitment delays and effects or possibly the same model used for routine stock assessments or a much simpler delay-difference or surplus production model). The important characteristic of the prediction model is that it predicts a unique F_{MSY} and associated B_{MSY} for each hypothesis, so that we can order the hypotheses from most conservative (i.e., $F_{MSY} << F_{now}$; major gain from reducing F) to most optimistic (i.e., $F_{MSY} = F_{now}$; no gain from reducing F). When the model is solved forward in time under some experimental reduced policy (F_{exp}), it should display a range (over the hypotheses about F_{MSY}) of expected experimental response patterns of catch. Such an experimental policy will start with an initial catch reduction for the lower F_{MSY} hypotheses followed by recovery of catch to above C_{now} (e.g., Fig. 1). If none of the included hypotheses results in eventual C_i above C_{now}, then none of these hypotheses imply the stock to be currently overfished, and there is no point in continuing the experimental design exercise.

Note that to create a range of hypothesized catch responses like Fig. 1, it may be necessary to assume that some previously estimated model parameter has changed over time so as to invalidate assessments of the parameter value based on historical data. For example, suppose the projections are made with a logistic model $dB/dt = rB(1 - B/K) - C_i$ with fitted parameter estimates r and K and that the stock is relatively stable at $B_{now} < K/2$. To represent the hypothesis that $F_{now} = F_{MSY} = r/2$, it would be necessary to also represent B_{now} as a stable biomass to assume that K has decreased over time, such that $B_{now} \approx K/2$. In more complex models, such changes can be represented as hypothesized decreases in natural mortality (M), decreases in growth rate, and (or) decreases in the maximum or equilibrium unfished recruitment rate.

A simple dynamic model that we have found useful for representing alternative hypotheses about F_{MSY} is the simple numbers dynamics equation (for definitions of symbols see List of Symbols):

© 2008 NRC Canada

Fig. 1. Predictions of expected catch changes for a hypothetical shrimp (Penaeidae) stock (parameters in List of symbols), under a range of alternative hypotheses about the maximum sustainable yield fishing mortality rate F_{MSY}. Each line represents an alternative hypothesis about the current F relative to F_{MSY}.

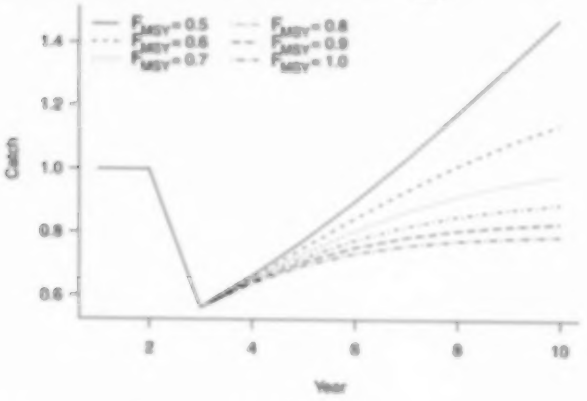

$$(1) \qquad dN/dt = R_t - (M + F_t)N_t$$

where recruitment rate R_t is assumed piecewise constant over annual time steps and is predicted for year t from the Beverton–Holt recruitment relationship

$$(2) \qquad R_t = aN_{t-k}/(1 + bN_{t-k})\, e^{\varepsilon_t}$$

where N_{t-k} is abundance at the start of year $t - k$, k is the age at recruitment to the harvestable stock N_t, and ε_t is an annual recruitment deviation (process error term in a mixed error model). The time dynamics for this model can be calculated as

$$(3) \qquad N_{t+1} = \frac{R_t}{Z_t} + \left(N_t - \frac{R_t}{Z_t}\right) e^{-Z_t}$$

$$(4) \qquad C_t = F_t \left[\frac{R_t}{Z_t} + \frac{(N_t - R_t/Z_t)(1 - e^{-Z_t})}{Z_t}\right]$$

where $Z_t = F_t + M_t$ is the total mortality rate, and C_t is the total catch for year t. For this model, we assume average body weight (w_t) remains constant at a mean, so that yield (biomass catch) is predicted to be $Y_t = C_t\bar{w}$ (i.e., we conservatively ignore effects of reduced F on $\bar{w}$). Given constant mean weight, F_{MSY} is given simply in terms of the maximum juvenile survival rate (a) and natural mortality rate (M) as

$$(5) \qquad F_{MSY} = \sqrt{aM} - M$$

and a is given when F_{MSY} is taken as the leading parameter (e.g., Schnute and Kronlund 1996) by $a = (F_{MSY} + M)^2/M$. To represent alternative hypotheses about changes in carrying capacity over time given no assumed change in M or F_{MSY}, we alter the stock–recruitment carrying capacity parameter (b). The equilibrium stock size (N_e) for eq. 2 given constant Z is given by $N_e = 1/b[a/(Z - 1)]$, which implies simple solutions for b, etc. when N_e is set to N_{now}.

Generally, the range of alternative hypotheses leading to a range of catch trajectories like Fig. 1 will be generated by varying a key leading parameter (preferably F_{MSY}) over a grid of discrete values, then calculating values of other model parameters from N_{now}, F_{now}, C_{now}, and possibly a using constraint relationships like eq. 5. For example, a can be derived using M and the hypothesis F_{MSY} as $a = (F_{MSY} + M)^2/M$ and

$$b = \left(\frac{a}{F_{now} + M} - 1\right)/N_{now}$$

The lower bound for the leading F_{MSY} value should be set a small fraction (e.g., 10%) of the estimated F_{MSY} in the historical stock assessments, and the maximum should be set to at least F_{now}. Setting the leading F_{MSY} value to F_{now} amounts to including a rationalizer hypothesis (see expected value of perfect information, page 195 in Walters 1986) in the set of alternative hypotheses, in the sense that assuming $F_{now} = F_{MSY}$ is equivalent to assuming that current management is already optimum (i.e., that hypothesis rationalizes the current management policy F_{now}). The hypothesis set should contain enough parameter combinations (discrete values of the leading parameter) to provide a relatively smooth representation of possible catch trajectories, and this can usually be achieved by using around 10 hypotheses or grid points.

Calculating the expected performance of a policy option

One thing that is certain is that response to any experimental F policy will not exactly follow any of the hypothesized average catch trajectories like in Fig. 1. Rather, there will be variations in realized F from the experimental target value (F_{exp}), and stock size will vary from the expected growth trajectory because of variations in recruitment, mortality, and growth, as well as implementation error. This means that at the end of any experiment of duration t_e years with experimental fishing rate F_{exp}, it is by no means certain that the correct production hypothesis (F_{MSY}) will be selected as most likely to have given rise to the observed experimental catch sequence $C_1 \ldots C_{t_e}$. Rather, we must admit that for each possible true F_{MSY}, there is a distribution of possible estimates, represented with the discrete hypothesis set as a frequency distribution of concluding that each hypothesis h is correct.

To calculate the expected performance (V) of an experimental policy, where performance is measured most simply by total catch over a time horizon (T years), we have to calculate the expected catch (summed over all hypotheses) during the experimental period plus the expected long-term catch averaged again over hypotheses and over the frequency distribution of possible long-term estimates ($\hat{h}$) of the best hypothesis:

$$(6) \qquad V = \sum_h \left[\sum_{t=1}^{t_e} \lambda^t C_{h,t} + \sum_{\hat{h}} \mathbf{P}(\hat{h}|h) \sum_{t=t_e+1}^{T} \lambda^t C_{h,\hat{h},t}\right]$$

Here, $C_{h,t}$ is the expected catch in experimental year t if hypothesis h is correct (e.g., catch sequence like in Fig. 1), and $C_{h,\hat{h},t}$ is the catch in later years t if hypothesis h is correct but if hypothesis $\hat{h}$ is assumed to be true in setting long-

© 2008 NRC Canada

term policy (i.e., if F is set to the F_{MSY} for hypothesis $\hat{h}$). $\mathbf{P}(\hat{h}|h)$ is the probability of concluding that $\hat{h}$ is most likely to have given rise to the data given that hypothesis h was actually correct; in traditional statistical terms, it essentially represents the power of the experiment. λ is a discount factor (e.g., $\lambda = 0.98$ represents a 2% annual discount rate). R code (R Development Core Team 2006) to implement eq. 6 is available from the authors upon request. Equation 6 can be easily modified to include more complex intergenerational discount factors (Sumaila and Walters 2005) and other economic terms such as fishing costs. Note that in simply averaging catch outcomes over hypotheses h, we are implicitly treating each h as an equally likely predictor of the future (assigning each h equal prior probability); an informative prior could be used for the averaging, but this would use historical experience as a predictor for future response and would violate the spirit of admitting wide uncertainty about future yield responses to the experimental rebuilding regime. That is, in using simple averaging we are essentially setting aside all historical data except insofar as the data have been used to estimate N_{MSY} and F_{MSY} and determining the range of alternative hypotheses about F_{MSY}. The reason for conducting the experiment in the first place is because the historical data are not informative about production patterns, and there is evidence of sustainable overfishing.

V can be easily calculated given models for the C_t responses and for the possible statistical outcomes $\mathbf{P}(\hat{h}|h)$ of the experiment. Random effects can be included in the calculations by calculating a large number of stochastic C_t sequences, with a single $\hat{h}$ outcome choice for each sequence, and averaging over these; however, in our experience nearly the exact same answer is obtained using average C_t for each model and F sequence and using a single assessment of the probability distribution $\mathbf{P}(\hat{h}|h)$.

Dual effects of control typically involve tradeoffs (see page 257 in Walters 1986), and these are quite evident in eq. 6. To make the second term of the equation larger, we want to make $\mathbf{P}(\hat{h}|h)$ as close to diagonal as possible (i.e., to make the probabilities of concluding $\hat{h}$ not equal to h as small as possible). But experimental choices that achieve this goal may require more informative choices for the first term of the equation (i.e., lower F_{exp} that lead to the highest contrast among h in predictions of $C_{exp,t}$).

Choosing among alternative hypotheses at the end of the experiment

The only serious technical difficulty in applying the value assessment eq. 6 is in assessing the error rate probability distribution ($\mathbf{P}(\hat{h}|h)$) of concluding that $\hat{h}$ is correct when h is actually correct, for each correct possibility h. Note that we can think of $\mathbf{P}$ as simply a matrix of probabilities or frequencies of occurrence, with a column for each true hypothesis and a row for each hypothesis that might be concluded to be true at the end of a period of experimental observation.

A straightforward way to estimate $\mathbf{P}(\hat{h}|h)$ is to conduct a large number of simulation trials under each h with a closed loop model that includes simulation of the full management data gathering and assessment process as well as the population dynamics responses (i.e., to repeatedly simulate the conduct of the management experiment, including simulation of resulting data patterns and data analysis; e.g., Cooke 1999). Then simply count the number of times that this closed loop model results in $\hat{h}$ being the most likely or best-fitting hypothesis as of time t_e.

To numerically construct the $\mathbf{P}(\hat{h}|h)$ matrix, we simplify the closed loop simulation approach by incorporating a total error term (v_t) that represents the combined effects of observation error, process error, and implementation error. Here we assume that the main data to be used in evaluating alternative hypotheses about stock productivity are the observed catch sequences over the experimental period ($C_{exp,t}$). All other indicators of population abundance and relative cohort strength will be used only as auxiliary information to validate that the intended experimental fishing mortality rate was achieved (and to correct $C_{exp,t}$ predictions when it has not). For a single, realized experiment, the negative log likelihood of the observed catch series for each hypothesis $\hat{h}$ is given by

$$(7) \qquad \ell_{\hat{h}} = n \ln(\sigma_v) + \frac{1}{2\sigma_v^2} \sum_{t=1}^{t_e} \left[\ln(C_{\hat{h},t}) - \ln(C_{h,t}) + v_t \right]^2$$

where σ_v is the standard deviation in the total errors, and v_t is a random normal deviate with mean equal to 0. Note that an autocorrelated sequence of random normal deviates can be used to represent error propagation over the duration of the experiment. In our simulation trials, we assume an autocorrelation coefficient of $\rho = 0.2$ in the total error terms. For each hypothesis h, the most likely alternative hypothesis $\hat{h}$ is the hypothesis with the lowest $\ell_{\hat{h}}$ value. For example, if there were no error in the experiment, then the diagonal elements of $\mathbf{P}(\hat{h}|h)$ would contain the most likely values.

To construct the $\mathbf{P}(\hat{h}|h)$ matrix, we conduct 1000 independent trials and keep track of the frequencies of the most likely model $\hat{h}$ for each of the h hypotheses. That is, each of the columns in $\mathbf{P}(\hat{h}|h)$ will contain 1000 selected models $\hat{h}$. The frequency of occurrence method greatly reduces the data simulation problem and assumes that $C_{exp,t}$ will vary from $C_{h,t}$ in a lognormal pattern $C_{\hat{h},t} = C_{h,t}\, e^{v_t}$. Although this method does not allow for explicit specification of observation error, process error, and implementation error, in practice, rarely do we have sufficient data to partition the total error into its specific components during the assessment phase.

Finding the best combination of F_{exp} and t_e

The basic concept of statistical decision analysis is to seek that policy option (in this case, combination of F_{exp}, t_e) that maximizes expected utility (V of eq. 6) over possible "states of nature" (h), with each possible outcome or state of nature weighted by its prior probability of being correct (equal weights are assumed in eq. 6). To do this search, we evaluate eq. 6 for V for a grid of F_{exp} and t_e, then simply pick out the combination that gives the highest V. The grid approach also allows direct and immediate evaluation of sensitivity of the results to the experimental choice, in terms of how V varies with changes in the two decision variables.

For example, for a grid of 10 F_{exp} values and 20 t_e experimental duration options, it is a fairly tedious computational

© 2008 NRC Canada

Fig. 2. Historical catch and effort patterns for two stocks that appear to have suffered recruitment overfishing based on fitting simple dynamic models to the catch time series: (*a*) shrimp (all penaeid species combined) off the west coast of Florida (FL, Florida; NMFS, National Marine Fisheries Service); (*b*) Japanese longline fishery for yellowfin tuna (*Thunnus albacares*) in the Atlantic Ocean. Effective effort for the tuna case is estimated as catch divided by spatial mean catch per effort estimated by method of Walters (2003).

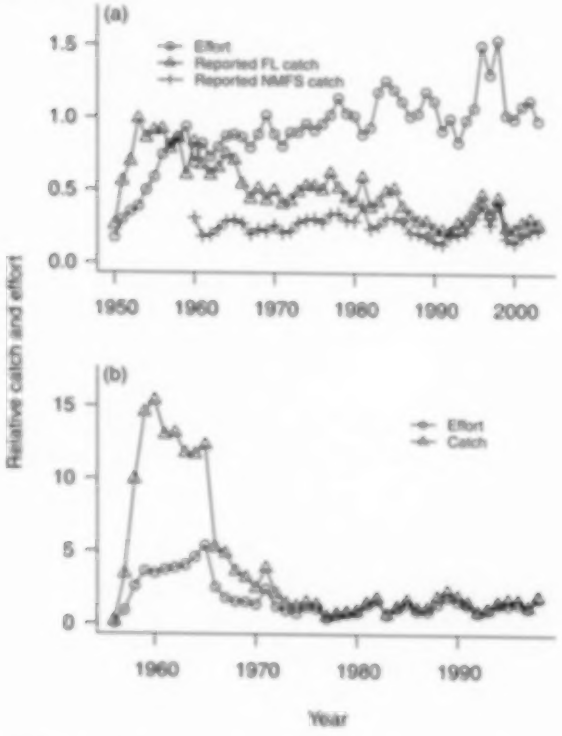

exercise to evaluate eq. 6 numerically. At each grid point, enough (at least 100) Monte Carlo simulation trials need to be done for each correct hypothesis h to provide a relatively stable estimate of the $\mathbf{P}(h|h)$ matrix. However, the whole exercise is relatively fast on personal computers, provided the dynamic model and likelihood calculations used to evaluate C_t trajectories are relatively simple (e.g., eqs. 2–4 combined with simple SS_h likelihood checks).

Case examples

Two very different fisheries illustrate that similar predictions about the best experimental strategy are likely to result from a wide range of population dynamics parameters (Fig. 2). Both examples appear to represent instances of "smooth collapse", as defined by Mullon et al. (2005). The West Florida shrimp fishery targets pink (*Farfantepenaeus duorarum*), brown (*Farfantepenaeus brasiliensis*), and white (*Litopenaeus setiferus*) shrimp and is the most valuable commercial fishery on the Gulf of Mexico coast of Florida. The Japanese longline fishery in the Atlantic Ocean takes a variety of species, with yellowfin tuna (*T. albacares*) being historically the largest biomass component. Both fisheries developed rapidly during the 1950s and 1960s, with early peak catches followed by declines to relatively stable levels by 2000. Both involve relatively short-lived species, for which it would be difficult to argue that the long-term decline in catch simply represents nonsustainable removal of accumulated older individuals from the populations; rather, we would likely conclude from the patterns in catch and effort data that these stocks are sustainably overfished.

Table 1. Assumed parameter values, priors, and median parameter estimates for a simple dynamic model of West Florida shrimp (Penaeidae) and Atlantic yellowfin tuna (*Thunnus albacares*) vulnerable to longline fisheries based on data shown in Fig. 2.

	Priors			Parameter estimates	
Stock	M	F_{MSY}	$\sigma_{F_{MSY}}$	F_{MSY}	R_{MSY}/R_o
Shrimp	2.0	1.0	0.5	0.51	0.16
Tuna	0.3	0.35	0.15	0.10	0.31

In the shrimp case, there is considerable uncertainty about what catch data to use for assessment (Fig. 2). Total catches reported by Florida shrimpers have declined over time, indicative of possible overfishing, but in earlier years a substantial proportion of these catches were likely taken in fishing areas as distant as the western Gulf of Mexico and the Campeche Bank off Mexico (R. Muller, Florida Marine Research Institute, 100 Eighth Avenue SE, St. Petersburg, FL 33701-5095, personal communication). National Marine Fisheries Service (NMFS) summaries of catch reported to have been taken in Florida waters (F. Patella and J. Nance, NMFS, 4700 Avenue U, Galveston, TX 77551, USA, personal communication) do not show a decline over time, but it is not clear how much to trust the catch reporting for earlier years because of obvious incentives for fishers to report their landings as having come from distant waters. The two catch series represent the limits of a range of hypotheses, from pessimistic (rather severe decline and overfishing) to optimistic (catches sustainable at current or possibly even higher levels).

We fit eqs. 2–4 to scaled catch time series (Fig. 2), assuming constant catchability (F per unit effort), known M, and estimate F_{MSY} and R_o (List of symbols) using a Bayesian approach (see Appendix B for details). Under these assumptions and given observed relative efforts E_t scaled so that $F_t = E_t$ and $F_{MSY} = E_{MSY}$ for the final year of the observed data, only the recruitment curve compensation parameter ($a = (F_{MSY} + M)^2/M$)) and the unfished natural recruitment rate (R_o) need to be estimated. In the case of the yellowfin tuna, we allow for both observation error and process error where we assume the variance in the process error terms $\sigma_w^2 = 0.12$. In the case of the Florida shrimp, an observation error only model was fitted to the data.

Considering catch declines under continuing high fishing efforts in the shrimp fishery, the resulting estimates of F_{MSY} (using the pessimistic catch series for Florida shrimp) were considerably lower than F_{MSY} (Table 1). Allowing F_{MSY} to vary in the parameter estimation, with a large value of $\sigma_{F_{MSY}}$, results in a relatively uninformative prediction about the present fishing mortality rate, but a rather informative prediction about F_{MSY} relative to F_{MSY} and estimates of cur-

© 2008 NRC Canada

Fig. 3. A random sample (N = 5000) of F_{MSY} and F_{now} points from the joint posterior distributions when F_{now} is allowed to vary subject to weak prior distribution on F_{now} (*a*: Florida shrimp; *c*: Atlantic yellowfin tuna). Panels *b* and *d* represent the distribution of R_{now}/R_o estimates for Florida shrimp and Atlantic yellowfin tuna, respectively. The vertical broken lines correspond to estimates of F_{MSY}, and the horizontal lines correspond to $F_{now} = F_{MSY}$. In both cases, overfishing is suspected.

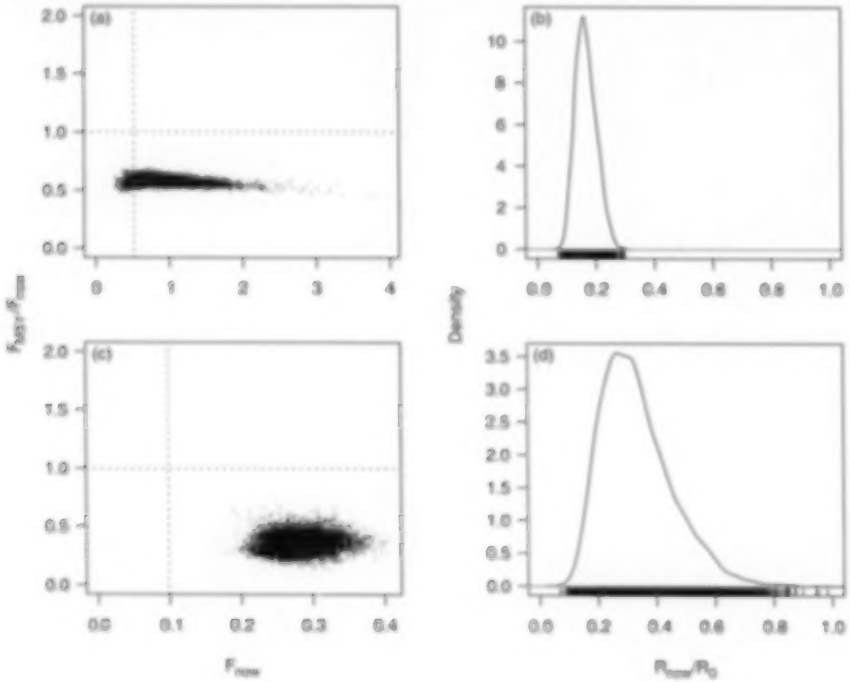

rent recruitment relative to unfished recruitment (R_{now}/R_o) (Figs. 3*a* and 3*b*). This pattern was maintained for a wide range of assumptions about prior distribution for F_{now}. Estimates of current recruitment relative to unfished natural recruitment were low, again indicative of fairly severe recruitment overfishing. We also tried various error assumptions in the fitting, involving alternative weighting of catch and mixed error models with recruitment deviations; none of these weighting schemes gave substantially different estimates of F_{MSY}/F_{now} or R_{now}/R_o than obtained by simply fitting the deterministic (pure catch observation error) version of the model. So from the standpoint of traditional fisheries assessment models (with stationary recruitment relationships), it seems quite certain for the Florida shrimp case that the stock has been overfished and that fishing mortality rates should be reduced.

In the case of the Atlantic yellowfin tuna, resulting estimates of F_{MSY} were also much lower than the current fishing rate (F_{now}) (Table 1). However, there is more uncertainty in the level of depletion as indicated by the R_{now}/R_o ratio (Fig. 3*d*). Similar patterns were obtained for F_{MSY}/F_{now} or R_{now}/R_o over a wide range of assumptions about variability in recruitment (σ_w^2). Admitting more recruitment variability results in more uncertainty in R_{now}/R_o, or levels of depletion, but the estimates of F_{MSY}/F_{now} suggest overfishing in the Atlantic yellowfin tuna case.

If such assessment results were presented to the fishing industries with recommendations for substantial reduction in fishing effort (roughly 50% for each example), it would be questioned if the immediate catch losses would ever be compensated for by higher future catches. In the shrimp case, it would be argued that urban development along the West Florida coast has caused decreases in juvenile nursery capacity for shrimp, causing catches to decline while F has remained near F_{MSY} all along. In the yellowfin tuna case, it would be argued that losses in catch of other tuna and billfish species might never be compensated by increases in the abundance of those other species, that any potential catch increases might be captured by other fishing fleets, and that recruitment to ages or sizes vulnerable to longline fishing has been reduced not by longline overfishing but by increases in fisheries targeting younger fish (e.g., purse seines). So for both examples, fishing industries would argue that effort reduction would lead to a future like one of the more pessimistic catch trajectories shown in Fig. 1, with immediate loss to them but no compensating, long-term increase.

It would be difficult for assessment scientists to dispute arguments about nonstationarity in production dynamics. There is no scientific way to discern whether or not the arguments are wrong, except through empirical testing. So these cases are ideal examples of situations where an expected value calculation like eq. 6 should be used to provide a balanced representation of possible future fishery values.

We calculated V values for time horizons (T) of 50 years and λ = 0.98, while evaluating $\mathbf{P}(\hat{h}|h)$ using 1000 simulations per h. Experimental catch observations were assumed

© 2008 NRC Canada

to have a coefficient of variation (CV, standard deviation of lognormal variation in v_t) of 0.2 for Florida shrimp and 0.3 for Atlantic yellowfin tuna, based on the average error for both case stocks in fitting historical catches using the eqs. 2–4 model; similar results were obtained for lower (0.05) variation and for autocorrelated versus independent deviations. The range of F_{MSY} hypotheses was taken to be 10 evenly spaced values ranging from the stock assessment best fit estimate as a lower bound to the current F (F_{curr}) as an upper bound, which meant a range from around $0.5F_{curr}$ to F_{curr}. Experimental period F_{exp} values were tested over a wider range, from 0.1 to 1.0 times F_{curr}, so as to include lower (and hence more quickly informative) experimental values than any F_{MSY} considered in the alternative hypotheses.

Qualitatively similar results were obtained for both case stocks (Fig. 4) in that there was a domain of experimental durations and intensities that maximized the experimental value V. V exhibited a relatively weak, dome-shaped relationship to F_{exp} and t_e, with optimum F_{exp} close to the most conservative (lowest) F_{MSY} and with optimum duration of experiment in the range 5–15 years depending on speed of population response (shorter experiment best for faster-growing shrimp stock without recruitment lag). Note that V was not expected to exhibit large changes over the experimental policy options, since it represents an average over a wide range of productivity hypotheses, so that potential gains under any particular hypothesis tended to be balanced by potential losses under other hypotheses. Note also that despite not being lower than any F_{MSY} considered, the optimum F_{exp} was certainly influenced strongly by the information value (reduction of spread in $\mathbf{P}(h|h)$) implied by adopting an F_{exp} quite different from F_{curr}; in the absence of such a value (e.g., in V calculations with very high observation variance), V is maximized by choosing F_{exp} roughly half way between the minimum and maximum F_{MSY} values included in the hypothesis range. Assuming unrealistically precise observations (v_t with CV < 0.05) led to shorter duration experiments, with lower (more extreme than any included F_{MSY}) F_{exp} being optimum. Assuming pessimistically high CV (0.4 or higher) led to a relatively flat value surface with no discernable benefit from following an experimental policy.

The yellowfin tuna example involves relatively low F_{MSY} and a substantial recruitment lag (L = 3 years in eq. 2), which imply relatively slow stock rebuilding and hence statistical difficulty in distinguishing among hypotheses even when F_{exp} is very low. So this case is near the edge of the domain of parameter combinations for which experimental management can improve (in an expected value sense) upon the simpler certainty equivalent or passively adaptive policy choice of simply adopting an assumed F_{MSY} near the middle of the range of hypotheses, without expectation that improved estimates of F_{MSY} will be obtained afterward. We can think of V as consisting of two expected value components: $V = V_{CE} + V_I$, where V_{CE} is a certainty equivalent value component estimated for any long-term (fixed) F choice by averaging values obtained under that choice over hypotheses without including changes in F due to future learning, and V_I is gain in value due to learning more about F_{MSY} (Ludwig and Walters 1982; Walters and Ludwig 1987). V_I increases for experimental choices F_{exp} further away from the base F_{curr}; however, the V_I component for the tuna example is barely large enough to imply an optimum F_{exp} different from the F that maximizes V_{CE}. (It is not uncommon for the policy choice based on maximization of V_{CE} to look as good or better than any more extreme policy choice involving experimental probing for better information — see for example Johnson and Williams 1999.)

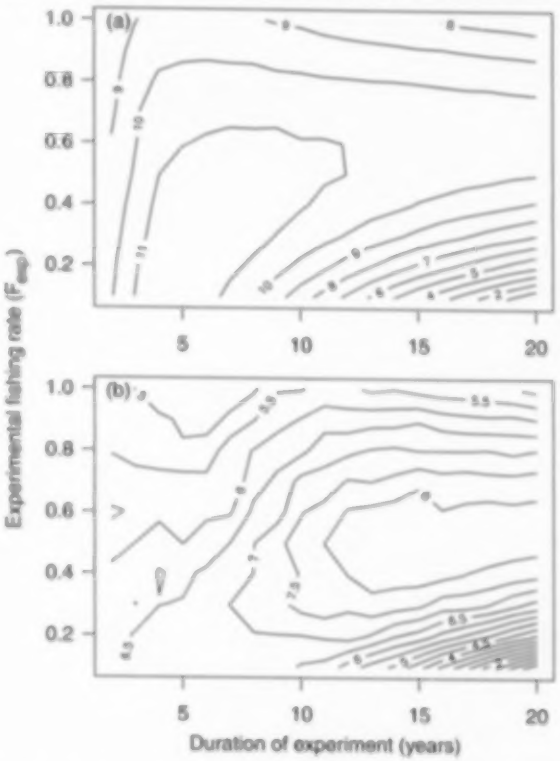

Fig. 4. Variation in expected long-term value of catches (V of eq. 6 scaled relative to its maximum value), with changes in experimental fishing mortality rate relative to current fishing rate (F_{exp}/F_{curr}, respectively) and with planned duration t_e of the experimental period before F is set to a long-term F_{MSY} value based on the most likely F_{MSY} hypothesis: (*a*) shrimp off the west coast of Florida; (*b*) yellowfin tuna (*Thunnus albacares*) in the Atlantic Ocean.

Discussion

There are at least three major issues that could cause an experimental plan based on the methods described above to fail upon implementation. The first issue is a "none of the above" response, where the stock exhibits some more extreme behavior during the experimental period than predicted under the range of response hypotheses. This happened for example with the Newfoundland northern cod stock and is a substantial risk in any situation where the stock has been severely reduced by fishing and or there has been substantial change in habitat or ecosystem structure. Change in the productivity regime during the course of the experiment, or during the transition from experiment period

© 2008 NRC Canada

to the new policy, would obviously lower the perceived value of conducting the experiment in the first place. However, the alternative is to continue with sustainable overfishing and justifying this practice despite legislation that states otherwise (e.g., US Sustainable Fisheries Act). Obviously, the best way to guard against this cause of failure is to ensure that the range of hypothesized responses is very wide.

The second and far more likely cause is implementation failure, where the target fishing mortality rate reduction ($F_{now} - F_{exp}$) is simply not achieved. This can happen, for example, if the implementation tactic is to reduce fishing effort, and if the stock is undergoing a range collapse such that the catchability coefficient q (where $F = qE$, E = effort) is increasing rapidly. If F is to be reduced through tactics involving spatial or seasonal closure(s), increases in fishing effort in the remaining open areas or times may be enough to prevent overall F from decreasing. In a growing number of situations in North America, there may be a strong numerical response of fishing effort from components of the fishery for which effort is difficult to regulate, in particular, recreational fisheries. The best way to guard against such failures is to make substantial investment as part of the experimental program in monitoring programs aimed explicitly at measuring fishing activity (swept area) and F as accurately as practical, using the best possible logbook (and observer) programs for swept area analysis and possibly tagging programs for direct assessment of changes in F (Martell and Walters 2002).

The third and most likely cause is to have the planned immediate change from F_{now} to F_{exp} replaced by an incremental or titration scheme due to pressure from fisheries managers and other stakeholders, where F is to be reduced gradually over time so as to minimize socio-economic disruption. The intuitive view of such gradual change from an experimental perspective is that response to the change can be monitored so as to see when the best F has been reached; this intuitive view presumably derives from experience in elementary chemistry courses, where titration experiments typically produce sudden and clear results as experimental inputs are changed. The basic problem with such an approach is that the intuitive imagery of clear and sudden response to finding the right input level is wrong in the first place when learning depends on gathering multiple observations over time from a complex system. A gradual change in F will radically slow the learning process (i.e., slow the convergence of $\mathbf{P}(\hat{h}|h)$ to a strongly diagonal structure) and to assure confounding of fishing effects with other progressive changes (e.g., habitat, regime shifts) that may be occurring at the same time.

Despite these implementation risks, an experimental approach to deciding on target F reductions may be much easier to justify to managers and fishing stakeholders than the usual assessment approach of presenting dubious probability distributions for those estimates, then hoping that the management process will somehow use such information wisely. It has recently become fashionable to present assessment results in probabilistic terms, to emphasize uncertainty and hopefully encourage precautionary policy choices; unfortunately, the probabilistic results typically depend heavily on strong assumptions about stationarity in at least some key population parameters (to avoid completely flat probability distributions) and hence tend to severely underestimate real uncertainty and to make the assessments less rather than more credible. In the experimental approach, debate about how much uncertainty to admit is reduced to debate about the width of the range of F_{MSY} hypotheses to admit and about how much unexplained variability to expect in prediction of how long it will take to distinguish among alternative hypotheses. Further, management advice is typically couched in terms of the need to err in cautious directions, which really just reveals that most scientists and managers are highly (and perhaps inappropriately) risk averse rather than showing it is wise to be precautionary in the first place. The expected value (V) calculations used to compare experimental alternatives force either a risk-neutral comparison or an explicit choice to replace catch as a performance measure with some risk-averse utility measure.

The expected value calculation provides an estimate of future catch benefits averaged over a fairly wide range of alternative hypotheses about stock response, if a particular fixed fishing rate F_{exp} is maintained for some years without adaptive correction part way through the experimental period. Using the value calculation to find a best initial F_{exp} does not in fact commit or require managers to not do such adaptive responses later in time; so the calculation can be viewed as providing a minimum estimate of the benefits of an experimental approach.

Acknowledgements

Support for this study was from a Natural Sciences and Engineering Research Council of Canada Discovery Grant to the C.J. Walters and from a National Science Foundation grant to James F. Kitchell. We thank Pierre Kleiber, Elizabeth Martell, Olaf Jensen, and two anonymous reviewers for useful discussions and comments on this manuscript.

References

Caddy, J.F., and Agnew, D.J. 2004. An overview of recent global experience with recovery plans for depleted marine resources and suggested guidelines for recovery planning. Rev. Fish Biol. Fish. **14**: 43–112. doi:10.1007/s11160-004-3770-2.

Cooke, J.G. 1999. Improvement of fishery-management advice through simulation testing of harvest algorithms. ICES J. Mar. Sci. **56**: 797–810. doi:10.1006/jmsc.1999.0552.

Johnson, F., and Williams, K. 1999. Protocol and practice in the adaptive management of waterfowl harvests. Conserv. Ecol. [online] **3**(1): 8. Available from www.consecol.org/vol3/iss1/art8/.

Ludwig, D., and Walters, C.J. 1982. Optimal harvesting with imprecise parameter estimates. Ecol. Model. **14**: 273–292. doi:10.1016/0304-3800(82)90023-0.

Martell, S.J.D., and Walters, C.J. 2002. Implementing harvest rate objectives by directly monitoring exploitation rates and estimating changes in catchability. Bull. Mar. Sci. **70**: 695–713.

Mullon, C., Fron, P., and Cury, P. 2005. The dynamics of collapse in world fisheries. Fish Fish. **6**: 111–120.

R Development Core Team. 2006. R: a language and environment for statistical computing. R Foundation for Statistical Computing, Vienna, Austria. ISBN 3-900051-07-0.

Schnute, J.T., and Kronlund, A.R. 1996. A management oriented approach to stock recruitment analysis. Can. J. Fish. Aquat. Sci. **53**: 1281–1293. doi:10.1139/cjfas-53-6-1281.

© 2008 NRC Canada

Shelton, P.A., Sinclair, A., Chouinard, G.A., Mohn, R., and Duplisea, D.E. 2006. Fishing under low productivity conditions is further delaying recovery of Northwest Atlantic cod (*Gadus morhua*). Can. J. Fish. Aquat. Sci. **63**: 235–238. doi:10.1139/F05-253.

Sumaila, U.R., and Walters, C.J. 2005. Intergenerational discounting: a new intuitive approach. Ecol. Econ. **52**: 135–142. doi:10.1016/j.ecolecon.2003.11.012.

Walters, C.J. 1986. Adaptive management of renewable resources. MacMillan Publishing Co., New York.

Walters, C.J. 2003. Folly and fantasy in the analysis of spatial catch rate data. Can. J. Fish. Aquat. Sci. **60**: 1433–1436. doi:10.1139/f03-152.

Walters, C.J., and Green, R. 1997. Valuing large scale management experiments for natural resources. J. Wildl. Manage. **61**: 987–1006. doi:10.2307/3802096.

Walters, C.J., and Ludwig, D. 1987. Adaptive management of harvest rates in the presence of a risk averse utility function. Nat. Resour. Model. **1**: 321–337.

Walters, C.J., and Martell, S.J.D. 2004. Fisheries ecology and management. Princeton University Press, Princeton, N.J.

List of symbols

t	index for time
k	age at recruitment (years)
F_{exp}	experimental fishing rate
t_e	duration (in years) of experimental treatment
MSY	maximum sustainable yield
B_t	biomass at time t
C_t	yield at time t
R_t	recruitment (in numbers)
λ	discount rate
	Estimated parameters
F_{MSY}	fishing rate corresponding to MSY
R_o	unfished recruitment
F_{term}	terminal fishing rate
ε_t	annual recruitment deviations (process errors)
	Derived parameters
a	maximum juvenile survival rate
b	recruitment capacity parameter
F_t	instantaneous fishing mortality rate
Z_t	total instantaneous mortality rate
V	expected performance (landings or landed value)

Appendix A. Proof of $F_{MSY} = \sqrt{aM} - M$

Assuming steady-state conditions, the catch equation can be written as

$$\text{(A1)} \qquad C = FN = \frac{FR}{M+F}$$

Note that R can be expressed as

$$R = -\frac{M+F-a}{b}$$

under steady-state conditions (i.e., set $N = R/Z$ and substitute this for N in eq. 2 and solve for R). Substituting this expression into eq. A1 results in

$$\text{(A2)} \qquad C = -\frac{F(M+F-a)}{(M+F)b}$$

Next, differentiate eq. A2 with respect to F, set this expression equal to zero, and solve the quadratic expression for the positive root that corresponds to F_{MSY}:

$$\frac{\partial C}{\partial F} = -\frac{M+F-a}{(M+F)b} + \frac{F(M+F-a)}{(M+F)^2 b} - \frac{F}{(M+F)b}$$

$$0 = -\frac{M^2 + 2MF + F^2 - aM}{(M+F)^2 b}$$

$$0 = -M^2 + 2MF + F^2 - aM$$

Solve for positive root of F:

$$\text{(A3)} \qquad F = \sqrt{aM} - M$$

which proves eq. 5.

Appendix B. Bayesian parameter estimation

In fitting eqs. 2–4 to catch conditional on effort data for Florida shrimp and Atlantic yellowfin tuna, we assume lognormal errors in reported catches. The posterior distribution is given by

$$\text{(B1)} \qquad P(C_t|E_t,\Theta) \propto L(C_t|E_t,\Theta)P(\Theta)$$

where $P(\Theta)$ represents the prior probability on model parameters. The negative log likelihood for each catch observation is

$$\text{(B2)} \qquad L(C_t|E_t,\Theta) = \ln(\sigma) + \frac{[\ln(C_t) - \ln(\hat{C}_t)]^2}{2\sigma^2}$$

where $\hat{C}_t$ is the observed removals, and σ is estimated from the data. Uninformative prior distributions for estimated parameters (List of symbols) were assumed, with the exception of the terminal fishing rate (F_{term}) and annual recruitment deviations (ε_t). $P(F_{term})$ was assumed lognormal with mean and variance specified in Table 1. Recruitment deviations were also assumed lognormal with mean = 0 and a fixed variance (σ_w^2). In the Florida shrimp case, $\sigma_w^2 = 0$, which is equivalent to fitting an observation error only model. In the Atlantic yellowfin tuna case, $\sigma_w^2 = 0.12$, and the total combined error was estimated at $\sigma^2 + \sigma_w^2 = 0.3$ (i.e., this is a mixed process and observation error assessment model).

We sampled the posterior distribution using the Metropolis–Hastings algorithm (Gelman et al. 1995) implemented in AD Model Builder (Otter Research Ltd. 1994). Chain convergence was assessed by visual inspection of running medians (length = 50) in trace plots. Data for Fig. 3 were generated using 5000 random samples from the posterior distribution.

References

Gelman, A., Carlin, J., Stern, H., and Rubin, D. 1995. Bayesian data analysis. Chapman and Hall, London.

Otter Research Ltd. 1994. An introduction to AD Model Builder for use in nonlinear modeling and statistics. Otter Research Ltd., Nanaimo, B.C.

© 2008 NRC Canada

Forage fish of the Pacific Rim as revealed by diet of a piscivorous seabird: synchrony and relationships with sea surface temperature

Julie A. Thayer, Douglas F. Bertram, Scott A. Hatch, Mark J. Hipfner, Leslie Slater, William J. Sydeman, and Yutaka Watanuki

Abstract: We tested the hypothesis of synchronous interannual changes in forage fish dynamics around the North Pacific Rim. To do this, we sampled forage fish communities using a seabird predator, the rhinoceros auklet (*Cerorhinca monocerata*), at six coastal study sites from Japan to California. We investigated whether take of forage fishes was related to local marine conditions as indexed by sea surface temperature (SST). SST was concordant across sites in the eastern Pacific, but inversely correlated between east and west. Forage fish communities consisted of anchovy (*Engraulis* spp.), sandlance (*Ammodytes* spp.), capelin (*Mallotus* spp.), and juvenile rockfish (*Sebastes* spp.), among others, and take of forage fish varied in response to interannual and possibly lower-frequency oceanographic variability. Take of primary forage species were significantly related to changes in SST only at the eastern sites. We found synchrony in interannual variation of primary forage fishes across several regions in the eastern Pacific, but no significant east–west correlations. Specifically in the Japan Sea, factors other than local SST or interannual variability may more strongly influence forage fishes. Predator diet sampling offers a fishery-independent, large-scale perspective on forage fish dynamics that may be difficult to obtain using conventional means of study.

Résumé : Nous testons l'hypothèse qui veut qu'il y ait des changements interannuels synchrones dans les dynamiques des poissons fourrage autour de la bordure du Pacifique Nord. C'est pourquoi nous avons échantillonné les peuplements de poissons fourrage à l'aide d'un oiseau marin prédateur, le macareux rhinocéros (*Cerorhinca monocerata*), à six sites d'étude côtiers du Japon à la Californie. Nous avons vérifié si les captures de poissons fourrage sont reliées aux conditions marines locales, telles que représentées par la température de surface de la mer (SST). Les SST s'accordent d'un site à l'autre dans l'est du Pacifique, mais il y a une corrélation inverse entre l'est et l'ouest. Les peuplements de poissons fourrage consistent, entre autres, d'anchois (*Engraulis* spp.), de lançons (*Ammodytes* spp.), de capelans (*Mallotus* spp.) et de jeunes sébastes (*Sebastes* spp.) et la capture de poissons fourrage varie en réaction à la variabilité océanographique interannuelle ou aussi peut-être de fréquence moins élevée. La capture de poissons fourrage principaux est en corrélation significative avec SST seulement dans les sites de l'est. Nous observons un synchronisme dans la variation interannuelle des poissons fourrage principaux entre plusieurs régions de l'est du Pacifique, mais aucune corrélation significative entre l'est et l'ouest. Tout particulièrement dans la mer du Japon, des facteurs autres que la SST locale et la variabilité interannuelle peuvent influencer plus fortement les poissons fourrage. L'échantillonnage du régime alimentaire des prédateurs permet d'obtenir, indépendamment de la pêche commerciale, une perspective à grande échelle de la dynamique des poissons fourrage qu'il serait peut-être difficile d'acquérir par les méthodes d'étude conventionnelles.

[Traduit par la Rédaction]

Received 30 March 2007. Accepted 8 November 2007. Published on the NRC Research Press Web site at cjfas.nrc.ca on 12 July 2008. J19924

J.A. Thayer.[1] Department of Wildlife, Fish and Conservation Biology, University of California, One Shields Avenue, Davis, CA 95616, USA; Marine Ecology Division, PRBO Conservation Science, 3820 Cypress Drive #11, Petaluma, CA 94954, USA.
D.F. Bertram[2,3] **and M.J. Hipfner.**[3] Centre for Wildlife Ecology, Simon Fraser University and the Canadian Wildlife Service, RR#1 5421 Robertson Road, Delta, BC V4K 3N2, Canada.
S.A. Hatch.[3] US Geological Survey, Alaska Science Center, 1011 East Tudor Road, Anchorage, AK 99503, USA.
L. Slater.[3] US Fish and Wildlife Service, Alaska Maritime National Wildlife Refuge, 95 Sterling Highway, Suite 1, Homer, AK 99603, USA.
W.J. Sydeman.[3,4] Marine Ecology Division, PRBO Conservation Science, 3820 Cypress Drive #11, Petaluma, CA 94954, USA.
Y. Watanuki.[3] Graduate School of Fisheries Sciences, Hokkaido University, Minato-cho, Hakodate, Japan.

[1]Corresponding author (e-mail: jthayer@prbo.org).
[2]Present address: Canadian Wildlife Service, Institute of Ocean Sciences, Sidney, BC V8L 4B2, Canada.
[3]Co-authors are listed in alphabetical order.
[4]Present address: Farallon Institute for Advanced Ecosystem Research, P.O. Box 750756, Petaluma, CA 94975, USA.

 doi:10.1139/F08-076 © 2008 NRC Canada

Introduction

An extensive body of literature compares population dynamics of marine organisms at various trophic levels with temporal and spatial environmental variation. In the northeastern Pacific, opposing trends in the abundance of zooplankton (Brodeur et al. 1996), salmon (Hare et al. 1999), and some flatfish stocks (Hollowed et al. 2001) have been hypothesized between the Alaska Current and California Current ecosystems. These trends have been linked to the Pacific Decadal Oscillation (PDO) and other large-scale environmental forcing such as the El Niño Southern Oscillation (ENSO; Hare et al. 1999; Hollowed et al.2001). On an even greater scale, global synchronies (or "out-of-phase" fluctuations) have been identified for various commercial species of anchovy (*Engraulis* spp.), sardine, herring, Pacific salmon (*Oncorhynchus* spp.), cod, pollock, and mackerel (Klyashtorin 1998; Beamish et al. 1999; Schwartzlose et al. 1999). Some of these quasi-global-scale observations relate to climate indices such as the Atmospheric Circulation Index, but are poorly correlated with interannual climate indices (e.g., Aleutian Low Pressure Index; Klyashtorin 1998). Freon et al. (2003) found little quantitative evidence for global synchronies of commercial coastal pelagic species worldwide and suggested that regional synchronies forced by climatic changes at the basin scale may be easier to demonstrate and understand.

Time series from fisheries landings are typically based on harvest of a single age class (adults) and may be fraught with socio-economic biases (Bakun and Broad 2003; Freon et al. 2003). Net surveys may also have some limitations in that standardized station sampling may miss patchily distributed species (Larson et al. 1994). Instead, sampling by upper trophic level predators offers an alternative tool for studying forage species (Reid et al. 1996; Mills et al. 2007). Because predators target patchy prey resources, may target juvenile age classes, and can be sampled at low cost compared with traditional net surveys, this technique is garnering substantial attention (Boyd et al. 2006). In this paper, we characterized changes in forage fish communities from the late 1970s to the early 2000s, as sampled by a piscivorous seabird, rhinoceros auklet (*Cerorhinca monocerata*), in six continental shelf regions representing at least three large marine ecosystems in the North Pacific (Fig. 1). The associated forage fish communities included small coastal pelagic species as well as juvenile, large predatory fish. We quantified change in primary forage fishes over a 10-year period (1994–2003). We tested the hypothesis that changes in primary forage species abundance in the auklet diet covaried among regions and were related to synchronous changes in local marine conditions. Fish populations in the different systems may be driven by regional processes, so we used sea surface temperature (SST) as an index of local ocean conditions. Specifically, our objectives were to (*i*) determine rhinoceros auklet diet composition from different shelf systems around the Pacific Rim, (*ii*) examine how diet composition varied spatially and temporally, and (*iii*) describe variation in relation to marine climate on local to basin scales.

Materials and methods

Ocean ecosystems

We conducted studies in three coastal ocean current systems and one transition zone. These contained six study sites: one in the western Pacific and five in the eastern Pacific.

The Tsushima Current branches off from the warm Kuroshio Current into the Sea of Japan and dominates surface flows northeastward along the western margin of the Japanese Archipelago (Park et al. 2004). Other major physical transport mechanisms in this system include mixing at the northern polar front and winter storms (Chiba and Saino 2002). The study site of Teuri Island (TEI; 44°25′N, 141°19′E) is located ~30 km off the coast of northwestern Hokkaido.

The Subarctic Current pushes water eastward across the North Pacific, bifurcating off the coast of British Columbia. To the north in the Gulf of Alaska, persistent coastal downwelling leads to nutrient depletion in the euphotic zone and low productivity following the initial spring bloom (Coyle and Pinchuk 2003). However, other influences contribute to nutrient supply in surface waters, such as freshwater runoff, coastal and bottom topography and strong tides that generate numerous eddies and meanders, frequent storms, surface Ekman flux, and episodic upwelling (Okkonen et al. 2001; Stabeno et al. 2004). St. Lazaria Island (SLI; 56°59′N, 135°42′W) lies in the southeastern Gulf of Alaska, 8 km west of Sitka Sound. Middleton Island (MI; 59°15′N, 146°15′W) is located in the northern Gulf of Alaska, ~80 km south of Prince William Sound and 15 km north of the shelf break.

In the California Current eastern boundary system, northwest winds cause coastal upwelling, particularly near capes and headlands (Chavez et al. 2002). Upwelling is strongest during the spring and summer and leads to nutrient enrichment and cool SST, but mixed-layer depth modifies this relationship (Chavez et al. 2002). Southeast Farallon Island (SFI; 37°42′N, 123°00′W) is situated 29 km south of Pt. Reyes, California, and 8 km east of the shelf break. Año Nuevo Island (ANI; 37°06′N, 122°20′W) lies 1 km off Pt. Año Nuevo, California, and 11 km northeast of submarine canyons extending in from the shelf break.

The Eastern Coastal Transition Zone off British Columbia shares physical characteristics with both the Gulf of Alaska and California Current. Interannually, the position and intensity of the Aleutian Low and North Pacific High atmospheric pressure centers may affect strength of horizontal transport to the north versus south (McGowan et al. 1998). Seasonally, the winter Aleutian Low drives prevailing southerly coastal winds that promote downwelling, but northward movement of the North Pacific High in summer triggers upwelling-favorable northerly winds and equatorward surface currents along the shelf break (Mackas et al. 2001). Triangle Island (TRI; 50°52′N, 129°05′W) lies in the Eastern Coastal Transition Zone ~45 km northwest of Vancouver Island, British Columbia, and 40 km from the shelf break.

Environmental indices

Given the many different atmospheric and oceanographic processes that influence productivity in the study systems, we chose SST as an index that represented the outcome of myriad bottom-up processes in each of the various systems that could be used for comparison. Local SST measurements were not available at all sites or in all years during our

© 2008 NRC Canada

Fig. 1. Map of North Pacific Ocean with study sites and simplified current flows (arrows). MI, Middleton Island; SLI, St. Lazaria Island; TRI, Triangle Island; SFI, Southeast Farallon Island; ANI, Año Nuevo Island; TEI, Teuri Island.

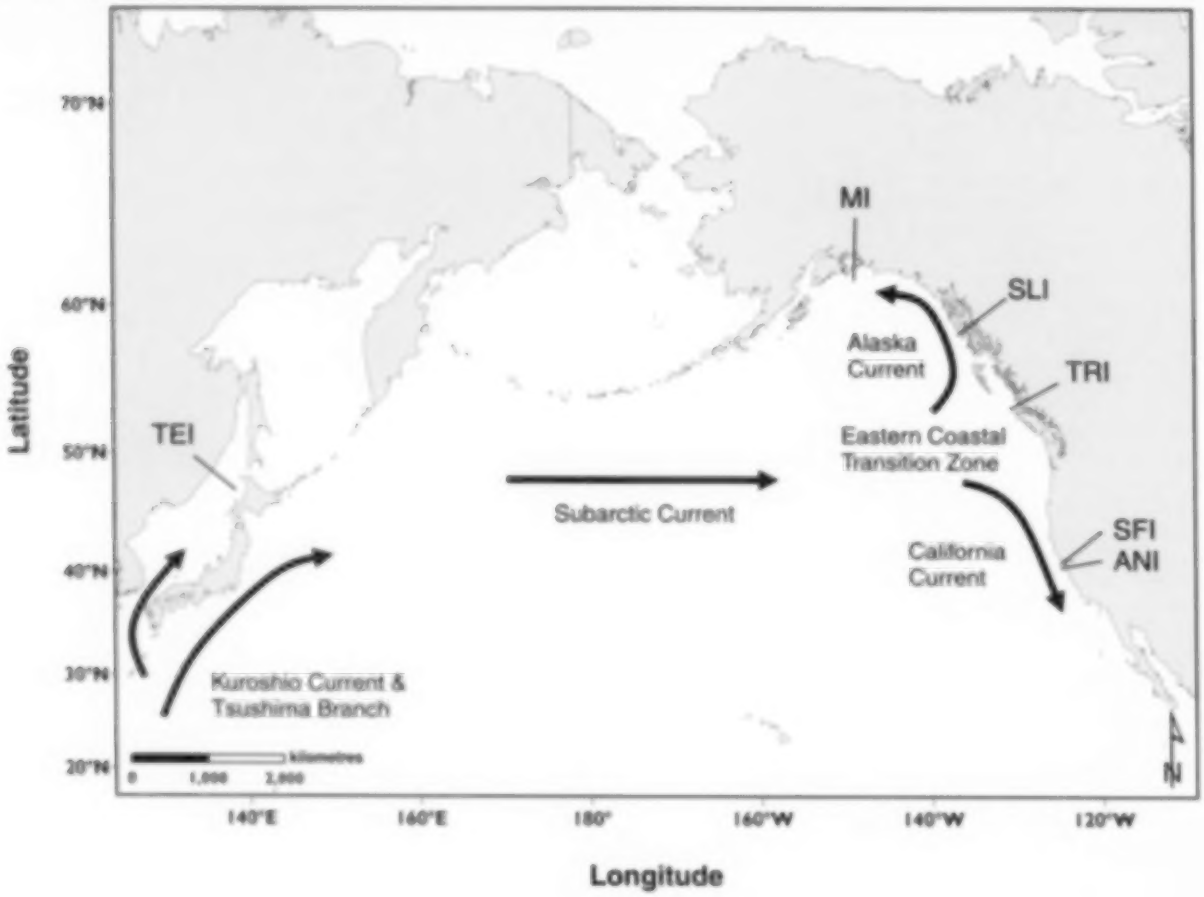

study. Therefore, we derived SST indices from the Advanced Very High Resolution Radiometer (AVHRR) satellite remote sensing system (9 km × 9 km cells; poet.jpl.nasa.gov/), available since 1985. We computed 3-month seasonal indices for a 50 km radius around each site (excluding land), comparable with auklet foraging ranges around the colonies (Kato et al. 2003; McFarlane-Tranquilla et al. 2005). AVHRR data were fairly complete within the 50 km radius around most sites in most months (see Appendix A). We compared satellite-derived SST with in situ measurements where possible (Appendix A). All correlations were highly significant, though less so as the year progressed, which we interpreted as reflecting the effects of insolation.

Forage fishes

Fishes were sampled by a piscivorous, diving marine bird (rhinoceros auklet), which is closely related to puffins and ranges throughout the North Pacific Rim. This seabird can forage to depths of 60 m, but has mean dive depths of 10–30 m (Burger et al. 1993; Kuroki et al. 2003). Fishes were collected from auklets provisioning offspring in summer (June–August), either by netting or hand-capturing the adults as they returned to the colony. Fishes were measured, weighed, and identified to species. Rhinoceros auklets are "multiple prey loaders", which typically bring 1–10 prey back to the colony in their bill following a foraging bout.

We used percent number of prey species, since we were interested in community composition. As multiple prey from one bill load are not statistically independent, individual prey items were summarized in terms of a bill-load sampling unit (Appendix B, Table B1). We calculated the proportion diet composition by number for each bill load averaged over each year as an index of prey harvest (or take). Forage communities were described using the entire time series available at each site, in some cases dating back to 1976.

Statistical analysis

Since fish data were expressed as proportions, we used a logit-transformation ($\ln[p/(1-p)]$) prior to analysis, where p was the proportion. All analyses were performed using STATA statistical software (v.8.0, 2003; StataCorp LP, College Station, Texas). Statistical comparisons were done only

© 2008 NRC Canada

Fig. 2. Seasonal anomalies of sea surface temperature (SST, °C) during December–February (stippled bars), March–May (black bars), and June–August (gray bars) from 1985 to 2003 within 50 km around (*a*) Middleton Island (MI, 59°N), (*b*) St. Lazaria Island (SLI, 56°N), (*c*) Triangle Island (TRI, 50°N), (*d*) Southeast Farallon Island (SFI, 37°N), and (*e*) Año Nuevo Island (ANI, 37°N) in the eastern Pacific and (*f*) Teuri Island (TEI, 44°N) in the western Pacific. Note different scales of various panels.

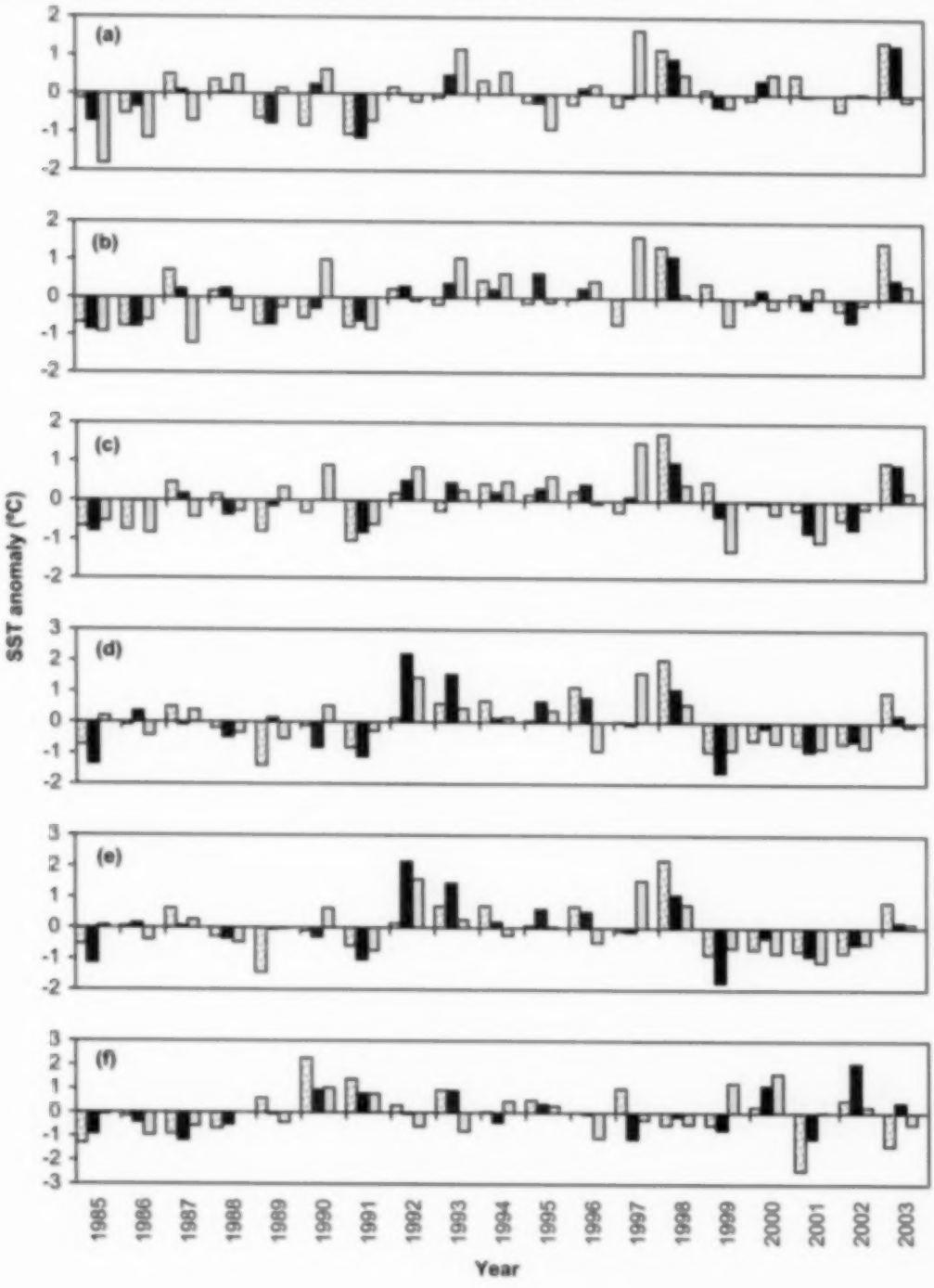

© 2008 NRC Canada

Table 1. Spearman rank correlations of sea surface temperature (SST) between sites in (*i*) December–February, (*ii*) March–May, and (*iii*) June–August 1985–2003.

			Eastern Pacific			
Latitude (°N)	Site	Western Pacific (TEI)	MI	SLI	TRI	SFI
December–February						
59	MI	−0.79**				
56	SLI	−0.60**	0.90**			
50	TRI	−0.51**	0.82**	0.96**		
37	SFI	−0.21	0.47**	0.56**	0.63**	
37	ANI	−0.25	0.46**	0.51**	0.57**	0.96**
March–May						
59	MI	0.33				
56	SLI	0.12	0.67**			
50	TRI	0.14	0.63**	0.80**		
37	SFI	0.20	0.39*	0.64**	0.86**	
37	ANI	0.19	0.45**	0.70**	0.92**	0.97**
June–August						
59	MI	0.07				
56	SLI	−0.15	0.75**			
50	TRI	−0.11	0.56**	0.70**		
37	SFI	−0.21	0.23	0.32	0.68**	
37	ANI	−0.45**	0.23	0.39*	0.73**	0.90**

Note: TEI, Teuri Island; MI, Middleton Island; SLI, St. Lazaria Island; TRI, Triangle Island; SFI, Southeast Farallon Island; *, $p \leq 0.10$; **, $p \leq 0.05$.

for years in which sampling took place at all sites for 1994–2003. Species richness was calculated for each site using fish species that made up ≥10% of predator diet in at least 1 year. For SST indices and the predominant prey at each site, we used linear and quadratic regression to infer trends between years. Time series were tested for first-order effects of serial autocorrelation (Prais–Winsten regression for small sample sizes). No autocorrelation coefficients were significant (all $p > 0.5$). Series were detrended if necessary by taking residuals. We then used Spearman's rank correlations to examine spatio-temporal concordance of ocean conditions and take of primary forage fish species at each location.

Results

Spatio-temporal SST variability

Relative to latitude, SST anomalies are thought to be greatest in the tropical Pacific (Chavez et al. 2002; Mantua and Hare 2002). In this study, we focused on extratropical regions and found the largest SST anomaly values at lower latitudes (Fig. 2). For a given time period, however, relative anomalies were sometimes higher in northern latitudes. For example, positive SST anomalies during the 1992–1993 ENSO were strongest in the lower latitudes of the eastern Pacific, the positive signal in 1997–1998 was strong at all latitudes, whereas positive anomalies in 2003 were stronger in the northeastern sites.

In general, and particularly between 1994 and 2003 (Table 1) when fish data were also available at all sites, changes in SST were similar in the eastern boundary currents and predominantly inversely related between east and west. This supports the inverse spatial pattern shown by the PDO (Mantua and Hare 2002). Inverse east–west relationships were always observed during ENSO events. Between 1985 and 1989, however, some positive east–west relationships were observed.

In 1994–2003, correspondence between the Gulf of Alaska and California Current decreased from winter to summer, presumably owing to effects of insolation. SST between eastern and western Pacific sites covaried negatively in winter and more weakly in summer. In spring, relationships were positive even though none were significant. Conditions around TEI in the Sea of Japan were subarctic in the winter (3–9 °C), changing to subtropical in summer (12–23 °C) as the Tsushima Current moved northward. The inverse east–west relationship was strongest relative to the Gulf of Alaska sites in winter (5–9 °C, subarctic system) and to the California Current sites in summer (11–18 °C, relatively subtropical) as the Gulf of Alaska and California Current shifted out of phase and the Tsushima Current moved northward through the Sea of Japan. We found no temporal trends in SST from 1994 to 2003 (linear regressions: $R^2 \leq 0.29$, $p \geq 0.13$).

Forage fish communities

Seabird diets reflect different forage fish communities around the North Pacific Rim, but transitions from one region to another showed largely the loss of one or two species that were replaced by others. In other words, communities appeared as a continuum in species composition, with species replacements occurring incrementally along latitudinal–longitudinal gradients. Forage species included both small schooling fishes and 0-age classes of juvenile predatory fishes (Fig. 3). The small schooling fishes con-

© 2008 NRC Canada

Fig. 3. Rhinoceros auklet (*Cerorhinca monocerata*) take of forage species for 1976–2003 at (*a*) Middleton Island (MI) in the northern and (*b*) St. Lazaria Island (SLI) in the southern Gulf of Alaska, (*c*) Triangle Island (TRI) in the Eastern Coastal Transition Zone, (*d*) Southeast Farallon Island (SFI) and (*e*) Año Nuevo Island (ANI) in the California Current, and (*f*) Teuri Island (TEI) in the Sea of Japan.

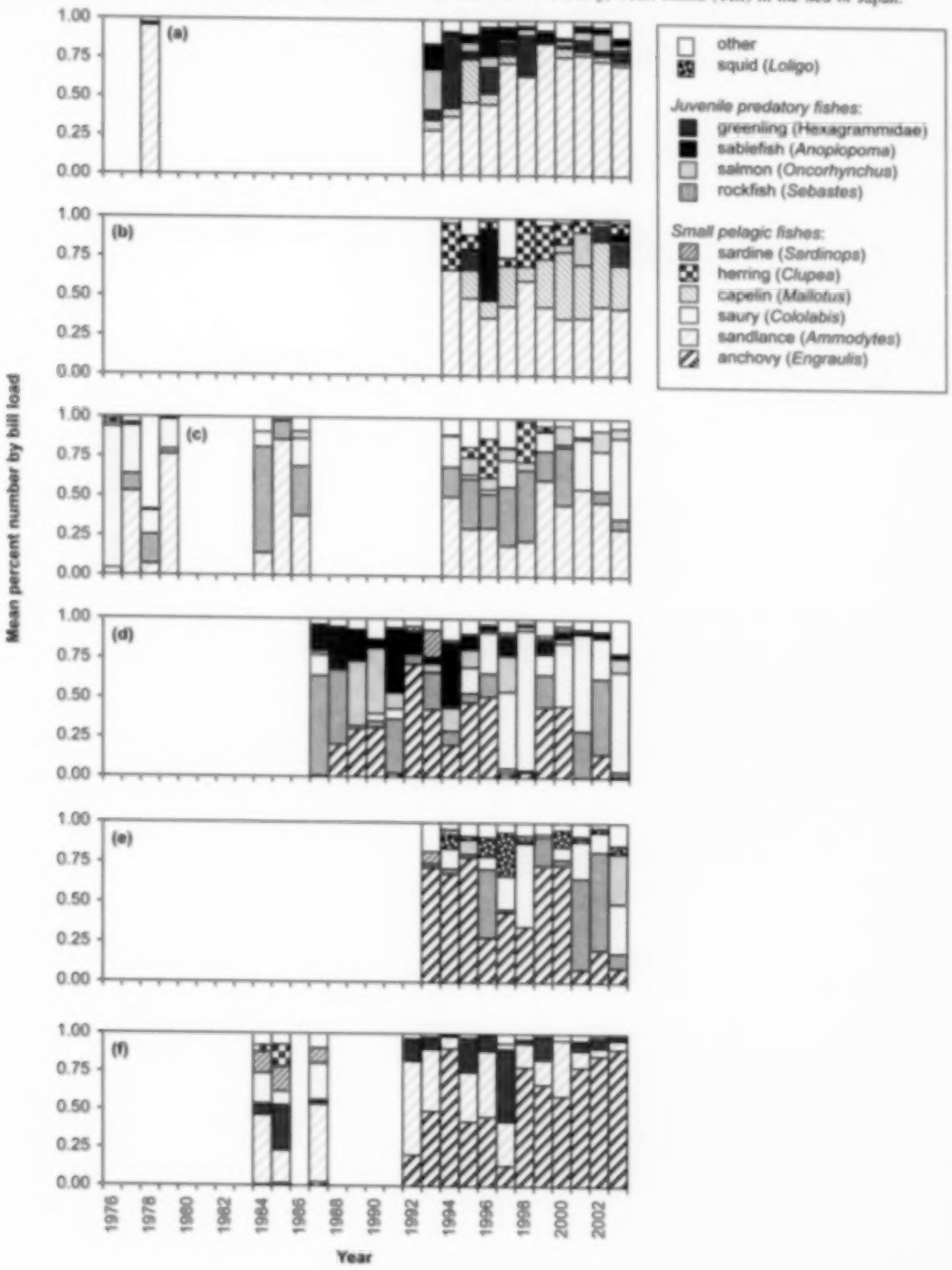

© 2008 NRC Canada

Table 2. Temporal trends (R^2 values) for take of primary forage fish at each sampling location, 1994–2003.

Latitude (°N)	Site	Species	Trend
59	MI	Sandlance	0.56**
56	SLI	Capelin	0.51**
50	TRI	Sandlance	0.06
44	TEI	Anchovy	0.47 (quad)*
37	SFI	Rockfish	0.01
37	ANI	Rockfish	0.20

Note: Trends are positive linear regression slopes (unless specified as quadratic (quad). MI, Middleton Island; SLI, St. Lazaria Island; TRI, Triangle Island; TEI, Teuri Island; SFI, Southeast Farallon Island; ANI, Año Nuevo Island; *, $p \leq 0.10$; **, $p \leq 0.05$.

sisted largely of anchovy (*Engraulis mordax* in the east, *Engraulis japonicus* in the west), sandlance (*Ammodytes hexapterus* in the east, *Ammodytes personatus* in the west), Pacific saury (*Cololabis saira*), capelin (*Mallotus villosus*), Pacific herring (*Clupea pallasii*) and Pacific sardine (*Sardinops sagax*). Juvenile predatory fishes included rockfish (*Sebastes* spp.), salmon (*Oncorhynchus* spp.), sablefish (*Anoplopoma fimbria*) and greenling (*Hexagrammos* spp. in the east, *Pleurogrammus azonus* in the west). California market squid (*Loligo opalescens*) were also present in the diet.

Subarctic species at mid- to high latitudes included capelin and sandlance, while saury, sardine, and anchovy dominated in mid-latitudes. Herring, greenling, salmon, rockfish, and squid were sampled at all locations, but herring and greenling were more prevalent at northern sites. Salmon were eaten more often at eastern sites, while rockfish and squid were most prevalent at southern sites. Sablefish were observed in eastern Pacific samples only. The northern Sea of Japan forage community consisted of anchovy, sandlance, saury, and juvenile greenling. Gulf of Alaska fishes included sandlance, capelin, herring, juvenile greenling, sablefish, and salmon. Sandlance, saury, herring, juvenile rockfish, salmon, and sablefish were present in the Eastern Coastal Transition Zone. California Current forage species included anchovy, saury, squid, juvenile rockfish, sablefish, and salmon. Overall, species richness in the diet was higher in the eastern Pacific (three–seven species each year) versus the western Pacific (two–four species).

Low-frequency variability

The most striking change in community composition occurred in the northern Sea of Japan (see also Deguchi et al. 2004). In 1984, 1985, and 1987, sardine, herring, and saury each comprised up to 15%–25% of birds' diet. However, these species virtually disappeared from the diet in the 1990s, while anchovy increased in 1992–1997, becoming the dominant prey after 1998 (Fig. 3).

Variations in the California Current were more complicated. While shifts in the Sea of Japan involved primarily coastal pelagic species, community changes in the California Current were due to both small pelagic and juvenile predatory fishes. Prior to 1989, juvenile rockfish were abundant (Ralston and Howard 1995; Miller and Sydeman 2004), as also indicated by SFI data here. Take of anchovy was high between 1989 and 1996, but as rockfish increased again after the 1997–1998 ENSO, saury also increased. This was especially evident at SFI, where saury replaced juvenile predatory species sablefish and salmon.

At TRI in the Eastern Coastal Transition Zone, saury replaced rockfish and herring in 2001–2003, while the presence of salmon remained relatively unchanged. Yet data from the late 1970s also show a large amount of saury, especially during the 1976 ENSO.

In the Gulf of Alaska, juvenile sablefish, salmon, and greenling declined at MI after 1998, while sandlance increased. Capelin, a small pelagic fish, increased at SLI, but there were no visible shifts in take of other species at that location.

We quantified trends in the take of primary prey species at each sampling location from 1994–2003. There were significant linear increases in take of sandlance at MI and capelin at SLI (Table 2). There was a U-shaped quadratic trend in anchovy at TEI.

Interannual covariation between sites

We found some evidence for interannual synchrony among main forage species across sites (Table 3). The take of rockfish at both SFI and ANI was positively correlated with that of sandlance at TRI. Correlations were also found between capelin at SLI and sandlance at MI and between capelin at SLI and rockfish at ANI. Rockfish covaried strongly between the two sampling sites in the California Current; however, no significant east–west relationships were observed.

Ocean conditions and forage species

During the 1992 ENSO event, SFI exhibited a reduction in primary forage species, with fewer rockfish during anomalously high temperatures in the eastern Pacific (Figs. 2, 3). Changes at TEI in the western Pacific were less clear because of a gap in data prior to 1992. During the 1997–1998 ENSO, high SST signals appeared at all latitudes, yet noticeable changes in main forage species occurred mainly at lower latitudes. Rockfish were practically nonexistent in the California Current, fewer sandlance were taken in the Eastern Coastal Transition Zone, and anchovy were extremely low at TEI in 1997. During the 2003 ENSO, when the SST signal was actually higher in the subarctic than in the subtropics, the most definitive changes in forage species were nevertheless recorded in the California Current.

In 1994–2003 in the southern Gulf of Alaska, take of capelin at inshore SLI was inversely correlated with local SST in winter (Fig. 4). In the northern Gulf of Alaska, however, capelin was not as abundant in samples from offshore MI. Rather, sandlance dominated the diet at MI and was inversely correlated with SST in spring (Fig. 4). At TRI in the Eastern Coastal Transition Zone, take of sandlance was most negatively correlated with summer SST (Fig. 4), but also with spring SST (Spearman's rho = –0.66, $p = 0.038$). Rockfish take in the California Current was also inversely related to SST. Relationships were strongest in summer (Fig. 4), but were also significant in spring at ANI (rho = –0.64, $p = 0.048$). In the western Pacific, we expected anchovy take at TEI in the northern Sea of Japan

© 2008 NRC Canada

Table 3. Covariation (Spearman's rho value) in take of primary forage fish between sites.

			Eastern Pacific			
Latitude (°N)	Species, location	Western Pacific (Anchovy, TEI)	Sandlance, MI	Capelin, SLI	Sandlance, TRI	Rockfish, SFI
59	Sandlance, MI	–0.12				
56	Capelin, SLI	–0.09	0.84**			
50	Sandlance, TRI	0.48	0.48	0.41		
37	Rockfish, SFI	0.14	0.22	0.18	0.59*	
37	Rockfish, ANI	0.24	0.41	0.56*	0.67**	0.76**

Note: TEI, Teuri Island; MI, Middleton Island; SLI, St. Lazaria Island; TRI, Triangle Island, SFI, Southeast Farallon Island; ANI, Año Nuevo Island; *, $p \leq 0.10$; **, $p \leq 0.05$.

to be positively correlated with SST. A positive relationship was observed with summer SST, yet it was not significant (Fig. 4).

Discussion

We used a piscivorous seabird to sample forage fish around the North Pacific Rim. The use of seabird diet as an indicator of prey is not a new idea (Cairns 1987; Barrett 2002; Mills et al. 2007), but this is the first study to use a single seabird species to sample multiple locations over an entire ocean basin. We found that forage species at many sites responded to marine conditions on interannual scales, although indications of lower-frequency change were strongest in the Sea of Japan. There was spatial synchrony (i.e., similarities) in the relationships between SST and certain forage fish species in seabird diet in the northeast Pacific.

Seabirds as indicators of forage fish

As indicators, "puffins" such as the rhinoceros auklet are especially useful in that they are abundant, widely distributed, and samples of forage fish are easily obtained by catching the birds as they return to colonies to feed dependent offspring. In a single feeding episode, puffins may also bring multiple forage fish to the nestlings. While predator-based sampling avoids certain problems inherent in studies of forage fish (e.g., patchy distributions), this technique also presents some difficult interpretive challenges given prey age or size classes and general prey preferences. If independent measures of prey abundance are available, these are valuable to calibrate predator diets. However, once preferences are well established, predator diet may be used to track dynamics of forage species (Reid et al. 1996, 2005).

Prey preferences have been examined at several of our study sites. Auklet take of juvenile rockfish in the California Current has been correlated with midwater trawl surveys for juvenile rockfish over many years (Thayer and Sydeman 2007); auklets in this region preferentially prey on rockfish when they are abundant in the ecosystem. In the Sea of Japan, auklet harvest of anchovy has been linked to annual stock size estimates (1996–2001; Deguchi et al. 2004). In both situations, the take of preferred prey was correlated with increased bird productivity (Takahashi et al. 2001; Thayer and Sydeman 2007). Unfortunately, there were no independent measures of prey availability in the environment that were available for other regions. However, in the Eastern Coastal Transition Zone (British Columbia, Canada), auklet take of sandlance has been related to the take of sandlance by other predators in the system (groundfish; Bertram and Kaiser 1993) as well as to high offspring survival (Hedd et al. 2006). Ongoing studies in the Gulf of Alaska indicate an increase in capelin since the mid-1990s (Brown 2002), similar to the trend in auklet take of capelin in this study.

Other high-lipid forage fish, though perhaps not known to be "preferred" as described above, may be taken opportunistically by the birds (e.g., sardine, juvenile salmon and sablefish). The appearance of such prey in the diet indicates their presence in the fish community at any given time. Thus, we interpret marine bird diet as useful for examining fish community composition in addition to its potential value as an indicator of dynamics of primary prey relative abundance in the environment. In conjunction with fisheries-independent data, an eventual goal is to use one or more marine birds and possibly other predators at multiple locations to provide a more complete picture of long-term fish community changes.

Forage species' response to interannual marine variability

Relationships of primary forage fishes with SST were observed in the California Current (rockfish), Eastern Coastal Transition Zone (sandlance), and southern (capelin) and northern Gulf of Alaska (sandlance). A mechanistic explanation for these relationships may be related to changes in food availability and larval fish survival. In the California Current, upwelling and cooler SST favors production (Chavez et al. 2002). Changes in the prey base for rockfish that affect adult fecundity or timing of parturition and (or) juvenile survival are likely explanations for the SST–rockfish relationship observed at multiple sites (Miller and Sydeman 2004). Rhinoceros auklets consume multiple age classes of forage fishes, but all of the rockfish taken in the California Current were classified as young of the year, which supports this explanation.

In the Eastern Coastal Transition Zone, Hedd et al. (2006) suggest linkages among 0-age class sandlance survival, copepod abundance, and spring SST rather than temperature-induced distributional shifts in sandlance. As sandlance feed primarily on copepods, cool years would provide favorable feeding conditions for young fish and thus contribute to strong recruitment. Indeed, we observed a strong relationship between spring SST and sandlance in this region. Both 0-age and 1+ age class sandlance were taken by the birds in our study, although 0-age fish were predominant.

Studies in the northern Gulf of Alaska, eastern Bering

© 2008 NRC Canada

Fig. 4. Relationships of forage fish indices with mean local sea surface temperature (SST) values between 1994 and 2003 at (*a*) Middleton Island (MI), (*b*) St. Lazaria Island (SLI), (*c*) Teuri Island (TEI), (*d*) Triangle Island (TRI), (*e*) Southeast Farallon Island (SFI), and (*f*) Año Nuevo Island (ANI). Trend lines reflect Spearman rank correlations at $p \leq 0.10$. Series are detrended if necessary. Outlying years are labeled.

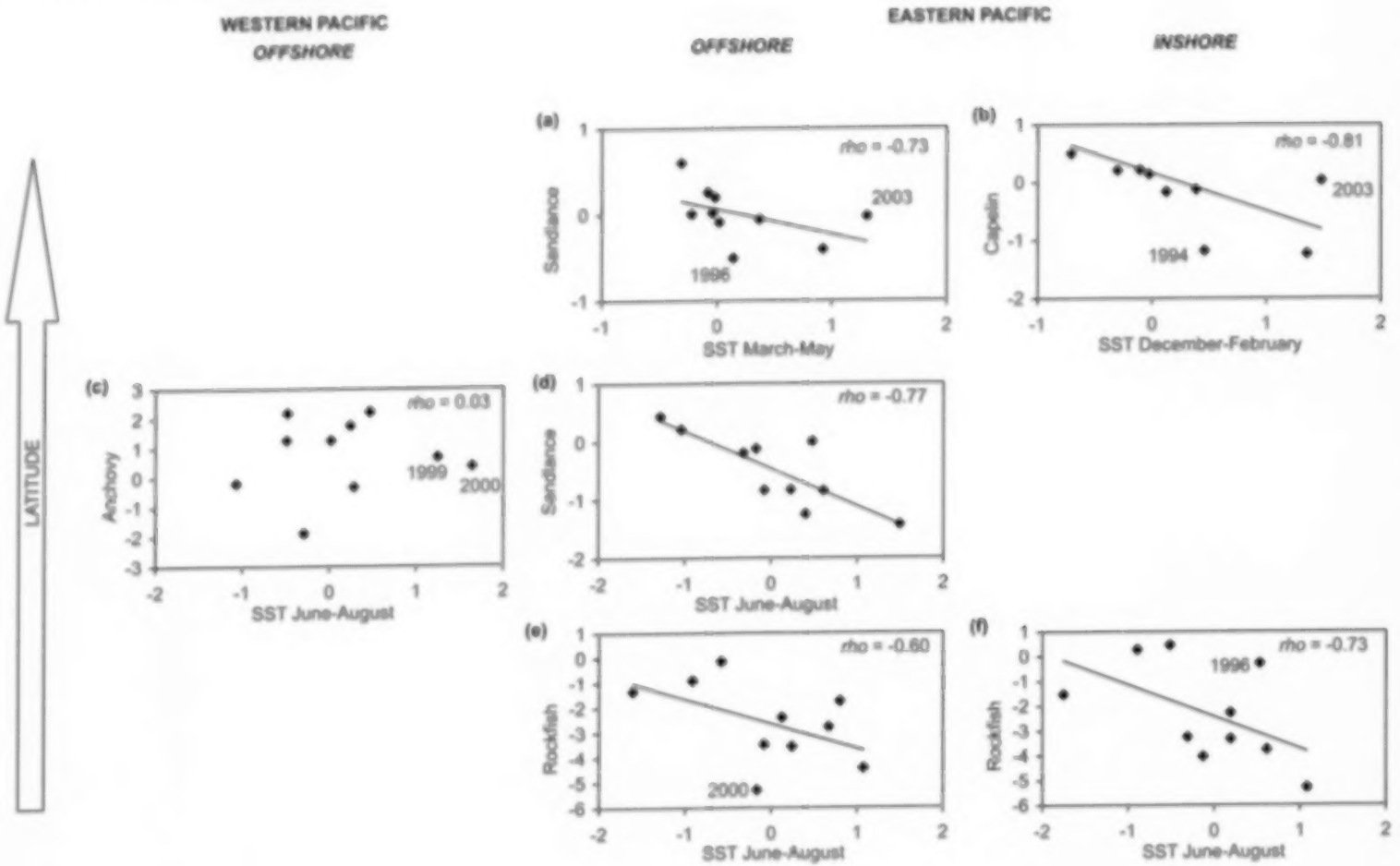

© 2008 NRC Canada

Sea, and Barents Sea indicate that capelin prefer colder waters and that they are found over a wider range in cooler years (Methven and Piatt 1991; Brodeur et al. 1999; Hollowed et al. 2007). Capelin feed on euphausiids and copepods (Hart 1973), and the abundance of these species was higher at lower temperatures in the Gulf of Alaska (Wang and Foy 2006). Therefore, cooler conditions could promote capelin survival. The negative correlation of capelin with winter SSTs in the Gulf of Alaska may be related to food availability and survival prior to reaching age class 1, the age at which they are taken by auklets. This explanation is more probable than one related to direct influence of SST on spawning distribution and behavior. Capelin come inshore to spawn in late spring and early summer (Naumenko 2002), but the relationship we observed with SST occurred during winter. Most importantly, capelin do not mature before ages 2 or 3 (Brown 2002), yet our samples consisted of almost exclusively 1+ age class fish.

In the northern Gulf of Alaska, both 0 and 1+ age class sandlance were harvested by the birds, and we found a strong relationship of sandlance with spring SST. In this region, wind mixing, topographic steering, and periodic upwelling introduce nutrients into surface layers in spring (Okkonen et al. 2001; Stabeno et al. 2004), promoting zooplankton blooms and positively influencing sandlance recruitment (Robards et al. 2002; Hedd et al. 2006).

Pan-Pacific comparisons

SST indices covaried negatively between the eastern and western Pacific Rim and positively within the eastern regions. While we did not find evidence of inverse east–west relationships in take of forage fishes, there was regional synchrony in the take of primary prey in the east. Forage fish take covaried more strongly between sites in proximity to each other and in adjacent ecosystems. We interpret this synchrony as suggestive of bottom-up processes across the entire eastern North Pacific.

In the west, we found no relationships between SST and forage fish. We expected a positive relationship between anchovy in the diet and SST, because the mechanism (advection of fish with intensification of the warm Tsushima Current) has been well described previously (Deguchi et al. 2004). Moreover, Deguchi et al. (2004) observed a correlation between June SST and anchovy in seabird diet between 1992 and 2001. Differences in the SST measurements used for analyses may explain this discrepancy. We used a 50 km radius around TEI based on AVHRR-derived SST, while Deguchi et al. (2004) used shipboard conductivity–temperature–depth (CTD) measurements covering a much larger area. Insolation can cause variation between ocean surface and subsurface temperature measurements (see Appendix A), increasing disparity between satellite and shipboard data. There were also slight differences in the time series. The relationship between June SST from the shipboard surveys and our satellite-derived index was extremely weak during the years of temporal overlap (1994–2001; $R^2_{June} = 0.25$, $p = 0.21$), suggesting that the scale of observation explains these differences. The radius of our measurements may have affected our results, since SST in the Sea of Japan can change drastically along a latitudinal gradient, depending on the location of the frontal zone between the Tsushima Current and subarctic waters to the north.

Temporal mismatch may have also obscured a temperature – forage fish relationship in the Sea of Japan. If the warm-water front of the Tsushima Current moved northward much earlier or later than average, a temporal mismatch may have occurred between auklet breeding and the anchovy prey around TEI (Takahashi et al. 2001; Deguchi et al. 2004). Auklets will adjust their timing of breeding to match prey availability as much as possible, but auklets may not be able to match extreme phenological and (or) distributional shifts in prey (Takahashi et al. 2001).

Long-term change

Our data sets were too sparse to adequately evaluate decadal changes in forage fish, but indications of shifts in the Sea of Japan and the California Current do support changes reported in the literature. In the California Current, a reduction of rockfish after the climate regime shift in 1989 and an increase after 1997–1998 were suggested by our data at SFI and supported by other studies (Ralston and Howard 1995; Miller and Sydeman 2004). In the Sea of Japan, Tian et al. (2006) showed stronger evidence for decadal versus interannual variations of fish community structure with ocean climate. Shifts in anchovy, sardine, saury, and herring stocks in 1988–1989 and (or) 1992–1993 were aligned with our observations of changes of these species at TEI. Furthermore, we found a significant relationship between anchovy at TEI and the PDO (1994–2003; $rho_{June-August} = -0.72$, $p = 0.02$), supporting evidence of influence by large-scale, low-frequency climatic changes.

In conclusion, based on the diet of a piscivorous seabird, we found regional synchrony in changes in forage fish communities throughout the northeastern coastal Pacific Ocean. Many other studies of synchrony or covariance in fish population dynamics have found relationships with long-term, temporal, environmental variability (Klyashtorin 1998; Hare et al. 1999, although see Hollowed et al. 2001 for shorter periodicities related to ENSO), whereas we observed synchrony on an interannual time scale. This study demonstrates the potential utility of predator-sampled data for obtaining a basin-wide perspective on mid-trophic-level forage species of key importance in food web dynamics. Coupling these data with other sources of forage fish data may be a valuable comparative tool. In the future, longer time series of predator diet will allow examination of forage species dynamics in relation to lower-frequency climate variability.

Acknowledgements

We gratefully acknowledge the US Fish and Wildlife Service Farallon National Wildlife Refuge, Año Nuevo State Park, British Columbia Parks, and the Centre for Wildlife Ecology (CWE) at Simon Fraser University. We thank the numerous biologists, students, and interns who helped collect field data. SST data at Yoichi were provided by A. Nakata, Hokkaido Fisheries Experimental Station. Research was funded in part by the National Fish and Wildlife Foundation, Japan Society for the Promotion of Science (JSPS) and Centers of Excellence (COE) program (Neo-Science of Natural History), Nestucca Trust Fund, CWE, Canadian

© 2008 NRC Canada

Wildlife Service (CWS), Oracle Corporation, and Exxon/Mobil Corporation, crucial components in sustaining our long-term data series.

References

Bakun, A., and Broad, K. 2003. Environmental 'loopholes' and fish population dynamics: comparative pattern recognition with focus on El Niño effects in the Pacific. Fish. Oceanogr. **12**: 458–473. doi:10.1046/j.1365-2419.2003.00258.x.

Barrett, R.T. 2002. Atlantic puffin *Fratercula arctica* and common guillemot *Uria aalge* chick diet and growth as indicators of fish stocks in the Barents Sea. Mar. Ecol. Prog. Ser. **230**: 275–287. doi:10.3354/meps230275.

Beamish, R.J., Noakes, D.J., McFarlane, G.A., Klyashtorin, L., Ivanov, V.V., and Kurashov, V. 1999. The regime concept and natural trends in the production of Pacific salmon. Can. J. Fish. Aquat. Sci. **56**: 516–526. doi:10.1139/cjfas-56-3-516.

Bertram, D.F., and Kaiser, G.W. 1993. Rhinoceros Auklet (*Cerorhinca monocerata*) nestling diet may gauge Pacific sandlance (*Ammodytes hexapterus*) recruitment. Can. J. Fish. Aquat. Sci. **50**: 1908–1914. doi:10.1139/f93-213.

Boyd, I., Wanless, S., and Camphuysen, C.J. (*Editors*). 2006. Top predators in marine ecosystems: their role in monitoring and management. Cambridge University Press, Cambridge, UK.

Brodeur, R.D., Frost, B.W., Hare, S.R., Francis, R.C., and Ingraham, W.J., Jr. 1996. Interannual variations in zooplankton biomass in the Gulf of Alaska, and covariation with California Current zooplankton biomass. Calif. Coop. Ocean. Fish. Investig. Rep. **37**: 80–98.

Brodeur, R.D., Wilson, M.T., Walters, G.E., and Melnikov, I.V. 1999. Forage fishes in the Bering Sea: distribution, species associations, and biomass trends. *In* Dynamics of the Bering Sea. *Edited by* T.R. Loughlin and K. Ohtani. Alaska Sea Grant College Program, Fairbanks, Alaska. AK-SG-99-03. pp. 509–536.

Brown, E.D. 2002. Life history, distribution, and size structure of Pacific capelin in Prince William Sound and the northern Gulf of Alaska. ICES J. Mar. Sci. **59**: 983–996. doi:10.1006/jmsc.2002.1281.

Burger, A.E., Wilson, R.P., Garnier, D., and Wilson, M.-P.T. 1993. Diving depths, diet, and underwater foraging of Rhinoceros Auklets in British Columbia. Can. J. Zool. **71**: 2528–2540. doi:10.1139/z93-346.

Cairns, D.K. 1987. Seabirds as indicators of marine food supplies. Biol. Oceanogr. **5**: 161–171.

Chavez, F.P., Pennington, J.T., Castro, C.G., Ryan, J.P., Michisaki, R.P., Schlining, B., Walz, P., Buck, K.R., McFadyen, A., and Collins, C.A. 2002. Biological and chemical consequences of the 1997–1998 El Niño in central California waters. Prog. Oceanogr. **54**: 205–232. doi:10.1016/S0079-6611(02)00050-2.

Chiba, S., and Saino, T. 2002. Interdecadal change in the upper water column environment and spring diatom community structure in the Japan Sea: an early summer hypothesis. Mar. Ecol. Prog. Ser. **231**: 23–35. doi:10.3354/meps231023.

Coyle, K.O., and Pinchuk, A.I. 2003. Annual cycle of zooplankton abundance, biomass and production on the northern Gulf of Alaska shelf, October 1997–2000. Fish. Oceanogr. **12**: 327–338. doi:10.1046/j.1365-2419.2003.00256.x.

Deguchi, T., Watanuki, Y., Niizuma, Y., and Nakata, A. 2004. Interannual variations of the occurrence of epipelagic fish in the diets of the seabirds breeding on Teuri Island, northern Hokkaido, Japan. Prog. Oceanogr. **61**: 267–275. doi:10.1016/j.pocean.2004.06.010.

Freon, P., Mullon, C., and Voisin, B. 2003. Investigating remote synchronous patterns in fisheries. Fish. Oceanogr. **12**: 443–457. doi:10.1046/j.1365-2419.2003.00242.x.

Hare, S.R., Mantua, N.J., and Francis, R.C. 1999. Inverse production regimes: Alaska and West coast Pacific salmon. Fisheries, **24**: 6–14. doi:10.1577/1548-8446(1999)024<0006:IPR>2.0.CO;2.

Hart, J.L. 1973. Pacific fishes of Canada. Bull. Fish. Res. Board Can. No. 180. pp 141–143.

Hedd, A., Bertram, D.F., Ryder, J.L., and Jones, I.L. 2006. Effects of interdecadal climate variability on marine trophic interactions: rhinoceros auklets and their fish prey. Mar. Ecol. Prog. Ser. **309**: 263–278. doi:10.3354/meps309263.

Hollowed, A.B., Hare, S.R., and Wooster, W.S. 2001. Pacific basin climate variability and patterns of Northeast pacific marine fish production. Prog. Oceanogr. **49**: 257–282. doi:10.1016/S0079-6611(01)00026-X.

Hollowed, A.B., Wilson, C.D., Stabeno, P.J., and Salo, S.A. 2007. Effect of ocean conditions on the cross-shelf distribution of walleye pollock (*Theragra chalcogramma*) and capelin (*Mallotus villosus*). Fish. Oceanogr. **16**: 142–154. doi:10.1111/j.1365-2419.2006.00418.x.

Kato, A., Watanuki, Y., and Naito, Y. 2003. Time allocation of chick-rearing rhinoceros auklets in Teuri Island, Japan, determined by acceleration-depth recording micro data loggers. J. Avian Biol. **34**: 282–287. doi:10.1034/j.1600-048X.2003.03134.x.

Klyashtorin, L.B. 1998. Long-term climate changes and main commercial fish production in the Atlantic and Pacific. Fish. Res. **37**: 115–125. doi:10.1016/S0165-7836(98)00131-3.

Kuroki, M., Kato, A., Watanuki, Y., Niizuma, Y., Takahashi, A., and Naito, Y. 2003. Diving behavior of an epipelagically feeding alcid, the Rhinoceros Auklet (*Cerorhinca monocerata*). Can. J. Zool. **81**: 1249–1256. doi:10.1139/z03-112.

Larson, R.J., Lenarz, W.H., and Ralston, S. 1994. The distribution of pelagic juvenile rockfish of the genus *Sebastes* in the upwelling region off central California. Calif. Coop. Ocean. Fish. Investig. Rep. **35**: 175–221.

Mackas, D.L., Thomson, R.E., and Galbraith, M. 2001. Changes in the zooplankton community of the British Columbia continental margin, 1985–1999, and their covariation with oceanographic conditions. Can. J. Fish. Aquat. Sci. **58**: 685–702. doi:10.1139/cjfas-58-4-685.

Mantua, N.J., and Hare, S.R. 2002. The Pacific Decadal Oscillation. J. Oceanogr. **58**: 35–44. doi:10.1023/A:1015820616384.

McFarlane-Tranquilla, L., Ryder, J.L., Boyd, W.S., Shisko, S.G., Amey, K., Bertram, D.F., and Hipfner, J.M. 2005. Diurnal marine distributions of marked Cassin's and rhinoceros auklets breeding at Triangle Island, British Columbia. Can. Wildl. Ser. Tech. Rep. Ser. No. 423.

McGowan, J.A., Cayan, D.R., and Dorman, L.M. 1998. Climate–ocean variability and ecosystem response in the Northeast Pacific. Science (Washington, D.C.), **281**: 210–217. doi:10.1126/science.281.5374.210. PMID:9660743.

Methven, D.A., and Piatt, J.F. 1991. Seasonal abundance and vertical distribution of capelin (*Mallotus villosus*) in relation to water temperature at a coastal site off eastern Newfoundland. ICES J. Mar. Sci. **48**: 187–193. doi:10.1093/icesjms/48.2.187.

Miller, A.K., and Sydeman, W.J. 2004. Rockfish response to low-frequency ocean climate change as revealed by diet of a marine bird over multiple time scales. Mar. Ecol. Prog. Ser. **281**: 207–216. doi:10.3354/meps281207.

Mills, K.L., Laidig, T., Ralston, S., and Sydeman, W.J. 2007. Diets of top predators indicate pelagic juvenile rockfish (*Sebastes* spp.) abundance in the California Current System. Fish. Oceanogr. **16**: 273–283. doi:10.1111/j.1365-2419.2007.00429.x.

Naumenko, E.A. 2002. The dynamics of prespawning caplin (*Mal-*

© 2008 NRC Canada

lotus villosus socialis) off the west Kamchatka coast. ICES J. Mar. Sci. **59**: 1006–1010. doi:10.1006/jmsc.2002.1280.

Okkonen, S.R., Jacobs, G.A., Metzger, E.J., Hurlburt, H.E., and Shriver, H.F. 2001. Mesoscale variability in the boundary currents of the Alaska Gyre. Cont. Shelf Res. **21**: 1219–1236. doi:10.1016/S0278-4343(00)00085-6.

Park, K.-A., Chung, J.Y., and Kim, K. 2004. Sea surface temperature fronts in the East (Japan): sea and temporal variations. Geophys. Res. Lett. **31**: L07304. doi:10.1029/2004GL019424.

Ralston, S., and Howard, D.F. 1995. On the development of year-class strength and cohort variability in two northern California rockfishes. Fish. Bull. (Washington, D.C.), **93**: 710–720.

Reid, K., Trathan, P.N., Croxall, J.P., and Hill, H.J. 1996. Krill caught by predators and nets: differences between species and techniques. Mar. Ecol. Prog. Ser. **140**: 13–20. doi:10.3354/meps140013.

Reid, K., Croxall, J.P., Briggs, D.R., and Murphy, E.J. 2005. Antarctic ecosystem monitoring: quantifying the response of ecosystem indicators to variability in Antarctic krill. ICES J. Mar. Sci. **62**: 366–373. doi:10.1016/j.icesjms.2004.11.003.

Robards, M.D., Roseb, G.A., and Piatt, J.F. 2002. Growth and abundance of Pacific sand lance *Ammodytes hexapterus* under differing oceanographic regimes. Environ. Biol. Fishes, **64**: 429–441. doi:10.1023/A:1016151224357.

Schwartzlose, R.A., Alheit, J., Bakun, A., Baumgartner, R.R., Cloete, R., Crawford, R.J.M., Fletcher, W.J., Green-Ruiz, Y., Hagen, E., Kawasaki, T., Lluch-Belda, D., Lluch-Cota, W.E., MacCall, A.D., Matsuura, Y., Nevarez-Martinez, M.O., Parrish, R.H., Roy, C., Serra, R., Shust, K.V., Ward, M.N.B., and Zuzunaga, J.Z. 1999. Worldwide large-scale fluctuations of sardine and anchovy populations. S. Afr. J. Mar. Sci. **21**: 289–347.

Stabeno, P.J., Bond, N.A., Hermann, A.J., Kachel, N.B., Mordy, C.W., and Overland, J.E. 2004. Meteorology and oceanography of the northern Gulf of Alaska. Cont. Shelf Res. **24**: 859–897. doi:10.1016/j.csr.2004.02.007.

Takahashi, A., Kuroki, M., Niizuma, Y., Kato, A., Saitoh, S., and Watanuki, Y. 2001. Importance of the Japanese anchovy *Engraulis japonicus* to breeding rhinoceros auklets *Cerorhinca monocerata* on Teuri Island, Sea of Japan. Mar. Biol. (Berl.), **139**: 361–371. doi:10.1007/s002270100594.

Thayer, J.A., and Sydeman, W.J. 2007. Spatio-temporal variability in prey harvest and reproductive ecology of a piscivorous predator *Cerorhinca monocerata* in an upwelling system. Mar. Ecol. Prog. Ser. **329**: 253–265. doi:10.3354/meps329253.

Tian, Y., Kidokoro, H., and Watanabe, T. 2006. Long-term changes in the fish community structure from the Tsushima warm current region of the Japan/East Sea with an emphasis on the impacts of fishing and climate regime shift over the last four decades. Prog. Oceanogr. **68**: 217–237.

Wang, X., and Foy, R.J. 2006. Spatial variability in mesozooplankton distribution related to seasonal temperature and salinity gradients on the Gulf of Alaska shelf. EOS Trans. Am. Geophys. Union, **87**(36): Suppl.

Appendix A

Advanced Very High Resolution Radiometer (AVHRR) data were fairly complete within the 50 km radius around most North Pacific sites in most months. In the California Current, >70% of cells contained data in all months in all years. However, data were patchier in the Gulf of Alaska and Sea of Japan – Tsushima Current in winter owing to cloud cover. While there was a minimum of 60% of cells with data at most sites in most months, sea surface temperature (SST) values were obtained at TRI for 5% and 28% of cells in December 2002 and 2003, respectively. Around MI, 45% of cells contained data in January 2003. At SLI, SST was available from 36% of cells in February 1997. Coverage at TEI averaged 44% in the month of January. Since SST values in adjacent cells were highly correlated, we maintained that averaging available values to obtain an SST value for the entire 50 km radius was appropriate for our purposes.

Satellite-derived SST data may be biased somewhat by insolation compared with subsurface measurements, so we compared AVHRR data with in situ measurements of temperature at up to 1 m depth where such data were available near three of our study sites. Satellite SST around SFI was correlated with in situ data, but more so before intense spring–summer solar heating began (linear regression: 1985–2003: $R^2_{\text{December–February}} = 0.93$, $R^2_{\text{March–May}} = 0.88$, $R^2_{\text{June–August}} = 0.74$; $p_{\text{all}} < 0.001$).

In situ measurements in the Eastern Coastal Transition Zone were available at both Kains Island (50°16′N, 128°1′W) at the northwestern edge of Vancouver Island, and Pine Island (50°35′N, 127°26′W) located further inshore towards mainland Canada. An average of SST at these locations was used as a proxy for comparing in situ data with a satellite-derived SST index around TRI. Correlations were significant ($R^2_{\text{December–February}} = 0.78$, $R^2_{\text{March–May}} = 0.88$, $R^2_{\text{June–August}} = 0.74$; $p_{\text{all}} < 0.001$).

In the Tsushima Current, SST measurements for all years were available at Yoichi (Hokkaido Fisheries Experimental Station; 43°12′N, 141°48′E), ~150 km south of TEI. These in situ measurements were significantly correlated with satellite-derived SST at TEI ($R^2_{\text{December–February}} = 0.53$, $R^2_{\text{March–May}} = 0.69$, $R^2_{\text{June–August}} = 0.73$; $p_{\text{all}} < 0.001$), but not as highly linked in December–May prior to the northward warm-water influx in summer, likely due to the latitudinal distance between sites.

Appendix B

Table B1 appears on the following page.

© 2008 NRC Canada

Table B1. Sample sizes (number of rhinoceros auklet (*Cerorhinca monocerata*) prey loads) at each study location, 1994–2003.

Site	1994	1995	1996	1997	1998	1999	2000	2001	2002	2003
MI	180	124	68	110	305	99	106	116	95	97
SLI	38	45	32	37	77	31	46	76	54	67
TRI	85	117	107	90	88	86	83	93	110	96
SFI	61	58	59	46	70	60	33	93	53	38
ANI	25	22	26	19	24	24	34	52	46	33
TEI	88	88	66	117	112	109	109	99	78	127

Note: MI, Middleton Island; SLI, St. Lazaria Island; TRI, Triangle Island; SFI, Southeast Farallon Island; ANI, Año Nuevo Island; TEI, Teuri Island.

© 2008 NRC Canada

Modeling cadmium accumulation in indigenous yellow perch (*Perca flavescens*)

Lisa D. Kraemer, Peter G.C. Campbell, and Landis Hare

Abstract: We used field data from transplantation and caging studies with juvenile yellow perch (*Perca flavescens*) to test a kinetic bioaccumulation model for cadmium (Cd). The model, which considers both dietary and aqueous sources of Cd, was first used to predict the dynamics of Cd accumulation in perch exposed to high ambient Cd for 70 days. Model simulations for hepatic Cd agreed well with the observed time course of Cd accumulation in the liver, but for the gills and gut, the predicted accumulations after 70 days were about three times higher than the observed values, suggesting that these latter organs can alter their ability to take up and (or) eliminate Cd. The model was also used to predict steady-state Cd concentrations in the gills, gut, and liver of perch living in lakes along a Cd gradient. Agreement between predicted and observed steady-state Cd concentrations was reasonable in lakes with low to moderate Cd concentrations, but in lakes with high dissolved Cd (>1.5 nmol·L^{-1}), the model overestimated Cd accumulation, particularly in the gills and gut. These results suggest that kinetic bioaccumulation models may better apply to some organs than to others. Because metal-induced toxicity is normally organ-specific, their application in a risk assessment context should be undertaken with caution.

Résumé : Nous avons testé un modèle cinétique de bioaccumulation du cadmium (Cd) chez la perchaude juvénile (*Perca flavescens*; branchies, intestin et foie) en nous servant de données obtenues dans le cadre d'expériences antérieures menées sur le terrain (transplantation; manipulation du régime alimentaire). Ce modèle biodynamique tient compte de l'accumulation du Cd à partir de l'eau et de la nourriture et il a d'abord été utilisé pour prédire l'accumulation du Cd chez des poissons exposés à des concentrations élevées en Cd pendant 70 jours. Les simulations pour le Cd hépatique se conformaient bien aux valeurs observées, mais pour les branchies et l'intestin, les valeurs prédites à la fin de la période de 70 jours étaient environ trois fois supérieures à celles observées, ce qui suggère que ces organes peuvent changer leur capacité de prendre en charge ou d'éliminer le Cd. Le modèle a également été utilisé pour prédire les concentrations en Cd à l'état stationnaire dans les branchies, l'intestin et le foie de perchaudes indigènes vivant dans des lacs situés le long d'un gradient en Cd. L'accord entre les simulations et les concentrations en Cd observées à l'état stationnaire était acceptable dans des lacs ayant des concentrations en Cd faibles ou modérées, mais dans les lacs les plus contaminés en Cd ([Cd] > 1.5 nmol·L^{-1}), le modèle a de nouveau surestimé l'accumulation, surtout dans les branchies et l'intestin. Ces résultats suggèrent que les modèles cinétiques de bioaccumulation s'appliquent mieux à certains organes qu'à d'autres. Puisque la toxicité induite par les métaux varie généralement d'un organe cible à un autre, l'application de ces modèles dans l'évaluation des risques posés par les métaux dans l'environnement doit être faite avec prudence.

Introduction

Kinetic bioaccumulation models have become powerful tools for explaining and predicting metal accumulation by aquatic animals (Blust 2001; Borgmann et al. 2005; Luoma and Rainbow 2005). Their strength comes from the fact that they are simple and thus practical to use and yet include enough mechanistic information to allow predictions of metal concentrations in animals living in the field (Luoma et al. 1992; Fisher et al. 2000; Croteau et al. 2002*a*). One reason for their success is that they explicitly consider metal uptake from water (e.g., via the gills) and from food (i.e., via the gut). For fish, it is particularly important to include both vectors for metal uptake, rather than assume that all of the metal is taken up from solution; metal bioaccumulation by many fish species is known to be influenced by dietborne metals (Harrison and Klaverkamp 1989; Mount et al. 1994; Kraemer et al. 2006).

One of the potential extensions to kinetic bioaccumulation models would be to use them to predict metal toxicity. However, to do so would require certain refinements, notably with respect to metal dynamics within the animal. Metal toxicity in animals is normally an organ-specific phenomenon, yet the current generation of field-tested metal bioaccumulation models does not consider metal distributions among various target organs (Luoma and Rainbow 2005).

In the present study, we used field data (Kraemer et al. 2005*a*, 2005*b*, 2006) describing Cd dynamics in yellow perch (*Perca flavescens*) to test the ability of a kinetic bioaccumulation model to predict Cd concentrations in individual organs. Data were available for Cd uptake from both food and water and for Cd loss. We chose Cd because of

Received 5 July 2007. Accepted 8 February 2008. Published on the NRC Research Press Web site at cjfas.nrc.ca on 16 July 2008. J20085

L.D. Kraemer. Trent University, 1600 West Bank Drive, Peterborough, ON K9J 7B8, Canada.
P.G. Campbell[1] and L. Hare. INRS – Eau, Terre et Environnement, Université du Québec, 490 de la Couronne, Québec, QC G1K 9A9, Canada.

[1]Corresponding author (e-mail: peter.campbell@ete.inrs.ca).

 doi:10.1139/F08-081 © 2008 NRC Canada

the toxic effects that it can exert on animals in mining areas (Campbell et al. 2003; Borgmann et al. 2004) and yellow perch because they are present in lakes covering a wide range of metal concentrations (Sherwood et al. 2000; Couture and Rajotte 2003; Giguère et al. 2004) and thus have great potential as a metal biomonitor. Recent work within our group (Giguère et al. 2005, 2006) and by others (Couture and Rajotte 2003; Levesque et al. 2003; Gravel et al. 2005) has demonstrated that although yellow perch can survive and reproduce in lakes with high ambient metal concentrations, they nevertheless manifest clear symptoms of metal-induced stress in a dose-dependent manner. We modeled Cd concentrations in several of its organs: the gills and gut, as they are important for Cd exchange with the external environment, and the liver, as it is an organ important for Cd storage (Giguère et al. 2004). We first tested the ability of a kinetic model to describe Cd dynamics in these three organs and then used the model to predict steady-state Cd concentrations in perch collected from lakes located along a Cd concentration gradient.

Our results demonstrate that the ability of metal accumulation and elimination experiments to predict steady-state concentrations in various organs of indigenous fish was dependent on the organ examined. Organs in contact with the external environment (i.e., the gills and gut) responded very differently than did the liver, presumably because of the ability of these "interface" organs to adjust their rates of metal uptake and (or) loss.

Materials and methods

The study lakes

The lakes that we studied are located in the Abitibi region near the city of Rouyn-Noranda, approximately 600 km northwest of Montréal, Québec, Canada. A copper smelter has been in operation since 1927 in the city of Rouyn-Noranda, and although emissions are now largely controlled (Croteau et al. 2002*b*), lakes located downwind from this smelter are contaminated with metals such as Cd as a result of historical atmospheric deposition. In addition to these direct inputs from the smelter, some lakes in this region are also contaminated by runoff from mine tailings and mineralized outcrops. For model development, we chose two lakes: Lake Opasatica (OP, reference lake) and Lake Dufault (DU, metal-contaminated lake). For the subsequent testing of the model, in addition to these two lakes, we added one reference lake (OL, Ollier), one moderately contaminated lake (VA, Vaudray), and another highly contaminated lake (OS, Osisko). We also considered previously published data from six additional sites: Lakes Bousquet, Dasserat, and Héva from the Rouyn-Noranda area (gill, gut and liver data; Giguère et al. 2004) and Lakes Raft, Laurentian, Hannah, and Wavy from the Sudbury region (liver data only; Giguère et al. 2005).

Relative importance of dietary and aqueous Cd as metal sources for juvenile yellow perch

A detailed description of this experiment can be found in Kraemer et al. (2006). Briefly, juvenile yellow perch (1.5 ± 0.1 g dry weight, mean ± standard error (SE)) were collected from Lake Opasatica and held in cages located in both Lake Opasatica (two cages per treatment) and Lake Dufault (two cages per treatment). Each cylindrical cage (height 1.2 m, diameter 0.5 m) was made of Nitex netting (64 µm mesh aperture) topped by Styrofoam floats and was anchored to the lake bottom (Munger et al. 1999). The floats held the cage opening well above the surface to prevent zooplankton from entering by wave action. Each cage initially contained 10 fish.

The cages were filled by passive entry of lake water through the netting, which prevented the entry of macrozooplankton. Yellow perch were allowed to acclimate to their cages for 24 h and were not fed during this time period. The caged fish in both lakes were then fed daily with macrozooplankton collected from either the reference lake (OP) or the Cd-contaminated lake (DU), creating four treatment regimes: reference lake water and reference diet (REF); reference lake water and contaminated food (FO); contaminated lake water and reference food (WO); and contaminated lake water and contaminated food (WF). Fish were sampled after 15 and 30 days of exposure, and the gills, gut, and liver were analyzed for Cd (see description of the analytical protocol below).

Cd uptake and efflux in juvenile yellow perch

Details of the Cd uptake and efflux experiments are outlined in Kraemer et al. (2005*a*) and Kraemer et al. (2005*b*), respectively. For the Cd-uptake experiments, juvenile yellow perch (<5 g fresh weight) were collected from a reference lake (OP) and held in cages in a metal-contaminated lake (DU) for up to 70 days. For the Cd-efflux experiments, juvenile yellow perch were collected from the contaminated lake (DU) and kept within cages in the reference lake (OP) for up to 75 days to measure Cd loss. Because this size class of perch feeds mainly on zooplankton and small aquatic insects (Gingras and Boisclair 2000), we designed enclosures to allow these prey to enter freely, thereby exposing perch to both contaminated food and contaminated water. The enclosures measured 2.5 m deep and 1.7 m in diameter (volume 5.7 m^3) and were made from 0.5 cm mesh aperture polypropylene netting. They were suspended from floating rafts made of plastic tubing (10 cm diameter), and each raft supported four cages. Each cage initially contained 30–40 fish.

The fish in individual cages were sacrificed five or six times during the 70-day Cd-exposure period and 75-day Cd-loss period. Fish were transported live to a nearby laboratory (<2 h away) where they were killed by a blow to the head. The fish were then immediately dissected, and the gills, gut, and liver were collected for metal analyses (see description below).

Cd concentrations in perch collected from lakes along a Cd concentration gradient

For the current study, juvenile yellow perch (n = 13–15) were collected with a seine net from the five principal study lakes (Dufault, Osisko, Vaudray, Ollier, Opasatica) at the end of May 2003. Fish were transported live to a nearby laboratory (<2 h) where they were killed by spinal dislocation. The fish were then dissected, and the liver, gills, and gut were removed for metal analyses (see description below). Additional data on Cd concentrations in perch from lakes in the Rouyn-Noranda and Sudbury regions were taken from

© 2008 NRC Canada

Giguère et al. (2004, 2005); hepatic Cd concentrations were available for all these lakes, but gill and gut Cd concentrations were only available for fish from the Rouyn-Noranda lakes.

Liver, gills, and gut metal analyses

For metal analyses, the organs were lyophilized, weighed, and digested in 70% HNO_3 (~3 mL of acid per gram dry weight of tissue). Digestions were carried out in an autoclave (120–125 °C, 1.1–1.3 kg·cm^{-2}, 3 h). The digested samples were then analyzed for Cd by inductively coupled plasma atomic emission spectrometry (ICP-AES; model Vista AX, Varian Inc., Mulgrave, Victoria, Australia) or by inductively coupled plasma mass spectrometry (ICP-MS; model X7, Thermo Elemental, Cheshire, UK). During each digestion run, both blanks (HNO_3 and MilliQ water) and certified reference samples (lobster hepatopancreas, National Research Council of Canada (NRCC) TORT-1 and TORT-2) were included; blanks indicated negligible contamination (undetectable, i.e., <0.33 μg Cd·L^{-1}, <1 ng Cd·g^{-1} organ dry weight), and the recovery of Cd in the TORT reference samples (n = 5; mean ± SE) was 90% ± 2%.

Environmental Cd concentrations

Water

Water samples were collected in June 2003 from the primary study lakes (Dufault, Osisko, Vaudray, Ollier, Opasatica) using diffusion samplers. Each sampler consisted of eight adjacent 4 mL cells separated from the lake water by a polysulphone membrane (0.2 μm nominal pore size) (HT-200, Pall Gelman Sciences, Ville St-Laurent, Québec). These samplers (one per lake) were deployed approximately 30 cm above the sediment and anchored in place with a brick. The samplers were allowed to equilibrate for 3 days in each lake. After equilibration with the surrounding waters, the samplers were recovered, carefully sealed, and sent on ice to our laboratory in Québec City within 24 h of retrieval from the lakes. At the time of retrieval, the ambient pH was also measured in both lakes near the diffusion samplers at a depth of 0.5 m with a pH meter (HI 9025, Hanna Instruments, Laval, Quebec, Canada). In the Quebec City laboratory, subsamples of water were removed from the samplers under a class-100 laminar flow hood for analysis of major anions (SO_4, PO_4, NO_3, Cl), cations (Ca, Mg, K, Na), total dissolved trace metals (Al, Fe, Cd, Cu, Zn), and dissolved organic and inorganic carbon. These solutes were measured as follows: major cations and trace metal cations by ICP-AES (Vista AX, Varian Inc.); anions by ion chromatography (DX300, Dionex Autolon, Sunnyvale, California, USA); inorganic carbon by a hot wire detector (HWD) gas chromatograph (Sigma 300, Perkin Elmer, Uberlingen, Germany), and organic carbon by a total organic carbon analyzer (TOC-5000A, Shimadzu, Kyoto, Japan). Blanks and appropriate standard reference materials for these analyses were included, and the analytical results were within the expected ranges. Using the above lake water analyses, we estimated free Cd^{2+} ion concentrations for lake water from the five principal study lakes using the Windermere humic aqueous model (WHAM 6.0.1; Tipping 1998); the free Cd^{2+} ion represented from 10% to 50% of the dissolved metal, with the remainder of the metal being complexed with humic and fulvic acids (inorganic complexation was negligible).

Zooplankton prey

Zooplankton were collected from the five primary lakes in June 2003 to measure diet-borne Cd. They were collected by horizontal tows with a plankton net (64 μm aperture) in the top 1–2 m of each of the primary study lakes. In each lake, the collected zooplankton was divided into three samples and stored frozen (–20 °C) in acid-washed containers until Cd analysis.

For Cd analyses, the zooplankton samples were lyophilized, weighed, and digested in 70% HNO_3 (~3 mL acid per gram dry weight sample). Digestions were carried out in an autoclave (120–125 °C, 1.1–1.3 kg·cm^{-2}, 3 h). During each digestion run, both blanks (HNO_3 and MilliQ water) and certified reference samples (lobster hepatopancreas, National Research Council of Canada (NRCC) TORT-2) were included. The digested samples were then analyzed for Cd by ICP-AES. Negligible contamination was detected in the digestion blanks (n = 4): <0.33 μg Cd·L^{-1}, <1 ng Cd·g^{-1} dry weight. Certified samples were quantitatively recovered (n = 4, 108% ± 2%, mean ± SE).

Statistical analyses

Statistical analyses on all experimental data were performed with SigmaStat 3.11 (SPSS Inc., Chicago, Illinois, USA). Errors (standard deviation) around the model predictions were estimated with parametric bootstrap resampling techniques using a Microsoft Excel add-in (Crystal ball 2000, Decisioneering, Denver, Colorado, USA) (500 bootstrap samples; Wehrens et al. 2000). Increases in liver, gill, and gut mass over time in transplanted fish were examined initially with a scatterplot, and a simple linear regression model was then tested by calculating determination coefficients (R^2).

Results and discussion

To understand the bioaccumulation of metals such as Cd, one must consider the influx and efflux rates of the metal, as well as the possible impact of growth dilution on bioaccumulated metal concentrations. Furthermore, because fish in nature are exposed to metals via both their diet and the water, a predictive model should ideally take into account these two exposure routes. A simple modeling construct has been proposed by N.S. Fisher, S.N. Luoma, and their coworkers to describe metal bioaccumulation (for a recent review, see Luoma and Rainbow 2005). In its simplest form, for a particular organ or for the whole organism, this biodynamic approach assumes a one-compartment, first-order model:

$$(1)\quad \frac{d[Cd]_{organ}}{dt} = k_u[Cd^{2+}] + (AE \times IR \times [Cd]_{food}) - k_e[Cd]_{organ} - k_g[Cd]_{organ}$$

where k_u, k_e, and k_g are rate constants for Cd influx from water (L·g^{-1}·day^{-1}), Cd efflux (day^{-1}), and growth (day^{-1}), respectively. $[Cd^{2+}]$ is the free Cd ion concentration in lake

© 2008 NRC Canada

water (nmol·L^{-1}), $[Cd]_{organ}$ is the Cd concentration in the organ of interest (nmol·(g dry weight)$^{-1}$), $[Cd]_{food}$ is the Cd concentration in the food of perch (nmol·(g dry weight)$^{-1}$), AE is the efficiency (%) with which perch assimilate Cd from their food, and IR is the rate at which food is ingested by perch (g prey·(g perch)$^{-1}$·day^{-1}). In the following section, we discuss how k_g and k_e were obtained for juvenile yellow perch from our experimental results. We then consider uptake for each organ separately and test the model predictions.

Model parameterization

Growth considerations

Although we could ignore fish growth during our Cd-uptake experiment (Figs. 1*a*, 1*c*, 1*e*), we could not do so for the Cd-efflux experiment because there was a significant increase in gill ($R^2 = 0.78$, $p < 0.05$), gut ($R^2 = 0.69$, $p < 0.05$), and liver ($R^2 = 0.82$, $p < 0.01$) mass during this latter experiment (Figs. 1*b*, 1*d*, 1*f*). Because the Cd-efflux experiment involved the transplantation of fish from a Cd-contaminated lake (Lake Dufault) to a reference lake (Lake Opasatica), these differences in growth response were likely linked either to increased food availability in the reference lake or to differences in how these transplanted fish converted available food to additional mass. Note that previous studies on adult yellow perch collected from a series of metal-impacted lakes reported that growth rates of fish from Cd-contaminated lakes were generally lower than those from reference lakes (Sherwood et al. 2000). The data from this earlier study also suggest that for a given amount of food consumed, adult yellow perch living in a Cd-impacted lake have a lower conversion efficiency (percentage of food intake allocated for growth) than yellow perch from reference lakes.

We can estimate the value of the growth rate constant, k_g, for the gills, gut, and liver from our Cd-efflux experiment using the following equation:

$$W = W_0 e^{k_g t} \quad (2)$$

where W is the weight (milligrams dry weight) at time t (days) and W_0 is the initial weight. The resulting k_g estimate (± standard deviation, SD) was 0.014 ± 0.008·day^{-1} for the gills, 0.007 ± 0.002·day^{-1} for the gut, and 0.008 ± 0.003·day^{-1} for the liver.

Cd efflux

The efflux rate constant (k_e) was estimated in a similar manner for the gills, gut, and liver. To estimate the value of k_e, we used data from our Cd-efflux experiment in which Cd-contaminated yellow perch were transplanted to a lake with low ambient $[Cd^{2+}]$ (Lake Opasatica; Kraemer et al. 2005*b*). If we assume that Cd uptake by perch was negligible in this low-Cd lake, then the integrated form of eq. 1 becomes

$$[Cd]_{organ} = [Cd]^0_{organ} \cdot e^{-(k_g + k_e)t} \quad (3)$$

where $[Cd]^0_{organ}$ is the Cd concentration (nmol Cd·(g dry weight)$^{-1}$) in the organ (i.e., gills, gut, or liver) at time 0 of the Cd-efflux experiment and $[Cd]_{organ}$ is the concentration of Cd at the end of the depuration period. Because Cd concentrations in the organs continued to decline up to the end of the depuration experiment (75 days), we are confident that the assumption of negligible uptake was reasonable. Using the k_g calculated for each of the organs, as well as changes in Cd concentrations during the transplantation, we estimated the value of the loss rate constant k_e to be 0.024 ± 0.016·day^{-1} (mean ± SD) for the gills, 0.012 ± 0.006·day^{-1} for the gut, and 0.002 ± 0.001·day^{-1} for the liver.

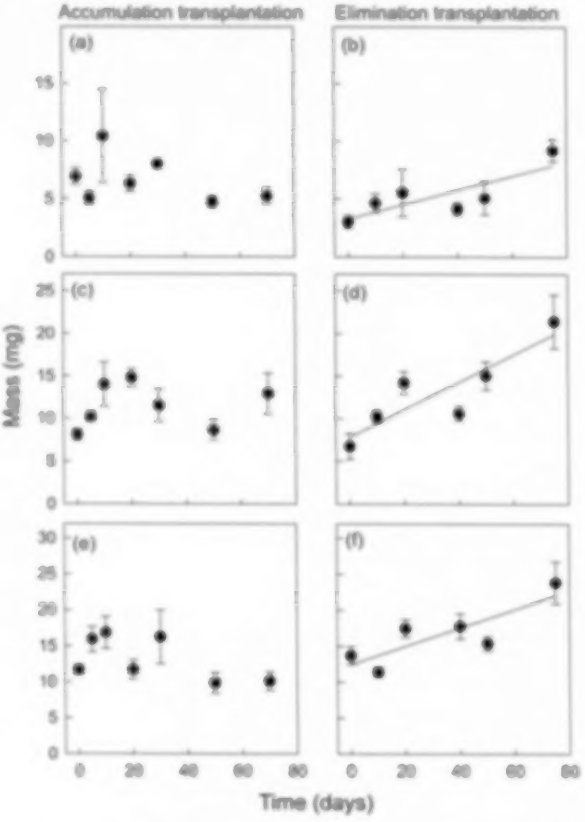

Fig. 1. Changes in (*a*, *b*) gill mass, (*c*, *d*) gut mass, and (*e*, *f*) liver mass of yellow perch (*Perca flavescens*) during the accumulation (Lake Opasatica to Lake Dufault, left-hand panels) and elimination (Lake Dufault to Lake Opasatica, right-hand panels) transplantation experiments. The data are represented by means ± standard deviation, SD. Although no significant correlation was observed for (*a*), (*c*), and (*e*), a linear regression model ($p \leq 0.05$) could be fitted to (*b*), (*d*), and (*f*).

Model application to the gills

Cd uptake

In a previous field experiment, we examined the relative importance of dissolved and dietary Cd as sources of exposure for yellow perch (Kraemer et al. 2006). Results from this study showed that the gills were only influenced by dissolved Cd. Therefore, in the model, we could ignore terms describing Cd uptake from food (AE × IR × $[Cd]_{food}$). Furthermore, we assumed that Cd loss from perch was negli-

© 2008 NRC Canada

Table 1. Summary of mean model parameters (± standard deviation, SD) estimated from the various field studies used in the model simulations.

	Growth rate constant (k_g) (day^{-1})			
	Efflux transplantation	Average used in steady-state estimations	Efflux rate constant (k_e) (day^{-1})	Uptake rate constant (k_u) (L·g^{-1}·day^{-1})
Gills	0.007±0.002	0.015±0.002	0.024±0.016	1.2±0.43
Gut	0.008±0.003	0.011±0.001	0.012±0.006	1.5±0.41
Liver	0.007±0.002	0.014±0.003	0.002±0.001	1.8±0.60

gible early in the Cd-uptake experiment (Kraemer et al. 2005*a*). Lastly, because changes in gill mass were negligible during the Cd uptake experiment (Fig. 1*a*), we ignored Cd dilution due to gill growth. Thus, eq. 1 becomes

$$(4) \qquad \frac{d[Cd]_{gill}}{dt} = k_u^{gill}[Cd^{2+}]$$

where $[Cd]_{gill}$ is the Cd concentration in the gills and k_u^{gill} is the rate constant for Cd uptake into the gills.

We estimated $\frac{d[Cd]_{gill}}{dt}$ to be the slope of the linear phase of the Cd-uptake experiment (i.e., from day 0 to day 10; Kraemer et al. 2005*a*) in which fish were exposed to Cd in ambient food and water, that is, 2.7 ±1.03 nmol·g^{-1}·day^{-1} ($R^2 = 0.99$, $p < 0.05$). Substituting this value into eq. 2, as well as that for $[Cd^{2+}]$ in Lake Dufault during the transplantation period (2.4 nmol·L^{-1}), yields a value for k_u^{gill} of 1.2 ± 0.4 L·g^{-1}·day^{-1} (Table 1). It is important to note that k_u^{gill} (as well as the other k_u estimates reported in this article) is calculated using the concentration of the free Cd^{2+} ion, not total dissolved Cd as is commonly used in this type of modelling approach.

Using the biodynamic model to explain Cd dynamics in the gills

Using our estimates for k_u^{gill} and k_e^{gill} and ignoring the impact of diet (as dietary Cd did not affect gill Cd concentrations) and growth dilution (as gill mass did not increase during the accumulation experiment), the dynamics of Cd accumulation in the gills could be modelled using the integrated form of eq. 1:

$$(5) \qquad [Cd]_{gill} = \left(\frac{k_u^{gill}[Cd^{2+}]}{k_e^{gill}}\right)(1 - e^{-k_e^{gill}t}) + [Cd]_{gill}^{0}e^{-k_e^{gill}t}$$

The model curve agrees reasonably well with the observed data for the first 10 days of exposure (Fig. 2*a*, broken line), but after 10 days, the model predicts that Cd concentrations in the gills will continue to increase, whereas the observed data tend towards a plateau in Cd concentrations (Fig. 2*a*, solid line). A likely explanation for the divergence of the model predictions from the observed results is that once concentrations reached a certain level within the gill, perch were able to moderate accumulation by altering k_u^{gill} and (or) k_e^{gill}. In support of this explanation, Glynn (1996) reported that apical uptake of Cd into zebrafish (*Brachydanio rerio*) gills was a linear function of aqueous Cd concentrations for exposures up to 15 nmol·L^{-1}, but between 15 and 30 nmol·L^{-1}, uptake appeared to plateau. Glynn (1996) also showed that the intracellular distribution of Cd changed as the Cd exposure concentrations increased and that this change in distribution coincided with a marked increase in the movement of Cd across the basolateral membrane of the gills into the other internal organs, suggesting that k_e^{gill} increased in response to increasing gill Cd concentrations. Similar results indicating the capacity of fish gills to respond to sublethal Cd exposure were recently reported by Gonzalez et al. (2006), who studied the time course of Cd accumulation in the gills of *Danio rerio* and followed the associated effects on gene expression. For fish exposed continuously to Cd concentrations of ~87 nmol·L^{-1}, both Cd accumulation and gene expression increased from day 0 to day 7, but by the end of the exposure (day 21), gill Cd concentrations had declined and the expression of almost all of the genes had returned to basal levels. This previous work suggests that yellow perch might similarly be able to alter k_e^{gill} (either by transferring Cd to other organs or by excreting Cd to the external environment) when Cd accumulated in the gill exceeds a certain threshold (i.e., after day 10 in our transplant experiment), resulting in a plateau in observed gill Cd concentrations. Further adding support to our hypothesis, Thomann et al. (1997) used a seven-compartment modelling approach to examine Cd dynamics within rainbow trout. In their modelling simulations, the flux of Cd into the gills dropped from approximately 20 pg·day^{-1} at the beginning of the exposure to 10 pg·day^{-1} by day 60.

Using the biodynamic model to predict steady-state gill Cd concentrations

Using our estimates for the rate constants for Cd uptake from water into the gills (k_u^{gill}, eq. 4), Cd elimination from the gill (k_e^{gill}, eq. 3), and gill growth (k_g^{gill}, eq. 2), as obtained from our transplant and diet manipulation studies, we can now proceed to model Cd concentrations in the gills of indigenous perch, which are assumed to be at steady state. To test this model, we used data for perch collected from a series of lakes varying in metal contamination (for lake descriptions, see Table 2). Using the integrated form of eq. 1, gill Cd concentrations at steady state can be described by

$$(6) \qquad [Cd]_{ss}^{gill} = \frac{k_u^{gill}[Cd^{2+}]}{k_e^{gill} + k_g^{gill}}$$

where k_g^{gill} in the model represents an average k_g (0.015 ± 0.002·day^{-1}; Table 1) for the gills of juvenile yellow perch collected from three different lakes during the summer (May to August): Opasatica (mean ± SD, 0.014 ± 0.001·day^{-1}), Vaudray (mean ± SD, 0.017 ± 0.002·day^{-1}), and Osisko (mean ± SD, 0.013 ± 0.001·day^{-1}). The values for $[Cd^{2+}]$ were calculated from the water chemistry of

© 2008 NRC Canada

Fig. 2. (*a*) Changes in gill Cd concentrations during the accumulation transplantation in which yellow perch (*Perca flavescens*) were transplanted from Lake Opasatica to Lake Dufault. The solid circles represent the means of observed Cd concentrations in the gills ± standard deviation, SD. The broken line represents the model simulations; the solid line represents a nonlinear regression ($p \leq 0.05$). (*b*) Predicted versus measured gill Cd concentrations for juvenile yellow perch (*Perca flavescens*) collected from both the Sudbury and Rouyn-Noranda areas. (*c*) The same information as in (*b*) except that Lakes Osisko and Dufault have been removed for clarity. Predictions were based on the assumption that Cd uptake was from water only. Data are represented by means ± SD, and the broken lines in (*b*) and (*c*) represent the 1:1 relationship. See Table 1 for lake codes.

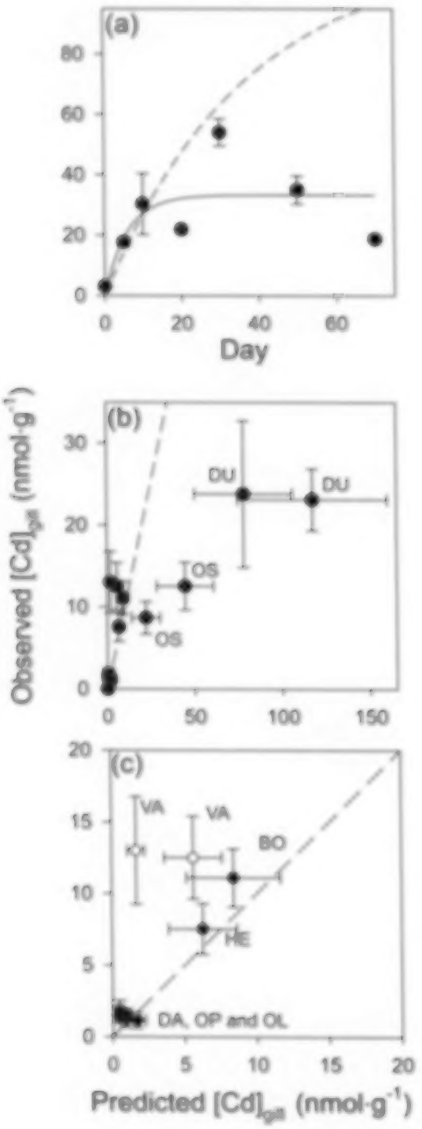

Table 2. Geographical location of the lakes in the current study and the chemical composition of their epilimnetic water.

Region	Lake (code)	Location	pH	Dissolved [Ca] (μmol·L^{-1})	Dissolved [Mn] (nmol·L^{-1})	Dissolved [Cd] (nmol·L^{-1})	Dissolved [Cu] (nmol·L^{-1})	Dissolved [Zn] (nmol·L^{-1})
Rouyn-Noranda	Bousquet (BO)[a]	48 13′N, 78 40′W	6.6	NR	NR	1.1	56	164
	Daserat (DA)[b]	48 13′N, 79 22′W	7.5	NR	NR	0.18	32	57
	Dufault (DU)[a]	48 05′N, 79 20′W	7.7	442	461	5.55	225	1015
	Héva (HE)[b]	48 11′N, 78 19′W	6.1	NR	NR	0.54	35	56
	Ollier (OL)[b]	48 11′N, 79 17′W	7.7	374	117	0.28	66	668
	Opasatica (OP)[a]	48 05′N, 79 20′W	7.7	372	639	0.11	47	5
	Osisko (OS)[a]	48 15′N, 79 0′W	7.8	645	378	1.45	89	204
	Vaudray (VA)[a]	48 05′N, 78 40′W	7.3	87	71	0.81	57	62
Sudbury	Hannah (HA)[c]	46 26′N, 81 02′W	7.0	270	NR	2.4	370	50
	Laurentian (LA)[c]	46 26′N, 80 57′W	6.4	110	NR	0.6	140	30
	Raft (RA)[c]	46 24′N, 80 56′W	6.7	90	NR	1.7	130	160
	Wavy (WA)[c]	46 18′N, 81 06′W	5.0	40	NR	1.5	110	120

Note: NR, not reported.
[a]Data collected in this study.
[b]Data from Giguère et al. (2004).
[c]Data from Giguère et al. (2005).

© 2008 NRC Canada

each lake (Table 2) using the WHAM chemical equilibrium model (Tipping 1998).

When all the lakes are considered together, there is an obvious tendency for the model to overestimate Cd concentrations for perch sampled from lakes with high Cd concentrations (Lakes Osisko and Dufault; Fig. 2*b*). In a previous study carried out on indigenous yellow perch in lakes in the same region, Giguère et al. (2004) showed that gill Cd concentrations increased linearly as a function of aqueous $[Cd^{2+}]$ in lakes where free Cd^{2+} concentrations were below a threshold of ~1 nmol·L^{-1}. In lakes above this threshold (i.e., Lakes Dufault and Osisko), gill Cd concentrations tended towards a plateau and no longer increased linearly with increasing aqueous Cd^{2+} concentrations. These earlier results, in combination with the inability of the present model to predict the dynamics of gill Cd concentrations above a certain gill Cd threshold, as seen in the Cd accumulation transplantation, support the hypothesis that perch living in lakes with elevated Cd concentrations have altered their ability to take up and (or) eliminate Cd via their gills.

If Lakes Dufault and Osisko are not considered in the steady-state simulations, there is a reasonable fit between observed and predicted values for Lakes Opasatica, Ollier, Bousquet, Dasserat, and Héva (Fig. 2*c*). However, there remains one notable exception in which the model fails to predict gill Cd concentrations. In Lake Vaudray, observed gill Cd concentrations were more than two times higher than predicted values, even though measured ambient aqueous Cd concentrations are relatively low in this lake (intermediate between those in Lakes Héva and Bousquet; Table 2). Differences in water chemistry may contribute to these higher than expected gill Cd concentrations for perch from Lake Vaudray. Ambient concentrations of Ca and Mn are low in this lake (Table 2); Ca is a known competitor for Cd uptake at the gill surface (Wood 2001), and dietary Mn has been shown to reduce Cd uptake in previous studies on rats (Sarhan et al. 1986) and mouse cell lines (Yanagiya et al. 2000; Noel et al. 2006). In the present case, we discount the possible effect of Ca, as earlier work has shown that lake-to-lake variations in Cd accumulation by yellow perch were not related to differences in ambient Ca concentrations (Giguère et al. 2004). On the other hand, Cd concentrations in the gills of perch from Lake Vaudray were inversely correlated with gill Mn concentrations in fish sampled over the summer (May to August), supporting the suggestion that Mn is potentially an important competitor with Cd in this lake (L.D. Kraemer, unpublished data).

Model application to the gut

Cd uptake

Results from diet manipulation experiments (Kraemer et al. 2006) in which perch were exposed to Cd via their food or water showed that gut tissues were influenced by both aqueous and dietary Cd, with 70% ± 21% (mean ± SD) of the accumulated Cd coming from aqueous sources and 30% ± 12% coming from dietary sources. We used this information to extract a value for k_u^{gut} from the 70-day transplantation experiment (Kraemer et al. 2005*a*). Because perch in the transplantation experiment were exposed to Cd via both their food and water, the slope of the linear phase of the Cd-uptake experiment reflected total influx (i.e., from both dietary and aqueous routes). Given that approximately 70% of accumulated Cd came from aqueous sources, we estimated k_u^{gut} from the transplantation experiment by multiplying the total influx by 70% (representing influx from just aqueous sources; eq. 7):

$$(7) \qquad I \times 70\% = k_u^{gut}[Cd^{2+}]$$

where I is the total influx rate (nmol·g^{-1}·day^{-1}) estimated from the linear phase of the Cd-uptake experiment (i.e., from day 0 to day 10; Kraemer et al. 2005*a*) in yellow perch exposed to Cd via food and water. Using a $[Cd^{2+}]$ of 2.4 nmol·L^{-1}, k_u^{gut} for the gut was estimated to be 1.5 ± 0.4 L·g^{-1}·day^{-1}. Clearly the gut itself is not in contact with waterborne Cd (freshwater fish do not drink appreciably); thus, the value for k_u^{gut} represents influx into the gut from aqueous sources, e.g., via the gills and internal circulation.

Using the biodynamic model to explain Cd dynamics in the gut

In an approach similar to that used for the gill data set, we used our estimations of k_u^{gut} and k_e^{gut} (ignoring the impact of growth dilution because gut mass did not increase during the accumulation experiment) to model the dynamics of Cd accumulation in the gut (Kraemer et al. 2005*a*). However, because dietary Cd also played a role in gut Cd accumulation (Kraemer et al. 2006), the importance of the diet could not be ignored, and thus eq. 5 was expanded to include the dietary parameters:

$$(8) \qquad [Cd]_{gut} = \left(\frac{k_u^{gut}[Cd^{2+}] + (AE \times IR \times [Cd]_{food})}{k_e^{gut}}\right) \times (1 - e^{-k_e^{gut}}) + [Cd]_{gut}^{0} e^{-k_e^{gut}}$$

Concentrations of Cd in the food were estimated by measuring Cd concentrations in bulk zooplankton samples taken from Lake Dufault (Table 3). For the other two dietary parameters, assimilation efficiency and ingestion rate, we referred to previously published data (see below).

For ingestion rates, Trudel et al. (2000) estimated IR for age 1+ yellow perch living at a low-metals site to be 0.028 g·g^{-1}·day^{-1}. Sherwood et al. (2000) estimated somewhat lower ingestion rates for older yellow perch (age 4+) collected from some of the lakes in our study area (0.016–0.018 g·g^{-1}·day^{-1}). As the age of our perch was closer to that of those studied by Trudel et al. (2000) and because ingestion rates are likely to vary with age, we used the higher value of 0.028 g·g^{-1}·day^{-1} for our modeling exercise.

For Cd assimilation efficiencies, Liu et al. (2002) estimated that zebrafish (*Danio rerio*) fed zooplankton (*Daphnia magna*) assimilated 3%–8% of the Cd in these prey. These results are comparable with the AE of 2.7% estimated for juvenile silversides (*Menidia menidia* and *Menidia beryllina*) feeding on zooplankton (Reinfelder and Fisher 1994). Much higher AEs of 23%, 14%–33%, and 10%–26% have been reported for juvenile striped bass (*Morone saxatilis*), glassy fish (*Ambassis urotaenia*), and mudskipper (*Periophthalmus cantonensis*), respectively, all of which were fed Cd-contaminated zooplankton (Ni et al. 2000; Baines and Fisher 2002). As juvenile yellow perch eat mainly zooplank-

© 2008 NRC Canada

Table 3. Cadmium concentrations (mean ± standard deviation, SD) measured in bulk zooplankton from six of our study lakes.

Lake	[Cd] in bulk zooplankton (nmol·(g dry weight)$^{-1}$)
Bousquet[a]	18±1
Dufault	87±2
Ollier	17±7
Opasatica	16±4
Osisko	56±6
Vaudray	32±4

[a]Data from Croteau et al. (2003).

tion, we assumed that the assimilation efficiency of Cd would be comparable with these previous laboratory studies, and therefore for our modelling simulations, we chose an assimilation efficiency of 33%, a value representative of the high end of these reported values.

The model curve for gut Cd uptake showed very similar trends to that observed for the gills (compare Figs. 2*a* and 3*a*). During the first 10 days, the model curve fit the observed data well, but after 10 days, the observed data showed a plateau in Cd concentrations, whereas the model predicted that concentrations would continue to increase during the 10- to 70-day period (Fig. 3*a*). Reducing the assimilation efficiency to 10% did not appreciably improve the fit. Similar to the case for the gills, it appears that perch are able to alter accumulation in the gut when Cd concentrations accumulated in this organ surpass a certain threshold. The biodynamic model was unable to take these biological changes into account.

Using the biodynamic model to predict steady-state gut Cd concentrations

For the steady-state predictions, we used an average k_2^{gut} of 0.011 ± 0.001·day^{-1} as determined for juvenile yellow perch sampled from three different lakes during the summer (May to August): Opasatica (0.012 ± 0.003·day^{-1}, mean ± SD), Vaudray (0.012 ± 0.004·day^{-1}), and Osisko (0.010 ± 0.003·day^{-1}). Using our estimations of k_u^{gut}, k_e^{gut}, and k_2^{gut} and expanding eq. 5 to include the importance of dietary Cd uptake (see eq. 9 below), we were able to model steady-state gut Cd concentrations in yellow perch living in a series of lakes impacted by this metal.

$$(9)\qquad [Cd]_{ss}^{gut} = \frac{k_u^{gut}[Cd^{2+}] + (AE \times IR \times [Cd]_{food})}{k_e^{gut} + k_2^{gut}}$$

The values for $[Cd^{2+}]$ were calculated from the water chemistry of each lake (Table 2), as in the case of the gills, and those for $[Cd]_{food}$ correspond to Cd concentrations measured in bulk zooplankton samples collected from six lakes in the Rouyn-Noranda area (Table 3).

Not surprisingly, our steady-state model simulations of Cd in the gut tissue yielded very similar results to those obtained for the gills. Once again, the model had an obvious tendency to overestimate Cd concentrations in perch sampled from the more Cd-contaminated lakes (Dufault and Osisko), whereas the model predicted Cd concentrations in perch sampled from lakes with lower Cd concentrations

Fig. 3. (*a*) Changes in gut Cd concentrations during the accumulation transplantation in which yellow perch (*Perca flavescens*) were transplanted from Lake Opasatica to Lake Dufault. The solid circles represent the means of observed Cd concentrations in the gut ± standard deviation, SD. The broken line represents the model simulations; the solid line represents a nonlinear regression ($p \leq 0.05$). (*b*) Predicted versus measured gut Cd concentrations for juvenile yellow perch (*Perca flavescens*) collected from the Rouyn-Noranda area. (*c*) The same information as in (*b*) except that Lakes Osisko and Dufault have been removed for clarity. Predictions were based on the assumption that Cd uptake was from water and food. Data are represented by means ± SD, and the broken line represents the 1:1 relationship. The model could not be extended to the Sudbury lakes because metal concentrations in the zooplankton from these lakes were not available. See Table 1 for lake codes.

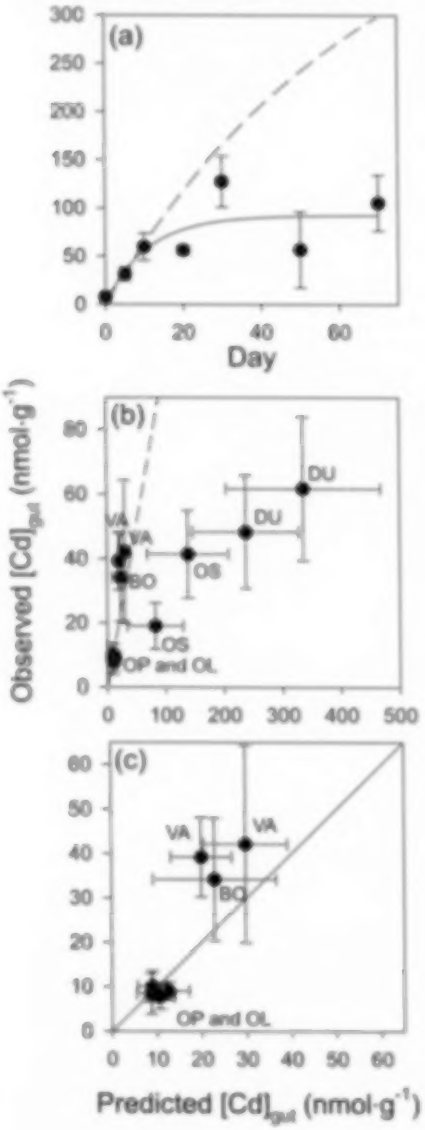

© 2008 NRC Canada

Fig. 4. (*a*) Changes in hepatic Cd concentrations during the accumulation transplantation in which yellow perch (*Perca flavescens*) were transplanted from Lake Opasatica to Lake Dufault. The solid circles represent the means ± standard deviations (SD) of observed Cd concentrations in the liver. The broken line represents the model simulations. (*b*) Predicted versus measured liver Cd concentrations for juvenile yellow perch collected from both the Sudbury and Rouyn-Noranda areas. Predictions were based on the assumption that Cd uptake was from water only. Data are represented by means ± SD, and the broken line represents the 1:1 relationship. See Table 1 for lake codes.

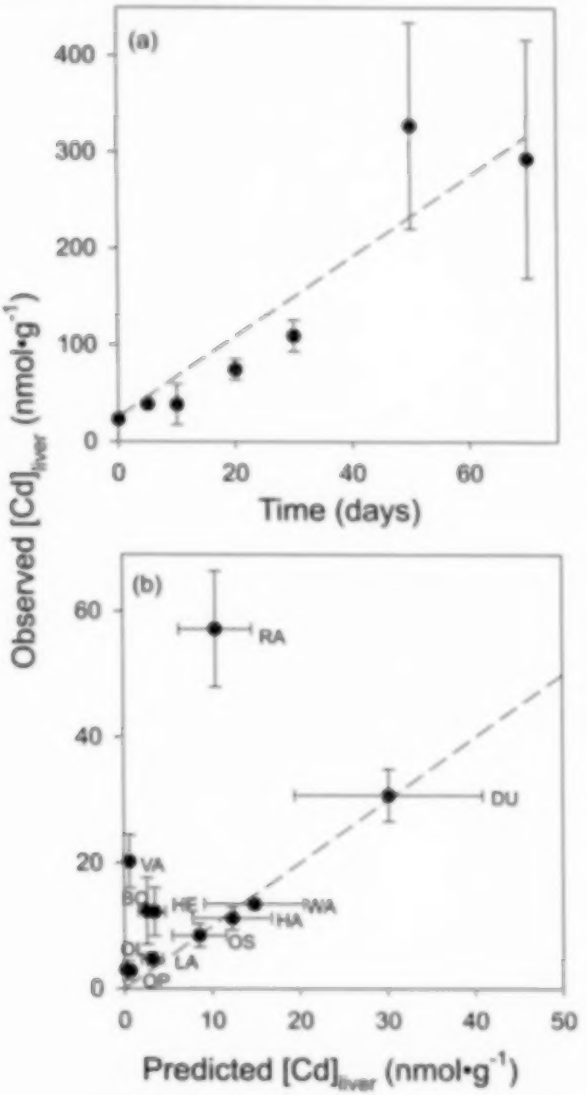

with reasonable accuracy (Fig. 3*b*). In their field study of perch collected from lakes in the Rouyn-Noranda area, Giguère et al. (2004) showed that Cd concentrations in the gut tissue of perch increased linearly with increasing $[Cd^{2+}]$ in lakes having low to moderate Cd concentrations (i.e., less than 1 nmol Cd^{2+}·L^{-1}), whereas above this threshold, gut Cd concentrations tended towards a plateau and no longer increased linearly with increasing $[Cd^{2+}]$. These data support the hypothesis that both the gills and the gut, the two organs important for Cd uptake, are able to alter their rates of uptake and (or) elimination when their internal concentrations exceed a certain threshold (Glynn 1996; Thomann et al. 1997).

Model application to the liver

Cd uptake

Applying the biodynamic model to the liver proved to be more complicated than for the gut and gills, mainly because of the physiological processes that govern the transfer of metals from these two external organs to the liver. Cadmium uptake into the gills is believed to occur mainly through Ca-selective channels on the apical side of the gill (Wood 2001). It is not known exactly how Cd is transferred to other internal organs once it is in the gill tissue, but a mechanism involving facilitated diffusion across the basolateral membrane of the gill has been suggested (Verbost et al. 1989; Wood 2001). Less is known about Cd uptake in the gut of fish, but evidence from mammalian research suggests that Cd is taken up across the apical membrane of the gut epithelium by an energy-independent process (Zalups and Ahmad 2003). Once inside the gut tissue, Cd forms a complex with metallothionein and this complex may cross the basolateral membrane by facilitated transport.

In our caging experiments, when perch were exposed to Cd via the diet and (or) water, Cd accumulation in the liver was not additive (i.e., amount of hepatic Cd accumulated in dietary-exposed perch + amounts of hepatic Cd accumulated in aqueous-exposed fish > amounts of hepatic Cd accumulated in perch exposed to Cd via both routes; Kraemer et al. 2006). Because the biodynamic model is designed to account for uptake from water and the diet separately and because perch were exposed to both sources during the 70-day transplantation experiment, this lack of additivity complicates the derivation of k_u^{liver}. However, given that aqueous Cd exposure accounts for approximately 100% of gill Cd and approximately 70% of gut Cd, we can surmise that aqueous Cd is also the dominant source of Cd for internal organs such as the liver. On this basis, as a first approximation, we decided to ignore the possible contribution of dietary Cd to hepatic accumulation.

Using the biodynamic model to explain Cd dynamics in the liver

Ignoring the possible contribution of diet-borne Cd to liver accumulation, we used the same form of equation as was used for the gills (eq. 5). The rate of Cd accumulation was estimated from data for the linear phase of uptake of the 70-day transplantation (day 10 to day 30), yielding a k_u^{liver} of 1.8 ± 0.6 L·g^{-1}·day^{-1}. Using this uptake rate constant, an elimination rate constant, k_e^{liver}, of 0.002·day^{-1} derived from our depuration experiment (Table 1) and ignoring the importance of growth (because liver mass did not increase during the transplantation), we were able to model Cd accumulation in the liver of perch during the transplantation period (Fig. 4*a*).

The modelling results for the liver contrast with those

© 2008 NRC Canada

observed for the gills and gut. Here the model agrees reasonably well with the observed data for the entire transplantation period, unlike the case for the gills and gut where the modelled results only agreed with observed data for the first 10 days. These results suggest that the rate constants for Cd uptake and loss from the liver are relatively insensitive to changes in liver Cd concentration, in contrast to the situation with gills and gut, which are affected by feedback changes that occur when bioaccumulated Cd exceeds a certain threshold. That Cd continues to accumulate in the liver, despite the tendency of Cd concentrations to plateau in the gills and gut, suggests that the metal-induced changes occurring in these latter organs involve accelerated movement of Cd into the internal circulatory system (rather than just decreased uptake or increased excretion across the apical epithelial membrane).

Unlike the gills or the gut, the liver obviously does not have direct contact with either the ambient water or the ingested food. The preceding analysis is thus analogous to the approach used by the current generation of biodynamic models, which consider the whole organism as a "black box" and ignore metal movement within the organism. In the present case, we explored an alternative approach to predict the steady-state hepatic Cd accumulation in the metal uptake caging experiment. If we assume that k_e^{gill} and k_e^{gut} represent movement of metal into the perch circulatory system and if we assume that all Cd lost from the gills and gut ends up in the liver, then we can equate loss from the two interfacial organs with inputs to the liver. Steady-state Cd concentrations in the liver would then be given by eq. 10:

$$(10) \qquad [Cd]_{ss}^{liver} = \frac{(k_e^{gill} \times [Cd]_{ss}^{gill}) + (k_e^{gut} \times [Cd]_{ss}^{gut})}{(k_u^{liver} + k_e^{liver})}$$

where $[Cd]_{ss}^{liver}$ is the steady-state liver Cd concentration, $[Cd]_{ss}^{gills}$ is the steady-state gill Cd concentration (32 nmol·g^{-1}; Fig. 2*a*), $[Cd]_{ss}^{gut}$ is the steady-state gut Cd concentration (80 nmol·g^{-1}; Fig. 3*a*), and the other constants have the same signification and units as described above. Using this equation and the efflux rate constants given in Table 1 and considering that k_u^{liver} was negligible in the uptake experiment, we calculate that steady-state hepatic Cd concentrations should have attained ~860 nmol Cd·g^{-1} in the uptake experiment; actual values were close to 300 nmol Cd·g^{-1} (Fig. 4*a*). Our initial assumption that all Cd lost from the gills and gut ends up in the liver likely overestimates the hepatic inputs; some of the observed decrease in gill and gut Cd in the depuration experiment may well have involved losses to the external environment. Additionally, Cd lost from the gills and gut will also be deposited in other organs, notably the kidney, which has been shown to accumulate high concentrations of Cd (Giguère et al. 2004; Kraemer et al. 2005*a*). Note also that the calculation is inherently sensitive to the value chosen for k_e^{liver} in the denominator (0.002·day^{-1}).

Using the biodynamic model to predict steady-state liver Cd concentrations in perch from other lakes

Using a similar approach as was used for the gills (i.e., ignoring the importance of dietary Cd), we modelled steady-state concentrations of Cd in the liver for perch collected from a series of lakes (using an equation analogous to eq. 6). Because k_e^{liver} is an order of magnitude lower than either k_e^{gill} or k_e^{gut}, hepatic turnover of Cd is lower than in the other organs and Cd accumulates to higher levels in this organ. For most of the lakes considered, the model predicted observed concentrations with reasonable accuracy (Fig. 4*b*). This agreement between model simulations and field observations is consistent with the results of Giguère et al. (2004), who found that steady-state liver Cd concentrations increased linearly with increasing aqueous $[Cd^{2+}]$ in yellow perch collected from the same series of lakes as the current study, with no plateau being observed. In the present study, however, there were a few notable exceptions, namely Lakes Vaudray, Bousquet, and Raft, where the observed hepatic Cd concentrations were much higher than those predicted by the model. As previously discussed for the gills, lake-to-lake variations in water chemistry may have contributed to these discrepancies between the model and observed data.

Future modeling perspectives

In this study, we calibrated a simple biokinetic model for Cd accumulation in juvenile yellow perch using the initial rates of Cd uptake and loss as measured in field experiments. The resulting model was unable to predict long-term Cd bioaccumulation in the gills and gut of yellow perch from contaminated lakes, likely because changes in the rate constants for uptake and (or) elimination of this metal occur when bioaccumulated Cd concentrations exceed a certain threshold. However, unlike the gill and gut simulations, there was reasonably good agreement between modelled and observed hepatic Cd concentrations. We previously reported that although perch accumulate Cd from both dietary and aqueous sources, aqueous Cd is the main source of accumulated metal (Kraemer et al. 2006). Indeed, the model was able to predict hepatic Cd concentrations with reasonable accuracy using just aqueous Cd information and omitting any dietary information.

Similar modeling simulations carried out on zebra mussels (Roditi et al. 2000) and copepods (Fisher et al. 2000) showed good agreement between model simulations and observed concentrations for many metals (Ag, Co, Zn, Hg), but for Cd, the model predictions were up to four times lower than observed concentrations. Because Cd had the longest half-life of the metals considered, Roditi et al. (2000) speculated that metals with long biological half-life periods are less closely related to ambient metal concentrations than are metals that are subject to more rapid turnover. In yellow perch, the opposite trend was observed; the model was most accurate in the liver, the organ with the slowest turnover rate. In our case, we believe that the inability of the model to accurately predict gill and gut Cd concentrations was linked to biological changes in the gills and gut (i.e., changes in the rate of transfer of Cd across the basolateral membranes) related to high concentrations of bioaccumulated Cd in these organs. Zhang and Wang (2007) reported that whole-body k_u values for Cd decrease as a function of body size in juvenile black sea bream (*Acanthopagrus schlegi*). The decrease in k_u was attributed primarily to a decrease in ingestion rates, with AE being independent of size. Although these results are not directly comparable with our organ-specific study, nevertheless, they do illustrate

© 2008 NRC Canada

that uptake parameters in biodynamic models may indeed vary as a function of many different biological factors.

In their recent review of the use of biodynamic modeling to predict species-specific metal bioaccumulation in the field, Luoma and Rainbow (2005) identified 15 publications in which model predictions could be compared with field observations. Over the entire suite of seven metals and 14 animal species, including one marine teleost, *Hippoglossoides platessoides* (plaice), whole-organism metal concentrations covered seven orders of magnitude. When all of the data were log-transformed and pooled, the overall coefficient of determination (R^2) between predictions and observations was an impressive 0.98; most forecasts agreed with observations within a factor of two. In the present study, we modelled Cd bioaccumulation not at the whole-organism level, but rather for specific organs known to be involved in metal uptake (gills, gut) or storage (liver). Our results suggest that because influx and (or) efflux rate constants for some organs are not, in fact, constant, then assuming constancy could lead to erroneous predictions when using kinetic bioaccumulation models to make organ-specific predictions. However, the ability to make such predictions is clearly important because toxic effects are likely to occur in specific organs and thus modeling their accumulation of metals is important for predicting impacts on individuals.

Acknowledgements

This study was supported by a grant from the Metals in the Environment Research Network (MITE-RN). We are grateful to the Société de la Faune et des Parcs de l'Abitibi–Témiscamingue (Government of Québec) for their logistical help with the field study. We also thank Caroline Durand and Philipe Bourret for their field assistance and Michelle Geoffroy-Bordeleau, Pauline Fournier, and Sébastien Duval for their help in the laboratory. Constructive comments from two anonymous reviewers helped improve the manuscript. PGCC is supported by the Canada Research Chair programme. This is contribution No. 49 from MITE-RN (http://www.mithe-rn.org).

References

Baines, S.B., and Fisher, N.S. 2002. Assimilation and retention of selenium and other trace elements from crustacean food by juvenile striped bass (*Morone saxatilis*). Limnol. Oceanogr. **47**: 646–655.

Blust, R. 2001. Radionuclide accumulation in aquatic organisms: concepts and models. *In* Radioecology: radioactivity and ecosystems. *Edited by* R. Kirchmann and E. Van der Stricht. International Union of Radioecology, Liège, Belgium. pp. 275–307.

Borgmann, U., Nowierski, M., Grapentine, L.C., and Dixon, D.G. 2004. Assessing the cause of impacts on benthic organisms near Rouyn-Noranda, Quebec. Environ. Pollut. **129**: 39–48. doi:10.1016/j.envpol.2003.09.023. PMID:14749068.

Borgmann, U., Janssen, C.R., Blust, R.J.P., Brix, K.V., Dwyer, R.L., Erickson, R.J., Hare, L., Luoma, S.N., Paquin, P.R., Roberts, C.A., and Wang, W.-X. 2005. Incorporation of dietborne metals exposure into regulatory frameworks. *In* Toxicity of dietborne metals to aquatic organisms. *Edited by* J.S. Meyer, W.J. Adams, K.V. Brix, S.N. Luoma, D.R. Mount, W.A. Stubblefield, and C.M. Wood. SETAC Press, Pensacola, Florida, USA. pp. 153–189.

Campbell, P.G.C., Hontela, A., Rasmussen, J.B., Giguère, A., Gravel, A., Kraemer, L., Kovecses, J., Lacroix, A., Levesque, H., and Sherwood, G.D. 2003. Differentiating between direct (physiological) and food-chain mediated (bioenergetic) effects on fish in metal-impacted lakes. Human Ecol. Risk Assess. **9**: 847–866. doi:10.1080/713610012.

Couture, P., and Rajotte, J.W. 2003. Morphometric and metabolic indicators of metal stress in wild yellow perch (*Perca flavescens*) from Sudbury, Ontario: a review. J. Environ. Monit. **5**: 216–221. doi:10.1039/b210338a. PMID:12729257.

Croteau, M.-N., Hare, L., and Tessier, A. 2002*a*. Influence of temperature on Cd accumulation by species of the biomonitor *Chaoborus*. Limnol. Oceanogr. **47**: 505–514.

Croteau, M.-N., Hare, L., and Tessier, A. 2002*b*. Increases in food web cadmium following reductions in atmospheric inputs to some lakes. Environ. Sci. Technol. **36**: 3079–3082. doi:10.1021/es011485+. PMID:12141486.

Croteau, M.-N., Hare, L., and Marcoux, P. 2003. Feeding patterns of migratory and non-migratory fourth instar larvae of two coexisting *Chaoborus* species in an acidic and metal contaminated lake: importance of prey ingestion rate in predicting metal bioaccumulation. Arch. Hydrobiol. **158**: 57–74. doi:10.1127/0003-9136/2003/0158-0057.

Fisher, N.S., Stupakoff, I., Sanudo-Wilhelmy, S., Wang, W.X., Teyssie, J.L., Fowler, S.W., and Crusius, J. 2000. Trace metals in marine copepods: a field test of a bioaccumulation model coupled to laboratory uptake kinetics data. Mar. Ecol. Prog. Ser. **194**: 211–218. doi:10.3354/meps194211.

Giguère, A., Campbell, P.G.C., Hare, L., McDonald, D.G., and Rasmussen, J.B. 2004. Influence of lake chemistry and fish age on Cd, Cu, and Zn concentrations in various organs of indigenous yellow perch (*Perca flavescens*). Can. J. Fish. Aquat. Sci. **61**: 1702–1716. doi:10.1139/f04-100.

Giguère, A., Campbell, P.G.C., Hare, L., and Cossu-Leguille, C. 2005. Metal bioaccumulation and oxidative stress in yellow perch (*Perca flavescens*) collected from eight lakes along a metal contamination gradient (Cd, Cu, Zn, Ni). Can. J. Fish. Aquat. Sci. **62**: 563–577. doi:10.1139/f04-224.

Giguère, A., Campbell, P.G.C., Hare, L., and Couture, P. 2006. Sub-cellular partitioning of cadmium, copper, nickel and zinc in indigenous yellow perch (*Perca flavescens*) sampled along a polymetallic gradient. Aquat. Toxicol. **77**: 178–189. doi:10.1016/j.aquatox.2005.12.001. PMID:16430977.

Gingras, J., and Boisclair, D. 2000. Comparison between consumption rates of yellow perch (*Perca flavescens*) estimated with a digestive tract model and with a radioisotope approach. Can. J. Fish. Aquat. Sci. **57**: 2547–2557. doi:10.1139/cjfas-57-12-2547.

Glynn, A.W. 1996. The concentration dependency of branchial intracellular cadmium distribution and influx in the zebrafish (*Brachydanio rerio*). Aquat. Toxicol. **35**: 47–58. doi:10.1016/0166-445X(96)00006-9.

Gonzalez, P., Baudrimont, M., Boudou, A., and Bourdineaud, J.-P. 2006. Comparative effects of direct cadmium contamination on gene expression in gills, liver, skeletal muscles and brain of the zebrafish (*Danio rerio*). Biometals, **19**: 225–235. doi:10.1007/s10534-005-5670-x. PMID:16799861.

Gravel, A., Campbell, P.G.C., and Hontela, A. 2005. Disruption of the hypothalamo-pituitary-interrenal axis in 1+ yellow perch (*Perca flavescens*) chronically exposed to metals in the environment. Can. J. Fish. Aquat. Sci. **62**: 982–990. doi:10.1139/f05-011.

Harrison, S.E., and Klaverkamp, J.F. 1989. Uptake, elimination and tissue distribution of dietary and aqueous cadmium by rainbow trout (*Salmo gairdneri*) and lake whitefish (*Coregonus clupea-*

© 2008 NRC Canada

formis). Environ. Toxicol. Chem. **8**: 87–97. doi:10.1897/1552-8618(1989)8[87:UEATDO]2.0.CO;2.

Kraemer, L.D., Campbell, P.G.C., and Hare, L. 2005*a*. Dynamics of Cd, Cu and Zn accumulation in organs and sub-cellular fractions in field transplanted juvenile yellow perch (*Perca flavescens*). Environ. Pollut. **138**: 324–337. doi:10.1016/j.envpol.2005.03.006. PMID:15951079.

Kraemer, L.D., Campbell, P.G.C., and Hare, L. 2005*b*. A field study examining metal elimination kinetics in juvenile yellow perch (*Perca flavescens*). Aquat. Toxicol. **75**: 108–126. doi:10.1016/j.aquatox.2005.07.007. PMID:16125800.

Kraemer, L.D., Campbell, P.G.C., and Hare, L. 2006. A field study examining the relative importance of food and water as sources of Cd for juvenile yellow perch (*Perca flavescens*). Can. J. Fish. Aquat. Sci. **63**: 549–557. doi:10.1139/f05-236.

Levesque, H., Dorval, J., Van Der Kraak, G.J., Campbell, P.G.C., and Hontela, A. 2003. Hormonal, morphological and physiological responses of yellow perch (*Perca flavescens*) to chronic environmental metal exposures. J. Toxicol. Environ. Health, **66**: 657–676. doi:10.1080/15287390306377.

Lin, X.-J., Ni, I.-H., and Wang, W.-X. 2002. Trophic transfer of heavy metals from freshwater zooplankton *Daphnia magna* to zebrafish *Danio rerio*. Water Res. **36**: 4563–4569. doi:10.1016/S0043-1354(02)00180-X. PMID:12418659.

Luoma, S.N., and Rainbow, P.S. 2005. Why is metal bioaccumulation so variable? Biodynamics as a unifying principle. Environ. Sci. Technol. **39**: 1921–1931. doi:10.1021/es048947e. PMID:15871220.

Luoma, S.N., Johns, C., Fisher, N.S., Steinberg, N.A., Oremland, R.S., and Reinfelder, J. 1992. Determination of selenium bioavailability to a benthic bivalve from particulate and solute pathways. Environ. Sci. Technol. **26**: 485–491. doi:10.1021/es00027a005.

Mount, D.R., Barth, A.K., Garrison, T.D., Barten, K.A., and Hockett, J.R. 1994. Dietary and waterborne exposure of rainbow trout (*Oncorhynchus mykiss*) to copper, cadmium, lead and zinc using a live diet. Environ. Toxicol. Chem. **13**: 2031–2041. doi:10.1897/1552-8618(1994)13[2031:DAWEOR]2.0.CO;2.

Munger, C., Hare, L., and Tessier, A. 1999. Cadmium sources and exchange rates for *Chaoborus* larvae in nature. Limnol. Oceanogr. **44**: 1763–1771.

Ni, I.-H., Wang, W.X., and Tam, K.K. 2000. Transfer of Cd, Cr and Zn from zooplankton prey to mudskipper *Periophthalmus cantonensis* and glassy *Ambassis urotaenia* fishes. Mar. Ecol. Prog. Ser. **194**: 203–210. doi:10.3354/meps194203.

Noel, L., Huynh-Delerme, C., Guerin, T., Huet, H., Fremy, J.-M., and Kolf-Clauw, M. 2006. Cadmium accumulation and interactions with zinc, copper, and manganese, analysed by ICP-MS in a long-term Caco-2 TC7 cell model. Biometals, **19**: 473–481. doi:10.1007/s10534-005-5147-y. PMID:16937253.

Reinfelder, J.R., and Fisher, N.S. 1994. Retention of elements absorbed by juvenile fish (*Menidia menidia*, *Menidia beryllina*) from zooplankton prey. Limnol. Oceanogr. **39**: 1783–1789.

Rodriti, H.A., Fisher, N.S., and Sanudo-Wilhelmy, S.A. 2000. Field testing a metal bioaccumulation model for zebra mussels. Environ. Sci. Technol. **34**: 2817–2825. doi:10.1021/es991442h.

Sarhan, M.J., Roels, H., Lauwerys, R., Reyners, H., and Gianfelici de Reyners, E. 1986. Influence of manganese on the gastrointestinal absorption of cadmium in rats. J. Appl. Toxicol. **6**: 313–316. doi:10.1002/jat.2550060503. PMID:3772006.

Sherwood, G.D., Rasmussen, J.B., Rowan, D.J., Brodeur, J., and Hontela, A. 2000. Bioenergetic costs of heavy metal exposure in yellow perch (*Perca flavescens*): in situ estimates with a radiotracer (^{134}Cs) technique. Can. J. Fish. Aquat. Sci. **57**: 441–450. doi:10.1139/cjfas-57-2-441.

Thomann, R.V., Shkreli, F., and Harrison, S. 1997. A pharmacokinetic model of cadmium in rainbow trout. Environ. Toxicol. Chem. **16**: 2268–2274. doi:10.1897/1551-5028(1997)016<2268:APMOCI>2.3.CO;2.

Tipping, E. 1998. Humic ion-binding model VI: an improved description of the interactions of protons and metal ions with humic substances. Aquat. Geochem. **4**: 3–48. doi:10.1023/A:1009627214459.

Trudel, M., Tremblay, A., Schetagne, R., and Rasmussen, J.B. 2000. Estimating food consumption rates of fish using a mercury mass balance model. Can. J. Fish. Aquat. Sci. **57**: 414–428. doi:10.1139/cjfas-57-2-414.

Verbost, P.M., Van Rooij, J., Flik, G., Lock, R.A.C., and Bonga, S.E.W. 1989. The movement of cadmium through freshwater trout branchial epithelium and its interference with calcium transport. J. Exp. Biol. **145**: 185–197.

Wehrens, R., Putter, H., and Buydens, L.M.C. 2000. The bootstrap: a tutorial. Chem. Intell. Lab. Syst. **54**: 35–52. doi:10.1016/S0169-7439(00)00102-7.

Wood, C.M. 2001. Toxic responses of the gill. *In* Target organ toxicity in marine and freshwater teleosts. *Edited by* D. Schlenk and W.H. Benson. Taylor & Francis, New York. pp. 1–89.

Yanagiya, T., Nobumasa, I., Shuichi, E., Yukihiro, K., and Seiichiro, H. 2000. Suppression of a high-affinity transport system for manganese in cadmium-resistant metallothionein-null cells. J. Pharmacol. Exp. Therap. **292**: 1080–1086.

Zalups, R.K., and Ahmad, S. 2003. Molecular handling of cadmium in transporting epithelia. Toxicol. Appl. Pharmacol. **186**: 163–188. doi:10.1016/S0041-008X(02)00021-2. PMID:12620369.

Zhang, L., and Wang, W.-X. 2007. Size-dependence of the potential for metal biomagnification in early life stages of marine fish. Environ. Toxicol. Chem. **26**: 787–794. doi:10.1897/06-348R.1. PMID:17447565.

© 2008 NRC Canada

Effects of marine-derived nutrients on population dynamics of sockeye salmon (*Oncorhynchus nerka*)

Tadayasu Uchiyama, Bruce P. Finney, and Milo D. Adkison

Abstract: The effects of marine-derived nutrients (MDN) on the productivity of sockeye salmon (*Oncorhynchus nerka*) stocks in Alaska, USA, were examined through nitrogen stable isotope analysis of smolts and mathematical models of the sockeye stock–recruit relationship. Smolt $\delta^{15}N$ was used to infer the degree to which smolts depend on MDN for their growth. We found that characteristics of sockeye nursery lakes and watersheds significantly affected the availability of MDN to juvenile sockeye. The magnitude of escapement and water residence time were the most important factors affecting the MDN availability to juvenile salmon. Analysis of stock–recruit models indicated that regional environmental fluctuations had a large effect on stock productivities. However, stock–recruitment data showed little evidence that increasing MDN input to nursery lakes increased stock productivities. Stock–recruitment data may be poorly suited to detection of the influence of MDN because of the multitude of factors that influence juvenile survival in the first several years of their life.

Résumé : Nous examinons les effets des nutriments d'origine marine (MDN) sur la productivité des stocks de saumons sockeye (*Oncorhynchus nerka*) en Alaska, É.-U., par l'analyse des ions stables d'azote chez les saumoneaux et l'utilisation de modèles mathématiques de la relation stock–recrutement chez les saumons sockeye. À l'aide des valeurs de $\delta^{15}N$ des saumoneaux, nous avons déduit dans quelle mesure les saumoneaux dépendent des MDN pour leur croissance. Les caractéristiques des lacs de nourricerie des saumons sockeye et des bassins versants affectent significativement la disponibilité des MDN aux jeunes saumons sockeye. L'importance de l'échappement et le temps de résidence de l'eau sont les facteurs les plus importants à affecter la disponibilité des MDN aux jeunes saumons. L'analyse des modèles de stock–recrutement indique que les fluctuations régionales du milieu ont un important effet sur la productivité des stocks. Cependant les données de stock–recrutement donnent peu d'indications que l'augmentation de l'apport des MDN dans les lacs de nourricerie accroît la productivité des stocks. Les données de stock–recrutement peuvent être peu appropriées pour détecter l'influence des MDN à cause de la multitude de facteurs qui influencent la survie des jeunes durant plusieurs des premières années de leur vie.

[Traduit par la Rédaction]

Introduction

A distinguishing characteristic of sockeye salmon (*Oncorhynchus nerka*) is their extensive use of lake rearing habitat during the juvenile stage of their life history. After emerging from the gravel, sockeye fry typically migrate to lakes associated with their natal spawning habitats, where they exhibit a pelagic life style, feeding mainly on limnetic zooplankton for 1 to 3 years before seaward migration (Burgner 1991). The biological productivity in sockeye nursery lake habitat is important for the survival and growth of juvenile sockeye salmon. Although sockeye salmon acquire 99% of their body weight in the ocean, survival in the freshwater stage is much lower than ocean survival (2% and 8%, respectively (Bradford 1995); 2.1% and 13.1%, respectively (Quinn 2004)). In addition, most marine mortality occurs soon after entering the ocean (Healey 1982; Bax 1983; Fisher and Pearcy 1988) and is inversely related to size attained in freshwater (Pearcy 1992; Koenings et al. 1993).

Spawning adult salmon returning to their natal freshwater habitats may bring in large quantities of nutrients annually in the form of their body mass (Kline et al. 1993; Bilby et al. 1996; Schmidt et al. 1998). For example, one million sockeye transport an estimated 64 100 kg·year^{-1} of nitrogen to Karluk Lake, Kodiak, Alaska, while 43 200 kg·year^{-1} and 800 kg·year^{-1} are supplied by the other main nitrogen sources, rivers and rain, respectively (Finney 1998). Many of the lakes in Alaska used as the nursery by sockeye salmon are

Received 31 May 2007. Accepted 2 April 2008. Published on the NRC Research Press Web site at cjfas.nrc.ca on 16 July 2008. J20025

T. Uchiyama.[1,2] School of Fisheries and Ocean Sciences, University of Alaska Fairbanks, Fairbanks, AK 99775, USA.
B.P. Finney.[3] Institute of Marine Science, School of Fisheries and Ocean Sciences, University of Alaska Fairbanks, Fairbanks, AK 99775-7720, USA.
M.D. Adkison. School of Fisheries and Ocean Sciences, Juneau Center, University of Alaska Fairbanks, 11120 Glacier Highway, Juneau, AK 99801, USA.

[1]Corresponding author (e-mail: tadayasu.uchiyama@email.ucr.edu).
[2]Present address: Department of Biology, University of California, Riverside, CA 92521, USA.
[3]Present address: Department of Biological Sciences, Idaho State University, Pocatello, ID 83209, USA.

 doi:10.1139/F08-085 © 2008 NRC Canada

classified as oligotrophic, where nutrients limit primary production. In such systems, the nutrients supplied by salmon might be very important in maintaining the productivity of the lake and the carrying capacity for juvenile salmon.

Nitrogen derived from adult salmon is enriched in ^{15}N relative to nitrogen from other terrestrial sources. The $\delta^{15}N$ of adult sockeye averages about 11‰–12‰, whereas terrestrial sources of nitrogen have $\delta^{15}N$ values closer to zero (Kline et al. 1993; Welch and Parsons 1993; Satterfield and Finney 2002). This large difference in $\delta^{15}N$ makes it possible to trace and quantify marine-derived nutrients (MDN) in freshwater systems (Kline et al. 1990). The $\delta^{15}N$ value of sockeye smolts has been shown to have a strong positive correlation with the number of adult sockeye spawning in the system and can be used to estimate the relative importance of MDN in the growth of juveniles (Kline et al. 1993; Finney et al. 2000).

It has been postulated that declines of some sockeye stocks may be partly due to reduced nutrient loading because of low escapement (Finney et al. 2000; Stockner et al. 2000). In many lakes, the input of MDN was much higher prior to the advent of commercial fisheries. A reduction in MDN has been advanced as a possible explanation for reduced sockeye returns to some formerly highly productive systems, such as Karluk Lake (Schmidt et al. 1998; Finney et al. 2000).

The objectives of this study were to assess whether physical characteristics of sockeye nursery lakes could affect the relative availability of MDN to juvenile sockeye and thus mediate the effects of MDN on stock productivity. The importance of MDN in the growth of juvenile salmon depends on the abundance of such nutrients in the system relative to the nutrients derived from terrestrial sources. The quantity of nutrients exported from watersheds into lakes rises with increasing watershed area (Kalff 2002). Lakes with large watershed areas are more likely to experience large inputs of terrestrial nutrients relative to the nutrients derived from spawning salmon. In such lakes, MDN should be of secondary importance to the productivity of the system and to the growth of juvenile salmon. Because the stable isotope signature of terrestrial nitrogen is much lighter (i.e., contains less ^{15}N) than that of nitrogen derived from adult salmon, juvenile salmon rearing in a lake in which nutrients from terrestrial sources are abundant would have a low $\delta^{15}N$ value.

Productivity of lake ecosystems can be limited by factors other than nutrients, such as the availability of light for photosynthesis by phytoplankton. Because of limited light availability, the productivity of glacial lakes with high concentrations of suspended silt may not respond to increased nutrient input. Past study showed that primary production in glacial lakes was much lower than primary production in clear-water lakes in British Columbia (Stockner 1987). Also, it has been shown that both smolt and adult sockeye productions were strongly correlated to the euphotic volume of nursery lakes (Koenings and Burkett 1987). We expected that increased spawner abundance has little effect in increasing productivity glacial lakes and that juvenile salmon in such lakes benefit less from the addition of MDN compared with their counterpart in nonglacial lakes. This would also be reflected in the nitrogen stable isotope signature of the juvenile salmon rearing in such lakes. Because phytoplankton preferentially assimilates the lighter isotope of nitrogen, ^{14}N, over the heavier ^{15}N, the nitrogen isotope signature of phytoplankton, and of all organisms the lives of which depend on the primary production of the lake, will be lighter than that of the source nitrogen if there is an excess of nitrogen in the environment.

Salmon typically cease feeding before entering their natal streams and depend entirely on their body energy reserves for migration, maturation of gonads, and spawning. In addition to the intense physical activity of the migration, the physical, chemical, and physiological changes that they must undergo during migration extensively deplete their body reserves of fat and protein (Burgner 1991). Sockeye salmon can consume a significant portion of their energy reserves in up-river migration (Idler and Clemens 1959), even when the distances are relatively small (Hendry and Berg 1999). It is possible that salmon that travel long distances to their spawning grounds lose more body protein than the ones who travel shorter distances during migrations. Therefore, we examined whether the distance from the coast to the mouth of a particular nursery lake affects the availability of MDN to the growth of juvenile sockeye.

Stratification of the water column in lakes limits exchange of materials, including nutrients, between layers of water within the lake. Most temperate lakes stratify during summer months because of a density gradient in the water column created by solar energy input to the lake surface. As the lake water is cooled at the surface in fall, the density gradient in the water column diminishes to the point at which wind is able to mix the entire water column. Mixing of the water column refurnishes the euphotic zone with nutrients from the hypolimnion, allowing nutrients to be recycled within the lake. Incomplete mixing of the water column (meromixis) limits nutrient supply to the epilimnion by reducing nutrient recycling and affects primary production. Three of the lakes included in this study (Coghill, Hugh Smith, and Redoubt) are known to have a persistent stratified state with a dense, anoxic layer of saline water that does not mix with the surface layer above (Edmundson et al. 1992; Geiger et al. 2003; Geiger 2003). It is likely that some nutrients entering these lakes are trapped in the bottom layer and thus do not contribute to the productivity of the lake. We examined the effect of stratification on MDN availability to smolts.

We analyzed nitrogen stable isotopes of smolts from 21 Alaska lakes and compared these data with both spawner abundance and lake characteristics as discussed above that might affect the importance of MDN in salmon growth. We also examined the effect of spawner abundance and lake characteristics on the productivity of 16 Alaska sockeye stocks, as reflected in the relationship between spawning adults and the number of adult offspring they produce. In this second analysis, we tried to quantify the effects of MDN by first fitting mathematical models to historical escapement and return data and then examining our estimates to see if the magnitude of the effect differed for various lake types.

Materials and methods

Study sites

Twenty-three sockeye stocks and associated nursery lakes in Alaska were included in this study (Table 1). Particular stocks of sockeye salmon (and their nursery lakes) were

© 2008 NRC Canada

Table 1. Morphometric and hydrological data for 23 sockeye salmon nursery lakes in Alaska.

Region	Lake	Area (km^2)	Volume ($10^6 m^3$)	Watershed area (km^2)	Glacier cover (km^2)	Residence time (years)	Distance from coast (km)	Mixing state
Alaska Peninsula	Black	41.1	61.65	715.47	9.96	0.058	47.30	Holomictic
	Chignik	24.1	626.60	1 567.37	36.16	0.270	7.01	Holomictic
	Sapsuk	11.0	443.1	133.28	0	1.74	—	Holomictic
Bristol Bay	Becharof	1 142.7	64 795	3 375.35	8.74	16.39	51.40	Holomictic
	Iliamna	2 642.9	115 310	16 862.41	839.38	7.21	112.16	Holomictic
	Ugashik (Upper and Lower)	381.7	12 188	1 968.84	0	5.78	71.73	Holomictic
Kodiak	Akalura	4.9	48.0	40.98	0	0.741	1.97	Holomictic
	Frazer	16.6	551.1	191.70	0	1.82	13.70	Holomictic
	Karluk	39.4	1 920.0	275.08	0	4.64	41.72	Holomictic
	Red	8.4	207.7	56.31	0	2.35	27.37	Holomictic
	Spiridon	9.2	319.2	54.18	0	7.97	2.51	Holomictic
Cook Inlet	Hidden	6.8	138.1	56.17	0	2.83	107.88	Holomictic
	Russian, Upper	4.6	122.2	66.95	1.500	1.81	147.11	Holomictic
	Tustumena	294.5	36 518	1 781.10	382.09	18.85	26.75	Holomictic
Prince William Sound	Coghill	12.7	381[a]	121.54	22.72	0.90	5.21	Meromictic
	Eshamy	3.6	122	23.66	0	1.21	—	Holomictic
Southeast	Anke	0.9	17.0	10.16	0	1.09	0.78	Holomictic
	Chilkat	9.8	319	97.20	3.17	2.03	31.03	Holomictic
	Chilkoot	7.0	382	333.86	76.67	0.48	1.96	Holomictic
	Hugh Smith	3.2	192.0[b]	49.41	0	0.94	0.27	Meromictic
	McDonald	4.2	191.5	120.77	0	0.38	2.01	Holomictic
	Redoubt	16.6	1 660[c]	108.58	0	4.30	0.00	Meromictic
	Speel	1.7	5.12	16.51	0	0.075	13.59	Holomictic

[a]The volume of the lake was adjusted for the depth of a meromictic layer at 30 m.
[b]The volume of the lake was adjusted for the depth of a meromictic layer at 60 m.
[c]The volume of the lake was adjusted for the depth of a meromictic layer at 100 m.

chosen based on the availability of smolt samples, escapement and return data, and lake morphometric data. The morphometric data (lake surface area, mean depth, and (or) lake volume) for the nursery lakes were obtained from Alaska Department of Fish and Game (ADF&G) reports and other literature. The distances from the coasts to the outlets of the study lakes were measured on digital spatial data obtained from the National Hydrography Dataset (NHD; US Geological Survey (USGS) 2004*a*). The stream feature of the NHD is a set of vector data that represent segments of rivers and streams. We measured the distance from the coast as the total length of the stream segments that connect the study lake to the coast with the shortest distance. The study sites encompassed a large geographic area (130.67 W – 161.02 W, 55.10 N – 61.10 N) with climatic differences. Because sockeye stocks in the same geographic region have been shown to exhibit a similar pattern in their productivity (Peterman et al. 1998), for the purpose of population modeling, the stocks in this study were grouped into five geographic regions: Alaska Peninsula, Bristol Bay, Kodiak, Cook Inlet – Prince William Sound, and Southeast. The study lakes varied in size, with surface area ranging from 0.9 to 2642 km^2 and volume ranging from 5.1 × 10^6 to 115 310 × 10^6 m^3. The volumes of the three meromictic (incomplete mixing of water column) lakes included in this study (Coghill, Hugh Smith, and Redoubt) were calculated using the depths of the top mixed layer because there is no exchange of water and materials between the top and bottom layers in these lakes.

Watershed area and annual discharge

The watershed areas of the nursery lakes were estimated based on the National Elevation Dataset (NED; resolution 2 arcseconds) obtained from the National Center for Earth Resources Observations and Science (2004), using the Watershed function in ArcGIS (version 9.0; ESRI, Redlands, California) spatial analyst tools.

We estimated the annual discharge from the nursery lakes using stream flow data obtained from the US Geological Survey Water Resources Web site (USGS 2004*b*). The annual mean flow values between 1910 and 2002 were averaged for each of 382 gauging stations in Alaska. The averaged flow values were divided by the drainage area for each gauging station to express the annual flow on a per unit drainage area basis ($m^3 \cdot year^{-1} \cdot km^{-2}$). Where direct flow measurements were not available, the values of annual flow/drainage area at the outlet of the nursery lakes were interpolated from the measured values at the nearest 15 gauging stations by inverse distance weighted interpolation using an ArcGIS geospatial analyst tool with a power value of 2. These values were then multiplied by the drainage area of each lake to estimate annual discharge ($m^3 \cdot year^{-1}$). The water residence time (year) of each nursery lake was obtained by dividing the lake volume by the estimated annual discharge.

Escapement and return data

Sockeye escapement and brood year total return data for

© 2008 NRC Canada

16 sockeye stocks were obtained from ADF&G Division of Commercial Fisheries regional offices and from ADF&G publications.

Two lakes in Southeast region (Chilkat and Speel) have been stocked with sockeye fry in the past. For the purpose of modeling stock–recruit relationships, a number of spawners equivalent to the number of stocked fry released was calculated by dividing the number of fry by a typical egg-to-fry survival rate (0.127; Quinn 2004) and by fecundity (3654), and this value then was added to the escapement of the corresponding years.

Analysis of smolt stable isotope data

Seven hundred and sixty-three sockeye smolts collected from 21 sockeye-producing systems in Alaska were analyzed for nitrogen stable isotope composition (Table 2). Smolts from Southeast region were analyzed by David Barto of ADF&G (Barto 2004). The number of smolt samples from a particular system and year ranged from 5 to 68. Muscle tissues from smolt samples were removed with a scalpel and either oven- or freeze-dried and then homogenized. Nitrogen stable isotope compositions were analyzed using a continuous-flow isotope ratio mass spectrometer (Europa Scientific 20/20 (Sercon, Cheshire, UK) or ThermoFinnigan Delta+ (Thermo Fisher Scientific Inc., Waltham, Mass., USA)) and were expressed in conventional δ^{15}N notation (Satterfield and Finney 2002).

The effects of characteristics of sockeye nursery lakes (watershed area, glacial coverage in the watershed, distance from the coast, and permanent stratification) on the level of MDN in juvenile salmon were examined by multiple linear regression, using the lake characteristics as explanatory variables and the mean of observed smolt δ^{15}N for each lake and year as a response variable. The multiple regression model was fitted to the data by weighted least squares using the number of observations in each lake and year as the weights. The multiple regression model was formulated as follows:

$$(1)\quad \delta^{15}N_{smolt,i,t} = \alpha + \beta_1\left(\frac{\text{MDN input}}{\text{lake volume}}\right)_{i,t-1} + \beta_2\left(\frac{\text{watershed area}}{\text{lake volume}}\right)_i + \beta_3\left(\frac{\text{glacier coverage}}{\text{watershed area}}\right)_i + \beta_4(\text{distance traveled})_i + \beta_5(\text{mixing})_i$$

where i represents stock/drainage, and t is brood year. MDN input in the regression equation was calculated as

$$(2)\quad \text{MDN input}_{i,t} = \sum_{j=0} S_{i,t-j}e^{[-(j+0.5)/RT_i]}$$

where S_i represents salmon escapement in lake i, RT_i represents water residence time of lake i, and j is the number of years before year t. We expected the effects of MDN to persist over several years from the time that the nutrients are introduced as the carcasses of spawning adults because of retention of nutrients in the system. Over time, these nutrients are lost from the system, and their effects on the productivity are also expected to diminish. We assumed that the amount of nutrients brought in by salmon is proportional to the escapement. We also assumed that the amount of nutrients retained in the system was proportional to the amount of water retained in the lake annually. Because our assumption was that nutrients were exported from a lake with outflowing water, some of the nutrients derived from the carcasses of spawning salmon would be lost from the system before the nutrients could be used by newly emerged fry during next spring. To account for this loss of nutrients, a half (0.5) year was added to the number of years passed

Table 2. Sockeye salmon smolt mean δ^{15}N values.

Lake	Sample year	No. of samples	Smolt δ^{15}N (‰)
Alaska Peninsula			
Black	2001	32	8.63
	2002	68	9.34
Chignik	1999	6	10.90
	2000	50	10.80
	2001	29	8.99
	2002	20	9.87
Bristol Bay			
Becharof	1999	15	8.13
	2000	24	8.53
	2001	19	7.46
Iliamna	1997	5	8.69
	1999	34	9.36
	2000	50	9.65
	2001	60	9.01
Ugashik	1999	16	9.51
	2000	25	9.61
	2001	20	9.76
Cook Inlet			
Hidden	2004	20	10.79
Tustumena	2004	19	8.57
Upper Russian	1995	20	8.10
Kodiak			
Akalura	1997	5	13.71
Frazer	1997	5	12.60
	2001	20	10.06
Karluk	1994	7	12.76
	1997	12	15.74
	1999	18	13.97
	2001	19	13.21
Red	1994	20	16.05
Spiridon	1997	10	11.29
Prince William Sound			
Coghill	1997	20	9.06
Southeast			
Auke[a]	1997	10	12.57
Chilkat[a]	1996	10	13.00
	1997	10	13.40
Chilkoot[a]	1996	10	9.47
Hugh Smith[a]	1996	10	8.38
McDonald[a]	1997	10	10.99
Redoubt[a]	1996	10	7.72
Speel[a]	1996	10	7.07

[a]Data from Barto 2004.

© 2008 NRC Canada

since the spawning (j). Because MDN input was calculated based on recorded escapement data in our model, MDN input for the first year in the stock–recruitment data would be zero as there was no record of escapement in previous years. MDN input would then show a sudden increase after the first year of the data set. To avoid an artificial abrupt increase in MDN input at the beginning of the recorded escapement data, we used the average escapement in calculating MDN input for each of the 100 years previous to the beginning of the escapement record. The period of 100 years was chosen arbitrarily, just to allow calculated MDN input to reach a stable level. This stabilized MDN input value was used strictly to provide a neutral starting value at the beginning of the stock–recruitment data and was not meant to reflect actual escapement in these 100 years.

One of the lakes in this study, Chignik Lake, was a special case in the sense that another nursery lake, Black Lake, is located upstream. Because Black Lake has a spawning stock distinct from that of Chignik Lake and the fish of the Black stock spawn and die upstream of Chignik Lake, the Chignik stock was expected to receive the benefit of MDN not only from the spawning fish of its own stock, but also from those of the Black stock as well. To reflect this additional MDN input, we estimated the MDN exported from Black Lake (eq. 3), and this quantity was added to the number of spawners in eq. 2 for Chignik Lake.

$$\text{(3)}\qquad \text{MDN export}_{\text{Black},t} = S_{\text{Black},t} - S_{\text{Black},t}e^{(-0.5/\text{RT}_i)}$$

To account for the size of lakes to which nutrients are imported, both MDN input and watershed area were divided by the lake volume. The fraction of watershed area covered by glaciers was used to assess the influence of glaciers to the lake ecosystem. The term "mixing" in the regression equation is a dummy variable (meromictic = 0, holomictic = 1).

All independent variables except the categorical variable ("mixing") were standardized by dividing by the maximum value for each variable to eliminate the effect of scale on the regression and to make the coefficients roughly comparable with one another. The significance of each regression coefficient was assessed using t tests. The importance of each term in the regression was further examined by backward stepwise model selection, using the Akaike information criterion corrected for small sample size (AIC_c) to determine whether explanatory variables should be retained. The AIC_c was calculated as

$$\text{(4)}\qquad \text{AIC}_c = n\ln(\text{RSS}) + \frac{2np}{n-p-1}$$

where RSS is the residual sum of squares from model fitting, n is the number of observations, and p is the number of parameters included in the model.

Stock–recruit models

To test the effect of MDN on the productivity of sockeye salmon stocks, we fit several stock–recruit models to available sockeye escapement–total return data. We assumed density-dependent compensation in the stock–recruit relationship and used the classic Ricker model (eq. 5) as a basis of model development.

$$\text{(5)}\qquad \ln\frac{R_{i,t}}{S_{i,t}} = \ln(\alpha_i) - \frac{S_{i,t}}{\beta_i} + \varepsilon_{i,t}$$

$S_{i,t}$ and $R_{i,t}$ denote sockeye escapement and return, respectively, for stock i in brood year t; α_i is the intrinsic productivity parameter for stock i, β_i is a parameter that determines the carrying capacity for stock i, and $\varepsilon_{i,t}$ is normally distributed random error for stock i in year t.

We modified the Ricker stock–recruit model (eq. 5) to include the effect of MDN from the carcasses of spawning salmon on future salmon production. For parsimony and because it had the largest effect in analyses of smolt isotope data, the only lake characteristic considered in this analysis was the effect of water residence time on MDN retention. The MDN input to the lake was modeled as in eqs. 2–3 and incorporated in stock–recruit models as in eqs. 6–8.

$$\text{(6)}\qquad \ln\frac{R_{i,t}}{S_{i,t}} = \ln(\alpha_{i,t}) - \frac{S_{i,t}}{\beta_{i,t}} + \varepsilon_{i,t}$$

$$\text{(7)}\qquad \alpha_{i,t} = \overline{\alpha}_i + k_{i,\alpha}\sum_{j=0} S_{i,t-j}e^{(-(j+0.5)/\text{RT}_i)}$$

$$\text{(8)}\qquad \beta_{i,t} = \overline{\beta}_i + k_{i,\beta}\sum_{j=0} S_{i,t-j}e^{(-(j+0.5)/\text{RT}_i)}$$

In this model (eqs. 6–8), the productivity of the stock ($\alpha_{i,t}$) and the carrying capacity ($\beta_{i,t}$) are formulated to have two parts: the baseline values ($\overline{\alpha}_i$, $\overline{\beta}_i$) and the effect of MDN ($k_i\sum_{j=0} S_{i,t-j}e^{(-(j+0.5)/\text{RT}_i)}$) additive to these baseline values. The effect of MDN is assumed to be proportional to the amount of MDN retained in the nursery lake. The factors $k_{i,\alpha}$ and $k_{i,\beta}$ scale the effect that the retained MDN have relative to the baseline productivity and carrying capacity. Accordingly, this model form will be referred to as "the $k_{i,\alpha,\beta}$ model." The $k_{i,\alpha}$ and $k_{i,\beta}$ were constrained to be positive.

We also considered models in which MDN only affected either the intrinsic productivity of the stock ($\alpha_{i,t}$ (eq. 9); referred to as "the k_α model") or the carrying capacity ($\beta_{i,t}$ (eq. 10); referred to as "the k_β model").

$$\text{(9)}\qquad \ln\frac{R_{i,t}}{S_{i,t}} = \ln(\alpha_{i,t}) - \frac{S_{i,t}}{\overline{\beta}_i} + \varepsilon_{i,t}$$

$$\text{(10)}\qquad \ln\frac{R_{i,t}}{S_{i,t}} = \ln(\overline{\alpha}_i) - \frac{S_{i,t}}{\beta_{i,t}} + \varepsilon_{i,t}$$

For all of the model forms above, we also examined the effects of climate on the spawner–recruit relationship by including additional parameters (eq. 11). Previous studies have shown that climate has a profound effect on the stock–recruitment relationship in many sockeye salmon stocks (Hare and Francis 1995; Beamish and Bouillon 1993; Adkison et al. 1996). Climatic influences are large enough that they should be included in any model of a long time series of stock and recruitment data. Such climate-related increases in productivity often result in increases in escapement (Bocking and Peterman 1988), which might hinder separation of the effect of climate and the effect brought about by

© 2008 NRC Canada

Table 3. Estimated coefficients, standard errors (SE), and p values for the multiple linear regression analysis on smolt $\delta^{15}N$ values (mean values for each lake-year).

Coefficient	Estimate	SE	t	p
α (intercept)	8.261	0.983	8.407	1.32×10^{-9}
β_1 (MDN input)	7.414	1.204	6.157	6.89×10^{-7}
β_2 (watershed area)	–0.434	0.654	–0.663	0.512
β_3 (glacier)	–0.0225	1.022	–0.022	0.983
β_4 (distance)	–2.409	0.757	–3.181	0.00325
β_5 (mixing)	1.804	0.999	1.804	0.0807

Note: The independent variables (lake characteristics) include MDN·lake volume^{-1}, watershed area·lake volume^{-1}, glacier·watershed area^{-1}, distance from coast, mixing state of lake. All independent variables (except the mixing state – dummy variable) were standardized by dividing by the maximum value for each variable. The regression model was fitted to the data by weighted least squares using the number of observations (smolt samples) in each lake-year as the weights.

MDN input. We attempted to separate the effect of climate from the MDN effect by considering several stocks in close proximity simultaneously. Climate-induced changes are usually similar for stocks in the same region (Peterman et al. 1998). Therefore, it should be possible to distinguish a shared, climate-driven pattern from localized fluctuations in recruitment, including those due to MDN. Accordingly, the effect of climate was modeled as

$$\ln\frac{R_{i,t}}{S_{i,t}} = \ln(\alpha_{i,t}) - \frac{S_{i,t}}{\beta_{i,t}} + c_i E_{r,t} + \varepsilon_{i,t} \quad (11)$$

where $E_{r,t}$ was an environmental influence that affects all stocks in a region r in the same fashion; the magnitude can vary from stock to stock, according to the stock-specific parameter c_i. Models including the parameters c_i and $E_{r,t}$ will be referred to as "the cE model". The environmental effect $E_{r,t}$ was estimated for all years for which stock–recruit data were available for more than one stock within a region. To ensure a consistent climatic effect among stocks in a region, the parameters c_i were constrained to be positive. The sum of the estimates of E was constrained to zero for each region over time, so that $c_i E_{r,t}$ and $\alpha_{i,t}$ would not be confounded.

Parameter estimation and model selection

Model parameters were estimated using a maximum likelihood method by fitting the models to the sockeye escapement and total return data. The models were fit to all stocks in the same region simultaneously. AIC_c was used to select the model forms that best explained the variability in the escapement–return data for each region. AIC_c was calculated using eq. 4.

Calculation of MDN effects on the stock–recruit relationship

To assess the magnitude of the influence of MDN on the productivity of sockeye stocks, we calculated indices of the influence of MDN on productivity (I_α) and carrying capacity (I_β) for each stock based on estimated parameters as follows:

Table 4. Estimated coefficients, standard errors (SE), and p values for the best multiple regression model of smolt $\delta^{15}N$.

Coefficient	Estimate	SE	t	p
α (intercept)	8.228	0.860	9.563	3.61×10^{-11}
β_1 (MDN input)	7.697	1.054	7.300	1.87×10^{-8}
β_4 (distance)	–2.306	0.724	–3.185	0.0031
β_5 (mixing)	1.668	0.923	1.806	0.0797

Note: The best regression model was selected using backward stepwise model selection, based on the Akaike information criterion corrected for small sample size (AIC_c) for each successive model. The independent variables retained were MDN·lake volume^{-1}, distance from coast, mixing state of lake.

$$I_{\alpha,i} = \frac{k_{i,\alpha}\sum_{j=0} S_{i,t-j}e^{(-(j+0.5)/RT_i)}}{\overline{\alpha} + k_{i,\alpha}\sum_{j=0} S_{i,t-j}e^{(-(j+0.5)/RT_i)}} \quad (12)$$

$$I_{\beta,i} = \frac{k_{i,\beta}\sum_{j=0} S_{i,t-j}e^{(-(j+0.5)/RT_i)}}{\overline{\beta} + k_{i,\beta}\sum_{j=0} S_{i,t-j}e^{(-(j+0.5)/RT_i)}} \quad (13)$$

The indices I_α and I_β represent the proportion of the overall productivity and carrying capacity, respectively, due to MDN. I_α and I_β were calculated for each brood year and then averaged for each stock.

We calculated stock–recruit relationships for the stocks where MDN effects were significant. Because of the cumulative effect of past escapement, the intrinsic productivity (α) and the carrying capacity (β) parameters of our MDN models (the $k_{i,\alpha}$, $k_{i,\beta}$ and $k_{i,\alpha,\beta}$ models) will change from one year to the next. To predict the equilibrium recruitment for a particular level of escapement, the selected model was projected 100 years with escapement held constant. This projection was repeated for 100 different levels of escapement between zero and the highest historical escapement for each stock.

Results

Analysis of smolt stable isotope data

The regression coefficients, standard errors, and p values for the multiple regression analysis of the smolt $\delta^{15}N$ data are presented (Table 3). In conformance with our hypothesized mechanisms, the estimated coefficient for MDN·lake volume^{-1} (β_1) was positive, whereas the coefficients for watershed area·lake volume^{-1} (β_2), glacier·watershed area^{-1} (β_3), and distance traveled (β_4) were all negative.

Also in conformance with expectations, the coefficient for mixing (β_5) predicted that the smolt $\delta^{15}N$ would be 1.804‰ higher in holomictic lakes than in meromictic lakes, given the same level of MDN, watershed area, glacier coverage, and distance from the coast. At $\alpha = 0.05$, MDN input and distance traveled were significant. The adjusted R^2 of the model fit was 0.61.

The amount of MDN input had by far the largest estimated effect on smolt $\delta^{15}N$ ($\beta_1 = 7.41$, $p = 6.89 \times 10^{-7}$). Among the lake characteristics examined, the distance from the coast affected the smolt $\delta^{15}N$ most ($\beta_4 = -2.41$, $p =$

© 2008 NRC Canada

Table 5. Multiple and adjusted R^2, residual sum of squares (RSS), and AIC_c for selected multiple regression models.

Model	Parameters included	Multiple R^2	Adjusted R^2	RSS	AIC_c
Null model	α	0	0	203.55	171.74
MDN input	β_1	0.546	0.534	107.53	144.08
Watershed area	β_2	0.056	0.029	189.64	171.93
Glacier cover	β_3	0.047	0.020	193.55	172.28
Distance from coast	β_4	0.058	0.032	190.80	171.83
Mixing state	β_5	0.030	0.003	193.00	172.95
Lowest AIC_c	α, β_1, β_4, β_5	0.658	0.627	75.39	138.55
Full model	α, β_1, β_2, β_3, β_4, β_5	0.662	0.610	72.94	143.87

Table 6. Estimated parameter values of the density-dependent population model without the MDN effect or the climatic effect (the Ricker model), with climatic effect but without the MDN effect (Ricker + climate; the cE model), with the MDN effect but without the climatic effect (the MDN model), and with both the MDN and climatic effects (MDN + climate).

Region	Model	No. of parameters	AIC_c	Percent explained
Alaska Peninsula	Ricker	6	688	47.0
	Ricker + climate	83	772	88.3
	MDN	12	699	47.8
	MDN + climate	89	800	90.1
Bristol Bay	Ricker	6	540	0.8
	Ricker + climate	47	554	68.0
	MDN	12	555	0.8
	MDN + climate	53	591	68.3
Kodiak	Ricker	6	560	25.1
	Ricker + climate	38	571	60.1
	MDN	12	573	25.8
	MDN + climate	38	571	60.1
Prince William Sound – Cook Inlet	Ricker	6	434	25.6
	Ricker + climate	42	496	67.4
	MDN	12	447	26.8
	MDN + climate	42	496	67.4
Southeast	Ricker	8	241	49.9
	Ricker + climate	30	301	74.5
	MDN	16	246	63.9
	MDN + climate	30	301	74.5

0.00325). The mixing state of the lake had the third largest effect ($\beta_5 = 1.80$).

The backward stepwise model selection based on AIC_c retained MDN input, distance traveled, and mixing state of the lake. The regression coefficients, standard errors, and p values were very similar to those from the full model (Table 4). The adjusted R^2 for the reduced model was 0.63 (Table 5).

Population models

The classic Ricker model (i.e., density-dependent compensation) explained about half of the variation in the productivity of Alaska Peninsula and Southeast stocks and about one-quarter of the variation in the productivity of Kodiak and Cook Inlet – Prince William Sound stocks (Table 6). This model explained <1% of the variation in the productivity of Bristol Bay stocks.

The inclusion of an environmental term ($E_{r,t}$) common to all stocks in the same region explained a large amount of variation in the productivity of the sockeye stocks. The increase in total variance explained ranged from 24.5% to 67.2% (Table 6). Especially notable were the Bristol Bay stocks, where the variation explained by the model increased from ≤0.1% to 66.7% for the Egegik stock, from ≤0.1% to 34.7% for the Kvichak stock, and from 1.7% to 90.2% for the Ugashik stock. Despite explaining such large portions of the variation in recruitment, including the environmental effect reduced model performance (resulted in higher AIC_c) compared with models without the environmental effect (Table 6) because of the large number of parameters estimated.

The estimates of the influence of climate (c_i) were comparable among stocks in the same region, except for the Southeast stocks. This suggests that the productivity of the stocks in the Alaska Peninsula, Bristol Bay, Kodiak, and Cook Inlet – Prince William Sound regions indeed have responded to some common environmental factor. In the Southeast region, only one stock (Chilkoot) had a large enough c_i for the estimated environmental effect to make any change in

© 2008 NRC Canada

Table 7. Proportions of the intrinsic productivity (I_α) and carrying capacity (I_β) attributed to MDN based on estimated parameters in comparison to the baseline productivity ($\bar{\alpha}$) and carrying capacity ($\bar{\beta}$).

Region	Lake	I_α	I_β
Alaska Peninsula	Black		0.73
	Chignik		0.26
	Sapsuk		
Bristol Bay	Egegik		
	Kvichak		0.01
	Ugashik		0.66
Kodiak	Frazer		
	Karluk	0.28	
	Red		
Prince William Sound	Coghill		0.18
	Eshamy		>0.99
Cook Inlet	Kasilof		
Southeast	Chilkat		0.51
	Chilkoot	>0.99	
	Redoubt		0.11
	Speel		0.64

Note: The values less than 0.001 were left blank.

model fit; the resultant estimates of the environmental factor (E_t) were thus stock-specific and not useful for separating environmental fluctuations from the influence of MDN.

Including the effect of MDN ($k_{\alpha,\beta}$ and $k_{\alpha,\beta}$) in addition to the density-dependent compensation in the model resulted in only small increases in the variation explained by the model, except for the Southeast stocks for which an additional 14% of the variation was explained (Table 6). When compared to the classic Ricker model, the inclusion of the MDN terms did not significantly improve the model in any region. When the model with MDN effects was compared with the model with environmental effects, it performed more poorly (higher AIC_c) for the Bristol Bay stocks and Kodiak stocks, despite large differences in the number of parameters estimated. MDN effects also did not explain much more of the variation in recruitment when added to the model that included environmental effects, except, again, for the Southeast stocks.

We calculated the proportion of the intrinsic productivity and the carrying capacity attributed to MDN (I_α and I_β) from the estimated parameters for the $k_{\alpha,\beta}$ model with climatic effects, irrespective of whether they were found significant based on our AIC_c criterion. These proportions ranged from <0.1% to, in some extreme cases, nearly 100% (Table 7). For most of the stocks, the effect of MDN was restricted to their carrying capacity β, while only two of the stocks (Karluk, Chilkoot) showed some sign of an MDN effect on intrinsic productivity α. The influences of MDN were estimated to be especially large for the Chilkoot (on intrinsic productivity, α), Black, Ugashik, Eshamy, Chilkat, and Speel (on carrying capacity, β) stocks. No strong relationship was found between the magnitude of MDN influence and any of the lake and watershed characteristics examined. Contrary to our original hypothesis, among the lakes that showed strong MDN influences were two of the fastest flushing lakes in this study, Black (residence time = 0.058 years) and Speel (residence time = 0.075 years).

Except for the $k_{\alpha,\beta}$ models in the Bristol Bay and Kodiak regions, environmental effects were never found to be statistically significant. However, the purpose of including these effects in our model was to eliminate the possible confounding of climate-driven changes in productivity (e.g., favorable climate results in increased escapements and productivity) with the effects of MDN. For this reason, we more closely examined the two best-supported models for each region that included climatic effects. Among the models selected were the k_β and the $k_{\alpha,\beta}$ models for the Black stock (Alaska Peninsula), the k_β model for the Ugashik stock (Bristol Bay), the k_α model for the Karluk stock (Kodiak), the k_β model for the Eshamy stock (Prince William Sound), and the k_β and $k_{\alpha,\beta}$ models for the Speel stock (Southeast). The models selected roughly corresponded to those in which the largest estimated proportions of the intrinsic productivity and carrying capacity were attributed to MDN (Table 7).

The equilibrium stock–recruit relationships for these MDN-influenced models are shown along with the stock–recruit relationship based on the climate-influenced Ricker model (the *cE* model; Figs. 1*a*–1*e*) without the MDN effect. For the Black and Speel stocks, k_β model returns were predicted to increase more rapidly than *cE* model returns and reach the maximum at lower levels of escapement (Figs. 1*a*, 1*e*). For these two stocks, the maximum sustainable yields (MSY) predicted by the k_β models were higher and the escapements that produced the MSY (S_{MSY}) were lower than those predicted by the *cE* model (Table 8). Carrying capacities (β) were lower than those predicted by the *cE* model.

The effects of MDN on the Karluk stock–recruitment relationship showed opposite changes to those estimated for the Black and Speel stocks (Fig. 1*c*). At low escapement levels, the predicted returns from the k_α model were slightly lower than those predicted from the *cE* model, but became higher at high levels of escapement. The MSY predicted by the k_α model was lower than that predicted by the *cE* model, but the carrying capacity predicted by the k_α model was higher than that predicted by the *cE* model (Table 8).

For the Ugashik and Eshamy stocks, the predicted returns from the k_β model were lower than those from the *cE* model at low levels of escapement (Figs. 1*b*, 1*d*). However, the carrying capacities for these two stocks continued to increase without reaching equilibrium at high spawner densities, and so did the predicted returns. Because the predicted returns never decreased, MSYs were not calculated for these two stocks.

Discussion

Smolt isotope analysis

The results of smolt nitrogen stable isotope analysis indicated that sockeye escapement and water residence time (explaining 53% of the variance in smolt $\delta^{15}N$ values) are the most important determinants of the availability of MDN to juvenile sockeye among the variables examined in this study. The estimated coefficient for MDN input (β_1) of 7.41 implies that input of 3.97 adult sockeye per 10^3 m^3 of lake water (the maximum MDN input value in the data set, recorded from Red Lake, Kodiak) would increase smolt $\delta^{15}N$ value by 7.41‰.

© 2008 NRC Canada

Fig. 1. Simulated stock–recruit relationships using the marine-derived nutrient (MDN) models selected by the Akaike information criteria (AIC_c) (solid line) for (*a*) Black Lake (the k_3 model), (*b*) Ugashik Lake (the k_2 model), (*c*) Karluk Lake (the k_{12} model), (*d*) Eshamy Lake (the k_2 model), and (*e*) Speel Lake (the k_3 model). The MDN models were run for 100 years at each escapement level using estimated parameters to obtain an equilibrium return. The simulations using the models including the environmental effect but without the MDN effect (the cE models) are also shown by asterisks (*). Open circles are observed returns. Broken line is the 1:1 replacement line.

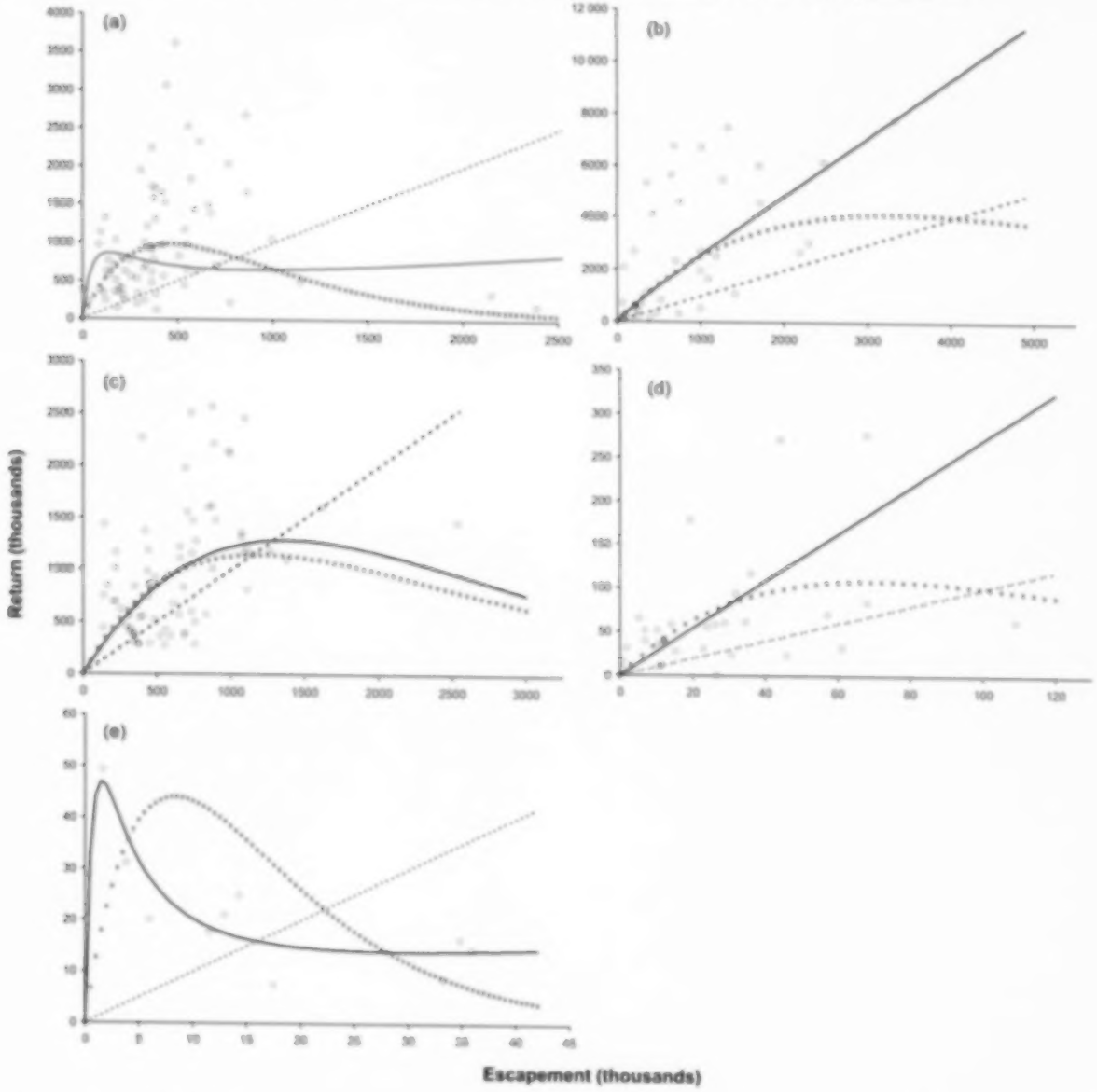

Although not explicit in the regression equation, the water residence time of a nursery lake also had a strong influence on the MDN availability to juvenile salmon. Because our assumption was that MDN imported to the system would be exported with the water leaving the system, we also expected a positive relationship between residence time and $\delta^{15}N$ of smolts. However, because residence time is related directly to lake volume (residence time = lake volume·lake discharge^{-1}) and indirectly to watershed area (lake discharge = watershed area·discharge estimate per unit watershed area), the relationship between residence time and the MDN availability was unclear. Furthermore, moderate to high correlations between residence time and other potential covariates made it necessary to exclude residence time as a covariate in the multiple regression analysis. Instead, the effect of residence time was included in the estimates of MDN input, influencing the persistence of nutrients in the system as described in eq. 2.

© 2008 NRC Canada

Table 8. MSY, S_{MSY}, and carrying capacity (β) for the equilibrium stock–recruit relationship.

Stock	Model	MSY	S_{MSY}	Maximum return	β
Black	k_3	765 934	90 259	866 601	113 842
	cE	599 844	307 022	977 275	464 168
Ugashik	k_3	—	—	—	—
	cE	1 748 139	1 699 476	4 153 167	3 351 644
Karluk	k_3	348 660	601 642	1 288 198	1 372 307
	cE	359 980	501 046	1 150 882	1 198 440
Eshamy	k_3	—	—	—	—
	cE	55 129	40 328	108 332	69 829
Speel	k_3	45 509	1 491	47 038	1 568
	cE	36 467	7 002	44 107	8 347

To assess the effects of residence time on MDN availability, we re-ran our regression analyses, substituting sockeye escapement a year previous to the smolt sampling for the MDN input variable in the regression equation, i.e., we did not account for nutrients from escapements from more than one previous year, which should be important in lakes with long water residence times. Although the original regression model explained 66% of variance in the data, the model with escapement limited to the previous year explained only 37% of variance. This result suggests that the water residence time of lakes positively affects MDN availability to juvenile salmon and that our assumption that hydrology affects the MDN contribution from previous years' spawners was reasonable.

Distance from the coast had the second largest effect on smolt δ^{15}N. The estimated coefficient β_3 of –2.41 indicates that smolt δ^{15}N value decreased by 2.41‰ for a distance of 147 km, the distance to the nursery lake located farthest from the point of freshwater entry among the lakes included in this study (Upper Russian Lake). This supported our assumption that having ceased feeding upon entering freshwater, salmon would continually lose nutrients in their bodies through metabolic activity during their upriver migration. Therefore, the longer they have to migrate, the less MDN they bring into their spawning and nursery habitats for their offspring. However, there are other possible explanations for this relationship. Some sockeye spawn downstream of the primary nursery lake in the drainage, and the fry later migrate upstream to the lake where they rear. In such a case, the estimate of MDN based on escapement would overestimate the MDN input to the nursery lake. The Upper Russian Lake sockeye stock is likely an example of this factor. Most adults have been observed to spawn downstream of Upper Russian Lake, and this seems to be reflected in the relatively low δ^{15}N value in these smolts. The amount and use of suitable spawning habitat both downstream and upstream of nursery lakes needs to be considered when assessing the MDN input to the lake based on escapement, although this information is often lacking. Another potential confounding factor is differences in growth rates or age at return among systems, which might result in differences in body mass among stocks. The age composition of spawning adult varies among populations (Burgner 1991), and the fish maturing at an older age tend to be larger than the ones maturing younger. For example, the average mid-eye–fork lengths of male sockeye salmon in Bristol Bay from 1958 through 2002 were 512.9, 527.1, 582.1, and 586.3 mm for 1.2, 2.2, 1.3, and 2.3 fish, respectively (Quinn 2004).

The third most important factor affecting smolt δ^{15}N values was whether lake water completely mixed; smolt δ^{15}N was estimated to be 1.80‰ higher in the holomictic lakes than in the meromictic lakes.

As expected, the estimated effect of watershed area per volume of lake (β_2) was negative, indicating that smolt δ^{15}N decreases with watershed area, a proxy for terrestrial input of nutrients. However, the small coefficient and large standard error made the estimate insignificant at $\alpha = 0.05$. The relatively small effect of watershed area on smolt δ^{15}N might mean that the nutrient export from watershed is not controlled by watershed area per se; biologic, climatologic, and geologic processes within watersheds have a large influence on nutrient export through factors such as soil composition and precipitation, which may vary significantly among watersheds.

As expected, the estimated effect of the fraction of the watershed covered by glaciers was negative, but the effect was also found to be statistically insignificant. This was most likely caused by the large variability in smolt δ^{15}N among watersheds with little glacial influence. Among the 21 lakes included in the multiple regression, 12 lakes do not have glaciers within their watersheds. Another six lakes have between 0.2% and 5% glacier coverage in their watersheds, and only three lakes (Chilkoot, Coghill, and Tustumena) have glacier coverage greater than 19% of watershed. Although the smolt δ^{15}N content in the three lakes with high glacier coverage were invariably low (9.03‰ ± 0.90‰, mean ± 2σ), the smolt δ^{15}N for the rest of lakes were highly variable (10.50‰ ± 4.74‰), although on average higher than those from the highly glaciated watersheds.

There can be considerable variability in the nitrogen isotope composition of zooplankton among species, seasons, and lakes (Matthews and Mazumder 2005). Such variability clearly occurs in systems without salmon, and therefore factors that affect baseline δ^{15}N levels may not have been recognized by our analysis. Although the isotopic signals in our smolt samples varied as we would expect, given the interaction of salmon-derived nutrients and hydrology, it is possible that the hydrology itself could be responsible for the patterns

© 2008 NRC Canada

Fig. 2. Simulated ln(*R*/*S*) for (*a*) Ugashik, (*b*) Karluk, and (*c*) Eshamy stocks using the marine-derived nutrient (MDN) models selected by the Akaike information criteria (AIC_c) (solid line). The MDN models were run for 100 years at each escapement level using estimated parameters to obtain an equilibrium ln(*R*/*S*). The simulated ln(*R*/*S*) using the models including the environmental effect but without the MDN effect (the *cE* models) are also shown by asterisks (*). Open circles are observed ln(*R*/*S*) for each stock. Solid circles are residuals obtained by subtracting the product of the parameters c_i and $E_{c,i}$ estimated for the MDN models from the observed ln(*R*/*S*).

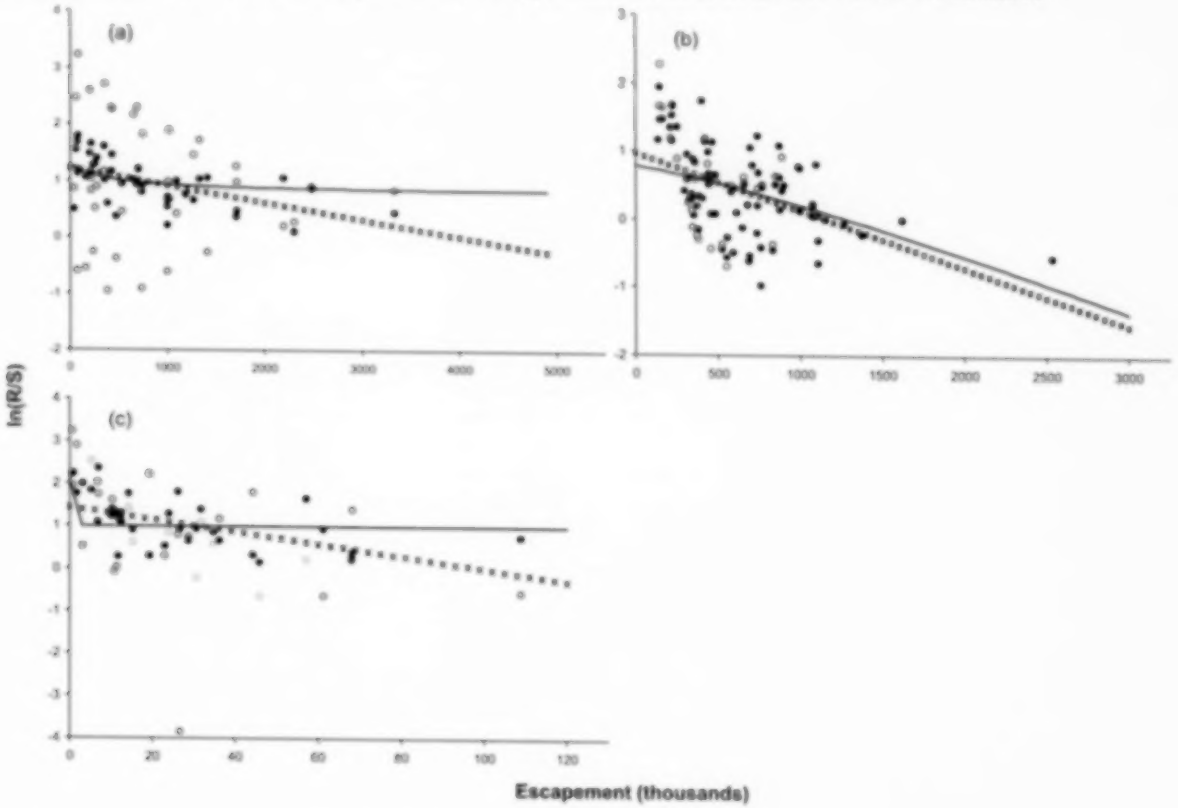

that we observed. However, analysis of biota in non-salmon lakes, though somewhat limited in extent, indicates lower $\delta^{15}N$ levels in non-salmon lakes relative to nearby salmon lakes of similar hydrologic conditions (Satterfield and Finney 2002; Gregory-Eaves et al. 2007). The trophic level of zooplankton preyed on by juvenile sockeye salmon will affect their $\delta^{15}N$ signature. We have not assessed the importance of this factor in our analysis because data on juvenile sockeye stomach contents are not systematically available. However, the range in smolt $\delta^{15}N$ that we observed across systems is too large to be explained predominantly by changes in trophic level of feeding.

Population models

Although the smolt isotope evidence suggests that MDN imported to freshwater ecosystems by adult salmon are used by juvenile sockeye salmon, it is still not clear whether the addition of MDN to sockeye fry rearing habitats results in increased productivity of stocks. Our stock–recruit modeling suggested that the variation in stock productivity was driven mostly by the environment, rather than by MDN input to the sockeye nursery lakes. The exception to this was the Southeast stocks for which the MDN input also explained a large portion of variation in the productivity. However, this might have been due to lack of a common pattern in the productivity among the Southeast stocks. If the variation due to environmental factors was not properly accounted for, some of the variation in the productivity due to environmental factors could have been incorrectly attributed to the MDN effect. The converse could be true for the other regional groups, i.e., that the effects of MDN were incorrectly assigned to the environmental factor. Because of the practical difficulties that managers face in attaining a target escapement goal, favorable environmental conditions that lead to higher returns will often result in a high escapement (Bocking and Peterman 1988), and the benefits of the resultant MDN could be attributed to the environment. However, we found little evidence of MDN effects on the stock–recruitment relationships even when climatic effects were not included in the models.

Surprisingly, the MDN effects were not estimated to be particularly important for the productivity of the stocks from nursery lakes with characteristics favoring the transfer of nutrients from adult carcasses to juvenile salmon. For example, smolt isotope analysis indicated that a long water residence time favors MDN transfer from adult to juvenile

© 2008 NRC Canada

salmon. However, two of the lakes, Black and Speel, that showed particularly large effects of MDN on the carrying capacity parameter have two of the fastest flushing rates among our study lakes.

Model selection results suggest that the MDN effects in the stock–recruit relationship were significant for one of the stocks studied in each region. Also, the proportions of the intrinsic productivity (α) and (or) carrying capacity (β) attributed to MDN were large for the stocks with significant MDN terms (either k_α or k_β or both). However, these models implied stock–recruitment relationships with counterintuitive management implications. For example, the models predicted a higher maximum yield and a higher maximum return for the Black and Speel stocks, respectively, compared with the prediction by the *cE* model. However, these high yields and returns occurred at low escapement levels, suggesting that MDN effects imply lower escapement goals. These results are undoubtedly spurious.

Including MDN terms resulted in an entirely different effect on the estimated stock–recruitment relationship for Ugashik and Eshamy stocks, as the predicted returns kept increasing with increasing escapement. Because regional environmental fluctuations explained so much variation in the data for these two stocks, there was very little variation in $\ln(R/S)$ left unexplained. As a consequence, the residuals show only a slight relationship to the number of spawners (Figs. 2*a*, 2*c*) except at very low levels of escapement. It is possible that compensatory density dependence was masked by the environmental variation, leading to an inability to estimate the limits to recruitment.

In contrast, the plot of $\ln(R/S)$ against escapement for the Karluk stock (Fig. 2*b*) shows high variability even after the variation due to the regional environmental fluctuations is removed. This resulted in a more distinct slope, which translated to a well-defined density-dependent compensation. Additional variation in the productivity of the Karluk stock explained by including a MDN effect was also small (1.9%). However, the AIC_c suggested that inclusion of the k_α parameter was important in explaining the Karluk stock–recruitment data.

The inability of our models to detect systematic influences of MDN on productivity could suggest that overall effects are minor and not felt in a regular fashion. Alternatively, it may indicate that the way that we chose to model MDN input to lakes did not accurately capture the mechanisms by which MDN is imported and retained in lakes. However, MDN input modeled the same way explained a large portion of variation in smolt $\delta^{15}N$, suggesting that our estimates of MDN input were reasonable.

Stock–recruitment data may be intrinsically ill suited for detecting the influence of MDN. Salmon carcasses would be expected to contribute most of their nutrients in the year immediately following spawning. However, the effects of parents on survival of their own offspring are already included in conventional stock–recruit relationships; the distinct effects of MDN can only be detected when they persist into subsequent years, where they undoubtedly would be weaker. MDN effects would be most distinguishable in slowly flushing lakes where historical spawner abundances included several multiyear periods of low escapements separated by multiple years of high escapements. In addition, although MDN effects should affect the freshwater stage of salmon's life, numerous other factors influence whole life-cycle survival, which is highly variable in salmon. For all of these reasons, the power to detect even fairly strong effects of MDN in the stock–recruitment relationship may be low.

Our study showed that the nutrients released from carcasses of adult salmon are incorporated into lentic ecosystems of sockeye nursery lakes and can make an important contribution to the nutrition of juvenile salmon. This contribution is highly variable among sockeye lake systems and is strongly correlated with the relative magnitude of escapement. In addition, hydrological conditions of the nursery lakes such as water residence time, distance from the coast, and whether the water column mixes were found to affect the availability of MDN to juvenile salmon. Conditions under which juvenile salmon benefit most from MDN input from spawning sockeye are lakes with long water residence times, short distances from the coast, and water columns that undergo complete mixing annually.

Watershed area and glacial coverage of watershed were not found to significantly affect the content of MDN in juvenile salmon, although the estimated effects were in the expected direction (i.e., reduction in smolt $\delta^{15}N$). We speculate that the biology, geology, and climate of watersheds complicate estimating terrestrial nutrient import into lakes based on watershed area.

Although there was strong evidence for MDN influences on sockeye smolt and strong evidence that hydrological characteristics of nursery lakes affected the strength of this effect, we did not find much evidence in our stock–recruitment analyses to support our hypothesis that increases in MDN input to sockeye nursery lakes will result in increased productivity of sockeye stocks. The analysis of stock–recruit data for 16 Alaska sockeye stocks suggests that environmental conditions have a much larger influence on sockeye stock productivity than MDN. However, stock–recruitment data may be poorly suited to detecting the influence of MDN on productivity, and separating the direct effect of environmental change and nutrient feedbacks resulting from environmental change is difficult.

A more fruitful approach in estimating the effects of MDN might be to investigate more directly the mechanisms by which MDN influences stock productivity. The MDN concentration in smolts should be compared with smolt growth, age at emigration to the ocean, total biomass of smolt produced, and subsequent marine survival. Additional fruitful areas of research would be further investigations of the transfer of MDN through the limnetic ecosystem and studies on how MDN are recycled and retained in sockeye nurseries, including watersheds and hyporheic zones.

Acknowledgements

We thank the Alaska Department of Fish and Game (ADF&G) Commercial Fisheries Division, especially the following personnel for providing sockeye escapement and return data: Randy Bachman, Lowell Fair, Dave Gordon, Steve Heinl, Kathleen Jensen, Jim McCullough, Rick Merizon, Steven Moffitt, Gary Timothy, Mark Willette, and Mark Witteveen. We also thank Jerry Taylor of NOAA Auke Bay Laboratories for providing the Auke Lake sock-

© 2008 NRC Canada

eye stock data. Smolt stable isotope data was compiled with the help of many collaborators. We especially thank Dave Barto (ADF&G) for providing stable isotope data for smolts from Southeast Alaska and Trent Dodson (Cook Inlet Aquaculture Association), Steve Honnold (ADF&G), Jim Larson (US Fish and Wildlife Service), and Ole Mathisen (School of Fisheries and Ocean Sciences, University of Alaska Fairbanks) for providing smolts for this study. This publication is the result of research sponsored by Alaska Sea Grant with funds from the National Oceanic and Atmospheric Administration Office of Sea Grant, Department of Commerce, under grant no. NA 16RG2321 (project no. R/31–08), and from the University of Alaska with funds appropriated by the state. This study was also funded by School of Fisheries and Ocean Sciences, University of Alaska Fairbanks.

References

Adkison, M.D., Peterman, R.M., Lapointe, M.F., Gillis, D.M., and Korman, J. 1996. Alternative models of climatic effects on sockeye salmon (*Oncorhynchus nerka*) production in Bristol Bay, Alaska, and the Fraser River, British Columbia. Fish. Oceanogr. **5**: 137–152. doi:10.1111/j.1365-2419.1996.tb00113.x.

Barto, D.L. 2004. Assessing the production of sockeye salmon (*Oncorhynchus nerka*) at Chilkat Lake, southeast Alaska, using current trophic conditions and the paleolimnologic sediment record. M.Sc. thesis, School of Fisheries and Ocean Sciences, University of Alaska Fairbanks, Fairbanks, Alaska.

Bax, N.J. 1983. Early marine mortality of marked juvenile chum salmon (*Oncorhynchus keta*) released in Hood Canal, Puget Sound, Washington, in 1980. Can. J. Fish. Aquat. Sci. **40**: 426–435. doi:10.1139/f83-061.

Beamish, R.J., and Bouillon, D.R. 1993. Pacific salmon production trends in relation to climate. Can. J. Fish. Aquat. Sci. **50**: 1002–1016. doi:10.1139/f93-116.

Bilby, R.E., Fransen, B.R., and Bisson, P.A. 1996. Incorporation of nitrogen and carbon from spawning coho salmon into the trophic system of small streams: evidence from stable isotopes. Can. J. Fish. Aquat. Sci. **53**: 164–173. doi:10.1139/cjfas-53-1-164.

Bocking, R.C., and Peterman, R.M. 1988. Preseason forecasts of sockeye salmon (*Oncorhynchus nerka*): comparison of methods and economic considerations. Can. J. Fish. Aquat. Sci. **45**: 1346–1354. doi:10.1139/f88-158.

Bradford, M.J. 1995. Comparative review of Pacific salmon survival rates. Can. J. Fish. Aquat. Sci. **52**: 1327–1338. doi:10.1139/f95-129.

Burgner, R.L. 1991. Life history of sockeye salmon (*Oncorhynchus nerka*). *In* Pacific salmon: life histories. *Edited by* C. Groot and L. Margolis. UBC Press, Vancouver, B.C. pp. 1–117.

Edmundson, J.A., Kyle, G.B., and Willette, M. 1992. Limnological and fisheries assessment of Coghill Lake relative to sockeye salmon (*Oncorhynchus nerka*) production and lake fertilization. Report No. 118, Alaska Department of Fish and Game, Division of Fisheries Rehabilitation, Enhancement, and Development, Juneau, Alaska.

Finney, B.P. 1998. Long-term variability of Alaskan sockeye salmon abundances determined by analysis of sediment cores. N. Pac. Anadr. Fish. Comm. Bull. **1**: 388–395.

Finney, B.P., Gregory-Eaves, I., Sweetman, J., Douglas, M.S.V., and Smol, J. 2000. Impacts of climatic change and fishing on Pacific salmon abundance over the past 300 years. Science (Washington, D.C.), **290**: 795–799. doi:10.1126/science.290.5492.795. PMID:11052941.

Fisher, J.P., and Pearcy, W.G. 1988. Movements of coho, *Oncorhynchus kisutch*, and chinook, *Oncorhynchus tshawytscha*, salmon tagged at sea off Oregon, Washington, and Vancouver Island during the summers 1982–1985. Fish. Bull. (U.S.), **85**: 819–826.

Geiger, H.J. 2003. Sockeye salmon stock status and escapement goal for Redoubt Lake in southeast Alaska. Regional Information Report No. 1J03–01, Alaska Department of Fish and Game, Division of Commercial Fisheries, Juneau, Alaska.

Geiger, H.J., Zadina, T.P., and Heinl, S.C. 2003. Sockeye salmon stock status and escapement goal for Hugh Smith Lake in southeast Alaska. Regional Information Report No. 1J03–05, Alaska Department of Fish and Game, Division of Commercial Fisheries, Juneau, Alaska.

Gregory-Eaves, I., Demers, M.J., Kimpe, L., Krummel, E.M., Macdonald, R.W., Finney, B.P., and Blais, J.M. 2007. Tracing salmon-derived nutrients and contaminants in freshwater food webs across a pronounced spawner density gradient. Environ. Toxicol. Chem. **26**: 1100–1108. doi:10.1897/06-402R.1. PMID:17571673.

Hare, S.R., and Francis, R.C. 1995. Climate change and salmon production in the northeast Pacific Ocean. *In* Climate change and northern fish populations. *Edited by* R.J. Beamish. Can. Spec. Publ. Fish. Aquat. Sci. No. 121. pp. 357–372.

Healey, M.C. 1982. Juvenile Pacific salmon in estuaries: the life support system. *In* Estuarine comparisons. *Edited by* V.S. Kennedy. Academic Press, New York. pp. 315–341.

Hendry, A.P., and Berg, O.K. 1999. Secondary sexual characters, energy use, senescence, and the cost of reproduction in sockeye salmon. Can. J. Zool. **77**: 1663–1675. doi:10.1139/cjz-77-11-1663.

Idler, D.R., and Clemens, W.A. 1959. The energy expenditures of Fraser River sockeye salmon during the spawning migration to Chilko and Stuart lakes. Int. Pac. Salmon. Fish. Comm. Prog. Rep. No. 6, Pacific Salmon Commission, Vancouver, B.C.

Kalff, J. 2002. Limnology. Prentice-Hall, Inc., Upper Saddle River, N.J.

Kline, T.C., Jr., Goering, J.J., Mathisen, O.A., Poe, P.H., and Parker, P.L. 1990. Recycling of elements transported upstream by runs of Pacific salmon: I. δ^{15}N and δ^{13}C evidence in Sashin Creek, southeastern Alaska. Can. J. Fish. Aquat. Sci. **47**: 136–144. doi:10.1139/f90-014.

Kline, T.C., Goering, J.J., Mathisen, O.A., Poe, P.H., Parker, P.L., and Scalan, R.S. 1993. Recycling of elements transported upstream by runs of Pacific salmon: II. δ^{15}N and δ^{13}C evidence in the Kvichak River watershed, Bristol Bay, southwestern Alaska. Can. J. Fish. Aquat. Sci. **50**: 2350–2365. doi:10.1139/f93-259.

Koenings, J.P., and Burkett, R.D. 1987. Population characteristics of sockeye salmon (*Oncorhynchus nerka*) smolts relative to temperature regimes, euphotic volume, fry density, and forage base within Alaskan lakes. *In* Sockeye salmon (*Oncorhynchus nerka*) population biology and future management. *Edited by* H.D. Smith, L. Margolis, and C.C. Wood. Can. Spec. Publ. Fish. Aquat. Sci. No. 96. pp. 216–234.

Koenings, J.P., Geiger, H.J., and Hasbrouck, J.J. 1993. Smolt-to-adult survival patterns of sockeye salmon (*Oncorhynchus nerka*): effects of smolt length and geographic latitude when entering the sea. Can. J. Fish. Aquat. Sci. **50**: 600–611. doi:10.1139/f93-069.

Matthews, B., and Mazumder, A. 2005. Consequences of large temporal variability of zooplankton δ^{15}N for modeling fish trophic position and variation. Limnol. Oceanogr. **50**: 1404–1414.

National Center for Earth Resources Observations and Science. 2004. National elevation database [online]. Available from

© 2008 NRC Canada

http://eros.usgs.gov/products/elevation/ned.html [accessed 12 December 2004].

Pearcy, W.G. 1992. Ocean ecology of North Pacific salmonids. University of Washington Press, Seattle, Wash.

Peterman, R.M., Pyper, B.J., Lapointe, M.F., Adkison, M.D., and Walters, C.J. 1998. Patterns of covariation in survival rates of British Columbia and Alaskan sockeye salmon (*Oncorhynchus nerka*) stocks. Can. J. Fish. Aquat. Sci. **55**: 2503–2517. doi:10.1139/cjfas-55-11-2503.

Quinn, T.P. 2004. The behavior and ecology of Pacific salmon and trout. University of Washington Press, Seattle, Wash.

Satterfield, F.R., and Finney, B.P. 2002. Stable isotope analysis of Pacific salmon: insight into trophic status and oceanographic conditions over the last 30 years. Prog. Oceanogr. **53**: 231–246. doi:10.1016/S0079-6611(02)00032-0.

Schmidt, D.C., Carlson, S.R., Kyle, G.B., and Finney, B.P. 1998. Influence of carcass-derived nutrients on sockeye salmon productivity of Karluk Lake, Alaska: importance of the assessment of an escapement goal. N. Am. J. Fish. Manage. **18**: 743–761. doi:10.1577/1548-8675(1998)018<0743:IOCDNO>2.0.CO;2.

Stockner, J.G. 1987. Lake fertilization: the enrichment cycle and lake sockeye salmon (*Oncorhynchus nerka*) production. *In* Sockeye salmon (*Oncorhynchus nerka*) population biology and future management. *Edited by* H.D. Smith, L. Margolis, and C.C. Wood. Can. Spec. Publ. Fish. Aquat. Sci. No. 96. pp. 198–215.

Stockner, J.G., Rydin, E., and Hyenstrand, P. 2000. Cultural oligotrophication: causes and consequences for fisheries resources. Fisheries, **25**: 7–14. doi:10.1577/1548-8446(2000)025<0007:CO>2.0.CO;2.

US Geological Survey. 2004*a*. National hydrography dataset [online]. Available from http://nhd.usgs.gov/index.html [accessed 12 December 2004].

US Geological Survey. 2004*b*. Calendar year streamflow statistics for the nation [online]. Available from http://nwis.waterdata.usgs.gov/nwis/annual.html [accessed 21 October 2004].

Welch, D.W., and Parsons, T.R. 1993. $\delta^{13}C$ and $\delta^{15}N$ values as indicators of trophic position and competitive overlap for Pacific salmon (*Oncorhynchus* spp.). Fish. Oceanogr. **2**: 11–23. doi:10.1111/j.1365-2419.1993.tb00008.x.

© 2008 NRC Canada

Seasonal variation in size-dependent survival of juvenile Atlantic salmon (*Salmo salar*): performance of multistate capture–mark–recapture models

Benjamin H. Letcher and Gregg E. Horton

Abstract: We estimated the magnitude and shape of size-dependent survival (SDS) across multiple sampling intervals for two cohorts of stream-dwelling Atlantic salmon (*Salmo salar*) juveniles using multistate capture–mark–recapture (CMR) models. Simulations designed to test the effectiveness of multistate models for detecting SDS in our system indicated that error in SDS estimates was low and that both time-invariant and time-varying SDS could be detected with sample sizes of >250, average survival of >0.6, and average probability of capture of >0.6, except for cases of very strong SDS. In the field ($N \sim 750$, survival 0.6–0.8 among sampling intervals, probability of capture 0.6–0.8 among sampling occasions), about one-third of the sampling intervals showed evidence of SDS, with poorer survival of larger fish during the age-2+ autumn and quadratic survival (opposite direction between cohorts) during age-1+ spring. The varying magnitude and shape of SDS among sampling intervals suggest a potential mechanism for the maintenance of the very wide observed size distributions. Estimating SDS using multistate CMR models appears complementary to established approaches, can provide estimates with low error, and can be used to detect intermittent SDS.

Résumé : Nous avons estimé l'importance de la survie dépendante de la taille (SDS) et la forme de la courbe correspondante sur une gamme étendue d'intervalles d'échantillonnage chez deux cohortes de jeunes saumons atlantiques (*Salmo salar*) vivant dans des cours d'eau à l'aide de modèles multi-états de capture–marquage–recapture (CMR). Des simulations destinées à vérifier l'efficacité des modèles multi-états pour détecter la SDS dans notre système indiquent que l'erreur dans les estimations de SDS est faible et qu'il est possible de détecter tant la SDS invariable dans le temps que la SDS variable dans le temps avec des tailles d'échantillons > 250, une survie moyenne > 0,6 et une probabilité moyenne de capture > 0,6, excepté lorsque SDS est très élevée. En nature ($N \sim 750$, survie de 0,6–0,8 dans les divers intervalles d'échantillonnage, probabilité de capture 0,6–0,8 dans les différentes occasions d'échantillonnage), environ un tiers des intervalles d'échantillonnage montrent des signes de SDS, avec une survie moindre des poissons plus grands durant l'automne de l'âge 2+ et une survie quadratique (de direction opposée dans les deux cohortes) durant le printemps de l'âge 1+. La variation de l'importance de SDS et de la forme de la courbe parmi les intervalles d'échantillonnage laisse croire à l'existence d'un mécanisme potentiel pour le maintien des distributions très étendues de tailles observées. La détermination de SDS par les modèles multi-états CMR semble être complémentaire aux méthodes établies, elle fournit des estimations avec une erreur faible et elle peut servir à détecter une SDS intermittente.

[Traduit par la Rédaction]

Introduction

Many ecological and evolutionary processes depend on body size (e.g., Roff 1992), and the relationship between body size and survival, in particular, has been the focus of a large number of studies (e.g., Cooch 2002; Blums et al. 2005). Typically, individuals with an observable body size are tagged and released for a set time interval. At the end of the interval, variation in recaptures among sizes can indicate size-dependent survival (SDS) or selection (Arnold and Wade 1984; Schluter 1988; Brodie et al. 1995), as long as there is no size dependency in probability of recapture (Zabel et al. 2005) or emigration (Kingsolver and Smith 1995; Letcher et al. 2005). SDS over a single interval has been estimated for many systems (Kingsolver et al. 2001), but single-interval estimates may not be generalizable if the direction of SDS changes over time (Preziosi and Fairbairn 2000) or if there is significant change in body size rank among individuals over time (Pfister and Stevens 2002).

Further complicating multiple-interval estimates of SDS are sparse capture histories of growing individuals. In certain rare cases (e.g., Clutton-Brock et al. 2002; Coulson et al. 2005), probabilities of observation are close to one, so that a complete longitudinal accounting of the size of survivors is possible. In this case, there will be no (or very few) missing observations. Missing observations will introduce little bias in SDS estimates when individuals do not grow

Received 14 September 2007. Accepted 26 February 2008. Published on the NRC Research Press Web site at cjfas.nrc.ca on 16 July 2008.
J20172

B.H. Letcher[1] and G.E. Horton.[2] S.O. Conte Anadromous Fish Research Center, US Geological Survey Leetown Science Center, One Migratory Way, Turners Falls, MA 01376, USA.

[1]Corresponding author (e-mail: ben_letcher@usgs.gov).
[2]Present address: 6489 Dry Creek Road, Healdsburg, CA 95448, USA.

 doi:10.1139/F08-083 © 2008 NRC Canada

during the period of observation, but this is rarely the case for field studies. More often, studies encompass enough size change, both over time across individuals and in relative rank among individuals, that a single estimate of initial or average size will not adequately describe size-dependent dynamics. Suggested techniques for interpolating missing values in a capture–mark–recapture (CMR) framework (Bonner and Schwarz 2004) will be effective when there are few missing values, but not for the more common case of a large number of missing values. Thus, for reliable, multiple-interval estimates of SDS in settings common to many field studies, we need an approach that can account for growing individuals with probabilities of capture substantially less than one.

CMR models that are based on the Cormack–Jolly–Seber (CJS) model offer a way to address this problem by providing methods to test hypotheses about SDS while accounting for individual heterogeneity in growth and probability of capture (Lebreton et al. 1992; Brownie et al. 1993). Investigators have used CMR modeling to estimate differences in survival for individuals with fixed, time-invariant traits (e.g., sex (Couch 2002) and size at one occasion (Zabel and Achord 2004)), as well as for individuals with time-varying traits (e.g., location (Lebreton et al. 2003)). However, although time-invariant individual traits (e.g., sex) are often modeled as covariates in survival analyses (Covas et al. 2002), time-varying traits can only be analyzed using covariates in situations in which there are no missing observations because covariate models accommodating missing observations (sparse capture histories) are not currently available. Instead, time-varying traits can be modeled with multistate models (Hestbeck et al. 1991; Brownie et al. 1993; Lebreton and Pradel 2002). To employ this family of models, traits are divided into a number of discrete "states" for each sampling occasion. These states are a representation of the trait for each observed individual on a given sampling occasion. The resulting state-specific estimates of the probability of survival are based only on those individuals actually observed (Lebreton and Pradel 2002). A drawback of multistate models is that the trait is reduced to a discrete category analogous to the way in which stages are defined in a stage-based matrix population projection model (Caswell 2001). Provided that the trait is divided into enough states, continuous distributions can be approximated, but the parameter space increases very rapidly with the number of states (states × (states – 1)) and can lead to estimability and power issues. The choice of the number of states will depend on the tradeoff between parameter estimate precision and parameter number (degree of approximation of a continuous distribution). Importantly, multistate models can also account for other size-dependent processes such as emigration and probability of capture. Because of their flexibility, multistate models have been championed as having the potential to offer a general framework for CMR models based on the CJS model (Lebreton and Pradel 2002).

We are interested in estimating SDS for juvenile stream-dwelling Atlantic salmon (*Salmo salar*). This species typically exhibits very wide size ranges resulting from variation in timing of emergence from redds (Einum and Fleming 2000) and in individual growth rates (Letcher and Gries 2003). This wide size variation is interesting because of its relationship with life history expression (Metcalfe 1998). Within the same population, some males mature as parr and these individuals tend to be the fastest growers (Letcher and Gries 2003; Aubin-Horth and Dodson 2004). The timing of seaward migration (smolt age) can also differ among individuals within the same population and is influenced by previous individual growth (Elson 1957). The maintenance of size-related life history expression in systems with wide size distributions (in Atlantic salmon, the size range often equals the mean) suggests either that SDS is weak or that it exists but is variable (opposing) over time. For example, Good et al. (2001) found opposing directions of selection on body size in Atlantic salmon for different years and the direction correlated with variation in stream flow. Hendry et al. (2003) also reported variable strengths and directions of selection on Atlantic salmon body size within years during stream residence. Based on wide distributions of body size, the relation between body size and life history, relatively high recapture probabilities (Letcher et al. 2004), and the suggestion of variable selection regimes over time, Atlantic salmon in freshwater provide a good model species for evaluating the extent of temporal variation in SDS.

Our objectives were (*i*) to determine the extent of temporal variation in the strength of SDS in a field population, (*ii*) to determine the effectiveness of the multistate CMR model for estimating the strength and shape of SDS under a variety of conditions, and (*iii*) to compare multistate model estimates of SDS with traditional methods for estimating selection on body size (Lande and Arnold 1983; Schluter 1988). We first characterized size-dependent processes (growth, emigration, probability of capture) that could affect detection of SDS. We then ran a series of simulations in the context of these size-dependent processes to evaluate the power of multistate CMR models to uncover shapes and strengths of SDS under a range of conditions (samples sizes, probabilities of survival and capture). Simulation results indicated that even very subtle forms of SDS could be detected in our system with multistate models. Finally, we estimated the magnitude and shape of SDS for two cohorts of juvenile Atlantic salmon during freshwater residence.

Materials and methods

Field data

Study area

Atlantic salmon in a 1 km long West Brook study area have been individually tagged (12 mm passive integrated transponder (PIT) tags; Digital Angel Corp., Delray Beach, Florida) since 1997 (for details of the study area and sampling, see Letcher et al. (2002) and Letcher and Gries (2003)). Here we report data from two cohorts of fish (2000 and 2001) from first tagging to the fall following age-2+ smolt emigration (Table 1) and for which we can estimate emigration (PIT tag detection antennas (efficiency = 91%) at the downstream end of the study area (Letcher et al. 2004; Zydlewski et al. 2006)). For both study cohorts, fry for stocking were obtained from the White River National Fish Hatchery (US Fish and Wildlife Service, Bethel, Vermont) and were stocked in the spring. The unfed fry (~26 mm) were first-generation offspring of sea-run adult re-

© 2008 NRC Canada

Table 1. Timing and numbers captured for sampling events by cohort for West Brook.

Cohort	Sample name	Sample number	Sample start date	Sample end date	Number captured
2000	0+ Fall	30	22 Sept. 2000	2 Oct. 2000	527
	0+ Prewinter	31	1 Dec. 2000	15 Dec. 2000	306
	1+ Spring	32	8 Mar. 2001	19 Mar. 2001	261
	1+ Summer	34	5 Jun. 2001	14 June 2001	293
	1+ Fall	36	4 Sept. 2001	14 Sept. 2001	298
	1+ Prewinter	37	3 Dec. 2001	10 Dec. 2001	157
	2+ Spring	38	25 Mar. 2002	6 Apr. 2002	75
	2+ Summer	40	6 June 2002	19 June 2002	50
	2+ Fall	41	17 Sept. 2002	3 Oct. 2002	41
2001	0+ Fall	36	4 Sept. 2001	14 Sept. 2001	432
	0+ Prewinter	37	3 Dec. 2001	10 Dec. 2001	368
	1+ Spring	38	25 Mar. 2002	6 Apr. 2002	360
	1+ Summer	40	6 June 2002	19 June 2002	323
	1+ Fall	41	17 Sept. 2002	3 Oct. 2002	279
	2+ Spring	43	2 Apr. 2003	18 Apr. 2003	111
	2+ Summer	45	10 June 2003	24 June 2003	83
	2+ Fall	46	3 Sept. 2003	16 Sept. 2003	68

turns to the Connecticut River and were stocked at a density of 50·m^{-2}. There is no natural salmon reproduction in our study area. Brook trout (*Salvelinus fontinalis*), brown trout (*Salmo trutta*), and an occasional blacknose dace (*Rhinichthys atratus*) are the only other fish species present.

Fish sampling

We electrofished (300–400 V, unpulsed DC) the study sections 12 times, covering the time from first tagging to the fall following age-2+ smolting (migration to the sea) for each cohort (Table 1). There was no 1+prewinter sampling for the 2001 cohort because ice cover during a particularly cold December precluded sampling. Each sampling occasion took about 10 days to complete (details in Letcher and Gries 2003). Overall, there were 797 individuals available for analysis for the 2000 cohort and 747 individuals for the 2001 cohort. Numbers of fish for analysis ranged from 527 to 41 among sampling occasions for the 2000 cohort and from 432 to 68 among sampling occasions for the 2001 cohort (Table 1).

Multistate models

We divided body size distributions for each sampling occasion into discrete states (s). Separate probabilities of survival ($\widehat{S}$) and capture ($\widehat{p}$) can be estimated for each state. The ability of multistate models to identify SDS was estimated by comparing output from models that included variation in survival among states with null models that did not include variation in survival among states. These two model sets differed in the number of model parameters ("beta parameters") necessary to estimate each S. Models in which survival was not allowed to vary among states required the least number of beta parameters, whereas models with state-specific survival required more beta parameters. In addition to state-specific survival estimates, we also estimated both linear and nonlinear (quadratic) forms of SDS ("state-trend" models), which required an intermediate number of parameters (details in Appendix A, Table A1). Instead of the five beta parameters needed to estimate S for each size state with a state-specific model, the trend model uses two (linear) or three (quadratic) beta parameter estimates to estimate each size-specific S during each interval. We used five size states, because preliminary results based on our field data indicated that five was the largest number that provided reasonable parameter estimates. Assumptions of multistate models are that (*i*) marks are not lost, (*ii*) individuals act independently, (*iii*) all marked individuals assigned to a state have the same probabilities of survival, movement, and capture (Hestbeck 1995), and (*iv*) $\widehat{S}$ and $\widehat{p}$ do not depend on earlier values of $\widehat{S}$ and $\widehat{p}$ (Brownie et al. 1993).

Model selection

We used the model selection procedures (Burnham and Anderson 1998) to estimate the extent of SDS. This approach estimates the likelihood that a model is the most parsimonious one in the model set. The two sources of complexity in our analysis were variation in survival (S) and capture probability (p) among states and variation in S and p over time (t). Model selection involves comparison of models of varying complexity in S, p, and transition probabilities among states using Akaike's information criterion (AIC; Burnham and Anderson 1998). Models with a higher likelihood (given the data) will have smaller AIC values. Throughout, we report AIC_c values, an AIC estimator that accounts for sample size effects (Burnham and Anderson 1998). Models of varying complexity are then compared using the difference in AIC_c values (ΔAIC_c) between a given model and the model with the minimum AIC_c value. ΔAIC_c values greater than 10 indicate that the model is a much less parsimonious fit to the data than the best model, whereas values between 2 and 10 indicate some support for the model. Values below 2 suggest that the model might be as parsimonious as the best model in the set (Burnham and Anderson 1998). Model weights indicate the relative likelihood of candidate models and can be interpreted as representing the "weight of evidence" that a model provides the best de-

© 2008 NRC Canada

scription of the data (Burnham and Anderson 1998) among the set of candidate models. Throughout, model naming conventions followed Lebreton et al. (1992). For example, a model with variation in S among states (s) and over time (t) would be expressed as $S(s,t)$ and a model with no variation (°) among states or time would be represented as $S(°,°)$.

Beta parameter analysis

Intermittent SDS may be difficult to detect using model selection procedures alone because of the very large number of models that would be needed to fully evaluate interval-specific SDS and the associated risk of overfitting the data (Burnham and Anderson 1998). For our field data, we conducted both model selection and beta parameter analysis (overlap of the 95% CI for each beta parameter with a value of 0) to determine the extent of SDS. We used beta parameter analysis for specific states on a given interval and also for the coefficients of trend models for a given interval. For the simulations, most of the analyses were conducted using model selection approaches, but we also compared beta parameter analysis with model selection to determine the ability of each approach to detect known SDS.

States

In analyses using field data, individuals were assigned a state value (1, 2, 3, 4, or 5) based on quintiles of the size distribution for each sample (i.e., the smallest 20% were assigned a 1 and the largest 20% were assigned a 5). Body sizes (wet mass, grams) were standardized to a mean of zero and standard deviation of one for each sample occasion by subtracting the mean from each individual's size and dividing by the standard deviation of the size distribution for the sample. We used standardized sizes rather than absolute sizes to reduce the overall number of size states that would be required to cover the entire range of absolute sizes during growth and at the same time provide reasonably small state bins. This resulted in estimates of SDS on relative size or size ranks instead of on absolute size. In the simulation analyses, each individual was assigned a starting size from a normal distribution with mean zero and standard deviation of one. Individual sizes were not fixed over time in the simulations but were allowed to vary in a random walk based on a normal distribution with mean of ~0 and standard deviation of ~0.4 (based on the distribution of standardized size change over a sampling interval from our field data). To avoid the problem of size-dependent losses (mortality, emigration) influencing the assignment of individuals to bins at the end of a sampling interval, we used the standardized size bin boundaries from the beginning of an interval ($k - 1$) as the boundaries for the occasion of interest (k). Individual encounter histories (input data to MARK) were represented by the integers 1 through 5 (states) for occasions on which individuals were captured and by zeros for occasions when they were not captured. Permanent emigrants (last observation of an individual was on the downstream pair of PIT tag antennas) were coded with a frequency value of –1 in the encounter history file (input file).

Preliminary evaluation of model structure

Before estimating SDS for the field data, we needed to conduct preliminary analyses to limit the number of possible model constructions. The time-dependent parameterization for our multistate analyses (five size states and multiple sampling intervals) resulted in a very large set of possible candidate models. Lebreton et al. (1992) suggested narrowing the possibilities first by seeking the appropriate time structure from simpler models and then applying this structure to models of varying complexity in the focal parameter (in our case, survival). To provide a reasonable set of candidate models, we evaluated time structure in apparent survival, possible transitions among states (Ψ), and the potential for size-dependence in p. First, we used the CJS model with a single state to evaluate general patterns over time in apparent survival (Φ) and p. Although there were many permutations of time structure, our only a priori expectation was fully time-dependent parameter structure; therefore, we ran CJS models with four combinations of Φ and p for each cohort: ($\Phi(°), p(°)$; $\Phi(°), p(t)$; $\Phi(t), p(°)$; $\Phi(t), p(t)$). Second, we determined the best structure on Ψ for each cohort by evaluating a multistate model set without state-specific survival but with the most appropriate time structure on survival and p from the CJS analysis. Third, we estimated the weight of evidence for size-dependent probability of capture for each cohort by comparing models with ($p(s,t)$) and without ($p(°,t)$) size-dependence in p (using the best structure on Ψ). In all analyses of SDS in the field, we used the best structure for each parameter as a starting model. To adjust estimates of S to a common time scale, time intervals were set as a proportion of the longest interval for each cohort.

Simulations

Based largely on the results of the preliminary evaluation of model structure, we ran a series of simulations to determine the effectiveness of multistate CMR models for estimating the strength and shape (directional or stabilizing) of SDS for our system. With this analysis, we determined the weakest form of SDS that was detectable under a variety of conditions and estimated error in survival estimates. We report percent relative error in estimated survival ((estimated – expected)/expected × 100) as our measure of parameter estimate error.

Size-dependent survival simulation

For both directional and stabilizing forms of SDS (Fig. 1), we varied the number of individuals (N; 50, 100, 250, 500, 1000), average survival (S; 0.4, 0.6, 0.8), average probability of capture (p; 0.4, 0.6, 0.8), and the strength of SDS (b; values in Fig. 1). We ran three replicates for each combination of input variables (each combination of input variables represented a simulation model or simulated scenario). SDS for each interval was simulated using either a cumulative density function (directional form of SDS)

$$(1) \qquad F(x) = \left(1 + e^{-\frac{x-a}{b}}\right)^{-1}$$

or probability density function (stabilizing form of SDS)

$$(2) \qquad f(x) = \frac{1}{b}\left(e^{-\frac{x-a}{b}}\right) \cdot \left(1 + e^{-\frac{x-a}{b}}\right)^{-2}$$

of the logistic distribution, where x was standardized body size (mean = 0, standard deviation (SD) = 1), and a and b

© 2008 NRC Canada

Fig. 1. (*a*) Directional and (*b*) stabilizing size-dependent survival (SDS) curves used in the power analysis. Numbers associated with each curve are the shape parameters (*b* on *x* axis) defining the strength of SDS in eqs. 1 and 2.

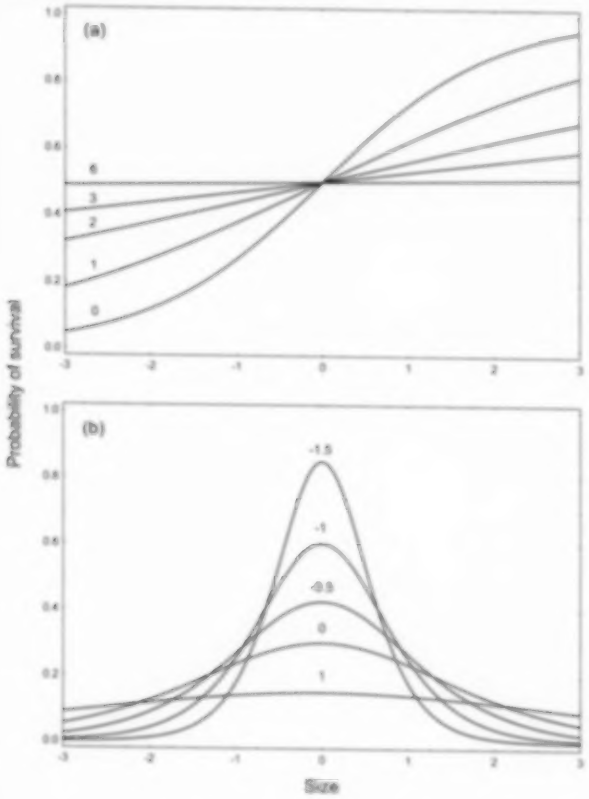

were constants. The value of *a* was set to 0, so *b* alone determined the strength of SDS (Fig. 1). To adjust eqs. 1 and 2 to provide the different input survival probabilities in the simulations, we multiplied each equation by 2*S*. For each value of *S*, this generated either an average survival of *S* across sizes for eq. 1 or a maximum value of *S* for eq. 2. The largest values of *b* (6 for directional, 1 for stabilizing) represented conditions of minimal SDS (Fig. 1). For each time step interval, individual survival was determined by comparing a deviate from a uniform distribution [0, 1] with the expected survival generated by calculating $F(x)$ or $f(x)$ for each individual's size at the beginning of the interval. An individual was scored as captured if it was alive and captured (uniform deviate [0, 1] < *p*) for an occasion. Because our preliminary evaluation of model structure for the field data did not support size dependence in *p*, we did not include size dependence in *p* in the simulations. Each simulation was run for nine sampling occasions (constant interval durations), and the encounter histories were constructed accordingly based on an individual's survival (yes or no), size state (1–5), and capture (yes or no). Batches of estimation models were run using Program MARK and Markwait (available from Jim Hines, US Geological Survey Patuxent Wildlife Research Center, 12100 Beech Forest Road, Laurel, MD 20708-4017, USA). The program to generate input files and to collect output data from MARK runs was written in Visual Basic (Microsoft Corporation, Redmond, Washington).

Time-invariant size-dependent survival

To test the power of multistate models to uncover known size dependence in survival (*S*), we compared AIC_c values of multistate models with (*i*) no variation in survival among states ($S(\cdot, \cdot)$), (*ii*) state-specific survival ($S(s, \cdot)$), (*iii*) a linear trend in survival, and (*iv*) a quadratic trend in survival (see Appendix A, Table A1). For this first set of simulations, we did not include time variation in the estimation models because there was no time structure on average *S* in the simulation input model. Model structure was $(\cdot, \cdot)$ for *p* and $(s, \cdot)$ for Ψ. To evaluate the ability of these models to uncover SDS, we took two steps with each estimation model. First, we evaluated whether any of the three models with size dependence provided a better fit to the data than the model with no size dependence ($S(\cdot, \cdot)$) by evaluating the ΔAIC_c values of the $S(\cdot, \cdot)$ model from each set of simulation models. Values of $\Delta AIC_c > 10$ indicated that size dependence was detectable. Second, to indicate the degree of relative support for the three size-dependent models when SDS could be detected ($\Delta AIC_c > 10$), we compared model weights for the three models for each combination of input values.

Time-varying size-dependent survival

Using an approach similar to that for the time-invariant SDS analysis, we also evaluated the performance of multistate models when SDS acted for one interval (*i*) only (2, 4, 6, or 8). We analyzed effects of time-varying SDS using both directional (eq. 1) and stabilizing (eq. 2) forms of SDS for one of the intervals. We conducted the simulations under the same set of conditions as above, except *p* equaled 0.8 for all simulated data sets (preliminary analyses indicated that variation in *p* had a marginal effect on results). Structure on *p* and Ψ was $p(\cdot, \cdot)$ and $\Psi(s, \cdot)$. We analyzed the patterns in the results using mean squared error (MSE) from analysis of variance (ANOVA) with ΔAIC_c for the $S(\cdot, t)$ model as the dependent variable and *N*, *S*, *i*, and *b* as the independent variables. For this same set of simulation runs, we also compared the ability of the beta overlap analysis and model selection procedures based on ΔAIC_c to detect SDS.

We assessed the error in $\hat{S}$ by comparing survival estimates for each state with expected survival based on eq. 1 or eq. 2 (depending on the form of SDS) for all combinations of *N*, *S*, *i*, *b*, and *s*. We analyzed error only for the specific interval during which SDS acted. For simplicity, we only present data for the $S(s, t)$ model because the error results from this model were similar to those of the linear model for directional SDS and were similar to those of the quadratic model for stabilizing SDS. To generate a survival estimate for each state and form of SDS, we input the size value from the center of each quintile of the normal distribution with mean = 0 and SD = 1 (–1.28, –0.52, 0, 0.52, 1.28) into eq. 1 or eq. 2. To provide a relative assessment of the effects of the input variables (*N*, *S*, *p*, *b*, and *s*) on error, we report MSE from ANOVA models with error as the dependent factor and the input variables as the independent variables.

© 2008 NRC Canada

Table 2. Cormack–Jolly–Seber (CJS) results with a single state for the 2000 and 2001 cohorts.

Cohort	Model	No. of par	AIC_c	ΔAIC_c	Model weight
2000	$\Phi(t)$, $p(t)$	15	3871.5	0.0	1
	$\Phi(\cdot)$, $p(t)$	9	3910.5	39.0	0
	$\Phi(t)$, $p(\cdot)$	9	4007.0	135.5	0
	$\Phi(\cdot)$, $p(\cdot)$	2	4091.8	220.4	0
2001	$\Phi(t)$, $p(t)$	13	3762.6	0.0	0.994
	$\Phi(\cdot)$, $p(t)$	8	3773.0	10.4	0.006
	$\Phi(t)$, $p(\cdot)$	8	3822.2	59.6	0
	$\Phi(\cdot)$, $p(\cdot)$	2	3851.3	88.7	0

Sample sizes to detect SDS

In our simulations, the number of individuals alive at a certain sampling occasion depended on N, S, and i, making it difficult to determine the numbers of individuals required to detect SDS successfully at any one sampling occasion. To provide a guide for the number of individuals that need to be present to detect SDS (independent of S, i, or initial values of N), we ran logistic regression models for each form and strength of SDS. In these models, beta estimate confidence interval overlap of 0 (yes or no) for the interval during which SDS was acting was the dependent variable and the expected number of individuals surviving to the interval (NS^i) was the independent variable. Numbers of individuals in this analysis are the number alive; for field applications, they should be adjusted by p to give numbers needed to capture. When testing for overlap with 0, we used the linear coefficient for linear models and the quadratic coefficient only for quadratic models.

Field data

Goodness of fit

Goodness of fit (GOF) tests for CMR models indicate violations of model assumptions and are an important first step in a CMR analysis. Pradel et al. (2003) provide an approach for GOF testing of multistate models (implemented in program U-care; ftp://ftp.cefe.cnrs-mop.fr/biom/Soft-CR). We conducted GOF tests for each cohort and report statistics for the AS model (for details, see Pradel et al. 2003).

Size-dependent survival

Based on results from the preliminary evaluation of model structure, we settled on full time dependency in both S and p, and no state dependence for p for survival estimates in the field. For both cohorts, we ran four models with varying structure on S ($S(s,t)$, $S(\cdot,t)$, linear trend, and quadratic trend) and fixed structure on $p(\cdot,t)$ and Ψ (best structure, see Results). We compared AIC_c values among models to determine the overall evidence for SDS. We also examined beta parameter overlap of 0 for specific intervals to help identify temporal variation in strength and shape of SDS.

Standard selection analysis

To allow comparison of multistate SDS analysis results with standard selection analysis (Lande and Arnold 1983; Schluter 1988), we plotted cubic splines for absolute fitness as a function of body size. For each sampling occasion, fish that were captured on subsequent occasions or that emigrated during the sampling interval were assigned an absolute fitness of one and fish that were never captured following the occasion and did not emigrate were assigned an absolute fitness of zero. Thus, we assumed that emigrants survived to the end of the interval, an assumption that did not add significant bias to estimates (Letcher et al. 2005). Splines were derived using a generalized additive model with a logit link function and binomial response. Because estimates of multistate survival (see below) were adjusted for the relative duration (scaled where value of longest duration = 1) of each sampling interval (I), we also adjusted the spline values (SV) in the same manner (reported spline values = SV^I).

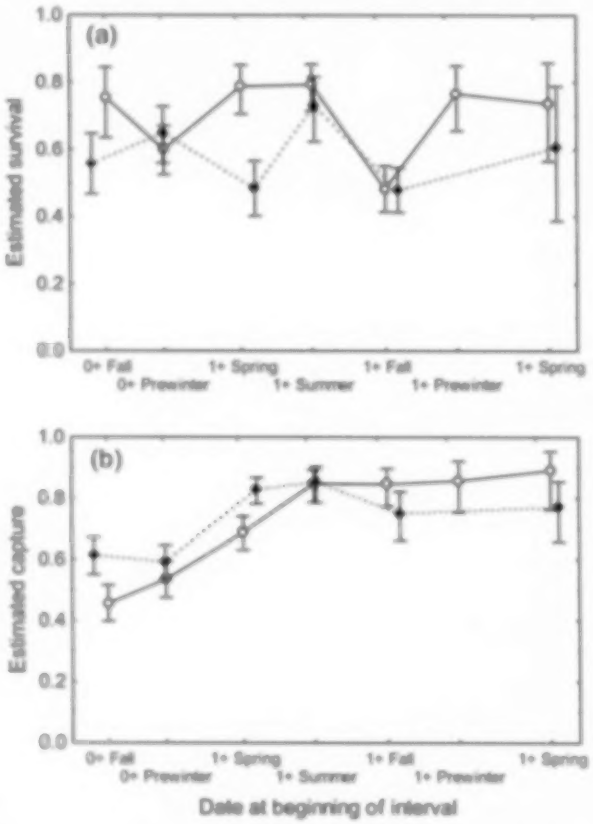

Fig. 2. Estimated (*a*) survival (±95% confidence interval) and (*b*) capture probability (p) for each sample and cohort from a Cormack–Jolly–Seber capture–mark–recapture (CJS CMR) estimation model with a single state. $\hat{S}$ is scaled to the longest interval for each cohort. Cohort: 2000, open circles; 2001, solid diamonds.

Results

Preliminary evaluation of model structure

Structure on Φ and p

Results from the single-state analysis clearly demonstrated a time trend in both Φ and p; $\Phi(t),p(t)$ was the best model for each cohort (ΔAIC_c for all other models was >10) (Table 2), and both Φ and p clearly varied over time

© 2008 NRC Canada

Table 3. Analysis of variance (ANOVA) results (mean squared error (MSE) and proportional MSE) from simulations to test relative effects of the input variables on the ability to detect time-invariant (ΔAIC_c for $S(\cdot,\cdot)$ model) and time-varying (ΔAIC_c for $S(\cdot,t)$ model) size-dependent survival (ΔAIC_c).

				Directional		Stabilizing	
SDS	Dependent variable	Input variable	df	MSE	Proportional MSE	MSE	Proportional MSE
Time-invariant	ΔAIC_c	N	4	457 673	0.28	88 784	0.27
		S	2	519 522	0.31	64 542	0.20
		p	2	9 049	0.01	5 317	0.02
		b	4	663 215	0.40	172 133	0.52
Time-varying	ΔAIC_c	N	4	9 844	0.19	18 418	0.22
		S	2	8 688	0.17	12 588	0.15
		I	3	11 188	0.22	21 942	0.27
		b	4	20 838	0.41	29 064	0.35
	Error in $\hat{S}$	N	4	2.84	0.32	8.13	0.05
		S	2	1.4	0.16	84.53	0.51
		I	3	3.67	0.41	28.71	0.17
		b	4	0.55	0.06	17.12	0.10
		s	4	0.55	0.06	28.78	0.17

Note: Results are also shown for error in $\hat{S}$ for the time-varying simulations. Results shown for directional and stabilizing forms of size-dependent survival (SDS).

(Fig. 2). Φ ranged from about 0.6 to 0.8 and p ranged from about 0.5 to 0.9. Therefore, all analyses using multistate models included time structure for both S and p.

Structure on Ψ

Model structure varied in the extent to which individuals could transition up or down states. In general, results indicated that probabilities of getting bigger were different than the probabilities of getting smaller and that probabilities of transitioning one or two or more than two states were also different for fish getting bigger or smaller. The top model structure for Ψ (data not shown) for each cohort was used in all subsequent analyses.

Size dependence of p

There was no evidence for size dependence in p; models without size dependence in p ($p(\cdot,t)$) had smaller AIC_c values than models with size dependence in p ($p(S,t)$). ΔAIC_c for the comparison between $p(\cdot,t)$ and $p(s,t)$ were 17.0 (2000 cohort) or 40.8 (2001 cohort). Therefore, structure on p for all following analyses using multistate models was $p(\cdot,t)$.

Simulations

Time-invariant size-dependent survival (ΔAIC_c)

Patterns in relative effects of input variables on ΔAIC_c for both directional and stabilizing forms of survival were similar, with b accounting for most of the variance, p accounting for very little, and intermediate levels accounted for by N and S (Table 3).

When there was no SDS (maximum b values for both directional and stabilizing SDS; Fig. 1), ΔAIC_c values for the $S(\cdot,\cdot)$ model were <2, indicating no support for SDS (top panels of Figs. 3 and 4). This result indicates that multistate models will not generate false positive results. When there was SDS (b < maximal values; Fig. 1), the ability to detect SDS (ΔAIC_c < 10 in Fig. 3) depended on N, S, and b and on whether SDS was directional (Fig. 3) or stabilizing (Fig. 4). With high survival (0.8), the strongest SDS (smallest value of b) was detectable with even as few as 50 individuals, but the weakest SDS was only detectable with 500 and 1000 individuals (directional) or only 1000 individuals (stabilizing). With lower S, the weakest SDS detectable with 1000 individuals was b = 2 for directional SDS and b = –0.5 for stabilizing SDS.

For directional SDS, model weights for $S(s,\cdot)$ models generally decreased and model weights for linear models generally increased as the strength of SDS decreased (Fig. 3), indicating that linear models provided a better description of the data than the other models. For stabilizing SDS, quadratic models generally gave the highest model weights, except when survival and strength of SDS were high (Fig. 4).

Time-varying size-dependent survival (ΔAIC_c)

For both directional and stabilizing SDS, b accounted for the most variation in ΔAIC_c, whereas N, S, and i accounted for similar, but lower, levels of variation (Table 3). SDS was much more readily detectable (ΔAIC_c for $S(\cdot,t)$ model > 10) when it occurred during an early sampling interval, with higher survival and larger N (Table 4). With i = 8, only stronger forms of SDS were detectable and only when N and S were large. With i = 2, strong SDS was detectable for most values of N and S, but weaker SDS was only detectable with larger values of N and S (Table 4). Using the criterion of ΔAIC_c > 10, the two weakest SDS were never detectable when SDS was time-varying.

Overall, weaker SDS was detected testing whether the confidence intervals of the appropriate beta value from the trend model overlapped zero compared with model selection procedures (Table 4). For some combinations of input values (e.g., i = 6, S = 0.6, N > 250, stabilizing), the trend models could detect SDS, whereas model selection procedures could not detect SDS. In most cases, evaluation of the beta parameters allowed detection of weaker forms of SDS than model

© 2008 NRC Canada

Fig. 3. (*a*) ΔAIC_c values for the $S(\cdot,\cdot)$ model for directional time-invariant size-dependent survival (SDS). Larger values indicate more support for SDS. Symbols represent different levels of N and the horizontal line is at $\Delta AIC_c = 10$. (*b*) Average model weights of the four candidate models when ΔAIC_c for the $S(\cdot,\cdot)$ model was >10 for $N = 1000$. Values of b are strengths of SDS. When $b = 6$ (no SDS), $S(\cdot,\cdot)$ models achieved the greatest support for all levels of S.

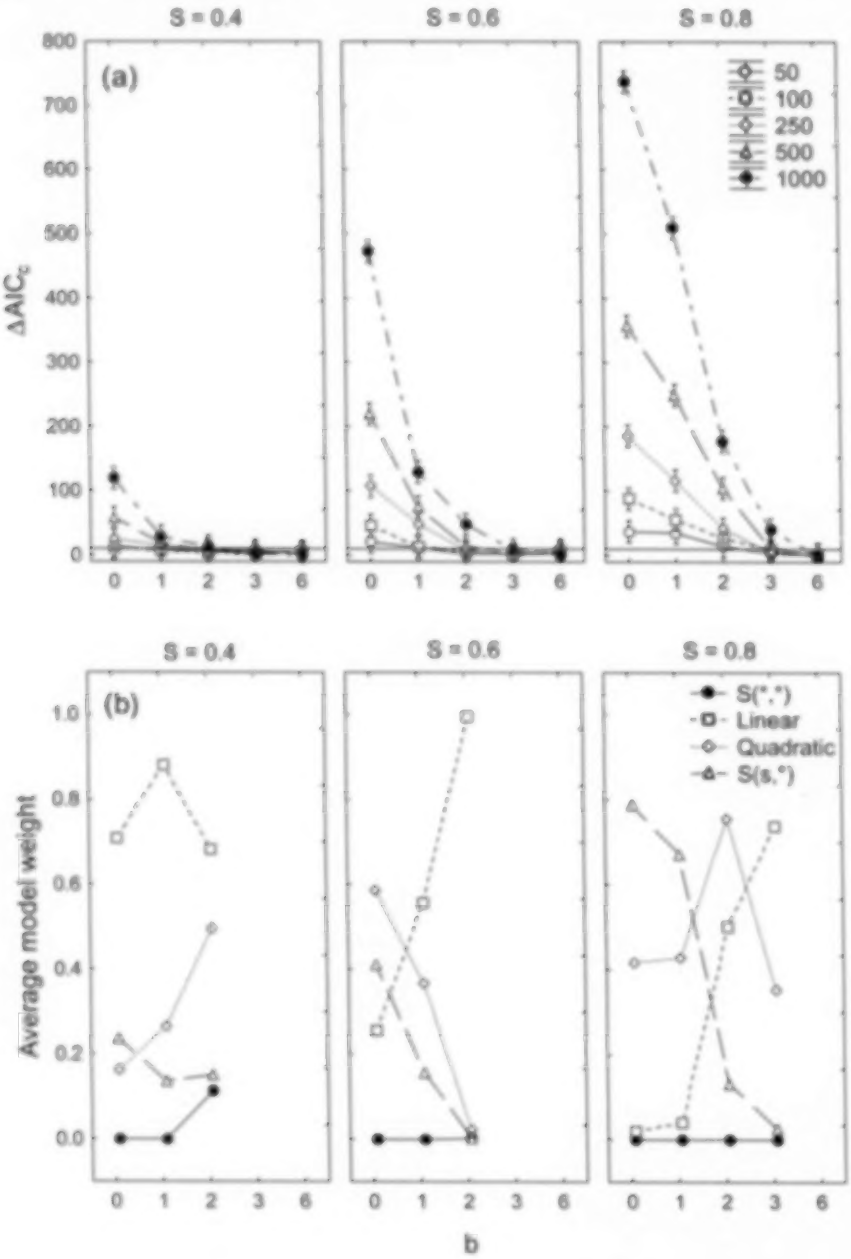

selection, and in some cases (e.g., $i = 2$, $S = 0.8$, $N = 1000$, directional), even the weakest SDS was detectable (Table 4).

Error in parameter estimates

The overall patterns of average error across simulation model parameters were similar between time-invariant and time-varying SDS. Interval accounted for the most variation in error in $\hat{S}$ when SDS was directional, but accounted for less variation with stabilizing SDS (Table 3). Error on the interval during which SDS acted tended to be low except when $i = 8$ (Fig. 5). S explained a medium level of variation for directional SDS and the highest variation in average

© 2008 NRC Canada

Fig. 4. (*a*) ΔAIC_c values for the *S*(°, °) model for stabilizing time-invariant size-dependent survival (SDS). Larger values indicate more support for SDS. Symbols represent different levels of *N* and the horizontal line is at $\Delta AIC_c = 10$. (*b*) Average model weights of the four candidate models when ΔAIC_c for the *S*(°, °) model was >10 for $N = 1000$. Values of *b* are strengths of SDS. When $b = 0$ or $b = 1$ (weak or no SDS, respectively), *S*(°, °) models achieved the greatest support for all levels of *S*.

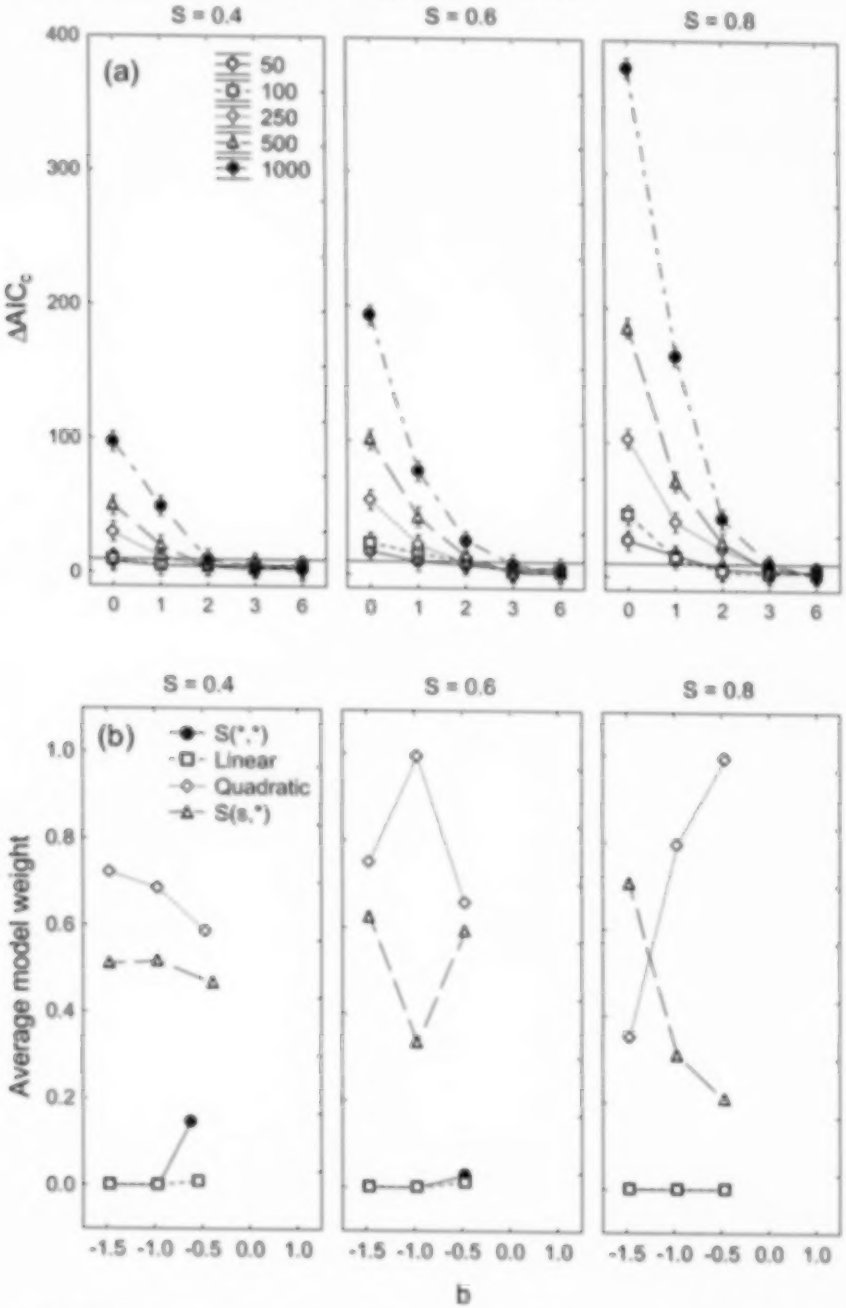

error for stabilizing SDS (Table 3). Average error was quite high (~0.35) at the lowest *S*, but was <0.1 for the other values of *S* for stabilizing SDS and for all values of *S* for directional SDS (Fig. 5). Average error was also high (~0.18) for the lowest value of *N* (50) and decreased to <0.1 across all values of *N* greater than 250 (Fig. 5). Average error was high for the strongest stabilizing SDS, but was <0.1 for all strengths of directional SDS and for the remaining *b* values for stabilizing SDS (Fig. 5). There was little variation in average error across size states for directional SDS, but error

© 2008 NRC Canada

Table 4. Weakest strength of size-dependent survival (SDS; table entries are *b* values from Fig. 1) detectable using either model selection procedures ($\Delta AIC_c > 10$ for $S(*,t)$ model) or analysis of beta value confidence intervals (interval does not cover 0) for the specific interval (i) during which SDS acted for N = 50, 100, 250, 500, and 1000.

			Model selection					Beta value				
Form of SDS	i	S	50	100	250	500	1000	50	100	250	500	1000
Directional	2	0.4	—	—	0	0	1	—	0	0	1	1
		0.6	0	0	1	1	1	0	0	2	2	2
		0.8	0	0	1	2	2	0	2	2	2	3
	4	0.4	—	—	—	—	0	—	—	—	—	0
		0.6	—	—	0	0	0	—	—	—	0	1	1
		0.8	—	—	1	1	2	—	0	1	2	2
	6	0.4	—	—	—	—	—	—	—	—	—	—
		0.6	—	—	—	—	0	—	—	0	1	1
		0.8	—	—	0	0	2	—	—	1	2	2
	8	0.4	—	—	—	—	—	—	—	—	—	—
		0.6	—	—	—	—	—	—	—	0	—	—
		0.8	—	—	—	0	0	—	—	1	1	2
Stabilizing	2	0.4	—	–1.5	–1.5	–1.5	–0.5	—	–1.5	–1	–1	–0.5
		0.6	—	–1.5	–1	–1	–0.5	—	–1	–0.5	–0.5	0
		0.8	–1.5	–1.5	–1	–0.5	–0.5	–1	–1	–0.5	0	0
	4	0.4	—	—	—	—	–0.5	—	—	—	—	–0.5
		0.6	—	—	–1.5	–1	–1	—	—	–1.5	–1	–0.5
		0.8	—	—	–1	–1	–0.5	–1.5	–1.5	–0.5	–0.5	0
	6	0.4	—	—	—	—	—	—	—	—	—	—
		0.6	—	—	—	—	—	—	—	—	–1.5	–1
		0.8	—	—	–1.5	–1.5	–1	—	—	–1	–0.5	–0.5
	8	0.4	—	—	—	—	—	—	—	—	—	—
		0.6	—	—	—	—	—	—	—	—	—	–1
		0.8	—	—	—	–1.5	–1	—	—	–1	–1.5	–0.5

Note: Probability of capture = 0.8. A dash (—) indicates that no SDS was detectable.

was higher for the smallest (0.12) and largest (0.36) size states when SDS was stabilizing (Fig. 5).

Sample sizes to detect SDS

Stronger SDS required fewer individuals to obtain a 95% probability of detecting SDS (Table 5). With the strongest SDS, as few as about 30 individuals were required during the interval of SDS, whereas many more (1219, directional; 455, stabilizing) were required for the most subtle strengths of SDS.

Field data

Goodness of Fit

GOF tests revealed that our data did not violate assumptions of the CJS multistate model for either cohort (2000, P value = 0.99, df = 245; 2001, P value = 0.94, df = 250).

Multistate estimates of size-dependent survival

For our field data, N was approximately 750 and S ranged from 0.6 to 0.8. Given these values and the numbers of fish captured on each sampling occasion (Table 1), results of the simulation indicated that we should be able to detect all but the weakest directional SDS for early intervals (Table 5). For the later intervals, lower fish numbers make detection of weak SDS unlikely, but sufficient numbers remained for detection of stronger SDS (Tables 1 and 5).

Size-dependent survival

There was strong evidence for SDS for both cohorts (Table 6). ΔAIC_c values for the $S(*,t)$ model were 11.0 for the 2000 cohort and 19.5 for the 2001 cohort. For the 2000 cohort, strength of evidence supported a linear trend (model weight = 0.99 and ΔAIC_c = 10.3), whereas a quadratic trend was supported, albeit with weaker evidence, for the 2001 cohort (model weight = 0.84 and ΔAIC_c = 3.3) (Table 6).

The patterns of SDS suggested for each interval from the state-trend models reflected the results of the trend model comparisons for each cohort. For the 2000 cohort, there was generally weaker evidence for SDS but strong support for a linear trend in SDS compared with a quadratic trend (disruptive or stabilizing) (Fig. 6). For the 2001 cohort, the reverse was true: generally stronger evidence overall for SDS and greater support for a quadratic trend than for a linear trend (Fig. 7). For the 2000 cohort, SDS was significantly quadratic (disruptive) in the third interval and significantly linear (negative) in the fifth interval (Fig. 6) based on the 95% confidence intervals of the beta parameters estimated from the state-trend models. For the 2001 cohort, there were significant SDS trends in three out of six intervals (Fig. 7). SDS was significantly linear (positive) in the first interval, significantly quadratic in the third interval (stabilizing), and significant for both linear (negative) and quadratic SDS (stabilizing) for the fifth interval (Fig. 7). The patterns of the trend lines also generally matched selection patterns esti-

© 2008 NRC Canada

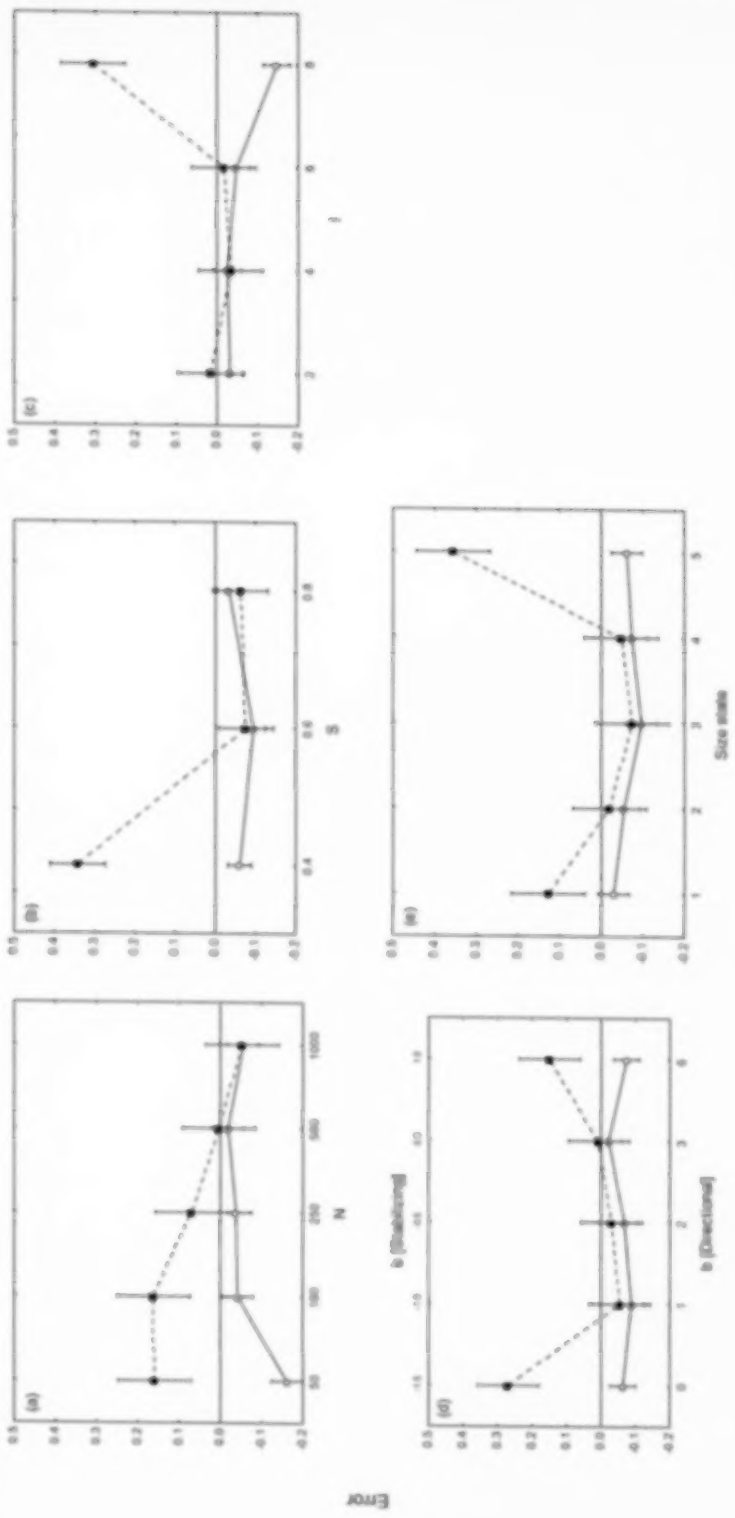

Fig. 5. Average relative error for the five input variables (*a*) *N*, (*b*) *S*, (*c*) *t*, (*d*) *b* (directional), and (*e*) size state) when size-dependent survival was time varying. Error is averaged over groups of four input variables and plotted as a function of each remaining input variable. Solid lines indicate directional size-dependent survival (SDS) and broken lines indicate stabilizing SDS.

© 2008 NRC Canada

Table 5. Logistic regression parameter estimates for the relationship between the probability of either the linear (directional) or quadratic (stabilizing) terms encompassing 0 and the expected number of individuals alive for the sampling occasion during which SDS (i) occurred, $y = \exp(x + zN)/(1 + \exp(x + zN))$.

Form of SDS	b	x	z	p value	Expected no. alive at 0.05
Directional	0	0.387	−0.070	<0.00001	47
	1	1.508	−0.054	<0.00001	83
	2	1.900	−0.025	<0.00001	191
	3	1.417	−0.004	0.036	1219
Stabilizing	−1.5	0.337	−0.097	<0.00001	34
	−1	0.585	−0.048	<0.00001	74
	−0.5	0.825	−0.030	<0.00001	126
	0	1.031	−0.009	<0.00001	455

Note: b is the parameter defining the strength of SDS (Fig. 1); expected number alive at 0.05 is the number of individuals alive at the beginning of the interval of SDS that yielded a value $y = 0.05$ (95% probability of not encompassing 0). $N = 180$ for each regression.

Table 6. Model selection results from a Cormack–Jolly–Seber (CJS) multistate analysis with five size states (s) using ($\cdot$, t) structure on p and "best structure" for Φ.

Cohort	Model	No. of parameters	AIC_c	ΔAIC_c	Deviance	Model weight
2000	S(linear trend, t)	55	6317.0	0.0	2800.0	0.99
	S(quadratic trend, t)	63	6327.3	10.3	2793.2	0.01
	$S(\cdot, t)$	47	6328.0	11.0	2828.0	0.00
	$S(s, t)$	77	6339.9	22.9	2775.5	0.00
2001	S(quadratic trend, t)	54	6053.5	0.0	2445.0	0.84
	S(linear trend, t)	49	6056.7	3.3	2458.9	0.16
	$S(\cdot, t)$	44	6073.0	19.5	2485.7	0.00
	$S(s, t)$	76	6083.9	30.5	2427.8	0.00

Note: Trend models estimated linear or quadratic trend in state-specific survival (S) over each time interval.

mated with cubic splines for each interval (Figs. 6 and 7), indicating that multistate estimates of size selection provide estimates similar to those derived using traditional selection techniques. Wide confidence intervals for the last samples reflect the poor ability to detect SDS in the later intervals.

Discussion

Using multistate CMR models to estimate SDS on juvenile Atlantic salmon, we found that the strength and shape of SDS varied between cohorts and among seasons. Between cohorts, model selection results indicated generally weaker evidence for SDS for the 2000 cohort than for the 2001 cohort and that the shape of the SDS curve was more linear (negative) for the 2000 cohort and stabilizing for the 2001 cohort. Annual variation in the shape of SDS has also been reported for age-0+ Atlantic salmon (Good et al. 2001), and yearly variation in the strength and shape of SDS has been observed in other systems (e.g., Grant and Grant 2002; Mcadam and Boutin 2003) but is not always the case (Merila et al. 2001). Variation in the timing and shape of SDS during freshwater residence could play a part in the maintenance of the wide Atlantic salmon size distributions observed in the field by preserving genetic variability for this trait.

Seasonal variation in the shape of SDS could play a more immediate role in the maintenance of wide size distributions by limiting the effect of size-selective mortality. Among seasons, SDS was strong but acted in varying directions in about one-half of the sampling intervals. SDS was strong during the period of very fast growth in the spring (Letcher and Gries 2003) when SDS was disruptive (2000) or stabilizing (2001). SDS was also strong during the age-1+ fall when SDS was linear (negative 2000) or generally stabilizing with relatively poor survival for the largest fish (2001). Seasonal variation in the strength and shape of SDS suggests that yearly estimates of SDS will not be of fine enough grain to relate environmental variation to variation in SDS in our system.

Earlier selection estimates from our study site for a different Atlantic salmon cohort (Hendry et al. 2003) and for brook trout (*Salvelinus fontinalis*) and brown trout (*Salmo salar*) (Carlson et al. 2004) also found weak and variable selection. The median linear selection differential from Hendry et al. (2003) of 0.04 was lower than the median of 0.09 from a review of selection coefficients from 62 species (Kingsolver et al. 2001). Results from both the fully time-dependent and state-trend multistate models provide an easy visualization of these complex patterns of variable selection. Although SDS was variable among sampling intervals, for

© 2008 NRC Canada

Fig. 6. Estimated survival (±95% confidence interval, CI) as a function of size state for the first six intervals (*a*–*f*) for the 2000 cohort. Points represent estimates from a $S(s,t)$ model and solid lines represent the predicted relationship from quadratic state-trend models. Solid squares are cubic splines based on the raw data. Letters in boxes on plots indicate that estimated 95% CI of linear (L) or quadratic (Q) state-trend beta parameters did not overlap zero.

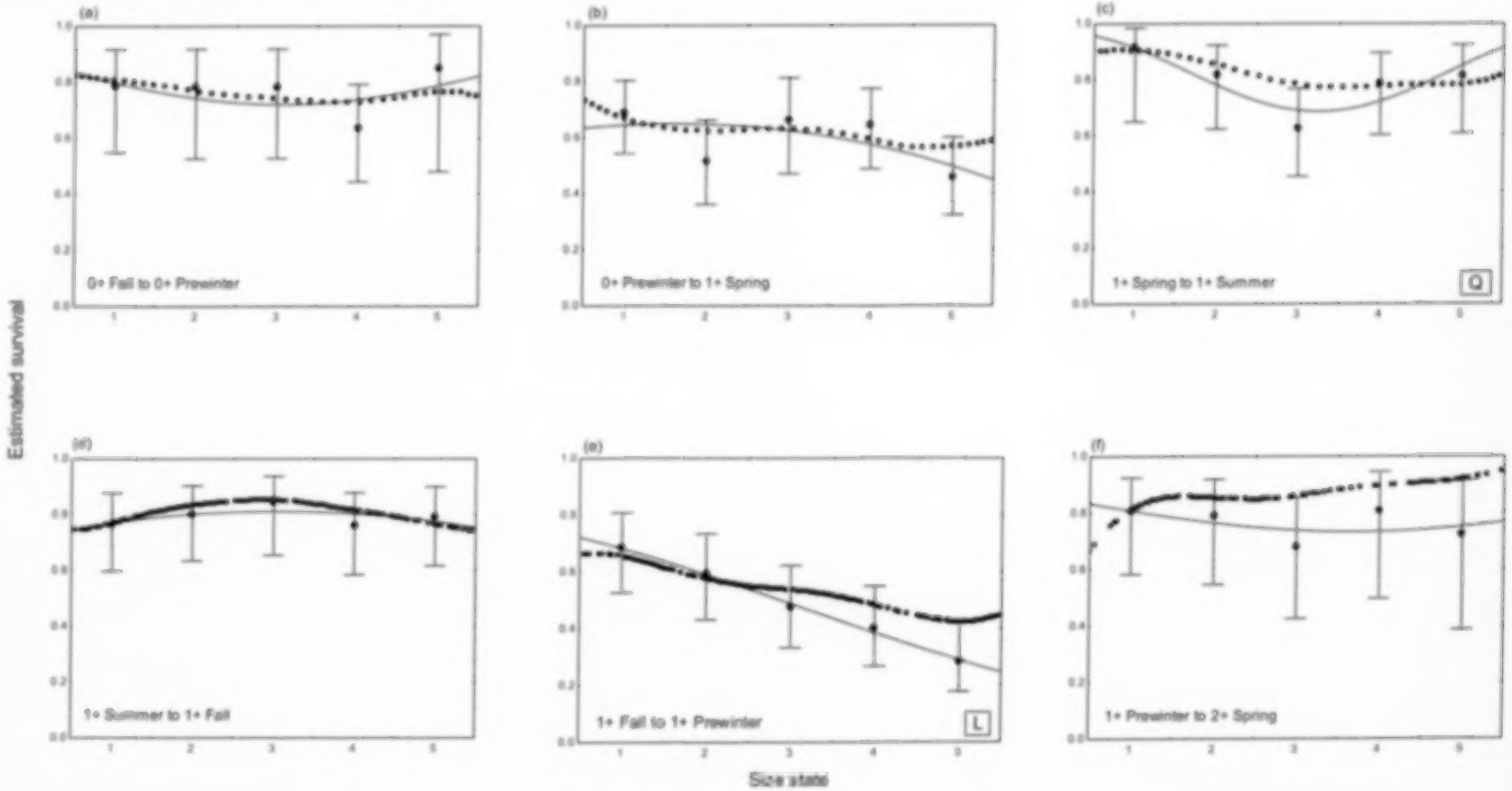

© 2008 NRC Canada

Fig. 7. Estimated survival (±95% confidence interval, CI) as a function of size state for the first six intervals for the 2001 cohort (*a–f*). Points represent estimates from a $S(s, t)$ model and solid lines represent the predicted relationship from quadratic state-trend models. Solid squares are cubic splines based on the raw data. Letters in boxes on plots indicate that estimated 95% CI of linear (L) or quadratic (Q) state-trend beta parameters did and overlap zero.

© 2008 NRC Canada

each cohort, there were intervals in which multistate-trend model results indicated relatively strong SDS. The interval with the clearest pattern was the age-1+ fall interval for which smaller fish generally survived better. This is also the interval with considerable emigration; however, based on our estimated emigration detection efficiency of 91%, we believe that we accounted for most of the size-dependent emigration that could have biased survival estimates (Letcher et al. 2005). A possible explanation for the lower survival of larger fish during this interval may be habitat limitation. Salmon tend to seek shelter in crevices in the rocky stream substrate (Gries et al. 1997), and it may be more difficult for larger fish to find sufficiently large shelters (Finstad et al. 2007). This could result in greater energy expenditure or greater exposure to large predators. Although data are currently insufficient to establish the extent of size-dependent predation in our system, we have recorded instances of predation on salmon by brook and brown trout and have found PIT tags from tagged salmon in the scat of mink, *Mustela vison* (see also Heggenes and Borgstrom 1988).

The other sampling interval with relatively strong SDS for each cohort was the age-1+ spring interval, although the pattern of SDS was opposite for each cohort (2000, disruptive; 2001, stabilizing). With the present analysis, it is not clear why the SDS curve shapes were opposing for the two cohorts, but there are some interesting relationships among survival, growth, and environmental variables. Over the spring interval, the cohort with disruptive SDS (2000) had higher overall survival (0.79 compared with 0.48 from CJS model), was on average 21% heavier, exhibited faster average growth (17% higher), and experienced 77% higher average stream discharge and cooler average water temperatures (8.1 °C compared with 9.0 °C) than the cohort that exhibited stabilizing SDS (2001). These results suggest that fish at the extremes of the size distribution in the spring experience lower mortality under better conditions for growth, such as those present in 2000. Future analyses that incorporate environmental variables as group covariates could help clarify the relationship between relative fish body size, survival, and environmental variables.

Analysis of our simulations indicated that multistate CMR models can provide estimates of SDS with low error (<5%) provided that population sizes are sufficiently large (≥250), average probabilities of survival and capture are greater than 0.6, and SDS is not unrealistically strong. An important advantage of multistate models compared with individual covariate-based models is an ability to accommodate missing observations. Our simulations demonstrated that the probability of capture had very little effect on either detectability of SDS or error of SDS estimates. The main disadvantage of multistate modeling is that data from the independent variable are necessarily classified into discrete states. However, the favorable comparison of multistate estimates with established techniques (Bonner and Schwarz 2004) suggests that generating state-trend estimates using five states can provide a suitable approximation to the continuous SDS functions.

Collectively, the results from our simulations suggest that analyses of SDS using multistate models have good power (based on model selection using AIC_c) and result in low error in $\bar{S}$ across most strengths of SDS when SDS is time-invariant. However, intermittent SDS, especially in later sampling occasions, will be more difficult to detect using these same model selection procedures, except when parameter conditions are ideal (high S, large N). Evaluation of beta parameters from trend models was more sensitive for detecting intermittent SDS. We share the view of Burnham and Anderson (1998) and view model selection as most useful as a guide to the relative importance of SDS across all intervals for a cohort. However, we suggest that the second step of examining the beta parameters of the highest ranked model (based on AIC_c) with appropriate time structure will be necessary to fully understand the timing and extent of SDS. This assertion is based on the premise that the "real" parameter estimates from CMR models (e.g., S, p, Ψ) are actually computed through a linear combination of estimated beta parameters. This linear combination is completely analogous to the linear combinations of beta terms in general linear modeling (GLM). Just as in GLM, the beta terms are normally distributed with a mean, standard error, and associated confidence interval (CI; based on α). The outcome of failure of the CI for each beta term in the model to encompass zero indicates that the associated independent variable for that beta term (in this case size) has an effect (with α) on the dependent variable of interest (in this case S).

Based on our results, an important constraint on the use of multistate models to estimate SDS is the fairly large sample sizes required; however, sample size limitations are not unique to multistate models. Our simulation analysis identified that error was generally high and the ability to detect SDS was low when sample sizes were 100 or less, especially when SDS was stabilizing. Minimum acceptable sample sizes appear to be 250. In their review, Kingsolver et al. (2001) found that median sample size for selection analyses was 134. Kingsolver et al. (2001) suggested that the low sample sizes of most studies may compromise ability to detect weak levels of selection. Hersch and Phillips (2004) demonstrated that power to detect linear selection gradients increased to about 0.8 with sample sizes close to 500 and that power decreased nonlinearly with smaller sample sizes. Our results showing that SDS will be harder to detect when it occurs later in the sampling sequence support the idea that small sample sizes will be magnified for multiple-interval estimates of selection or SDS relative to single-interval estimates because of the inevitable losses due to emigration and mortality. Therefore, for investigators interested in studying SDS over multiple intervals, study design must encompass areas that provide an adequate number of taggable individuals given a priori expectations of S and p.

We simulated two ends of the continuum of time-varying SDS: constant and occurring during a single interval. In the field, SDS will very rarely be constant and is unlikely to operate only for a single interval. Although our simulations were not intended to represent actual field conditions in detail, they do bracket likely field conditions from difficult to detect (single-interval SDS) to easiest to detect (constant SDS). To help assess numbers of individuals required to detect different strengths of SDS for any interval, we ran logistic regressions using the expected numbers of individuals alive while SDS was operating. From this analysis, we conclude that very strong SDS could be detected with as

© 2008 NRC Canada

few as 30 individuals alive at the beginning of a sampling occasion, but that subtle SDS will require hundreds of individuals. Combined with prior estimates of S and p, investigators could use the logistic regressions from Table 5 to estimate the numbers of tagged individuals required at the beginning of a study to detect different levels of expected SDS (after adjusting for p).

Estimates of size selection over a single interval can be biased by size-dependent probability of capture (Kingsolver and Smith 1995; Bradshaw et al. 2003; Zabel et al. 2005) as uncaptured individuals typically are coded as mortalities. Using a simple measure of selection, Zabel et al. (2005) found strong biases in size-selection estimates when probability of capture varied with size. Although not explored here because there was no evidence of size-dependent capture in our study system, multistate CMR models provide the additional possibility of explicitly modeling state-dependent capture probabilities in essentially the same way as survival was modeled above. Multistate models, or other approaches that account for variability in capture (e.g., Kingsolver and Smith 1995), may be essential for deriving reasonable selection estimates on body size when the probability of capture varies with size. In fact, the good match between traditional selection estimates and multistate estimates found here probably is largely a consequence of the lack of size dependence in probability of capture in our system.

The CJS class of models provides estimates of apparent survival (the confounded rates of true survival and site fidelity) unless study areas are closed to emigration. Although apparent survival may represent a useful parameter in some research settings, losses from the study areas other than mortality, such as emigration from the study site, must be measured explicitly to avoid error in estimates of SDS. For example, Atlantic salmon (*Salmo salar*) in a field study exhibited substantial size-dependent emigration in some intervals (Letcher et al. 2005). By ignoring this information, the effects of emigration could have masked or accentuated SDS estimates, possibly resulting in erroneous conclusions about the important SDS processes that structure these populations. In the field, Letcher et al. (2005) determined that ignoring the effects of emigration could change conclusions about the strength of selection for approximately one-half of the sampling intervals. In our study area, we can account for about 91% of the individual emigrants from the study area with in-stream tag reading antennas (Zydlewski et al. 2006) thus approaching an estimate of true survival (even though partial confounding undoubtedly remained). Clearly, sources of size-dependent sampling biases (capture, emigration) must be accounted for to avoid misleading SDS estimates.

Finally, it is important to consider the potential effects of sampling interval duration and individual growth variation on SDS estimates. Size-dependent survival estimates are based on individual size at the time of the first sampling occasion for each interval. Biased SDS estimates could result if the sampling interval is so long that size at the time of death might not reflect size at the beginning of the sampling interval. Body size rank change is unlikely for short sampling intervals or if mortality occurs early in the interval, but size rank change preceding mortality is more likely for longer intervals and for populations exhibiting stronger individual growth rate variation. In our input simulations, individual body sizes could change based on a random walk, but we did not specifically model the strength of the potential interaction between intensity of individual growth variation and sample interval duration. Useful future work could identify optimal sampling interval durations for given levels of growth variation that would minimize error in SDS estimates.

Acknowledgements

We thank the many people who helped sample in the field (especially Todd Dubreuil and Matt O'Donnell), G. White for quickly updating MARK, and the anonymous reviewers, B. Mitchell, N. Aubin-Horth, A. Hendry, D. Sigourney, K. Nislow, M. O'Donnell, and S. Carlson for reading and commenting on manuscript drafts. The US Forest Service, Northern Research Station provided partial support.

References

Arnold, S.J., and Wade, M.J. 1984. On the measurement of natural and sexual selection: theory. Evolution, **38**: 709–719. doi:10.2307/2408383.

Aubin-Horth, N., and Dodson, J.J. 2004. Influence of individual body size and variable thresholds on the incidence of a sneaker male reproductive tactic in Atlantic salmon. Evolution, **58**: 136–144. PMID:15058726.

Blums, P., Nichols, J.D., Hines, J.E., Lindberg, M.S., and Mednis, A. 2005. Individual quality, survival variation and patterns of phenotypic selection on body condition and timing of nesting in birds. Oecologia (Berl.), **143**: 365–376. doi:10.1007/s00442-004-1794-x.

Bonner, S.J., and Schwarz, C.J. 2004. Continuous time-dependent individual covariates and the Cormack–Jolly–Seber model. Anim. Biodivers. Conserv. **27**: 149–155.

Bradshaw, C.J.A., Barker, R.J., Harcourt, R.G., and Davis, L.S. 2003. Estimating survival and capture probability of fur seal pups using multistate mark–recapture models. J. Mammal. **84**: 65–80. doi:10.1644/1545-1542(2003)084<0065:ESACPO>2.0.CO;2.

Brodie, E.D., Moore, A.J., and Janzen, F.J. 1995. Visualizing and quantifying natural-selection. Trends Ecol. Evol. **10**: 313–318. doi:10.1016/S0169-5347(00)89117-X.

Brownie, C., Hines, J.E., Nichols, J.D., Pollock, K.H., and Hestbeck, J.B. 1993. Capture–recapture studies for multiple strata including non-Markovian transitions. Biometrics, **49**: 1173–1187. doi:10.2307/2532259.

Burnham, K.P., and Anderson, D.R. 1998. Model selection and inference: a practical information-theoretic approach. Springer-Verlag, New York.

Carlson, S.M., Hendry, A.P., and Letcher, B.H. 2004. Natural selection acting on size, growth rate, and compensatory growth: an empirical test in a wild trout population. Evol. Ecol. Res. **6**: 1–19.

Caswell, H. 2001. Matrix population models: construction, analysis, and interpretation. Sinauer Associates, Sunderland, Mass.

Clutton-Brock, T.H., Coulson, T.N., Milner-Gulland, E.J., Thomson, D., and Armstrong, H.M. 2002. Sex differences in emigration and mortality affect optimal management of deer populations. Nature (London), **415**: 633–637. doi:10.1038/415633a. PMID:11832944.

Cooch, E.G. 2002. Fledging size and survival in snow geese: timing is everything (or is it?). J. Appl. Stat. **29**: 143–162. doi:10.1080/02664760120108494.

Coulson, T., Gaillard, J.M., and Festa-Bianchet, M. 2005. Decomposing the variation in population growth into contributions

© 2008 NRC Canada

from multiple demographic rates. J. Anim. Ecol. **74**: 789–801. doi:10.1111/j.1365-2656.2005.00975.x.

Covas, R., Brown, C.R., Anderson, M.D., and Brown, M.B. 2002. Stabilizing selection on body mass in the sociable weaver *Philetairus socius*. Proc. R. Soc. Lond. Ser. B Biol Sci. **269**: 1905–1909. doi:10.1098/rspb.2002.2106.

Einum, S., and Fleming, I.A. 2000. Selection against late emergence and small offspring in Atlantic salmon (*Salmo salar*). Evolution, **54**: 628–639. PMID:10937238.

Elson, P.F. 1957. The importance of size in the change from parr to smolt in Atlantic salmon. Can. Fish Cult. **21**: 1–6.

Finstad, A.G., Einum, S., Forseth, T., and Ugedal, O. 2007. Shelter availability affects behaviour, size-dependent and mean growth of juvenile Atlantic salmon. Freshw. Biol. **52**: 1710–1718. doi:10.1111/j.1365-2427.2007.01799.x.

Good, S.P., Dodson, J.J., Meekan, M.G., and Ryan, D.A.J. 2001. Annual variation in size-selective mortality of Atlantic salmon (*Salmo salar*) fry. Can. J. Fish. Aquat. Sci. **58**: 1187–1195. doi:10.1139/cjfas-58-6-1187.

Grant, P.R., and Grant, B.R. 2002. Unpredictable evolution in a 30-year study of Darwin's finches. Science (Washington, D.C.), **296**: 707–711. doi:10.1126/science.1070315. PMID:11976447.

Gries, G., Whalen, K.G., Juanes, F., and Parrish, D.L. 1997. Nocturnal activity of juvenile Atlantic salmon (*Salmo salar*) in late summer: evidence of diel activity partitioning. Can. J. Fish. Aquat. Sci. **54**: 1408–1413. doi:10.1139/cjfas-54-6-1408.

Heggenes, J., and Borgstrom, R. 1988. Effect of mink, *Mustela vison* Schruber, predation on cohorts of juvenile Atlantic salmon, *Salmo salar* L., and brown trout, *S. trutta* L., in three small streams. J. Fish Biol. **33**: 885–894. doi:10.1111/j.1095-8649.1988.tb05536.x.

Hendry, A.P., Letcher, B.H., and Gries, G. 2003. Natural selection in a restoration program for an extirpated population: size, condition and growth of Atlantic salmon in the Connecticut River. Conserv. Biol. **17**: 795–805. doi:10.1046/j.1523-1739.2003.02075.x.

Hersch, E.I., and Phillips, P.C. 2004. Power and potential bias in field studies of natural selection. Evolution, **58**: 479–485. PMID:15119432.

Hestbeck, J.B. 1995. Bias in transition-specific survival and movement probabilities estimated using capture–recapture data. J. Appl. Stat. **22**: 737–750. doi:10.1080/02664769524586.

Hestbeck, J.B., Nichols, J.D., and Malecki, R.A. 1991. Estimates of movement and site fidelity using mark resight data of wintering Canada geese. Ecology, **72**: 523–533. doi:10.2307/2937193.

Kingsolver, J.G., and Smith, S.G. 1995. Estimating selection on quantitative traits using capture–recapture data. Evolution, **49**: 384–388. doi:10.2307/2410350.

Kingsolver, J.G., Hoekstra, H.E., Hoekstra, J.M., Berrigan, D., Vignieri, S.N., Hill, C.E., Hoang, A., Gibert, P., and Beerli, P. 2001. The strength of phenotypic selection in natural populations. Am. Nat. **157**: 245–261. doi:10.1086/319193.

Lande, R., and Arnold, S.J. 1983. The measurement of selection on correlated characters. Evolution, **37**: 1210–1226. doi:10.2307/2408842.

Lebreton, J.D., and Pradel, R. 2002. Multistate recapture models: modelling incomplete individual histories. J. Appl. Stat. **29**: 353–369. doi:10.1080/02664760120108638.

Lebreton, J.D., Burnham, K.P., Clobert, J., and Anderson, D.R. 1992. Modeling survival and testing biological hypotheses using marked animals: a unified approach with case studies. Ecol. Monogr. **62**: 67–118. doi:10.2307/2937171.

Lebreton, J.D., Hines, J.E., Pradel, R., Nichols, J.D., and Spendelow, J.A. 2003. Estimation by capture–recapture of recruitment and dispersal over several sites. Oikos, **101**: 253–264. doi:10.1034/j.1600-0706.2003.11848.x.

Letcher, B.H., and Gries, G. 2003. Effects of life history variation on size and growth in stream-dwelling Atlantic salmon. J. Fish Biol. **62**: 97–114. doi:10.1046/j.1095-8649.2003.00009.x.

Letcher, B.H., Gries, G., and Juanes, F. 2002. Survival of stream-dwelling Atlantic salmon: effects of life history variation, season and age. Trans. Am. Fish. Soc. **131**: 838–854. doi:10.1577/1548-8659(2002)131<0838:SOSDAS>2.0.CO;2.

Letcher, B.H., Dubreuil, T.D., O'Donnell, M.J., Obedzinski, M., Griswold, K., and Nislow, K.H. 2004. Long-term consequences of variation in timing and manner of fry introduction on juvenile Atlantic salmon growth, survival and life history expression. Can. J. Fish. Aquat. Sci. **61**: 2288–2301. doi:10.1139/f04-214.

Letcher, B.H., Horton, G.E., Dubreuil, T.L., and O'Donnell, M.J. 2005. A field test of the extent of bias in selection estimates after accounting for emigration. Evol. Ecol. Res. **7**: 643–650.

Mcadam, A.G., and Boutin, S. 2003. Variation in viability selection among cohorts of juvenile red squirrels (*Tamiasciurus hudsonicus*). Evolution, **57**: 1689–1697. PMID:12940371.

Merila, J., Sheldon, B.C., and Kruuk, L.E.B. 2001. Explaining stasis: microevolutionary studies in natural populations. Genetica, **112–113**: 199–222. doi:10.1023/A:1013391806317. PMID:11838766.

Metcalfe, N.B. 1998. The interaction between behavior and physiology in determining life history patterns in Atlantic salmon (*Salmo salar*). Can. J. Fish. Aquat. Sci. **55**(Suppl. 1): 93–103. doi:10.1139/cjfas-55-S1-93.

Pfister, C.A., and Stevens, F.R. 2002. The genesis of size variability in plants and animals. Ecology, **83**: 59–72.

Pradel, R., Wintrebert, C.M.A., and Gimenez, O. 2003. A proposal for a goodness-of-fit test to the Arnason–Schwarz multisite capture–recapture model. Biometrics, **59**: 43–53. doi:10.1111/1541-0420.00006. PMID:12762440.

Preziosi, R.F., and Fairbairn, D.J. 2000. Lifetime selection on adult body size and components of body size in a waterstrider: opposing selection and maintenance of sexual size dimorphism. Evolution, **54**: 558–566. PMID:10937232.

Roff, D.A. 1992. The evolution of life histories. Chapman and Hall, New York.

Schluter, D. 1988. Estimating the form of natural-selection on a quantitative trait. Evolution, **42**: 849–861. doi:10.2307/2408904.

Zabel, R.W., and Achord, S. 2004. Relating size of juveniles to survival within and among populations of chinook salmon. Ecology, **85**: 795–806. doi:10.1890/02-0719.

Zabel, R.W., Wagner, T., Congleton, J.L., Smith, S.G., and Williams, J.G. 2005. Survival and selection of migrating salmon from capture–recapture models with individual traits. Ecol. Appl. **15**: 1427–1439. doi:10.1890/04-0940.

Zydlewski, G., Horton, G.E., Dubreuil, T.L., Letcher, B.H., Zydlewski, J., and Casey, S. 2006. Remote monitoring of fish in small streams: a unified approach using PIT tags. Fisheries, **31**: 492–502. doi:10.1577/1548-8446(2006)31[492:RMOFIS]2.0.CO;2.

Appendix A

Table A1 appears on the next page.

© 2008 NRC Canada

Table A1. Design matrix for estimating a quadratic state-trend in *S*. In this example, there are five states and five intervals.

		Beta parameters														
State	Interval	1	2	3	4	5	6	7	8	9	10	11	12	13	14	15
1	1	1	1	1	0	0	0	0	0	0	0	0	0	0	0	0
1	2	0	0	0	1	1	1	0	0	0	0	0	0	0	0	0
1	3	0	0	0	0	0	0	1	1	1	0	0	0	0	0	0
1	4	0	0	0	0	0	0	0	0	0	1	1	1	0	0	0
1	5	0	0	0	0	0	0	0	0	0	0	0	0	1	1	1
2	1	1	2	4	0	0	0	0	0	0	0	0	0	0	0	0
2	2	0	0	0	1	2	4	0	0	0	0	0	0	0	0	0
2	3	0	0	0	0	0	0	1	2	4	0	0	0	0	0	0
2	4	0	0	0	0	0	0	0	0	0	1	2	4	0	0	0
2	5	0	0	0	0	0	0	0	0	0	0	0	0	1	2	4
3	1	1	3	9	0	0	0	0	0	0	0	0	0	0	0	0
3	2	0	0	0	1	3	9	0	0	0	0	0	0	0	0	0
3	3	0	0	0	0	0	0	1	3	9	0	0	0	0	0	0
3	4	0	0	0	0	0	0	0	0	0	1	3	9	0	0	0
3	5	0	0	0	0	0	0	0	0	0	0	0	0	1	3	9
4	1	1	4	16	0	0	0	0	0	0	0	0	0	0	0	0
4	2	0	0	0	1	4	16	0	0	0	0	0	0	0	0	0
4	3	0	0	0	0	0	0	1	4	16	0	0	0	0	0	0
4	4	0	0	0	0	0	0	0	0	0	1	4	16	0	0	0
4	5	0	0	0	0	0	0	0	0	0	0	0	0	1	4	16
5	1	1	5	25	0	0	0	0	0	0	0	0	0	0	0	0
5	2	0	0	0	1	5	25	0	0	0	0	0	0	0	0	0
5	3	0	0	0	0	0	0	1	5	25	0	0	0	0	0	0
5	4	0	0	0	0	0	0	0	0	0	1	5	25	0	0	0
5	5	0	0	0	0	0	0	0	0	0	0	0	0	1	5	25

Note: Each column is the estimate for a single beta parameter. This model estimates a quadratic trend across states for each interval. For example, parameter 1 is the intercept, parameter 2 is the linear coefficient, and parameter 3 is the quadratic coefficient for the state-trend estimate for interval 1. The matrix does not include parameters for estimating p and Ψ, which followed the conventional $(*.t)$ design.

© 2008 NRC Canada

Are wild populations ideally distributed? Variations in density-dependent habitat use by age class in juvenile Atlantic salmon (*Salmo salar*)

A. Jamie F. Gibson, Heather D. Bowlby, and Peter G. Amiro

Abstract: We examined relationships between abundance and habitat use in three age classes of juvenile Atlantic salmon (*Salmo salar*) in the Stewiacke River, Nova Scotia, Canada. Using stream gradient as a proxy for habitat quality, we used a double half normal function, modified to include density dependence, to model the relationship between habitat quality and fish density. We found that density was asymmetrically distributed around a similar optimum gradient for all three age classes regardless of abundance. Habitat use was highly density-dependent for age-0 and age-1 juveniles, but not for age-2+ salmon. As abundance of age-0 and age-1 salmon increased, their relative density decreased in low-gradient habitat and increased in higher-gradient habitat, although their absolute density increased in all stream gradient categories. Variation in habitat use was consistent with ideal free theory for age-1 juveniles in high-gradient habitat, but not in low-gradient habitat. Age-2+ individuals appeared not to modify their distribution among habitats, even though increasing competition changes the relative benefit of low-gradient habitat in terms of resource acquisition. In contrast, age-1 individuals responded to increased competition by modifying their distribution along the habitat gradient, even though this may have slightly reduced an individual's potential for growth.

Résumé : Nous examinons les relations entre l'abondance et l'utilisation des habitats chez trois classes d'âge de saumons atlantiques (*Salmo salar*) juvéniles dans la rivière Stewiacke, Nouvelle-Écosse, Canada. En utilisant la pente du cours d'eau comme variable de remplacement de la qualité de l'habitat, nous modélisons, à l'aide d'une fonction normale semi-double modifiée pour inclure la densité dépendance, la relation entre la qualité de l'habitat et la densité des poissons. Nous observons que la densité se répartit de façon asymétrique autour d'une pente optimale similaire pour les trois classes d'âge, indépendamment de la densité. L'utilisation de l'habitat est fortement dépendante de la densité chez les jeunes d'âges 0 et 1, mais non chez les saumons d'âge 2+. À mesure que la densité des saumons d'âge 0 et 1 augmente, leur densité relative diminue dans les habitats à pente faible et augmente dans les habitats à pente forte, alors que leur densité absolue augmente dans toutes les catégories de pentes du cours d'eau. La variation dans l'utilisation des habitats s'accorde avec la théorie de la distribution libre idéale chez les jeunes d'âge 1 dans les habitats à forte pente, mais non dans les habitats à pente faible. Les individus d'âge 2+ semblent ne pas modifier leur répartition dans les divers habitats, bien la compétition croissante modifie les avantages relatifs des habitats de pente faible en ce qui a trait à l'acquisition des ressources. En revanche, les individus d'âge 1 réagissent à l'augmentation de la compétition en modifiant leur répartition le long du gradient des habitats, bien que ce déplacement réduise légèrement leur potentiel de croissance individuelle.

[Traduit par la Rédaction]

Introduction

Density-dependent habitat selection is an important conceptual framework that has been developed to explain how distribution patterns change in response to interactions among individuals within a population (Morris et al. 2001; Jonzen et al. 2004). Habitat selection facilitates coexistence and provides a convenient mechanism for measuring competition and describing the form of competitive interactions (Morris 2003). Several mechanisms leading to density-dependent habitat selection have been proposed, based on ideal distribution assumptions (that individuals act to maximize fitness) (Kramer et al. 1997). Under the ideal free distribution (Fretwell and Lucas 1970), individuals have equal access to resources and choose habitat so as to balance mean habitat quality, and thus individual fitness, throughout the population's distribution (Morris 2003; Girard et al. 2004). In contrast, unequal access to resources (resulting from territoriality, for example) can result in one of two habitat selection patterns, an ideal despotic or an ideal pre-emptive distribution. Under the ideal despotic distribution (Fretwell 1972), intraspecific competition forces inferior individuals to occupy suboptimal habitats once available territories in optimal habitats are saturated (Morris 2003; Hedger et al. 2005). The ideal pre-emptive distribution (Pulliam and Danielson 1991) is similar, although prior residency rather than competitive ability determines habitat occupancy (Rodriguez 1995). Although these theories predict similar patterns of variation in density among habitats as population abundance increases, the relative fitness of individuals in different habitat types would be expected to

Received 13 April 2007. Accepted 25 February 2008. Published on the NRC Research Press Web site at cjfas.nrc.ca on 16 July 2008.
J19941

A.J.F. Gibson,[1] H.D. Bowlby, and P.G. Amiro. Population Ecology Division, Science Branch, Department of Fisheries and Oceans, P.O. Box 1006, Dartmouth, NS B2Y 4A2, Canada.

[1]Corresponding author (e-mail: gibsonajf@mar.dfo-mpo.gc.ca).

 doi:10.1139/F08-087 © 2008 NRC Canada

vary only if they had unequal access to resources (Rodriguez 1995; Hedger et al. 2005).

In juvenile Atlantic salmon (*Salmo salar*), density-dependent processes (potentially affecting habitat selection, growth, mortality, and dispersal) are thought to occur exclusively in the freshwater environment (Jonsson et al. 1998; Armstrong 2005). Although density-dependent growth and mortality in wild populations has been well documented (Milner et al. 2003; Armstrong 2005), density-dependent habitat selection has rarely been investigated outside an experimental setting (but refer to Rodriguez (1995) and Hedger et al. (2005) for examples). Therefore, it is unknown how large an impact habitat selection has on population regulation relative to other density-dependent processes and environmental variation. One hypothesis is that density dependence is strongly expressed very early in ontogeny (egg-to-fry stage) as mortality (Crozier and Kennedy 1995; Cunjak and Therrien 1998; Milner et al. 2003), whereas later stages respond to local density in terms of increased dispersal and (or) slower growth rates (Einum et al. 2006). Given that dispersal ability is a prerequisite for habitat choice, one might expect that density-dependent habitat selection would be expressed primarily in older individuals because of their increased ability to disperse to, and defend, favourable areas (Blanchet et al. 2006). A second hypothesis is that exploitative competition for food occurs at much lower densities than interference competition for space over various temporal and spatial scales (Imre et al. 2005). In this scenario, density-dependent habitat selection could be masked by other behavioural processes within the range of fish densities observable in the wild. Furthermore, behavioural responses to density may be small relative to environmental influences on juvenile distribution. Although the distribution of many teleost species (Marshall and Frank 1995; Gaston et al. 1997; Fromentin et al. 2001), including juvenile salmonids (Milner et al. 2003; Armstrong 2005), has been found to expand with increasing abundance, variation in habitat suitability over time (caused by environmental change) could conceivably produce similar patterns (Shepherd and Litvak 2004, Einum 2005).

Mobile organisms make decisions to enter and (or) occupy certain areas based on the relative benefit to the individual (Kramer et al. 1997), so the patterns of habitat use in a population can provide evidence of habitat selection. However, to reliably investigate the importance of density-dependent habitat selection on localized distribution patterns in the presence of density-independent environmental variation requires a data set with unique characteristics: (*i*) monitoring effort must be distributed randomly across a habitat gradient, (*ii*) data collection must be long term and over the spatial scale at which density dependence likely operates, (*iii*) localized population density must be measured in such a way as to be indicative of total population abundance, (*iv*) the species of interest must undergo substantial changes in population density over the course of the study, (*v*) population monitoring must target the life stage or stages affected by density dependence, and (*vi*) a proxy for individual fitness (such as growth, fecundity, or age-at-maturity) must be measured concurrently with density (Rose et al. 2001; Shepherd and Litvak 2004; Freckleton et al. 2006). In a natural situation, such data cannot be collected unless a population undergoes significant changes in abundance while extensive monitoring programs are in place.

To determine if the distribution of juvenile Atlantic salmon provides evidence for density-dependent habitat selection in the wild, we developed a set of models to describe potential density-dependent and density-independent patterns in habitat use. These were fit to juvenile density data collected by electrofishing in the Stewiacke River, Nova Scotia, a data set with all of the above prescribed features. The Stewiacke River salmon population is part of the Inner Bay of Fundy Atlantic salmon population assemblage designated as endangered by the Committee on the Status of Endangered Wildlife in Canada (COSEWIC 2006). The electrofishing survey used a random stratified design for site selection in which sampling locations were randomly selected from stratified habitat types, thus controlling for environmental variation. Coupled with this approach was an evaluation of the effect of density on individual fitness, here represented by length-at-age, to assess whether individuals were choosing habitat as predicted by ideal distribution theory. Length-at-age, indicative of individual growth rate, is known to be a fitness-related trait in salmonids (Hutchings and Jones 1998; Blanchet et al. 2006) and was used as a proxy for individual fitness. Of particular interest (relative to ideal distribution theory) were (*i*) differences among age classes in optimal habitat selection, where the habitat gradient at which an age class was most densely distributed was considered to be optimal, (*ii*) changes in distribution among habitats as population abundance changed through time, and (*iii*) changes in the average fitness of individuals as populations declined over time relative to mean fitness in different habitats.

Materials and methods

Data collection

Juvenile abundance in this river was monitored continuously from 1984 to 2002 by electrofishing at sites that were randomly selected from strata defined by habitat type. Habitat classification and site selection along the Stewiacke River is explained in detail by Amiro (1984, 1993). In brief, the river was partitioned into reaches, based on contour intervals from orthographic maps, and grouped into 11 gradient categories (strata; 0.25% intervals). The area-weighted surface gradient (AWSG) of randomly selected reaches within each category was measured in situ and used to determine the relationship between AWSG and the gradient measured on orthographic maps. Habitat types within the stream were classified according to similarities in bottom type and flow characteristics, and gradients were weighted according the proportion of each habitat type they contained (Amiro 1993). This controls for potential biases related to heterogeneity in habitat type among sampling units. Based on these results, electrofishing sampling sites (~100 m in length) were chosen using a random stratified design, where gradient strata (range = 0% to 2.5% AWSG) were sampled in proportion to the amount of juvenile habitat (based on stream gradient and distance from the river mouth) in each (Amiro et al. 1989; Amiro 1993). AWSG is a determinant of water flow characteristics, a reflection of channel morphology and sediment sorting processes (Yang 1971), and a useful indicator of the amount of energy required to occupy a habitat (Armstrong et al. 2003; Blanchet et al. 2006).

© 2008 NRC Canada

These factors have been shown to strongly influence habitat use and distribution in juvenile salmon (Armstrong et al. 2003).

Between 27 and 44 sites on the Stewiacke River were electrofished on an annual basis, starting in July and finishing in August of each year (Gibson and Amiro 2003). Sites were fished in a random order to control for temporal variation in growth among juvenile assemblages. Although the selection of sites varied among years, each gradient category was sampled representatively each year (the proportion of sites sampled annually in each gradient category remained constant). Provided that a sufficient number of juveniles was captured initially, salmon abundance within a site was estimated using Peterson mark–recapture methods, and catchability was estimated by dividing the number of marked fish by the number caught during the recapture pass (Amiro et al. 1989). Annual mean catchability was used to estimate fish abundance for sites where mark–recapture was not possible. The densities of three age classes, age-0, age-1, and age-2+ (age-2 plus the small proportion of individuals that remained in the river for longer than 2 years) were estimated for each site based on the aging of scale samples. For all juveniles age-1 and older, fork length was measured to the nearest millimetre.

Habitat-abundance models

In the analyses that follow, we used the AWSG as the habitat variable. For each age class, we used a double half normal function to model the relationship between the density of juvenile salmon in year t at site i, $D_{i,t}$, and the AWSG of the site:

$$(1)\qquad D_{i,t} = \beta_0(\overline{D}_t)\begin{Bmatrix} \exp\left(\dfrac{-(\mu - \mathrm{AWSG}_i)^2}{\sigma_L}\right) & \text{if } \mathrm{grad}_i \le \mu \\ \exp\left(\dfrac{-(\mu - \mathrm{AWSG}_i)^2}{\sigma_R}\right) & \text{if } \mathrm{grad}_i > \mu \end{Bmatrix}$$

In this model, the stream gradient at which an age class is most densely distributed is denoted by μ. The steepness of the decline away from maximum density is described by independent standard deviations for the left (σ_L) and right (σ_R) sides of the curve. The component of the function within the braces has a maximum value of 1. The term β_0 is the ratio of the maximum expected density at any site (for a given year and age class) to the mean density in a given year and age class ($\overline{D}_t$). The term $\beta_0\overline{D}_t$ thus rescales the range of the function from the interval [0, 1] to the expected range of densities for a given mean abundance. Previous research has used a second-order polynomial to model the relationship between abundance and distribution (e.g., Talbot 1994). This is equivalent to fitting our base model with symmetrical variation in density in suboptimal habitat ($\sigma_L = \sigma_R$).

Density dependence was incorporated into the modelling process by treating μ, σ_L, and σ_R as linear functions of the average density by substituting the following expressions into eq. 1:

Fig. 1. The double half normal function used to model the density of juvenile salmon (*Salmo salar*) in a river as a function of stream gradient and abundance. This function has three parameters: μ, which is the preferred gradient category, σ_L, which determines how rapidly fish density decreases as stream gradient decreases from μ, and σ_R, which determines how rapidly fish density decreases as stream gradient increases from μ. Density dependence is included by modelling μ, σ_L, and σ_R as linear functions of abundance within the river. The slopes of these equations, β_2, β_4, and β_6, respectively, modify the shape of the habitat-density model as abundance changes.

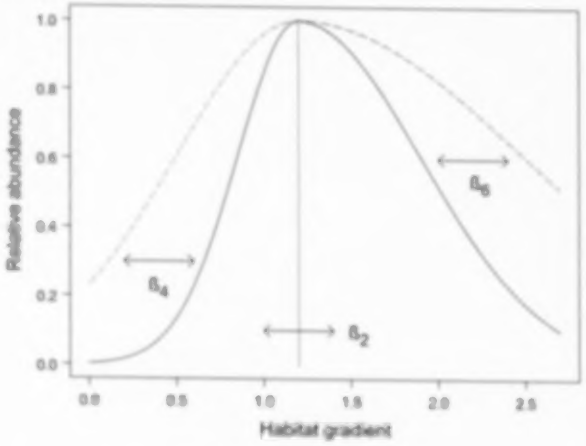

$$(2)\qquad \mu = \beta_1 + \beta_2\overline{D}_t$$

$$(3)\qquad \sigma_L = \beta_3 + \beta_4\overline{D}_t$$

and (or)

$$(4)\qquad \sigma_R = \beta_5 + \beta_6\overline{D}_t$$

where β_1, β_3, and β_5 are intercept terms, and the coefficients β_2, β_4, and β_6, if different from zero, modify the relationship between the density of fish and stream gradient as the mean abundance changes (Fig. 1). The coefficient β_2 shifts the function to the right or left through its effect on μ, whereas β_4 and β_6 change the way in which fish are distributed with respect to stream gradient through their effect on σ_L and σ_R.

With slight changes to its formulation, this model is sufficiently flexible to compare several biological scenarios, making it possible to describe and evaluate changes in the relationship between stream gradient and salmon density. The biological hypotheses represented by these models describe potential population-level responses to local changes in density, which could be manifested in several ways: (*i*) the preferred habitat type of each age class may shift, (*ii*) individuals may redistribute into marginal habitats or become more concentrated in primary habitat, or (*iii*) do both concurrently. Here, we used nine model variants, five of which incorporated density dependence, to evaluate the above hypotheses for each age class of juvenile salmon (Table 1). The null model is simply that juvenile salmon are equally distributed over stream gradients, i.e., no relationship between density and AWSG exists. In this case, the

© 2008 NRC Canada

Table 1. Summary of the characteristics of the models used to evaluate the relationship between fish density and stream gradient, in addition to the influence of density dependence on this relationship.

Model	Relationship between fish density and habitat gradient	Hypothesis about density-dependent habitat use	Density-dependent parameters	Equations	Constraints	No. of parameters to be estimated
Null	None	Not density-dependent				1
1	Symmetrical	Not density- dependent		1	$\sigma_L = \sigma_R$	3
2	Symmetrical	Change in preferred habitat	μ	1, 2	$\sigma_L = \sigma_R$	4
3	Symmetrical	Redistribution in marginal habitat	σ_L	1, 3	$\sigma_L = \sigma_R$	4
4	Symmetrical	Change in both preferred habitat and redistribution in marginal habitat	μ, σ_L	1, 2, 3	$\sigma_L = \sigma_R$	5
5	Asymmetrical	Not density- dependent		1		4
6	Asymmetrical	Change in preferred habitat	μ	1, 2		5
7	Asymmetrical	Redistribution in marginal habitat	σ_L, σ_R	1, 3, 4		6
8	Asymmetrical	Both change in preferred habitat and redistribution in marginal habitat	μ, σ_L, σ_R	1, 2, 3, 4		7

Note: Equations are provided in the text.

expected fish density at site i is simply the average density for that age class in the given year:

$$(5) \qquad D_{i,t} = \overline{D}_t$$

In models 1 to 4 (Table 1), juvenile salmon are more concentrated in specific habitat, with symmetrical variation in density in suboptimal habitat, as described by eq. 1 with $\sigma_L = \sigma_R$. Habitat use is not density dependent in model 1. In model 2, preferred habitat (μ) varies in response to changes in abundance (one potential density-dependent response), but the rate of decline from maximum density remains constant and symmetrical with respect to abundance (substitute eq. 2 into eq. 1). In model 3, preferred habitat does not change with abundance, but the distribution of salmon in suboptimal habitat (σ_L) does change (a second potential density-dependent response) but remains symmetrical ($\sigma_L = \sigma_R$) (substitute eq. 3 into eq. 1). In model 4, both the preferred habitat and the symmetric distribution of salmon in suboptimal habitat change with abundance (both types of density dependence; substitute both eq. 2 and eq. 3 into eq. 1). Models 1 to 4 incorporate the assumption that individuals show no preference for lower-gradient or higher-gradient suboptimal habitats. If this assumption is relaxed, the function can be asymmetric around μ. The remaining models (models 5–8) allow for this asymmetry but are otherwise biologically equivalent to models 1 through 4. Within all models, note that the predictor $\overline{D}_t$ (mean density) could be any of five variables: age-class density (age-0, age-1, or age-2+, respectively), mean density of parr (age-1 and age-2+), or mean density of age-0, age-1, and age-2+ salmon combined. Although we examined all possible predictors, the lowest Akaike information criterion (AIC) was consistently found for models in which age-class density was the independent variable. In the analyses presented herein, we used age-class density as the index of annual abundance for each modeling scenario. This implies that density dependence represents competition within an age class, rather than among age classes, even though it is biologically plausible that intercohort relationships effect the distribution of juveniles among habitat types.

Parameter estimates for each age class and model combination were obtained using maximum likelihood assuming a Poisson error structure for the densities of salmon at each site (McCullagh and Nelder 1989). A quasi-Newton optimizer, "NLMIN" in S-Plus (Venables and Ripley 2002), was used to find the minimum of the negative of the log likelihood ($\ell(\mathbf{D}|\mathbf{AWSG}, g)$), given by

$$(6) \qquad \ell(\mathbf{D}|\mathbf{AWSG}, g) = \sum_{i,t}(D_{i,t}\ln(g(\mathrm{AWSG}_i)) - g(\mathrm{AWSG}_i) - \ln\Gamma(D_{i,t} + 1))$$

where g is one of the habitat-abundance models. We used AIC to assess the trade-off between model fit to the data and the number of parameters in the model (Hilborn and Mangel 1997). The model with the lowest AIC was selected as the preferred model.

To determine the statistical significance of parameters β_2, β_4, and β_6, we used profile likelihoods (Davison and Hinkley 1997). Using β_i to denote a model parameter and $\boldsymbol{\beta}$ to denote all other parameters in the model, the log profile likelihood for β_i, $\ell_p(\beta_i)$, is

$$(7) \qquad \ell_p(\beta_i) = \max_{\boldsymbol{\beta}} \ell(\beta_i, \boldsymbol{\beta})$$

The maximum likelihood estimate for β_i occurs where $\ell_p(\beta_i)$ achieves its maximum value. The plausibility of other possible values of β_i was evaluated by comparing their log likelihoods with the maximized log likelihood. A likelihood-based 95% confidence interval for β_i is

$$(8) \qquad \{\beta_i : 2[\ell_p(\beta_i^{\mathrm{MLE}}) - \ell_p(\beta_i)] \leq \chi_1^2(0.95)\}$$

We concluded that habitat use by juvenile salmon changed significantly with abundance if the 95% confidence interval for the slopes (β_2, β_4, or β_6) did not include zero.

© 2008 NRC Canada

Fig. 2. Box plots showing the distributions of densities of (*a*) age-0, (*b*) age-1, and (*c*) age-2+ juvenile Atlantic salmon (*Salmo salar*) in the Stewiacke River, Nova Scotia, from 1984 to 2002, as determined by electrofishing. The boxes show the interquartile spread, and the line in the box shows the median value. Whiskers are drawn to indicate lowest and highest values within 1.5 times the interquartile range from the quartile. Outliers are shown as points. (Modified from Gibson and Amiro 2003 with permission.)

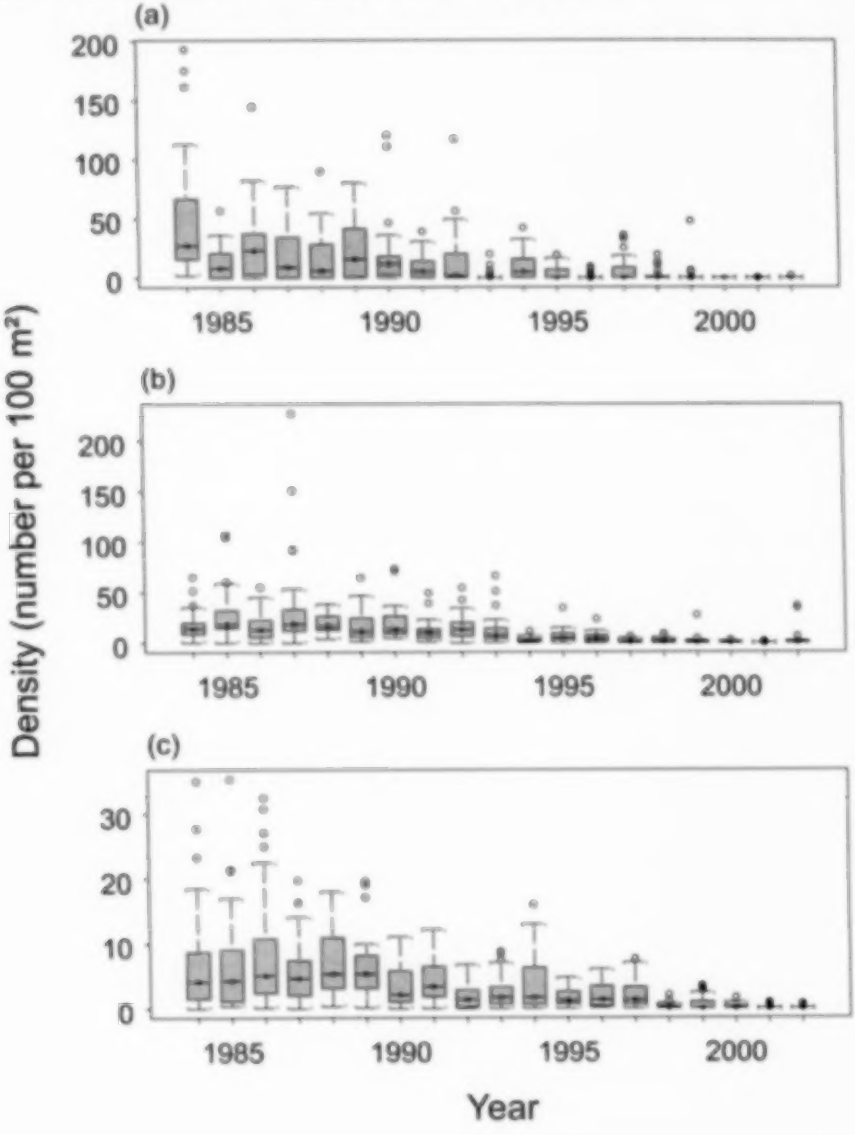

Testing predictions from ideal free theory

If the distribution of juvenile salmon in fresh water follows an ideal free distribution (Fretwell and Lucas 1970), mean habitat suitability (for individuals) should be equal in heterogeneous environments because of differences in juvenile density along the habitat gradient. Regardless of overall age-class abundance or the scale of observation, individual fitness should also be equal in all habitats (Shepherd and Litvak 2004). Here, we use a fitness-correlated trait, length-at-age, to evaluate this hypothesis based on the mean fork lengths of age-1 and age-2+ parr, stream gradients, and individual densities recorded at each site during each year. To identify density-dependent growth in either age class, we used a log linear model to describe the relationship between the length of age-1 or age-2+ parr and mean density:

$$(9) \qquad FL_{i,t} = a + b\left(\ln(\overline{D}_t)\right)$$

where $FL_{i,t}$ is the average fork length of salmon of a given age at site i in year t, and a and b are the regression coefficients estimated by least-squares, linear regression.

© 2008 NRC Canada

Fig. 3. Bubble plots showing how the distribution of three age classes of juvenile Atlantic salmon (*Salmo salar*) in the Stewiacke River, Nova Scotia, changed with respect to stream gradient as the populations declined. Bubble size is proportional to the density of salmon at each site, as determined by electrofishing. Maximum observed densities for (*a*) age-0, (*b*) age-1, and (*c*) age-2+ were 45.9, 33.6, and 8.2 fish·(100 m^2)$^{-1}$, respectively. Black dots indicate densities of zero.

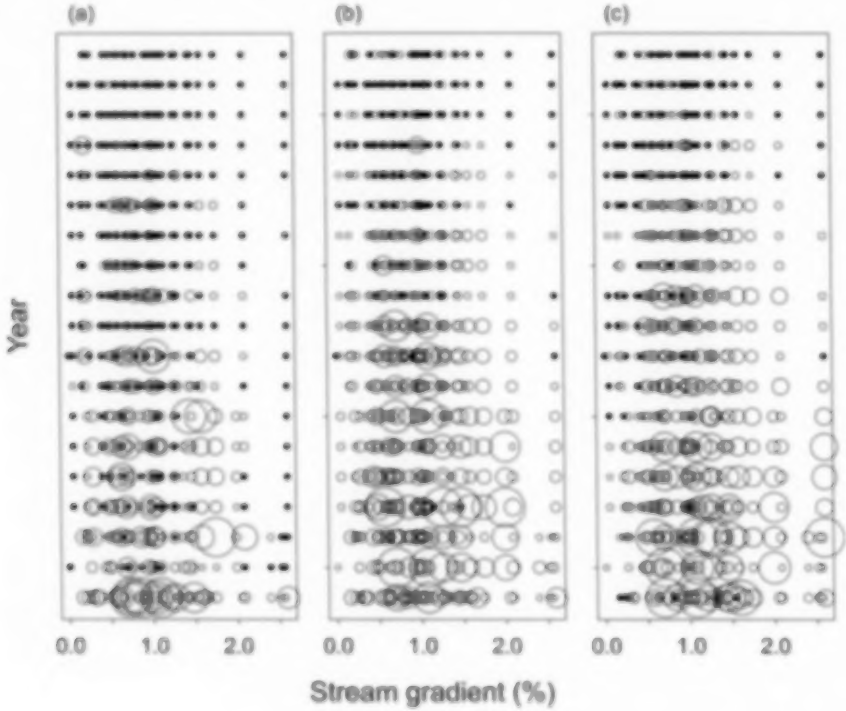

Next, we evaluated whether length-at-age varied with stream gradient using length-at-age – stream gradient linear mixed-effects models. Several types of relationships could exist. If juveniles occupied habitat in a manner described by an ideal free distribution, mean fitness among individuals would be equal and there would be no relationship between length-at-age and stream gradient. If competitively superior individuals occupied preferred habitat types (thus limiting access to resources for other individuals), individual fitness would be higher in preferred vs suboptimal habitat types (Bult et al. 1999), which would be reflected by positive slope estimates in habitat gradients below the optimum and negative estimates above the optimum. If competitive processes such as territoriality are the main factors leading to habitat selection in juvenile salmon, differences in fitness among habitat types should increase with abundance, and the slopes of the length-at-age – stream gradient regressions should become more positive or more negative. Note, however, that it would still be possible for the slope of the length-at-age – stream gradient regression to change with abundance irrespective of the presence of density-dependent habitat selection in the population. Finally, if length-at-age is not a good proxy for individual fitness, the slope of the length-at-age – gradient regression should vary randomly or in a manner not described above.

To investigate the above possibilities, data were split at the estimated optimal gradient (μ) for age-1 and age-2+ juveniles. Initially, the data for each year were considered separately to allow for annual variation in observed density. Linear regressions of mean fork length over stream gradient were fit separately to observations above and below the optimal habitat gradient. Next, we fit linear mixed-effects models (Pinheiro and Bates 2000) to determine the population-level relationship between stream gradient and length-at-age. Four categories were considered based on age and habitat gradient: age-1 below the optimum gradient, age-1 above the optimum, age-2+ below the optimum and age-2+ above the optimum. We assumed that the annual slopes and intercepts of the length-at-age – gradient relationship were normally distributed random variables and fit the mixed-effects models treating annual slopes and intercepts as random effects. Because habitat gradient could act in conjunction with population abundance in its effect on length, a second model considered the combination of habitat gradient and mean abundance as the predictor. In situations in which the interaction term was nonsignificant, it was dropped from the analysis.

Results

The highest densities of juvenile salmon were recorded within the first 4 years of sampling and generally declined

© 2008 NRC Canada

Table 2. Comparison of the negative log likelihoods (NLL) and Akaike information criterion (AIC) for eight models used to evaluate the relationship between density and habitat gradient relative to changes in abundance for three age classes of juvenile salmon in the Stewiacke River, Nova Scotia.

Age class		Model								
		Null	1	2*	3*	4*	5	6*	7*	8*
Age 0	NLL	5781.4	5427.9	5422.6	5423.1	5413.1	5381.9	5372.4	**5362.1**	5362.1
	AIC	5783.4	5433.9	5430.6	5431.1	5423.1	5389.9	5382.4	**5374.1**	5376.1
Age 1	NLL	3577.3	3341.6	3310.5	3339.8	3305.9	3321.0	3304.8	3291.4	**3277.5**
	AIC	3579.3	3347.6	3318.5	3347.8	3315.9	3329.0	3314.8	3303.4	**3291.5**
Age 2+	NLL	1649.2	1470.7	1470.6	1470.7	1469.9	**1434.4**	1434.4	1434.0	1431.6
	AIC	1651.2	1476.7	1478.6	1478.7	1479.9	**1442.4**	1444.4	1446.0	1445.6

Note: The values for preferred models are shown in bold, and those that include a density-dependent component are identified with an asterisk.

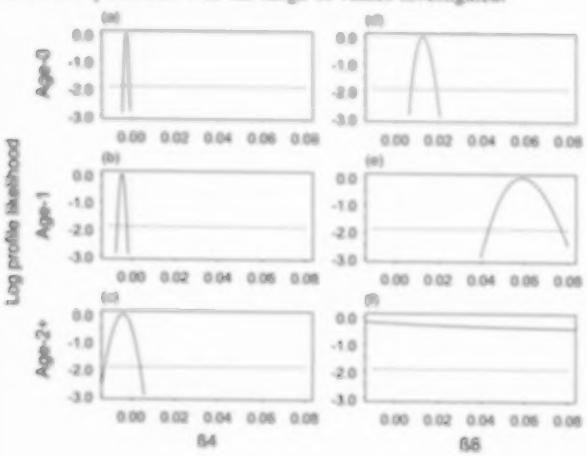

Fig. 4. Profile log likelihoods (solid lines) for (*a*, *b*, *c*) β_4 and (*d*, *e*, *f*) β_6 from model 7 fit to density data from three age classes of juvenile Atlantic salmon (*Salmo salar*) in the Stewiacke River, Nova Scotia. The log likelihoods are standardized to a maximum of zero by subtracting the maximum log likelihood from each estimate. Parameters are statistically different from zero (vertical, dotted line) if zero is not within the interval. The profile for β_6 for age-2+ salmon (*f*) is flat, indicating the data are uninformative about this parameter over the range of values investigated.

Table 3. Maximum likelihood estimates for the coefficients for the preferred models relating habitat use to abundance for three age classes of juvenile Atlantic salmon in the Stewiacke River, Nova Scotia.

	Age class			
	Age 0	Age 1	Age 1	Age 2+
Model	7	7	8	5
u	0.769	0.75		0.823
σ_L				0.281
σ_R				3.571
β_0	1.288	1.195	1.281	1.261
β_1			0.102	
β_2			0.053	
β_3	0.518	0.463	–0.0471	
β_4	–0.003	–0.004	0.039	
β_5	0.658	0.686	1.825	
β_6	0.013	0.058	–0.0418	

Note: Models and model selection are described in the text.

over time at all sites (Fig. 2). Maximum annual mean densities for age-0, age-1, and age-2+ salmon were 45.9, 33.6, and 8.2 fish·(100 m^2)$^{-1}$ in the 1980s, which dropped to minima of 0, 0.07, and 0.06 fish·(100 m^2)$^{-1}$, respectively, in the later years of the study. When changes in density were compared with stream gradient, two patterns were evident in the data: (*i*) age-class density was not equal among sites with different gradients in any year (excluding years with zero density at all sites), and (*ii*) the decline in age-class density within a site over time was not constant among sites with different gradients (Fig. 3). Generally, sites with intermediate gradients contained the highest densities of juvenile salmon when compared with either low-gradient or high-gradient habitat, although this difference was less pronounced for high-gradient sites. Similarly, sites with intermediate gradients tended to have higher recorded densities of juveniles for more years than either low-gradient or high-gradient sites. Again, this difference was less pronounced for high-gradient sites. Taken together, these patterns suggest that the distribution of each age class of juvenile salmon is influenced by habitat characteristics, as well as by fish density.

Based on model AIC and parameter profile likelihoods, a density-dependent model provided the best description of the observed variation in density among habitats over time for age-0 (model 7) and age-1 (model 8), but not age-2+ (model 5), juvenile salmon (Table 2). Models with symmetrical distributions about the preferred gradient category had much higher AICs than did models with asymmetric distributions, suggesting that high-gradient habitat has a higher carrying capacity than low-gradient habitat. The predicted center of distribution for each age class was similar, indicating that all ages of juvenile salmon were most concentrated in habitats where the AWSG was between 0.75 and 0.82 (Fig. 3).

For age-0 salmon, model 7 (asymmetric, density-dependent changes in distribution in suboptimal habitat) was the preferred model, although the AIC was not substantially lower than that for model 8 (in which the preferred habitat also changes). The profile likelihood plots for parameters β_4 and β_6 demonstrated that the distribution of age-0 salmon in low- or high-gradient habitats changed significantly

© 2008 NRC Canada

Fig. 5. Relationships between density and stream gradient for three age classes of juvenile Atlantic salmon (*Salmo salar*) in the Stewiacke River, Nova Scotia. The points in the left-column plots (*a*, *b*, *c*) are the observed densities from 1984 to 2002 and are coded based on whether they were collected in years when the annual mean density was above (open circles) or below (solid circles) its median value. The solid lines show the predicted densities obtained at the first and third quartiles of the annual mean abundance ($\bar{D}_i$), and the broken lines indicate the stream gradient with the highest predicted density. Right-column plots (*d*, *e*, *f*) show predicted relative densities from model 7 at the lowest (solid line), median (dotted line), and highest (broken line) annual mean abundances ($\bar{D}_i$) observed between 1984 and 2002.

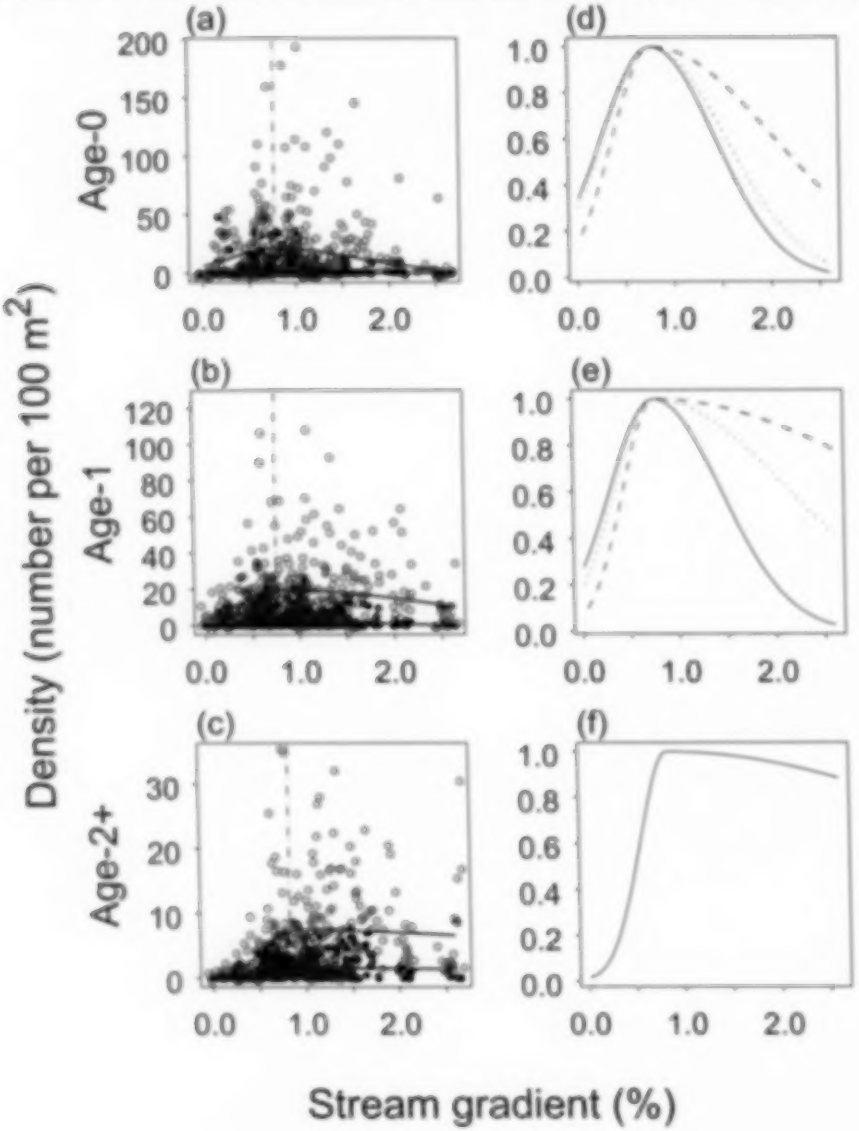

with abundance, as the 95% confidence limits for these parameters did not include zero (Fig. 4). Increased use of low- and high-gradient marginal habitats was expected as abundance increased. However, estimates for β_4 were negative (Table 3), indicating that as abundance increased, the "relative" density of juveniles in low-gradient habitat decreased (Fig. 5, right panels), although the "absolute" density in low-gradient habitat increased (Fig. 5, left panels). Over the range of abundances observed in this study, relative density of age-0 salmon at a stream gradient of 0% decreased by a factor of about 2.2 as abundance increased. In contrast, at a stream gradient of 2.5%, relative density increased with increasing abundance by a factor of 12.

Model 8 (in which preferred habitat and distribution in suboptimal habitat changed with abundance) had the lowest AIC for age-1 salmon. However, when attempting to generate the profile likelihoods, we found that this model was not very stable (it would converge to local rather than global

© 2008 NRC Canada

Fig. 6. The fitted (solid line) and observed (points) mean fork length of (*a*) age-1 and (*b*) age-2+ Atlantic salmon (*Salmo salar*) relative to density in the Stewiacke River, Nova Scotia, from 1984 to 2002. Each point shows the mean length of salmon at a single electrofishing site plotted against the average density for the year. Broken lines show the 95% confidence limits for the model fit.

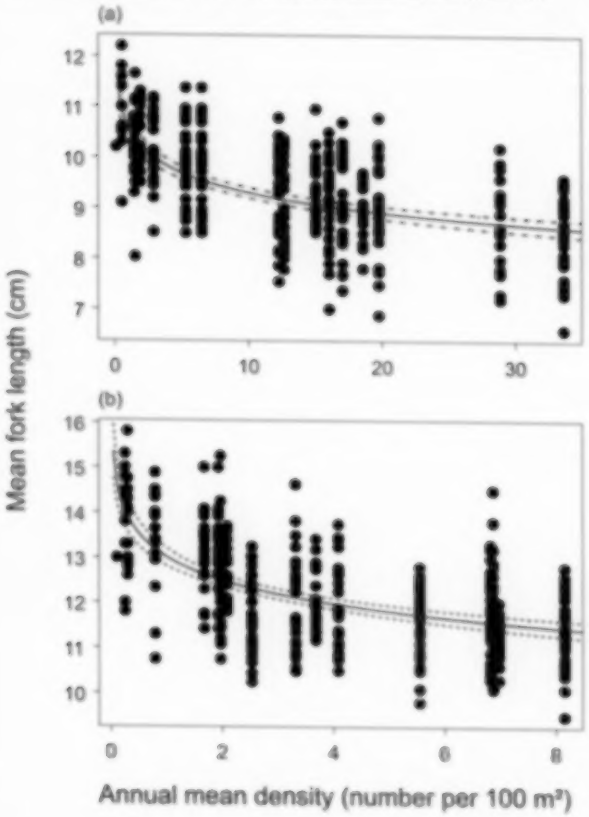

minima and was sensitive to starting values). Therefore, we focused on the second most likely scenario for age-1 parr (model 7), even though it is biologically plausible that preferred habitat changes with abundance for this age class. For model 7, the profile likelihood plots for parameters β_4 and β_5 demonstrated that the distribution of age-1 salmon in low- or high-gradient habitats changed significantly with density (Fig. 4) and the changes were in the same direction as for age-0 salmon (Table 3). Over the range of age-1 abundances observed in this study, relative density in low-gradient habitat (0% AWSG) decreased by 3.7 times as abundance increased (Fig. 5), whereas in high-gradient habitats (2.5% AWSG), relative density increased by a factor of 20 as abundance increased.

Model 5 (an asymmetric distribution without density dependence) had the lowest AIC for age-2+ salmon (Table 2). In contrast with the younger age classes, both 95% confidence intervals for β_4 and β_5 for age-2+ salmon obtained from model 7 included zero, further supporting the idea that the distribution of fish in low-gradient, as well as high-gradient, habitat did not vary significantly with abundance (Fig. 4). Large parr appeared to be more concentrated in high-gradient habitats than in low-gradient areas, regardless of overall abundance. Although model 6 (asymmetric distribution, preferred habitat changes with abundance) had a similar AIC value to that of model 5, the 95% confidence interval for parameter β_2 included zero (data not shown). Therefore, it is similarly unlikely that optimal habitat changed with abundance over the range of age-2+ densities observed in the wild.

One would expect an inverse relationship between abundance and fitness-related traits if the resources available to a population were limiting. For Stewiacke River salmon, we found that length-at-age decreased significantly with increasing abundance for age-1 (p value < 0.001) and age-2+ (p value < 0.001) fish (Fig. 6). On average, individuals of either age class were approximately 2 cm larger when juvenile abundance was low than when it was high, which is indicative of density-dependent growth in both age classes.

If an ideal free distribution characterizes the distribution of individuals among habitats, then individual fitness should not differ among habitat types. For Stewiacke River salmon, we found that the relationship between fork length and stream gradient varied among gradient categories, as well as among years (Fig. 7). For age-1 salmon in habitat gradients below the optimum, none of the slopes of the length-at-age – stream gradient regressions (Fig. 7) was significantly different from zero (95% confidence level; Fig. 8), but the estimated slopes were less than zero in 12 of 15 cases and the three positive slopes had relatively large confidence intervals. When the mixed-effects model with gradient as the predictor was fit to the data, all slope estimates were negative (Fig. 8) and the gradient term was significant in the model (p value = 0.0007). The random effects distribution for the slope of the length-at-age – stream gradient relationship had a mean of –1.261 and a standard deviation of 0.378. This suggests that length-at-age declines significantly as gradient increases up to the optimum gradient, but the relationship was relatively variable among years. For age-1 juveniles in gradients above the optimum, the slopes of the length-at-age – stream gradient regressions (Fig. 7) were not significantly different from zero and estimates had small confidence limits (95% confidence level; Fig. 8). In contrast to results from low-gradient habitat, the estimated mean slope from the random effects distribution was not significant (p value = 0.179) and slope was relatively less variable among years (standard deviation = 0.059). For age-2+ juveniles in habitat gradients below the optimum, the slopes of the length-at-age – stream gradient regressions (Fig. 7) were not significantly different from zero (95% confidence level; Fig. 8) and the estimated slopes were less than zero in 10 of 15 cases and had relatively large confidence intervals. The mean of the random effects distribution for the slopes was not significantly different from zero (p value = 0.859), and the standard deviation of the random effects distribution (1.196) was relatively high. This suggests that the relationship between fork length and gradient for age-2+ salmon parr is quite variable among years in low-gradient habitats. Similar nonsignificant results were obtained for age-2+ fish in habitat gradients above the optimum (p value = 0.319), except that the variability in estimated slopes was lower (Fig. 8), as was the standard deviation of the random effects distribution (0.402).

© 2008 NRC Canada

Fig. 7. Relationship between mean fork length and stream gradient for age-1 (open circles, solid lines) and age-2+ (solid circles, broken lines) Atlantic salmon (*Salmo salar*) in the Stewiacke River, Nova Scotia, for the years 1984 to 1999. Data are split into observations below and above the preferred habitat gradient (μ) for each age class. The points are the observed values and lines are least-squares, linear regression fits to the data.

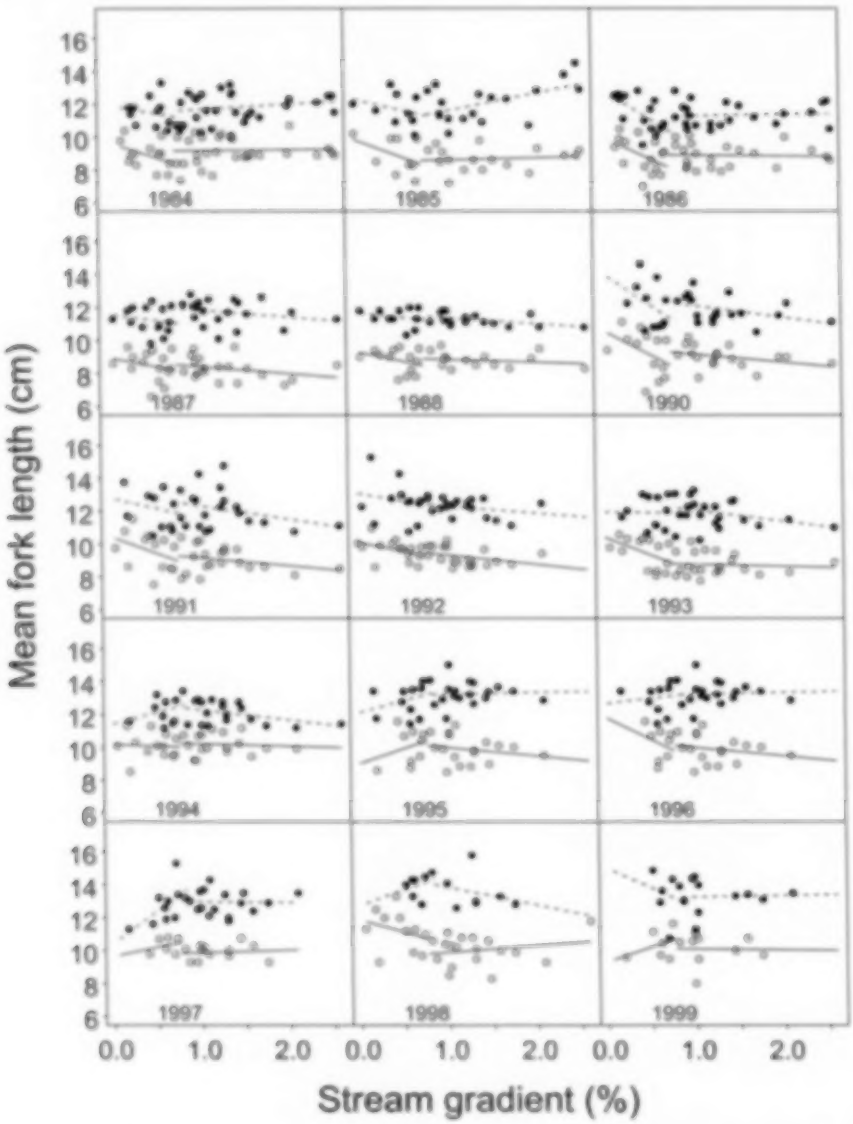

Given that population abundance had a significant independent effect on length-at-age (p value < 0.001; Fig. 6), habitat gradient could act in conjunction with abundance to determine the overall affect on length-at-age. When habitat gradient, mean abundance, and their interaction were used as predictors in the mixed-effects model, the results differed more noticeably among age classes and gradient categories (Table 4). For age-1 juveniles in habitat gradients below the optimum, AWSG and mean abundance had significant negative effects on length-at-age (Table 4), but the interaction between them was nonsignificant. The standard deviation of the random effects distribution for the gradient coefficient was 0.037, suggesting that very little of the variation in this relationship could be attributed to random variation among years (as opposed to the main effects). For age-1 juveniles in habitat gradients above the optimum, only mean abundance had a significant negative effect on length-at-age (Table 4). The standard deviation of the random effects distribution for the gradient coefficient was similar to that estimated for the below-optimum gradient category. For age-2+ juveniles in habitat gradients below the optimum, the interaction term between gradient and mean abundance had a significant negative effect on length-at-age, even though the independent effect of habitat gradient was positive (Table 4).

© 2008 NRC Canada

Fig. 8. The relationship between the slopes (points) of linear regressions of mean fork lengths on stream gradient and the annual mean abundance of Atlantic salmon (*Salmo salar*) in the Stewiacke River, Nova Scotia, for the years 1984 to 1999. Results are from (*a*, *b*) age-1 and (*c*, *d*) age-2+ juveniles in gradients below (*a* and *c*, respectively) and above (*b* and *d*, respectively) the preferred habitat gradient. The vertical solid lines indicate the 95% confidence interval for each slope, and the broken line corresponds to a slope of zero. Slope estimates from a linear mixed-effects model (open triangles) are shown for comparison.

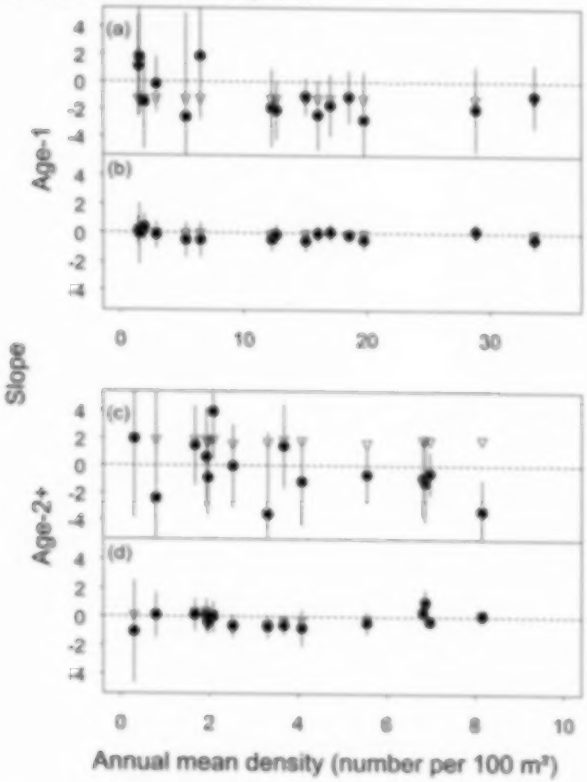

In this model, the annual variation in the relationship was greater, given that the standard deviation of the random effects distribution was 0.269. For age-2+ juveniles in habitat gradients above the optimum, only mean abundance had a significant negative effect on length-at-age (Table 4). The standard deviation of the random effects distribution for the gradient coefficient was higher than that estimated for the below-optimum category.

Discussion

Small-scale density-dependent habitat selection in wild fish populations has not been widely reported (but refer to Bult et al. (1999) and Young (2004) for examples of manipulative experiments), even though it is thought to be an important mechanism for reducing interannual variation in population size (Fromentin et al. 2001; Rose et al. 2001). Furthermore, although intracohort competition for food and space has been predicted for wild juvenile salmon (Bult et al. 1999; Armstrong 2005), this study is among the first to quantify its effects on distribution in a wild population. In the Stewiacke watershed, our results indicate that habitat use is density-dependent for age-0 and age-1 juvenile salmon but is not density-dependent for older juveniles over the ranges of abundance observed. In contrast to previous findings, the proportional usage of each habitat type did not remain constant as abundance increased for the two younger age classes (Hedger et al. 2005) and length-at-age differed significantly among habitat types (Girard et al. 2004).

One of the more surprising results of this study was that optimal habitat type (assumed to correspond to the stream gradient with maximum density) did not differ markedly among age classes. Such differences in microhabitat use were expected, based on previous observations of differential use of riffles, runs, and pools among age classes (Gibson 1993; Bult et al. 1999; Blanchet et al. 2006). Furthermore, juvenile salmon are highly territorial and their ability to defend territory increases with size (Einum and Nislow 2005; Blanchet et al. 2006), so one might expect larger juveniles to be able to exclude smaller ones from favourable areas. However, minimal separation with respect to weighted stream gradient was observed between age-0 and age-1 juveniles (cf. $\mu = 0.75$ and 0.76, respectively), while a slightly higher preferred gradient was estimated for age-2+ juveniles ($\mu = 0.82$). This suggests that all age classes require a similar combination of heterogeneity of habitat types (riffles, runs, and pools) and water flow (stream gradient) characteristics within stream reaches at a population level. However, it is consistent with previous findings of niche separation among age classes at smaller scales, with age-2+ juveniles preferring greater water velocities, depths, and substrate sizes than the younger age classes (Gibson 1993; Milner et al. 2003; Hedger et al. 2005). Most electrofishing sites in this study averaged over 100 m long. This distance is quite large relative to the daily movement of individuals (Johansen et al. 2005; Einum et al. 2006), the average territory size (Hedger et al. 2005; Blanchet et al. 2006), or the scale of habitat selection (Bult et al. 1999). Therefore, the scale may have been too coarse to fully capture any patterns in niche segregation.

Density-dependent habitat selection in conjunction with density-dependent growth was found only for the age-1 cohort, which is consistent with the hypothesis that increased use of marginal habitat (or increased competition among individuals) has negative consequences on overall fitness (Grant and Kramer 1990; Hutchings and Jones 1998). However, the inverse relationship between length and density for the age-2+ cohort suggests that competitive processes can also lower the overall fitness of an age class without a change in habitat use. Although density-dependent growth is a general phenomenon described for juvenile salmon populations (Grant and Imre 2005), the lack of substantial variation in length-at-age with stream gradient for either of the age-1 or age-2+ cohorts suggests that growth patterns do not result predominantly from spatial variation in habitat quality (Shepherd and Litvak 2004). This does not preclude the possibility that slight variation in growth patterns can be used to infer the form of competitive interactions leading to density-dependent habitat selection within an age class.

Variations in length-at-age as a function of habitat gradient were found in both the age-1 and age-2+ age classes,

© 2008 NRC Canada

Table 4. Population-level estimates, standard error, and significance for the fixed effects of habitat gradient (AWSG) and mean abundance (abundance) on the length-at-age of age-1 and age-2+ juveniles in habitat gradients below the optimum and above the optimum, respectively.

Category	Fixed effects	Estimate	Standard error	df	*p* value	Standard deviation
Age-1, below optimum	Intercept	11.151	0.246	157	<0.0001	0.273
	AWSG	–1.342	0.353	157	0.0002	0.037
	Abundance	–0.070	0.010	13	<0.0001	
Age-1, above optimum	Intercept	10.212	0.166	257	<0.0001	0.146
	AWSG	–0.133	0.099	257	0.1826	0.045
	Abundance	0.056	0.007	13	<0.0001	
Age-2+, below optimum	Intercept	12.326	0.506	149	<0.0001	0.096
	AWSG	1.743	0.857	149	0.0439	0.269
	Abundance	–0.015	0.098	13	0.8787	
	AWSG:abundance	–0.499	0.174	149	0.0049	
Age-2+, above optimum	Intercept	13.514	0.242	246	<0.0001	0.210
	AWSG	–0.137	0.167	246	0.4129	0.455
	Abundance	–0.278	0.036	13	<0.0001	

Note: The standard deviation of the random effects distribution for the intercept and slope for each linear mixed-effects model is shown.

but only in habitat gradients below the optimum. The fact that a relationship was observed (irrespective of population abundance) suggests that access to resources is not equivalent among individuals or among habitats, which is consistent with predictions from ideal despotic or ideal preemptive theory. However, no such variation was detected in high-gradient habitats. Previous research has found that inter- and intra-species competition does not influence distribution patterns in riffles (Rodriguez 1995), a finding consistent with our models, as well as ideal free theory. In contrast to our expectations, length-at-age declined (rather than increased) with gradient for habitat gradients below the optimum. This implies that factors other than intracohort competition have a significant influence on the distribution and fitness of age-1 juveniles. Although length-at-age is frequently used as a proxy for individual fitness (Girard et al. 2004; Armstrong 2005) and is known to be strongly correlated with fitness (Hutchings and Jones 1998), our results suggest that it is not the only determinant of lifetime reproductive success within juvenile salmon populations. Two factors that likely act in opposition to resource acquisition (reflected by growth) are interspecific competition and predator avoidance. In pool habitat types, brook or brown trout (which also inhabit the Stewiacke watershed) are able to exclude Atlantic salmon through interference and exploitative competition (Gibson 1993; Rodriguez 1995). Furthermore, predation rates on juvenile salmonids are higher in low-gradient habitats (Bult et al. 1999), presumably because of increased water clarity and greater mobility resulting from the defence of larger territories (Martel 1996). In the freshwater environment, juvenile salmon are known to trade off fast growth for high survival (e.g., Metcalfe et al. 1999). The results of our study support the hypothesis that predation and intraspecies competition are more important factors than resource acquisition in determining the distribution of individuals in low-gradient habitat.

Further support for the above hypothesis was found in the pattern of habitat usage in age-0 and age-1 juveniles as abundance increased. All age classes (regardless of abundance) were distributed asymmetrically along the habitat gradient, although only age-0 and age-1 juveniles exhibited patterns of habitat use consistent with density-dependent habitat selection. Under ideal distribution theory, individuals occupy the best habitat first, and new individuals will begin to occupy marginal areas only when high-quality habitat is saturated (Kramer et al. 1997). This pattern was exhibited by the age-0 and age-1 cohorts, which made use of more habitat types as abundance increased (as shown by the increase in absolute density across all stream gradients). However, an inverse relationship was found between relative density and abundance in low-gradient habitat, but a positive relationship was found at stream gradients above the preferred gradient value. Proportionately, age-0 and age-1 juveniles showed less preference for low-gradient habitat types even as intraspecies competition increased. This implies that the fitness benefits of predator avoidance and reduced interspecific competition in high-gradient habitat outweigh the benefits of increased growth in low-gradient habitat, particularly as abundance increases.

Where variations in length-at-age were detected, stream gradient and mean population abundance exerted independent effects on age-1 juveniles, but acted in conjunction for age-2+ juveniles. Although this first appears contradictory given that habitat use is density-dependent in the age-1 but not the age-2+ age class, it suggests that age-2+ individuals do not modify their distribution among habitats even though increasing competition changes the relative benefit of low-gradient habitat types in terms of resource acquisition. Given that prior residency is thought to be the single most important factor affecting the outcome of competitive interactions between individuals of similar size (Volpe et al. 2001; Harwood et al. 2002), habitat selection patterns in age-2+ individuals may result primarily from pre-emption (ideal pre-emptive theory). In contrast, age-1 individuals respond to increased competition by modifying their distribution along the habitat gradient, even though this may reduce an individual's potential for growth. Territorial defence would be strongest at low density and would weaken as intracohort competition increased, because of the increasing frequency of antagonistic interactions among individuals

© 2008 NRC Canada

(Imre et al. 2002; Morris 2003). This effect would be stronger in the age-1 age class than in the age-2+ age class because the range of densities sampled were an order of magnitude greater. Drift-feeding fishes (such as juvenile Atlantic salmon) have greater access to prey in high velocity environments (Poff and Huryn 1998; Nislow et al. 1999). However, any potential increase in feeding success would be offset by the energy required to occupy territory in fast-moving water (Johansen et al. 2005; Rosenfeld et al. 2005). As age-1 juveniles begin to redistribute among habitat types as abundance increases, it is likely that competitive ability largely determines habitat selection patterns, as predicted by ideal despotic theory.

In a practical context, understanding the consequences of density-dependent habitat selection on a population's distribution patterns is important for a species in decline. The relative success of fisheries management policies is often based on long-term monitoring of fish density, from which trends in abundance are inferred (Nislow et al. 1999; Fromentin et al. 2001), and variability in the extent, timing, and nature of density-dependent habitat selection would alter the effectiveness of monitoring programs. Density-dependent habitat selection is also relevant to resource conservation as it may affect the efficacy of various recovery strategies, particularly enhancement programs (Whalen et al. 2000; Milner et al. 2003). Future research should investigate the extent to which density-dependent habitat selection can be generalized among populations of Atlantic salmon (Armstrong 2005) and determine how habitat selection scales up to regional dynamics (Resetarits 2005).

Acknowledgements

The authors thank the many people who assisted with electrofishing and habitat surveys in this watershed. Robert Randall, Kurtis Trzcinski, Istvan Imre, Douglas Morris, and one anonymous reviewer provided comments and suggestions that considerably improved this manuscript.

References

Amiro, P.G. 1984. Stream gradients and Atlantic salmon parr densities. Can. Atl. Fish. Sci. Advisory Board (CAFSAC) Res. Doc. No. 1986/32.

Amiro, P.G. 1993. Habitat measurement and population estimation of juvenile Atlantic salmon (*Salmo salar*). Can. Spec. Publ. Fish. Aquat. Sci. No. 118. pp. 81–97.

Amiro, P.G., McNeill, A.J., and Longard, D.A. 1989. Results of surveys and electrofishing in the Stewiacke River, 1984 to 1988, and the St. Mary's River, 1985 and 1986. Can. Data Rep. Fish. Aquat. Sci. No. 764.

Armstrong, J.D. 2005. Spatial variation in population dynamics of juvenile Atlantic salmon: implications for conservation and management. J. Fish Biol. **76**: 35–52.

Armstrong, J.D., Kemp, P.S., Kennedy, G.J.A., Ladle, M., and Milner, N.J. 2003. Habitat requirements of Atlantic salmon and brown trout in rivers and streams. Fish. Res. **62**: 143–170. doi:10.1016/S0165-7836(02)00160-1.

Blanchet, S., Dodson, J.J., and Bernatchez, L. 2006. Influence of habitat structure and fish density on Atlantic salmon *Salmo salar* L. territorial behaviour. J. Fish Biol. **68**: 951–957. doi:10.1111/j.0022-1112.2006.00970.x.

Bult, T.P., Riley, S.C., Haedrich, R.L., Gibson, R.J., and Heggenes, J. 1999. Density-dependent habitat selection by juvenile Atlantic salmon (*Salmo salar*) in experimental riverine habitats. Can. J. Fish. Aquat. Sci. **56**: 1298–1306. doi:10.1139/cjfas-56-7-1298.

COSEWIC. 2006. COSEWIC assessment and update status report on the Atlantic salmon *Salmo salar* (Inner Bay of Fundy populations) in Canada. Committee on the Status of Endangered Wildlife in Canada (COSEWIC). Ottawa, Ontario (www.sararegistry.gc.ca/species/speciesDetails_e.cfm?sid=672).

Crozier, W.W., and Kennedy, G.J.A. 1995. The relationship between a summer fry (0+) abundance index, derived from semi-quantitative electrofishing, and egg deposition of Atlantic salmon, in the River Bush, Northern Ireland. J. Fish Biol. **47**: 1055–1062. doi:10.1111/j.1095-8649.1995.tb06029.x.

Cunjak, R.A., and Therrien, J. 1998. Inter-stage survival of wild juvenile Atlantic salmon, *Salmo salar* L. Fish. Manage Ecol. **5**: 209–223. doi:10.1046/j.1365-2400.1998.00094.x.

Davison, A.C., and Hinkley, D.V. 1997. Bootstrap methods and their application. Cambridge University Press, Cambridge, UK.

Einum, S. 2005. Salmonid population dynamics: stability under weak density dependence? Oikos, **110**: 630–633. doi:10.1111/j.0030-1299.2005.14088.x.

Einum, S., and Nislow, K.H. 2005. Local-scale density-dependent survival of mobile organisms in continuous habitats: an experimental test using Atlantic salmon. Oecologia, **143**: 203–210. doi:10.1007/s00442-004-1793-y. PMID:15654640.

Einum, S., Sundt-Hansen, L., and Nislow, K.H. 2006. The partitioning of density-dependent dispersal, growth and survival throughout ontogeny in a highly fecund organism. Oikos, **113**: 489–496. doi:10.1111/j.2006.0030-1299.14806.x.

Freckleton, R.P., Watkinson, A.R., Green, R., and Sutherland, W.J. 2006. Census error and the detection of density dependence. J. Anim. Ecol. **75**: 837–851. doi:10.1111/j.1365-2656.2006.01121.x. PMID:17009748.

Fretwell, S.D. 1972. Populations in a seasonal environment. Princeton University Press, Princeton, N.J.

Fretwell, S.D., and Lucas, H.L. 1970. On territorial behaviour and other factors influencing habitat distribution in birds. Acta Biotheor. **19**: 136–156.

Fromentin, J.-M., Myers, R.A., Bjørnstad, O.N., Stenseth, N.C., Gjosæter, J., and Christie, H. 2001. Effects of density-dependent and stochastic processes on the regulation of cod populations. Ecology, **82**: 567–579.

Gaston, K.J., Blackburn, T.M., and Lawton, J.H. 1997. Interspecific abundance–range size relationships: an appraisal of mechanisms. J. Anim. Ecol. **66**: 579–601.

Gibson, R.J. 1993. The Atlantic salmon in fresh water: spawning, rearing and production. Rev. Fish. Biol. **3**: 39–73.

Gibson, A.J.F., and Amiro, P.G. 2003. Abundance of Atlantic salmon (*Salmo salar*) in the Stewiacke River, NS, from 1965 to 2002. Can. Sci. Advisory Secretariat (CSAS) Res. Doc. No. 2003/108.

Girard, I.L., Grant, J.W.A., and Steingrimsson, S.O. 2004. Foraging, growth, and loss rate of young-of-the-year Atlantic salmon (*Salmo salar*) in relation to habitat use in Catamaran Brook, New Brunswick. Can. J. Fish. Aquat. Sci. **61**: 2339–2349. doi:10.1139/f04-216.

Grant, J.W.A., and Imre, I. 2005. Patterns of density-dependent growth in juvenile stream-dwelling salmonids. J. Fish Biol. **67**(Suppl. B): 100–110. doi:10.1111/j.0022-1112.2005.00916.x.

Grant, J.W.A., and Kramer, D.L. 1990. Territory size as a predictor of the upper limit to population density of juvenile salmonids in streams. Can. J. Fish. Aquat. Sci. **47**: 1724–1737. doi:10.1139/f90-197.

Harwood, A.J., Metcalfe, N.B., Griffiths, S.W., and Armstrong, J.C. 2002. Intra- and inter-specific competition for winter con-

© 2008 NRC Canada

cealment habitat to juvenile salmonids. Can. J. Fish. Aquat. Sci. **59**: 1515–1523. doi:10.1139/f02-119.

Hedger, R.D., Dodson, J.J., Bergeron, N.E., and Caron, F. 2005. Habitat selection by juvenile Atlantic salmon: the interaction between physical habitat and abundance. J. Fish Biol. **67**: 1054–1071. doi:10.1111/j.0022-1112.2005.00808.x.

Hilborn, R., and Mangel, M. 1997. The ecological detective: confronting models with data. Princeton University Press, Princeton, N.J.

Hutchings, J.A., and Jones, M.E.B. 1998. Life history variation and growth rate thresholds for maturity in Atlantic salmon, *Salmo salar*. Can. J. Fish. Aquat. Sci. **55** (Suppl 1): 22–47.

Imre, I., Grant, J.W.A., and Keeley, E.R. 2002. The effects of visual isolation on territory size and population density of juvenile rainbow trout (*Oncorhynchus mykiss*). Can. J. Fish. Aquat. Sci. **59**: 303–309. doi:10.1139/f02-010.

Imre, I., Grant, J.W.A., and Cunjak, R.A. 2005. Density-dependent growth of young-of-the-year Atlantic salmon *Salmo salar* in Catamaran Brook, New Brunswick. J. Anim. Ecol. **74**: 508–516.

Johansen, M., Elliott, J.M., and Klemetsen, A. 2005. A comparative study of juvenile salmon density in 20 streams throughout a very large river system in northern Norway. Ecol. Freshwat. Fish, **14**: 96–110.

Jonsson, N., Jonsson, B., and Hansen, L.P. 1998. The relative role of density-dependent and density-independent survival in the life cycle of Atlantic salmon *Salmo salar*. J. Anim. Ecol. **67**: 751–762. doi:10.1046/j.1365-2656.1998.00237.x.

Jonzen, N., Wilcox, C., and Possingham, H.P. 2004. Habitat selection and population regulation in temporally fluctuating environments. Am. Nat. **104**: E103–E114.

Kramer, D.L., Rangeley, R.W., and Chapman, L.J. 1997. Habitat selection: patterns of spatial distribution from behavioural decisions. *In* Behavioural ecology of teleost fishes. *Edited by* J-G.J. Godin. Oxford University Press, Oxford, UK. pp. 37–80.

Marshall, C.T., and Frank, K.T. 1995. Density-dependent habitat selection by juvenile haddock (*Melanogrammus aeglefinus*) on the southwestern Scotian Shelf. Can. J. Fish. Aquat. Sci. **52**: 1007–1017. doi:10.1139/f95-099.

Martel, G. 1996. Growth rate and influence of predation risk on territoriality in juvenile coho salmon (*Oncorhynchus kisutch*). Can. J. Fish. Aquat. Sci. **53**: 660–669. doi:10.1139/cjfas-53-3-660.

McCullagh, P., and Nelder, J.A. 1989. Generalized linear models. 2nd edition. Chapman and Hall, London, UK.

Metcalfe, N.B., Fraser, N.H.C., and Burns, M.D. 1999. Food availability and the nocturnal vs. diurnal foraging trade-off in juvenile salmon. J. Anim. Ecol. **68**: 371–381. doi:10.1046/j.1365-2656.1999.00289.x.

Milner, N.J., Elliott, J.M., Armstrong, J.D., Gardiner, R., Welton, J.S., and Ladle, M. 2003. The natural control of salmon and trout populations in streams. Fish. Res. **62**: 111–125. doi:10.1016/S0165-7836(02)00157-1.

Morris, D.W. 2003. Toward an ecological synthesis: a case for habitat selection. Oecologia, **136**: 1–13. doi:10.1007/s00442-003-1241-4. PMID:12690550.

Morris, D.W., Lundberg, P., and Ripa, J. 2001. Hamilton's rule confronts ideal free habitat selection. Proc. R. Soc. Lond. B Biol. Sci. **268**: 921–924.

Nislow, K.H., Folt, C.L., and Parrish, D.L. 1999. Favorable foraging locations for young Atlantic salmon: application to habitat and population restoration. Ecol. Appl. **9**: 1085–1099. doi:10.1890/1051-0761(1999)009[1085:FFLFYA]2.0.CO;2.

Pinheiro, J.C., and Bates, D.M. 2000. Mixed effects models in S and S-Plus. Springer-Verlag, New York.

Poff, N.L., and Huryn, A.D. 1998. Multi-scale determinants of secondary production in Atlantic salmon (*Salmo salar*) streams. Can. J. Fish. Aquat. Sci. **55**(Suppl 1): 201–217. doi:10.1139/cjfas-55-S1-201.

Pulliam, H.R., and Danielson, B.J. 1991. Sources, sinks and habitat selection: a landscape perspective on population dynamics. Am. Nat. **137**: S50–S66. doi:10.1086/285139.

Resetarits, W.J., Jr. 2005. Habitat selection behaviour links local and regional scales in aquatic systems. Ecol. Lett. **8**: 480–486. doi:10.1111/j.1461-0248.2005.00747.x.

Rodriguez, M.A. 1995. Habitat-specific estimates of competition in stream salmonids: a field test of the isodar model of habitat selection. Evol. Ecol. **9**: 169–184. doi:10.1007/BF01237755.

Rose, K.A., Cowan, J.H., Jr., Winemiller, K.O., Myers, R.A., and Hilborn, R. 2001. Compensatory density dependence in fish populations: importance, controversy, understanding and prognosis. Fish Fish. **2**: 293–327.

Rosenfeld, J.S., Leiter, T., Lindner, G., and Rothman, L. 2005. Food abundance and fish density alters habitat selection, growth, and habitat suitability curves for juvenile coho salmon (*Oncorhynchus kisutch*). Can. J. Fish. Aquat. Sci. **62**: 1691–1701. doi:10.1139/f05-072.

Shepherd, T.D., and Litvak, M.K. 2004. Density-dependent habitat selection and the ideal free distribution in marine fish spatial dynamics: considerations and cautions. Fish Fish. **5**: 141–152.

Talbot, A.J. 1994. Habitat-dependence of population abundance and variability in juvenile Atlantic salmon (*Salmo salar*). Ph.D. thesis, Dalhousie University, Halifax, N.S.

Venables, W.N., and Ripley, B.D. 2002. Modern applied statistics with S. 4th edition. Springer-Verlag, New York, Inc., New York.

Volpe, J.P., Anholt, B.R., and Glickman, B.W. 2001. Competition among juvenile Atlantic salmon (*Salmo salar*) and steelhead (*Oncorhynchus mykiss*): relevance to invasion potential in British Columbia. Can. J. Fish. Aquat. Sci. **58**: 197–207. doi:10.1139/cjfas-58-1-197.

Whalen, K.G., Parrish, D.L., Mather, M.E., and McMenemy, J.R. 2000. Cross-tributary analysis of parr to smolt recruitment of Atlantic salmon (*Salmo salar*). Can. J. Fish. Aquat. Sci. **57**: 1607–1616. doi:10.1139/cjfas-57-8-1607.

Yang, C.T. 1971. Formation of riffles and pools. Water Resour. Res. **7**: 1567–1574. doi:10.1029/WR007i006p01567.

Young, K.A. 2004. Asymmetric competition, habitat selection, and niche overlap in juvenile salmonids. Ecology, **85**: 134–149. doi:10.1890/02-0402.

© 2008 NRC Canada

Transoceanic migration rates of young North Pacific albacore, *Thunnus alalunga*, from conventional tagging data

Momoko Ichinokawa, Atilio L. Coan, Jr., and Yukio Takeuchi

Abstract: This study summarizes US and Japanese historical North Pacific albacore (*Thunnus alalunga*) tagging data and uses maximum likelihood methods to estimate seasonal migration rates of young North Pacific albacore. Previous studies related to North Pacific albacore migration have found that the frequency of albacore migrations is difficult to quantify because of inadequate amounts of tags released by the US tagging program in the western Pacific. Use of the combined Japan and US tagging data solves this problem. This study also incorporates specific seasonal migration routes, hypothesized in past qualitative analyses, to avoid overparameterization problems. The estimated migration patterns qualitatively correspond to those from previous studies and suggest the possibility of frequent westward movements and infrequent eastward movements in the North Pacific. This frequent westward movement of young albacore in the North Pacific would correspond to a part of albacore life history in which immature fish recruit into fisheries in the western and eastern Pacific and then gradually move near to their spawning grounds in the central and western Pacific before maturing.

Résumé : Notre étude fait la synthèse de données archivées américaines et japonaises de marquage du germon (*Thunnus alalunga*) du Pacifique Nord et utilise des méthodes de vraisemblance maximale pour estimer les taux saisonniers de migration des jeunes germons du Pacifique Nord. Des études antérieures sur la migration du germon dans le Pacifique Nord ont trouvé qu'il est difficile de quantifier la fréquence de migration du germon à cause du nombre insuffisant d'étiquettes libérées par le programme américain de marquage dans l'ouest du Pacifique. L'utilisation combinée des données de marquage japonaises et américaines résout ce problème. Notre étude incorpore aussi des routes spécifiques de migration saisonnière, fixées par hypothèse dans les études qualitatives antérieures, afin d'éviter les problèmes de surparamétrage. Les patrons de migration estimés correspondent qualitativement à ceux des études antérieures et laissent croire à la possibilité de nombreux déplacements vers l'ouest et des déplacements plus rares vers l'est dans le Pacifique Nord. Ces déplacements fréquents vers l'ouest des jeunes germons dans le Pacifique Nord devraient correspondre à la période du cycle biologique pendant laquelle les poissons immatures sont incorporés dans les pêches dans l'ouest et l'est du Pacifique; ils se déplacent ensuite graduellement vers leurs lieux de fraye dans le centre et l'ouest du Pacifique avant d'atteindre la maturité.

[Traduit par la Rédaction]

Introduction

The dispersion of individuals and populations in nature is usually a very difficult part of life history to quantify (Begon et al. 1996). This is especially true for transoceanic migrating pelagic fish. The causes of these transoceanic movements are ecologically important in explaining the spatial distribution of these organisms. In addition, the migration patterns of various pelagic fish stocks are important with respect to calculations of abundance indices, stock assessment model structures, and management strategies (cf. Walters and Martell 2004).

Young North Pacific albacore (*Thunnus alalunga*) are known to migrate into the cooler waters of the North Pacific Transition Zone (35–45°N) before moving into subtropical waters to spawn. Otsu and Uchida (1963) outlined possible seasonal migration patterns of young North Pacific albacore from a few conventional tagging experiments and catch patterns of various fisheries (Fig. 1*a*). They showed two circular migration trajectories for young North Pacific albacore: one between the western and central Pacific, and the other between the eastern and central Pacific. They hypothesized that the two groups of northern albacore congregate and mix in the central Pacific during autumn and winter.

Intensive tagging experiments, conducted by the US, only partially support the migration patterns suggested by Otsu and Uchida (1963). The US North Pacific tagging experiments showed that albacore migrate between areas near the US west coast and areas in the central Pacific (cf. Laurs and Lynn 1977). However, although growth and exploitation rates have been estimated using these tagging data (Laurs and Wetherall 1981; Bertignac et al. 1999), the previous

Received 21 July 2007. Accepted 22 April 2008. Published on the NRC Research Press Web site at cjfas.nrc.ca on 16 July 2008. J20104

M. Ichinokawa[1] and Y. Takeuchi. National Research Institute of Far Seas Fisheries, Fisheries Research Agency, 5-7-1 Orido, Shimizu-ku, Shizuoka 424-8633, Japan.
A.L. Coan, Jr. Southwest Fisheries Science Center, 8604 La Jolla Shores Drive, La Jolla, CA 92037, USA.

[1]Corresponding author (e-mail: ichimomo@fra.affrc.go.jp).

 doi:10.1139/F08-095 © 2008 NRC Canada

Fig. 1. (*a*) Seasonal migration patterns of young (≈≤5-year-old) albacore, *Thunnus alalunga*, hypothesized by Otsu and Uchida (1963) and (*b*) geographic distributions of major North Pacific albacore fisheries (redrawing of fig. 1 in Bertignac et al. (1999)). Four oceanic regions in the North Pacific (WP, CP, EP1, and EP2) used in this study to estimate migration among areas are also shown.

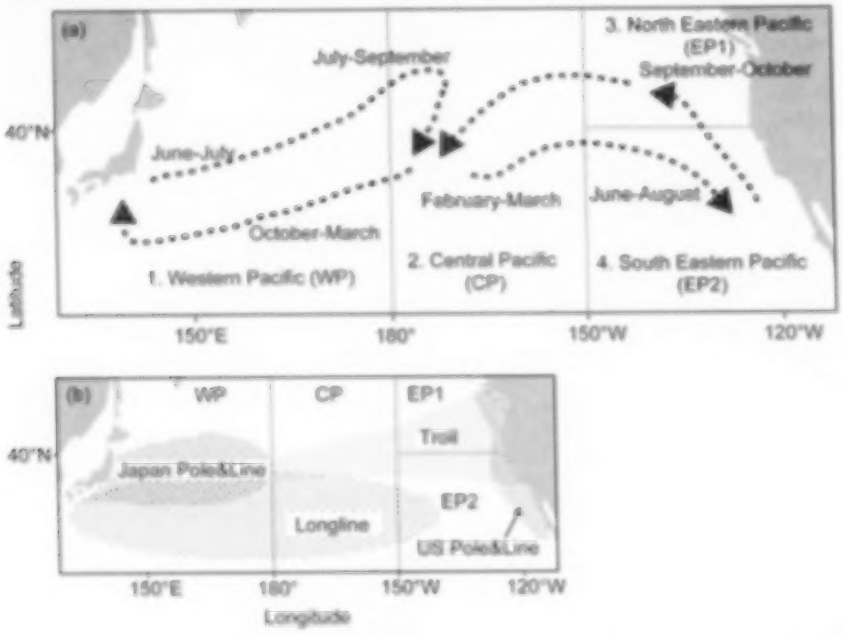

studies have found it difficult to quantify the frequency of albacore migrations because of inadequate amounts of tag releases in the western Pacific.

Japan also conducted albacore tagging experiments in the western areas of the North Pacific during the same period as the US (Kikawa et al. 1977). The data from the experiments by Japan only partially supported the migration hypothesis of Otsu and Uchida (1963). The study also suggested the necessity for comparative analysis of the tagging data from the US and Japan; however, tagging data from both experiments have never been fully analyzed. The additional Japanese tag releases from the western North Pacific would complete quantitative migration information for young North Pacific albacore and enable mathematical verification of the hypothesis by Otsu and Uchida (1963).

This study estimates seasonal migration of North Pacific albacore based on conventional tagging experiments conducted by Japan and the US. Results of tagging experiments conducted during 1970s and 1980s by Japan and US are summarized. Maximum likelihood methods are used on the tagging data and applied in a spatially structured population dynamics model to estimate albacore seasonal migration rates. The accuracy of these estimated migration rates and other types of information needed to sufficiently estimate North Pacific albacore migration rates are also discussed.

Materials and methods

Conventional tagging experiments for North Pacific albacore

Although Japanese North Pacific albacore tag release data date back to 1957, this study only uses data for the period from 1971 to 1986, the period in which both US and Japanese tagging programs were active. The US tagging data are archived at the Southwest Fisheries Science Center of the US National Marine Fisheries Service (NMFS), and the Japanese data are archived at the National Research Institute of Far Seas Fisheries of Japan (NRIFSF). The tagged albacore were released mainly from US and Japanese pole-and-line vessels. A limited number of US releases were also from vessels using jig fishing gear. Japanese pole-and-line fisheries during 1971 to 1986 generally caught albacore less than 90 cm in fork length from spring through early summer in the western Pacific north of 20 N (Fisheries and Oceans Canada 2004). US pole-and-line fisheries also caught fish less than 90 cm mainly in the North Pacific near the US west coast in July to October (Childers and Aalbers 2006). Because North Pacific albacore mature at ages greater than ~5 years old or larger than 90 cm (International Scientific Committee on Tuna and Tuna-like Species in the North Pacific Ocean (ISC) 2005), tag movement patterns should represent the movement of young (immature) albacore.

The US tagging program was conducted jointly by the NMFS and the albacore fishing industry through the American Fishermen's Research Foundation (AFRF). Albacore for the US tagging program were caught by commercial jig boats and pole-and-line vessels on charter to the AFRF. The Japanese tagging program was conducted by several institutes of Japan such as the Tohoku Regional Fisheries Research Laboratory and Nankai Regional Fisheries Research Laboratory, as well as NRIFSF. In the Japanese tagging program, albacore were caught by training vessels, NIRFSF research vessels, and chartered pole-and-line vessels. Only fish in very good condition were tagged and released in both tag-

© 2008 NRC Canada

Table 1. Number of (*a*) tag releases and (*b*) recoveries in area and quarter.

	WP				CP				EP1				EP2				
	Q1	Q2	Q3	Q4	Q1	Q2	Q3	Q4	Q1	Q2	Q3	Q4	Q1	Q2	Q3	Q4	Total
(a) Number of tag releases																	
1971																887	887
1972		289									246			1109	730		2 374
1973		239								21	168			1590	14	12	2 044
1974		509									812	9		1374	194	92	2 990
1975		642				2				3	293			379	609	41	1969
1976		561	25							2	523			368	567	17	2 063
1977		260	134			10	4				343		1	19	1244	273	2 288
1978		321	247	120		195	259				5	63		41	1896	227	3 374
1979		804	118	2		51	440				500			14	481		2 410
1980		1070	38			124	214				514			32	137	19	2 148
1981		300						10			100		56		89		555
1982		25		10	2	168	665				214		11	3	112	23	1 233
1983		40	31	5		445	73	1			262			18	218	14	1 107
1984					10	558	119				235	4			28	4	958
1985		13	10			422	18				230	2		23	83		801
1986						494	22				485			9	112		1 122
Total	0	5073	603	137	12	2469	1814	11	0	26	4930	78	68	4979	6514	1609	28 323
(b) Number of tag recoveries																	
1972		1									3				53	19	76
1973	1	18	2					2			11		1		30	42	107
1974		34	4		1						47	12			14	9	121
1975	2	55	9	1							48			1	13	11	140
1976	5	58	4	27	2			2			11	2	1	1	55	23	191
1977	2	14	1	5				1			1		1		64	32	121
1978	2	19	16	15	1		4				2	1	2	1	48	22	133
1979	3	31	20	11	1		11				7	2	4	1	37	21	149
1980	5	41	16	11			9	3			1		2		19	11	118
1981	6	47	3	6	1	2	11	3					9	2	4	4	98
1982	9	31	2	9	1	1	1				1		2		3	1	61
1983	2	24	2	4		3	1				2	1			2	1	42
1984		16		1		2	2	1			2				6		30
1985	3	17		5		1		1							2	1	30
1986	3	13	2	3	1						1				1		24
1987	3	6		2													11
1988	1	2	1														4
1989	1	1															2
Total	48	428	82	100	8	9	39	13	0	0	137	18	22	6	351	197	1 458

Note: Q1, January–March; Q2, April–June; Q3, July–September; Q4, October–December.

© 2008 NRC Canada

Table 2. Number of tag recoveries by areas where the tags were released and recovered.

	Recovered area					
Released area	WP	CP	EP1	EP2	Total no. of recoveries	Total no. of releases
WP	330	32	3	2	367	5 813
CP	114	11	4	0	129	4 306
EP1	119	6	39	20	184	5 034
EP2	95	20	109	554	778	13 170

Fig. 2. Number of tag recoveries by month and gear.

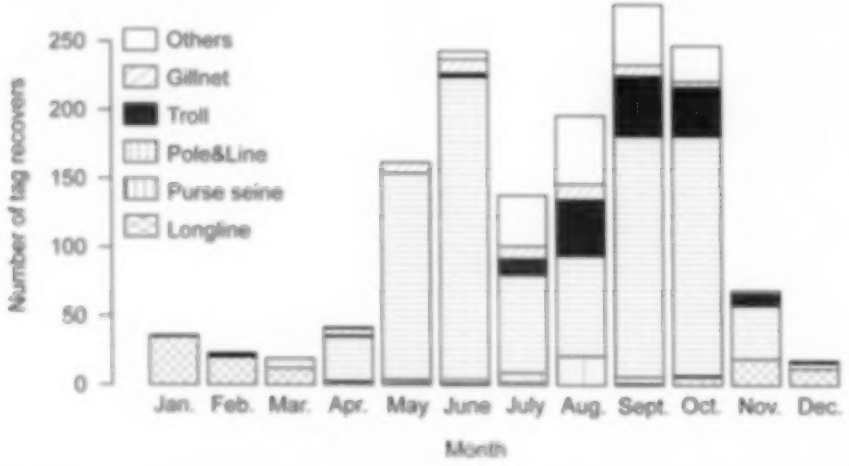

ging programs. Both programs used spaghetti-dart-type tags with 12–13 cm lengths of yellow polyvinyl tubing and a dart head made by Floy Tag and Manufacturing Inc. (Seattle, Washington). Further details of the US tagging program and results of tag analyses are described by Laurs et al. (1976), Laurs and Lynn (1977), Laurs and Wetherall (1981), and Bertignac et al. (1999). A brief summary of the Japanese tagging program is described in Kikawa et al. (1977).

Albacore tags were released in the Pacific between 30°N to 50°N and recaptured mainly by US and Japanese pole-and-line fisheries operating in the same area. Tag release and recapture data were grouped by four areas (WP, CP, EP1, and EP2; Fig. 1) and quarters (Q1, January–March; Q2, April–June; Q3, July–September; Q4, October–December). Young albacore recruit to the pole-and-line fisheries at approximately 2 years of age and mainly in the areas WP and EP2.

The total number of tags released during 1971 to 1986 was 28 323, and the total corresponding recoveries was 1458, which produces an overall recovery rate of 5.1% (Table 1). Recovery rates for Japan and the US tagging programs were 6.5% and 4.9%, respectively. Most of albacore tags released in area WP were from Japan, and most of tags released in areas CP, EP1, and EP2 were from the US. Twice the number of tags was released in the 1970s as in the 1980s. The number of tag returns in 1980s was also less than in the 1970s. Days at liberty of the tags was <1 year in 43% and 1–2 years in 38% of the total recoveries.

Tag releases and recoveries concentrated in certain years, quarters, and area strata, so some strata had very few releases and recoveries (Table 1). The largest number of tags were released in EP2, Q3, and recovered in WP, Q2. There were very few tag releases in Q1 for all regions, and there were no tag returns at EP1 in Q1 and Q2. In addition, a few thousand tags were released in Q2 and Q3 in area CP and in Q3 in area WP that were never recaptured.

Because most of tags were released and recaptured by pole-and-line fisheries (Fig. 2), the distribution of the albacore tag releases and recaptures between area–quarter strata are very dependent on the US and Japanese pole-and-line fishing seasons. Japanese pole-and-line fisheries operate mainly in the western Pacific during the second quarter of the year, and US fisheries operate mainly in the eastern Pacific during the third quarter (Fig. 1*b*). Consequently, the tag releases and recaptures were concentrated mainly at Q2 in the western Pacific and at Q3 in the eastern Pacific.

Movement patterns of the albacore tags between the four areas are summarized (Table 2). The patterns suggest that westward movements were more frequent than eastward movements. For example, of the 4306 tags released in area CP, 114 were recaptured in area WP, whereas only 11, 4, and 0 were recaptured in areas CP, EP1, and EP2, respectively. In addition, 119 tags released in area EP1 were recaptured in area WP, whereas only three tags released in area WP were recaptured in area EP1.

Tag dynamics model and likelihood function

A spatially structured tag dynamics model (Hilborn 1990;

© 2008 NRC Canada

Fig. 3. Probability distribution of the estimated migration rates calculated from the Markov chain Monte Carlo (MCMC). Black and shaded broken lines represent the results from the fully parameterized model with assumed tag-return rates of 0.7 and 0.5, respectively. Black and shaded solid lines represent the results from the simple parsimonious model with the rates of 0.7 and 0.5, respectively, although the two lines were almost overlapped and hardly seen. Because the fully parameterized model MCMC did not converge sufficiently, the distribution patterns shown here were only examples. The simple parsimonious model MCMC did converge. Migration routes assumed to be zero are outlined with broken lines and migration routes hypothesized by Otsu and Uchida (1963) are outlined with thick shaded lines.

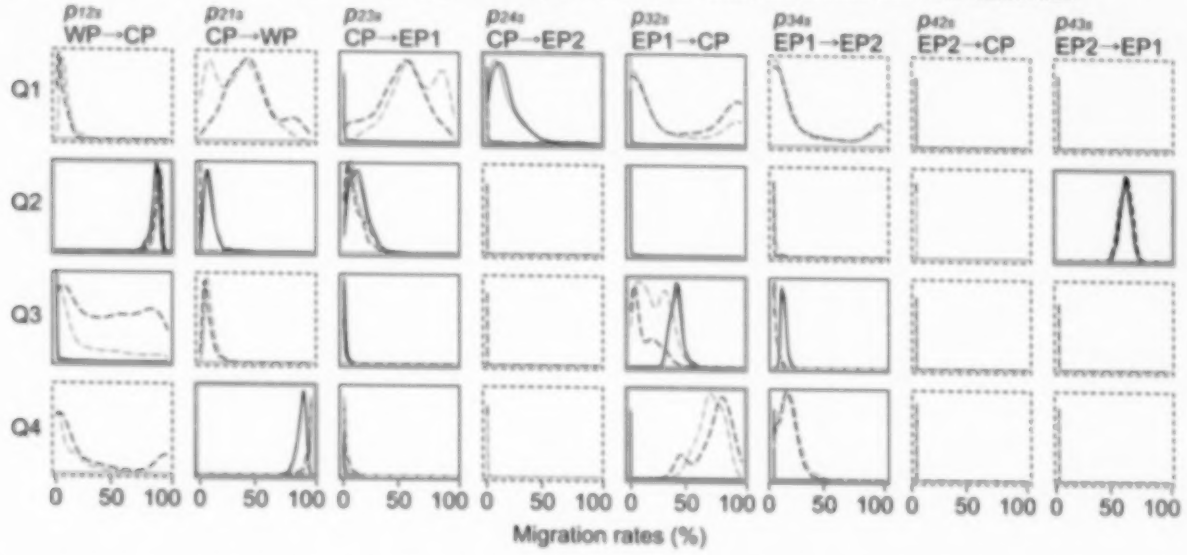

Xiao 1996) was used to describe the dynamics of the tagged group of albacore. Although the original equation by Hilborn (1990) did not explicitly include parameters related to natural mortality and tag loss, we modified the equation by including a term for natural mortality and instantaneous tag-shedding rates according to Xiao (1996). In this study, tagged groups of albacore were defined as albacore released in the same area, quarter, and year. The total number of albacore (N_{iat}) of tag group i in area a and time t is shown in eq. 1:

$$(1) \qquad N_{iat+1} = \sum_{j=1}^{n} [N_{ijt}(1 - h_{jt})p_{jas}]\exp(-M - \psi) + T_{iat}$$

where n is the total number of tag groups, M is the instantaneous natural mortality rate per quarter, h_{at} is the exploitation rate in area a and time t, p_{jas} is the migration rate from area j to area a in season s, T_{iat} is the number of tags released in tag group i in area a and time t, Ψ is the instantaneous tag-shedding rate. The parameter Ψ is assumed constant at 0.0245 based on an analysis that used double-tagging data for North Pacific albacore (Laurs et al. 1976). Japanese tagging data were assumed to have the same instantaneous tag-shedding rate, as both programs used the same type of tag.

The exploitation rate h_{at} in eq. 1 is modeled as the product of catchability by area and season (q_{as}) and year (q_y) (eq. 2):

$$(2) \qquad h_{at} = q_{as}q_y$$

Hilborn (1990) and Xiao (1996) used fishing effort data to estimate h_{at}. However, because there are no reliable historical spatially stratified effort data for the North Pacific albacore fishery in pole-and-line fisheries, the exploitation rates in this study were estimated with the multiplicative vector of the catchability of q_{as} and q_y. Note that this equation implicitly assumed that the relative ratio of exploitation rates between seasons and areas was constant through the whole period.

The expected number of tag recoveries in stratum *iat* ($\hat{R}_{iat}$) was calculated from the estimated number of tagged fish in stratum *iat* ($\hat{N}_{iat}$) (eq. 3):

$$(3) \qquad \hat{R}_{iat} = \hat{N}_{iat}h_{at}x$$

The parameter x is the tag-return rate of the proportion of tags returned after tag shedding. The actual value of the tag-recovery rate is unclear, but Bertignac et al. (1999) separate the tag-recovery rates into three components: proportions of tags returned after immediate tag shedding has occurred ($1 - \alpha$), returned after capture (β), and returned with complete information (γ). The parameter γ was estimated as 0.88 from tag-return data. The other constants of α and β were assumed to be 0.12 and 0.9, respectively, according to Bertignac et al. (1999). The tag-return rate of 0.7 was tentatively applied to base case. However, because the nuisance parameter is difficult to estimate but important in the estimation of some parameters, sensitivity tests were run on a range of tag return rates between 0.5 and 0.9 to test robustness. In addition, to consider different tag-recovery rates, especially reporting rates of Japan and US fishermen, we also conducted other sensitivity analyses assuming different tag-recovery rates between areas EP1 and EP2 and areas CP1 and WP. In summary, we estimated the parameters of M, p_{jas}, q_{as}, and q_y and assumed constant x and Ψ.

© 2008 NRC Canada

Table 3. Maximum likelihood estimates (MLE) and 90% confidence limits of the estimates under different assumptions of tag-recovery rates (x).

	x = 0.70 (–1696.6)			x = 0.50 (–1696.9)			x = 0.50 only in EP (–1697.02)		
	MLE	5% lower	5% upper	MLE	5% lower	5% upper	MLE	5% lower	5% upper
Natural mortality rates (per quarter)	0.122	0.104	0.134	0.117	0.100	0.130	0.119	0.115	0.128
Exploitation rates in 1981 (%)									
WP	20.7	15.6	28.4	27.7	20.3	35.8	20.7	14.8	28.3
CP	2.7	1.5	5.8	3.8	2.1	8.0	2.7	1.3	6.1
EP1	2.4	1.7	3.2	3.4	2.5	4.4	3.4	2.5	4.5
EP2	11.8	9.7	14.2	16.3	13.4	20.0	16.4	13.4	21.1
Migration rates from Q1 to Q2									
CP → EP1	0.0	0.0	21.7	0.0	0.0	17.7	0.0	0.0	16.7
CP → EP2	14.1	1.2	46.3	14.1	0.3	38.5	14.0	0.6	45.6
EP1 → CP	0.0	0.0	6.4	0.0	0.0	5.9	0.0	0.0	6.8
Migration rates from Q2 to Q3									
WP → CP	89.2	83.8	93.3	88.9	80.9	93.2	89.4	84.2	93.6
CP → WP	8.0	0.4	14.4	8.0	1.6	17.1	8.0	2.1	18.4
CP → EP1	11.6	3.3	29.2	11.7	1.8	30.0	11.5	2.7	32.0
EP1 → CP	0.0	0.0	7.6	0.0	0.0	8.1	0.0	0.0	8.4
EP2 → EP1	60.4	52.8	71.4	60.3	53.4	68.2	60.3	52.4	68.6
Migration rates from Q3 to Q4									
WP → CP	0.0	0.0	18.2	0.0	0.0	9.9	0.0	0.0	28.6
CP → EP1	1.5	0.0	3.7	1.5	0.2	4.3	1.5	0.0	3.9
EP1 → CP	42.1	31.9	51.9	41.8	32.6	48.2	42.4	34.3	49.7
EP1 → EP2	8.7	5.7	13.8	8.6	5.6	12.7	8.6	5.4	13.2
Migration rates from Q4 to Q1									
CP → WP	92.3	84.7	96.4	92.3	84.4	96.6	92.4	83.5	96.2
CP → EP1	0.0	0.0	1.1	0.0	0.0	0.9	0.0	0.0	1.2
EP1 → CP	0.0	0.0	0.0	0.0	0.0	0.0	0.0	0.0	0.0
EP1 → EP2	0.0	0.0	0.0	0.0	0.0	0.0	0.0	0.0	0.0

Note: The negative log likelihood is given in parentheses after the x value in the table heading. The 90% confidence limits were calculated with the Markov chain Monte Carlo (MCMC) method.

This study assumes seasonally different albacore migration rates (p_{ijs} from areas i to j in season s), which occur between quarters and adjacent ocean areas. Migration patterns are assumed to change by season, not between years. Assuming that tagged albacore can only move to adjacent areas from a current area in a season, the transition matrix of the movement in season s (P_s) can be written as follows. The number of 1, 2, 3, and 4 corresponds to areas WP, CP, EP1, and EP2, respectively.

$$(4)\quad P_s = \begin{pmatrix} 1-p_{12s} & p_{12s} & 0 & 0 \\ p_{21s} & 1-p_{21s}-p_{23s}-p_{24s} & p_{23s} & p_{24s} \\ 0 & p_{32s} & 1-p_{32s}-p_{34s} & p_{34s} \\ 0 & p_{42s} & p_{43s} & 1-p_{42s}-p_{43s} \end{pmatrix}$$

This transition matrix indicates that 32 (8 × 4) parameters of p_{ijs} should be estimated if different migration rates are assumed in different seasons. Considering 32 other parameters such as catchability (q_{ast}, q_t) and natural mortality rates (M), the total number of parameters to be estimated in this model was 64. The model with 64 parameters is referred to as a "fully parameterized", or simply "full", model in this study.

The number of expected recoveries ($\hat{R}_{ast}$) in each stratum is assumed to have a Poisson distribution (Hilborn 1990; Xiao 1996):

$$(5)\quad L(R_{ast}|\hat{R}_{ast}) = \frac{\exp(-\hat{R}_{ast})\hat{R}_{ast}^{R_{ast}}}{R_{ast}!}$$

where R_{ast} is the observed number of tag returns. The total likelihood function for all observed recoveries against expected recoveries is then

$$(6)\quad L(R_{ast}|q_{ast}, q_t, p_{ijs}, M) = \prod_t \prod_a \prod_t \frac{\exp(-\hat{R}_{ast})\hat{R}_{ast}^{R_{ast}}}{R_{ast}!}$$

The negative log of the likelihood function (eq. 6) was

© 2008 NRC Canada

Fig. 4. (*a* and *b*) Sensitivity of the assumed tag-return rates and estimated exploitation rates in 1981 and (*c* and *d*) examples of migration rates. Results are shown from the simple parsimonious model (*a* and *c*) and from those that assume different tag-return rates only in EP1 and EP2 (*b* and *d*).

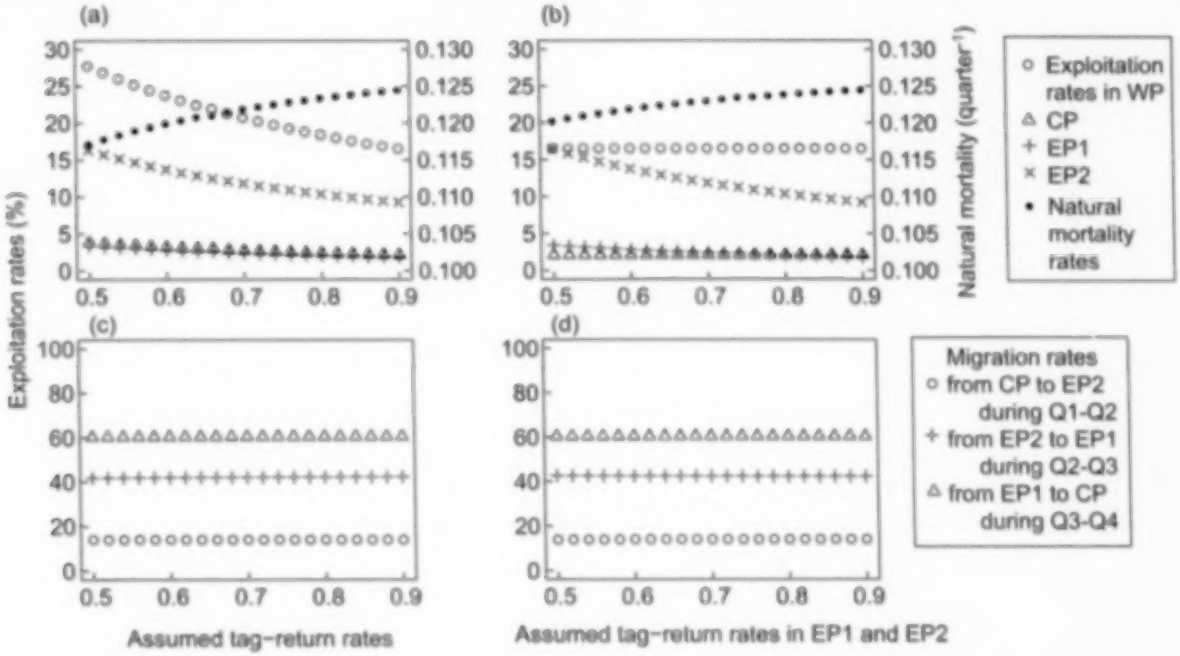

minimized to estimate the parameters. The minimization and estimation of parameters used a quasi-Newton method in AD Model Builder (Otter Research Ltd. 2001). A convergence criterion of the function minimization was set to be less than 10^{-6} of the maximum absolute value of the vector of derivatives of the objective function. In addition, several sets of initial values were tried to test the global convergence of the solutions. Estimated confidence intervals of the parameters were calculated through a Markov chain Monte Carlo (MCMC) chain of 1 000 000 iterations that sampled parameters every 1000 iterations.

Results

Model convergence and re-parameterization with assumed migration routes

In the fully parameterized model, the observed solutions showed a high dependency on sets of initial values and the assumed tag-return rates, even when each calculation obtained a maximum gradient value smaller than 10^{-6}. Parameter distributions for migration rates calculated by the MCMC (Fig. 3) clearly show the situation of unstability of the estimated parameters. Some estimated density distributions have multiple local peaks at 0% and 100%, e.g., the migration rates from EP1 to EP2 and EP1 to CP in Q1. In addition, most migration rates, such as those from EP2 to CP through the year, were 0%. Furthermore, the shape of the density distribution depended on the assumed tag-return rates. The results show that multiple local minimums in the likelihood function of the fully parameterized model exist and that the estimated parameters from the full model were not actual maximum likelihood estimates.

An alternative, simpler parsimonious model with fewer migration parameters was considered. In this model, some migration rates were previously assumed to be zero according to the results by the fully parameterized model, and some parameters were assumed to be nonzero (estimated) according to the hypothesized migration routes by Otsu and Uchida (1963, fig. 1*a*). For example, because most albacore in the eastern Pacific move north during summer, a southern summer migration rate (from EP1 to EP2 in Q2) was assumed to be zero, whereas northern migration rates were estimated. We also looked at tag-recovery data with short-term recoveries in adjacent areas and quarters. Among the 16 routes where migration rates were assumed to be zero, no fish were actually observed to have moved in 14 of the routes and only one fish in two of the routes. The following transition matrices were developed for the simpler model. In the following equation, migration rates fixed at zero are represented by $\underline{0}$. Parameters p_{ij}, represent the migration routes hypothesized by Otsu and Uchida (1963). Others are parameters without information, which will be estimated.

$$P_1 = \begin{pmatrix} 1 & \underline{0} & 0 & 0 \\ \underline{0} & 1-p_{231}-p_{241} & p_{231} & p_{241} \\ 0 & p_{321} & 1-p_{321} & \underline{0} \\ 0 & \underline{0} & \underline{0} & 1 \end{pmatrix}$$

© 2008 NRC Canada

$$p_2 = \begin{pmatrix} 1-p_{122} & p_{222} & 0 & 0 \\ p_{212} & 1-p_{212}-p_{232} & p_{232} & 0 \\ 0 & p_{322} & 1-p_{322} & 0 \\ 0 & 0 & p_{432} & 1-p_{432} \end{pmatrix}$$

$$p_3 = \begin{pmatrix} 1-p_{123} & p_{123} & 0 & 0 \\ 0 & 1-p_{233} & p_{233} & 0 \\ 0 & p_{323} & 1-p_{323}-p_{343} & p_{343} \\ 0 & 0 & 0 & 1 \end{pmatrix}$$

$$p_4 = \begin{pmatrix} 1 & 0 & 0 & 0 \\ p_{214} & 1-p_{214}-p_{234} & p_{234} & 0 \\ 0 & p_{324} & 1-p_{324}-p_{344} & p_{344} \\ 0 & 0 & 0 & 1 \end{pmatrix}$$

The number of parameters to be estimated in this simple model is 16 for migration.

The simple parsimonious model successfully converged with a maximum gradient smaller than 10^{-6} and results in a unimodal parameter distribution (Fig. 3). In addition, estimations from some different sets of initial values arrived at the same solutions. This suggests that relatively good estimations were obtained from the simple model. The maximum likelihood estimates and their 90% confidence intervals estimated from MCMC are summarized (Table 3). The estimated confidence intervals were relatively narrow in the routes with high migration rates, whereas ones with low rates such as p_{243} (the migration rate from CP to EP2 between Q2 and Q3) and p_{232} (from CP to EP1 between Q2 and Q3) show relatively wide confidence intervals, 1%–46% and 3%–29%, respectively.

Tag movement estimation with the simple parsimonious model

Assumed tag-recovery rates and estimated exploitation rates showed negative correlations, whereas assumed tag recovery rates and natural mortality rates showed positive correlations (Figs. 4*a*–4*b*). On the other hand, estimated migration rates (three examples of migration rates are shown) were not affected by the assumed changes in tag-recovery rates (Figs. 4*c*–4*d*). The different tag-recovery rates in areas EP1, EP2, WP, and CP (Figs. 4*b* and 4*d*) affected estimates of exploitation rates and natural mortality rates in EP1 and EP2. However, exploitation rates and migration rates in WP and CP were not affected. Similar results, although not shown here, were obtained when tag-return rates were changed only in areas WP and CP. The results of the sensitivity analysis indicate that the estimated migration rates, with changing tag-return rate, would be robust.

The number of tag returns estimated from the simple parsimonious model explained the observed patterns of number of tag returns by area reasonably well (Fig. 5). However, there were small differences between observed and expected tag returns in some years and regions. The number of expected tag returns in Q3, area EP1, in 1974 and 1975 was approximately half of the observed tag returns, whereas expected tag returns in area EP2 was about twice that observed during the same period. During 1979–1981, there were three unexpected peaks in returned tags in area CP, whereas the

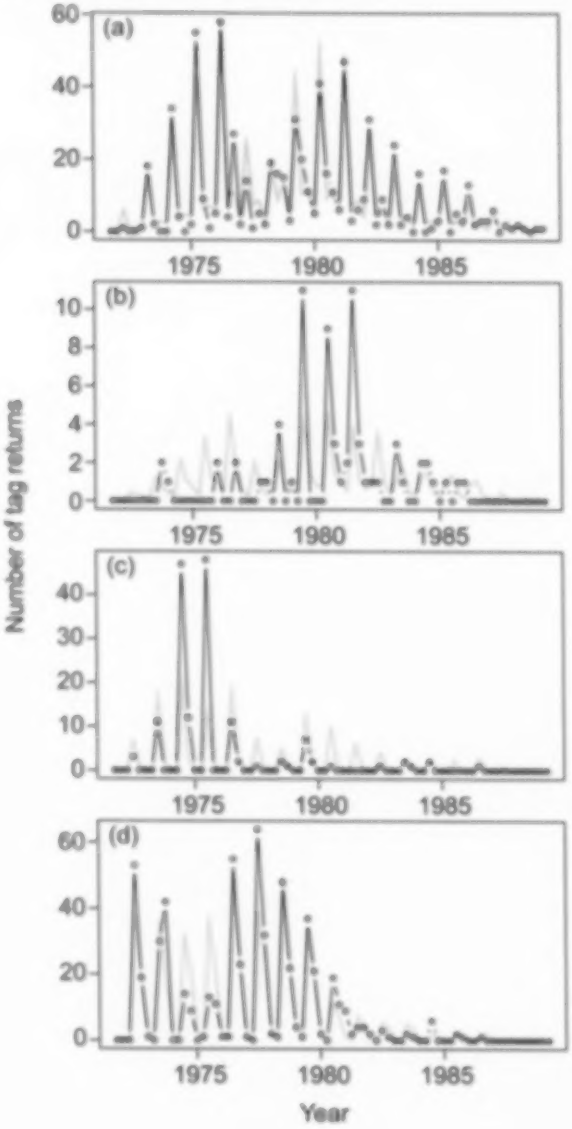

Fig. 5. Number of tag returns observed (solid lines with circles) and expected from the parsimonious model (shaded lines) in (*a*) WP, (*b*) CP, (*c*) EP1, and (*d*) EP2.

observed number of tag returns of EP1 was much smaller than expected during the same period. These unexpected tag returns would be caused by not considering possible annual changes of migration rates and (or) relative ratio of exploitation rates between seasons and areas in the model.

Estimated migration patterns derived from the parsimonious model (Table 3) and from Otsu and Uchida (1963) are summarized (Fig. 6). The estimated migration rates with high probabilities roughly correspond to the routes suggested by Otsu and Uchida (1963). Young albacore in area WP move to area CP during the summer and then back to area WP in winter. Young albacore in area EP2 move to area

© 2008 NRC Canada

Fig. 6. Movement patterns based on the estimated seasonal movement rates of young albacore, *Thunnus alalunga*, in the North Pacific. The black arrows show predicted movement patterns and rates in this study, and the shaded broken arrows show hypothesized patterns by Otsu and Uchida (1963), as shown in Fig. 1.

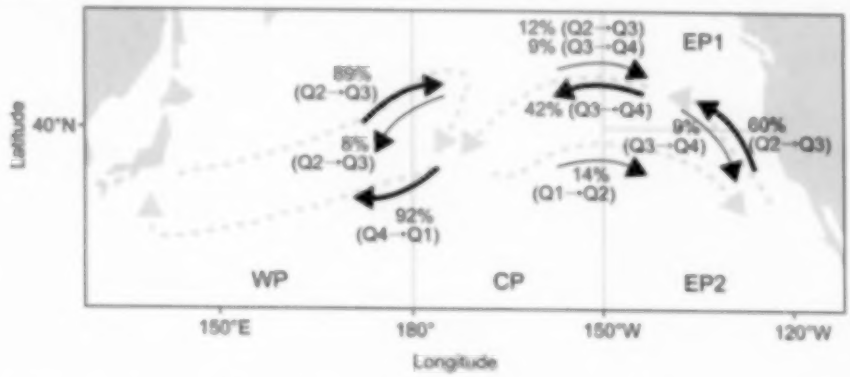

Fig. 7. Predicted probabilities that 2-year-old albacore, *Thunnus alalunga*, in area (*a*) WP and (*b*) EP2 will move into the other areas: WP, solid bars; CP, open bars; EP1, shaded bars; EP2, diagonally hatched bars. The probabilities were calculated from the estimated migration rates in Table 3. In this calculation, depression of albacore caused from fishing activities, the intensity of which would be different among the areas, and natural mortality were not considered.

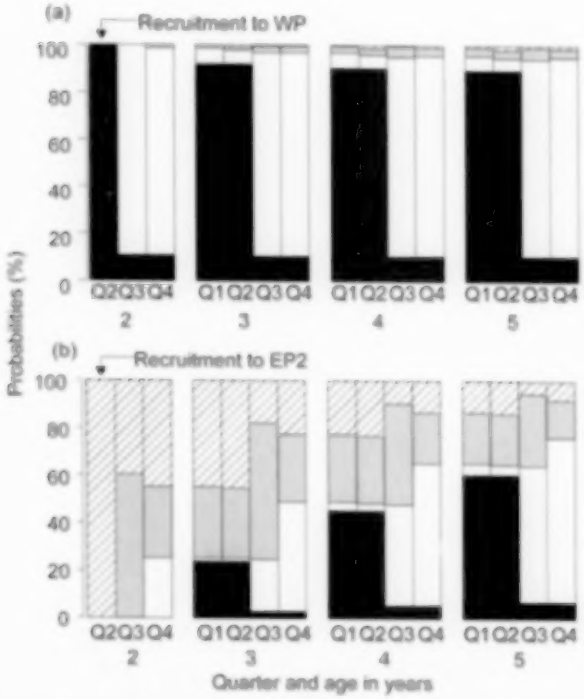

Fig. 8. Estimated exploitation rates by area and year and estimated 90% confidence intervals (vertical lines). The broken line starting in 1975 (described in the legend as VPA, virtual population analysis) represents exploitation rates of 2- to 4-year-old North Pacific albacore, *Thunnus alalunga*, calculated from numbers and catch at age of 2- to 4-year-old albacore estimated from tuning of the VPA used in the North Pacific albacore stock assessment (Fisheries and Oceans Canada 2004).

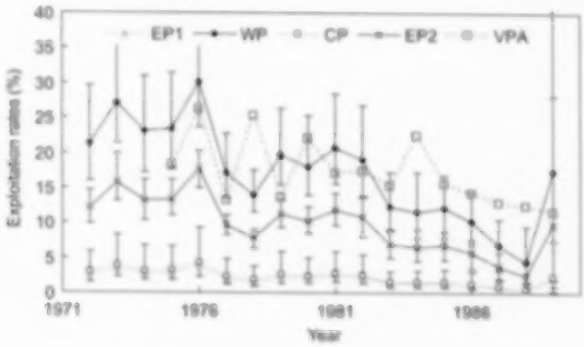

EP1 during the summer, about a half (42%) of them move to area CP during autumn to winter, and some (14%) of them move back to area EP2 in the spring. The probabilities of albacore moving to areas EP1 and EP2 from area CP were relatively low compared with those that moved to area CP. According to these patterns, most of the new recruitment (at about 2 years old) into pole-and-line fisheries in area EP2 was expected to gather into areas CP and WP within a few years (Fig. 7).

Discussion

This study summarized the combined US and Japanese historical albacore tagging data and estimated seasonal migration rates of young albacore in the North Pacific. By limiting the number of parameters and presuming rough seasonal migration routes, reasonable migration rates could be successfully estimated for young North Pacific albacore. The estimated migration patterns qualitatively correspond to those of the previous study by Otsu and Uchida (1963) and also suggest the possibility of frequent westward movement and infrequent eastward movement of young North Pacific albacore.

The frequent westward movement reflects a part of the life history migration pattern of North Pacific albacore. The youngest albacore generally appear in the pole-and-line fish-

© 2008 NRC Canada

eries in areas WP and EP2, where they grow and eventually spawn in the subtropical region in the north-central and western Pacific (ISC 2005). The estimated migration rates also suggested that new recruits move into EP2 at 2 years old and gradually move to the north-central and western Pacific near their spawning ground until they are 5 years old. Considering the fact that mature age is approximately 5 years old in North Pacific albacore (Fisheries and Oceans Canada 2004), this westward movement pattern of the young albacore might be a reasonable part of their life history. Qualitative descriptions about seasonal migrations of North Pacific albacore were made from a limited amount of tag data (Otsu and Uchida 1963; Laurs and Lynn 1977). This study quantified these qualitative descriptions and revealed young stage albacore movement patterns.

There are still many uncertainties in the estimated parameters, especially in exploitation rates, which directly depend on tag-return rates, and migration routes where low migration rates were estimated. The simple parsimonious model estimated higher exploitation rates in areas WP and EP2 than in areas CP and EP1 (Fig. 8). The exploitation rates in area WP were very similar to those of 2- to 4-year-old fish estimated from virtual population analyses (VPA; Fisheries and Oceans Canada 2004). The decreasing trend of the exploitation rates in the area WP was also roughly the same as trends produced by Fisheries and Oceans Canada (2004). However, exploitation rates estimated in this study declined more rapidly. Absolute values of exploitation rates should be compared more carefully because of their dependency on the assumed nuisance parameter of tag-return rates. This problem in estimating fishing and natural mortality rates was also suggested by Bertignac et al. (1999). Additional information about fishing effort should be used to estimate more accurate harvest rates and to stabilize our model structure for estimating migration rates. However, reliable historical fishing effort data stratified by area, season, and fisheries are currently not available, and rough approximations of historical trends in fishing effort may be obtained from stock assessments and used to refine harvest rates in future tag studies.

Consideration of other model structure would also be useful. Some extensions of the multiyear tag-recovery model from Brownie and Pollock (1985), which predicts recapture by tag groups, allow explicit inclusion of age-dependant effects on survival and movement parameters (cf. Brownie et al. 1993; Schwarz et al. 1993), although it certainly requires more data. Further accumulation of the tag data would make it possible to apply the model and estimate more stratified parameters by age and tag groups. Further studies aimed at removing or estimating the effects of tag-shedding rates (cf. Hearn et al. (1999) in the context of multiyear tagging model and Shirakihara and Kitada (2004) in two tag-release – one recovery experiments) are also needed for accurate estimates of exploitation rates and natural mortality rates from these tagging data.

This study investigated problems in reliably estimating seasonal migration rates with spatially and seasonally heterogeneously distributed tag data and ways to avoid these problems. Although the uneven distribution of the albacore tagging data prevented us from estimating migration patterns of young albacore in the fully parameterized model, this study demonstrated that partially quantitative estimation of migration rates could be obtained if we chose a range of migration pattern by setting up a rough migration path of North Pacific albacore on the basis of previous qualitative work by Otsu and Uchida (1963) and preliminary observation of the results with a fully parameterized model. Although our method would be very simplistic, the results show a good example of how to incorporate qualitative (old literature by Otsu and Uchida 1963) and quantitative (conventional tag experiment) knowledge and avoid the problems caused by fishery-dependent tag-release and recovery data. For future work, it would be very useful if we could integrate any qualitative and quantitative knowledge on migration, e.g., archival and conventional tagging data (Sibert and Fournier 2001), distribution of catch data (Kimura et al. 1997), and oceanographic conditions (Polovina et al. 2001), to delimit the migration hypotheses in a more effective manner.

Acknowledgements

The authors thank all of the scientific staff and crew who provided and complied the North Pacific albacore conventional tagging data. The authors also thank Hiroyuki Kurota (National Research Institute of Far Seas Fisheries) for his useful comments and all members of the ISC Albacore Working Group, who provided many useful scientific comments.

References

Begon, M., Harper, J.L., and Townsend, C.R. 1996. Ecology. Blackwell Science, Oxford, UK.

Bertignac, M., Hampton, J., and Coan, A.L., Jr. 1999. Estimates of exploitation rates for north Pacific albacore, *Thunnus alalunga*, from tagging data. Fish. Bull. (Washington, D.C.), **97**: 421–433.

Brownie, C., and Pollock, K.H. 1985. Analysis of multiple capture–recapture data using band-recovery methods. Biometrics, **41**: 411–420. doi:10.2307/2530866.

Brownie, C., Hines, J.E., Nichols, J.D., Pollock, K.H., and Hestbeck, J.B. 1993. Capture–recapture studies for multiple strata including non-Markovian transitions. Biometrics, **49**: 1173–1187. doi:10.2307/2532259.

Childers, J., and Aalbers, S. 2006. Summary of the 2005 U.S. North and South Pacific Albacore Troll Fisheries. Southwest Fisheries Science Center Administrative Report No. LJ-06-06, National Marine Fisheries Service, La Jolla, California.

Fisheries and Oceans Canada. 2004. Report of the Nineteenth North Pacific Albacore Workshop. Fisheries and Oceans Canada, Pacific Biological Station, Nanaimo, British Columbia. *Available at* http://www.dfo-mpo.gc.ca/Library/315833.pdf.

Hearn, W.S., Polacheck, T., Pollock, K.H., and Whitelaw, W. 1999. Estimation of tag reporting rates in age-structured multicomponent fisheries where one component has observers. Can. J. Fish. Aquat. Sci. **56**: 1255–1265. doi:10.1139/cjfas-56-7-1255.

Hilborn, R. 1990. Determination of fish movement patterns from tag recoveries using maximum likelihood estimators. Can. J. Fish. Aquat. Sci. **47**: 635–643. doi:10.1139/f90-071.

International Scientific Committee on Tuna and Tuna-like Species in the North Pacific Ocean. 2005. Report of the ISC Albacore Working Group Meeting 2005. NOAA Fisheries Southwest Fisheries Science Center, La Jolla, California. *Available at* http://isc.ac.affrc.go.jp/ISC_05_ALB/05ISC-ALBWG_Report.pdf.

© 2008 NRC Canada

Kikawa, S., Shiohama, T., Morita, Y., and Kume, S. 1977. Preliminary study on the movement of the North Pacific albacore based on the tagging. Bull. Far Seas Fish. Res. Lab. **15**: 101–113. [In Japanese with English abstract.]

Kimura, S., Nakai, M., and Sugimoto, T. 1997. Migration of albacore, *Thunnus alalunga*, in the North Pacific Ocean in relation to large oceanic phenomena. Fish. Oceanogr. **6**: 51–57. doi:10.1046/j.1365-2419.1997.00029.x.

Laurs, R.M., and Lynn, R.J. 1977. Seasonal migration of North Pacific albacore, *Thunnus alalunga*, into North American coastal waters: distribution, relative abundance, and association with transition zone waters. Fish. Bull. (Washington, D.C.), **75**: 795–822.

Laurs, R.M., and Wetherall, J.A. 1981. Growth rates of north Pacific albacore, *Thunnus alalunga*, based on tag returns. Fish. Bull. (Washington, D.C.), **79**: 293–302.

Laurs, R.M., Lenarz, W.H., and Nishimoto, R.N. 1976. Estimates of rates of tag shedding by North Pacific albacore, *Thunnus alalunga*. Fish. Bull. (Washington, D.C.), **74**: 675–678.

Otsu, T., and Uchida, R.N. 1963. Model of the migration of albacore in the North Pacific Ocean. Fish. Bull. (Washington, D.C.), **63**: 33–44.

Otter Research Ltd. 2001. An introduction to AD Model Builder. Version 6.0.2. Otter Research Ltd., Sidney, British Columbia.

Polovina, J.J., Howell, E., Kobayashi, D.R., and Seki, M.P. 2001. The transition zone chlorophyll front, a dynamic global feature defining migration and forage habitat for marine resources. Prog. Oceanogr. **49**: 469–483. doi:10.1016/S0079-6611(01)00036-2.

Schwarz, C.J., Schweigert, J.F., and Arnason, A.N. 1993. Estimating migration rates using tag-recovery data. Biometrics, **49**: 177–193. doi:10.2307/2532612.

Shirakihara, K., and Kitada, S. 2004. Estimating migration rates from two tag-release/one recovery experiments. ICES J. Mar. Sci. **61**: 821–828. doi:10.1016/j.icesjms.2004.01.006.

Sibert, J.R., and Fournier, D.A. 2001. Possible models for combining tracking data with conventional tagging data. *In* Electronic tagging and tracking in marine fisheries reviews: methods and technologies in fish biology and fisheries. *Edited by* J. Sibert and J. Nielsen. Kluwer Academic Press, Dordrecht, Netherlands. pp. 443–456.

Walters, C.J., and Martell, S.J.D. 2004. Fisheries ecology and management. Princeton University Press, Princeton, New Jersey.

Xiao, Y. 1996. A framework for evaluating experimental designs for estimating rates of fish movement from tag recoveries. Can. J. Fish. Aquat. Sci. **53**: 1272–1280. doi:10.1139/cjfas-53-6-1272.

© 2008 NRC Canada

Nature and nurture in dormancy: dissolved oxygen, pH, and maternal investment impact *Bythotrephes longimanus* resting egg emergence and neonate condition

Meghan Elizabeth Brown

Abstract: *Bythotrephes longimanus* (Onychopoda: Cercopagidae), an invasive zooplankter in North America, requires suitable habitat to satisfy its planktonic and resting stages, which occupy the pelagia and sediment of lakes, respectively. Thousands of resting eggs from hundreds of planktonic mothers were exposed to laboratory conditions that mimicked gradients observed in lake sediment (dissolved oxygen = 1.4–11.9 mg·L^{-1}; pH = 3–11). Eggs hatched in all treatments, which confirms the utility of dormancy and the robustness of the resting egg in *B. longimanus*. However, hatching success and neonate condition were greatest when dormancy conditions were maintained at near-saturated dissolved oxygen and near-neutral pH; deviations from these conditions resulted in prolonged development, smaller neonates, and the failure of many eggs to hatch. In addition to the influence of environmental conditions, heavier mothers produced larger eggs that hatched more frequently and resulted in heavier neonates. These maternal effects are likely due to greater energy investment by healthier mothers. This study suggests that nature and nurture influence dormancy success, and the results underscore that both life-cycle stages of *B. longimanus* need to be considered to understand its range expansion.

Résumé : *Bythotrephes longimanus* (Onychopoda: Cercopagidae), un organisme zooplanctonique envahissant en Amérique du Nord, requiert un habitat adéquat pour répondre aux besoins de ses stades planctoniques et son stade de repos qui vivent respectivement dans la zone pélagique et les sédiments des lacs. Nous avons exposé des milliers d'oeufs de repos provenant de centaines de mères planctoniques à des conditions de laboratoire qui miment les gradients observés dans les sédiments lacustres (oxygène dissous = 1,4–11,9 mg·L^{-1}; pH = 3–11). Les oeufs ont éclos dans toutes les conditions expérimentales, ce qui confirme l'importance de la dormance et la robustesse des oeufs de repos chez *B. longimanus*. Cependant, le succès de l'éclosion et la condition des nouveau-nés sont meilleurs lorsque les conditions de dormance se maintiennent à un niveau d'oxygène dissous s'approchant de la saturation et à un pH près de la neutralité; les écarts à partir de ces conditions ont pour résultat, un développement prolongé, une taille réduite des nouveau-nés et un insuccès de l'éclosion chez de nombreux oeufs. En plus de l'influence des conditions du milieu, les mères plus lourdes produisent des oeufs plus grands qui ont un taux d'éclosion plus élevé et donnent des nouveau-nés plus lourds. Ces effets maternels sont vraisemblablement dus à un investissement énergétique plus important par des mères en meilleure santé. Notre étude laisse croire que la nature et les conditions d'élevage influencent le succès de la dormance; nos résultats soulignent qu'il est nécessaire de considérer les deux étapes du cycle biologique de *B. longimanus* pour comprendre l'expansion de son aire de répartition.

[Traduit par la Rédaction]

Introduction

To understand the ecology and evolution of a species, it is necessary to study its complete life cycle. In temperate environments, many species of crustacean zooplankton cycle between an active phase that maximizes growth during favorable conditions (i.e., suitable abiotic habitat, abundant prey, low predation, etc.) and a dormant phase that facilitates survival and dispersal when conditions are poor (e.g., Hairston et al. 1996, 1999; Cáceres 1997). Understanding how these two life stages are impacted by nature and nurture in crustacean zooplankton is especially critical when studying range expansion of an invasive taxon such as the spiny waterflea, *Bythotrephes longimanus* (Onychopoda: Cercopagidae).

Since the establishment of *B. longimanus* in North America over two decades ago, research has focused on its active (planktonic) stage, which reproduces parthenogenetically and can quickly reach high population densities during summer and fall (Rivier 1998; Yan et al. 2001). The planktonic stage of *B. longimanus*, which measures about 1 cm in length, poses multiple environmental and economic threats in all five Laurentian Great Lakes and over 100 inland lakes throughout Canada and the USA where it has established (MacIsaac et al. 2004; Branstrator et al. 2006; N. Yan, York University, Department of Biology, Toronto, ON M3J 1P3, Canada, personal communication). Invasions have been associated with decreased abundance of small-

Received 26 July 2007. Accepted 30 January 2008. Published on the NRC Research Press Web site at cjfas.nrc.ca on 19 July 2008.
20109

M.E. Brown. Department of Biology, Hobart and William Smith Colleges, Geneva, NY 14456, USA (e-mail: mbrown@hws.edu).

 doi:10.1139/F08-082 © 2008 NRC Canada

bodied crustaceans, its preferred prey, (Lehman and Cáceres 1993; Yan et al. 2001) and declines in zooplankton species richness (Yan and Pawson 1997). Further, *B. longimanus* may compete with young fishes for food resources (Hoffman et al. 2001) and becomes ensnared in fishing equipments and recreational gear.

In contrast with its planktonic life stage, *B. longimanus* survives poor growth conditions as a dormant gametogenetic egg. The gametogentic egg is referred to as a resting egg in this publication, instead of a diapausing or over-winter eggs, since there is slowed, but measurable, metabolic activity (Andrew and Herzig 1984). Resting eggs appear to be essential for the species' survival because the presence of its planktonic stage during winter has never been reported (Rivier 1998). The fertilized resting egg develops through the gastrula stage in the mother's brood pouch (~2–7 eggs per clutch) and upon release settles to the sediment where it typically remains dormant until cued to hatch (Yurista 1992, 1997; Jarnagin et al. 2004). Although, resting eggs are generally produced in autumn and hatch the following spring, summer production and hatching of resting eggs is reported and can occur within the same summer (e.g., Burkhardt 1994; Yan et al. 2001; Brown and Branstrator 2005). Upon hatching, resting eggs give rise to females that can reproduce parthenogenetically and thus restore the active planktonic stage of the life cycle. In addition to the essential role of the resting egg in the year-to-year persistence within lakes, when dormancy is sustained for periods longer than the poor growth conditions persist, an egg bank accumulates that can play an important role in the maintenance of genetic variation and diversity for some species of zooplankton (e.g., Hairston et al. 1996).

As for many invasive species, the resting egg is hypothesized to be the founding life stage of new invasions for *B. longimanus*. It can move between lakes ensnared on recreational equipment and in, or on, migrating animals (MacIsaac et al. 2000; Jarnagin et al. 2000; Charalambidou et al. 2003). As such, previous studies have documented the water column conditions that trigger resting egg production (Burkhardt 1994; Yan et al. 2001; Brown and Branstrator 2005), the survivorship of eggs ingested by fish (Jarnagin et al. 2000) or waterfowl (Charalambidou et al. 2003), and temperature cues for hatching (Yurista 1992, 1997).

However, for *B. longimanus*, the maternal influences prior to dormancy (nurture) and environmental conditions during dormancy (nature) that support or prevent the successful hatch of resting eggs, as well as the reactivation of the planktonic stage, are unknown. For many species of zooplankton, including *B. longimanus*, the role of nurture is well documented for parthenogenic neonates; neonate size increases as material size increases (e.g., Glazier 1992; Boersma 1997; Branstrator 2005). Similar trends have been observed for gametogenetic neonates of *Daphnia*, whereby larger ephippia (resting eggs) not only yield larger neonates that are more likely to hatch, but the neonates themselves are more fit than those from smaller ephippia (Boersma et al. 2000). Further, studies on the dormant stages of many zooplankton species have documented the role of nature in the reinitiation of the active stage from dormancy. Environmental conditions that impact dormancy success include light and temperature (Herzig 1985; Carvalho and Wolf 1989), oxygen level (e.g., Ban and Mindoa 1992; Clegg and Jackson 1998; Marcus and Lutz 1998), desiccation (Wood and Banta 1937; Doma 1979), pH (Arnott and Yan 2002), and various chemical reagents (Pancella and Stross 1963; Uye et al. 1979; George et al. 1998), but the responses are not consistent among or even within species (Schwartz and Herbert 1987; De Meester and De Jager 1993), and the aforementioned studies have mainly focused on hatching conditions during the brief emergence period instead of the entire dormancy.

The establishment of *B. longimanus* is affected by environmental conditions, as distributional patterns show that less productive (MacIsaac et al. 2000; Yan et al. 2001; Branstrator et al. 2006) and nonacidic (Nilssen and Sandøy 1990) lakes are more likely to support *B. longimanus* across its native and introduced range. However, which phase(s) of the life cycle is (are) impacted and the extent of this has not been studied. The chemical and biological conditions of lake sediments (i.e., dissolved oxygen (DO) concentration, reduction–oxidation byproducts (such as CO_2, CH_4, and SO_4), pH, temperature, sedimentation rates, predation, and bacterial and fungal attack) may impact the success of the resting stage of *B. longimanus*, as these conditions influence resting egg hatching success and neonate condition for other zooplankton species (Arnott and Yan 2002; Cáceres and Tessier 2003). The hypolimnetic environments of productive lakes are commonly hypoxic or anoxic and have non-neutral pH conditions (e.g., Boström et al. 1982; Jeppesen et al. 1990). Undersaturated oxygen conditions can influence emergence patterns of at least some cladoceran taxa (Arnott and Yan 2002), and anoxia inhibits development and metabolism of diapausing *Artemia* cysts (Hofmann and Hand 1990; Clegg 1997). Further, in many naturally productive lakes, elevated pH (9 to 11) is observed (Mortimer 1941; Jeppesen et al. 1990), which is toxic to some zooplankton (Vijverberg et al. 1996). Anthropogenic influences have also altered the pH of lakes across the native and introduced range of *B. longimanus*, resulting in both acidic (Wright et al. 1980; Eilers and Selle 1991) and basic conditions at the sediment surface (Yan et al. 1996; Arnott and Yan 2002).

To examine the role of nature and nurture in the hatching success and neonate condition of *B. longimanus*, this study exposed thousands of resting eggs from hundreds of mothers to a range of dormancy conditions that might be experienced at the sediment–water interface. The primary objectives were (*i*) to test the hypothesis that hatching success is negatively correlated with extreme environmental conditions (i.e., undersaturated DO and non-neutral pH) in the hypolimnetic environment during dormancy, (*ii*) to identify the lethal thresholds (conditions where no eggs hatch) for the dormant egg of single and interactive conditions typical in hypolimnetic environments during dormancy, and (*iii*) to examine the contribution of maternal effects on egg and neonate condition.

Materials and methods

Collection of resting eggs

Gravid planktonic *B. longimanus* from Island Lake Reservoir (St. Louis County, Minnesota, USA) served as the source for all resting eggs. Collecting the eggs while they

© 2008 NRC Canada

were still in the mother's brood pouch prevented their prior exposure to sediment conditions and standardized their age. *Bythotrephes longimanus* was first detected in the reservoir in 1990 (Gravelle 1990) and likely invaded from Lake Superior. It was the only inland lake in Minnesota with an established population of *B. longimanus* at the time this study was initiated. Surface sediment conditions in Island Lake Reservoir are variable; temperatures range between 4 and 16 °C, DO range between 0.5 and 11 mg·L^{-1}, and pH range between 6 and 8.5.

In the laboratory, single females carrying resting eggs were reared in wells of tissue culture plates at ambient lake temperature until the release of their clutches, which took between 12 and 120 h. Females were maintained in Percival Intellus environmental chambers with red light (12 h light : 12 h dark cycle, <5 μE·m^{-2}·s^{-1}) to approximate lake light conditions and enabled *B. longimanus* to locate prey. Every 12 h, they were supplied with fresh, filtered Island Lake Reservoir water (hereafter called filtered water) and live food (immature *B. longimanus* without their caudal spines or *Daphnia* spp.). Any released resting eggs were removed with a large-bore pipette and placed individually in wells of tissue culture plates with 5 mL of filtered water.

The condition of each egg was inspected under a microscope with red light (Leica MZ125, 50×), and all mature golden-brown eggs (see Jarnagin et al. 2000 for further description) that were free of cracks, dents, and fungal growth were selected for experiments. Egg diameter was measured with an ocular micrometer. Egg volume (V) was calculated from egg diameter as the equivalent spherical volume. Each egg was assigned a unique identification number and position in the tissue culture plate to keep a record of its maternal lineage, sibling relationship, size, and collection and storage information. Resting eggs were maintained in dark environmental chambers at 3.5 °C until experimentation (maximum storage time was 14 days). Once a sufficient number of eggs had been collected each year (n_{2002} = 275, n_{2003} = 1200, n_{2004} = 1750), resting eggs were randomly placed into treatments.

Mothers were preserved in 70% ethanol, and 2–4 weeks later the body and caudal spine length were measured according to Burkhardt (1994). Subsequently, mothers were dried (24 h at 60 °C) and weighed (Cahn C-33 microbalance, KHK Enterprises, Inc.). Individual weights were recorded to the nearest microgram (accuracy of ±2 μg). To account for weight loss resulting from chemical preservation, maternal weights were corrected by increasing the preserved weight by a factor of 1.74 (Giguere et al. 1989).

Laboratory DO and pH experiments

Resting eggs were exposed to controlled pH and DO concentrations during a 120-day dormancy period in 2002, 2003, and 2004 (see Appendix A, Table A1 for experimental combinations and the mean dormancy conditions for each treatment). In 2002, experiments were conducted (*i*) to ensure that near-constant pH and DO conditions could be maintained for the entire 120-day dormancy, (*ii*) to test for differences in hatching success at two different DO concentrations, and (*iii*) to confirm that hatching cues reported by Yurista (1992) were accurate for eggs collected from Island Lake. Four treatments (48 eggs per treatment) were established in 2002 at neutral pH, two at 7.5 mg DO·L^{-1}, and two at 11.9 mg DO·L^{-1} (53% and 85% saturation, respectively, at 3.5 °C and 435 m above sea level (Mortimer 1981)). Following the success of the 2002 experiments, in 2003, 20 treatments (48 eggs per treatment) were established to investigate hatching patterns and potential lethal thresholds (treatments where no eggs hatched) for pH (3, 5, 7, 9, and 11) and DO (2.5, 4.2, 7.5, and 11.9 mg·L^{-1}; approximately 18%, 30%, 53%, and 85% saturation, respectively, at 3.5 °C and 435 m above sea level (Mortimer 1981)) by testing all possible combinations of these factors. In 2004, experiments were conducted to further examine the hatching patterns observed in 2003; treatments (48 eggs per treatment) were established at 1.4 mg DO·L^{-1} for pH 3, 5, 6, 7, 9, and 11 and at 11.9 mg DO·L^{-1} for pH 5, 6, and 7.

Treatments in all years were conducted in dark environmental chambers. Single eggs were contained in individual wells of tissue culture plates and submersed in a 4 L glass jar filled with filtered water. Each treatment consisted of six plates per jar with eight eggs per plate. Plates were covered with 210 μm mesh windows to allow water circulation. Compressed nitrogen gas or compressed air was bubbled into the jars to maintain assigned DO levels, and 10% sulfuric acid or 10% sodium hydroxide was periodically added to maintain assigned pH levels. Temperature (YSI 5500), DO (YSI 5500), and pH (VWR symphony SB10) were measured every other day.

After the 120-day dormancy period, temperature in the environmental chamber was increased to promote hatching (hatching period). In 2002, one of the treatments from each assigned DO level was subjected to a 6.5 °C hatching cue and the other to a 10 °C hatching cue to establish proper hatching cues. In 2003 and 2004, all treatments received a 6.5 °C hatching cue. In all years, at the start of the hatching period, water in each treatment jar was flushed with fresh filtered water to produce neutral pH and saturated DO conditions (see Appendix A, Table A1 for mean hatching conditions for each treatment). The levels of DO and pH maintained during dormancy were not continued during the hatching phase to standardize hatching conditions. Therefore, abiotic condition during dormancy and maternal line were the only known variables contributing to variation in hatching success and neonate condition.

The developmental condition of each egg was scored weekly for 20 weeks following the hatching cue. Plates were individually removed from treatment jars, and each egg was examined with the aid of a microscope under red light (<5 μE·m^{-2}·s^{-1}). This provided enough light to see the egg, but based on Yurista (1997), it should not provide an additional hatching cue and had no observable effect on hatching (M. Brown, unpublished data). Eggs were scored as "hatched" when two halves of the egg and the thin pop-up stage membrane (see Yurista 1992) were present and (or) remains of the neonate were present. Eggs that had not hatched but appeared healthy were scored as "not hatched", and their development was further described as "no development," "initiated development", or "pop-up stage" based on figure 2 in Yurista (1992). Occasionally not hatched eggs were encountered that developed to the pop-up stage, but in the subsequent weeks did not hatch and eventually were surrounded by a thick film of growth. These eggs were scored

© 2008 NRC Canada

as "partially hatched". An egg that was cracked, smashed, degraded, or appeared empty was scored "not viable." All neonates were measured for total length and then immediately dried and weighed by the methods described for mothers.

Statistical methods

Statistical analyses were used to determine the role of nature in hatching success by (*i*) examining how hatching success and development time were influenced by DO concentration and pH and (*ii*) identifying differences between treatment levels and any lethal thresholds for the dormant egg of single and interactive conditions. Statistical analyses were also performed to study the role of nurture in hatching success by examining the relationship among maternal size, clutch size, and egg size, as well as the effect of these characteristics on hatching success. Lastly, statistics were performed to quantify how both nature and nurture impacted neonate dry weight. All analyses were performed in SYSTAT 10 (SPSS Inc., Chicago, Illinois) unless otherwise specified.

The role of nature in hatching success

Dormancy and hatching conditions are reported as arithmetic means of measurements taken every other day. Since pH is logarithmic, the mean pH was calculated by first back-transforming to the equivalent hydrogen ion concentration and finding its mean and then calculating the negative log of this value. Hatching results are reported as the mean proportions of eggs in each jar that either hatched, partially hatched, or were not viable. These means were calculated from the proportions of eggs in the aforementioned categories for each of the six plates in each treatment jar. Using the plate as the experimental unit was a more conservative approach than using the cell (i.e., individual eggs), but still allowed for a measure of variance, since all eggs for a treatment were contained in a single jar. It also was consistent with the egg scoring, since entire plates were removed to check for egg development.

For 2002, a one-way analysis of variance (ANOVA) was used to test for differences in hatching success between the 6.5 and 10 °C hatching cues. For all years, a mixed regression using restricted maximum likelihood estimation was used to determine whether DO, pH, and the interaction between DO and pH (fixed effects) were significant predictors of the proportion of eggs that hatched and whether the chamber (random effect) influenced the proportion of eggs that hatched (SPSS 14.0, SPSS Inc., Chicago, Illinois). The chamber effect reflects both the use of different chambers in 2002 (for the two hatching temperatures) and the use of the same chamber in different years. This was done since treatment combinations changed between years, and therefore it was not possible to separate a year from a treatment effect. The nontransformed data met normality and equal variance assumptions. Planned simple contrasts with a priori hypotheses were used to determine differences between specific treatments by levels of a factor (pH or DO) as follows: non-neutral pH treatments were compared with pH = 7, acidic treatments were compared with other acidic treatments, basic treatments were compared with other basic treatments, and undersaturated DO treatments were compared with saturated DO, with the hypotheses that the more extreme condition would have lower hatching success. Subsequently, pH treatments were grouped according to significant differences based on the planned contrasts, and linear trends among these pH groups were compared across DO concentrations using an analysis of covariance (ANCOVA). A slope homogeneity test was used to confirm that the slopes did not differ among the pH groupings before performing the ANCOVA.

The length of development following dormancy in the 2003 treatments was quantified by two measures: (*i*) the length of time it took for the first neonate to appear after the hatching cue (1st hatch) and (*ii*) the length of time it took for half of the number of neonates that would eventually hatch to emerge after the hatching cue (50% hatch). To determine if these developmental times were a function of dormancy conditions, four simple least-squared linear regression models were used (one for each combination of the independent variables (DO or pH distance from neutrality) and the dependent variables (50% or 1st hatch)). Regression slopes were compared with zero by F ratios to determine if linear trends were significant.

The role of nurture in hatching success

For all treatments combined, the mean diameter and volume of eggs that hatched and those that failed to hatch were compared with a t test that assumed equal variance (two-tailed p value). The slopes of simple least-squared linear regression models were used to evaluate the influence of egg diameter on the time it took to proceed through three stages: (*i*) from hatching cue to initial development, (*ii*) from initial development to pop-up, and (*iii*) from pop-up to emergence of the neonate. A multiple least-squared linear regression was used to examine the influence of maternal weight and clutch size (independent variables) on egg diameter (dependent variable). Data were grouped by clutch size for all eggs used in the experiments.

The role of nature and nurture in neonate size

A stepwise linear regression with a constant was used to determine if neonate dry weight was a function of egg diameter, dormancy condition, or both (DO or pH distance from 7). Slope homogeneity tests were used to look for an interaction between all statistically significant predictors. An ANCOVA was performed to look for differences in the y intercepts (main effect of dormancy condition) and to determine if the slope of the lines differed from zero (covariate effect of egg diameter).

Results

The role of nature in hatching success

Resting egg hatching success was indistinguishable between the 6.5 and 10 °C hatching cues ($F_{[1,275]} = 0.012$, $p = 0.913$), and at least one resting egg hatched following incubation in all combinations of dormancy DO and pH (Fig. 1*a*). The highest percentage of hatching occurred following dormancy at near-saturated DO and near-neutral pH during dormancy (Fig. 1*a*). Hatching success was never greater than 80%, and many eggs that failed to hatch appeared healthy, with only a small percentage of eggs in any

© 2008 NRC Canada

Fig. 1. The mean proportion (±1 standard deviation, SD) of resting eggs that hatched (*a*), were not viable (*b*), and partially hatched (*c*) at the conclusion of experiments that manipulated dormancy dissolved oxygen (DO) concentration (mg·L^{-1}) and pH. Symbols separate pH treatments following dormancy conditions at near-neutral pH (pH = 7 or pH = 6: ●), basic pH (pH = 9 or pH = 11: □), and acidic pH (pH = 3 or pH = 5: ×). Linear regressions are shown separately for near-neutral ($y = -0.0211x + 0.291$, $R^2 = 0.51$), basic ($y = -0.0254x + 0.170$, $R^2 = 0.76$), and acidic treatments ($y = -0.0174x + 0.1477$, $R^2 = 0.27$). A slope homogeneity test confirmed that linear trends did not differ in slope among pH groups ($F_{[8,192]} = 1.197$, $p = 0.303$), and a subsequent analysis of covariance (ANCOVA) showed that linear trends over DO concentrations were significant among the pH groups at the *y* intercept ($F_{[4,192]} = 20.66$, $p < 0.001$) and that all slopes differed significantly from zero ($F_{[1,192]} = 8.697$, $p = 0.004$).

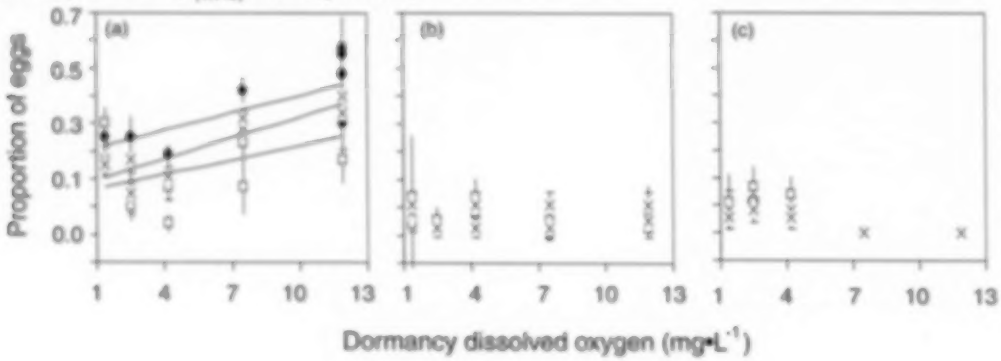

treatment scored as nonviable (<20%, Fig. 1*b*) or partially hatched (<15%, Fig. 1*c*).

The proportion of eggs that hatched declined with declining DO concentration (Fig. 1*a*, $F_{[4,171]} = 18.76$, $p < 0.0001$). Undersaturated DO concentration during dormancy resulted in significant decreases in hatching success (Fig. 1*a*). Hatching success for eggs maintained at DO = 11.9 was greater than eggs maintained at DO = 7.5 (contrast estimate = –0.246, standard error, SE = 0.038, $p < 0.001$), DO = 4.2 (contrast estimate = –0.263, SE = 0.038, $p < 0.001$), and DO = 2.5 (contrast estimate = –0.146, SE = 0.032, $p < 0.001$). However, the proportion of eggs that hatched was indistinguishable between the treatments with DO = 11.9 and DO = 1.4 (contrast estimate = –0.69, SE = 0.049, $p = 0.154$, see results below on chamber assignment and year effects). Among DO treatments, the proportion of eggs scored as not viable was consistent (Fig. 1*b*, statistics not performed); however, the presence of partially hatched eggs was associated with low DO concentration. Partially hatched eggs were always and only observed when the DO was below 4.2 mg·L^{-1}, but there was no increase in frequency with the level of DO stress (Fig. 1*c*, statistics not performed).

Deviations from non-neutral pH also resulted in significant decreases in hatching success (Fig. 1*a*, $F_{[5,171]} = 7.87$, $p < 0.0001$), but were independent of DO concentration ($F_{\text{interaction }[17,171]} = 0.101$, $p = 0.101$). Among pH treatments, the proportion of eggs that hatched was greater at pH = 7 than at pH = 5 (contrast estimate = –0.0.63, SE = 0.082, $p = 0.022$) and was greater at pH = 7 than at pH = 9 (contrast estimate = –0.135, SE = 0.040, $p = 0.002$). Hatching success did not differ within basic treatments (pH = 9 and pH = 11, contrast estimate = –0.017, SE = 0.038, $p = 0.658$) or acidic treatments (pH = 5 and pH = 3, contrast estimate = –0.063, SE = 0.038, $p = 0.98$). Hatching success was also indistinguishable between pH 6 and 7 (contrast estimate = –0.028, SE = 0.035, $p = 0.425$). Across pH levels, the proportion of eggs scored as not viable was nearly constant (Fig. 1*b*, no statistic performed), and there were no patterns observed with regard to partially hatched eggs (Fig. 1*c*).

When pH treatments were grouped by near-neutral, acidic, and basic treatments (based on the significant contrasts above), a slope homogeneity test confirmed that linear trends across DO concentrations did not differ in slope among the pH groups ($F_{[8,192]} = 1.197$, $p = 0.303$). Linear trends across DO concentrations were significantly different among pH groups ($F_{[4,192]} = 20.66$, $p < 0.001$), with all groups having slopes that differed significantly from zero ($F_{[1,192]} = 8.697$, $p = 0.004$). Near-neutral pH treatments had the greatest hatching success ($y = -0.0211x + 0.291$, $R^2 = 0.51$), followed by basic treatments ($y = -0.0254x + 0.170$, $R^2 = 0.76$) and acidic treatments ($y = -0.0174x + 0.1477$, $R^2 = 0.27$) (Fig. 1).

The chamber assignment had no statistically significant effect on hatching ($F_{[3,171]} = 0.957$, $p = 0.414$). Chamber level was assigned based on multiple chambers in a single year (2002 only) and the same chamber being used in different years. Although no statistics were performed on the year the experiment was conducted, since treatment combinations were not spread evenly across year, hatching success in 2002 and 2004 tended to be greater than that in 2003, despite identical methodology. This is evident, for example, in the 1.4 mg·L^{-1} treatments, which were conducted in 2004 only (Appendix A, Table A1) and exhibited greater hatching success at all pH levels than hypoxic treatments in 2003 (Fig. 1*a*).

For those eggs that did hatch, exposure to undersaturated DO concentrations and non-neutral pH conditions tended to lengthen development time as measured by the time to 1st hatch and 50% hatch (Fig. 2). The only significant relationship was between DO and time to 1st hatch; increasing DO concentration resulted in shorter mean time to 1st hatch (Fig. 2*a*, $F_{[3,120]} = 4.95$, $p = 0.039$).

© 2008 NRC Canada

Fig. 2. Mean time (weeks) for the first neonate to appear after the hatching cue (solid bars) and mean time (weeks) for half the number of the neonates that would eventually hatch to emerge after the hatching cue (open bars) for experiments conducted in 2003. Error bars are ± 1 standard deviation (SD). Each bar in panel (*a*) is the mean of five treatments with the same dissolved oxygen concentration but different pH; each bar in panel (*b*) is the mean four treatments with the same pH but different dissolved oxygen concentration.

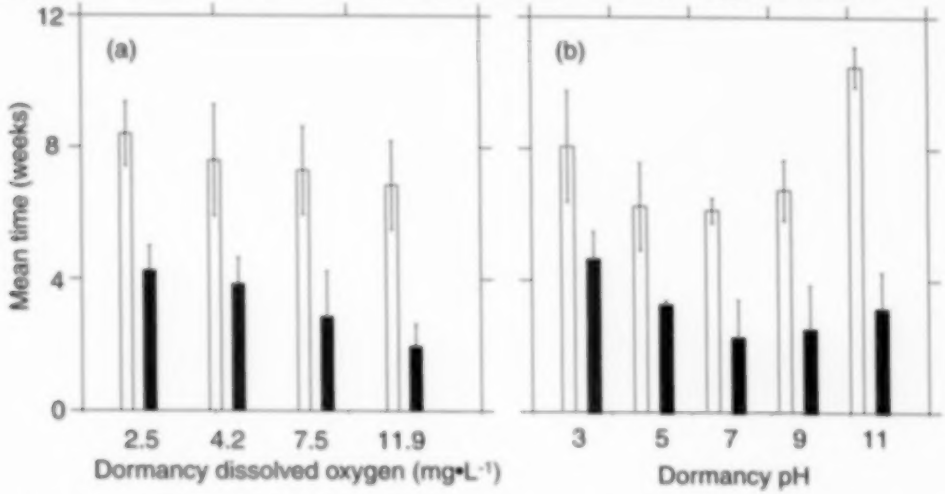

Fig. 3. Length of time (weeks) resting eggs of different diameters spend in developmental stages. Eggs from all experimental years (2002–2004) are included. Panel (*a*) displays the mean time it took eggs to show signs of initial development after the hatching cue was given. Panel (*b*) shows the length of time between initial development and the pop-up stage. Panel (*c*) displays the time between the pop-up stage and the neonate hatching. Error bars are ±1 standard deviation (SD). See Materials and methods and Yurista (1992) for developmental chronology.

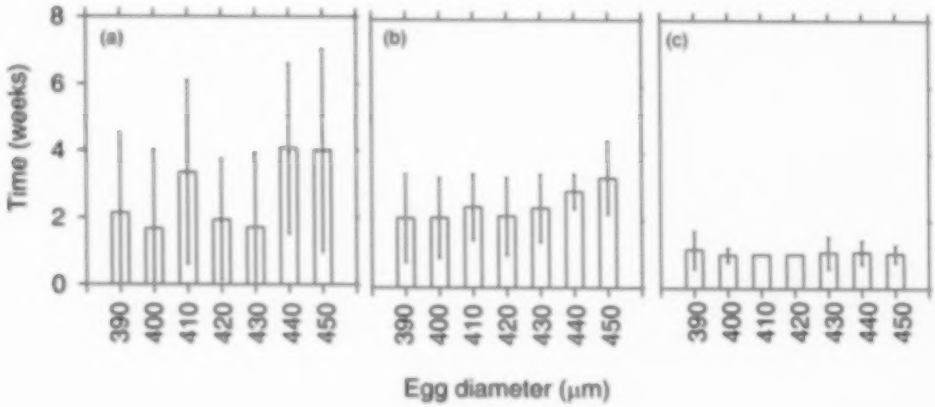

The role of nurture in hatching success

Larger diameter eggs developed more slowly than smaller diameter eggs on average (Fig. 3). Increased egg size resulted in a longer time between the start of the hatching cue and initial development (Fig. 3*a*: $F_{[1,651]} = 96.45$, $p < 0.001$) and a longer time between initial development and the pop-up stage (Fig. 3*b*: $F_{[1,651]} = 108.46$, $p < 0.001$). Eggs of all sizes proceeded from the pop-up stage to a hatched neonate in about 1 week (Fig. 3*c*: $F_{[1,651]} = 0.51$, $p = 0.475$).

Hatched eggs ($n = 1208$) had a greater mean diameter (432 μm) and mean volume (4.25×10^7 μm^3) than eggs that failed to hatch ($n = 1440$, mean diameter = 419 μm, mean volume = 3.86×10^7 μm^3) ($t = 7.9$, $p < 0.001$). Egg diameter was a function of maternal condition and brood size. Egg diameter increased with maternal weight ($n = 276$, $t = 1.95$, $p = 0.052$) and decreased with clutch size ($n = 276$, $t = -5.05$, $p < 0.001$) (Fig. 4, egg diameter = 415.34 + (123.14 × maternal weight) – (10.57 × clutch size) + (29.19 × maternal weight × clutch size], $R^2 = 0.47$). There was a significant interaction between clutch size and corrected maternal weight ($n = 276$, $t = 2.483$, $p = 0.014$).

The role of nature and nurture in neonate size

A slope homogeneity test confirmed that there was no significant interaction between egg diameter and DO concentration ($n = 571$, $t = 0.69$, $p = 0.49$), and a subsequent ANCOVA revealed that neonate weight increased with in-

© 2008 NRC Canada

Fig. 4. Mean resting egg diameter for clutches of various sizes as a function of corrected maternal weight. A regression model (egg diameter = 415.34 + (123.14 × maternal weight) – (10.57 × clutch size) + (29.19 × maternal weight × clutch size), $R^2 = 0.47$, $p < 0.001$, $n = 276$) indicated significant relationships between egg diameter and clutch size ($t = -5.05$, $p < 0.001$), egg diameter and corrected maternal dry weight ($t = 1.95$, $p = 0.05$), and egg diameter and the interaction between clutch size and corrected maternal dry weight ($t = 2.48$, $p = 0.014$).

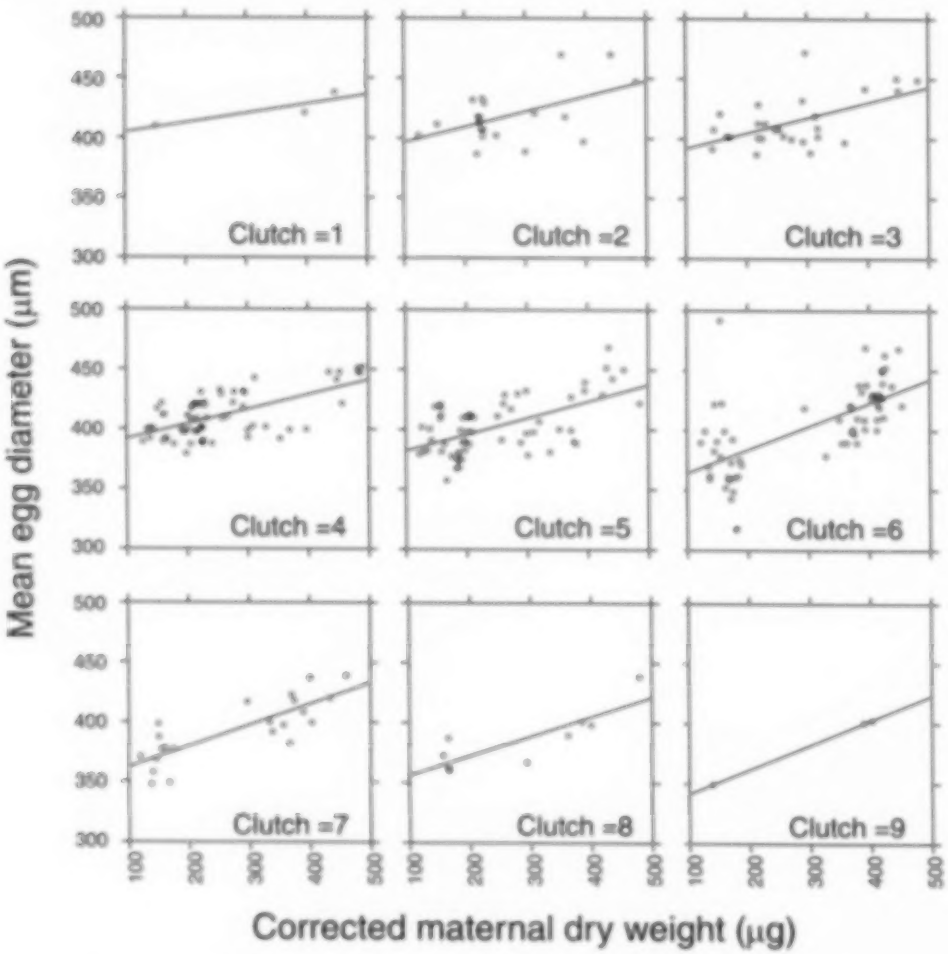

creasing dormancy DO ($F_{[4,571]} = 53.36$, $p < 0.001$) and increasing egg diameter ($F_{[7,571]} = 133.07$, $p < 0.001$) (Figs. 5*a*–5*e*). pH conditions during dormancy had no detectable influence on neonate weight ($n = 571$, $t = 0.146$, $p = 0.884$) (Figs. 5*f*–5*k*).

Discussion

The role of nature

Bythotrephes longimanus preferentially occupies clear, deep, oligotrophic lakes (MacIsaac et al. 2000; Branstrator et al. 2006). This reflects its ability to establish sustaining populations in these lake types, which includes successful completion of its planktonic (active) and resting egg (dormant) stages that occupy two different regions of a lake, the pelagia and the sediments, respectively. The abiotic tolerance of the planktonic stage and the low level of, or refuge from, planktivory in deep oligotrophic lakes have been suggested as possible explanations for this pattern (MacIsaac et al. 2000; Yan et al. 2001; Branstrator et al. 2006), but these hypotheses remain untested in a direct fashion. Further, they overlook that the habitat characteristics that *B. longimanus* prefers likely reflect a combination of its life-cycle requirements for both the planktonic and resting stages. The present study demonstrates that resting egg hatching success and neonate size are in part driven by environmental conditions that impact dormancy, which can vary considerably at the sediment–water interface of lakes across the native and introduced range of *B. longimanus*, depending on lake productivity and acidification (e.g., Mortimer 1941; Boström et al. 1982; Stoddard et al. 1999). Results also confirm that temperatures near 4.0 °C cue hatching for *B. longimanus* resting eggs, as reported by Yurista (1992), which is typical of spring sediments temperatures in lakes across the range of *B. longimanus* and in Island Lake Reservoir (M. Brown, unpublished data), the source lake for eggs in this experiment.

© 2008 NRC Canada

Fig. 5. (*a–e*) Relationships between resting egg diameter and neonate dry weight for eggs maintained during dormancy at 1.4 mg·L^{-1} (*a*: n = 49), 2.0 mg·L^{-1} (*b*: n = 43), 3.7 mg·L^{-1} (*c*: n = 55), 7.5 mg·L^{-1} (*d*: n = 141), and 11.9 mg·L^{-1} (*e*: n = 283). Overlapping points are shown with a slight offset. Panel (*a*) is 2004 data only. Panels (*b*) and (*c*) are 2003 data only. Panel (*d*) is 2002 and 2003 data. Panel (*e*) is data from 2002, 2003, and 2004. A slope homogeneity test showed that there was no interaction between egg diameter and dissolved oxygen (DO) (n = 571, t = 0.689, p = 0.49). An analysis of covariance (ANCOVA) revealed that the linear trends were significantly different from one another at the y intercept (main effect of DO: $F_{[4,571]}$ = 53.36, $p < 0.001$) and that the slopes were significantly different from zero (covariate effect of egg diameter: $F_{[1,571]}$ = 133.07, $p < 0.001$). (*f–k*) Relationships between resting egg diameter and neonate dry weight for eggs maintained during dormancy at pH = 3 (*f*: n = 36), 5 (*g*: n = 64), 6 (*h*: n = 369), 7 (*i*: n = 369), 9 (*j*: n = 28), and 11 (*k*: n = 44). Overlapping points are shown with a slight offset. Panel (*f*) is 2004 data only. Panels (*g*), (*h*), (*i*), (*j*), and (*k*) are data from 2002, 2003, and 2004.

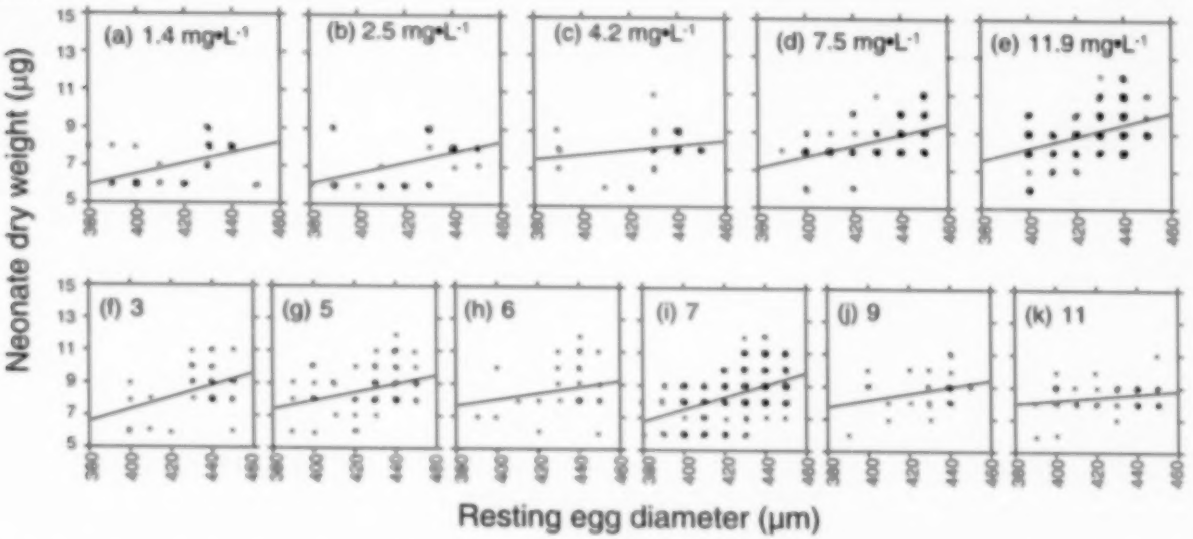

This finding permitted a single hatching cue of 6.5 °C in 2003 and 2004 treatments.

The first objective of this work was to test the hypothesis that hatching success was negatively correlated with extreme environmental conditions, which is supported in that declines in DO and deviations from neutral pH in general resulted in progressively more severe effects. Hatching success gradually declined as DO concentrations decreased, and partial hatches (initiated development, but failed to hatch) were always and only observed below 4.2 mg·L^{-1}. However, it is notable that fewer eggs hatched in all undersaturated treatments compared with saturated treatments (11.9 mg·L^{-1}) except for the most hypoxic treatment (1.4 mg·L^{-1}), which had comparable hatching success with the saturated condition. This could be the result of enhanced hatching at the most extreme DO conditions or potentially more robust eggs in 2004 when the 1.4 mg·L^{-1} treatment was conducted (see discussion of nurture below). The overall pattern of decreased hatching success in extreme conditions is consistent with previous work on dormant stages of other species of zooplankton that report lowered emergence rates in hypoxic conditions (e.g., Ban and Mindoa 1992; Clegg and Jackson 1998; Marcus and Lutz 1998). The present study expands this work by showing progressive effects of decreasing oxygen concentration during the dormant period on the embryo, exclusive of conditions during the hatching period, since DO was depressed only during the dormancy phase.

There were also progressive declines in neonate birth weight as oxygen concentrations declined, which may influence the ecology of the planktonic stage that establishes from these neonates. The variation observed was beyond the error of the microbalance used to measure individual neonate weight (10%–20%), but limited instrument accuracy may account for some of the range of neonate weights observed for eggs of similar diameter. Although it is unknown if the size of *B. longimanus* neonates impacts their fitness in the wild, smaller *B. longimanus* gametogenetic neonates, just like their parthenogenetic counterparts, may have restricted diets because of the size of their feeding appendages, take longer to reach reproductive maturity, mature at smaller size, and have smaller clutches and (or) smaller neonates (Ebert 1993; Arbačiauskas and Gasiūnaitė 1996; Branstrator 2005). In *Daphnia*, the larger the neonate that emerges from the gametogenetic egg, the larger her first brood will be (Boersma et al. 2000), and larger parthenogenetic animals are able to withstand starvation and low resource levels better than small offspring (Tessier and Consolatti 1989). Thus, in lakes with depressed oxygen in the hypolimnion, poor hatching success combined with potentially lowered fitness of neonates may have important consequences for the establishment of the planktonic phase each spring.

Hatching success also gradually declined in more acidic and more basic pH treatments, which may result from the resting eggs' inability to osmotically regulate essential elements, as has been observed in the active stage of other plankton (Potts and Fryer 1979; Vijverberg et al. 1996).

© 2008 NRC Canada

The fact that hatching success was greatest following dormancy conditions at near-neutral pH, depressed in basic dormancy conditions, and even further depressed in acidic treatments indicates that the eggs are most sensitive to acidified conditions. Unlike DO stresses, dormancy pH had no observable effect on the condition of the neonate, as has been reported in parthenogenetic *Daphnia* following exposure to non-neutral pH treatments (Vijverberg et al. 1996). For the experiments presented here, treatment wells were searched weekly, and neonates were immediately killed and weighed; therefore, effects of dormancy conditions on *B. longimanus* neonate locomotion and postbirth development remain unknown.

Combined, the negative effects of DO and pH on egg ontogeny suggest that the hypolimnetic environments of productive lakes are poor environments for recruitment. It is known that *B. longimanus* has limited establishment in productive (MacIsaac et al. 2000; Branstrator et al. 2006) and acidified or alkaline lakes (Nilssen and Sandøy 1990). Thus, a complementary, and experimentally supported explanation of *B. longimanus* establishment patterns lies in the habitat available to the dormant stage, not solely the planktonic habitat as discussed by MacIsaac et al. (2000) and Branstrator et al. (2006). Moreover, poor dormancy habitat may also explain, in part, the temporary disappearance of *B. longimanus* during periods of eutrophication in Lago Maggiore, Italy (Manca and Ruggiu 1998) and Lake Võrtsjärv, Estonia (Haberman 1998).

The second major objective of this work was to identify the lethal thresholds of *B. longimanus* resting eggs. Across the large range of DO and pH tested, no conditions were found that completely inhibited hatching. At least one egg hatched in every treatment, and the percentage of nonviable eggs did not differ among treatments. This suggests that at the population level, the resting egg is an effective means of temporal dispersal even during poor dormancy conditions for this zooplankter. This is consistent with the dormant stages of other crustacean zooplankton that can tolerate stresses that are lethal to the active life stages, including exposure to abiotic stresses such as high temperatures, freezing, desiccation, anoxia, and toxins (see references in Introduction) and biotic stresses such as passage through the digestive track of fish and waterfowl (Proctor 1964; Mellors 1975). The latter has also been documented for *B. longimanus* (Jarnagin et al. 2000; Charalambidou et al. 2003). It is notable that although no lethal thresholds were observed, egg hatching success was lower following dormancy in acidic treatments compared with basic treatments that were the same distance from neutral pH.

As opposed to killing the resting eggs, extreme conditions may instead promote eggs to remain in a dormant state, which has been observed in plant seeds that delay germination and in *Daphnia* ephippia that use bet-hedging strategies to insure that some eggs remain dormant despite a hatching cue, to provide for long-term persistence (i.e., greater than 1 year) (De Meester and De Jager 1993; Cáceres and Tessier 2003). Lengthened dormancy or prolonged development in undersaturated DO treatments might result from depressed egg metabolism. For eggs that did hatch, undersaturated DO condition resulted in longer development times following a hatching cue, which may result from longer dormancies. For example, the mean time to 50% hatch (half the eggs to hatch that would eventually hatch) for eggs incubated at 2.5 $mg \cdot L^{-1}$ was a little more than 4 weeks, whereas for eggs maintained at 11.9 $mg \cdot L^{-1}$, the mean time to 50% hatching was about 2 weeks. This near doubling of development time is consistent with the observation of Andrew (1993), who predicted increased dormancy length due to the slowed metabolic rate of *B. longimanus* resting eggs when DO concentrations were maintained below 40% saturation at 4.2 °C (about 5.5 $mg \cdot L^{-1}$).

Further, oxygen uptake rates can be depressed in acidic pH as concentration of free, hydrated CO_2 increases, inhibiting the diffusion of O_2 (Potts and Fryer 1979; Alibone and Fair 1981). For *B. longimanus*, the length of development following dormancy in acidic treatments tended to be longer, although these differences were not significant. Decreased affinity for oxygen at acidic pH is an intriguing explanation of low hatching success, since intracellular pH (pH_i) of gastrula-stage embryos of some species regulates the transition between dormancy and active development. In *Artemia*, carbon dioxide decreases pH_i and can be used to induce a state of dormancy (Busa and Crowe 1983).

Given the great variation in DO and pH levels possible at the sediment–water interface (e.g., Mortimer 1941; Jeppesen et al. 1990; Stoddard et al. 1999) and their relation to nutrient and acid pollution, the experimental results reported here are important for understanding the establishment of *B. longimanus* across the North American landscape. Nonetheless, it is important to note that *B. longimanus* within a single lake may be locally adapted to the conditions of that environment, and the present study only tested the response of eggs from a single reservoir where *B. longimanus* has existed for over a decade. Future study should address among-lake differences in resting egg tolerance, as well as response to actual sediment conditions, as the present study isolated DO and pH conditions without using lake sediments. Resting eggs are likely to experience stresses in addition to low DO and non-neutral pH, such as anoxic byproducts, predation, and bacterial and fugal attack. Abiotic stresses are likely to become more extreme below the sediment surface where conditions vary considerably at millimetre scales (Mortimer 1941) and thus may be especially important for buried eggs. Although older eggs retrieved from deep in the sediment often have poor hatching success, resting eggs of some cladoceran species can remain viable for centuries in lake sediments (Hairston et al. 1995); for these species, it will be fascinating to study the relation between egg age and resistance to stress.

The role of nurture

In addition to the role of nature during dormancy, variation in hatching success in *B. longimanus* is attributable to nurture. In other cladoceran species, environmental conditions during egg production (Davison 1969; Doma 1979; De Meester and De Jager 1993), heritability (De Meester and De Jager 1993), and interaction between genotype and environment (Schwartz and Herbert 1987) have all been shown to be important drivers of emergence from dormancy. The final objective of this study (i.e., to detail maternal effects on the *B. longimanus* resting egg) provides an additional lens to view dormancy.

© 2008 NRC Canada

The variations in clutch size and egg size observed in this study and the observed hatching patterns regarding egg size underscore the effect of each life-cycle phase on the other — larger mothers have more successful resting eggs, and better resting conditions result in larger neonates. Increased egg and neonate size with increased maternal size and greater hatching success of larger eggs is consistent with previous studies on cladocerans (Glazier 1992; Ebert 1993; Boersma 1997). Larger *Daphnia* ephippia produced by larger females are more likely to hatch and will hatch into larger neonates (Boersma et al. 2000). Further, *Daphnia* born from parthenogenic eggs have an increased survival rate from larger eggs owing to an increase in protein, lipid, and carbon content invested by the mother (Guisande and Gliwicz 1992). For *B. longimanus*, larger eggs may contain greater energy stores (Andrew and Herzig 1984), whereas smaller eggs may not have enough energy to sustain them through dormancy or limited energy for the subsequent development of the neonate, especially under stress. This explanation is consistent with the observation that larger resting eggs took longer to develop after the hatching cue than did smaller eggs. The fact that larger resting eggs resulted in heavier neonates lends additional weight to the idea that larger eggs contained greater energy stores and (or) larger embryos. If larger *B. longimanus* mothers invest more energy per offspring, this may help to overcome environmental stress (i.e., pH, DO, etc.) and perhaps serve an adaptive role in the resting eggs, as has been demonstrated for other cladocerans (De Meester et al. 1998; Boersma et al. 2000), plants (Philippi 1993), and insects (Mousseau and Dingle 1991).

It was not possible to separate maternal effects due to differences in energy investment, genetics, or the interaction between genetics and the environments. However, it seems likely that in *B. longimanus*, the physiological condition of the females could differ substantially, with the nutritional status of the mother and her overall health determining how much energy she can allocate to her resting eggs, which depend entirely on energy provisioned by the mother to survive dormancy and hatch successfully. Periods of intense predation, inadequate food resources, and abiotic stresses, which are all known to cue resting egg production in zooplankton (e.g., Cáceres 1997; Yan et al. 2001; Brown and Branstrator 2005), may result in insufficient resources being allocated to the resting egg, either because of nutritional deficiencies or shifts in resource allocation toward somatic growth. Further, gravid *B. longimanus* are known to be selected for by visually-feeding fishes, and although resting eggs can remain viable after gut passage (Jarnagin et al. 2000), these eggs may be deposited before they are fully mature. In both parthenogenetic and gametogenetic cladocerans, increasing neonate size with maternal size has been attributed to better condition of larger females during egg production and their ability to allocate proper energy stores (e.g., Pfrendor and Deng 1998; Boersma et al. 2000; Branstrator 2005). Future studies will need to tease apart the genetic and phenotypic drivers of egg dormancy in *B. longimanus* and also how the environment interacts with both.

In the present study, the greatest hatching success and largest neonates were observed when eggs were produced by large planktonic mothers and dormancy conditions were maintained at near-saturated DO and near-neutral pH. These maximum rates are comparable with estimates of annual egg bank turnover for *B. longimanus* in field sediment surveys, which are high (approximately 80%–90%) in both invaded and native lakes (Herzig 1985; Brown and Branstrator 2005). Andrew and Herzig (1984) hypothesize that dormancy in *B. longimanus* may last less than 1 year because of metabolic activity in the resting egg. Limited temporal viability could restrict establishment, as short dormancy times combined with environmental stress have been implicated in failed invasions for other zooplankton (Hairston et al. 1999). Poor dormancy conditions and (or) improper provisioning from their planktonic mothers may create a bottleneck for the *B. longimanus* resting egg, which appears to be essential for persistence within lakes and the likely vector for new invasions. Certainly other factors, such as predation throughout the life cycle of *B. longimanus* and resource limitation during the planktonic stage may be important, and unfolding the ecology of this and other species with multiple life stages requires study of the role of nature and nurture during the complete life cycle.

Acknowledgements

D. Brown, K. Heimgartner, M. Thabes, and W. Reynolds provided collection and laboratory assistance. D. Branstrator offered invaluable suggestions throughout the research, and he, J. Pastor, and M. Thabes provided insightful comments on earlier drafts of this manuscript. I also thank K. Cottingham and three anonymous reviewer for comments on organization and statistical suggestions. D. Droney provided support for the mixed regression analysis. This work was supported by funds awarded to D. Branstrator from the Minnesota Sea Grant College Program supported by the NOAA office of Sea Grant, United States Department of Commerce, under grant No. NOAA-NA16-RG1046. The US government is authorized to reproduce and distribute reprints for government purposes, not withstanding any copyright notation that may appear hereon. This research was also finically supported through a Doctoral Dissertation Fellowship awarded to M.E. Brown from the University of Minnesota.

References

Alibone, M.R., and Fair, P. 1981. The effects of low pH on the respiration of *Daphnia magna* Straus. Hydrobiologia, **85**: 185–188.

Andrew, T.E. 1993. The influence of oxygen concentration on the respiration rate of the resting eggs of *Leptodora kindti* (Focke 1844) and *Bythotrephes longimanus* Leydig 1860. Arch. Hydrobiol. **128**: 409–414.

Andrew, T.E., and Herzig, A. 1984. The respiration rate of the resting eggs of *Leptodora kindti* (Focke 1844) and by *Bythotrephes longimanus* Leydig 1860 (Crustacea, Cladocera) at environmentally encountered temperatures. Oecologia (Berl.), **64**: 241–244. doi:10.1007/BF00376877.

Arbačiauskas, K., and Gasiūnaitė, Z.R. 1996. Growth and fecundity of *Daphnia* after diapause and their impact on the development of a population. Hydrobiologia, **320**: 209–222. doi:10.1007/BF00016822.

Arnott, S.E., and Yan, N.D. 2002. The influence of drought and re-acidification on zooplankton emergence from resting stages.

© 2008 NRC Canada

Ecol. Appl. **12**: 138–153. doi:10.1890/1051-0761(2002)012[0138:TIODAR]2.0.CO;2.

Ban, S., and Minoda, T. 1992. Hatching of diapausing eggs of *Eurytemora affinis* (Copepoda: Calanoida) collected from lake-bottom sediments. J. Crustac. Biol. **12**: 51–56. doi:10.2307/1548718.

Boersma, M. 1997. Offspring size and parental fitness in *Daphnia magna*. Evol. Ecol. **11**: 439–450. doi:10.1023/A:1018484824003.

Boersma, M., Boriss, H., and Mitchell, S. 2000. Maternal effects after sexual reproduction in *Daphnia magna*. J. Plankton Res. **22**: 279–285. doi:10.1093/plankt/22.2.279.

Boström, B., Jansson, M., and Forsberg, C. 1982. Phosphorus release from lake sediments. Arch. Hydrobiol. Beih. Ergebn. Limnol. **18**: 5–59.

Branstrator, D.K. 2005. Contrasting life histories of the predatory cladocerans *Leptodora kindtii* and *Bythotrephes longimanus*. J. Plankton Res. **27**: 569–585. doi:10.1093/plankt/fbi033.

Branstrator, D.K., Brown, M.E., Shannon, L.J., Thabes, M.C., and Heimgartner, K.V. 2006. Range expansion of *Bythotrephes longimanus* in North America: evaluating habitat characteristics in the spread of an exotic zooplanker. Biol. Invasions, **8**: 1367–1379. doi:10.1007/s10530-005-5278-7.

Brown, M.E., and Branstrator, D.K. 2005. Seasonal dynamics in *Bythotrephes* diapause egg emergence and production, and the role of dormancy in range expansion. Verh. Internat. Verein. Limnol. **29**: 174–178.

Burkhardt, S. 1994. Seasonal size variation in the predatory cladoceran *Bythotrephes cederstroemii* in Lake Michigan. Freshw. Biol. **31**: 97–108. doi:10.1111/j.1365-2427.1994.tb00842.x.

Busa, W.B., and Crowe, J.H. 1983. Intracellular pH regulates transition between dormancy and development of brine shrimp (*Artemia salina*) embryos. Science (Washington, D.C.), **221**: 366–368. doi:10.1126/science.221.4608.366. PMID:17798891.

Cáceres, C.E. 1997. Dormancy in invertebrates. Invertebr. Biol. **116**: 371–383. doi:10.2307/3226870.

Cáceres, C.E., and Tessier, A.J. 2003. How long to rest: the ecology of optimal dormancy and environmental constraint. Ecology, **84**: 1189–1198. doi:10.1890/0012-9658(2003)084[1189:HLTRTE]2.0.CO;2.

Carvalho, G.R., and Wolf, H.G. 1989. Resting eggs of lake-*Daphnia* I. Distribution, abundance, and hatching of eggs collected from various depths in lake sediments. Freshw. Biol. **22**: 459–470. doi:10.1111/j.1365-2427.1989.tb01118.x.

Charalambidou, I., Ketelaars, H.A.M., and Santamaria, L. 2003. Endozoochory by ducks: influence of developmental stages of *Bythotrephes* diapause eggs on dispersal probability. Divers. Distrib. **9**: 367–374. doi:10.1046/j.1472-4642.2003.00026.x.

Clegg, J.S. 1997. Embryos of *Artemia franciscana* survive four years of continuous anoxia: the case for complete metabolic rate depression. J. Exp. Biol. **200**: 467–475. PMID:9318130.

Clegg, J.S., and Jackson, S.A. 1998. The metabolic status of quiescent and diapause embryos of *Artemia franciscana* (Kellogg). Arch. Hydrobiol. Adv. Limnol. **52**: 425–439.

Davison, J. 1969. Activation of the ephippial eggs of *Daphnia pulex*. J. Gen. Physiol. **53**: 562–575. doi:10.1085/jgp.53.5.562. PMID:5814069.

De Meester, L., Cousyn, C., and Vanoverbeke, J. 1998. Chemical interactions, maternal effects and the hatching of *Daphnia* diapausing eggs. Arch. Hydrobiol. **52**: 263–272.

De Meester, L., and De Jager, H. 1993. Hatching of *Daphnia* sexual eggs. I: intraspecific differences in hatching responses of *D. magna* eggs. Freshw. Biol. **30**: 219–226. doi:10.1111/j.1365-2427.1993.tb00803.x.

Dorna, S. 1979. Ephippia of *Daphnia magna* Straus — a technique for their mass production and quick revival. Hydrobiologia, **67**: 183–188. doi:10.1007/BF00126718.

Ebert, D. 1993. The trade-off between offspring size and number in *Daphnia magna*: the influence of genetic, environment, and maternal effects. Arch. Hydrobiol. **4**: 453–473.

Eilers, J.M., and Selle, A.R. 1991. Geographic overview of the regional case study areas. *In* Acid deposition and aquatic ecosystems. *Edited by* D.F. Charles. Springer-Verlag, New York. pp. 107–125.

George, C.L., Lindley, V.A., Evans, S.V., and Donkin, P. 1998. The effect of pollution of intertidal sediments on the viability of calanoid copepod eggs. Arch. Hydrobiol. Adv. Limnol. **52**: 175–183.

Giguere, L.A., St-Pierre, J.-F., Bernier, B., Vezina, A., and Rondeau, J.G. 1989. Can we estimate the true weight of zooplankton samples after chemical preservation? Can. J. Fish. Aquat. Sci. **46**: 522–527. doi:10.1139/f89-070.

Glazier, D.S. 1992. Effects of food, genotype, and maternal size and age on offspring investment in *Daphnia magna*. Ecology, **73**: 910–926. doi:10.2307/1940168.

Gravelle, J. 1990. Slimy species sneaks into inland lake. Duluth News Tribune, 13 September.

Guisande, C., and Gliwicz, Z.M. 1992. Egg size and clutch size in two *Daphnia* species grown at different food levels. J. Plankton Res. **14**: 997–1007. doi:10.1093/plankt/14.7.997.

Haberman, J. 1998. Zooplankton of Lake Võrtsjärv. Limnologica, **28**: 49–65.

Hairston, N.G., Jr., Kearns, C.M., and Ellner, S.P. 1996. Phenotypic variation in a zooplankton egg bank. Ecology, **77**: 2382–2392. doi:10.2307/2265740.

Hairston, N.G., Jr., Perry, L.J., Bohonak, A.J., Fellows, M.Q., Kearns, C.M., and Engstrom, D.R. 1999. Population biology of a failed invasion: paleolimnology of *Daphnia exilis* in upstate New York. Limnol. Oceanogr. **44**: 477–486.

Hairston, N.G., Jr., Van Brunt, R.A., Kearns, C.M., and Engstrom, D.R. 1995. Age and survivorship of diapausing eggs in a sediment egg bank. Ecology, **76**: 1706–1711. doi:10.2307/1940704.

Herzig, A. 1985. Resting eggs — a significant stage in the life cycle of crustaceans *Leptodora kindti* and *Bythotrephes longimanus*. Verh. Internat. Verein. Limnol. **22**: 3088–3098.

Hofmann, G.E., and Hand, S.C. 1990. Subcellular differentiation arrested in *Artemia* embryos under anoxia: evidence supporting a regulatory role of intercellular pH. J. Exp. Zool. **253**: 287–382. doi:10.1002/jez.1402530308.

Hoffman, J., Smith, M.E., and Lehman, J.T. 2001. Perch or plankton: top-down control of *Daphnia* by yellow perch (*Perca flavescens*) or *Bythotrephes cederstroemi* in an inland lake? Freshw. Biol. **46**: 759–775. doi:10.1046/j.1365-2427.2001.00716.x.

Jarnagin, S.T., Kerfoot, W.C., and Swan, B.K. 2004. Zooplankton life cycles: direct documentation of pelagic births and deaths relative to diapausing egg production. Limnol. Oceanogr. **49**: 1317–1332.

Jarnagin, S.T., Swan, B.K., and Kerfoot, W.C. 2000. Fish as vectors in the dispersal of *Bythotrephes cederstroemi*: diapausing eggs survive passage through the gut. Freshw. Biol. **43**: 579–589.

Jeppesen, E., Søndergaad, M., Mortesen, E., Kristensen, P., Riemann, B., Jensen, H., Müller, J.P., Sorthjaer, O., Jensen, J.P., Christofersen, K., Bosselmann, S., and Dall, E. 1990. Fish manipulation as a lake restoration tool in shallow eutrophic lakes 1: cross-analysis of three Danish case-studies. Hydrobiologia, **200/201**: 205–218. doi:10.1007/BF02530340.

Lehman, J.T., and Cáceres, C.E. 1993. Food-web responses to spe-

© 2008 NRC Canada

cies invasion by a predatory invertebrate: *Bythotrephes* in Lake Michigan. Limnol. Oceanogr. **38**: 879–891.

MacIsaac, H.J., Borbely, J.V.M., Muirhead, J.R., and Graniero, P.A. 2004. Backcasting and forecasting biological invasions of inland lakes. Ecol. Appl. **14**: 773–783. doi:10.1890/02-5377.

MacIsaac, H.J., Ketelaars, H.A.M., Grigorovich, I.A., Ramcharan, C.W., and Yan, N.D. 2000. Modeling *Bythotrephes longimanus* invasions in the Great Lakes basin based on its European distribution. Arch. Hydrobiol. **149**: 1–21.

Manca, M., and Ruggiu, D. 1998. Consequences of pelagic food-web changes during a long-term lake oligotrophication process. Limnol. Oceanogr. **43**: 1368–1373.

Marcus, N.H., and Lutz, R.V. 1998. Longevity of subitaneous and diapause eggs of *Centropages hamatus* (Copepoda: Calanoida) from the northern Gulf of Mexico. Mar. Biol. (Berl.). **131**: 249–257. doi:10.1007/s002270050317.

Mellors, W.K. 1975. Selective predation of ephippial *Daphnia* and the resistance of ephippial eggs to digestion. Ecology, **56**: 974–980. doi:10.2307/1936308.

Mortimer, C.H. 1941. The exchange of dissolved substances between mud and water in lakes (Parts I and II). J. Ecol. **29**: 147–329.

Mortimer, C.H. 1981. The oxygen content of air-saturated fresh waters over ranges of temperature and atmospheric pressure of limnological interest. Mitt. Int. Ver. Theor. Angew. Limnol. **20**: 1–23.

Mousseau, T.A., and Dingle, H. 1991. Maternal effects in insect life histories. Annu. Rev. Entomol. **36**: 511–534. doi:10.1146/annurev.en.36.010191.002455.

Nilssen, J.P., and Sandøy, S. 1990. Recent lake acidification and cladoceran dynamics: surface sediment and core analyses from lakes in Norway, Scotland and Sweden. Philos. Trans. R. Soc. Lond. B Biol. Sci. **327**: 299–309. doi:10.1098/rstb.1990.0066.

Pancella, J.R., and Stross, R.G. 1963. Light induced hatching of *Daphnia* resting eggs. Chesap. Sci. **4**: 135–140. doi:10.2307/1350746.

Pfrender, M.E., and Deng, H.W. 1998. Environmental and genetic control of diapause termination in *Daphnia*. Arch. Hydrobiol. Adv. Limnol. **52**: 237–251.

Philippi, T. 1993. Bet-hedging germination of desert annuals: variation among populations and maternal effects in *Lepidium lasiocarpum*. Am. Nat. **142**: 488–507. doi:10.1086/285551.

Potts, W.T.W., and Fryer, G. 1979. The effects of pH and salt content on sodium balance in *Daphnia magna* and *Acantholeberis curirostris* (Crustacea: Cladocera). J. Comp. Physiol. **129**: 289–294.

Proctor, V.W. 1964. Viability of crustacean eggs recovered from ducks. Ecology, **45**: 656–658. doi:10.2307/1936124.

Rivier, I.K. 1998. The predatory Cladocera (Onychopoda: Podonidae, Polyphemidae, Cercopagidae) and Leptodorida of the world. Backhuys Publishing, Leiden, The Netherlands.

Schwartz, S.S., and Herbert, P.D.H. 1987. Methods for the activation of the resting eggs of *Daphnia*. Freshw. Biol. **17**: 373–379. doi:10.1111/j.1365-2427.1987.tb01057.x.

Stoddard, J.L., Jeffries, D.S., Lükewille, A., Clair, T.A., Dillon, P.J., Driscoll, C.T., Forsius, M., Johannessen, M., Kahl, J.S., Kellogg, J.H., Kemp, A., Mannio, J., Monteith, D.T., Murdoch, P.S., Patrick, S., Rebsdorf, A., Skjelvåle, B.L., Stainton, M.P., Traaen, T., van Dam, H., Webster, K.E., Wieting, J., and Wilander, A. 1999. Regional trends in aquatic recovery from acidification in North America and Europe. Nature (London), **401**: 575–578. doi:10.1038/44114.

Tessier, A.J., and Consolatti, N.L. 1989. Variation in offspring size in *Daphnia* and consequences for individual fitness. Oikos, **56**: 269–279. doi:10.2307/3565347.

Uye, S., Kasahara, S., and Onbé, T. 1979. Calanoid copepod eggs in sea-bottom muds: effects of some environmental factors on the hatching of resting eggs. Mar. Biol. (Berl.), **51**: 151–156. doi:10.1007/BF00555194.

Vijverberg, J., Kalf, D.F., and Boersma, M. 1996. Decrease in *Daphnia* egg viability at elevated pH. Limnol. Oceanogr. **41**: 789–794.

Wood, T.R., and Banta, A.M. 1937. Hatchability of *Daphnia* and *Moina* sexual eggs without drying. Internationale Revue der Gesamten Hydrobiologie und Hydrographie, **359**(1–6): 229–243.

Wright, R.F., Conroy, N., Dickson, W.P., Harriman, R., Hendrickson, A., and Schofield, C.L. 1980. Acidified lake districts of the world: a comparison of water chemistry of lakes in southern Norway, southern Sweden, southwestern Scotland, the Adirondack mountains of New York State, and southeastern Ontario. *In* Ecological impacts of acid precipitation. *Edited by* D. Drablos and A. Tollan. Sur NedbØors Virking På Skog og Fisk Project, Oslo, Norway. pp. 377–379.

Yan, N.D., and Pawson, T.W. 1997. Changes in the crustacean zooplankton community of Harp Lake, Canada, following invasion by *Bythotrephes cederstroemi*. Freshw. Biol. **37**: 409–425. doi:10.1046/j.1365-2427.1997.00172.x.

Yan, N.D., Blukacz, A., Sprules, W.G., Kindy, P.K., Hackett, D., Girard, R.E., and Clark, B.J. 2001. Changes in zooplankton and the phenology of the spiny water flea, *Bythotrephes*, following its invasion of Harp Lake, Ontario, Canada. Can. J. Fish. Aquat. Sci. **58**: 2341–2350. doi:10.1139/cjfas-58-12-2341.

Yan, N.D., Keller, W., Scully, N.M., Lean, D.R.S., and Dillon, P.J. 1996. Increased UV-B penetration in a lake owing to drought-induced acidification. Nature (London), **381**: 141–143. doi:10.1038/381141a0.

Yurista, P.M. 1992. Embryonic and postembryonic development in *Bythotrephes cederstroemii*. Can. J. Fish. Aquat. Sci. **49**: 1118–1125. doi:10.1139/f92-124.

Yurista, P.M. 1997. *Bythotrephes cederstroemi* diapausing egg distribution and abundance in Lake Michigan and the environmental cues for breaking diapause. J. Great Lakes Res. **23**: 202–209.

Appendix A

Table A1 appears on the following page.

© 2008 NRC Canada

Table A1. Temperature, dissolved oxygen (DO), and pH conditions in each treatment during the dormancy period and the hatching period.

Treatment			Dormancy conditions (120 days)				Hatching conditions			
Year	DO (mg·L^{-1})	pH	Temp. (°C)	DO (mg·L^{-1})	DO (%)	pH	Temp. (°C)	DO (mg·L^{-1})	DO (%)	pH
2002	11.9	7	3.86 (0.72)	11.14 (1.32)	84.83 (7.72)	7.24 (0.21)	6.55 (0.33)	10.23 (0.54)	83.68 (4.22)	7.29 (0.36)
			3.82 (0.46)	11.67 (1.06)	88.34 (6.12)	7.31 (0.20)	10.09 (0.54)	9.12 (0.87)	93.10 (5.44)	7.25 (0.37)
	7.5	7	3.44 (0.65)	7.66 (0.65)	58.90 (6.45)	7.22 (0.18)	6.67 (0.48)	10.25 (0.44)	84.10 (0.65)	7.27 (0.26)
			3.75 (0.39)	7.22 (1.11)	54.55 (8.20)	7.01 (0.36)	10.21 (0.43)	9.44 (1.21)	85.10 (7.12)	7.33 (0.54)
2003	11.9	3	3.95 (1.14)	12.06 (0.87)	91.66(6.34)	3.09 (0.21)	6.12 (0.28)	11.15 (1.15)	89.93 (9.30)	7.21 (0.24)
		5	3.83 (1.27)	12.16 (1.08)	92.10 (7.36)	5.05 (0.40)	6.14 (0.30)	11.56 (1.61)	93.33 (13.00)	7.18 (0.56)
		7	3.72 (1.14)	11.82 (1.05)	89.31 (7.62)	7.24 (0.39)	6.14 (0.31)	10.84 (1.01)	87.53 (8.34)	7.23 (0.30)
		9	3.74 (1.17)	12.00 (1.00)	90.65 (7.15)	8.75 (0.35)	6.15 (0.29)	10.84 (1.22)	87.57 (10.00)	7.20 (0.29)
		11	3.92 (1.26)	12.15 (0.80)	90.54 (13.55)	10.80(0.48)	6.15 (0.25)	11.55 (1.61)	93.26 (12.90)	7.48 (0.56)
	7.5	3	3.84 (0.71)	7.21 (1.14)	54.37 (8.87)	3.08 (0.19)	6.36 (0.32)	10.80 (0.86)	87.73 (7.18)	7.20 (0.24)
		5	3.87 (0.72)	7.65 (0.75)	58.04 (5.84)	5.09 (0.39)	6.26 (0.25)	10.80 (1.07)	87.48 (8.78)	7.17 (0.23)
		7	3.82 (0.64)	7.55 (0.88)	57.17 (6.52)	7.13 (0.35)	6.32 (0.25)	10.92 (1.25)	88.63 (10.58)	7.18 (0.29)
		9	3.87 (0.71)	7.62 (0.99)	57.79 (7.64)	8.81 (0.41)	6.26 (0.36)	10.84 (1.06)	87.86 (9.00)	7.18 (0.24)
		11	3.85 (0.53)	7.27 (1.26)	55.09 (9.57)	10.90 (0.39)	6.32 (0.36)	10.89 (1.31)	88.41 (10.82)	7.29 (0.38)
	4.2	3	3.73 (0.46)	4.42 (1.11)	33.40 (8.39)	3.09 (0.21)	6.18 (0.44)	10.74 (0.97)	86.87 (8.52)	7.21 (0.25)
		5	3.75 (0.52)	4.37 (0.81)	33.09 (6.28)	4.88 (0.66)	6.29 (0.51)	10.84 (0.97)	87.94 (10.99)	7.16 (0.23)
		7	3.73 (0.35)	4.39 (0.84)	30.14 (6.34)	7.21 (0.27)	6.11 (0.56)	10.63 (1.35)	85.79 (10.93)	7.16 (0.21)
		9	3.73 (0.34)	4.07 (1.06)	30.71 (7.92)	8.83 (0.39)	6.17 (0.39)	10.67 (1.14)	86.28 (9.70)	7.25 (0.23)
		11	3.72 (0.39)	4.11 (1.03)	31.01 (7.72)	10.93 (0.39)	6.17 (0.45)	10.83 (1.37)	87.51 (11.23)	7.39 (0.39)
	2.5	3	3.72 (0.39)	2.65 (0.81)	20.01 (6.07)	3.11 (0.21)	6.39 (0.42)	10.53 (1.04)	85.65 (8.70)	7.25 (0.24)
		5	3.85 (0.32)	2.64 (0.74)	19.97 (5.60)	4.92 (0.59)	6.52 (0.34)	10.57 (1.28)	86.23 (10.12)	7.30 (0.28)
		7	3.84 (0.40)	2.38 (0.79)	18.03 (5.87)	7.26 (0.33)	6.44 (0.47)	10.39 (1.35)	84.60 (11.23)	7.35 (0.26)
		9	3.71 (0.30)	2.61 (1.00)	19.72 (7.57)	8.89 (0.38)	6.41 (0.35)	10.60 (1.12)	86.08 (9.11)	7.48 (0.58)
		11	3.82 (0.38)	2.34 (1.14)	17.76 (8.70)	10.84 (0.47)	6.42 (0.34)	10.35 (1.39)	84.20 (11.45)	7.41 (0.48)
2004	11.9	5	4.03 (0.43)	11.12 (0.91)	84.98 (6.51)	4.71 (0.54)	6.53 (0.48)	10.11 (0.50)	82.76 (4.03)	7.00 (0.28)
		6	3.90 (0.47)	11.06 (1.06)	84.28 (7.45)	6.27 (0.46)	6.77 (0.38)	10.25 (0.54)	84.45 (4.22)	7.04 (0.34)
		7	3.68 (0.45)	10.96 (0.63)	83.02 (4.20)	7.00 (0.38)	6.85 (0.32)	10.58 (0.49)	87.41 (4.08)	7.20 (0.24)
	1.4	3	3.84 (0.37)	1.31 (0.28)	9.95 (2.13)	3.32 (0.27)	6.67 (0.40)	10.20 (0.55)	83.82 (4.62)	6.78 (0.22)
		5	4.25 (0.32)	1.34 (0.37)	10.26 (2.87)	5.15 (0.53)	6.56 (0.46)	10.19 (0.48)	83.47 (3.76)	7.01 (0.43)
		6	4.10 (0.41)	1.36 (0.65)	10.41 (4.96)	6.08 (0.54)	6.53 (0.29)	10.02 (0.47)	82.05 (4.07)	7.11 (0.38)
		7	3.90 (0.49)	1.37 (0.46)	10.45 (3.46)	7.16 (0.47)	6.69 (0.33)	10.16 (0.67)	83.54 (5.36)	7.10 (0.22)
		9	3.95 (0.37)	1.65 (0.51)	12.58 (3.92)	8.61 (0.59)	6.68 (0.30)	10.23 (0.67)	84.12 (5.87)	7.32 (0.54)
		11	3.73 (0.40)	1.42 (0.94)	10.79 (7.08)	10.5 (0.27)	6.56 (0.31)	10.23 (0.41)	83.83 (3.77)	7.78 (0.39)

Note: Mean (±1 SD) dormancy and hatching conditions are shown for each of the laboratory pH and DO combinations tested. In 2002 only, treatment combination was conducted for hatching conditions at 6.5 and 10 °C.

© 2008 NRC Canada

Comparison between activity estimates obtained using bioenergetic and behavioural analyses[1]

Guillaume Guénard, Daniel Boisclair, Ola Ugedal, Torbjørn Forseth, and Bror Jonsson

Abstract: Activity rate of Arctic char (*Salvelinus alpinus*) held in 90 m^2 littoral enclosures were estimated using bioenergetic (with consumption estimated using stable caesium, ^{133}Cs) and behavioural approaches (with fish movements quantified using video cameras). We found no statistically significant difference between values of activity rate obtained using the two approaches for three of the six experiments we performed. However, there was no relationship between estimates of activity rate obtained using the two approaches. Discrepancies may arise from the difficulty to meet assumptions regarding the temporal stability of the concentration of ^{133}Cs in fish diet and of the assimilation coefficient of this tracer. When fish remain in an area where their behaviour can be well described (e.g., enclosure, habitat patches of littoral zones, coral reefs), the behavioural approach appears more robust to estimate activity rate because it depends most on a variable that is easiest to estimate (the number of movements performed). When these conditions are not met (low fish densities or major fish migrations), a reliable assessment of the concentration and assimilation of ^{133}Cs in stomach contents appears critical to implement the bioenergetic approach based on this tracer.

Résumé : Nous avons estimé les taux d'activité d'ombles chevaliers (*Salvelinus alpinus*) dans six enclos de 90 m^2 installés dans la zone littorale d'un lac en utilisant une méthode bioénergétique (basée sur l'estimation des taux de consommation par une analyse de l'accumulation de césium stable, ^{133}Cs) et une méthode comportementale (basée sur l'estimation des mouvements de nage à l'aide de paires de caméras vidéo en stéréo). Nous n'avons pas trouvé de différences statistiquement significatives entre les taux d'activité estimations par l'une ou l'autre des méthodes dans trois enclos sur six. De plus, aucune relation n'a été décelée entre les estimés de taux d'activité produites par les deux méthodes. Il est possible que les différences dans les taux d'activité obtenus par ces deux méthodes aient été la conséquence du non-respect des prémisses liées à la stabilité temporelle de la concentration de ^{133}Cs dans le régime des poissons, de même que des coefficients d'assimilation du marqueur. Lorsque la répartition des poissons est restreinte à des zones où leur comportement peut être décrit avec fiabilité (c.à.d. dans des enclos, des taches d'habitat en zone littorale, des récifs coralliens, etc.), la méthode comportementale semble la plus adéquate pour mesurer les taux d'activité, car elle dépend principalement de variables faciles à estimer (le nombre de mouvements effectués). Par contre, dans les cas où le comportement des poissons est difficile à décrire avec fiabilité (basses densités de poissons, mouvements majeurs de migration), un suivi fiable de la concentration et de l'assimilation de ^{133}Cs dans les contenus stomacaux devra nécessairement être effectué afin d'assurer que la méthode bioenergétique puisse être utilisée avec confiance.

Introduction

Bioenergetic models are mass-balanced equations that represent the energy budget (kJ·day^{-1}) of an organism (Kitchell et al. 1977; Hewett and Johnson 1992; Hanson et al. 1997):

$$(1) \qquad G = C - (F + E + \mathrm{SDA} + \mathrm{SMR} + \mathrm{ACT})$$

In these models, growth rate (G, which, in eq. 1, includes energy reserves for reproduction) is the difference between consumption rate and a series of energy losses (egestion (F), excretion (E)) and expenditures (standard metabolic rate (SMR), specific dynamic action (SDA), activity rate (ACT)). Bioenergetic models have been used to predict fish growth (Rice et al. 1983; Wieser and Medgyesy 1991; Brandt et al. 1992), to estimate the effect of fish on their prey (Kitchell and Breck 1980; Majkowski and Wairwood 1981; Stewart et al. 1981), to assess the role of fish on nutrient recycling (Kraft 1992; see Hansen et al. 1993 for a review), and to quantify the energy costs associated with heavy metal exposure (Sherwood et al. 2000).

Activity rate has long been recognized as the least understood component of bioenergetic models (Hewett and Johnson 1992; Ney 1993). Activity rate (the net cost of swimming at the exclusion of any other loss or expenditure) has been suggested to represent a variable and often impor-

Received 20 June 2007. Accepted 23 January 2008. Published on the NRC Research Press Web site at cjfas.nrc.ca on 22 July 2008. J20060

G. Guénard and D. Boisclair.[2] Université de Montréal, Département de sciences biologiques, C.P. 6128, Succursale Centre-ville, Montréal, QC H3C 3J7, Canada.
O. Ugedal and T. Forseth. Norwegian Institute for Nature Research, Tungasletta 2, No-7485 Trondheim, Norway.
B. Jonsson. Norwegian Institute for Nature Research, Forskningsparken A/S, Gaustadalleén 21, No-0349 Oslo, Norway.

[1]Contribution of the Groupe de Recherche Interuniversitaire en Limnologie (GRIL).
[2]Corresponding author (e-mail: daniel.boisclair@umontreal.ca).

 doi:10.1139/F08-080 © 2008 NRC Canada

tant component of fish energy budget. Boisclair and Leggett (1989) estimated activity rate of yellow perch (*Perca flavescens*) from three age classes in 12 lakes of the Eastern Township of Québec, Canada. Activity rate was estimated as the difference between consumption rate and the sum of growth rate, energy losses, and energy expenditures. In this study, consumption and growth rates were estimated in the field, while other components of the bioenergetic equation were obtained using published empirical models (Hewett and Johnson 1992). Consumption rate was calculated by combining the results of surveys of fish digestive tract contents and experiments of evacuation rates (Eggers 1977). Boisclair and Leggett (1989) found that perch activity rate ranged from 0% to 250% of SMR among their study lakes. Boisclair and Sirois (1993) estimated the activity rate of brook trout (*Salvelinus fontinalis*) reared in in situ enclosures. They estimated activity rate using underwater video cameras that allowed them to assess the number and the velocity of the movements performed by fish. Fish movements were transformed in energy expenditures using an empirical relationship between swimming cost, fish mass, and swimming speed (Boisclair and Tang 1993). Activity rate of brook trout ranged from 60% to 280% of SMR depending on the environmental conditions found in the enclosures in which they were held. These studies and others (see Boisclair 2001 for a review) are consistent with the suggestion that deficient modelling of activity rate may be responsible for the occasionally poor performance of bioenergetic models (Minton and McLean 1982; Wahl and Stein 1991; Madon and Culver 1993).

The development of reliable models of activity rate requires the repeated estimation of this component of bioenergetic models under variable environmental conditions (Sirois and Boisclair 1995; Boisclair and Rasmussen 1996). Approaches employed to estimate activity rate may be defined as either bioenergetic or behavioural. Following the bioenergetic approach, activity rate is estimated as the difference between consumption rate and the sum of growth rate, energy losses, and energy expenditures associated with standard metabolism and digestion. Studies using the bioenergetic approach differ in the methods used to estimate consumption rate. Consumption rate over specified time periods may be estimated either from the interpolation of temporally punctual surveys of digestive tract contents and evacuation rates (Boisclair and Leggett 1989; Post 1990; Fox 1991) or from the rate at which chemical tracers accumulate in the fish body (caesium: Davis and Foster 1958; Kolehmainen 1974; Forseth et al. 1992; mercury: Trudel et al. 2000). Following the behavioural approach, activity rate is estimated by interpolating data about fish behaviour transformed to energy expenditures using empirical relationships among fish mass, swimming speed, and respiration (Boisclair 1992*a*, 1992*b*; Boisclair and Tang 1993). The bioenergetic approach based on a chemical tracer has been presumed to be superior to alternate approaches because it allows one to obtain consumption and activity rates that are integrated over a time interval (Rowan and Rasmussen 1996). The accuracy of the bioenergetic approach based on a chemical tracer to estimate consumption rate has been demonstrated (Forseth et al. 1992; Gingras and Boisclair 2000). However, the ability of this approach to estimate activity rate remains to be assessed. In contrast, the behavioural approach has been shown repeatedly to provide realistic values of activity rate (Sirois and Boisclair 1995; Trudel and Boisclair 1996; Aubin-Horth et al. 1999). Unfortunately, the behavioural approach requires a sampling effort that is much larger than the bioenergetic approach (repeated sampling at 1- to 4-week intervals over a growing season instead of tracer concentration at the beginning and the end of this time interval). In this context, the corroboration of the bioenergetic approach based on a chemical tracer may improve our ability to develop models to predict fish activity rate. The purpose of this study was to compare activity rate estimated using the bioenergetic approach based on a chemical tracer with values estimated using the behavioural approach.

Materials and methods

Sites and enclosures

A total of six experiments were conducted in Lake Songsjøen (western Norway, 63°19′26″N, 9°39′55″E; elevation: 262 m above sea level; area: 70 ha) to estimate fish activity rate using the bioenergetic and the behavioural approaches. Lake Songsjøen is oligotrophic and holds populations of Arctic char (*Salvelinus alpinus*) and brown trout (*Salmo trutta*).

Experiments were conducted in two (2000) to four (2001) 9.5 m × 9.5 m square enclosures deployed 3–7 m from shore. Enclosures are further identified as E1 to E6. Depth at the shallow end of the enclosures ranged from 75 to 128 cm (average: 98 cm). Depth at the deep end of the enclosures ranged from 232 to 275 cm (average: 248 cm). The volume of the enclosures averaged 156 m^3 and ranged from 143 to 177 m^3. Enclosures were made of nets (7 mm mesh) attached to a frame anchored on the lake bottom. The bottom line of each net was sunk 10–30 cm into the sediments or anchored using gravel bags to prevent fish escape. The enclosures therefore allowed fish to feed on invertebrates that may be found at the water surface, in the water column, and on or in the sediments.

Fish for study

Juvenile Arctic char (ages 2+ and 3+) were captured in two Norwegian lakes using minnow traps. Lake Våvatn (63°19′41″N, 9°34′29″E; elevation: 298 m above sea level; area: 425 ha) is located 1.2 km upstream of Lake Songsjøen. Lake Øvre Nonshøtjønn (62°43′05″N, 9°32′03″E; elevation: 1004 m above sea level; area: 3.5 ha) is located 68 km south of Lake Songsjøen. These lakes were selected because they contain populations of char living under different environmental conditions (elevation, temperature, presence (Våvatn) or absence (Øvre Nonshøtjønn) of brown trout, etc.). We performed the experiments at similar fish density, but used fish from Lake Våvatn at two different times (2000 and 2001) and from two different lakes at the same time (2001). This strategy was used because it allowed us to obtain among-year and among-population variability in activity rate. Arctic char were collected in Lake Våvatn on 17–28 May 2000 and 3–12 June 2001. Arctic char were collected in Lake Øvre Nonshøtjønn only in 2001 (25 May to 12 June). Char were individually weighed (electronic balance, Mettler model BB1200, ±0.1 g) and marked using fin

© 2008 NRC Canada

colour markers (Sigma-Aldrich Alcian Blue 8GX). These operations were conducted under anaesthesia (immersion in an emulsion of clove oil 25 mg·L^{-1} for 30–90 s) to reduce the stress associated with fish handling. The fish were allowed to recover in aerated water for 15 min. The weight of the fish collected in Lake Vâvatn in 2000 (N = 58; range: 12.4–35.9 g fresh weight (fw); average: 22.30 g fw) was less variable than in 2001 (N = 41; range: 13.0–55.5 g fw; average: 24.4 g fw). Fish collected in Lake Øvre Nonshøtjønn ranged from 10.2 to 93.5 g fw (N = 42; average: 37.32 g fw).

Experimental procedures

Experiments conducted in the two enclosures deployed in 2000 took place from 4 June to 5 July (E1) and from 4 June to 3 July (E2). At the beginning of the experimental period, snorkelling was performed to insure that no fish were present in the enclosures. Each enclosure was stocked with 20 fish from Lake Vâvatn (average density: 10.8 fish·(100 m^3)$^{-1}$). Experiments conducted in the four enclosures deployed in 2001 began on 20 June and ended on 2 August (E3, E5) or 3 August (E4, E6). At the onset of the experiments, E3 and E4 were stocked with 15 Arctic char from Lake Vâvatn, while E5 and E6 were stocked with 15 fish from Lake Øvre Nonshøtjønn (average density: 10.3 fish·(100 m^3)$^{-1}$). Fish were distributed to minimize among-enclosure variations in average initial body mass. Arctic char that were not stocked in the enclosures (18 fish from Lake Vâvatn in 2000, 11 fish from Lake Vâvatn in 2001, and 12 fish from Lake Øvre Nonshøtjønn in 2001) were used to estimate the initial ^{133}Cs content of char (i.e., the initial ^{133}Cs burden; see Estimation of initial caesium burden).

At the end of the experiments, fish were recaptured by dragging a seine three times inside each enclosure and were killed by a 20 min immersion in clove oil emulsion (100 mg·L^{-1}). Each Arctic char was identified, weighed, and dissected. The stomach contents of the fish taken from a given enclosure were analysed to assess diet and then pooled to obtain sufficient material for ^{133}Cs analysis. Fish tissues and stomach contents were frozen for ^{133}Cs burden analyses.

Video sampling

We applied the behavioural approach using the method described by Boisclair (1992*a*) to estimate fish activity rate from swimming behaviour. Fish swimming behaviour was recorded with stereo video cameras (SVC). These consisted of a pair of cameras (either Panasonic WV-BL602 or Panasonic WV-BP312) enclosed in a water-resistant case. Two SVC were used, each producing two images. Fish behaviour could therefore be observed simultaneously at two locations of an enclosure. The four images produced by the two SVC were assembled into a single image using a Quad image processor (Panasonic WJ-410). A time–date generator (Panasonic WJ-810) was used to add the exact time of filming to the images (±0.001 s). The resulting images were recorded using a VHS videocassette recorder (Panasonic AG-1330). SVC were positioned to adequately estimate fish behaviour and activity rate in different areas of the enclosures. Snorkelling performed outside the enclosures indicated that during summer 2000, char were observed in the surface layer (surface to 1 m from the bottom) of the offshore-third of the enclosures. Hence, in 2000, we defined two sampling zones (Zones A and B; Fig. 1). Zone A consisted of the water volume formed by the shallowest two-thirds of the enclosures and the layer within 1 m from the bottom of the offshore-third of the enclosures. Zone B comprised the volume defined by the surface layer (from 1 m above the bottom to surface) of the offshore-third of the enclosures. The ratio of the volumes of Zones A and B was approximately 3:1. The SVC deployed to observe fish behaviour in Zone A were positioned 50 cm from the perpendicular (to shore) sides of the enclosures, 80 cm below water surface (40 to 80 cm above the bottom), and in the middle of the enclosure on the littoral–pelagic axis. These cameras were directed perpendicular to the side of the enclosures and parallel to water surface. The SVC sampling Zone B was positioned 50 cm from the middle of the deepest side of the enclosures, 180 cm below the surface. It was oriented perpendicular to the side of the enclosure and looking upward with an angle of 45° relative to water surface. Depending on the enclosure, the SVC sampling Zone B was thus between 50 and 100 cm above the bottom.

Fig. 1. Zones sampled by the stereo video camera (SVC) in the enclosure during the summers 2000 and 2001.

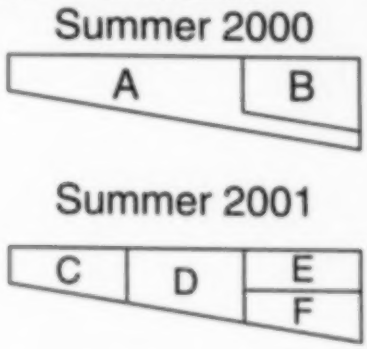

Observations made in 2001 resulted in the definition of four sampling zones for that year (Zones C, D, E, and F; Fig. 1). Zones C and D included, respectively, the water volume of the first- and second-shallowest thirds of the enclosures. Zone E was the volume defined by the surface layer (surface to a depth of 1.1 m) of the offshore-third of the enclosures. Zone F was the deepest layer (depth of 1.1 m to bottom) of the offshore-third of the enclosures. Volume ratios of Zones C, D, E, and F were approximately 1:1.45:1:1.

The SVC deployed to observe fish behaviour in Zones C and D were positioned 50 cm from the perpendicular sides of the enclosures, 75 cm below the surface, and 3.15 m from the shallowest side of the enclosures. The SVC was oriented parallel to the surface and was directed towards either Zones C or D (see the filming schedule below) by changing the angle relative to the enclosure side (45° to 60° shoreward for Zone C; 75° to 85° offshore for Zone D). The SVC sampling Zones E and F were positioned 50 cm from the middle of the deepest side of the enclosures and 110 cm below the surface (120–140 cm above the bottom). They were oriented perpendicularly with the side and directed upward with an angle of 20° to 30° relative to the surface

© 2008 NRC Canada

when sampling Zone E and downward with an angle of 10° relative to the surface when sampling Zone F.

Fish behaviour was quantified during 2 days in each enclosure. On any given sampling day, fish were filmed at 0400, 1000, 1600, and 2200. However, in 2001, the filming sessions were progressively shifted to 0630, 1030, 0330, and 2030 from 23 July (sunrise: 0315; sunset: 2130) to 3 August (sunrise: 0445; sunset: 2000) because of the decrease in daylight hours. In 2000, Zones A and B were filmed simultaneously for 1 h. However, in 2001, two of the four zones defined that year were filmed for 30 min, the SVC were repositioned (which would require 15–25 min), and the two other zones were filmed for 30 min. Hence, the filming schedule resulted in 48 h of films: sixteen 1 h recordings of two zones (2 enclosures × 2 filming days × 4 h of filming per day; Zones A and B were filmed simultaneously) in 2000 and sixty-four 30 min recordings of four zones (4 enclosures × 2 filming days × 8 periods of 30 min per day; pairs of zones filmed simultaneously were randomized) in 2001.

Analysis

Caesium analysis

Initial ^{133}Cs burden of char was estimated using predictive models based on fish origin and size (see Estimation of initial caesium burden). Final ^{133}Cs burden of char was estimated for each individual fish. Each fish was weighed (g fw), dried until no mass loss occurred (60 °C for 24 to 48 h), and weighed again to determine dry mass (g dry weight (g dw)) and the proportion of dry matter. Dry fish were homogenized and a 300 mg subsample was taken and digested with HNO_3. Measurements of ^{133}Cs concentration (ng·g^{-1} dw) were made on the digested sample using a high resolution inductively coupled plasma mass spectrometer (ICP-MS, Thermo Electron Corp., model Finnigan Element1). ^{133}Cs concentrations per gram of dry fish tissues were converted to ^{133}Cs concentration per gram of fresh fish tissues (ng·g^{-1} fw) by multiplication with the proportion of dry matter. ^{133}Cs burden in fish (ng) was obtained by multiplying ^{133}Cs concentration per gram of fresh fish tissue by the original fresh mass of the fish (g fw). ^{133}Cs concentration in the food consumed by fish (pooled stomach contents) was evaluated following the same procedure. In this case, dry weight concentrations were used (ng·g^{-1} dw).

Video analysis

We converted the recordings from VHS videotapes to numeric format using a PC-based interface (ATI video acquisition interface, resolution: 640 × 480 pixels) to ease the use of computer-based image analysis tools. Image analysis began by an observation of each recording for actively swimming fish (velocity > 1 cm·s^{-1}). For every second of filming, all moving fish were counted. Fish that were observed in only one camera of a given SVC were excluded from the count. Total moving fish-seconds (FS, fish·s) is the sum of the number of the active fish observed within every second of a recording. Image analysis was performed with software developed by the first author using XBasic Program Development Environment (2002, version 6.23). The analysis consisted of the manual positioning (in raw pixel coordinates) of the head and tail of fish (see Boisclair 1992*a* for details). To minimize the effects of pseudoreplication, swimming velocity was estimated on a single, randomly selected, 1 s interval per fish passage. A fish passage is the complete displacement of a fish in the volume sampled by the SVC. A maximum of 100 velocity measurements were taken per hour of filming. Random subsampling was thus conducted when more than 100 fish passages where available per hour of filming. Boisclair (1992*b*) reported that this sample size is sufficient to obtain reliable estimates of the mean swimming velocity of brook trout. We assumed that this finding is applicable to Arctic char.

Computations

Estimation of initial caesium burden

Because ^{133}Cs measurement requires killing the fish, the ^{133}Cs burden in fish at the beginning of the experiments was estimated from the ^{133}Cs concentration of the Arctic char that were not used to stock the enclosures. We treated Arctic char coming from Lake Våvatn in summer 2000 (Group 1), Lake Våvatn in summer 2001 (Group 2), and Lake Øvre Nonshøtjonn in summer 2001 (Group 3) as three distinct levels of treatment. ^{133}Cs concentration ($\log_{10}$-transformed) of Arctic char were different among groups ($F_{[2,30]} = 24.57$, $p = 1.42 \times 10^{-7}$). Moreover, ^{133}Cs concentration was not found dependent on the fresh body weight of the fish within every group (Group 1: Pearson's $r = 0.17$, $t_{[16]} = 0.71$, $p = 0.49$; Group 2: $r = -0.19$, $t_{[9]} = -0.58$, $p = 0.57$; Group 3: $r = 0.29$, $t_{[10]} = 0.97$, $p = 0.35$). As a consequence, the initial ^{133}Cs burden (ng) of an Arctic char belonging to one of the aforementioned groups was predicted by multiplying the mean ^{133}Cs concentration of that group (respectively 17.88, 19.42, and 27.79 ng·g^{-1} fw for Groups 1, 2, and 3) by its fresh body weight (g fw) at the beginning of the experiment.

Computation of activity rate using the bioenergetic approach

Calculation of activity (kJ) using the bioenergetic approach based on a chemical tracer was done by rearranging eq. 1 (see Introduction) to

$$\text{(2)} \qquad \text{ACT} = C - (G + F + E + \text{SMR} + \text{SDA})$$

Activity rate was calculated for individual fish following five steps. First, for any given day i, we calculated the (linearly) interpolated body mass (w_i (g fw)) and ^{133}Cs burden (Q_i (ng)) of the fish. Second, we estimated ^{133}Cs elimination rate (k_i (day^{-1})) from w_i and mean daily temperature (T_i (°C)) using the model of Ugedal et al. (1992). Daily food intake (I_i (ng·day^{-1})) was calculated for each 1-day interval according to the method proposed by Forseth et al. (1992; their eq. 3*b*). Food consumption for the complete duration of the experiment (C (kJ)) was calculated as

$$\text{(3)} \qquad C = \frac{\left(\sum_i I_i\right) \cdot S}{[\text{Cs}]_F \cdot \text{Eff}}$$

where $[\text{Cs}]_F$ (ng·g^{-1} dw) is the concentration of ^{133}Cs in the diet of fish from each enclosure, Eff is the assimilation effi-

© 2008 NRC Canada

ciency of ^{137}Cs (the proportion of the ^{137}Cs found in the diet that is effectively assimilated by the fish), and S (kJ·g^{-1} dw) is the energy density of the diet. Energy density of the diet was estimated using the relative contribution (dry mass percentage) of prey items to fish diet from each enclosure and prey energy density (kJ·g^{-1} dw; Cummin and Wuycheck 1971). When no specific information about prey energy content was available, we employed values of the nearest taxonomic group. Third, growth (G (kJ)) was obtained by multiplying predicted fish energy density (kJ·g^{-1} fw; Hartman and Brandt 1995, their eq. 13 developed for salmonids) by the body mass gained during the experiment and by dividing this product by the duration of the experiment. Fourth, we estimated the maximum consumption (C_{MAX} (kJ)) required to calculate F and E. C_{MAX} was estimated on a daily basis using values of w_i and T_i and was summed over the complete experimental period. Fifth, values of F (kJ), E (kJ), and SMR (kJ) were estimated on a daily basis using the models of Larsson and Berglund (2005: C_{MAX}), Elliott (1976: F and E), and Lyytikäinen and Jobling (1998: SMR) and summed over the complete experimental period. SDA was assumed to represent 17% of assimilated energy (consumption rate minus fecal loss, Hewett and Johnson 1992). Because the experiments had different durations, estimates of energy compartments in eq. 2 were converted to rates (kJ·day^{-1}) by dividing the number of experimental days. Models used to estimate C_{MAX} and SMR were developed from data on Arctic char (Lyytikäinen and Jobling 1998; Larsson and Berglund 2005), whereas models used to estimate k, F, and E were borrowed from brown trout (Elliott 1976; Ugedal et al. 1992).

Calibration of the SVC

Calibration of the video cameras was done underwater using a target consisting of a board having lines spaced both vertically and horizontally by 10, 20, and 30 cm. This target was placed at distances ranging from 40 to 240 cm from the cameras (increments of 40 cm). Calibration was done before the first filming day and was repeated each four filming days. We estimated real length of objects (L (cm)) from the relationship between virtual length (l (pixels)) and parallax (i.e., the offset between images from the cameras in abscissa: Δx (pixels)) using a nonlinear function:

$$(4) \qquad L = \frac{l}{\frac{c_1}{\Delta x + c_2} + c_3}$$

where c_1 is a scale parameter, and c_2 and c_3 are offset parameters estimated by least-squares nonlinear regression of known distances between pairs of landmarks on the calibration target against values of Δx and l obtained from image analysis. The quotient of real and virtual length (L/l) was used to evaluate the distance between the target and the SVC (D (cm)):

$$(5) \qquad D = c_4 \cdot \frac{L}{l} + c_5$$

where parameters c_4 and c_5 were estimated using linear regression of known values of distance of the calibration target and known values of L/l. Coefficients of determination associated with these relationships (eqs. 4 and 5) ranged from 92% to 99%.

Swimming cost model

The behavioural approach is based on the estimation of the energy spent swimming by fish per unit of volume observed using video cameras. Energy spent swimming is estimated using the number of movements performed by fish per unit of time, fish mass, and fish swimming speed (Boisclair 1992*a*). The cost of swimming is determined using a swimming cost model implemented with fish mass and swimming speed (Boisclair and Tang 1993; Tang and Boisclair 1995; Tang et al. 2000). Data sets needed to estimate the parameters of these models are obtained by quantifying the oxygen consumption of swimming fish using respirometry experiments. We developed a new swimming costs model integrating data sets from Boisclair and Tang (1993, routine swimming), Tang and Boisclair (1995), and Tang et al. (2000). The resulting data set consisted of results from 113 experiments for which oxygen consumption, body mass, and velocity of free-swimming fish (fish not forced to swim against a current nor constrained to swim in any given direction) were available. This data set comprised four fish species: goldfish (*Carassius auratus*, Smit 1965: 54 experiments), Hawaiian flagtail (*Kuhlia sandvicensis*, Muir et al. 1965: 11 experiments), largescale mullet (*Liza macrolepis*, Kutty 1969, three experiments), and brook trout (Tang and Boisclair 1995; Tang et al. 2000: 45 experiments). The model predicting swimming costs was obtained by regressing (loglinear multiple regression) oxygen consumption rate of fish (VO_2 (mgO_2·h^{-1})) against their body mass (M, g fw) and mean swimming speed ($\bar{v}$ (cm·s^{-1}))

$$(6) \qquad \log_{10}VO_2 = b_0 + b_{MASS} \cdot \log_{10}M + b_{SPEED} \cdot \log_{10}\bar{v}$$

Parameters of this new swimming cost model are provided in Activity rate: behavioural approach (see Results).

Evaluation of the volume sampled by video cameras

The volume filmed by the SVC has the shape of a rectangle-based pyramid with a volume that increases as the distance from the cameras increases. In our study, this volume crossed the bottom of the littoral zone or the surface of the lake at an angle. Hence, the volume sampled by the SVC was calculated as the volume of a truncated, rectangle-based pyramid. This volume began at 25 cm from the objective of the cameras (minimum distance to perceive a fish simultaneously in two cameras of a same SVC) and extended to the maximum distance of fish detection. The maximum distance of fish detection may vary with filming conditions (the zone sampled, the position and the orientation of the cameras, and the characteristics of the images such as pixel brightness and their frequency distribution) and with stochastic events (e.g., all fish swimming, by chance, near the video cameras). The effect of these elements on the calculation of activity rate was considered by classifying each video recording according to the filming conditions, by estimating the maximum fish detection distance for all video recordings belonging to a filming condition (pooling of all the fish coordinates estimated for all video recordings obtained under a filming condition), and by adopting the highest value of maximum fish detection distance for a given filming condition as the max-

© 2008 NRC Canada

imum fish detection distance used to estimate the volume sampled by the video cameras under this filming condition. Hence, the volume sampled by the video cameras for a given filming condition was identical for all video recordings obtained under this filming condition and was independent of the number of fish that moved during this specific video recording.

Computation of activity rate using the behavioural approach

The behavioural approach estimated the mean activity rate of fish within an enclosure over the complete duration of an experiment as the mean of the activity rate of fish in the different zones of an enclosure (two to four zones in 2000 and 2001, respectively) during four different times of the day (four filming sessions per day) and 2 days of filming. This was achieved in four steps. First, we estimated the active fish biomass ($B_{z,t}$ (g·m^{-3} fw)) observed in the volume sampled by the SVC in each zone z of an enclosure and for each combination t of time of day and day of filming as

$$(7) \qquad B_{z,t} = \frac{FS_{z,t} \cdot \overline{M}_t}{T_{z,t} \cdot V_{z,t}}$$

where $FS_{z,t}$ is the total number of moving fish-seconds (fish-s), $\overline{M}_t$ is the mean body mass of fish inside an enclosure (g fw; interpolated at the time of sampling), $T_{z,t}$ is the duration of the filming (s), and $V_{z,t}$ is the observed volume of water (m^3). $B_{z,t}$ is taken as a measure of the biomass of fish found in a zone at t weighted by the number of movements they performed per unit of volume and per unit of time. The number of $B_{z,t}$ values estimated for each enclosure was 16 in 2000 (two zones per enclosure × four filming sessions per day × 2 days of filming per enclosure) and 32 in 2001 (four zones per enclosure × four filming sessions per day × 2 days of filming per enclosure). Second, when fish were observed swimming, we calculated the mean swimming cost (MSC (J·g^{-1}·h^{-1})) in each zone z of an enclosure and for each combination t of time of day and day of filming using mean body mass, mean swimming speed, and coefficients of the swimming cost model (eq. 6) as

$$(8) \qquad MSC_{z,t} = 13.54 \times 10^{fs} \cdot \overline{M}_t^{(b_{MASS}-1)} \cdot V_{z,t}^{b_{SPEED}}$$

where 13.54 is the oxycaloric coefficient (J·mg O_2^{-1}, Elliott and Davison 1975). $MSC_{z,t}$ therefore represents the cost of swimming for a fish having the average weight and swimming at the average speed estimated in zone z of an enclosure and for the combination t of time of day and day of filming. When no fish were seen swimming in a zone at t, $MSC_{z,t}$ was assumed to be zero. The number of $MSC_{z,t}$ estimated was identical to that of $B_{z,t}$. Third, we calculated hourly activity rate (A_t (J·g^{-1}·h^{-1})) in a complete enclosure for each combination t of time of day and day of filming as

$$(9) \qquad A_t = \frac{\sum_{z=1}^{n} (B_{z,t} \cdot MSC_{z,t})}{n \cdot \overline{B}_{e,t}}$$

where $\overline{B}_{e,t}$ (g·m^{-3} fw) is the mean biomass of fish in an enclosure per unit of volume (i.e., the sum of the interpolated body masses at t divided by the volume of the enclosure), and n is the number of zones sampled in an enclosure (two in 2000, four in 2001). The numerator of this equation provided the sum of the cost of swimming in all zones z of an enclosure weighted by $B_{z,t}$ in each zone at t. The denominator of this equation averaged the sum of the cost of swimming over the zones sampled in an enclosure and over the biomass of fish present in this enclosure at t. Eight values of A_t (four filming sessions per day and 2 days of filming per enclosure) were estimated for each enclosure in 2000 and in 2001. Fourth, daily activity rate (A_e (J·day^{-1})) in an enclosure e over a complete experiment was estimated as

$$(10) \qquad A_e = 24 \cdot \overline{A}_t \cdot \overline{M}_e$$

where 24 is the number of hours in a day, $\overline{A}_t$ is the geometric mean of the hourly activity rate estimated in an enclosure e, $\overline{M}_e$ is the mean body mass of char (g fw) in this enclosure in the middle of the experiment (mean of the linear interpolation of individual fish mass).

Estimating the confidence intervals of activity rate

Confidence intervals around the activity rate obtained from the bioenergetic approach were estimated by bootstrapping (Efron and Tibshirani 1993, 10 000 recalculations used in every case). Confidence intervals on bioenergetic activity rate estimates were obtained following five steps. First, we calculated 10 000 bootstrapped sets of mean initial ^{133}Cs concentration in char. For each individual fish, these sets of means were used in a second step to calculate pseudovalues of initial ^{133}Cs burden (see Estimation of initial caesium burden). Third, assuming that the error associated with the estimates of final ^{133}Cs burden in individuals was low, we calculated 10 000 pseudovalues of ^{133}Cs intake for each fish using the corresponding pseudovalues of initial ^{133}Cs burden. Fourth, we calculated 10 000 pseudovalues of consumption rate by including the error associated with ^{133}Cs concentration in food and ^{133}Cs absorption coefficient used for the method of Forseth et al. (1992). Pseudovalues of ^{133}Cs concentration in food were calculated by bootstrapping the values obtained in this study. Pseudovalues of ^{133}Cs absorption coefficient were normally distributed random deviates using the means and standard deviations published by Forseth et al. (1992). Fifth, we applied the pseudovalues of consumption rate on the calculation of the energy budget to obtain 10 000 pseudovalues of activity rate for each individual char. The bilateral 95% confidence limits (CL) of activity rate were taken as the 2.5th and 97.5th percentiles of these pseudovalues. The error associated with the application of the models predicting k, C_{MAX}, F, E, SDA, and SMR was not included in error analysis because the variance–covariance of the parameters of these models were not available from original papers. The error analysis we performed may thus provide conservative values of 95% CL of activity rate obtained using the bioenergetic approach. The confidence limits around activity rate obtained using behavioural approach were estimated using the standard error of the generalized linear model (GLM) parameters.

Model comparison

Mean daily activity rates estimated with the bioenergetic approach were compared with values obtained with the behavioural approach using a major axis regression (type II re-

© 2008 NRC Canada

Table 1. Number of fish stocked in the experimental enclosures and their body masses (average (min, max)) at the beginning of the experiment.

Enclosure	Date of beginning	Volume (m^3)	No. of fish stocked	Duration (days)	Source lake	Initial body mass (g fw)
E1	4 June 2000	177	20	31	Våvatn	21.99 (15.2, 31.3)
E2	4 June 2000	175	20	29	Våvatn	21.38 (15.2, 32.7)
E3	20 June 2001	151	15	43	Våvatn	21.43 (14.2, 54.6)
E4	20 June 2001	143	15	44	Våvatn	21.24 (13.0, 55.5)
E5	20 June 2001	144	15	43	Øvre Nonshøtjønn	24.02 (10.2, 47.3)
E6	20 June 2001	147	15	44	Øvre Nonshøtjønn	23.21 (11.5, 51.8)

gression; Legendre and Legendre 1998). Confidence limits of parameters such as the correlation coefficients (Pearson), regression slope, and regression intercept were calculated using the pseudovalues of activity rate obtained from the bootstraps (bioenergetic approach) and GLM model parameters (behaviour approach). Only one pair of pseudovalues from each enclosure was allowed for every single recalculation of the parameters. The lower and upper 95% CL of a given parameter were taken as the 2.5 and 97.5 percentiles of its pseudovalues. Expectation was that if the bioenergetic and the behavioural approaches produced similar estimates of activity rate, these estimates would be correlated, and the confidence intervals of their type II regression slope and intercept would include, respectively, 1 and 0.

Statistical analysis

Computations and statistical analysis were performed using R language (R Development Core Team 2006). Tests of the statistical significance of among-enclosure differences were done using analysis of variance (ANOVA). When among-enclosure differences were statistically significant, a post hoc test (Scheffé's test: Scheffé 1953) was conducted to test for differences between every pair of enclosures. Normality of the residuals of ANOVA and regression models was tested using Shapiro–Wilk's test of normality (Shapiro and Wilk 1965). Homogeneity of within-group residual variance was tested using Bartlett's test (Snedecor and Cochran 1989). Homogeneity of the residual variance along regression lines was assessed by examining the plots of residual values (y) as a function of predicted values (x). The analysis of the effect of experimental and environmental factors on $B_{c,t}$ and A_t was done using GLM (McCullagh and Nelder 1989; quasi-Poisson likelihood model using logarithmic link function: Hastie and Pregibon 1992). This procedure was used because these variables featured an important level of skewness and overdispersion. Statistical significance of the resulting deviance tables were calculated using F tests. We used a statistical significance threshold of 5% for type I (α) error in all analyses.

Results

The mean body mass of individual char in the enclosures at the beginning of the experiments ranged from 21.38 (E2) to 24.02 (E5) g fw (Table 1). The initial body mass did not differ among enclosures ($F_{[5,94]} = 0.2718$, $p = 0.93$). At the beginning of the experiments, the density of char (initial fish density) inside the enclosures averaged 10.64 fish·(100 m)$^{-3}$ and ranged from 9.95 (E3) to 11.44 (E2) fish·(100 m)$^{-3}$. On average, 80% of the fish stocked were recaptured at the end of the experiments (from 60% in E2 to 95% in E1). At the end of the experiments, char density (final fish density) averaged 8.52 fish·(100 m)$^{-3}$ and ranged from 6.86 (E2) to 10.75 (E1) fish·(100 m)$^{-3}$. The mean body mass of fish recaptured at the end of the experiments ranged from 24.23 (E3) to 35.06 g fw (E5). Final body mass differed among enclosures ($F_{[5,74]} = 2.343$, $p = 0.05$; individual fish within each enclosure were used as replicates), but differences between pairs of enclosures were too small to be detected by post hoc tests. Individual growth rate averaged 203 mg·day^{-1} (fw) and ranged from –72.1 to 442 mg·day^{-1}. Only one fish (from E4) lost weight during the experiments. Growth rate was not related to initial fish body mass ($r = 0.099$, $t_{[78]} = 0.877$, $p = 0.383$) and differed among enclosures ($F_{[5,74]} = 7.27$, $p = 1.4 \times 10^{-5}$; individual fish within each enclosure were used as replicates). Fish in enclosure E3 (95 mg·day^{-1}) had growth rate, respectively, 2.6, 2.4, and 2.6 times lower than in enclosures E1, E2, and E5 (respectively 246, 232, and 244 mg·day^{-1}). Moreover, growth was positively influenced by initial and final fish density (respectively: adjusted R^2 (R^2_{adj}) = 0.15, $t_{[78]} = 3.88$, $p = 0.0002$; $R^2_{adj} = 0.057$, $t_{[78]} = 2.41$, $p = 0.02$).

During summer 2000, the average water temperature was 11.5 °C and ranged from 8.2 °C (4 June, first day of the experiment) to 15.8 °C (2 July). Water temperature increased throughout the experiment at a rate of 0.14 °C·day^{-1}. During summer 2001, average water temperature was 16.3 °C and ranged from 13.5 °C (2 August) to 19.6 °C (9 July). In 2001, water temperature tended to decrease from the beginning to the end of the experiments (–0.042 °C·day^{-1}).

Caesium intake

Predicted ^{133}Cs burden of char at the beginning of the experiments (initial ^{133}Cs burden) ranged from 252 to 1440 ng (mean = 464 ng), whereas the ^{133}Cs burden of char at the end of the experiments (final ^{133}Cs burden) ranged from 311 to 4129 ng (mean = 834 ng). Final ^{133}Cs burden differed among enclosures ($F_{[5,72]} = 33.74$, $p < 2.2 \times 10^{-16}$; Table 2). At the end of the experiments, char from Lake Øvre Nonshøtjønn (mean = 1716 ng) contained, on average, three times more ^{133}Cs than char from Lake Våvatn (mean = 562 ng). The ^{133}Cs daily intake of individual char ranged from 3.0 to 79.5 ng·day^{-1} (mean = 13.2 ng·day^{-1}). The mean daily ^{133}Cs intake of char differed among enclosures ($F_{[5,72]} = 43.74$; $p < 2.2 \times 10^{-16}$). Daily intake of ^{133}Cs for char from Lake Øvre Nonshøtjønn (average: 32.0 ng·day^{-1}) was four times higher than corresponding values for char from Lake Våvatn (average: 8.0 ng·day^{-1}). Among fish

© 2008 NRC Canada

Table 2. Number of fish recaptured in the experimental enclosures, their mean growth rate, final caesium burden, consumption rate, activity rate (obtained from the bioenergetic approach), and the mean percent contribution (volumetric) of prey from benthos and plankton to their diet at the end of the experiment.

Enclosure	No. of fish recaptured	Growth rate ($kJ \cdot day^{-1}$)	Final Cs burden (ng)	Consumption rate ($kJ \cdot day^{-1}$)	Activity rate ($kJ \cdot day^{-1}$)	Benthos (%)	Plankton (%)
E1	19	1.36	709	6.09	1.65	23	77
E2	12	1.20	594	4.72	1.14	36	63
E3	12	0.52	496	2.90	0.41	17	83
E4	11	0.86	478	2.82	–0.04	26	74
E5	13	1.42	1710	8.73	2.81	18	80
E6	13	1.14	1722	8.60	2.99	11	89

from Lake Våvatn, char in enclosure E1 (12.4 $ng \cdot day^{-1}$) had daily ^{133}Cs intake 2.1 times higher than char from enclosures E3 and E4 (summer 2001, average: 5.8 $ng \cdot day^{-1}$).

Stomach contents

Zooplankton crustaceans (mainly cladocerans and copepods) largely dominated the diet of char in all experiments (80% to 90% of stomach contents dw). Chironomids were the second most important prey item (10% to 15% of stomach contents). Energy densities used to transform consumption rate from a dry mass to an energy basis were 21.93 $kJ \cdot g^{-1}$ dw for cladocerans, 24.22 $kJ \cdot g^{-1}$ dw for copepods, 22.69 $kJ \cdot g^{-1}$ dw for chironomids, and 20.18 $kJ \cdot g^{-1}$ dw for surface insects (Cummin and Wuycheck 1971). For all other prey items, we used the mean value of arthropods (19.77 $kJ \cdot g^{-1}$ dw). The estimated energy content of fish diet ranged from 21.01 to 23.36 $kJ \cdot g^{-1}$ dw among enclosures (average = 22.47 $kJ \cdot g^{-1}$ dw).

Caesium concentration in fish diet averaged 96 $ng \cdot g^{-1}$ dw and varied up to 3.4-fold among enclosures (from 51 to 171 $ng \cdot g^{-1}$ dw). ^{133}Cs concentration found in the stomach contents of Arctic char from Lake Våvatn in 2000 (average = 127 $ng \cdot g^{-1}$ dw) was 2.4-fold higher than those in 2001 (average = 52 $ng \cdot g^{-1}$ dw), whereas in 2001, ^{133}Cs concentration of the stomach contents of fish originating from Lake Øvre Nonshøtjønn (average = 109 $ng \cdot g^{-1}$ dw) were twice as high as that of Arctic char from Lake Våvatn. Such high variation in the ^{133}Cs concentration of stomach contents may have originated from differences in the ^{133}Cs content of the consumed preys and (or) from the simultaneous ingestion of particulate matter. Because few differences were observed in diet composition (Table 2), we believe that the latter possibility deserves to be explored. Studies by Kolehmainen (1972) have shown that absorption of radioactive ^{137}Cs by bluegill (*Lepomis macrochirus*) from chironomid larvae was low when the larvae ingested contaminated sediments (containing clay 7%–16% of total ingested ^{137}Cs were absorbed) or contaminated detritus (3.0%), but higher when the larvae ingested algae growing in contaminated water (68.7%). The same author found that "Bluegill can absorb most of ^{137}Cs associated with tissues, but are able to absorb very little of ^{137}Cs that is in the detritus and on the clay in the alimentary canal of Chironomid larvae." This assertion may hold true for stable ^{133}Cs as well. Consequently, food may contain substantial amounts of ^{133}Cs that are adsorbed to sediment particles and may not be available for absorption by fish. In such situations, estimates of ^{133}Cs absorption in the field may be overestimated by coefficients obtained from laboratory studies (see Forseth et al. 1992; Tucker and Rasmussen 1999).

We assessed this possibility using concentrations of praseodymium (^{141}Pr), an element of the lanthanide group closely associated with sediment particles, measured at the same time as ^{133}Cs during mass spectrometry analysis. ^{141}Pr has strong adsorptive properties for sediments particles (Kyker 1961; Zhang and Chai 2004) and has been used by Ellis and Huston (1968) as an inert tracer for estimation of absorption in ruminants. We assumed that the same would hold true for fish as well. Concentrations of ^{141}Pr in stomach contents of Arctic char differed among groups ($F_{[2,11]}$ = 14.92, p = 0.0007). Char from Lake Våvatn in summer 2000 (average = 515 $ng \cdot g^{-1}$ dw) had 1.8 times higher ^{141}Pr concentrations than those in summer 2001 (mean = 283 $ng \cdot g^{-1}$ dw), indicating that char from Lake Våvatn ingested more sediments in 2000 than in 2001. However, no such difference was found in summer 2001 between char from Lake Våvatn and Lake Øvre Nonshøtjønn (average = 210 $ng \cdot g^{-1}$ dw). Moreover, concentrations of ^{141}Pr in the stomach contents of char from Lake Våvatn in 2000 were positively related to ^{133}Cs concentrations (R^2_{adj} = 91.1%, $F_{[1,4]}$ = 52.39, p = 0.002). This relationship between ^{133}Cs and ^{141}Pr concentrations in the stomach contents for char was not found in 2001 (Lake Våvatn: $F_{[1,2]}$ = 5.01, p = 0.155; Lake Øvre Nonshøtjønn: $F_{[1,2]}$ = 0.005, p = 0.948). Consequently, the total ^{133}Cs concentrations found in the stomachs of char in 2000 may not reflect the true exposition of char to ^{133}Cs because a substantial fraction of the ^{133}Cs found in the stomachs of char is likely bound to sediment particles. This situation may yield an underestimation of consumption rate through an overestimation of ^{133}Cs absorption. We avoided this problem by substituting the ^{133}Cs concentration in stomachs of char from Lake Våvatn in summer 2000 by the corresponding values available for char from Lake Våvatn on summer 2001.

Consumption rate

The ^{133}Cs-based daily consumption rate estimated for individual fish ranged from 1.47 to 21.5 $kJ \cdot day^{-1}$. The general mean ^{133}Cs-based daily consumption rate was 5.32 $kJ \cdot day^{-1}$. Consumption rate differed among enclosures ($F_{[5,72]}$ = 18.21, $p = 1.2 \times 10^{-11}$). Char from enclosures E5 and E6 (Lake Øvre Nonshøtjønn 2001: mean = 8.67 $kJ \cdot day^{-1}$) had a consumption rate 2.5 times higher than char from enclosures E2, E3, and E4 (mean = 3.48 $kJ \cdot day^{-1}$). Char from enclosure E1 (mean = 6.09 $kJ \cdot day^{-1}$) consumed 2.1 times more food that char in enclosures E3 and E4 (Lake Våvatn 2001:

© 2008 NRC Canada

Fig. 2. Bioenergetic budget for Arctic char (*Salvelinus alpinus*) in enclosures E1 to E6. Mean estimates of the components are shown with their respective confidence intervals (95%). Black dashes over consumption rates represent the maximum consumption rates (C_{MAX}) estimated from the models of Larsson and Berglund (2005). *C*, food consumption; *F*, egestion; *E*, losses from excretion; SDA, specific dynamic action; SMR, standard metabolic rate; *G*, growth rate; ACT, activity rate.

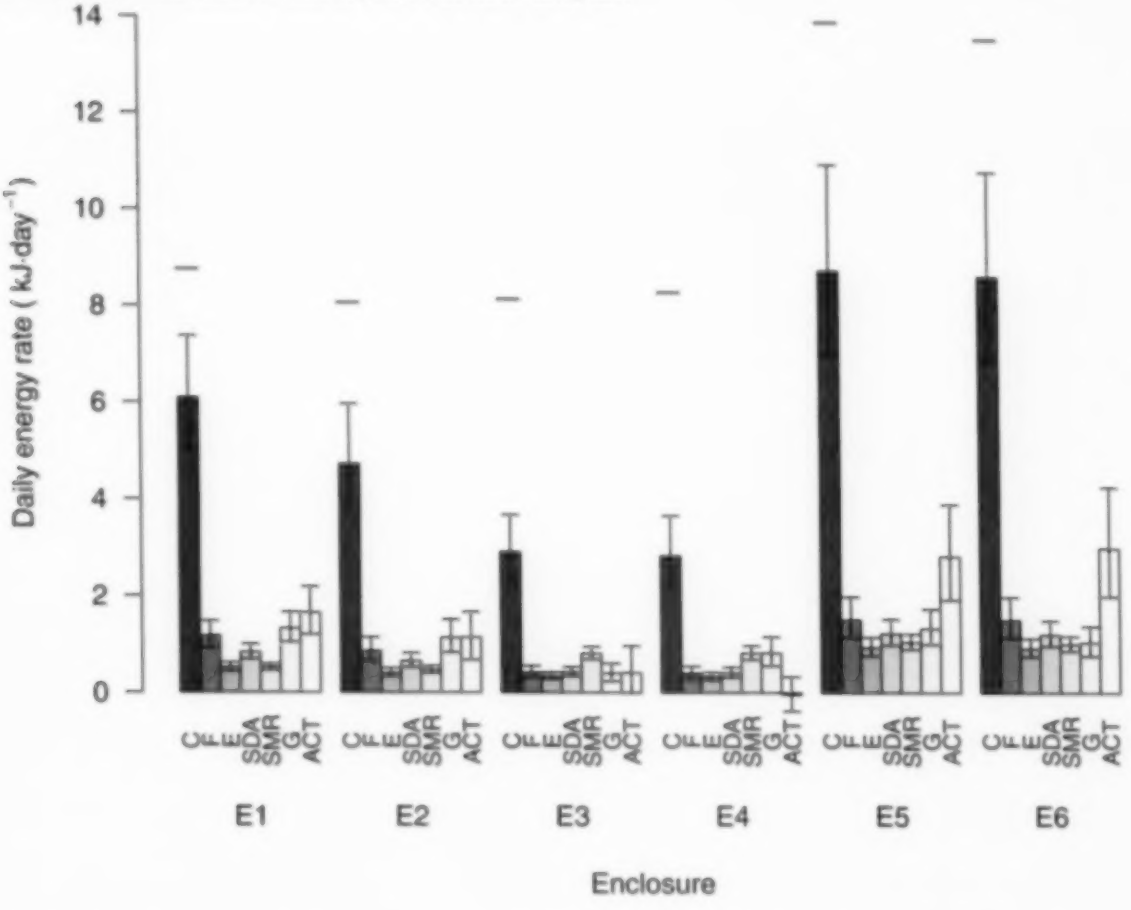

mean = 2.86 kJ·day^{-1}). Two of the 80 fish analysed were associated with estimates of consumption rate that were either unrealistically low (consumption rate represented only 4% of C_{MAX} and was lower than the growth rate of the fish; one fish in E1) or high (consumption rate represented 148% of C_{MAX}; one fish in E4). Keeping in our analysis an individual fish that apparently grew more than it fed or fed 48% more than maximum consumption rate for this fish species and size (C_{MAX} model of Larsson and Berglund 2005) was not only thermodynamically and physiologically incorrect, but it also would potentially introduce in the literature incorrect values of activity rate. These two fish were therefore excluded from further analysis. Consumption rate was employed to estimate most components of the energy budget of the fish found in all enclosures (Fig. 2).

Activity rate: bioenergetic approach

The mean activity rate per fish obtained from the bioenergetics approach was 1.41 kJ·day^{-1} (2.19 × SMR), and ranged from –0.709 kJ·day^{-1} (–0.895 × SMR) to 8.50 kJ·day^{-1} (6.11 × SMR). Negative values of activity rate arise when the model of eq. 1 does not balance. This occurred for 8 of the 78 fish analysed. The magnitude of the error around consumption rate was sufficient to explain the existence of negative activity rate. Negative values of activity rate estimated using the bioenergetic approach were taken to represent low values of activity rate and were not corrected during the comparison with activity rates estimated using the behavioural approach.

Mean activity rate per enclosure (Fig. 2) ranged from –0.035 (E4) to 2.99 kJ·day^{-1} (E6; from 0.08 × SMR in E4 to 3.20 × SMR in E1) and varied significantly among enclosures ($F_{[5,72]} = 16.210$, $p = 1.11 \times 10^{-10}$; SMR: $F_{[5,72]} = 14.76$, $p = 5.93 \times 10^{-10}$). Activity rate of char from enclosure E1, E5, and E6 (mean = 2.98 kJ·day^{-1}) was 13 times higher than activity rate of char from enclosures E3 and E4 (mean = 0.19 kJ·day^{-1}). Moreover, activity rate of char from enclosure E2 (mean = 1.14 kJ·day^{-1}) was six times higher than that of char from enclosures E3 and E4. Activity rate expressed in term of multiples of

© 2008 NRC Canada

Fig. 3. (*a*) Swimming costs model used to estimate activity rate of Arctic char (*Salvelinus alpinus*) using the swimming behavioural method. Respiration rates (tones of grey of the background of points) of goldfish (*Carassius auratus*; circles), Hawaiian flagtail (*Kuhlia sandvicensis*; diamonds), largescale mullet (*Liza macrolepis*; triangles), and brook trout (*Salvelinus fontinalis*; squares) are represented against their body mass (*x* axis) and swimming speed (*y* axis). Predictions of the model for any combination of body mass and swimming speed are displayed as tones of grey in the background of the plotting surface. (*b*) Difference between predictions of the swimming costs model developed in this study and the model published by Boisclair and Tang (1993). Absolute differences (mg $O_2 \cdot h^{-1}$) are displayed as background tones, whereas relative differences (%) are represented by overlying isopleths (broken lines).

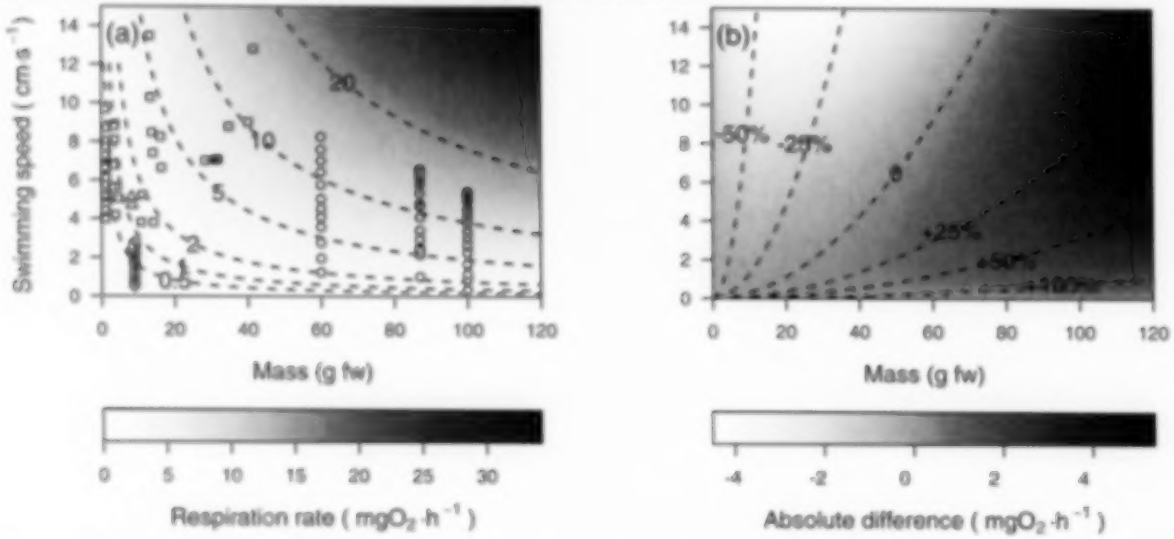

SMR was nine times higher for char from enclosures E1, E2, E5, and E6 (mean = 2.88 × SMR) than for char from enclosures E3 and E4 (mean = 0.32 × SMR). No differences in activity rate were found among enclosures E1, E2, E5, and E6 and between enclosures E3 and E4. The grand mean activity rate of all enclosures was 1.31 kJ·day^{-1} (2.03 × SMR), lower and upper 95% CL were, respectively, 1.06 and 1.59 kJ·day^{-1} (1.73–2.39 × SMR).

Activity rate: behavioural approach

Body mass of fish used to develop the swimming cost model ranged from 1.1 to 100 g fw, and their swimming speed ranged from 0.363 to 13.5 cm·s^{-1}. The $\log_{10}$ fresh body mass of fish explained 70.9% (R^2_{adj}) of the variation in their $\log_{10}$ respiration rate ($F_{[1,112]} = 247.0$, $p < 2.2 \times 10^{-16}$), and adding $\log_{10}$ swimming speed to the model increased R^2_{adj} to 84.2% (Fig. 3*a*; $F_{[2,111]} = 270.9$, $p < 2.2 \times 10^{-16}$). Both predictors were positively related with respiration rate ($b \pm 1$ standard error, b_0: −1.411 ± 0.092; b_{MASS}: 0.915 ± 0.039; b_{SPEED}: 0.886 ± 0.096).

The water volume sampled by the video cameras ranged from 0.1 to 4.8 m^3 (average = 0.6 m^3). Fish were observed in 126 of a total of 160 recordings (80%). Furthermore, it was possible to estimate swimming speed for 103 recordings (64%). The median value of fish-seconds (FS) observed for a 1 h recording was 28 FS·h^{-1} and the maximum was 1239 FS·h^{-1} (E1, Zone B, 13 June 2000, 10:00). Mean active fish biomass observed ($B_{r,i}$) was 1.17 g·m^{-3}, and values ranged from 0 to 9.14 g·m^{-3}, whereas estimates of biomass density in the enclosures ($B_{r,e}$) ranged from 2.26 to 3.69 g·m^{-3}. Char used preferentially the deepest sections of the enclosures, avoiding shallow areas. In 2000, the active fish biomass in zone B (mean = 2.50 g·m^{-3}) was 21 times as high as that in zone A (mean = 0.12 g·m^{-3}; $F_{[1,39]} = 28.55$, $p = 8.83 \times 10^{-6}$). Moreover, in 2001 active fish biomass in zones E and F (mean = 1.70 g·m^{-3}) were three times as high as that in zones C and D (mean = 0.56 g·m^{-3}; $F_{[3,124]} = 5.916$, $p = 0.000\,833$).

The mean swimming speed of char was 13.79 cm·s^{-1} (range: 3.63 to 31.4 cm·s^{-1}). Swimming speed varied significantly among enclosures (ANOVA $F_{[5,97]} = 8.3389$, $p = 1.37 \times 10^{-6}$). Fish from enclosures E2, E5, and E6 (mean = 16.01 cm·s^{-1}) swam 52% faster than fish from enclosures E3 and E4 (mean = 10.56 cm·s^{-1}). No differences in mean swimming speed were found among enclosures E1, E2, E5, and E6or among enclosures E1, E3, and E4. Char from Lake Vâvatn observed in 2000 therefore swam at speeds similar to those of char originating from Lake Øvre Nonshøtjønn observed in 2001, and both groups of fish swam faster than char from Lake Vâvatn in 2001. Swimming speed greater than the maximum value of swimming speed used to develop the swimming cost model (13.5 cm·s^{-1}) were observed in a total of 55 recording (53% of the recordings where swimming speed could be estimated).

The mean value of hourly activity rate was 2.18 kJ·kg^{-1}·h^{-1} (1.75 × SMR) and ranged from 0 to 6.55 kJ·kg^{-1}·h^{-1} (0–7.43 × SMR). Hourly activity rate did not differ among enclosures ($F_{[5,42]} = 0.5689$, $p = 0.72$; SMR: $F_{[5,42]} = 1.5218$, $p = 0.20$) and time of day ($F_{[3,44]} = 2.7608$, $p = 0.053$; SMR: $F_{[3,44]} = 1.3823$, $p = 0.26$). Daily activity rate ranged from 1.15 (E2) to 2.38 kJ·day^{-1} (E5) and from 1.04 (E6) to 2.81 (E1) × SMR. Mean daily activity rate (all enclosures) was 1.64 kJ·day^{-1} (1.75 × SMR), and

© 2008 NRC Canada

Fig. 4. Comparison of the daily activity rate estimates obtained using the behavioural (*y* axis) and the bioenergetic approach (*x* axis). Activity rate is presented in kJ·day^{-1} (*a*) or multiples of SMR (*b*). Errors bars represent the 95% confidence limits around estimates. The graphs feature a 1:1 line.

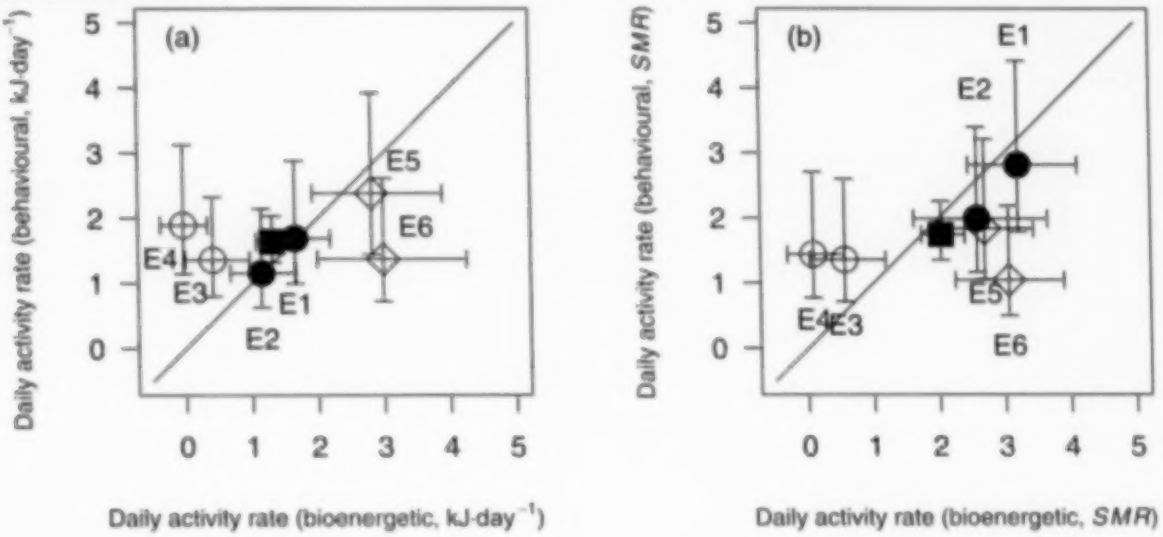

lower and upper 95% CL were, respectively, 1.32 and 2.03 kJ·day^{-1} (1.35–2.26 × SMR).

Comparison of activity estimates

There was no statistically significant relationship between estimates of activity rates obtained from the bioenergetic and the behavioural approaches (Fig. 4). The Pearson's correlation coefficient between estimates were 0.25 (0.45 × SMR), and the lower and upper 95% CL of this coefficient were, respectively, –0.56 and 0.80 (–0.32 and 0.82 × SMR). The null hypothesis that both approaches rendered unrelated estimates in a per enclosure basis thus cannot be ruled out. The slope of the major axis behaved accordingly (0.10, 95% CL: –0.41 and 0.88; 0.25 × SMR, 95% CL: –0.23 and 1.00 × SMR). Finally, the intercept of the major axis was 1.27 kJ·day^{-1} (95% CL: –0.57 and 2.47 kJ·day^{-1}; 1.51 × SMR, 95% CL: 0.01 and 2.46 × SMR). The best agreement between approaches was observed for enclosures E1, E2, and E5 (both confidence limits crossing the 1:1 line). Estimates of daily activity rate obtained using the behavioural approach were higher than corresponding values estimated using the bioenergetic approach in enclosures E3 and E4. The opposite trend was observed for enclosure E6.

Discussion

Daily activity rate estimated with the bioenergetic and the behavioural approaches were analogous in many respects: the mean daily activity rate (1.31 kJ·day^{-1} for the bioenergetic approach and 1.63 kJ·day^{-1} for the behavioural approach); the magnitude of the 95% CL of the mean daily activity rate (1.06–1.59 kJ·day^{-1} for the bioenergetic approach and 1.32–2.03 kJ·day^{-1} for the behavioural approach); the magnitude of individual estimates of daily activity rate obtained using the two approaches. In addition, the bioenergetic (0.08 to 3.20 × SMR) and the behavioural (1.04 to 2.81 × SMR) approaches provided values of daily activity rate that are within the range of published estimates (0.02 to 3.99 × SMR; Sirois and Boisclair 1995; Trudel and Boisclair 1996; Aubin-Horth et al. 1999). Despite these conditions, daily activity rate obtained using both approaches were significantly different for half of the experiments performed (E3, E4, E6). As a result, we found no statistically significant relationship between daily activity rate obtained using the bioenergetic approach and corresponding values estimated using the behavioural approach. The discrepancies between the estimates provided by the two approaches may be best analysed by comparing the strengths and the weaknesses of these approaches.

Bioenergetic approach

The validity of estimates of activity rate obtained using the bioenergetic approach depends, first and foremost, on the validity of estimates of consumption rate. The estimation of consumption rate based on chemical tracers requires the adequate representation of the initial and final tracer concentration in fish tissues, the elimination rate of the tracer, and the concentration of the tracer in fish diet. As in most studies that employed the bioenergetic approach based on chemical tracers (Davis and Foster 1958; Forseth et al. 1992; Rennie et al. 2005), concentration of a tracer in fish tissues at the beginning of a time period was assessed with fish assumed to represent the initial state of the same fish (i.e., same species, size, and origin) that assessed the concentration of the chemical tracer at the end of this time period. Given the content of most tracers in fish tissues, estimation of tracer concentration often requires the use of the complete fish, and hence, the killing of the fish. The assumption described above is therefore unavoidable. In the present study, the elimination rate of stable ^{133}Cs by Arctic char

© 2008 NRC Canada

was predicted using the model of Ugedal et al. (1992). This model was based on radioactive ^{137}Cs elimination by brown trout. Rowan and Rasmussen (1995) argued that the rate of radioactive ^{137}Cs elimination is independent of fish species. Although this claim has never been thoroughly tested, the use of this elimination rate model has been validated for Arctic char (Forseth et al. 1991). Moreover, as ^{133}Cs nuclei are only 3% lighter than ^{137}Cs nuclei, it is reasonable to assume that the elimination rate of ^{133}Cs, through the isotopic kinetic effects, would only differ from the elimination rate of ^{137}Cs by a similar magnitude (Kolehmainen 1972). Consequently, it appears realistic to use the model of Ugedal et al. (1992) to estimate the elimination of stable ^{133}Cs for Arctic char. Consumption rate estimated in the present study presumed that stomach contents at the end of the experiments (when fish were recuperated from the enclosures) are sufficient to obtain dependable concentrations of ^{133}Cs in fish diet during the experiment. Fish are generally not captured during experiments to minimize fish stress and environmental perturbations. Temporal variations of fish diet over a period of approximately 1 month are possible, and this may represent a weakness of the bioenergetic approach for experimental studies. This weakness may be circumvented but only at the expense of a major increase in the number of experimental units (Boisclair 1992*a*; Marchand and Boisclair 1998), which somewhat reduces the advantage, over the behavioural approach, of the lower sampling effort required by the bioenergetic approach based on chemical tracers (Forseth et al. 1992; Rowan and Rasmussen 1996). The present study suggests that a representative survey of fish stomach contents is useful not only to insure a proper temporal assessment of the fish diet and its ^{133}Cs concentration but also to warrant an adequate appraisal of variations of the ingestion of material (sediments, detritus) that may contribute to ^{133}Cs concentrations in fish stomachs but decrease the absorption of this tracer by fish. Substitution of ^{133}Cs concentrations in the stomachs of fish from enclosures E1 and E2, by values obtained from enclosures E3 and E4, was based on the analysis of the concentration of ^{141}Pr in fish stomach contents and applied to compensate for the presence in the stomach contents of ^{133}Cs bounded to sediments. This substitution increased estimates of consumption rate threefold. However, such corrections were done only on the basis of the stomach contents on the last experimental day. Whether important quantities of sediments or detritus were present in the stomach contents of fish from different enclosures on different days is not known and could affect the results of the bioenergetic approach based on chemical tracers. Problems associated with adsorption may be expected to vary among tracers and their forms. Hg^{+} and Hg^{2+}, because of their affinity with clay, organic matter, and iron oxide, may be subjected to the same adsorption problem noted with ^{133}Cs. However, methylmercury (MeHg) may be much less prone to this problem because it is generally associated with digestible particles such as proteins. It is presently impossible to identify why two of the 80 individual analyses of fish consumption rate provided aberrant values. However, it is worth noting that inclusion of these fish would not affect our finding about the lack of relationship between values of activity rate obtained using the bioenergetic and the behavioural approaches. The 95% CL of the correlation between values of activity rate obtained using both approaches were –0.56 to 0.80 without these two fish and would be –0.52 to 0.82 if the two aberrant fish were kept in the analyses.

The bioenergetic approach estimates activity rate by subtracting a series of energy expenditures (SMR; SDA) and losses (fecal and urinary) from consumption rate. These energy expenditures and losses were computed using models developed for brown trout feeding on invertebrates (*F* and *E*: Elliott 1976), other salmonid species (SDA: Hewett and Johnson 1992), or Arctic char itself (SMR: Lyytikäinen and Jobling 1998). The validity of activity rate estimates obtained using the bioenergetic approach also depends on the validity of these models for the species of interest. The effect of parameter or model borrowing from one species to another remains unresolved (Trudel et al. 2004; Trudel and Welch 2005). As such, it is impossible to determine the extent to which the negative estimates of activity rate provided by the bioenergetic approach (E3: three fish with negative activity rates; E4: five fish with negative activity rate) are related to weaknesses described above about the estimation of consumption rate or to parameter or model borrowing for SMR, SDA, *F*, and *E*. However, the SMR, SDA, *F*, and *E* models used in the present study were implemented in the same manner in all enclosures, and in the advent of species-specific models, these models would continue to be inputted with the same key variables (fish weight, water temperature, and consumption rate). Given that the mass exponent of the empirical relationship generally used to represent these components of fish energy budget are the most stable parameters of bioenergetic models (thereby minimizing the effect of changing allometric relationships) and that the initial and final fish mass varied, respectively, by 41% and 35% (thereby minimizing the effect of changing allometric relationships), we argue that the availability of species-specific models would not change the relative position of activity rate values obtained using the bioenergetic and the behavioural approaches.

The behavioural approach

Daily activity rate estimated using the behavioural approach could be affected by errors or biases on six key inputs: the mass of fish in the enclosure, the swimming speed of fish, the respiration predicted from the swimming cost model, the volume sampled by the SVC, the intensity of the filming schedule, and the number of FS estimated. Fish average mass on any given day was estimated by linear interpolation of the initial and final fish mass. The bioenergetic approach was also implemented following a linear interpolation of fish mass. Hence, errors or biases about fish mass may not be responsible for the discrepancies between both approaches. Boisclair (1992*a*) showed that measurement error associated with swimming speeds estimated using SVC is ± 4.5% of mean swimming speed. Such measurement error would have an impact on the order of ±8% on the estimates of mean swimming cost. Energy expenditures associated with swimming were obtained using a spontaneous swimming cost model developed using respiration data from four fish species other than Arctic char. While this model is expected to adequately predict the swimming cost of fish performing changes in speed and

© 2008 NRC Canada

direction (Boisclair 2001), the use of this model may be questioned because it implies the interspecific transfer of a model (model or parameter borrowing; Trudel et al. 2004; Trudel and Welch 2005). However, studies using the behavioural approach and the swimming costs model of Boisclair and Tang (1993) were successful in producing activity estimates that allowed numerous authors to balance the bioenergetic equation implemented with independent values of growth and consumption rates for brook trout (Boisclair and Sirois 1993; Sirois and Boisclair 1995; Marchand and Boisclair 1998), dace (*Phoxinus eos* × *P. neogaeus*) (Trudel and Boisclair 1996), and yellow perch (Aubin-Horth et al. 1999). Yet, none of these species were part of the data set employed by Boisclair and Tang (1993) to develop their model. In the present study, the swimming cost of Arctic char was estimated with a new model developed by combining the data set of Boisclair and Tang (1993) with respirometry experiments performed with brook trout (Tang and Boisclair 1995; Tang et al. 2000). This is expected to represent, if anything, an improvement to the model of Boisclair and Tang (1993) because Arctic char and brook trout belong to the same genus.

The volume sampled by the SVC was estimated using the geometric properties of the field of view of cameras and the maximum distance (from the SVC) beyond which fish detection was not possible as a consequence of water transparency and turbidity. The resulting polyhedron was further truncated to subtract the volume hidden by other obstacles (bottom, surface). These volumes were easy to estimate, as obstacles were visible and their dimensions were straightforward to measure. On the other hand, the maximum distance for fish detection had to be deducted from the position of fish and, consequently, could only be estimated reliably if a sufficient number of fish were observed. Fish were absent in 20% of the recordings, and 15 or fewer fish were observed in half of the remaining recordings. We assumed that grouping recordings performed in similar conditions would allow us to obtain a reasonable figure of maximum distance for fish detection, and we calculated sampled volumes accordingly.

The intensity of the filming schedule (4 h·day^{-1} and 2 days·month^{-1}) used in the present study was similar to that of numerous published studies that employed SVC (4–5 h·day^{-1} and 3–10 days·month^{-1}). These studies showed that this approach provided activity rate consistent with other components of the bioenergetic equation. The number of movements observed within the field of view of the SVC (FS) was the most reliable variable estimated. Arctic char was the only species present inside the enclosures, and the quality of the images obtained insured their detection. No large moving object (>10 cm) other than Arctic char was observed on any recording. Variation of the number of FS alone explained 87% of the variability of all hourly activity rate values obtained ($F_{[1,101]} = 119.12$, $p < 2.2 \times 10^{-16}$). Body mass and swimming speed explained, respectively, 3.2% and 0.2% of the variation of hourly activity rate. This result is consistent with the suggestion that estimates of activity rate obtained using the behavioural approach may be primarily driven by the number of FS when fish are defined as active (Trudel and Boisclair 1996). This situation emphasizes that errors on fish mass, swimming speed, and predictions of respiration models may have relatively minor effects on the relative magnitude of among-hour or among-day variations of activity rate, and hence, on the relative position of estimates of daily activity rate obtained using the bioenergetic and the behavioural approaches.

Daily activity rate estimated using the behavioural approach may not only be affected by inputs to the models but also by the structure of the models. Equations 7 to 10 involve the product or the ratio of means of variables that may be argued to affect daily activity rate through the "fallacy of averages" (e.g., $\mu(AB) \neq \mu A \cdot \mu B$ when A and B are correlated; Wagner 1969). In our study, some variables were estimated on an individual basis (e.g., the mass of fish No. 1 at t in 2000), but the SVC did not allow us to identify fish individually and hence to assess many variables on an individual basis (e.g., FS of fish No. 1 in a particular zone z at time t). Consequently, the structure of the data does not permit us to assess or to correct the fallacy of averages using the solution proposed by Welsh et al. (1988) ($\mu(AB) = \mu A \cdot \mu B + \mathrm{cov}(A,B)$). For instance, we have the individual masses fish Nos. 1 to 20 at any given time t of an enclosure in 2000, but we do not have the individual FS/(T·V) for fish Nos. 1 to 20 in zone z at t to which they should be paired to assess cov(FS/(T·V), M) to assess or to correct for the fallacy of averages in eq. 7. However, for each zone, time of day, and sampling day, we have $FS_{z,t}/T_{z,t}$·$V_{z,t}$ and the coordinates of the head and tail of a sample of the fish that were observed in this zone at that time. We transformed the coordinates of the head and tail of fish in swimming velocities, but these can also be transformed to fish length (Boisclair 1992*a*) and, with a length–weight relationship, to fish weight. This provided us with data on FS/(T·V), average fish mass (averaged over all fish observations), and average velocity (averaged over all fish observations) per zone and time of day. These data indicated that there is no correlation between FS/(T·V) and M ($-0.09 < R^2_{adj} < -0.01$; $0.40 < p < 0.99$) and between $A_{z,t}$ (estimated as $A_{z,t} = (B_{z,t}\text{·}\mathrm{MSC}_{z,t})/B_{e,t}$) and M ($-0.07 < R^2_{adj} < -0.01$; $0.41 < p < 0.90$). Given that the fallacy of averages occurs only when the two variables involved are correlated, that the variables for which the existence of a correlation could be tested is minor or small in our study, and that when correlations occur, the resulting bias is generally smaller than 20% (Welsh et al. 1988), we trust that the fallacy of averages may have a negligible impact on our interpretation about activity rate values that varied up to 53-fold between the bioenergetic and the behavioural approach.

The bioenergetic approach based on chemical tracers was developed to provide integrated values of consumption and, eventually, activity rates over extended periods of time with minimal sampling efforts. The quality of the consumption and activity rates obtained using this approach depends on the validity of numerous inputs and assumptions. For instance, the bioenergetic approach based on a chemical tracer assumes that the concentration of the tracer in the food and the assimilation of this tracer are constant over the time interval for which consumption and activity rates are estimated. As exemplified by the present study, the inclusion of sediments or detritus in fish diet may overestimate ^{133}Cs availability to fish and cause a threefold underestimation of

© 2008 NRC Canada

consumption rate. Once the effect of sediments and detritus in fish diet is considered, the confidence limits of consumption rate ranged from ± 14% (E5) to ± 26% (E3 and E4). Estimates of activity rate obtained using the bioenergetic approach represented from 0% (E4) to 32% (E6) of the consumption rate. Values of activity rate obtained using the bioenergetic approach were smaller than the width of the confidence intervals around estimates of consumption rate for 30 of the 80 individual char analysed (38%). Similarly, daily activity rate (mean activity rate within an enclosure) was smaller than the width of the confidence intervals of consumption rate for three of the six enclosures (namely E2, E3, and E4). While the bioenergetic approach based on ^{137}Cs may provide realistic estimates of consumption rate, the errors associated with consumption rate and the uncertainties associated with the use of other components of the bioenergetic equation (F, E, SDA, and SMR) presently question the validity of this approach to estimate activity rate. This is best illustrated by the presence of negative values of activity rate for eight of the fish analysed and by the wide range of activity rate estimates (0.08 to 3.20 × SMR) obtained under experimental conditions that were similar in many respects (same fish species, same fish origin, experiments in same lake with the same enclosures, approximately the same fish densities and biomass). The behavioural approach provides discrete values of activity rate over short time intervals (minutes to hours), a datum that cannot be obtained using the bioenergetic approach based on chemical tracers. The estimation of activity rate over time intervals of weeks to months with the behavioural approach requires more intense sampling and processing efforts than with the bioenergetic approach based on chemical tracers. The behavioural approach also involves the interpolation of hourly to daily activity rate and of daily to monthly activity rate. However, values of activity rate obtained using the behavioural approach depend mostly on a variable that is the easiest to estimate; the number of fish-seconds are observed active (the number of moving FS of eq. 7). In addition, the behavioural approach cannot provide negative activity values. Finally, values of activity rate obtained under similar experimental conditions (same fish species, same fish origin, experiments in same lake with the same enclosures, approximately the same fish densities and biomass), as may be anticipated, did not vary significantly among each other and covered a relatively small range (1.04 to 2.81 × SMR). The present study suggests that the behavioural approach may be more trustworthy than the bioenergetic approach implemented with ^{137}Cs to estimate fish activity when fish are known to remain in an area where their behaviour can be well described (enclosures, littoral zones, coral reefs). Whether using tracers less subjected to the problem of absorption would be sufficient to modify this interpretation remains to be tested. In addition, irrespective of the tracers used, isolation of activity rate using the bioenergetic approach requires dependable models of F, E, SMR, and SDA. The present study also emphasizes that in other situations (low fish densities, fish performing movements or migrations over ranges that do not permit an adequate description of their behaviour), where the bioenergetic approach may be the only approach amenable, efforts should be deployed to adequately estimate the diet of the fish (in particular detritus or sediment contents) and the assimilation efficiency of the tracer.

Acknowledgements

We thank Jean-François Bertrand, Judith Bouchard, Egil Land, Sigurd Einum, Ian Fleming, and Leidulf Fløystad for their assistance in the field; Syverin Lierhagen for measuring Cs; Guillaume Bourques, Nils Denuelle, Thibaut Jombard, and Claude Normand for their assistance with image analysis; and Saad Chidami for advices during redaction. Field experiment was conduced at Songli Research Facility, Norway. Financial support was provided by the Norwegian Research Council, the Norwegian Institute for Nature Research, the Natural Sciences and Engineering Research Council of Canada (NSERC), and the Freshwater Ecology Group of Université de Montréal. Guillaume Guénard was supported by NSERC ES-A and ES-B scholarships.

References

Aubin-Horth, N., Gingras, J., and Boisclair, D. 1999. Comparison of activity rates of 1+ yellow perch (*Perca flavescens*) from population of contrasting growth rates using underwater video observations. Can. J. Fish. Aquat. Sci. **56**: 1122–1132. doi:10.1139/cjfas-56-6-1122.

Boisclair, D. 1992*a*. An evaluation of the stereocinematographic method to estimate fish swimming speed. Can. J. Fish. Aquat. Sci. **49**: 523–531. doi:10.1139/f92-062.

Boisclair, D. 1992*b*. Relationship between feeding and activity rates for actively foraging juvenile brook trout (*Salvelinus fontinalis*). Can. J. Fish. Aquat. Sci. **49**: 2566–2573. doi:10.1139/f92-283.

Boisclair, D. 2001. Fish habitat modeling: from conceptual framework to functional tools. Can. J. Fish. Aquat. Sci. **58**: 1–9. doi:10.1139/cjfas-58-1-1.

Boisclair, D., and Leggett, W.C. 1989. The importance of activity in bioenergetic models applied to actively foraging fishes. Can. J. Fish. Aquat. Sci. **46**: 1859–1867. doi:10.1139/f89-234.

Boisclair, D., and Rasmussen, J.B. 1996. Empirical analysis of the influence of environmental variables associated with lake eutrophication on perch growth, consumption, and activity rate. Ann. Zool. Fenn. **33**: 507–515.

Boisclair, D., and Sirois, P. 1993. Testing assumptions of fish bioenergetics models using direct estimates of growth, consumption and activity rate. Trans. Am. Fish. Soc. **122**: 784–796. doi:10.1577/1548-8659(1993)122<0784:TAOFBM>2.3.CO;2.

Boisclair, D., and Tang, M. 1993. Empirical analysis of the influence of swimming pathern on the net energetic cost of swimming in fishes. J. Fish Biol. **42**: 169–183. doi:10.1111/j.1095-8649.1993.tb00319.x.

Brandt, S.B., Masson, D.M., and Patrick, E.V. 1992. Spatially-explicit models of fish growth rate. Fisheries, **17**: 23–33. doi:10.1577/1548-8446(1992)017<0023:SMOFGR>2.0.CO;2.

Cummin, K.W., and Wuycheck, J.C. 1971. Caloric equivalents for investigations in ecological energetics. Mitt. Int. Verein. Limnol. 18.

Davis, J.J., and Foster, R.F. 1958. Bioaccumulation of radioisotopes through acquatic food chain. Ecology, **39**: 530–535. doi:10.2307/1931764.

Efron, B., and Tibshirani, R.J. 1993. An introduction to the bootstrap. Monographs on Statistical and Applied Probability 57. Chapman and Hall, New York.

Eggers, D.M. 1977. Factors in interpreting data obtained by diel sampling of fish stomachs. J. Fish. Res. Board Can. **34**: 290–294.

© 2008 NRC Canada

Elliott, J.M. 1976. The energetics of feeding, metabolism and growth of brown trout (*Salmo trutta* L.) in relation to body weight, water temperature and ration size. J. Anim. Ecol. **45**: 923–948. doi:10.2307/3590.

Elliott, J.M., and Davison, W. 1975. Energy equivalent of oxygen consumption in animal energetics. Oecologia (Berl.), **19**: 195–201. doi:10.1007/BF00345305.

Ellis, W.C., and Huston, J.E. 1968. 144Ce-144Pr as a particulate digesta flow marker in ruminants. J. Nutr. **95**: 67–78. PMID:5653278.

Forseth, T., Ugedal, O., Jonsson, B., Langeland, A., and Njästad, O. 1991. Radiocesium turnover in Arctic charr (*Salvelinus alpinus*) and brown trout (*Salmo trutta*) in a Norwegian lake. J. Appl. Ecol. **28**: 1053–1067. doi:10.2307/2404225.

Forseth, T., Jonsson, B., Nærmann, R., and Ugedal, O. 1992. Radioisotope method for estimating food consumption by brown trout. Can. J. Fish. Aquat. Sci. **49**: 1328–1335. doi:10.1139/f92-148.

Fox, M.G. 1991. Food consumption and bioenergetics of young-of-the-year walleye (*Stizostedion vitreum vitreum*): model predictions and population density effects. Can. J. Fish. Aquat. Sci. **48**: 434–441. doi:10.1139/f91-057.

Gingras, J., and Boisclair, D. 2000. Comparison between consumption rates of yellow perch (*Perca flavescens*) estimated with a digestive tract model and with a radioisotope approach. Can. J. Fish. Aquat. Sci. **57**: 2547–2557. doi:10.1139/cjfas-57-12-2547.

Hansen, M.J., Boisclair, D., Brandt, S.B., Hewett, S.W., Kitchell, J.F., Lucas, M.C., and Ney, J.J. 1993. Applications of bioenergetics models to fish ecology and management: where do we go from here? Trans. Am. Fish. Soc. **122**: 1019–1030. doi:10.1577/1548-8659(1993)122<1019:AOBMTF>2.3.CO;2.

Hanson, P., Johnson, T., Kitchell, J.F., and Schindler, D.E. 1997. Fish bioenergetics 3.0. University of Wisconsin Sea Grant Institute, Madison, Wisc. Rep. WISCU-T-97-001.

Hartman, K.J., and Brandt, S.B. 1995. Estimating energy density of fish. Trans. Am. Fish. Soc. **124**: 347–355. doi:10.1577/1548-8659(1995)124<0347:EEDOF>2.3.CO;2.

Hastie, T.J., and Pregibon, D. 1992. Generalized linear models. *In* Statistical models in S. *Edited by* J.M. Chambers and T.J. Hastie. Pacific Grove, Wadsworth, Calif. pp. 195–248.

Hewett, S.W., and Johnson, B.L. 1992. Fish bioenergetics model 2. University of Wisconsin, Sea Grant Institute, Madisson, Wisc. Rep. WIS-SG-92-250.

Kitchell, J.F., and Breck, J.E. 1980. Bioenergetics model and foraging hypothesis for sea lamprey (*Petromyzon marinus*). Can. J. Fish. Aquat. Sci. **37**: 2159–2168. doi:10.1139/f80-258.

Kitchell, J.F., Stewart, D.J., and Weininger, D. 1977. Application of a bioenergetic model to yellow perch (*Perca flavescens*) and walleye (*Stizostedion vitreum vitreum*). J. Fish. Res. Board Can. **34**: 1922–1935.

Kolehmainen, S.E. 1972. The balances of ^{137}Cs, stable cesium and potassium of bluegill (*Lepomis macrochirus* Raf.) and other fish in White Oak Lake. Health Phys. **23**: 301–315. PMID:4642952.

Kolehmainen, S.E. 1974. Daily feeding rates of bluegill (*Lepomis macrochirus*) determined by refined radioisotope method. J. Fish. Res. Board Can. **31**: 67–74.

Kraft, C.E. 1992. Estimates of phosphorus and nitrogen cycling by fish using a bioenergetics approach. Can. J. Fish. Aquat. Sci. **49**: 2596–2604. doi:10.1139/f92-287.

Kutty, M.N. 1969. Oxygen consumption in the mullet *Liza macrolepsis* with special reference to swimming velocity. Mar. Biol. (Berl.), **4**: 239–242. doi:10.1007/BF00393900.

Kyker, G.C. 1961. Rare earths. *In* Mineral metabolism. Vol. 2. *Edited by* C.L. Comar and F. Bronner. Academic Press, New York. pp. 499–541.

Larsson, S., and Berglund, I. 2005. The effect of temperature on the energetic growth efficiency of Arctic charr (*Salvelinus alpinus* L.) from four Swedish populations. Journal of Thermal Biology, **30**: 29–36. doi:10.1016/j.jtherbio.2004.06.001.

Legendre, P., and Legendre, L. 1998. Numerical ecology. 2nd English ed. Elsevier Science BV, Amsterdam.

Lyytikäinen, T., and Jobling, M. 1998. The effect of temperature fluctuations on oxygen consumption and ammonia excretion of underyearling Lake Inari Arctic charr. J. Fish Biol. **52**: 1186–1198.

Madon, S.P., and Culver, D.A. 1993. Bioenergetics model for larval and juvenile walleyes: an *in situ* approach with experimental ponds. Trans. Am. Fish. Soc. **122**: 797–813. doi:10.1577/1548-8659(1993)122<0797:BMFLAJ>2.3.CO;2.

Majkowski, J., and Wairwood, K.G. 1981. A procedure for evaluating the food biomass consumed by a fish population. Can. J. Fish. Aquat. Sci. **38**: 1199–1208. doi:10.1139/f81-161.

Marchand, F., and Boisclair, D. 1998. Influence of fish density on the energy allocation pattern of juvenile brook trout (*Salvelinus fontinalis*). Can. J. Fish. Aquat. Sci. **55**: 796–805. doi:10.1139/cjfas-55-4-796.

McCullagh, P., and Nelder, P. 1989. Generalized linear models. Chapman & Hall, London, UK.

Minton, J.W., and McLean, R.B. 1982. Measurement of growth and consumption of sauger (*Stizostedion canadense*): implications for fish energetics studies. Can. J. Fish. Aquat. Sci. **39**: 1396–1403. doi:10.1139/f82-188.

Muir, B.S., Nelson, G.J., and Bridge, K.W. 1965. A method for measuring swimming speed in oxygen consumption studies on the aholehole *Kuhlia sandvicensis*. Trans. Am. Fish. Soc. **94**: 378–382. doi:10.1577/1548-8659(1965)94[378:AMFMSS]2.0.CO;2.

Ney, J.J. 1993. Bioenergetics modelling today: growing pains on the cutting edge. Trans. Am. Fish. Soc. **122**: 736–748. doi:10.1577/1548-8659(1993)122<0736:BMTGPO>2.3.CO;2.

Post, J.R. 1990. Metabolic allometry of larval and juvenile yellow perch (*Perca flavescens*): in situ estimates and bioenergetic models. Can. J. Fish. Aquat. Sci. **47**: 554–560. doi:10.1139/f90-063.

R Development Core Team. 2006. R: a language and environment for statistical computing (reference index). [online] Version 2.3.1. Available from cran.r-project.org/doc/manuals/fullrefman.pdf.

Rennie, M.D., Collins, N.C., Shuter, B.J., Rajotte, J.W., and Couture, P. 2005. A comparison of methods for estimating activity costs of wild fish populations: more active fish observed to grow slower. Can. J. Fish. Aquat. Sci. **62**: 767–780. doi:10.1139/f05-052.

Rice, J.A., Breck, J.E., Bartell, S.M., and Kitchell, J.F. 1983. Evaluating the constraints of temperature, activity and consumption on growth of largemouth bass. Environ. Biol. Fishes, **9**: 263–275. doi:10.1007/BF00692375.

Rowan, D.J., and Rasmussen, J.B. 1995. The elimination of radiocesium from fish. J. Appl. Ecol. **32**: 739–744. doi:10.2307/2404813.

Rowan, D.J., and Rasmussen, J.B. 1996. Measuring the bioenergetic cost of fish activity in situ using a globally dispersed radiotracer (^{137}Cs). Can. J. Fish. Aquat. Sci. **53**: 734–745. doi:10.1139/cjfas-53-4-734.

Scheffé, H. 1953. A method for judging all contrasts in the analysis of variance. Biometrika, **40**: 87–110.

Shapiro, S.S., and Wilk, M.B. 1965. An analysis of variance test for normality (complete samples). Biometrika, **52**: 591–611.

Sherwood, G.D., Rasmussen, J.B., Rowan, D.J., Brodeur, J., and

© 2008 NRC Canada

Hontela, A. 2000. Bioenergetic costs of heavy metal exposure in yellow perch (*Perca flavescens*): in situ estimates with a radiotracer (^{137}Cs) technique. Can. J. Fish. Aquat. Sci. **57**: 441–450. doi:10.1139/cjfas-57-2-441.

Sirois, P., and Boisclair, D. 1995. The influence of prey biomass on activity and consumption rates of brook trout. J. Fish Biol. **46**: 787–805. doi:10.1111/j.1095-8649.1995.tb01602.x.

Stewart, D.J., Kitchell, J.F., and Crowder, L.B. 1981. Dynamics of consumption and food conversion by Lake Michigan alewife: an energetics modeling synthesis. Trans. Am. Fish. Soc. **110**: 751–763. doi:10.1577/1548-8659(1981)110<751:FFATSP>2.0.CO;2.

Smit, H. 1965. Some experiments on the oxygen consumption of goldfish (*Carassius auratus* L.) in relation to swimming speed. Can. J. Zool. **43**: 623–633. doi:10.1139/z65-063. PMID: 5826307.

Snedecor, G.W., and Cochran, W.G. 1989. Statistical methods. 8th ed. Iowa State University Press, Ames, Iowa.

Tang, M., and Boisclair, D. 1995. Relationship between respiration rate of juvenile brook trout (*Salvelinus fontinalis*), water temperature, and swimming characteristics. Can. J. Fish. Aquat. Sci. **52**: 2138–2145. doi:10.1139/f95-806.

Tang, M., Boisclair, D., Ménard, C., and Downing, J. 2000. Influence of weight, swimming characteristics, and water temperature on the cost of swimming in brook trout (*Salvelinus fontinalis*). Can. J. Fish. Aquat. Sci. **57**: 1482–1488. doi:10.1139/cjfas-57-7-1482.

Trudel, M., and Boisclair, D. 1996. Estimation of fish activity cost using underwater video cameras. J. Fish Biol. **48**: 40–53. doi:10.1111/j.1095-8649.1996.tb01417.x.

Trudel, M., and Welch, D.W. 2005. Modeling the oxygen consumption rate in Pacific salmon and steelhead: model development. Trans. Am. Fish. Soc. **134**: 1542–1561. doi:10.1577/T04-156.1.

Trudel, M., Tremblay, A., Schetagne, R., and Rasmussen, J.B. 2000. Estimating food consumption rates of fish using a mercury mass balance model. Can. J. Fish. Aquat. Sci. **57**: 414–428. doi:10.1139/cjfas-57-2-414.

Trudel, M., Geist, D.R., and Welch, D.W. 2004. Modeling the oxygen consumption rate in Pacific salmon and steelhead: an assessment of current models and practices. Trans. Am. Fish. Soc. **133**: 326–348. doi:10.1577/02-116.

Tucker, S., and Rasmussen, J.B. 1999. Using ^{137}Cs to measure and compare bioenergetic budgets of Atlantic salmon (*Salmo salar*) and brook trout (*Salvelinus fontinalis*) in the field. Can. J. Fish. Aquat. Sci. **56**: 875–887. doi:10.1139/cjfas-56-5-875.

Ugedal, O., Forseth, T., and Jonsson, B. 1992. Effect of temperature and body size on radiocesium retention in brown trout, *Salmo trutta*. Freshw. Biol. **28**: 165–171. doi:10.1111/j.1365-2427.1992.tb00573.x.

Wagner, H.M. 1969. Principles of operation research. Prentice-Hall, Englewood Cliffs, N.J.

Wahl, D.H., and Stein, R.A. 1991. Food consumption and growth of three esocids: field tests of a bioenergetic model. Trans. Am. Fish. Soc. **120**: 230–246. doi:10.1577/1548-8659(1991)120<0230:FCAGOT>2.3.CO;2.

Welsh, A.H., Peterson, A.T., and Altmann, S.A. 1988. The fallacy of averages. Am. Nat. **132**: 277–288. doi:10.1086/284850.

Wieser, W., and Medgyesy, N. 1991. Metabolic rate and cost of growth in juvenile pike (*Esox lucius*) and perch (*Perca fluviatilis*): the use of energy budget as indicators of environmental changes. Oecologia (Berl.), **87**: 500–505. doi:10.1007/BF00320412.

Zhang, Z.Y., and Chai, Z.F. 2004. Isotopic tracer studies of chemical behavior of rare earth elements in environmental and biological sciences. Radiochim. Acta, **92**: 355–358. doi:10.1524/ract.92.4.355.35607.

© 2008 NRC Canada

Absorption properties of phytoplankton in the Lower Estuary and Gulf of St. Lawrence (Canada)

Suzanne Roy, Frédérick Blouin, André Jacques, and Jean-Claude Therriault

Abstract: Models of ocean colour rely on information about phytoplankton absorption, which varies according to community composition and photoacclimation. Here we show that pigment packaging, which is strongly determined by the size structure of local algal populations, represents a dominant factor in the Estuary and Gulf of St. Lawrence, accounting for ~50%–80% of the reduction in phytoplankton absorption at 440 nm during the spring bloom periods and for 24%–48% before and after the blooms. This is consistent with the importance of diatoms in this environment. Comparison between three methods of estimating packaging gave average values within less than 20% of each other during the blooms. Changes in pigment composition, which also affect phytoplankton absorption, were more important outside bloom periods (particularly in the Gulf), although this influence was relatively modest (11%–13%). This was accompanied by an increase in photoprotective pigments and an absorption peak in the ultraviolet range (~330 nm). Regional variations in phytoplankton absorption reflected bloom conditions, whereas detrital particulate material was highest in the upstream Saguenay region (often more than 60% of the absorption of total particulate material at 440 nm ($a_p(440)$)) and was at least 20%–30% elsewhere. This information is a first step towards the development of regional models of ocean colour.

Résumé : Les propriétés d'absorption de la lumière par le phytoplancton sont essentielles pour le développement des modèles bio-optiques de couleur de l'océan. Dans ce travail, nous montrons que l'empaquetement des pigments algaux (« packaging effect »), qui est principalement déterminé par la structure de taille des populations locales, explique 50–80 % de la réduction du spectre d'absorption du phytoplancton à 440 nm pendant les périodes de floraisons printanières de diatomées dans l'estuaire et le golfe du Saint-Laurent. Ce facteur est de 24–48 % avant et après les floraisons, reflétant l'importance des diatomées dans cet environnement. Une comparaison entre trois méthodes d'estimation du « packaging » donne des valeurs moyennes variant de moins de 20 % entre elles. La composition pigmentaire a une influence relativement plus modeste (11–13 %) sur l'absorption phytoplanctonique et elle est importante principalement dans le golfe après la floraison printanière, liée à une augmentation des pigments photoprotecteurs et à un maximum dans la bande UV (autour de 330 nm). Les variations régionales de l'absorption phytoplanctonique sont le reflet des conditions de floraisons algales, alors que pour le matériel détritique particulaire, les valeurs sont généralement entre 20 et 30 % de l'absorption particulaire totale ($a_p(440)$), sauf dans la région du Saguenay où elles sont nettement plus élevées (souvent plus de 60 %).

Introduction

The interpretation of ocean colour detected from space or from airplanes relies increasingly on a detailed understanding of the dominant optical constituents of the water, particularly for coastal waters (Bukata et al. 1995). Phytoplankton is an optical constituent of great interest for biological oceanography, as it determines the biomass and productivity at the base of aquatic food webs. Phytoplankton absorption is currently used to estimate the biomass of phytoplankton from remote-sensing observations through the use of semi-analytical bio-optical models (e.g., Bricaud et al. 1995; Ciotti et al. 1999; Sathyendranath et al. 2004). It is also used in models of primary productivity (Longhurst et al. 1995; Behrenfeld and Falkowski 1997) and has recently been proposed as a strong predictor of primary productivity in surface waters of the oceans (Marra et al. (2007), but see also Huot et al. (2007)). There is thus a need to understand the factors that control the variability of phytoplankton absorption, along with those of co-occurring detrital particulate and dissolved material that can influence the interpretation of remote-sensing observations of ocean colour, particularly in coastal regions (International Ocean-Colour Coordinating Group (IOCCG) 2000).

The Lower Estuary and Gulf of St. Lawrence system constitutes a large coastal environment (226×10^3 km^2) that is very important for fishing populations surrounding this region. The general circulation pattern in this system is typically estuarine, with an important annual freshwater input of about 424 km^3 in the surface waters of the Estuary

Received 30 May 2007. Accepted 25 February 2008. Published on the NRC Research Press Web site at cjfas.nrc.ca on 29 July 2008. J20021

S. Roy[1] **and F. Blouin.**[2] Institut des Sciences de la Mer de Rimouski (ISMER), Université du Québec à Rimouski, Rimouski, QC G5L 3A1, Canada.
A. Jacques. Département de mathématiques, informatique et génie, Université du Québec à Rimouski, Rimouski, QC G5L 3A1, Canada.
J. Therriault.[3] Maurice Lamontagne Institute, Department of Fisheries and Oceans, Mont-Joli, QC G5H 3Z4, Canada.

[1]Corresponding author (e-mail: suzanne_roy@uqar.qc.ca).
[2]Present address: Centre de recherche sur les biotechnologies marines, Rimouski, QC G5L 9H3, Canada.
[3]Retired.

 doi:10.1139/F08-089 © 2008 NRC Canada

(Bugden et al. 1982) moving out to the Atlantic Ocean. This outgoing flow is compensated for by an inflow of denser Atlantic waters at depth. The large width of this estuary results in relatively complex mesoscale circulation features (Ingram and El-Sabh 1990; Vézina et al. 1995), which can be observed from space (Fuentes-Yaco et al. 1997). The Gulf has been characterized as an inland sea with several biophysical subregions (de Lafontaine et al. 1991). Optically, this system has been described as predominantly "case 2" in the Estuary and "case 1" in the Gulf (Babin et al. 1993). Case 1 waters are typically oceanic, whereas case 2 waters are essentially coastal and optically more complex, with constituents other than phytoplankton contributing significantly to the optical properties.

Previous work by Babin et al. (1993, 1995) examined the spatial variability of the specific absorption coefficient of phytoplankton in this region during the summer. They showed that variability was greatest at large scale, mostly between the Estuary and the Gulf. In a series of satellite (CZCS) images from both regions, Fuentes-Yaco et al. (1997) showed that the Estuary had a higher biomass of phytoplankton than the Gulf during most of the year. High biomass is generally associated with larger-sized cells for which the packaging effect (self-shading leading to a decreased specific absorption) is greater (e.g., Bricaud et al. 2004). We thus hypothesized that the packaging effect was important, particularly in the Estuary and during phytoplankton blooms. The other major factor influencing phytoplankton absorption is pigment composition, particularly the relative concentrations of photoprotective and photosynthetic (light-harvesting) pigments (Sathyendranath et al. 1987; Bricaud et al. 1995). Photoprotective carotenoids often make a significant contribution to the changes in cell pigmentation, particularly in high light environments (Bricaud et al. 1995). Because the Gulf waters have a more oceanic optical character (case 1 waters) and light penetrates deeper (Babin et al. 1993), we hypothesized that the photoprotective pigments had a greater influence on phytoplankton absorption in the Gulf than in the Lower St. Lawrence Estuary. These variables have never before been measured concurrently with phytoplankton absorption over this whole system. There were also no previous measurements of particulate and phytoplankton absorption during spring in this region, because the access is usually restricted by ice cover. The major goal of this study was thus to test the hypothesis that the packaging effect had a strong influence on phytoplankton absorption, particularly during the spring algal bloom in the Lower Estuary and Gulf of St. Lawrence. The factors that can account for the variability in phytoplankton absorption were also examined during and after this bloom. This information is fundamental for developing regional models of ocean colour.

Materials and methods

Sampling

Two field campaigns were conducted on 17–30 May 2000 and 17 April – 4 May 2001 in the Estuary and Gulf of St. Lawrence on board the NGCC *Martha L. Black* (the locations of the stations are shown in Fig. 1). Water sampling was conducted with a Rosette sampler equipped with 30 L Niskin bottles. Only the surface (1.5 m) data were utilized in this study, as chlorophyll *a* (Chl *a*) values from the surface and top 10 m were strongly correlated ($r = 0.92$, $n = 44$) and these represent most of the signal received by remotely sensed ocean colour sensors. Filtrations for pigments and phytoplankton absorption were done rapidly after collection on Whatman GF/F filters (2.5 cm) using a vacuum pressure not exceeding 8 psi. Filters were frozen in liquid nitrogen immediately after filtration and kept in a –80 °C freezer until further analysis in the laboratory. For absorption measurements, the filters were kept flat in tissue capsule holders (Fisher HistoPrep; Thermo Fisher Scientific Inc., Waltham, Mass.); they were folded and put into cryovials for pigment determination.

Physical and chemical variables

Temperature and salinity were determined using a conductivity–temperature–depth (CTD) profiler (model SBE19; SeaBird Electronics Inc., Bellevue, Wash.). Vertical profiles of downwelling irradiance (E_d) were obtained with an underwater photosynthetically active radiation (PAR) sensor (SPMR model; Satlantic Inc., Halifax, Nova Scotia, Canada). The attenuation coefficient was calculated from the ratio of $\ln(E_d(0)/E_d(z))$ and the depth interval. Values for E_d just below the surface ($E_d(0)$) were extrapolated from linear regressions of $\ln(E_d)$ against depth (z). The concentration of nutrients was determined using a Technicon Autoanalyser (Technicon Instruments Corp., Tarrytown, N.Y.) following the methods of Strickland and Parsons (1972). Samples for nutrients (50 mL) were filtered on 0.2 µm Acrodisc filters (Pall Corporation, East Hills, N.Y.), collected in acid-washed cryovials, and stored at –80 °C until analysis. The concentration of suspended particulate material was determined from weight determinations on samples of 100 mL, following JGOFS standard protocols. Whatman GF/F filters were preburned and preweighed before the field campaigns, and filters were stored at –80 °C aboard the ship and in the laboratory prior to analysis. The concentration of particulate organic carbon (POC) was determined using a CHN elemental analyser (model 2400; PerkinElmer Life and Analytical Sciences, Inc., Waltham, Mass.).

Absorption

The absorption spectra of the particulate material on the filter were determined with the quantitative filter method (Mitchell et al. 2002) using a spectrophotometer (model Lambda 2; PerkinElmer) equipped with an integrating sphere (model RSA-PE-20; Labsphere Inc., North Sutton, N.H.). All spectra were first corrected for background by subtracting an average spectrum of blank filters from the same lot and then for scattering by subtracting the mean optical density between 790 nm and 800 nm for each sample. A quadratic fit equation was used to estimate the optical pathlength amplification factor due to the filters. This equation was determined in our laboratory from phytoplankton cultures (Laurion et al. 2003). Optical density values from filters (OD_f) were transformed into equivalent OD values in suspension (OD_s) with the following equation: $OD_s(\lambda) = 0.339[OD_f(\lambda)] + 0.583[OD_f(\lambda)^2]$. The values were then transformed into absorption coefficients ($a_p(\lambda)$, m^{-1}) by multiplying by 2.303 (transforming base-10 to base-e loga-

© 2008 NRC Canada

Fig. 1. Map of the study area: (*a*) map of eastern Canada, with the box showing the study area; (*b*) map of the Lower Estuary and Gulf of St. Lawrence showing the location of the sampling stations.

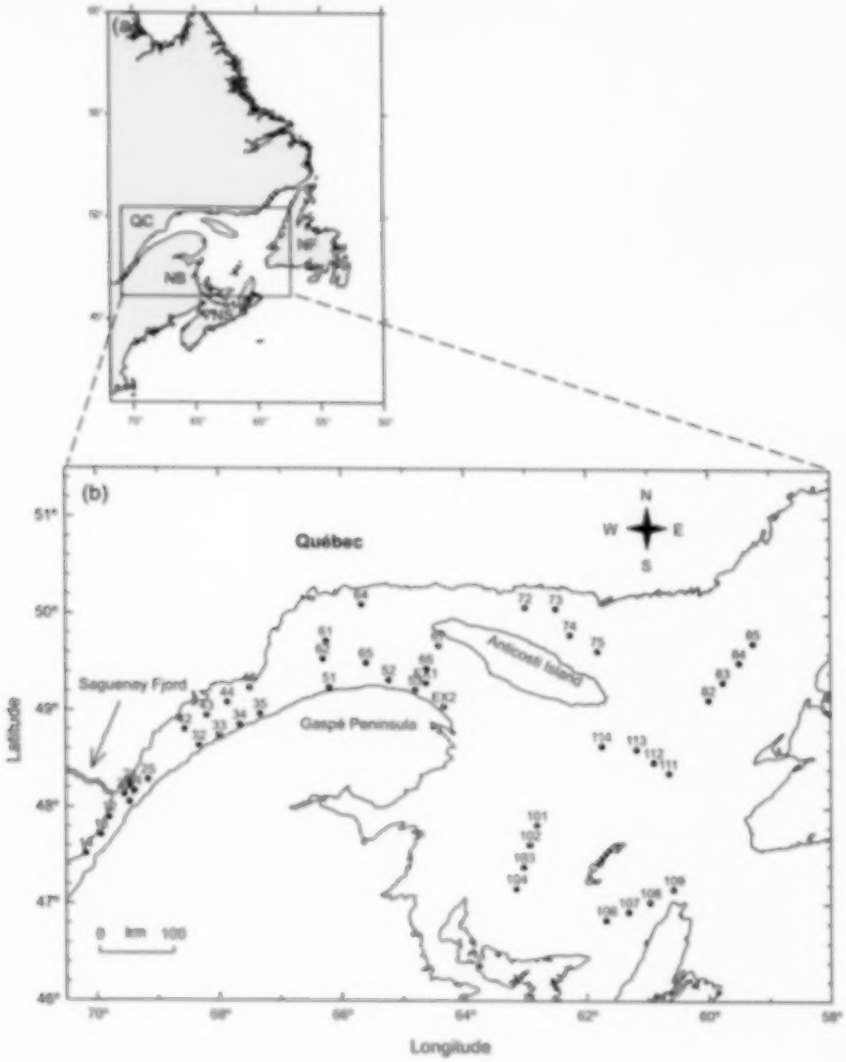

rithm) and dividing by the pathlength of light passing through the sample (= volume filtered divided by the area of filtration). The coefficient of variation was generally <5% for scans of triplicate filters (available for April 2001 only). Detrital absorption, $a_d(\lambda)$, was obtained using the method developed by Kishino et al. (1985), after extracting pigments from the filters (using absolute methanol followed by filtered seawater) and rescanning the bleached filters. Variability for a_d was slightly higher than for a_p, with a coefficient of variation generally <8%. Phytoplankton absorption, $a_{ph}(\lambda)$, was finally determined by subtracting $a_d(\lambda)$ from $a_p(\lambda)$. To obtain chlorophyll-specific absorption coefficients ($a^*_{ph}(\lambda)$), $a_{ph}(\lambda)$ was normalized by HPLC-determined total chlorophyll *a* (TChl *a* = Chl *a* + epimers and allomers of Chl *a* + chlorophyllide *a*). The average coefficient of variation for replicates of a_{ph} was 17%.

Pigments

Pigment analysis was performed on a separation HPLC system (Thermo Fisher Scientific Inc.) equipped with a fluorometer (model ABI Spectroflow 980; Applied Biosystems International, Foster City, Calif.) set at 412 nm and a SpectraFocus fast scanning absorbance detector (Thermo Fisher Scientific Inc.). The separation of the various pigments was done on a RP-C8 Symmetry column (150 × 4.6 mm, 3.5 µm; Waters, Milford, Mass.) at a temperature of 25 °C. The frozen filters were extracted in 95% methanol using sonication. The elution followed the method of Zapata et al. (2000) (mobile phases A and B1, flow rate = 1 mL·min^{-1}). Peak identification and standardization used commercial pigment standards from DHI Water and Environment (Denmark). Extinction coefficients were obtained from Jeffrey et al. (1997). Errors based on the analysis of

© 2008 NRC Canada

Table 1. Range of values (minimum, maximum) for selected oceanographic variables for the May 2000 and April 2001 field campaigns and stations (S followed by the station number) where these values can be found in the Lower Estuary and Gulf of St. Lawrence system.

Variable	Year	Minimum	Maximum
Surface temperature (°C)	May 2000, April 2001	1.7 (S 51), 0.0 (S 84)	9.1 (S 13), 4.0 (S 14)
Surface salinity	May 2000, April 2001	12.1 (S 13), 12.1 (S 14)	31.6 (S 85), 31.9 (S 72)
First optical depth (K_d^{-1}) (m)	May 2000, April 2001	0.7 (S 14), 0.8 (S 14)	13.2 (S 111), 6.5 (S 66)
Euphotic depth (1% E_0) (m)	May 2000, April 2001	4.6 (S 14), 4.3 (S 14)	60.7 (S 111), 30.6 (S 66)
Total suspended matter ($g \cdot m^{-3}$)	May 2000, April 2001	0.0 (S 107), 1.1 (S 62)	17.7 (S 14), 24.5 (S 14)
POC ($\mu mol \cdot L^{-1}$)	May 2000, April 2001	7.2 (S 104), 12.0 (S 42)	113.7 (S 35), 82.8 (S 102)
$NO_2 + NO_3$ ($\mu mol \cdot L^{-1}$)	May 2000, April 2001	0.1 (S 43), 0.1(S 104)	29.7 (S 12), 41.3 (S 14)
PO_4 ($\mu mol \cdot L^{-1}$)	May 2000, April 2001	0.0(S 35), 0.3 (S 104)	1.3 (S 103), 1.2 (S 53)
Si ($\mu mol \cdot L^{-1}$)	May 2000, April 2001	0.1(S 43), 0.2 (S 113)	34.5 (S 13), 40.3 (S 14)
TChl *a* ($\mu g \cdot L^{-1}$)	May 2000, April 2001	0.06 (S 107), 0.07 (S 12)	16.22 (S 42), 9.40 (S 102)
Sum of pheopigments ($\mu g \cdot L^{-1}$)	May 2000, April 2001	0.01 (S 103), 0.01 (S 21)	2.25 (S 52), 0.30 (S 82)
$a_p(440)$ (m^{-1})	May 2000, April 2001	0.007 (S 103), 0.041 (S 84)	0.363 (S 52), 0.983 (S 14)
$a_d(440)$ (m^{-1})	May 2000, April 2001	0.003 (S 104), 0.010 (S 84)	0.262 (S 14), 0.918 (S 14)
$a_{ph}(440)$ (m^{-1})	May 2000, April 2001	0.002 (S 107), 0.006 (S 21)	0.279 (S 66), 0.205 (S 64)

triplicate samples from most stations gave a coefficient of variation of 10% on average for Chl *a* (both years). Errors were larger for minor pigments, present in lower concentrations (for example, the average coefficient of variation for Chl c_3 was 18% in May 2000 and 29% in April 2001).

Taxonomic identification

Identification and enumeration of phytoplankton (no replicates) were done on samples fixed with acid Lugol, using an inverted microscope (Leitz Labovert FS, Wetzlar, Germany). Surface water samples of 100 mL were mixed and poured in settling columns and examined after a sedimentation period of 24 h by L. Bérard-Therriault at the Maurice-Lamontagne Institute (Mont-Joli, Quebec).

Statistical analysis

Cluster analysis was performed using the NTSYS software (Ver. 2.01; Exeter Software, Setauket, N.Y.) using the Bray and Curtis dissimilarity coefficient on the phytoplankton absorption data.

Results and discussion

General characteristics

The region sampled covers a range of oceanographic conditions from the lower salinity waters upstream near the Saguenay fjord to the more oceanic waters downstream towards Newfoundland (Fig. 1). The range of values for selected water properties is provided (Table 1). Waters from the upstream region were warmer and less saline, with more suspended material, shallower light penetration, and higher nutrient concentrations. Maximum algal biomass (Chl *a*) was found in the Lower Estuary in May 2000 and in the Gulf in April 2001.

Particulate absorption

Particulate absorption at 440 nm ranged from 0.007 to 0.363 m^{-1} in May 2000 and from 0.041 to 0.983 m^{-1} in April 2001 (Table 1). The particulate absorption spectra were strongly influenced by the presence of phytoplankton for most of the stations sampled (Fig. 2). Phytoplankton absorption accounted for an average of 63% and 58% of total particle absorption at 440 nm for May 2000 and April 2001, respectively. One exception was the upstream Saguenay Fjord region (stations 11 to 24, Fig. 2*a*), where $a_p(\lambda)$ was often similar to the detrital absorption spectrum ($a_d(\lambda)$), and phytoplankton absorption was virtually absent (generally less than 20% of particulate absorption). When stations from this region were omitted, a linear relationship between a_p(443 nm or 675 nm) and the concentration of TChl *a* ([TChl *a*]) gave a good fit for both years ($a_p(675) = 0.0132[\text{TChl } a] + 0.0116$, $r^2 = 0.97$, $n = 40$ for May 2000; $a_p(675) = 0.0118[\text{TChl } a] + 0.0151$, $r^2 = 0.87$, $n = 25$ for April 2001). The regression slope value for May 2000 is similar to the value obtained by Cleveland (1995) for subpolar environments (0.0132). The relationship between particulate absorption and chlorophyll has been alternatively described by a power function (e.g., Bricaud et al. 1998). For our data set (without the Saguenay region stations), this would give a fit slightly worse than above, with $a_p(440) = 0.059[\text{TChl } a]^{0.666}$ ($r^2 = 0.96$, $n = 37$) for May 2000 and $a_p(440) = 0.091[\text{TChl } a]^{0.289}$ ($r^2 = 0.63$, $n = 28$) for April 2001. The May 2000 results are more consistent than the April 2001 ones with Bricaud et al.'s. (1998) findings ($a_p(440) = 0.052[\text{TChl } a]^{0.598}$, $r^2 = 0.92$, $n = 260$), because their results came from an extensive oceanic database and our May 2000 samples showed more resemblance to oceanic waters, especially for the Gulf postbloom samples.

Detrital absorption

Detrital absorption at 440 nm ranged from 0.003 to 0.262 m^{-1} in May 2000 and from 0.010 to 0.918 m^{-1} in April 2001 (Table 1). For both years, the detrital absorption at 440 nm contributed about 20%–30% of the total particulate absorption for most stations, except for stations near the Saguenay Fjord where the detrital component contributed for more than 60% (e.g., Fig. 2*a*). The range of values obtained is consistent with those from previous studies from various environments (e.g., Cleveland 1995; Bricaud et al. 1998), as well as studies from the St. Lawrence during the summers of 1988 to 1990 ($a_d(440) = 33\%$ to 40% of $a_p(440)$; Babin et al. 1993). The relative contribution of de-

© 2008 NRC Canada

Fig. 2. Selected absorption spectra for total particulate material (a_p, solid line), detrital particulate material (a_d, shaded dotted–dashed line), and phytoplankton (a_{ph}, shaded broken line), all with units of m^{-1}: (*a*) station 13; (*b*) station 42; (*c*) station 85, and (*d*) station 102. Refer to Fig. 1 and the May 2000 field campaign for station numbers.

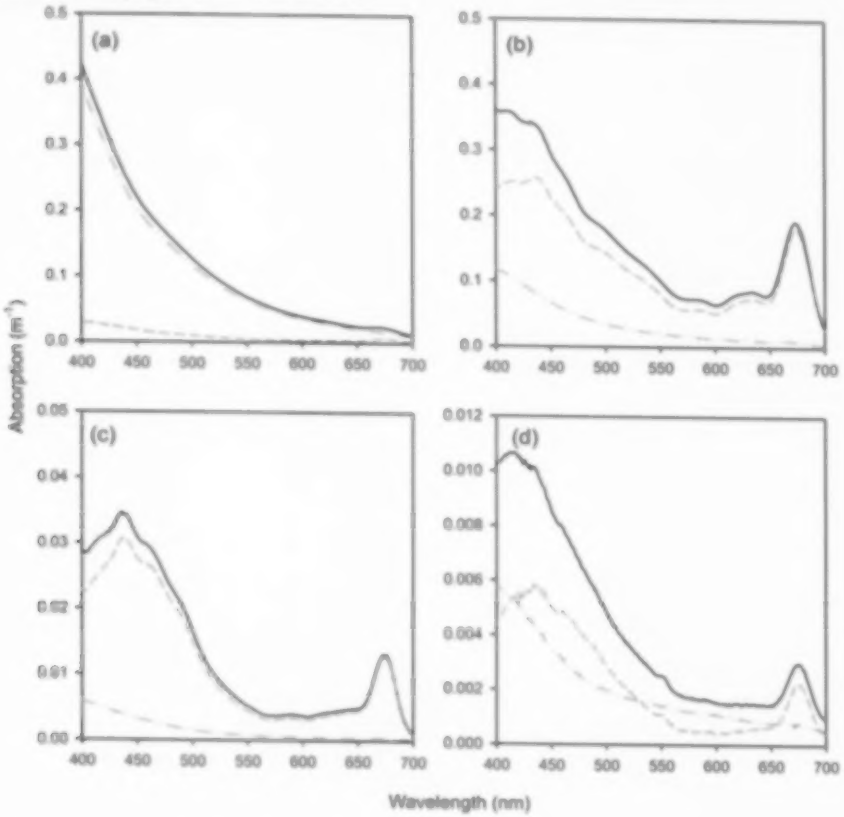

trital to particulate absorption at 440 nm was inversely related to the concentration of TChl *a* (data not shown), as in Bricaud and Stramski (1990). This inverse trend was strongly influenced by the high detrital contributions in the Saguenay region, likely related to locally strong vertical mixing currents (El-Sabh 1988) and to the spring freshwater discharge (Nelson and Guarda 1995; Lutz et al. 2006). Outside of this region, the relative contribution of detrital particulate material was still significant in all our samples (20%–30%), indicating that a correction for detrital particulate material will be necessary to run accurate ocean colour models in this region.

There was a strong positive correlation between $a_d(440)$ and either TChl *a* or $a_{ph}(440)$ in May 2000 only when the upstream stations near the Saguenay fjord were removed ($r = 0.72$, $n = 40$, for the correlation between $a_d(440)$ and TChl *a*). No significant correlations were found when these upstream stations were included, suggesting that the detrital material in the upstream stations was not related to algae (more likely resuspended particles; d'Anglejan 1990). For the rest of the Estuary and the Gulf, the particulate detrital material covaried with algal biomass, as often reported for oceanic waters (Arrigo et al. 1998; IOCCG 2000). The detrital absorption spectra showed a characteristic rise with decreasing wavelength (Fig. 2; Kishino et al. 1985; Roesler et al. 1989; Bricaud and Stramski 1990). The spectral slope, *S*, obtained from a nonlinear regression fit of the expression $a_d(\lambda) = a_d(400)\exp[-S(\lambda - 400)]$ (as in Arrigo et al. (1998)), averaged 0.014 ± 0.002 nm^{-1} over all stations in May 2000 and 0.013 ± 0.002 nm^{-1} for the April 2001 samples. These values are similar to those found by Arrigo et al. (1998) for Antarctic waters (their average = 0.0143 nm^{-1}) and in the range of several other studies (e.g., average of 0.011 ± 0.002 nm^{-1} in Roesler et al. (1989)). Roesler et al. (1989) indicated that there is little change in the value of the a_d spectral slope between case 1 and case 2 waters.

Phytoplankton absorption

At 440 nm, phytoplankton absorption ranged from 0.002 to 0.279 m^{-1} in May 2000 and from 0.006 to 0.205 m^{-1} in April 2001 (Table 1). The a_{ph} spectra differed in shape, particularly in May 2000, between the Estuary, where a bloom was taking place (see pigment results below), and the Gulf, where the annual spring bloom was already over. These differences in a_{ph} are highlighted in Fig. 2, in which selected stations show the variety of spectra obtained. The blue peak and the blue–red peak ratio were generally larger in the Gulf in May 2000.

To simplify the presentation of the data, we summarized the information based on regional variations in phytoplankton

© 2008 NRC Canada

Table 2. Groups identified using a cluster analysis on $a^*_{ph}(\lambda)$ from five wavelengths (412, 443, 490, 555, and 670 nm) using the Bray and Curtis dissimilarity coefficient (NTSYS software (Ver. 2.01); Exeter Software, Setauket, N.Y.).

May 2000		
Estuary		
Subgroup 1 (Saguenay)	Subgroup 2 (Estuary)	Group 3 (Gulf)
S 11	S 21	S 13
S 12	S 22	S 61
S 14	S 24	S 72
S 25	S 35	S 73
S 32	S 43	S 74
S 33	S 45	S 75
S 34	S 51	S 82
S 42	S 62	S 83
S 44	S 106	S 84
S 52	S 107	S 85
S 53	S 108	S 101
S 66	S EX1001	S 102
	S EX2001	S 103
		S 104
		S 109
		S 111
		S 112
		S 113
		S 114
April 2001		
	Estuary and Gulf	
Group 1 (Saguenay)	Subgroup 2 (Estuary)	Subgroup 3 (Gulf)
S 12	S 21	S 32
S 13	S 34	S 33
S 14	S 35	S 42
S 22	S 43	S 51B
S 24	S 44	S 64
S 51	S 61	S 72
	S 62	S 73
	S 65	S 74
	S 66	S 84
	S 82	S 101
	S 114	S 102
		S 104
		S 111
		S 113

Note: Stations (S followed by the station number) from Fig. 1.

absorption. The different regions were determined using a cluster analysis on a_{ph} at five wavelengths: 412, 443, 490, 555, and 670 nm. The selected wavelengths are based on their use in ocean colour sensors such as SeaWiFS. When using phytoplankton absorption values not normalized to chlorophyll, three major groups were detected in May 2000: (*i*) the Estuary (up to stations north of Anticosti Island), (*ii*) the Magdalen Islands (stations 102 to 104 and 107), and (*iii*) the rest of the Gulf (for the list of stations in each group, see Table 2). When the algal biomass influence was removed by using chlorophyll-specific phytoplankton absorption instead, only two groups showed up, the Estuary and the Gulf, with the Magdalen Islands stations included this time with the Gulf (Table 2). These stations were set apart in the first analysis because of their lower a_{ph} and chlorophyll concentration values, but their chlorophyll-specific spectra were similar to those of other stations in the Gulf. The major difference between the Estuary and Gulf groups in May 2000 was the much lower values of a^*_{ph} in the Estuary, particularly for the blue

Fig. 3. Average spectra and standard deviation (SD; shown as the average minus SD, dotted lines) for specific phytoplankton absorption for the three regions identified from the cluster analysis of a^*_{ph} at five wavelengths (412, 443, 490, 555, and 670 nm): (*a*) May 2000 and (*b*) April 2001. The dotted SD lines are shown below their parent regional average spectrum.

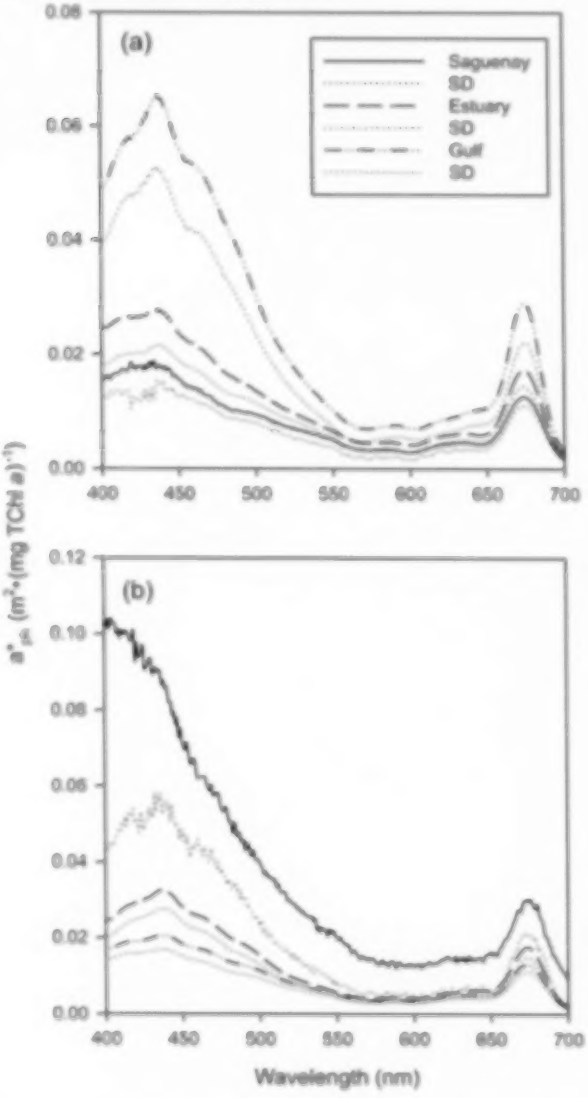

© 2008 NRC Canada

peak (Fig. 3*a*). The Estuary group could be further subdivided into a group of upstream stations where the seasonal bloom was underway (average TChl a = 9.2 μg·L^{-1}) and the rest of the Estuary. The bloom stations showed the lowest specific absorption at all wavelengths (Fig. 3*a*). The values observed for $a^*_{ph}(443)$ ranged from 0.020 to 0.065 m^2·(mg Chl a)$^{-1}$. This range was slightly larger than that reported by Babin et al. (1993, 1995) for studies in the same region during summer.

In April 2001, when the spring bloom was underway in the Gulf, two major groups emerged, one for the Saguenay region and the other covering the Estuary and Gulf, which could be subdivided in two subgroups, one for the Estuary and the other for the Gulf (Table 2). Although both subgroups had relatively low a^*_{ph} values, the Gulf stations were distinguished by their lowest specific absorption (Fig. 3*b*). The Saguenay region (stations 12 to 24) had particularly high a^*_{ph} values, along with very low pigment concentration (TChl a = 0.1 μg·L^{-1}, on average). The Estuary and Gulf regions were more similar in April 2001 than in May 2000 (Figs. 3*a*, 3*b*), reflecting the diatom bloom that was underway in a large portion of the St. Lawrence marine waters at that time. Considering results from both years, we decided to present separately the data for the Saguenay region, the Estuary, and the Gulf for the rest of this paper.

The relationships between $a_{ph}(675)$ and TChl a concentration are shown and the fit of different functions is compared (Fig. 4). As observed by Lutz et al. (1996), a Michaelis–Menten type equation of the form $a_{ph}(\lambda) = (a_m a_m^*[\mathrm{Chl}])(a_m + a_m^*[\mathrm{Chl}])^{-1}$, where a_m and a_m^* are two fitted parameters corresponding, respectively, to the asymptote value and the initial slope near the origin of the absorption versus TChl a concentration curve, gave a good fit to these data (a_m = 0.543, a_m^* = 0.023, r^2 = 0.88, n = 44, in May 2000; a_m = 0.196, a_m^* = 0.030, r^2 = 0.83, n = 32, in April 2001). Our fitted curve for May 2001 was relatively close to the fit obtained for a group of stations dominated by diatoms in Lutz et al. (1996), whereas closest agreement for the April 2001 results was found using the parameters for group D in Lutz et al. (1996), where a mixture of prymnesiophytes and diatoms dominated.

We also tested the recent nonlinear model of Sathyendranath et al. (2004), where phytoplankton absorption is viewed as the sum of the absorption by two different phytoplankton populations with different specific absorption coefficients (a^*_{ph}) and expressed as $a_{ph}(\lambda) = (1/S(\lambda))(a_1^*(\lambda) - a_2^*(\lambda))[1 - \exp(-S(\lambda)[\mathrm{Chl}])] + a_2^*(\lambda)[\mathrm{Chl}]$, where a_1^*, a_2^*, and S are parameters fitted as a function of wavelength λ (Devred et al. 2006). The nonlinear regression fit of this model is shown in Fig. 4 (broken curve). The fit with this function was slightly better at low TChl a concentrations when there were different phytoplankton populations present in the same data set (as in May 2000 with bloom and postbloom stations). The curvature of all of these relationships indicates that pigment packaging was present, reducing absorption at high chlorophyll concentration.

Fig. 4. Relationships between $a_{ph}(675)$ and TChl a concentration for the field campaigns of (*a*) May 2000 and (*b*) April 2001. The circles indicate actual data and the lines show various fits: the best fit for this data set according to Lutz et al.'s (1996) approach (solid line, parameters of the equation fitted to our data set), the best fit using the parameters determined in Lutz et al. (1996) (broken lines) for (*a*) their group A (diatom-dominated) or (*b*) their group D (dominated by prymnesiophytes and diatoms), and the fit using Sathyendranath et al.'s (2004) model (dotted–dashed line).

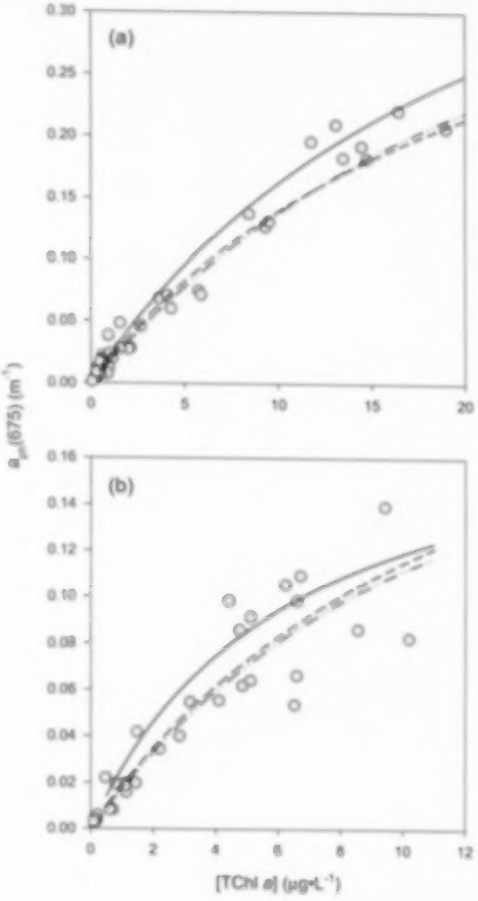

Pigment composition and taxonomy

The average concentration of TChl a over the top 10 m ranged from 0.06 to 16.22 μg·L^{-1} in May 2000 and from 0.07 to 9.40 μg·L^{-1} in April 2001 (Table 1). In May 2000, the highest TChl a concentration was found in the Saguenay region, decreasing downstream (Fig. 5*a*). In April 2001, this pattern was reversed, with the highest concentration in the Gulf (Fig. 5*b*). The phytoplankton spring bloom typically takes place at an earlier time in the Gulf than in the Estuary, notably because of a decreased exchange between the deeper layer and the surface during the high freshwater runoff period, preventing the seeding of the photic layer with resting spores of diatoms (Levasseur et al. 1984; Therriault and Levasseur 1985, 1986). Pheopigments were observed in relatively low concentration. They were more prevalent in the shallower region of Magdalen Islands in the Gulf in May 2000. The average proportion of pheopigments relative to TChl a was 15% in May 2000 (ranging from 4% to 40%) and 8% in April 2001 (ranging from 2% to 55%). The sea-

© 2008 NRC Canada

Fig. 5. (*a* and *b*) Relative concentration of various marker pigments (relative to the sum of all accessory pigments, weight units) for the various regions: (*a*) May 2000 and (*b*) April 2001. The average concentration of TChl *a* (in $\mu g \cdot L^{-1}$) for each region is shown near the bottom of the bars. Pigment abbreviations: Fuco, fucoxanthin; Peri, peridinin; BFU, 19′-butanoyloxyfucoxanthin; Chl c3, chlorophyll *c*3; Allox, alloxanthin; Chl b, chlorophyll *b*; Prasino, prasinoxanthin; SumPPC, sum of photoprotective carotenoids. Only major marker pigments are shown, which explains why the summed bars do not reach a value of 1.0. (*c* and *d*) Relative abundance of the major algal groups (as a fraction of total cell abundance) for the various regions in (*c*) May 2000 and (*d*) April 2001. Abbreviations: Dinoflag., dinoflagellates; Chryso., chrysophytes; Prymnesio., prymnesiophytes; Crypto., cryptophytes; Chloro., chlorophytes; Prasino., prasinophytes; St.51, station 51.

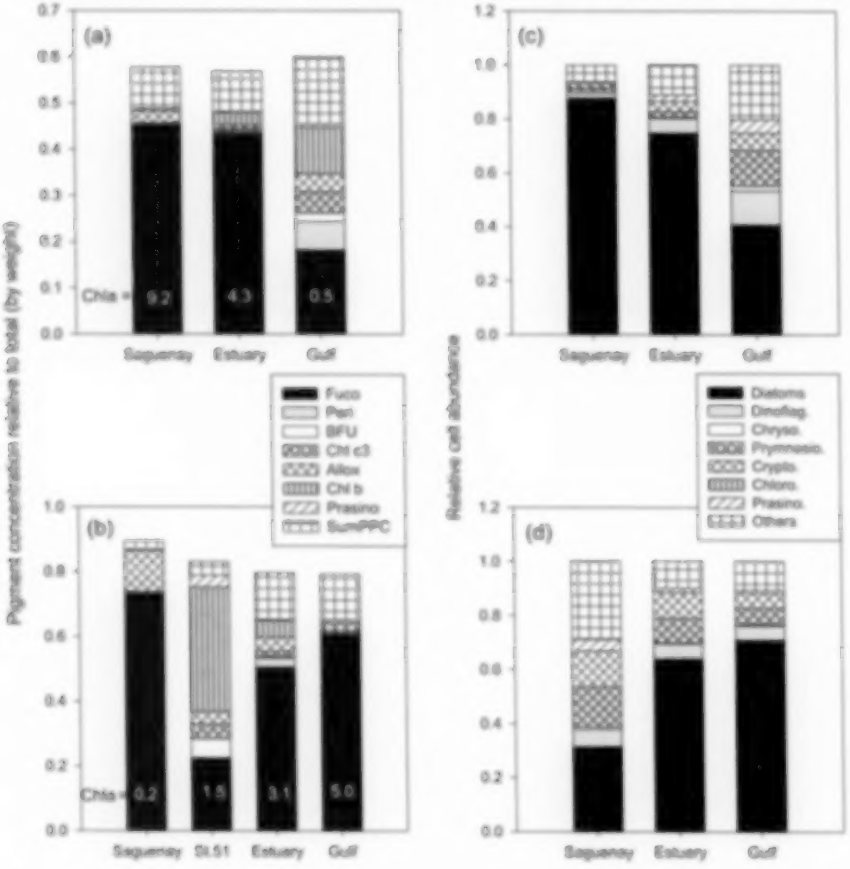

Table 3. Community composition based on the diagnostic pigment approach of Uitz et al. (2006), where f_{pico} is the fraction of TChl *a* concentration associated with picoplankton, f_{nano} is the fraction of TChl *a* associated with nanoplankton, and f_{micro} is the fraction of TChl *a* associated with microplankton. These fractions (in percentage ± standard deviation, SD) are determined relative to the sum of diagnostic pigments, according to the formulae given in Uitz et al. (2006).

Region, year	f_{pico} (%)	f_{nano} (%)	f_{micro} (%)
Saguenay, May 2000	1 (±0)	3 (±6)	96 (±6)
Estuary, May 2000	4 (±5)	1 (±2)	95 (±6)
Gulf, May 2000	23 (±13)	7 (±3)	71 (±14)
Saguenay, April 2001	11 (±21)	7 (±10)	82 (±23)
Estuary, April 2001	7 (±7)	4 (±3)	90 (±8)
Gulf, April 2001	2 (±2)	1 (±2)	97 (±3)

sonal increase in the zooplankton population (de Lafontaine et al. 1991) likely contributed to the May 2000 increase in pheopigments. No divinyl Chl *a* or Chl *b* were present in the samples.

To illustrate the variety of accessory pigments present, the relative pigment proportion (ratio of each pigment over the sum of accessory pigments, in weight units) was plotted for each of the groups determined above (Figs. 5*a*, 5*b*). Clear differences are seen in May 2000 between the Gulf, with a varied pigment composition, and the Estuary and Saguenay groups, where fucoxanthin clearly dominated (Fig. 5*a*). Microscopic identification confirmed these trends and supported the association of fucoxanthin with diatoms (Fig. 5*c*). The dominant diatoms in the Estuary and Saguenay region in May 2000 were *Chaetoceros socialis* (5–14 μm diameter) and *Chaetoceros furcellatus* (5–19 μm diameter). Individual cells of these species are relatively small (nanoplankton size) but are generally found in chain form, possibly shifting them to the microplankton size category. The postspring bloom

© 2008 NRC Canada

Fig. 6. Influence of TChl *a* concentration on the size fractions and of these on phytoplankton specific absorption at 440 nm. Size fractions were estimated based on pigments, as in Uitz et al. (2006). (*a–c*) Relationship between size fractions and TChl *a* for (*a*) the fraction of TChl *a* associated with picoplankton (f_{pico}), (*b*) the fraction associated with nanoplankton (f_{nano}), and (*c*) the fraction associated with microplankton (f_{micro}). (*d–f*) Relationship between $a^*_{ph}(440)$ and these size fractions: (*d*) f_{pico}, (*e*) f_{nano}, and (*f*) f_{micro}. Symbols: circles, Saguenay stations; squares, Estuary stations; triangles, Gulf stations; shaded symbols, May 2000; solid symbols, April 2001.

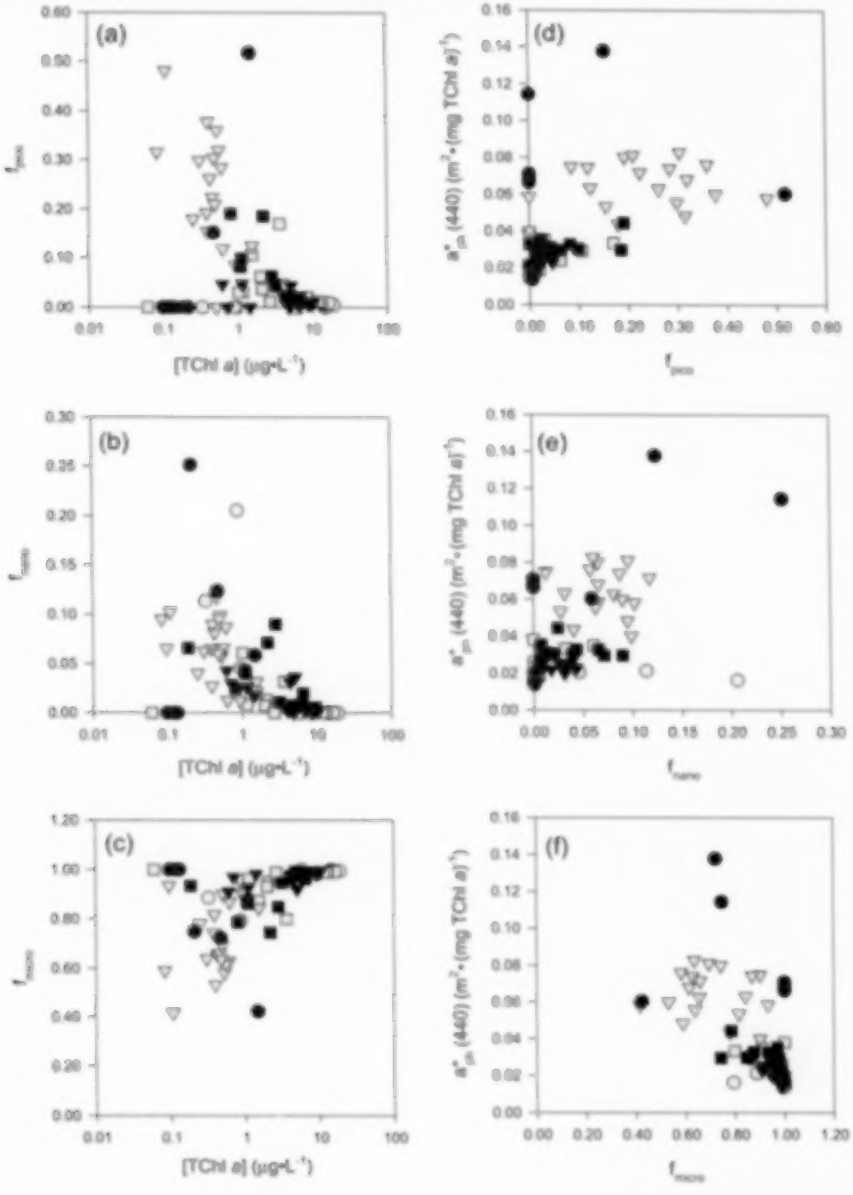

situation in the Gulf in May 2000 was characterized by a greater abundance of peridinin-containing dinoflagellates, alloxanthin-containing cryptophytes, chrysophytes, and prymnesiophytes (with Chl c_3, 19′-hexanoyloxyfucoxanthin (HFU), 19′-butanoyloxyfucoxanthin (BFU)), as well as chlorophytes and prasinophytes (with Chl *b*, lutein, prasinoxanthin).

In April 2001, fucoxanthin was dominant in all regions (apart from station 51 mentioned below; Fig. 5*b*), reflecting an abundance of diatoms (Fig. 5*d*). The dominant diatom species for the Estuary and Gulf were *Neodenticula seminae* (8 µm wide × 20 µm long), *Chaetoceros debilis* (10–40 µm diameter), *Chaetoceros socialis* (5–14 µm diameter), *Skeletonema costatum* (3–16 µm diameter), and *Thalassiosira nordenskioldii* (11–41 µm diameter). For the Saguenay region, the taxonomic identification indicated a relatively low

© 2008 NRC Canada

Fig. 7. Relationship between PPC to total carotenoid ratio and TChl *a* for (*a*) May 2000 and (*b*) April 2001. Relationship between $a^*_{ph}(440)$ and PPC to total carotenoid ratio for (*c*) May 2000 and (*d*) April 2001. PPC, photoprotective carotenoids; solid circles, Saguenay stations; open circles, Estuary stations; solid triangles, Gulf stations.

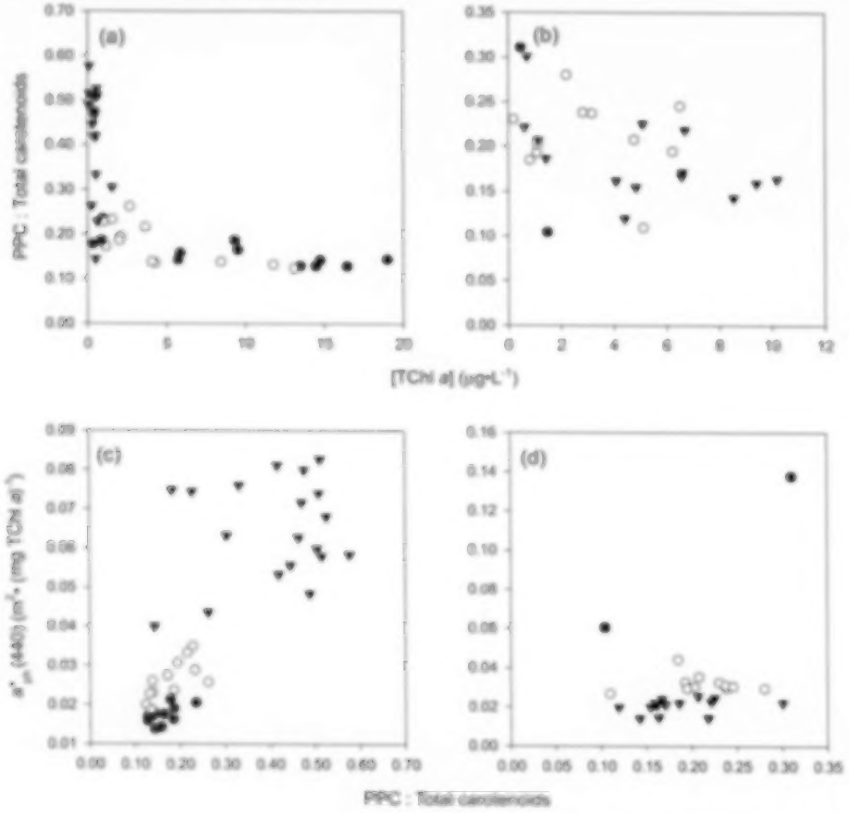

abundance of diatoms (Fig. 5*d*), in contrast with the pigment analysis, which indicated a dominance of fucoxanthin (Fig. 5*b*). The low cell abundance of the Saguenay group stations (5.8×10^4 cells·L^{-1}) explains why few accessory pigments were detected, making pigment analysis less informative for taxon identification. Microscopy indicated that cryptophytes and prasinophytes were present in the Saguenay region. These cells are generally small-sized, so a large abundance would have been necessary for good pigment detection. Station 51, which was classified by the cluster analysis along with the Saguenay region stations but which had a higher pigment concentration (1.5 µg Chl *a*·L^{-1} compared with 0.2 for the other Saguenay region stations), showed an abundance of Chl *b*, prasinoxanthin (both present in prasinophytes), and BFU (Fig. 5*b*), more in agreement with cell identification for this region (Fig. 5*d*).

Photoprotective carotenoids (PPC; diadinoxanthin, diatoxanthin, violaxanthin, antheraxanthin, zeaxanthin, and β,β-carotene) were abundant only outside of the bloom periods, showing marked differences between regions (Fig. 5). Highest relative values were found in the Gulf in May 2000 after the spring bloom (Fig. 5*a*), and lowest values were found in the Saguenay region in April 2001 (Fig. 5*b*). Highest PPC values in the Gulf matched with high UV peaks (maximum around 330 nm, with UV absorption three to four times the absorption of the red chlorophyll maximum, data not shown). This indicates that cells were previously exposed to high irradiance levels (Arrigo et al. 1998; Moisan and Mitchell 2001).

Influence of cell size on specific phytoplankton absorption

Diagnostic pigments have been used to derive community composition and major size groups in field samples when no other cell taxonomy information was available (Uitz et al. 2006). This pigment-derived approach generally concurs with the preceding description. The fraction of TChl *a* associated with picoplankton (f_{pico}), nanoplankton (f_{nano}), and microplankton (f_{micro}) are shown from a multiple regression that relates TChl *a* with major diagnostic pigments (Table 3; Uitz et al. 2006, database of 120 field campaigns). The fraction of picoplankton is expressed in this work as (1.01[Chl *b*] + 0.86[Zeaxanthin])/sum of all diagnostic pigments (SDP); the fraction of nanoplankton is (1.27[HFU] + 0.35[BFU] + 0.60[alloxanthin])/SDP, and the fraction of microplankton is (1.41[fucoxanthin] + 1.41[peridinin])/SDP. Using this pigment approach, microplankton dominated during the bloom periods (f_{micro} = 95% in the Estuary in May 2000 and 97% in the Gulf in April 2001). Smaller-sized phytoplankton were more abundant outside of the

© 2008 NRC Canada

Fig. 8. Influence of photoprotective pigments on the slope of the absorption spectra between 488 and 532 nm. The normalized slope of a_{ph} spectra between 488 and 532 nm ($(a_{ph}(488) - a_{ph}(532))/(a_{ph}(676)(488–532))$) is plotted as a function of the relative abundance of photoprotective pigments (PPC:PSC) for May 2000. Symbols: solid circles, Saguenay stations; open circles, Estuary stations; solid triangles, Gulf stations. Linear regression lines are shown: solid line for all the stations from the Saguenay and Estuary regions; broken line for the Gulf region. PPC, photoprotective carotenoids; PSC, photosynthetic carotenoids.

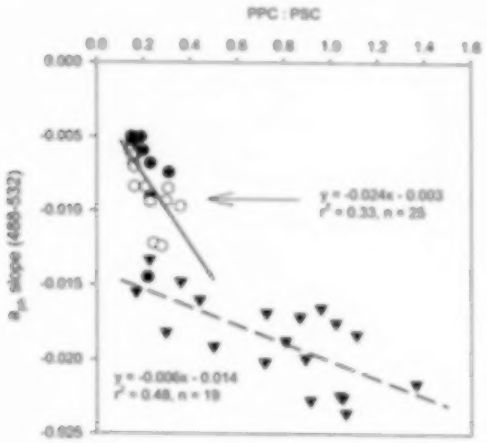

bloom periods (30% for picoplankton + nanoplankton in the Gulf in May 2000 and 18% in the Saguenay region in April 2001). This analysis also points out that the fraction represented by the pigment-defined microplankton was always >50% during this study, even after the seasonal spring bloom. We note that this method may not fully agree with microscopic cell identification, as the size categories are established based on marker pigments. For instance, the major diatoms found during this study included nanoplankton- and microplankton-sized cells, and this distinction would not be possible based solely on the presence of the marker pigment fucoxanthin.

The relationships between these pigment-determined size fractions and the specific absorption of phytoplankton, as well as TChl *a*, are examined (Fig. 6). The relative abundance of small cells (pico- and nano-plankton, containing pigments such as Chl *b* or Chl c_3) showed an increasing upper boundary at low ambient chlorophyll concentration for both years (Figs. 6*a*, 6*b*). Hence, small cells, when present, were in greater relative abundance in low TChl *a* waters. In contrast, microplankton was always high at high chlorophyll concentrations (Fig. 6*c*). An increase in $a^*_{ph}(440)$ was generally associated with increased fractions of pico- and nano-plankton and decreased fractions of microplankton (Figs. 6*d*, 6*e*, 6*f*), as observed elsewhere (e.g., Uitz et al. 2006).

Influence of pigment composition on specific phytoplankton absorption

Pigments characteristic of green algae (Chl *b* and prasinoxanthin) and pheopigments contributed significantly to

Fig. 9. Relationship between the efficiency factor for absorption, $Q^*_a(675)$, and TChl *a* concentration for the three regions: solid circles, Saguenay stations; open circles, Estuary stations; solid triangles, Gulf stations. (*a*) May 2000; (*b*) April 2001.

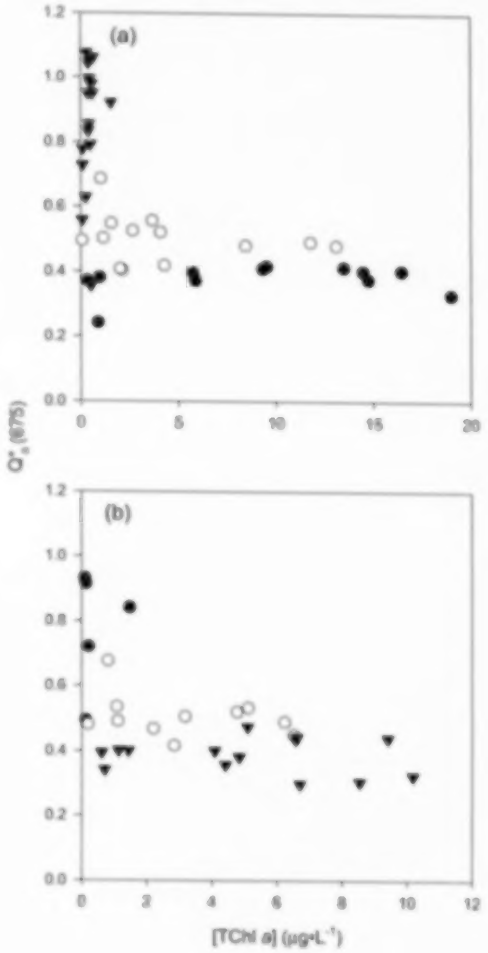

the variability of $a^*_{ph}(440)$ in this coastal environment (multiple regression of a^*_{ph} as a function of chlorophyll-normalized marker pigments, results not shown). Photoprotective pigments can also affect phytoplankton absorption particularly in the blue-green region of the spectrum. As observed by Bricaud et al. (1995) and Stuart et al. (1998), the relative concentration of PPC tended to decrease logarithmically with increasing TChl *a* concentration in May 2000 (Fig. 7*a*). The upper bound of the relative concentration of PPC increased at low TChl *a* concentrations, and high values of PPC were only found in the Gulf region. This trend was absent in April 2001 because of the overall low concentration of photoprotective pigments (Fig. 7*b*). High concentrations of PPC, generally found in high irradiance acclimated cells, result in high values of the specific absorption of phytoplankton (Morel and Bricaud 1981), as observed for the May 2000 results

© 2008 NRC Canada

Fig. 10. Gaussian band heights (in m^{-1}) as a function of the corresponding pigment concentration ($\mu g \cdot L^{-1}$) for the May 2000 field campaign. A few selected bands are shown: (*a*) Chl *a*: 435 nm; (*b*) Chl *b*: 460 nm; and (*c*) total carotenoids: 489 nm. Regression lines are shown only when significant. Solid circles, Saguenay stations; open circles, Estuary stations; solid triangles, Gulf stations.

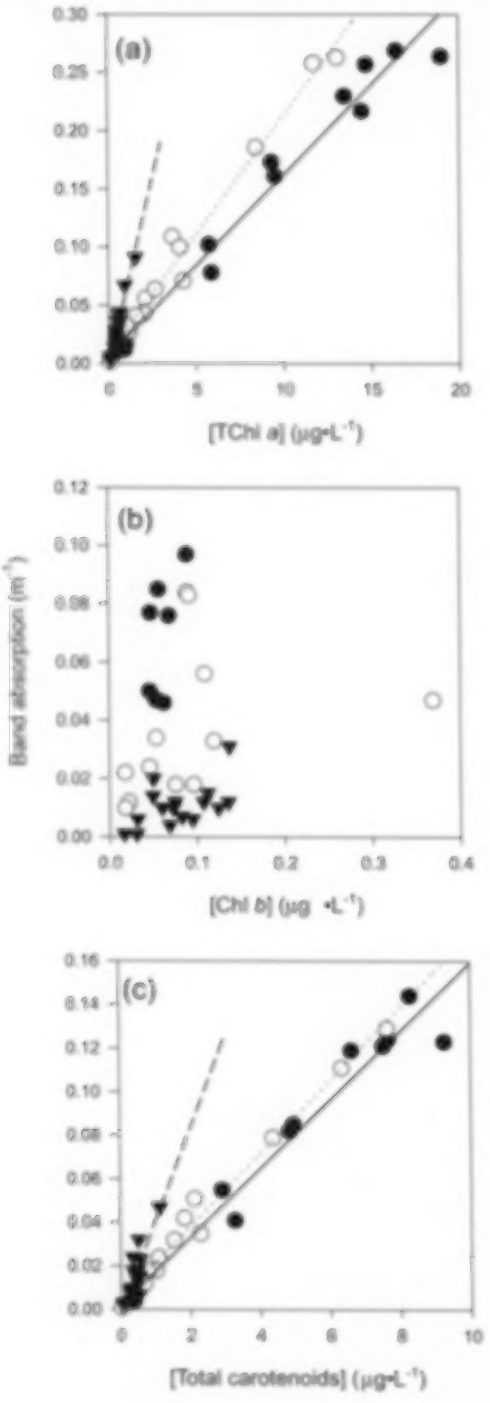

(Fig. 7*c*). No trend was visible in April 2001 because of the limited spread in both a^*_{ph} and relative PPC values (Fig. 7*d*).

The relative contribution of photoprotective pigments to phytoplankton absorption can be estimated using pigment reconstruction (Babin et al. 1996). This approach calculates the relative contribution of PPC to phytoplankton absorption using the ratio $(\Sigma(p_i a^*_i)):(\Sigma(p_j a^*_j))$, where i refers to PPC and j refers to all pigments, p is pigment concentration, and a^* is the weight-specific absorption coefficient of a particular pigment in solution (from Bricaud et al. 2004). The relative contribution of photoprotective pigments to phytoplankton absorption at 440 nm calculated in this way amounted to a maximum of 13% (average for the Gulf in May 2000, data not shown).

Photoprotective pigments also affect the shape of the absorption spectrum, as they contribute specifically to absorption in the range 450–500 nm. This influence can be examined through changes in the slope of the $a_{ph}(\lambda)$ spectrum between 488 and 532 nm (Eisner et al. 2003). In this approach, the normalized slope between 488 and 532 nm in the $a_{ph}(\lambda)$ spectra ($= (a_{ph}(488) - a_{ph}(532))\cdot(a_{ph}(676)(488–532))^{-1}$) is plotted against the ratio of PPC to photosynthetic carotenoids (PSC, the difference between total carotenoids and PPC; as shown in Fig. 8). Values for this normalized slope were between –0.015 and –0.025 in the Gulf in May 2000 (Fig. 8), in the range of the high irradiance samples from the work of Eisner et al. (2003). We have several indications that the Gulf samples were indeed exposed to high irradiance, including the UV peaks, high PPC concentrations, and deeper euphotic layer (Table 1). Lower normalized slopes, in the range of –0.005 to –0.013, were observed for the more upstream stations where light penetration was reduced because of higher loads of suspended matter (Table 1). When all stations were considered in May 2000, the linear regression between the a_{ph} normalized slope and the PPC–PSC ratio was a_{ph} slope = –0.015(PPC:PSC) – 0.006 ($r^2 = 0.73$, $n = 43$). The slope of this regression (–0.015) is close to that found by Eisner et al. (2003) for the Washington coast (–0.013 for discrete samples, their fig. 3). However, a closer look at our data set indicated that this relationship differed between regions. The Gulf showed a regression slope (–0.006) significantly smaller (*t* test) than the other two regions (–0.024; Fig. 8). Changes in community composition and photoacclimation likely contributed to this variability, as mentioned in Eisner et al. (2003). The difference in the normalized slopes between the Gulf and the other two regions in May 2000 could also be related to changes in the packaging effect (see below). No relationship was found between the normalized slopes and PPC:PSC in April 2001 (data not shown), likely because PPCs were in low concentration then.

Pigment packaging effect

The pigment packaging effect can be assessed in several ways, for example, by using parameters derived from a Gaussian spectral decomposition method (Hoepffner and Sathyendranath 1993; Lohrenz et al. 2003) or by comparison of measured spectra with spectra reconstructed based on pigment features (Bidigare et al. 1990; Nelson et al. 1993; Bricaud et al. 2004). A precise determination of the efficiency

© 2008 NRC Canada

Table 4. Slopes of model II linear regressions between selected Gaussian band heights at specified wavelengths and corresponding pigment concentrations (these slopes are equivalent to specific absorption coefficients with units of m^2·(mg pigment)$^{-1}$).

	Chl *a*			
Region, year	435 nm	676 nm	461 nm	Carotenoids, 489 nm
Saguenay, May 2000	0.016	0.013	0.020	0.016
Saguenay, April 2001	0.065	0.029	nd	0.075
Estuary, May 2000	0.021	0.016	0.024	0.017
Estuary, April 2001	0.029	0.016	0.036	0.020
Gulf, May 2000	0.066	0.035	0.050	0.048
Gulf, April 2001	0.017	0.013	0.027	0.015
Comparison with other studies				
Hoepffner and Sathyendranath 1993 (ocean)	0.047	0.021	0.110	0.035
Hoepffner and Sathyendranath 1993 (diatoms)	0.031	0.017	0.081	0.029
Stuart et al. 1998 (Vancouver)	0.034	0.024	0.094	0.029
Stuart et al. 1998 (Arabesque 2)	0.083	0.037	0.298	0.081
Lohrenz et al. 2003 (West Florida)	0.066	0.032	0.170	0.056

Note: nd, no data (too few data points for regression).

Table 5. Mean peak heights of the Gaussian bands centered at 435 nm, normalized to the peak height at 623 nm, for each of the regions for the two field campaigns. These values are compared with a similarly measured estimate from a nonpackaged sample from the Arabesque 2 campaign (which had a value of 13 for the 435 nm band; Stuart et al. 1998).

Region, year	Normalized peak height	Relative to Arabesque 2	PE, %
Saguenay, May 2000	5.41	0.42	58
Saguenay, April 2001	7.29	0.56	44
Estuary, May 2000	5.11	0.39	61
Estuary, April 2001	7.28	0.56	44
Gulf, May 2000	9.86	0.76	24
Gulf, April 2001	5.36	0.41	59

Note: Ratios between the normalized peaks observed for our cruises and the Arabesque 2 cruise are shown in the column entitled "Relative to Arabesque 2". A ratio of one suggests there is no packaging effect (PE), whereas decreasing values indicate increased packaging (assessed as 1 – (normalized peak height:Arabesque 2 value) and reported as a percentage value in this table).

factor for absorption, Q^*_a (Morel and Bricaud 1981), cannot generally be determined from bio-optical theory for field samples because intracellular pigment concentration and cell size are usually not known precisely. Different packaging assessment methods were thus compared here.

The simplest approach consisted of comparing the value of measured phytoplankton absorption at 675 nm (where other pigments have little effect) with the value of absorption of Chl *a* in solution (given as 0.0207 m^2·(mg Chl *a*)$^{-1}$ in Bricaud et al. (1995), but reassessed at 0.027 by Johnsen et al. (1994) and more recently at 0.033 by Johnsen and Sakshaug (2007)). Estimating packaging by this simple method may require the removal of the influence by other pigments, e.g., Chl *b*, on absorption at 675 nm. Alternatively, the Gaussian band for Chl *a* at 675 nm may be used (this method is described below), as there is no interference by other pigments. $Q^*_a(675)$ was then determined as the ratio between this chlorophyll-specific band absorption and the specific absorption coefficient of Chl *a* in solution (0.033 m^2·(mg Chl *a*)$^{-1}$). The relationships between $Q^*_a(675)$ and TChl *a* for both years are shown (Fig. 9). Low packaging (high Q^*_a values, because packaging is (1 – Q^*_a)), was found outside the bloom periods (e.g., in the Gulf in May 2000), whereas around 55% packaging at 675 nm was observed during the bloom periods.

Packaging was then assessed using the spectral decomposition method developed by Hoepffner and Sathyendranath (1991, 1993). The $a_{ph}(\lambda)$ spectra were decomposed into 13 Gaussian bands corresponding to the absorption of the major phytoplankton pigments using a curve-fitting approach. Initial peak centres and half-widths of each band were taken from Hoepffner and Sathyendranath (1993). The relationship between the final Gaussian band heights and the concentration of the corresponding pigments was linear in most cases, regressions were significant ($r^2 > 0.66$, generally > 0.9), and intercepts were not significantly different from zero (Fig. 10). Chl *b* was an exception (as in Stuart et al. (1998) and Lohrenz et al. (2003)), showing no clear relation to the bands at 460 and 653 nm (Fig. 10*b*). The slopes of the model II regressions between the height of the Gaussian band and the corresponding pigment concentration constitute an estimate of the specific absorption coefficient of the pigments contributing to the specified Gaussian band. Selected slopes are shown (Table 4) and are generally within the range of values from previous studies. These weight-specific absorption coefficients for each band can be used in a reconstitution of absorption in the absence of packaging, as in Lohrenz et al. (2003), but we preferred the simpler approach of Stuart et al. (1998), based on a comparison with results from one of their cruises where packaging was minimal (Arabesque 2; Table 4). The actual magnitude of the package effect was estimated by comparing the mean peak heights of the Chl *a* band, normalized to the peak height at 623 nm where packaging is close to zero. These normalized peak heights for the Chl *a* band at 435 nm are shown for our data set (Table 5). The highest normalized peak heights were found in the Gulf in May 2000. The value of 9.9 at

© 2008 NRC Canada

Table 6. The influence of the packaging effect and of pigment composition on the variability of $a^*_{ph}(440)$ for the various regions from this study.

Region, year	Packaging effect, %	Packaging effect Gaussian bands, %	Packaging effect reconstruction, %	Pigment composition, %
Saguenay + Estuary, May 2000	66	58–61	73–81	6–9
Gulf, May 2000	20	24	48	11
Saguenay, April 2001	20	44	38	13
Estuary + Gulf, April 2001	66	44–59	68–79	6–7

Note: Columns 2 to 4 compare the three methods used to estimate packaging. Column 2 refers to the method of Bricaud et al. (1995), where $Q^*_a(675)$ is determined from the ratio of measured $a^*_{ph}(675)$ to the absorption of chlorophyll in solution (taken as 0.027 m^2 (mg Chl $a)^{-1}$) and where the packaging effect is $1 - Q^*_a(675)$. Because packaging is about 20% more at the blue peak than at the red peak (Geider and Osborne 1987), the packaging effect at 440 nm was assessed as 20% + $(1 - Q^*_a(675))$. Column 3 refers to the Gaussian band approach detailed in Table 5 (also for the blue peak). Column 4 estimates the packaging effect at 440 nm from spectral reconstruction based on pigments, as in Bricaud et al. (2004, including the missing absorption term determined in that publication). The last column gives the relative contribution of accessory pigments to phytoplankton absorption at 440 nm, as determined from the difference between measured phytoplankton absorption at 440 nm and the Gaussian peak height of Chl *a* absorption at the same wavelength (Stuart et al. 1998).

435 nm can be compared with a value of 13 observed in the Arabesque 2 field campaign where packaging was negligible (Stuart et al. 1998). This indicates that phytoplankton absorption from the Gulf in May 2000 was still packaged to a certain extent. Assuming that packaging can be expressed as 1 minus the ratio of these normalized band heights between our data and the Arabesque 2 campaign, packaging at 435 nm amounted to 24% in May 2000 (Table 5). A similar estimation of packaging at 435 nm amounted to 58% and 61%, respectively, for the Saguenay and Estuary regions in May 2000 (bloom conditions), showing increased packaging compared with the Gulf. In April 2001, the Gulf (then undergoing a diatom bloom) showed much higher packaging compared with May 2000 (59%). The Estuary showed slightly lower values (44%), as did the Saguenay region (44%). Hence high packaging (~60%) was observed when bloom diatoms dominated.

The last approach used to assess packaging was based on a comparison of measured spectra with spectra reconstructed from the sum of the contributions by the various pigments at each wavelength, measured as the product of weight-specific absorption coefficients in solution with the concentration of each pigment (Bidigare et al. 1990; Nelson et al. 1993; Bricaud et al. 2004). This reconstruction is based on pigments that are not packaged (in solution), so that $Q^*_a(\lambda)$ can be expressed as the ratio between measured and reconstructed absorption (respectively with and without packaging; Bricaud et al. 2004). The weight-specific absorption coefficients of the major pigments used in the present reconstruction approach were taken from fig. 1 in Bricaud et al. (2004). As the Q^*_a values estimated in this way sometimes surpassed the theoretically maximum value of 1.0, we included a "missing absorption term" as in Bricaud et al. (2004), where this empirically determined missing absorption (= 0.0525[TChl a]$^{0.855}$) is added to the reconstructed absorption for complete absorption of phytoplankton material in solution. The package effect (= $1 - Q^*_a(675)$) estimated with this approach gave values between 68% and 81% during the bloom periods and lower values outside of these periods (38%–48%). These values are shown along with the previous estimations of packaging (Table 6). All three methods gave roughly similar values, with a coefficient of variation for the mean of the three methods less than 20% for the bloom periods and slightly higher (35%) for the Gulf in May 2000, when packaging was smallest. From these results, there are no obvious reasons to prefer the Gaussian bands or pigment reconstruction approaches to estimate packaging, because the simple ratio approach (column 3 of Table 6, values adjusted for 440 nm), using the updated value of specific absorption of chlorophyll in solution from Johnsen and Sakshaug (2007), gave values generally between the other two approaches.

Relative influence of pigmentation and packaging

Among the factors contributing to the changes in specific phytoplankton absorption, pigment composition was the least important. The maximum contribution of photoprotective pigments mentioned above was around 13%. This compares well with an estimate of the contribution of all pigments other than Chl *a* to the measured absorption at 440 nm using the Gaussian bands approach by determining the difference between measured phytoplankton absorption at 440 nm and the Gaussian peak height of Chl *a* absorption at the same wavelength (Stuart et al. 1998). This contribution was less than 6%–9% during phytoplankton bloom periods and 11%–13% outside these periods (Table 6). These values are slightly lower than those reported by several other studies (Lazzara et al. 1996; Allali et al. 1997; Stuart et al. 1998), but closer to those from coastal waters where microplankton is likely a strong contributor (Lohrenz et al. 2003). As in Lohrenz et al. (2003), the highest contribution of nonphotosynthetic pigments to phytoplankton absorption was in the region where the relative proportion of Chl *b* (green algae) was highest (Gulf, May 2000; Fig. 7*c*). This was also the region where the largest diversity of pigments was found (Fig. 5*c*), as well as the highest fraction of picoplankton and nanoplankton (Table 3), as generally found in oceanic environments (Lazzara et al. 1996; Allali et al. 1997; Stuart et al. 1998).

The packaging effect had a much larger influence than pigment composition on phytoplankton absorption in the St. Lawrence waters. Our estimation varied according to the method used to determine packaging, but a packaging effect at 440 nm of at least 50% was observed during the bloom periods (Table 6). Values were smaller outside these periods, but still relatively high for all three methods (24%–48%; Table 6). Packaging varies mostly with cell size and

© 2008 NRC Canada

intracellular pigment concentration (Morel and Bricaud 1981). Regions where small cells dominate generally show high Q^*_a values (low packaging), although photoacclimation may affect this relationship through changes in intracellular pigment concentration (Bricaud et al. 2004). A bulk size index can be calculated from the fractions of picoplankton, nanoplankton, and microplankton, as described in Bricaud et al. (2004). This bulk size index ($= (1[f_{pico}] + 5[f_{nano}] + 50[f_{micro}])/100$) gave values of 48 μm during the bloom periods and 36 μm in the postbloom period (May 2000) in the Gulf. Because the smallest average size observed (36 μm) is still in the microplankton category, it is thus not surprising to find a large influence of packaging in this environment. Packaging associated with cells of this size range was found to be more than 50% in the extensive data set analyzed by Bricaud et al. (2004). Lohrenz et al. (2003) found a packaging effect of up to 62% in a coastal environment where large phytoplankton dominated.

Our results thus confirm that packaging is the dominant factor responsible for the variation of phytoplankton absorption in the St. Lawrence, as suggested by Babin et al. (1993). They also show that the size structure of local algal populations strongly determines both the packaging effect and phytoplankton absorption (Finkel 2001; Bricaud et al. 2004). Furthermore, phytoplankton absorption during spring varied from year to year in the two adjoining regions of the Estuary and the Gulf of St. Lawrence. This was related primarily to the presence or absence of local phytoplankton blooms. Specific phytoplankton absorption can vary by at least a factor of three in the Gulf and should not be taken as constant. Values in the Estuary seem to be less variable, around 0.026 m^2·(mg TChl a)$^{-1}$ both in previous studies and in the present work, consistent with the generally high algal biomass observed in this region (Fuentes-Yaco et al. 1997). Estimates of Chl a concentration based on bio-optical models will need to take this variability into consideration, as well as the packaging effect, which significantly reduces phytoplankton absorption for a given Chl a concentration. These models will also need to consider the detrital contribution to particulate absorption, particularly high in the upstream regions of the Estuary, near the Saguenay fjord.

Acknowledgements

We thank the captains and crews of the CCG *Martha L. Black*, as well as P. Larouche, the chief scientist, and his scientific crew for their excellent work during the 2000 and 2001 field sampling. We are grateful to D. Blondeau-Patissier and M.-H. Brisson for help with the laboratory analyses and we thank J. Bouchard, A. Silio-Calzada, and I. Laurion for help during the field work. We also acknowledge S. Sathyendranath and V. Stuart for their helpful comments on the manuscript. This work was supported by Natural Sciences and Engineering Research Council of Canada (NSERC) Strategic and Discovery grants, by a team grant from FQRNT (Québec) to S. Roy, and by Fisheries and Oceans Canada (Maurice Lamontagne Institute in Mont-Joli).

References

Allali, K., Bricaud, A., and Claustre, H. 1997. Spatial variations in the chlorophyll-specific absorption coefficients of phytoplankton and photosynthetically active pigments in the equatorial Pacific. J. Geophys. Res. **102**(C6): 12413–12423. doi:10.1029/97JC00380.

Arrigo, K.R., Robinson, D.H., Worthen, D.L., Schieber, B., and Lizotte, M.P. 1998. Bio-optical properties of the southwestern Ross Sea. J. Geophys. Res. **103**(C10): 21683–21695. doi:10.1029/98JC02157.

Babin, M., Therriault, J.-C., Legendre, L., and Condal, A. 1993. Variations in the specific absorption coefficient for natural phytoplankton assemblages: impact on estimates of primary production. Limnol. Oceanogr. **38**: 154–177.

Babin, M., Therriault, J.-C., Legendre, L., Nieke, B., Reuter, R., and Condal, A. 1995. Relationship between the maximum quantum yield of carbon fixation and the minimum quantum yield of chlorophyll *a* in vivo fluorescence in the Gulf of St. Lawrence. Limnol. Oceanogr. **40**: 956–968.

Babin, M., Morel, A., Claustre, H., Bricaud, A., Kolber, Z., and Falkowski, P.G. 1996. Nitrogen- and irradiance-dependent variations of the maximum quantum yield of carbon fixation in eutrophic, mesotrophic and oligotrophic marine systems. Deep Sea Res. Part I Oceanogr. Res. Pap. **43**: 1241–1272. doi:10.1016/0967-0637(96)00058-1.

Behrenfeld, M.J., and Falkowski, P.G. 1997. Photosynthetic rates derived from satellite-based chlorophyll concentration. Limnol. Oceanogr. **42**: 1–20.

Bidigare, R.R., Ondrusek, M.E., Morrow, J.E., and Kiefer, D.A. 1990. In vivo absorption properties of algal pigments. Proc. SPIE, **1302**: 290–302. doi:10.1117/12.21451.

Bricaud, A., and Stramski, D. 1990. Spectral absorption coefficients of living phytoplankton and nonalgal biogenous matter: a comparison between the Peru upwelling area and the Sargasso Sea. Limnol. Oceanogr. **35**: 562–582.

Bricaud, A., Babin, M., Morel, A., and Claustre, H. 1995. Variability in the chlorophyll-specific absorption coefficients of natural phytoplankton: analysis and parameterization. J. Geophys. Res. **100**(C7): 13321–13332. doi:10.1029/95JC00463.

Bricaud, A., Morel, A., Babin, M., Allali, K., and Claustre, H. 1998. Variations of light absorption by suspended particles with chlorophyll *a* concentration in oceanic (case 1) waters: analysis and implications for bio-optical models. J. Geophys. Res. **103**(C13): 31033–31044. doi:10.1029/98JC02712.

Bricaud, A., Claustre, H., Ras, J., and Oubelkheir, K. 2004. Natural variability of phytoplanktonic absorption in oceanic waters: influence of the size structure of algal populations. J. Geophys. Res. **109**(C11010): 1–12. doi:10.1029/2004JC002419.

Bugden, G.L., Hargrave, B.T., Sinclair, M.M., Tang, C.L., Therriault, J.C., and Yeats, P.A. 1982. Freshwater runoff effects in the marine environment: the Gulf of St. Lawrence example. Can. Tech. Rep. Fish. Aquat. Sci. No. 1078.

Bukata, R.P., Jerome, J.H., Kondratyev, K.Y., and Pozdnyakov, D.V. 1995. Optical properties and remote sensing of inland and coastal waters. CRC Press, Boca Raton, Florida.

Ciotti, A.M., Cullen, J.J., and Lewis, M.R. 1999. A semi-analytical model of the influence of phytoplankton community structure on the relationship between light attenuation and ocean colour. J. Geophys. Res. **104**(C1): 1559–1578. doi:10.1029/1998JC900021.

Cleveland, J.S. 1995. Regional models for phytoplankton absorption as a function of chlorophyll concentration. J. Geophys. Res. **100**(C7): 13333–13344. doi:10.1029/95JC00532.

d'Anglejan, B. 1990. Recent sediments and sediment transport processes in the St. Lawrence Estuary. *In* Oceanography of a large-scale estuarine system: the St. Lawrence. *Edited by* M.I. El-Sabh

© 2008 NRC Canada

and N. Silverberg. Coastal and Estuarine Studies, Vol. 39. Springer-Verlag, New York. pp. 109–129.

de Lafontaine, Y., Demers, S., and Runge, J. 1991. Pelagic food web interactions and productivity in the Gulf of St. Lawrence: a perspective. *In* The Gulf of St. Lawrence: small ocean or big estuary? *Edited by* J.-C. Therriault. Can. Spec. Publ. Fish. Aquat. Sci. **113**: 99–123.

Devred, E., Sathyendranath, S., Stuart, V., Maass, H., Ulloa, O., and Platt, T. 2006. A two-component model of phytoplankton absorption in the open ocean: theory and applications. J. Geophys. Res. **111**(C03011): 1–11. doi:10.1029/2005JC002880.

Eisner, L.B., Twardowski, M.S., Cowles, T.J., and Perry, M.J. 2003. Resolving phytoplankton photoprotective:photosynthetic carotenoid ratios on fine scales using in situ spectral absorption measurements. Limnol. Oceanogr. **48**: 632–646.

El-Sabh, M.I. 1988. Physical oceanography of the St. Lawrence estuary. *In* Hydrodynamics of estuaries. Vol. II. Estuarine case studies. *Edited by* B. Kjerfve. CRC Press, Boca Raton, Florida. pp. 61–78.

Finkel, Z.V. 2001. Light absorption and size scaling of light-limited metabolism in marine diatoms. Limnol. Oceanogr. **46**: 86–94.

Fuentes-Yaco, C., Vézina, A.F., Larouche, P., Vigneau, C., Gosselin, M., and Levasseur, M. 1997. Phytoplankton pigment in the Gulf of St. Lawrence, Canada, as determined by the Coastal Zone Colour Scanner — Part I: spatio-temporal variability. Cont. Shelf Res. **17**: 1421–1439. doi:10.1016/S0278-4343(97)00021-6.

Geider, R.J., and Osborne, B.A. 1987. Light absorption by a marine diatom: experimental observations and theoretical calculations of the package effect in a small *Thalassiosira* species. Mar. Biol. (Berl.). **96**: 299–308. doi:10.1007/BF00427030.

Hoepffner, N., and Sathyendranath, S. 1991. Effect of pigment composition on absorption properties of phytoplankton. Mar. Ecol. Prog. Ser. **73**: 11–23. doi:10.3354/meps073011.

Hoepffner, N., and Sathyendranath, S. 1993. Determination of the major groups of phytoplankton pigments from the absorption spectra of total particulate matter. J. Geophys. Res. **98**(C12): 22789–22803. doi:10.1029/93JC01273.

Huot, Y., Babin, M., Bruyant, F., Grob, C., Twardowski, M.S., and Claustre, H. 2007. Relationship between photosynthetic parameters and different proxies of phytoplankton biomass in the subtropical ocean. Biogeosci. **4**: 853–868.

Ingram, R.G., and El-Sabh, M.I. 1990. Fronts and mesoscale features in the St. Lawrence estuary. *In* Oceanography of a large-scale estuarine system: the St. Lawrence. *Edited by* M.I. El-Sabh and N. Silverberg. Coastal and Estuarine Studies, Vol. 39. Springer, New York. pp. 71–93.

International Ocean-Colour Coordinating Group (IOCCG). 2000. Remote sensing of ocean colour in coastal, and other optically-complex, waters. *Edited by* S. Sathyendranath. Reports of the International Ocean-Colour Coordinating Group, No. 3. IOCCG, Dartmouth, Nova Scotia, Canada.

Jeffrey, S.W., Mantoura, R.F.C., and Wright, S.W. 1997. Phytoplankton pigments in oceanography. Monographs on oceanographic methodology, Vol. 10. UNESCO Publishing, Paris, France

Johnsen, G., and Sakshaug, E. 2007. Biooptical characteristics of PSII and PSI in 33 species (13 pigment groups) of marine phytoplankton, and the relevance for pulse-amplitude-modulated and fast-repetition-rate fluorometry. J. Phycol. **43**: 1236–1251. doi:10.1111/j.1529-8817.2007.00422.x.

Johnsen, G., Nelson, N.B., Jovine, R.V.M., and Prézelin, B.B. 1994. Chromoprotein- and pigment-dependent modeling of spectral light absorption in two dinoflagellates, *Prorocentrum minimum* and *Heterocapsa pygmaea*. Mar. Ecol. Prog. Ser. **114**: 245–258. doi:10.3354/meps114245.

Kishino, M., Takahashi, M., Okami, N., and Ichimura, S. 1985. Estimation of the spectral absorption coefficients of phytoplankton in the sea. Bull. Mar. Sci. **37**: 634–642.

Laurion, I., Blouin, F., and Roy, S. 2003. The quantitative filter technique for measuring phytoplankton absorption: interference by MAAs in the UV waveband. Limnol. Oceanogr. Methods, **1**: 1–9.

Lazzara, L., Bricaud, A., and Claustre, H. 1996. Spectral absorption and fluorescence excitation properties of phytoplanktonic populations at a mesotrophic and an oligotrophic site in the tropical North Atlantic (Eumeli program). Deep Sea Res. Part I Oceanogr. Res. Pap. **43**: 1215–1240. doi:10.1016/0967-0637(96)00057-X.

Levasseur, M., Therriault, J.-C., and Legendre, L. 1984. Hierarchical control of phytoplankton succession by physical factors. Mar. Ecol. Prog. Ser. **19**: 211–222. doi:10.3354/meps019211.

Lohrenz, S.E., Weidemann, A.D., and Tuel, M. 2003. Phytoplankton spectral absorption as influenced by community size structure and pigment composition. J. Plankton Res. **25**: 35–61. doi:10.1093/plankt/25.1.35.

Longhurst, A.R., Sathyendranath, S., Platt, T., and Caverhill, C. 1995. An estimate of global primary production in the ocean from satellite radiometer data. J. Plankton Res. **17**: 1245–1271. doi:10.1093/plankt/17.6.1245.

Lutz, V.A., Sathyendranath, S., and Head, E.J.H. 1996. Absorption coefficient of phytoplankton: regional variations in the North Atlantic. Mar. Ecol. Prog. Ser. **135**: 197–213. doi:10.3354/meps135197.

Lutz, V.A., Subramaniam, A., Negri, R.M., Silva, R.I., and Carreto, J.I. 2006. Annual variations in bio-optical properties at the 'Estación Permanente de Estudios Ambientales (EPEA)' coastal station, Argentina. Cont. Shelf Res. **26**: 1093–1112. doi:10.1016/j.csr.2006.02.012.

Marra, J., Trees, C.C., and O'Reilly, J.E. 2007. Phytoplankton pigment absorption: a strong predictor of primary productivity in the surface ocean. Deep Sea Res. Part I Oceanogr. Res. Pap. **54**: 155–163. doi:10.1016/j.dsr.2006.12.001.

Mitchell, B.G., Kahru, M., Wieland, J., and Stramska, M. 2002. Determination of spectral absorption coefficients of particles, dissolved material and phytoplankton for discrete water samples. *In* Ocean optics protocols for satellite ocean color sensor validation. Revision 3. *Edited by* J.L. Mueller and G.S. Fargion. NASA Technical Memorandum, 2002-21004/Rev 3, Vol. 2. NASA Goddard Space Center, Greenbelt, Maryland. pp. 231–257.

Moisan, T.A., and Mitchell, B.G. 2001. UV absorption by mycosporine-like amino acids in *Phaeocystis antarctica* Karsten induced by photosynthetically available radiation. Mar. Biol. (Berl.). **138**: 217–227. doi:10.1007/s002270000424.

Morel, A., and Bricaud, A. 1981. Theoretical results concerning light absorption in a discrete medium, and application to specific absorption of phytoplankton. Deep Sea Res. Part I Oceanogr. Res. Pap. **28A**: 1375–1393. doi:10.1016/0198-0149(81)90039-X.

Nelson, J.R., and Guarda, S. 1995. Particulate and dissolved spectral absorption on the continental shelf of the southeastern United States. J. Geophys. Res. **100**(C5): 8715–8732. doi:10.1029/95JC00222.

Nelson, N.B., Prézelin, B.B., and Bidigare, R.R. 1993. Phytoplankton light absorption and the package effect in California coastal waters. Mar. Ecol. Prog. Ser. **94**: 217–227. doi:10.3354/meps094217.

© 2008 NRC Canada

Roesler, C.S., Perry, M.-J., and Carder, K.L. 1989. Modeling in situ phytoplankton absorption from total absorption spectra in productive inland marine waters. Limnol. Oceanogr. **34**: 1510–1523.

Sathyendranath, S., Lazzara, L., and Prieur, L. 1987. Variations in the spectral values of specific absorption of phytoplankton. Limnol. Oceanogr. **32**: 403–415.

Sathyendranath, S., Watts, L., Devred, E., Platt, T., Caverhill, C., and Maass, H. 2004. Discrimination of diatoms from other phytoplankton using ocean colour data. Mar. Ecol. Prog. Ser. **272**: 59–68. doi:10.3354/meps272059.

Strickland, J.D.H., and Parsons, T.R. 1972. A practical handbook of seawater analysis. 2nd ed. (revised). Bull. Fish. Res. Board Can. No. 167. pp. 1–310.

Stuart, V., Sathyendranath, S., Platt, T., Maass, H., and Irwin, B.D. 1998. Pigments and species composition of natural phytoplankton populations: effect on the absorption spectra. J. Plankton Res. **20**: 187–217. doi:10.1093/plankt/20.2.187.

Therriault, J.-C., and Levasseur, M. 1985. Control of phytoplankton production in the lower St. Lawrence estuary: light and freshwater runoff. Naturaliste Can. **112**: 65–76.

Therriault, J.-C., and Levasseur, M. 1986. Freshwater runoff control of the spatio-temporal distribution of phytoplankton in the lower St. Lawrence estuary (Canada). *In* Proceedings of the NATO Freshwater/Sea Workshop. *Edited by* S. Skreslet. Springler-Verlag, New York. pp. 251–260.

Uitz, J., Claustre, H., Morel, A., and Hooker, S.B. 2006. Vertical distribution of phytoplankton communities in open ocean: an assessment based on surface chlorophyll. J. Geophys. Res. **111**(C08005). doi:10.1029/2005JC003207.

Vézina, A.F., Gratton, Y., and Vinet, P. 1995. Mesoscale physical–biological variability during a summer phytoplankton bloom in the lower St. Lawrence Estuary. Estuar. Coast. Shelf Sci. **41**: 393–411. doi:10.1016/0272-7714(95)90001-2.

Zapata, M., Rodriguez, F., and Garrido, J.L. 2000. Separation of chlorophylls and carotenoids from marine phytoplankton: a new HPLC method using a reversed phase C8 column and pyridine-containing mobile phases. Mar. Ecol. Prog. Ser. **195**: 29–45. doi:10.3354/meps195029.

© 2008 NRC Canada

No indications of Atlantic salmon (*Salmo salar*) shoaling with kin in the Baltic Sea

Stefan Palm, Johan Dannewitz, Torbjörn Järvi, Marja-Liisa Koljonen, Tore Prestegaard, and K. Håkan Olsén

Abstract: Several studies have shown that fish shoals may consist of closely related individuals. It has been found, for example, that released out-migrating salmon smolts tend to aggregate with kin, including when sibling groups have been reared separately. We used genetic microsatellite markers to test whether "shoals" of adult Atlantic salmon (*Salmo salar*) during the marine phase (i.e., aggregations of fish caught in drift nets at offshore feeding areas in the Baltic Sea) consisted of closely related individuals (full-siblings, half-siblings). We found no evidence of kin cohesiveness related to shoals, however. Despite a weak overall tendency for individuals assigned to the same population (river or stock) to occur together, estimates of genetic relatedness in combination with consistent heterozygote deficiencies, and results from mixed-stock analyses and assignment tests collectively indicated that shoals consisted of unrelated fish from multiple populations.

Résumé : Plusieurs études ont montré que les bancs de poissons peuvent être constitués d'individus fortement apparentés. On a trouvé, par exemple, que des saumoneaux libérés lors de la migration vers la mer tendent à se regrouper avec des poissons apparentés, même lorsque des groupes de même fratrie ont été élevés séparément. Nous avons utilisé des marqueurs génétiques microsatellites pour vérifier si des « bancs » de saumons atlantiques (*Salmo salar*) adultes durant leur phase marine (c'est-à-dire des regroupements de poissons capturés dans des filets dérivants dans des sites d'alimentation du large dans la Baltique) consistent en des individus fortement apparentés (de même fratrie, de demi-fratrie). Nous ne trouvons, cependant, aucune indication de cohésion en fonction de la parenté dans les bancs. Malgré une tendance globale faible pour les individus assignés à la même population (rivière ou stock) à se retrouver ensemble, les estimations de parenté génétique, combinées aux déficits constants d'hétérozygotes, ainsi que les résultats des analyses de stocks mixtes et des tests d'assignation indiquent tous ensemble que les bancs sont constitués de poissons non apparentés provenant de multiples populations.

[Traduit par la Rédaction]

Introduction

Shoaling is a common behavior among bony fishes. Formation of shoals is thought to convey advantages such as increased predator protection and reduced aggression and feeding competition (Ward et al. 2003). Laboratory studies have documented that shoals within several species may consist of close relatives (kin), and some such observations also exist from the wild (e.g., Pouyaud et al. 1999; Gerlach et al. 2001; Behrmann-Godel et al. 2006). It has been suggested that kin cohesiveness could increase the inclusive fitness of the shoaling individuals (e.g., Olsén et al. 2004), and in anadromous salmonids, to increase their navigation accuracy to the home stream (Larkin and Walton 1969). The exact mechanism(s) responsible for kin recognition in fish is not known, but several experiments with salmonids have revealed that olfactory cues are used to discriminate between unfamiliar siblings and non-siblings. There are also abilities to discriminate between populations and odors suggested to be part of the home stream "bouquet" (earlier studies reviewed by Olsén 1999).

It has recently been observed that Atlantic salmon (*Salmo salar*) smolts tend to aggregate with kin when migrating towards the sea. By following the downstream movement of marked fish after release in an experimental stream, it was demonstrated that siblings tended to move together also when they had been reared in different tanks (Olsén et al. 2004). Hence, it may appear plausible that kin groups could

Received 27 May 2007. Accepted 25 February 2008. Published on the NRC Research Press Web site at cjfas.nrc.ca on 31 July 2008. J20016

S. Palm.[1] Population Biology, Department of Ecology and Evolution, Evolutionary Biology Centre, Uppsala University, Norbyvägen 18D, SE-752 36 Uppsala, Sweden.
J. Dannewitz. Population Biology, Department of Ecology and Evolution, Evolutionary Biology Centre, Uppsala University, Norbyvägen 18D, SE-752 36 Uppsala, Sweden; Institute of Freshwater Research, National Board of Fisheries, SE-178 93 Drottningholm, Sweden.
T. Järvi. Institute of Freshwater Research, National Board of Fisheries, SE-178 93 Drottningholm, Sweden; Division of Population Genetics, Department of Zoology, Stockholm University, SE-106 91 Stockholm, Sweden.
M.-L. Koljonen. Finnish Game and Fisheries Research Institute, P.O. Box 2, FIN-00791 Helsinki, Finland.
T. Prestegaard. Institute of Freshwater Research, National Board of Fisheries, SE-178 93 Drottningholm, Sweden.
K.H. Olsén. School of Life Sciences, Södertörn University College, SE-141 89 Huddinge, Sweden.

[1]Corresponding author (e-mail: Stefan.Palm@ebc.uu.se).

 doi:10.1139/F08-088 © 2008 NRC Canada

remain aggregated for longer periods during the marine phase. A similar observation was made by Fraser et al. (2005) in a molecular genetic evaluation of adult and subadult migratory brook trout (*Salvelinus fontinalis*) in a Canadian lake, where a major portion of the analyzed shoals was found to contain closely related individuals from the same population.

Traditional tagging studies and more recent genetic work has revealed that local salmon populations from the Baltic Sea area may differ considerably with respect to migration routes and feeding areas in the marine environment (e.g., Carlin 1969; Kallio-Nyberg et al. 1999; Koljonen 2006). Overall, however, knowledge of the behavior of postsmolts in marine waters is sparse, and studying kin cohesiveness in the open sea represents a particular challenge. First, direct detection and sampling of shoals is difficult and typically has to be substituted by indirect measures such as catch data. Second, open sea fisheries typically include a mixture of salmon from multiple populations. Any detailed molecular assessment of individual relationships, therefore, has to be preceded by tests for presence of multiple populations as a basis for a proper statistical analysis.

In this study, we use microsatellite markers to test whether shoals of adult Atlantic salmon caught in the open sea (Baltic Sea) consist of closely related individuals from the same river. We have analyzed samples of salmon closely aggregated in drift nets, possibly representing shoals that were caught at the same time. Access to a comprehensive baseline database with microsatellite genotypes representing 32 Baltic Sea salmon stocks further permitted mixed-stock analyses (MSA), assignment of individuals to populations (stocks or rivers), and assessment of genetic signs of close relatedness. Our results indicate that shoals, as defined herein, do not consist of closely related individuals.

Material and methods

Sampling

Adult salmon were caught using floating gill nets at open sea in the Baltic Sea main basin in October–November 2002 and 2003. The drift nets were set by commercial fishermen about 30–50 nautical miles (1 n.m. = 1.852 km) south-southeast of the Island of Gotland, close to the border between International Council for the Exploration of the Sea (ICES) subdivisions 26 and 28-2. Each "link" in the drift net chains was 600 m long, 7–8 m deep, and with a mesh size of 160 mm. The number of links set per day varied between 13 and 38, corresponding to total net lengths between 7800 and 22 800 m. The nets were left for about 14 h (on average) before being hauled in.

About 2600 salmon were caught during 7 fishing days, and of these, we sampled and analyzed 325 (Table 1). Fin clips for DNA extraction and basic fishery statistics (sex, length, etc.) were taken at sea directly after capture. The reason for not sampling all salmon was that (*i*) many individuals were not classified into a shoal, and (*ii*) the number of fish caught was larger than was considered necessary for the present study (especially in 2003).

Our definition of a shoal was a group of salmon placed closely together in the net (at most 20 m between each fish, usually less) with a minimum distance to the next such

Table 1. Catch and sampling statistics for Atlantic salmon (*Salmo salar*) caught in drift nets in the Baltic Sea main basin in 2 consecutive years.

Year	Date	Position	No. of drift nets	Total no. of fish caught	No. of fish DNA sampled	Total no. of shoals	No. of shoals (of size *n*)					
							n = 2	*n* = 3	*n* = 4	*n* = 5	*n* = 6
2002	30 October	56 26′N, 18 43′E	32	—	32	11	8	2	1	0	0
	31 October	56 23′N, 18 55′E	36	—	34	13	6	6	1	0	0
	1 November	56 11′N, 18 44′E	30	—	11	4	3	0	1	0	0
	Subtotal 2002		98	307	77	28	17	8	3	0	0
2003	5 October	56 13′N, 19 12′E	38	—	63	28	21	7	0	0	0
	6 October	56 04′N, 19 03′E	30	—	121	45	21	18	5	1	0
	7 October	56 00′N, 19 05′E	13	—	24	7	3	1	1	1	1
	8 October	55 59′N, 19 03′E	32	—	40	14	7	4	1	2	0
	Subtotal 2003		113	2300	248	94	52	30	7	4	1
Both years			211	2607	325	122	69	38	10	4	1

Note: Position refers to where the first net in each "chain" was set. Not all salmon caught were included, but the shoals were always sampled completely. Poor DNA quality for a few salmon in 2002 resulted in seven "shoals", with only one fish remaining after genotyping; those individuals have been retained for some of the basic statistical analyses.

© 2008 NRC Canada

group of at least 200 m. In total, we have analyzed 122 shoals with an average size of 2.6 individuals (Table 1). The shoals included were selected independently of size, and they were always sampled completely (i.e., DNA from all fish included was collected).

Testing for nonrandom distributions in drift nets

Our study is based on the assumption that a majority of the shoals are real and not merely random aggregations of individuals. Hence, we evaluated statistically if the number of shoals is larger than would be expected under a null hypothesis of random distribution of fish. To this end, we devised a randomization test where uniform random numbers were used to allocate positions of hypothetical salmon along an artificial drift net (using PopTools; Hood 2006). The total net length and number of simulated salmon were identical to our data in 2002 and 2003 (Table 1). The procedure was repeated 1000 times. After each run, we counted the resulting number of random shoals using the same criteria as applied to our authentic data. Finally, we evaluated whether the real number of shoals was significantly large by comparing it with the simulated distribution (yielding a one-sided P value). Since only a subset of the salmon was sampled, the test is expected to be conservative, especially in 2003 when only about 11% of the caught fish had been classified into shoals.

Microsatellite genotyping

DNA was extracted from ethanol-preserved fin tissue using the Chelex protocol described by Walsh et al. (1991). The following eight polymorphic microsatellite loci were scored: *Ssa289* (McConnell et al. 1995), *Ssa85*, *Ssa197*, *Ssa171*, *Ssa202* (O'Reilly et al. 1996), *StOsl85*, *StOsl311*, and *StOsl417* (Slettan et al. 1995). All loci were coamplified in the same 25 μL polymerase chain reaction (PCR) reaction (multiplex PCR) using Pharmacia Ready-To-Go PCR beads (Amersham Pharmacia Biotech Inc., Piscataway, New Jersey, USA) and approximately 100 ng of template DNA. Primers were end-labeled with fluorescent dyes to enable co-migration of all loci in the same capillary during electrophoresis (i.e., loci labeled with the same dye had nonoverlapping size ranges). Uniform signal intensity among loci was achieved by adjusting primer concentrations. The PCR amplification was initiated with a denaturation step at 94 °C for 5 min, followed by 35 cycles of 30 s at 94 °C, 30 s at an annealing temperature of 53 °C, and 1 min at 72 °C. The process was terminated with a 10 min elongation step at 72 °C. Electrophoresis and size determination of alleles was made on an ABI Prism 310 Genetic Analyzer (Applied Biosystems, Foster City, California, USA) according to the manufacturer's recommendations (www.appliedbiosystems.com).

Baseline data and marker calibration

As baseline for MSA and when assigning individuals to populations, we used microsatellite genotypes for 2368 individuals collected from 32 Atlantic salmon stocks of wild and hatchery origin from rivers around the Baltic Sea (Sweden, Finland, Russia, Estonia, and Latvia), including the most productive ones. The baseline file represents a slightly extended version of the one used by Koljonen (2006) when assessing stock proportions in salmon catches from the Baltic Sea. The data have been collected between 1993 and 2006 within an ongoing joint project coordinated by the Finnish Game and Fisheries Research Institute, and the current average sample size per stock is 74 individuals.

The shoal and baseline samples have been scored for the same set of microsatellite loci but at different laboratories, using different scoring methods and equipments (gel- vs. capillary-based electrophoresis, etc.). The present analysis therefore had to be preceded by a marker calibration. Genotypes were compared for 40 salmon scored both at the Finnish Game and Fisheries Institute and at the Swedish Institute of Freshwater Research (responsible for the present data set). As expected, allele designations (lengths in base pairs) differed systematically at most loci. After having accounted for these differences, only a limited number of conflicting genotype scorings remained (~3%, distributed over five loci and 10 individuals), indicating a reasonable degree of data consistency. The reliability of the genotypic data was further checked by MICRO-CHECKER (van Oosterhout et al. 2004), which tests for potential signs of stuttering, large allele drop-outs, and null alleles.

Statistical genetic analyses

The programs FSTAT (Goudet 1995) and HIERFSTAT (Goudet 2005) were used for estimating F statistics and when testing for genetic differentiation. FSTAT was also used for tests of deviations from Hardy–Weinberg proportions and genotypic equilibrium. All the statistical tests were based on permutations using 10 000 randomizations.

For MSA and subsequent population assignments of individual genotypes, we used the Bayesian-based mixture modeling procedure implemented in BAYES (Pella and Masuda 2001; Masuda 2002). This approach has some important advantages over previous MSA and assignment tests (Koljonen et al. 2007). First, the resulting mixed stock estimates are typically less biased than those from previous (maximum likelihood based) methods. Second, the multilocus genotype distribution in the mixture is taken into account when assigning individuals. This way, an individual is not necessarily assigned to the baseline stock, where its genotype has the overall highest expected frequency (as in classical assignment), but to the stock where it appears most likely after having combined this information with the estimated stock proportions for the mixture. In a recent evaluation of stock composition and assignment methods, Koljonen et al. (2005) demonstrated that Bayesian MSA, when applied to mixed Baltic Sea salmon samples of known population composition, markedly improved both estimates of stock proportions and individual assignments.

BAYES was used to analyze the samples from year 2002 and 2003 separately, as well as in combination. The initial chain length was set to 5000, and when necessary (i.e., if diagnostic tests in the program indicated lack of convergence) additional iterations were run. In each analysis, 32 chains (one per baseline population) were run with prior stock proportions dominated by a single population (84.5%) and the remaining ones set at equally low percentages (0.5%). Contingency tests for independence among shoal and assigned population were performed with an extension of Fisher's ex-

© 2008 NRC Canada

act test for general $r \times c$ tables using StatXact 3.1 (Cytel Software Corporation 1997).

Relatedness

The relatedness coefficient is defined as the fraction of alleles identical by descent shared among individuals. It may be estimated using marker data as the genetic similarity between individuals relative to that between random individuals in some reference population (e.g., Blouin 2003). We assessed relatedness (r) between pairs of individuals (dyads) using the estimator of Wang (2002) as implemented in SPAGeDi (Hardy and Vekemans 2002) and KINGROUP (Konovalov et al. 2004). The Wang estimator was chosen since it exhibited somewhat higher precision and less bias for closely related dyads than alternative ones in computer simulations using the present loci and allele frequencies (not shown). A permutation procedure implemented in KINGROUP was used for testing whether single r estimates were significantly larger than zero.

In a single outbreeding population, r for unrelated dyads is expected to be zero, whereas its expectation increases with the true level of relatedness (0.25 and 0.5 for half- and full-sibs, etc.). In a mixed population sample, however, estimates of relatedness are expected to be biased. The magnitude and direction of this bias is difficult to predict, as it depends on multiple factors, including the number of admixed populations, their relative proportions, the amount of genetic differentiation, and the used r estimator.

The ideal way of accounting for population admixture is to first use an assignment procedure and to then assess relatedness separately for each population. This may be conceivable when the number of populations is small and (or) when the degree of confidence in individual assignments is high (e.g., Fraser et al. 2005). In the present case, a large number of putative populations in combination with a fairly limited number of loci precluded that approach. Hence, we used simulation to assess bias and precision expected for relatedness estimates in the present case, given the results of the MSA. The expected bias was found to be small enough to allow meaningful estimation of average relatedness (within and between shoals) without accounting for stock admixture (Appendix A).

As an alternative to pairwise relatedness, we also used a group-likelihood method that tries to partition individuals into families (half- and full-sib groups) on the basis of their multilocus genotype (COLONY 1.2; Wang 2004). Group approaches have been proven to be quite powerful (e.g., Smith et al. 2001), and the present method has the particular advantage that it also may account for typing errors (e.g., mutations, large allele drop outs, and null alleles) that are expected to have more devastating effects for group relatedness approaches than for pairwise ones. A basic assumption, however, is that the individuals are from a single cohort within a large, randomly mating population (Wang 2004, p.1965). Therefore, before applying the group-likelihood method, simulated data was used to evaluate its performance on a mixed population sample mimicking the present one. We found that the group method was quite powerful in detecting closely related individuals when present, but that population admixture may also result in suggestion of false family groups (Appendix A).

When analyzing our real data with COLONY, we used the total sample (2002 and 2003 combined) and allowed for occurrence of both full- and half-sibs (full-sib families nested within half-sib groups). The effect of three error rates (0, 0.02, and 0.05) was evaluated, always using the same value for both error types included ("dropouts" and "other") across all loci.

Results

Most individuals (68%) were females, as expected for a species with a large proportion of nonmigrating males. No age data have been collected, but the average standard length (66 cm; range 52–95 cm) corresponds to salmon with 1–2 sea years caught in the southern Baltic Sea at this time of the year (L. Karlsson, Swedish Board of Fisheries, Institute of Freshwater Research, SE-814 94 Alvkarleby, Sweden, personal communication, 2007).

The randomization procedure devised for testing whether the number of shoals was larger than expected under a random scenario yielded a significant result ($P = 0.006$) for year 2002; only in six out of 1000 runs was the number of random shoals larger than or equal to the observed number. Further, both the average number of randomized shoaling individuals and the proportion of shoals above minimum size (i.e., $n > 2$) was markedly lower than what was really observed (52 vs. 85 and 10% vs. 34%, respectively). The corresponding test for 2003 was not informative because of lack of power; the low proportion of fish and shoals sampled (reflecting a much higher catch per effort in that year; Table 1) resulted in numbers of randomized shoals that always exceeded the observed one ($P = 1$).

Genetic variation

The number of alleles per locus in the total material varied between 5 and 26 with a mean of 14.8, and the average expected heterozygosity was 0.76 (Table 2). Eight out of 28 pairwise tests for genotypic disequilibrium in the total sample (both years combined) were significant ($P < 0.05$), and four of the significances (including seven out of the eight loci) remained also after sequential Bonferroni correction. With the exception for locus *Ssa289* (see below), the diagnostic routines in MICRO-CHECKER found no indications of potential genotyping problems or null alleles.

Deviations from Hardy–Weinberg expectations

The total material displays an overall heterozygote deficiency; each locus exhibits a positive F_{IS} estimate, and the average across loci is 0.035 and strongly significant (Table 2). Statistically significant heterozygote deficiencies are also present within the 2 sampling years when these are analyzed separately (average F_{IS} is 0.046 and 0.031). A hierarchical analysis of genetic variation between years and shoals (within years) further revealed that a major part of the total heterozygote deficiency exists within shoals and that allele frequency differences between years and shoals are marginal (Table 3). The deviations from Hardy–Weinberg (and genotypic) equilibrium most likely represent a Wahlund effect caused by genetic differences among populations that are admixed.

The heterozygote deficiency at *Ssa289* may appear con-

© 2008 NRC Canada

Table 2. Basic genetic statistics (eight microsatellite loci; data for both years combined, $n = 325$).

Locus	A	H	F_{IS}	Simulated F_{IS} (95% CI)
Ssa171	17	0.62	0.014	0.006 (–0.045; 0.059)
Ssa197	19	0.90	0.020	0.020 (–0.015; 0.059)
Ssa202	9	0.67	0.036	0.042 (–0.015; 0.107)
Ssa289	5	0.62	0.103**	0.063 (–0.013; 0.136)
Ssa85	15	0.81	0.027	0.025 (–0.025; 0.073)
SsOsl311	26	0.88	0.025	0.053 (0.013; 0.095)
SsOsl417	14	0.84	0.019	0.048 (0.000; 0.098)
SsOsl85	13	0.77	0.053*	0.038 (–0.016; 0.092)
All loci	14.8	0.76	0.035***	0.037 (0.019; 0.056)
All (without *Ssa289*)			0.028**	

Note: A, number of alleles; H, expected heterozygosity; F_{IS} quantifies the deviation from Hardy–Weinberg proportions; simulated F_{IS} estimates were obtained through resampling of baseline genotypes from a population admixture mimicking the present one (see Appendix B for details); CI, confidence interval; *, $P < 0.05$; **, $P < 0.01$; ***, $P < 0.001$.

Table 3. Hierarchical F statistics for Atlantic salmon (*Salmo salar*) shoals sampled at open sea in 2 consecutive years.

Locus	$F_{Year/Total}$	$F_{Shoals/Year}$	$F_{Individuals/Shoal}$	$F_{Individuals/Total}$
Ssa171	–0.002	–0.013	0.028	0.012
Ssa197	0.001	0.011	0.009	0.021
Ssa202	0.006	0.009	0.031	0.045
Ssa289	0.003*	0.011	0.092**	0.104**
Ssa85	0.000	0.006	0.021	0.027
SsOsl311	0.004	–0.003	0.026	0.027
SsOsl417	0.001	0.001	0.018	0.020
SsOsl85	0.007*	0.025	0.031	0.061*
All loci	0.002*	0.006	0.030**	0.038***
All (without *Ssa289*)	0.002*	0.006	0.023*	0.030***

Note: *, $P < 0.05$; **, $P < 0.01$; ***, $P < 0.001$.

spicuously large when compared with the other loci (Tables 2 and 3), and MICRO-CHECKER suggested that the general excess of homozygotes for most allele size classes at this locus could reflect presence of null alleles. We have reasons to believe, however, that it rather represents a particularly pronounced Wahlund effect caused by random sampling error in combination with comparably large genetic differentiation at this locus among the populations admixed in our samples (Table 2; Appendix B).

MSA and individual assignments

The resulting estimates from the Bayesian mixture analyses are presented in Table 4. About the same stocks from the northernmost Baltic Sea (Bothnian Bay) predominate in both 2002 and 2003, although some temporal differences among years exist (see, e.g., Kalixälven; Table 4). As a side issue, we note that a majority of the fish is estimated to be of wild, naturally propagated origin. These results are similar to those of Koljonen (2006), who also observed a dominance of wild northern stocks when analyzing drift net samples collected during 2002–2004 in the southern Baltic Sea main basin.

In most cases, the population origin of single individuals could not be unambiguously resolved. Assignment of genotypes to the baseline populations yielded an average maximum assignment probability per individual ($P_{i[Max]}$) of only 66% (range 19%–100%). Nevertheless, it seems clear that fish from multiple populations occur admixed within shoals. As much as 98 of the 122 shoals contained individuals assigned to different populations. When restricting the analysis to individuals assigned with a relatively high degree of confidence ($P_{i[Max]} > 0.7$), all 29 remaining shoals included individuals from more than one population. Using an even more stringent criteria ($P_{i[Max]} > 0.9$) did not change the proportion of shoals with individuals assigned to different populations (the remaining seven shoals were all admixed).

Still, we found an overall tendency for individuals assigned to the same population to occur together within shoals. An exact contingency test for independence between shoal and stock was significant for year 2003 (df = 1196; $P = 0.0132$), whereas no significance was obtained for the considerably smaller table of 2002 (df = 286; $P = 0.731$). The contingency tests were performed using all fish (no restriction on $P_{i[Max]}$), indicating that an unknown proportion of misclassified individuals may have reduced the statistical power somewhat. On the other hand, restricting the analysis to those individuals with high assignment probabilities may also result in decreased power due to a reduced table size.

© 2008 NRC Canada

Table 4. Mixed stock proportions for Atlantic salmon (*Salmo salar*) from the southern Baltic Sea in 2002 and 2003.

		Mixture proportion (95% probability interval)		
Stock (country code)	Main propagation	2002 (n = 77)	2003 (n = 248)	Both years (n = 325)
Tornionjoki wild (FI,SE)	Wild	0.35 (0.20; 0.49)	0.39 (0.24; 0.54)	0.38 (0.26; 0.50)
Kalixälven (SE)	Wild	0 (0; 0.14)	0.24 (0.11; 0.39)	0.19 (0.08; 0.30)
Iijoki (FI)	Hatchery	0.09 (0.03; 0.19)	0.09 (0.04; 0.17)	0.09 (0.05; 0.16)
Luleälven (SE)	Hatchery	0.18 (0.07; 0.30)	0.03 (0; 0.10)	0.09 (0.04; 0.14)
Vindelälven (SE)	Wild	0.04 (0; 0.12)	0.05 (0.02; 0.09)	0.05 (0.02; 0.08)
Tornionjoki H (FI)	Hatchery	0 (0; 0.11)	0.04 (0; 0.11)	0.03 (0; 0.09)
Byskeälven (SE)	Wild	0.11 (0.03; 0.23)	0 (0; 0.02)	0.03 (0; 0.06)
Ångermanälven (SE)	Hatchery	0 (0; 0.05)	0.04 (0; 0.10)	0.02 (0; 0.05)
Skellefteälven (SE)	Hatchery	0 (0; 0.04)	0.02 (0; 0.05)	0.02 (0; 0.04)
Oulujoki (FI)	Hatchery	0 (0; 0.02)	0.02 (0; 0.04)	0.02 (0; 0.04)
Ljusnan (SE)	Hatchery	0 (0; 0.02)	0.02 (0; 0.06)	0.02 (0; 0.05)
Simojoki (FI)	Wild	0.01 (0; 0.06)	0.01 (0; 0.04)	0.01 (0; 0.04)
Gauja (LV)	Hatchery	0.02 (0; 0.08)	0.01 (0; 0.02)	0.01 (0; 0.03)
Neva-Fi (RU)	Hatchery	0.04 (0.01; 0.10)	0 (0; 0.02)	0.01 (0; 0.03)
Åbyälven (SE)	Wild	0.02 (0; 0.12)	0 (0; 0.03)	0 (0; 0.05)
Ljungan (SE)	Wild	0 (0; 0.08)	0 (0; 0.01)	0 (0; 0.03)
Dalälven (SE)	Hatchery	0 (0; 0.04)	0 (0; 0.03)	0 (0; 0.02)
Råneälven (SE)	Wild	0.02 (0; 0.08)	0	0 (0; 0.02)
Indalsälven (SE)	Hatchery	0 (0; 0.01)	0 (0; 0.03)	0 (0; 0.01)
Lögdeälven (SE)	Wild	0 (0; 0.01)	0 (0; 0.01)	0 (0; 0.01)
Venta (LV)	Wild	0 (0; 0.04)	0	0 (0; 0.01)
Öreälven (SE)	Wild	0 (0; 0.01)	0	0 (0; 0.01)
Daugava (LV)	Hatchery	0 (0; 0.06)	0	0
Emån (SE)	Wild	0 (0; 0.01)	0	0
Luga (RU)	Wild	0 (0; 0.01)	0	0
Mörrumsån (SE)	Wild	0	0	0
Narva (EE,RU)	Hatchery	0 (0; 0.01)	0	0
Neva-Rus (RU)	Hatchery	0	0	0
Keila (EE)	Wild	0	0	0
Kunda (EE)	Wild	0	0	0
Pärnu (EE)	Wild	0	0	0
Umeälven (SE)	Hatchery	0 (0; 0.01)	0 (0; 0.01)	0

Note: The estimates (median with 95% probability interval) were obtained using the Bayesian method implemented in BAYES (Pella and Masuda 2001). The baseline file represented an extended version of the one in Koljonen (2006). Country codes: Estonia, EE; Finland, FI; Latvia, LV; Russia, RU; and Sweden, SE.

Table 5. Estimates of average pairwise relatedness (r ± standard deviation (SD); Wang 2002) within and between Baltic Sea salmon shoals.

	No. of pairwise comparisons (dyads)	Average r ± SD (range)	No. of significances
Within shoals	298	0.002±0.18 (–0.42; 0.57)	20 (6.7%)
Between shoals	52 352	–0.009±0.19 (–0.48; 0.81)	2 924 (5.6%)

Note: Number of significances refers to dyads with an r estimate significantly larger than zero (P < 0.05; one-sided permutation test).

Relatedness

Estimates of pairwise relatedness in the total sample (2002 and 2003) provided no evidence for kin cohesiveness. Average relatedness within shoals was close to zero and almost identical to that for dyads representing different shoals (Table 5). Corresponding analyses for 2002 and 2003 (samples analyzed separately) also gave estimates of average r within and between shoals that were very close to zero (not shown). No more than 6.7% (20 of 298) of the single r values for dyads within shoals in Table 5 were significantly larger than zero at the 5% level, and only in 4 of these 20 significant cases had both individuals been assigned to the same population. Likewise, when computing average r within each of the 122 shoals, these values varied symmetrically around zero (range –0.42 to 0.43). We could see no trend of larger shoals to have higher and more significant r values, as could be anticipated when analyzing a mix of real and false–random shoals (where a majority of the latter ones are expected to be small).

The group-likelihood analyses with COLONY, on the other hand, suggested presence of closely related individuals in our material (Table 6). The number of the suggested fam-

© 2008 NRC Canada

Table 6. Results from group-likelihood analyses (Wang 2004) at three typing error rates.

Error rate	No. of half-sib groups	No. of full-sib families	No. of pairwise comparisons (dyads)		
			Unrelated	Half-sibs	Full-sibs
0	62	217	51 796 (98.4%)	725 (1.4%)	129 (0.2%)
0.02	52	196	51 633 (98.1%)	850 (1.6%)	167 (0.3%)
0.05	41	162	51 306 (97.4%)	1 086 (2.1%)	258 (0.5%)

Note: The total sample (n = 325) was analyzed. Displayed for each error rate are the proposed numbers of half- and full-sib families and the corresponding number of dyads.

ily groups varied somewhat depending on the assumed error rate, and the average size of the full-sib families and half-sib groups was ~1–2 and 5–8 individuals, respectively.

We could see no tendency for the family groups proposed to occur together within shoals, however. When focusing on the result for the intermediate error rate (0.02), for example, exact contingency tests (tables with shoals × half- and full-sib groups, respectively) were nonsignificant ($P > 0.3$). In contrast, individuals previously assigned to the same population had often been grouped together by COLONY (exact P values < 0.001). Since our simulations (Appendix A) revealed an obvious risk for unrelated individuals from the same population to be erroneously grouped into families, it is unclear to what extent true family groups actually exist in our data. A more detailed examination of this matter is beyond the scope of the present study.

Discussion

This investigation was prompted by a previous observation that Atlantic salmon smolts tend to aggregate with kin when migrating towards the sea (Olsén et al. 2004), suggesting that groups of closely related individuals could possibly remain aggregated during the marine phase. Our results demonstrate, however, that shoals of adult salmon in the open Baltic Sea do not consist of kin. Rather, consistent heterozygote deficiencies in combination with low estimates of relatedness and individual assignments collectively indicate that shoals herein consist of largely unrelated fish from multiple populations (stocks or rivers). The tendency in year 2003 for fish assigned to the same population to occur together (significant contingency test) is interesting, but may rather reflect some overall spatial affinity in the sea by fish from the same river, leading to being caught in the same part of a drift net (and shoal) more often than expected under a completely random scenario.

Assumptions

Our analysis is based on the basic assumption that salmon placed closely together in the drift nets do represent shoals (i.e., cohesive groups of salmon that actively have moved together), rather than random aggregations of individuals. The significant randomization test for the sample from 2002 yields indirect support for this assumption. Still, it is a fact that we have not observed shoaling or any of our analyzed shoals directly (before capture), and other explanations for the observed clustering of small groups of salmon in the drift nets can not be dismissed. Such alternatives include the grouping of individuals that in fact were moving in different directions but that intersected at the same place (the "direction" of the fish in the nets turned out to be hard to record in practice), and also the fact that salmon may follow distinct routes or "common corridors" at sea (cf. Lacroix et al. 2005), which could explain clustering without shoaling.

Formation of shoals is nevertheless well documented for many salmonids, particularly in freshwater habitats. It is a common observation, for example, that juveniles of anadromous species tend to aggregate when migrating towards the sea (Hoar 1976; Groot and Margolis 1991; Olsén et al. 2004). In contrast, likely because of practical constraints, much less is known about shoaling of adult fish at open sea. Still, it seems to be a common opinion among researchers as well as sport and commercial fishermen that anadromous salmonids often appear aggregated during feeding migrations in the sea; however, it is hard to find published results that directly confirm that belief. Jákupsstovu et al. (1985) did evaluate statistically whether Atlantic salmon caught using longline haulbacks outside the Faroe Islands were distributed nonrandomly on the lines, which indirectly could reflect shoaling; only in 3 out of 11 analyzed sets did the observed distribution of salmon deviate significantly from its random expectation. Likewise, no large shoals were detected in recent trawling surveys of Atlantic salmon postsmolts outside the North American east coast (Lacroix and Knox 2005).

With respect to other salmonid species, a review by Takagi et al. (1981; cited by Groot and Margolis 1991, p. 186) of offshore echogram images and gillnet samples of pink salmon (*Oncorhynchus gorbuscha*) from the North Pacific Ocean suggested existence of small cohesive groups (a few tens of individuals or less, often pairs) that possibly could represent shoals. Some data from recaptured coded-wire tags also provide indirect evidence for shoaling. Potter (1985, cited by Elliott 1994, p.20) found that marked postsmolts of sea-run brown trout (*Salmo trutta*) tended to aggregate in the sea with individuals from the same English river. Similarly, McKinnell et al. (1997) identified several cases with recaptured steelhead (sea-run rainbow trout, *Oncorhynchus mykiss*), released at the same place and time, which were recovered simultaneously up to 3 years later in the North Pacific. In conclusion, these findings obtained using different indirect approaches indicate that shoaling of salmonids at open sea exists, albeit in a less structured and more loosely organized manner than in lakes and rivers.

It is often stressed (e.g., Fraser et al. 2005) that precise estimates of pairwise relatedness typically requires a large number of hypervariable loci, say, around 20 microsatellites or even more. Even though this may be true when it comes to accurately estimating relatedness for single dyads, we feel pretty confident that access to a larger number of loci in the

© 2008 NRC Canada

present study would not have changed our general conclusion. It is quite possible that a few kin dyads may have remained undetected in our analysis owing to lack of power. Our simulation of bias and precision for r (Appendix A) indicated, however, that a significant proportion of kin within shoals would have resulted in a detectable signal (i.e., average r within shoals would have been larger than zero). If anything, the present approach to estimate relatedness without accounting for population admixture should yield somewhat elevated r values for close relatives.

Comparisons with previous studies

Other studies of relatedness in marine fish species have focused on issues such as reproductive success and family relationships within cohorts (e.g., Herbinger et al. 1997; Planes and Lenfant 2002; Selkoe et al. 2006), and to our knowledge this is the first analysis of a putative relationship among individual relatedness and shoaling at open sea. Previous results on shoaling in relation to kin in freshwater species are contradictory, ranging from indications of strong such relationships in studies of blackchin tilapia (*Sarotherodon melanotheron*) and Eurasian perch (*Perca fluviatilis*) (Pouyaud et al. 1999; Gerlach et al. 2001), to lack of any detectable association in threespine sticklebacks (*Gasterosteus aculeatus*) and guppies (*Poecilia reticulata*) (Peuhkuri and Seppa 1998; Russell et al. 2004). Multiple ecological, evolutionary, and methodological factors may probably explain the pronounced variation among studies, and further work appears warranted before any general patterns may become apparent.

A number of reasons may lie behind the apparent lack of kin cohesiveness in the present study. Since the analyzed salmon left their natal rivers as out-migrating smolt, they have spent about 1–2 years in the sea. During this period they have experienced substantial mortality, traveled long distances, and come across fish from other populations. All of these factors are anticipated to gradually reduce the size of shoals and to dissolve existing kin associations.

Nonetheless, in their study of adult and subadult brook trout in a Canadian lake, Fraser et al. (2005) found a significant proportion of kin within shoals. We can only speculate about reasons for the discrepancy among that and the current result, but beside potential species differences, it appears likely that the large dissimilarities with respect to migration distances (lake vs. the Baltic Sea) and the numbers of populations that may be admixed could play major roles. A higher mortality rate in the Baltic Sea, where the fishing pressure is considerable, may also be part of the explanation. A further possibility is that shoaling with relatives is not obligatory during feeding migrations in the marine environment, but is, as suggested by Larkin and Walton (1969), of importance primarily when navigating back to the home river. Finally, it remains to be investigated to what extent shoals of adult salmon in the sea are temporally stable or if shoaling merely represents a recurrent behavioral phenomenon that, for example, is associated with increased feeding activity (cf. Foster et al. 2001). If so, this could well be a main explanation for the apparent lack of kin cohesiveness in the present study.

Acknowledgements

We thank two anonymous reviewers and the associate editor Michael Hansen for comments on an earlier version of the manuscript. Bengt-Åke Jansson is acknowledged for assistance with the fieldwork. Financial support was provided by a grant to KHO from The Swedish Research Council for Environment, Agricultural Sciences and Spatial Planning (FORMAS; contract 22.3/2001-1905) and by a postdoctoral scholarship to SP from the Sven and Lilly Lawski foundation.

References

Behrmann-Godel, J., Gerlach, G., and Eckmann, R. 2006. Kin and population recognition in sympatric Lake Constance perch (*Perca fluviatilis* L.): can assortative shoaling drive population divergence? Behav. Ecol. Sociobiol. **59**: 461–468. doi:10.1007/s00265-005-0070-3.

Blouin, M.S. 2003. DNA-based methods for pedigree reconstruction and kinship analysis in natural populations. Trends Ecol. Evol. **18**: 503–511. doi:10.1016/S0169-5347(03)00225-8.

Carlin, B. 1969. Salmon conservation in Sweden, salmon tagging experiments, the migration of salmon. Series of lectures. The Atlantic Salmon Association, Montréal, Que.

CYTEL Software Corporation. 1997. StatXact 3.1: statistical software for exact nonparametric inference. CYTEL Software Corporation, Cambridge, Mass., USA.

Elliott, J.M. 1994. Quantitative ecology and the brown trout. Oxford University Press, Oxford, UK.

Foster, E.G., Ritz, D.A., Osborn, J.E., and Swadling, K.M. 2001. Schooling affects the feeding success of Australian salmon (*Arripis trutta*) when preying on mysid swarms (*Paramesopodopsis rufa*). J. Exp. Mar. Biol. Ecol. **261**: 93–106. doi:10.1016/S0022-0981(01)00265-9. PMID:11438107.

Fraser, D.J., Duchesne, P., and Bernatchez, L. 2005. Migratory charr schools exhibit population and kin associations beyond juvenile stages. Mol. Ecol. **14**: 3133–3146. doi:10.1111/j.1365-294X.2005.02657.x. PMID:16101779.

Gerlach, G., Schardt, U., Eckmann, R., and Meyer, A. 2001. Kin-structured subpopulations in Eurasian perch (*Perca fluviatilis* L.). Heredity, **86**: 213–221. doi:10.1046/j.1365-2540.2001.00825.x. PMID:11380667.

Goudet, J. 1995. FSTAT (Version 1.2): a computer program to calculate F-statistics. J. Hered. **86**: 485–486.

Goudet, J. 2005. HIERFSTAT, a package for R to compute and test hierarchical F-statistics. Mol. Ecol. Notes, **5**: 184–186. doi:10.1111/j.1471-8286.2004.00828.x.

Groot, C., and Margolis, L. 1991. Pacific salmon life histories. UBC Press, Vancouver, B.C.

Hardy, O.J., and Vekemans, X. 2002. SPAGeDi: a versatile computer program to analyse spatial genetic structure at the individual or population levels. Mol. Ecol. Notes, **2**: 618–620. doi:10.1046/j.1471-8286.2002.00305.x.

Herbinger, C.M., Doyle, R.W., Taggart, C.T., Lochmann, S.E., Brooker, A.L., Wright, J.M., and Cook, D. 1997. Family relationships and effective population size in a natural cohort of Atlantic cod (*Gadus morhua*) larvae. Can. J. Fish. Aquat. Sci. **54**(Suppl. 1): 11–18. doi:10.1139/cjfas-54-S1-11.

Hoar, W.S. 1976. Smolt transformation: evolution behaviour and physiology. J. Fish. Res. Board Can. **33**: 1234–1252.

Hood, G.M. 2006. PopTools version 2.7.5 [online]. Available from www.cse.csiro.au/poptools [accessed 24 May 2007].

Jákupsstovu, S.H.Í., Jorgensen, P.T., Mouritsen, R., and Nicolajsen, Á. 1985. Biological data and preliminary observations on the spatial distribution of salmon within the Faroese fishing zone in February 1985. International Council for the Exploration of the Sea, C.M.1985/M:30.

© 2008 NRC Canada

Kallio-Nyberg, I., Pelkonen, H., and Rita, H. 1999. Effects of stock-specific and environmental factors on the feeding migration of Atlantic salmon (*Salmo salar*) in the Baltic Sea. Can. J. Fish. Aquat. Sci. **56**: 853–861. doi:10.1139/cjfas-56-5-853.

Koljonen, M.-L. 2006. Annual changes in the proportions of wild and hatchery Atlantic salmon (*Salmo salar*) caught in the Baltic Sea. ICES J. Mar. Sci. **63**: 1274–1285. doi:10.1016/j.icesjms.2006.04.010.

Koljonen, M.-L., Pella, J.J., and Masuda, M. 2005. Classical individual assignments versus mixture modeling to estimate stock proportions in Atlantic salmon (*Salmo salar*) catches from DNA microsatellite data. Can. J. Fish. Aquat. Sci. **62**: 2143–2158. doi:10.1139/f05-128.

Koljonen, M.-L., King, T., and Nielsen, E. 2007. Genetic identification of populations and individuals. *In* The Atlantic salmon: genetics, conservation and management. *Edited by* E. Verspoor, L. Stradmeyer, and J. Nielsen. Blackwell Publishing, Oxford, UK. pp. 270–298.

Konovalov, D.A., Manning, C., and Henshaw, M.T. 2004. KINGROUP: a program for pedigree relationship reconstruction and kin group assignments using genetic markers. Mol. Ecol. Notes, **4**: 779–782. doi:10.1111/j.1471-8286.2004.00796.x.

Lacroix, G.L., and Knox, D. 2005. Distribution of Atlantic salmon (*Salmo salar*) postsmolts of different origins in the Bay of Fundy and Gulf of Maine and evaluation of factors affecting migration, growth, and survival. Can. J. Fish. Aquat. Sci. **62**: 1363–1376. doi:10.1139/f05-055.

Lacroix, G.L., Knox, D., and Stokesbury, M.J.W. 2005. Survival and behaviour of post-smolt Atlantic salmon in coastal habitat with extreme tides. J. Fish Biol. **66**: 485–498. doi:10.1111/j.0022-1112.2005.00616.x.

Larkin, A., and Walton, A. 1969. Fish school size and migration. J. Fish. Res. Board Can. **26**: 1372–1374.

Masuda, M. 2002. User's manual for BAYES: Bayesian stock-mixture analysis program. National Marine Fisheries Service, Alaska Fisheries Science Center, Auke Bay Laboratory, Juneau, Alaska.

McConnell, S.K., O'Reilly, P., Hamilton, L., Wright, J.N., and Bentzen, P. 1995. Polymorphic microsatellite loci from Atlantic salmon (*Salmo salar*): genetic differentiation of North American and European populations. Can. J. Fish. Aquat. Sci. **52**: 1863–1872. doi:10.1139/f95-779.

McKinnell, S., Pella, J.J., and Dahlberg, M.L. 1997. Population-specific aggregations of steelhead trout (*Oncorhynchus mykiss*) in the North Pacific Ocean. Can. J. Fish. Aquat. Sci. **54**: 2368–2376. doi:10.1139/cjfas-54-10-2368.

Olsén, H. 1999. Present knowledge of kin discrimination in salmonids. Genetica, **104**: 295–299. doi:10.1023/A:1026413404363.

Olsén, K.H., Petersson, E., Ragnarsson, B., Lundqvist, H., and Järvi, T. 2004. Downstream migration in Atlantic salmon (*Salmo salar*) smolt sibling groups. Can. J. Fish. Aquat. Sci. **61**: 328–331. doi:10.1139/f04-067.

O'Reilly, P.T., Hamilton, L.C., McConnell, S.K., and Wright, J.M. 1996. Rapid analysis of genetic variation in Atlantic salmon (*Salmo salar*) by PCR multiplexing of dinucleotide and tetranucleotide microsatellites. Can. J. Fish. Aquat. Sci. **53**: 2292–2298. doi:10.1139/cjfas-53-10-2292.

Pella, J., and Masuda, M. 2001. Bayesian methods for analysis of stock mixtures from genetic characters. Fish. Bull. (Washington, D.C.), **99**: 151–167.

Peuhkuri, N., and Seppa, P. 1998. Do three-spined sticklebacks group with kin? Ann. Zool. Fenn. **35**: 21–27.

Planes, S., and Lenfant, P. 2002. Temporal change in the genetic structure between and within cohorts of a marine fish, *Diplodus sargus*, induced by a large variance in individual reproductive success. Mol. Ecol. **11**: 1515–1524. doi:10.1046/j.1365-294X.2002.01521.x. PMID:12144670.

Potter, E.C.E. 1985. Growth and survival of sea trout (*Salmo trutta* L.) in the sea. Proceedings of the 4th British Freshwater Fish Conference, Liverpool, University of Liverpool, Liverpool, UK. pp. 91–98.

Pouyaud, L., Desmarais, E., Chenuil, A., Agnese, T.F., and Bonhomme, F. 1999. Kin cohesiveness and possible inbreeding in the mouthbrooding tilapia *Sarotherodon melanotheron* (Pisces Cichlidae). Mol. Ecol. **8**: 803–812. doi:10.1046/j.1365-294X.1999.00632.x.

Russell, S.T., Kelley, J.L., Graves, J.A., and Magurran, A.E. 2004. Kin structure and shoal composition dynamics in the guppy, *Poecilia reticulata*. Oikos, **106**: 520–526. doi:10.1111/j.0030-1299.2004.12847.x.

Selkoe, K.A., Gaines, S.D., Caselle, J.E., and Warner, R.R. 2006. Current shifts and kin aggregation explain genetic patchiness in fish recruits. Ecology, **87**: 3082–3094. doi:10.1890/0012-9658(2006)87[3082:CSAKAE]2.0.CO;2. PMID:17249233.

Slettan, A., Olsaker, I., and Lie, O. 1995. Atlantic salmon, *Salmo salar*, microsatellites at the SsOsl25, SsOsl85, SsOsl311, SsOsl417 loci. Anim. Genet. **26**: 281–282. PMID:7661406.

Smith, B.R., Herbinger, C.M., and Merry, H.R. 2001. Accurate partition of individuals into full-sib families from genetic data without parental information. Genetics, **158**: 1329–1338. PMID:11454779.

Takagi, K., Ito, K.V., Hartt, A.G., and Dell, M.B. 1981. Distribution and origin of pink salmon (*Oncorhynchus gorbuscha*) in offshore waters of the North Pacific Ocean. Int. North Pac. Fish. Comm. Bull. **40**: 1–195.

van Oosterhout, C., Hutchinson, W.F., Wills, D.P.M., and Shipley, P. 2004. MICRO-CHECKER: software for identifying and correcting genotyping errors in microsatellite data. Mol. Ecol. Notes, **4**: 535–538. doi:10.1111/j.1471-8286.2004.00684.x.

Walsh, P.S., Metzger, D.A., and Higuchi, R. 1991. Chelex-100 as a medium for simple extraction of DNA for PCR-based typing from forensic material. Biotechniques, **10**: 506–513. PMID:1867860.

Wang, J.L. 2002. An estimator for pairwise relatedness using molecular markers. Genetics, **160**: 1203–1215. PMID:11901134.

Wang, J.L. 2004. Sibship reconstruction from genetic data with typing errors. Genetics, **166**: 1963–1979. doi:10.1534/genetics.166.4.1963. PMID:15126412.

Ward, A.J.W., Axford, S., and Krause, J. 2003. Cross-species familiarity in shoaling fishes. Proc. R. Soc. Biol. Sci. Ser. B, **270**: 1157–1161. doi:10.1098/rspb.2003.2337.

Appendix A

Simulated data was used for assessing bias and precision for pairwise and group-likelihood relatedness estimates for the present population admixture.

Pairwise approach

We used KINGROUP to generate 1000 multilocus genotypes (our eight microsatellite loci) of known population origin and individual relatedness. The simulated individuals represented the five baseline stocks that according to our mixture analyses are most common in our data (stocks with median proportions ranging from 0.376 to 0.047; Table 4).

© 2008 NRC Canada

Table A1. Pairwise relatedness (r; Wang 2002) in a simulated population mixture with stock proportions mimicking those observed empirically.

		Simulated r values				
Relatedness	Population	No. of dyads	Average (SD)	Expectancy	Bias	Prop. significant r values ($P < 0.05$)
Unrelated (between populations)	—	332 500	–0.05 (0.19)	0	–0.05	0.036
Unrelated (within populations)	Tornionjoki wild	100 000	0.03 (0.20)	0	0.03	
	Kalixälven	25 000	0.03 (0.21)	0	0.03	
	Iijoki	4 000	0.12 (0.20)	0	0.12	
	Luleälven	4 000	–0.02 (0.21)	0	–0.02	
	Vindelälven	1 000	0.13 (0.21)	0	0.13	
	Total	134 000	0.03 (0.21)	0	0.03	0.112
Half-sibs	Tornionjoki wild	20 000	0.27 (0.18)	0.25	0.02	
	Kalixälven	5 000	0.22 (0.18)	0.25	–0.03	
	Iijoki	800	0.29 (0.17)	0.25	0.04	
	Luleälven	800	0.22 (0.19)	0.25	–0.03	
	Vindelälven	200	0.35 (0.20)	0.25	0.10	
	Total	26 800	0.26 (0.18)	0.25	0.01	0.425
Full-sibs	Tornionjoki wild	4 750	0.52 (0.19)	0.5	0.00	
	Kalixälven	1 125	0.48 (0.18)	0.5	–0.02	
	Iijoki	150	0.53 (0.18)	0.5	0.03	
	Luleälven	150	0.46 (0.20)	0.5	–0.04	
	Vindelälven	25	0.56 (0.17)	0.5	0.06	
	Total	6 200	0.51 (0.19)	0.5	0.01	0.860

Note: Expectancy refers to expected r in a single outbreeding population. The proportion of significant r values (i.e., larger than zero) was determined using a permuted reference distribution. SD, standard deviation.

On the basis of population-specific allele frequency distributions, a nested mating design was used when simulating full-sibs, half-sibs, and unrelated individuals. For each of the included populations, five "sires" were mated with five unique "dames", resulting in a total of 25 full-sib groups that in turn were related as half-sibs "within" each sire. Further, to obtain relative mixture proportions mimicking (roughly) those really observed, we let the number of offspring per family vary from 20 (Tornionjoki wild) to 2 (Vindelälven).

In a next step, r was estimated between the simulated genotypes, resulting in a total of 499 500 pairwise comparisons, whereof 6200, 26 800, and 466 500 represented full-sibs, half-sibs, and unrelated (within and between populations), respectively. Bias was assessed by comparing the means for the simulated r values with those expected in a single outbreeding population, whereas the standard deviations yielded information on precision. All r estimators included in the program SPAGeDi were evaluated, but we restrict the presentation to the estimator by Wang (2002) that was found to display somewhat less bias and higher precision for full- and half-sib dyads (not shown).

The simulation results for r are presented in Table A1. Average bias at different levels of relatedness was relatively minor (between –0.05 and +0.03), between 4 and 20 times smaller than the standard deviation.

Group-likelihood approach

We similarly evaluated the efficiency and bias of the group method implemented in COLONY (Wang 2004) when violating the basic assumption of having data from a single population and cohort. First, we analyzed the same simulated data set as above (i.e. 1000 genotypes representing half- and full-sibs from five populations). For comparison, we also included a second simulated sample of the same size that only contained unrelated genotypes (in the same population proportions as before). In both cases we assumed no genotyping errors (correct for our simulated data) and allowed the program to search for both full-sib families and half-sib groups.

The analysis of simulated half- and full-sib families worked well despite population admixture. In total, the number of full- and half-sib dyads proposed was close to the true numbers (Table A2). Moreover, COLONY suggested a total of 126 full-sib families (true number 125). Of these, 112 were 100% correctly identified, whereas the remaining groups (with a single exception) also included occasional half-sibs (10 families) or unrelated individuals from the same population (3 families). Similarly, 9 out of the 28 proposed half-sib groups (true number 25) consisted entirely of true half-sibs, whereas the additional 19 groups to various extents encompassed unrelated full-sib families from the same population. For the second simulated data set only containing unrelated genotypes, COLONY (erroneously) suggested 628 small full-sib families (average size 1.6) distributed within 148 half-sib groups, corresponding to a fairly limited number of false half- and full-sib pairwise comparisons (Table A2). There was a significant excess of proposed full-sib families with all members from a single population ($\chi^2 = 19.4$; df = 1; $P < 0.001$), as compared with the proportion expected had the individuals been grouped randomly with respect to population origin (given the present admixture proportions). In contrast, a majority (86%) of the half-sib groups included individuals from more than a single population.

© 2008 NRC Canada

Table A2. Number of family groups and corresponding pairwise comparisons as estimated using a group-likelihood approach (COLONY; Wang 2004) when applied to two simulated population mixtures of known relatedness.

			No. of pairwise comparisons (dyads)		
	No. of half-sib groups	No. of full-sib families	Unrelated	Half-sibs	Full-sibs
Simulation 1: full- and half-sib groups					
True number	25	125	466 500 (93.4%)	26 800 (5.4%)	6 200 (1.2%)
Estimated	28	126	467 231 (93.5%)	26 124 (5.2%)	6 145 (1.2%)
Simulation 2: all offspring unrelated					
True number	0	0	499 500 (100%)	0 (0%)	0 (0%)
Estimated	628	148	496 082 (99.3%)	2 970 (0.6%)	448 (0.1%)

References

Wang, J.L. 2002. An estimator for pairwise relatedness using molecular markers. Genetics, **160**: 1203–1215. PMID:11901134.

Wang, J.L. 2004. Sibship reconstruction from genetic data with typing errors. Genetics, **166**: 1963–1979. doi:10.1534/genetics.166.4.1963. PMID:15126412.

Appendix B

The heterozygote deficiency at locus *Ssa289* (F_{IS} = 0.103; $P < 0.01$) is two–seven times larger than at the other loci (Table 2), and the diagnostic tests in MICRO-CHECKER suggested this deficiency to reflect potential problems with null alleles. We find that reason unlikely, however. When analyzing the baseline data for all 32 Baltic Sea stocks, *Ssa289* does not deviate notably from the other loci with respect to conformances to Hardy–Weinberg expectations (not shown), as would be expected in the presence of a significant frequency of null alleles. Further, our data calibration did not indicate any systematic scoring problems or differences between laboratories at this or any other locus.

Rather, we suggest that the conspicuously large heterozygote deficiency at *Ssa289* reflects comparatively large allele frequency differences among the populations that occur mixed in our sample, having resulted in a particularly pronounced Wahlund effect. We further note that the number of alleles at *Ssa289* is smaller than that for the other loci (5 vs. 9–26; Table 2), indicating an increased probability to obtain a conspicuously large (or small) F_{IS} estimate due to random sampling error.

To test our hypothesis, we used bootstrapping to assess the likelihood of observing heterozygote deficiencies as large as those observed, using baseline data and median point estimates from the mixed stock analysis (MSA) (both years combined; Table 4). Using PopTools, random samples of 325 multilocus genotypes were drawn with replacement from the baseline file with population proportions mimicking those of the MSA analysis (including 14 populations with median mixture proportions of 1% or larger). The procedure was repeated 1000 times. For each bootstrap sample, F_{IS} was calculated at each locus and overall.

The resulting means and confidence intervals are presented in Table 2. With respect to *Ssa289*, as much as 148 (14.8%) of the bootstrapped samples had an F_{IS} value larger than or equal to the observed value. Hence, in the present case, it appears fairly likely to obtain a conspicuously large F_{IS} estimate at this locus by random chance.

© 2008 NRC Canada

Landscape-scale evaluation of genetic structure among barrier-isolated populations of coastal cutthroat trout, *Oncorhynchus clarkii clarkii*

Troy J. Guy, Robert E. Gresswell, and Michael A. Banks

Abstract: Relationships among landscape structure, stochastic disturbance, and genetic diversity were assessed by examining interactions between watershed-scale environmental factors and genetic diversity of coastal cutthroat trout (*Oncorhynchus clarkii clarkii*) in 27 barrier-isolated watersheds from western Oregon, USA. Headwater populations of coastal cutthroat trout were genetically differentiated (mean F_{ST} = 0.33) using data from seven microsatellite loci (2232 individuals), but intrapopulation microsatellite genetic diversity (mean number of alleles per locus = 5, mean H_e = 0.60) was only moderate. Genetic diversity of coastal cutthroat trout was greater (P = 0.02) in the Coast Range ecoregion (mean alleles = 47) than in the Cascades ecoregion (mean alleles = 30), and differences coincided with indices of regional within-watershed complexity and connectivity. Furthermore, regional patterns of diversity evident from isolation-by-distance plots suggested that retention of within-population genetic diversity in the Coast Range ecoregion is higher than that in the Cascades, where genetic drift is the dominant factor influencing genetic patterns. Thus, it appears that physical landscape features have influenced genetic patterns in these populations isolated from short-term immigration.

Résumé : L'examen des interactions entre les facteurs du milieu à l'échelle du bassin versant et la diversité génétique chez des truites fardées (*Oncorhynchus clarkii clarkii*) côtières dans 27 bassins versants isolés par des barrières dans l'ouest de l'Oregon, É.-U., a permis d'évaluer les relations entre la structure du paysage, la perturbation stochastique et la diversité génétique. D'après les données provenant de sept locus microsatellites (2232 individus), les populations des eaux d'amont de truites fardées côtières sont différenciées génétiquement (F_{ST} moyen = 0,33), mais la diversité génétique des microsatellites à l'intérieur des populations (nombre moyen d'allèles par locus = 5, H_e moyen = 0,60) n'est que modérée. La diversité génétique des truites fardées côtières est plus forte (P = 0,002) dans l'écorégion de la chaîne côtière (allèles moyens = 47) que dans l'écorégion des Cascades (allèles moyens = 30) et ces différences coïncident avec des indices de complexité et de connectivité régionales à l'intérieur des bassins versants. De plus, les patrons régionaux de diversité, illustrés par des graphiques d'isolement par la distance, laissent croire que la rétention de la diversité génétique à l'intérieur des populations est plus élevée dans l'écorégion de la chaîne côtière que dans les Cascades, où la dérive génétique est le facteur dominant à influencer les patrons génétiques. Ainsi, il apparaît que les caractéristiques physiques du paysage ont influencé les patrons génétiques dans ces populations protégées de l'immigration à courte échelle temporelle.

[Traduit par la Rédaction]

Introduction

Understanding the processes that control genetic variation in space and time is fundamental for conserving biological diversity and understanding the processes of species evolution (Waples 1991; Moritz 1994; Bernatchez 1995). Genetic analyses are commonly used to determine geographic structuring among populations that are subdivided spatially and temporally by limited dispersal among local breeding populations (Hanski 1998). These local populations are subject to extinction through stochastic environmental dynamics and demographic effects such as bottlenecks, founder effects, and drift (Lacy 1987).

In salmonid fishes, genetic structuring has been shaped by large-scale historical events such as range expansions or contractions following glacial retreat and pluvial periods (Taylor et al. 2001; Nielsen and Sage 2002; Castric and Bernatchez 2003). Recent research suggests, however, that the contribution of contemporary landscape features to the structure of genetic diversity supersedes or moderates the histori-

Received 26 June 2007. Accepted 25 February 2008. Published on the NRC Research Press Web site at cjfas.nrc.ca on 31 July 2008. 20073

T.J. Guy.[1,2] Department of Fisheries and Wildlife, Oregon State University, 104 Nash Hall, Corvallis, OR 93331, USA.
R.E. Gresswell.[3] US Geological Survey, Forest and Rangeland Ecosystem Science Center, 777 NW 9th St., Suite 400, Corvallis, OR 97330, USA.
M.A. Banks. Coastal Oregon Marine Experiment Station, Marine Fisheries Genetics Program, Hatfield Marine Science Center, Department of Fisheries and Wildlife, Oregon State University, 2030 SE Marine Sciences Dr., Newport, OR 97365, USA.

[1]Corresponding author (e-mail: troy.guy@noaa.gov).
[2]Present address: Cooperative Institute for Marine Resources Studies, Point Adams Research Station, 520 Heceta Pl., Hammond, OR 97121-0155, USA.
[3]Present address: US Geological Survey, Northern Rocky Mountain Science Center, 1648 S 7th Ave., Bozeman, MT 59717, USA.

 doi:10.1139/F08-090 © 2008 NRC Canada

cal genetic signature, at least at small spatial scales (Angers et al. 1999; Costello et al. 2003). For example, landscape features such as drainage network complexity and among-habitat differences in channel gradient can limit dispersal among populations (Angers et al. 1999; Hebert et al. 2000; Castric et al. 2001). Increasingly, studies have shown that patterns of genetic diversity are strongly influenced by populations above migration barriers (Hebert et al. 2000; Costello et al. 2003; Wofford et al. 2005). Similarly, natural cascades and waterfalls can influence patterns of genetic variability by acting as filters or barriers to dispersal from adjacent downstream populations (Currens et al. 1990; Griswold et al. 1997; Carlsson and Nilsson 2001).

Genetic diversity is generally assumed to be lower in populations isolated from gene flow because of demographic effects that act on populations of small effective sizes (N_e). However, the relative effects of ecological processes and habitat features (e.g., disturbance regime, habitat size, topologic complexity, and within-stream connectivity) on genetic diversity have not been thoroughly evaluated (Angers et al. 1999; Hebert et al. 2000; Castric et al. 2001). Headwater stream fishes existing above waterfalls provide a unique opportunity to examine the linkages between habitat features and population genetic structuring, because their genetic composition is not confounded by serial dispersal from downstream populations, at least over recent time scales.

Coastal cutthroat trout (*Oncorhynchus clarkii clarkii*), a salmonid subspecies commonly found in barrier-isolated populations in headwater streams of the Pacific Northwest, are an excellent model for examining the influence of landscape on genetic structure. Individual populations exist in climatic, hydrologic, and geomorphic conditions that vary across the historic range of the subspecies from Humboldt Bay, California, to Prince William Sound, Alaska (Fig. 1). Much of the Pacific Northwest lies on an active tectonic margin characterized by large uplifting mountain ranges that are actively eroded by substantial winter precipitation (160–230 cm) and complex river systems with numerous small tributaries. Glacial ice covered the majority of the northern region as recently as 10 000 years before present, but coastal cutthroat trout may have persisted south of the Cordilleran ice sheet in the Cascadia refugia for up to a million years (Fig. 1; McPhail and Lindsey 1986, Behnke 1992).

Coastal cutthroat trout exhibit a diverse array of life-history types, including anadromous, amphidromous, potamodromous, and nonmigratory forms (Trotter 1989). In the last few decades, range-wide declines in abundance and distribution have raised concerns about the long-term persistence of the subspecies, especially the anadromous form (Nehlsen et al. 1991; Trotter et al. 1993). The relatively abundant potamodromous and nonmigratory forms have received little attention despite the fact that they exist in complex assemblages of small headwater populations, potentially isolated from immigration and gene flow. These populations are especially vulnerable to large-scale landscape disturbances acting disproportionately on dendritic headwater stream networks (Fagan 2002).

Ecologists have long recognized the importance of disturbance regimes for creating and maintaining a mosaic of habitats that form the physical template for evolution (Southwood 1977; White and Pickett 1985). In the Pacific Northwest, mass wasting events, such as landslides and debris flows, are common processes that affect habitat for stream-dwelling organisms, especially headwater fishes (Reeves et al. 1995). Landslides and debris flows are responsible for sediment and wood input to stream channels that provide habitat structure for stream fishes (Swanson et al. 1987; Benda and Dunne 1997; May and Gresswell 2004); however, these stochastic events can potentially extirpate or severely reduce local populations and (or) connectivity among subpopulations (Lamberti et al. 1991; Gresswell 1999; Roghair et al. 2002).

The interaction of disturbance and habitat formation is especially important for coastal cutthroat trout because strong population structuring is often apparent at all levels of population organization, even within individual streams and tributaries (Campton and Utter 1987; Wenburg and Bentzen 2001; Wofford et al. 2005). Coastal cutthroat trout are common in small streams and are frequently the only fish species encountered in headwater surveys (McPhail 1967; Wydoski and Whitney 1979; Reeves et al. 1998). Individuals often occur above waterfalls in relatively small, isolated populations that have direct contact with mass wasting events (May and Gresswell 2003). Population demographics may rebound quickly following disturbance (Lamberti et al. 1991; Gresswell 1999; Roghair et al. 2002), but genetic diversity will remain low if connectivity (low-gradient channels that facilitate fish movement) between neighboring populations is poor (Dunham et al. 1999).

We hypothesize that the genetics of small populations isolated from frequent immigration and recolonization will be strongly differentiated depending upon the level of stream channel connectivity and network complexity within an isolated watershed. For example, habitat with high connectivity will be rapidly repopulated after a disturbance by individuals surviving in areas unaffected by the event, and thus genetic diversity within the watershed will be maintained. Additionally, diversity should be retained in watersheds with greater network complexity because multiple tributaries in an isolated watershed will provide a buffer against a genetic bottleneck if the population in a single tributary is extirpated.

On the landscape scale, habitats can be classified by ecoregions, large areas of land that contain similar physical and biological characteristics (Omernik 1987). For example, western Oregon contains the Coast Range, Cascades, and Klamath Mountains ecoregions (Level III ecoregions; see Pater et al. 1998). Because evidence for stochastic disturbance is very common throughout western Oregon, we hypothesize that the genetic diversity of isolated coastal cutthroat trout will be shaped by landscape differences among the ecoregions. Coast Range watersheds are characterized by low gradient, erosive sedimentary geology, and highly dendritic stream networks. Potentially, these streams retain greater genetic diversity following extirpating disturbance events than predominantly single-channel Cascades and Klamath Mountain watersheds characterized by steeper channel gradient and more resistant bedrock geology.

The National Marine Fisheries Service (NMFS) has used an alternative way to conceptualize genetic organization for salmonid populations under the Endangered Species Act (Waples 1991, 1995). According to this policy-related

© 2008 NRC Canada

Fig. 1 Sampling locations, ecoregion boundaries, geographic range, and relationship to the southern extent of Cordilleran ice sheet for coastal cutthroat trout (*Oncorhynchus clarkii clarkii*). For creek name codes, see Table 1.

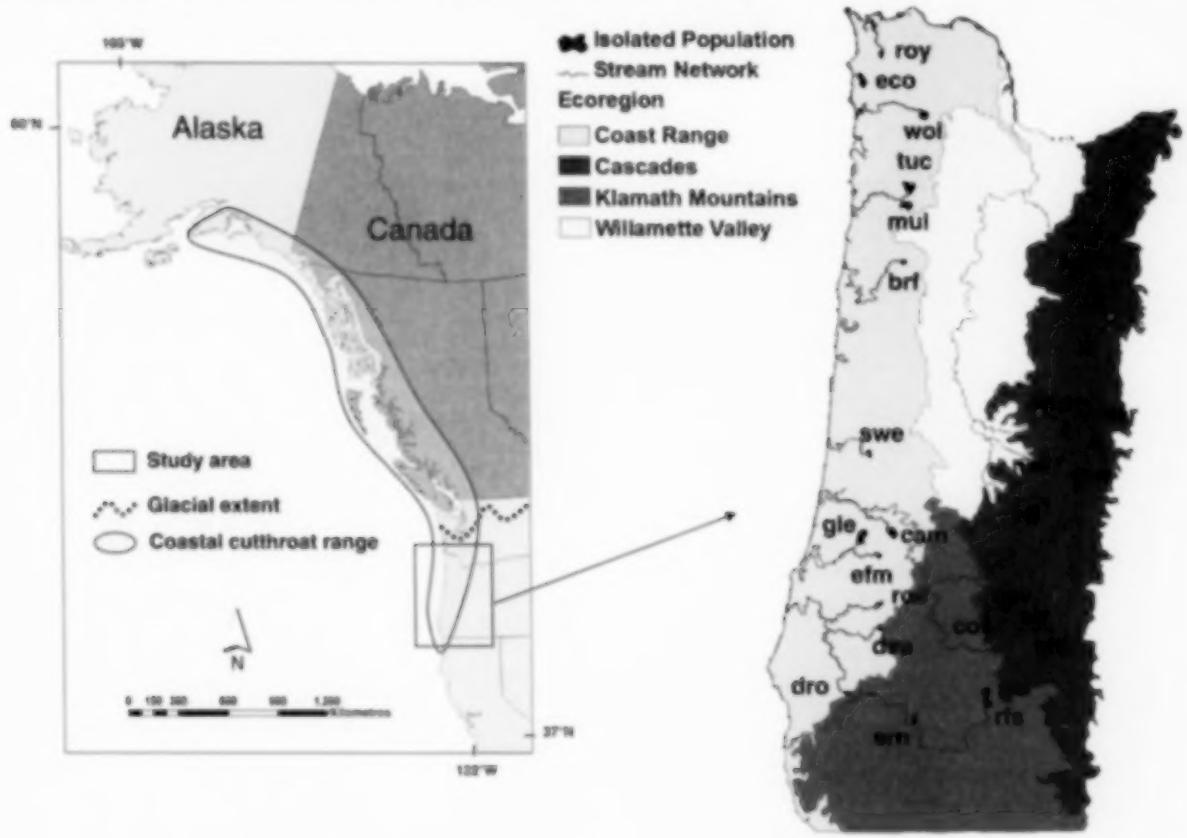

framework, a population or group of populations is considered distinct if it represents an evolutionarily significant unit (ESU) of the biological species (Johnson et al. 1999). Criteria for designation include (*i*) substantial reproductive isolation from conspecific groups and (*ii*) importance in the evolutionary legacy of the species (Waples 1991); major physical features of individual watersheds are not specifically considered except in relation to population isolation. Therefore, we hypothesize that this type of classification, although potentially valid for policy decisions, may not be closely related to landscape features that may explain genetic differentiation among isolated populations.

To this end, we analyzed genetic variation in 27 isolated populations of coastal cutthroat trout across western Oregon. Study objectives were (*i*) to determine the extent of differentiation and hierarchical genetic structure among isolated coastal cutthroat trout populations in headwater streams and (*ii*) assess how watershed-scale environmental factors correlate with the structure of genetic diversity.

Materials and methods

Sample collection

To develop a sampling frame, we identified 269 headwater watersheds (approximately third-order, 500–1500 ha) where coastal cutthroat trout were the only salmonid above natural barriers to upstream migration (cascades and waterfalls >4 m high) and where there was no record of hatchery stocking (Gresswell et al. 2004). Because ecoregions and geology were expected to influence habitat–genetic relationships across western Oregon, six sampling strata were created by integrating the watersheds with geographic information system (GIS) coverages of ecoregions (Coast Range, Cascades, and Klamath Mountain ecoregions; Oregon Natural Heritage Program, 1 : 250 000 ecoregion coverage) and high and low erosion potential (reclassified US Geological Survey, 1 : 500 000 geology coverage). A total of 25 watersheds were randomly selected for study in proportion to the number of watersheds in each stratum. Rainbow trout (*Oncorhynchus mykiss*) were visually identified in one watershed (Straight Creek) during sample collection; thus, this population was excluded from further analysis. Three additional populations (EF Laying Creek, Sweet Creek, and Camp Creek) from a larger random sample (n = 40) of watersheds in western Oregon (Gresswell et al. 2006) were added to yield a total of 27 sample watersheds (Fig. 1; Table 1).

Because of logistical constraints in field sampling and to avoid potentially comparing watersheds with large differences in effective population sizes (N_e), watershed size was

© 2008 NRC Canada

Table 1. Sampling date, location, and group classifications for coastal cutthroat trout (*Oncorhynchus clarkii clarkii*) for populations included in this study.

Creek name	Code	*n*	Year	Northing	Easting	Geology	Ecoregion	ESU*	Watershed	Strategy
Cavitt Creek	cav	94	2000	4776923.50	509350.34	Hard	Cascades	CO	Umpqua River	Component
Coffee Creek	cof	95	2000	4763899.50	500567.38	Soft	Cascades	CO	Umpqua River	Component
Miller Creek	mil	65	2000	4801471.00	507303.81	Hard	Cascades	CO	Umpqua River	Complete
NF,EF Rock Creek	nec	19	2000	4808921.00	513817.53	Hard	Cascades	CO	Umpqua River	Complete
SF Buckeye Creek	sfb	89	2001	4764867.50	535899.38	Hard	Cascades	CO	Umpqua River	Component
EF Laying Creek	efl	96	2000	4837587.50	533377.75	Hard	Cascades	UW	Willamette River	Component
Grasshopper Creek	gra	91	1999	4862816.00	566035.00	Hard	Cascades	UW	Willamette River	Component
Hardy Creek	har	89	2000	4871060.50	561125.38	Hard	Cascades	UW	Willamette River	Complete
Lukens Creek	luk	95	2001	4988354.00	559505.69	Hard	Cascades	UW	Willamette River	Component
Nevergo Creek	nev	15	2000	4861509.00	540977.63	Hard	Cascades	UW	Willamette River	Component
WF Deer Creek	wfd	74	2000	4878597.50	543431.19	Soft	Cascades	UW	Willamette River	Complete
Bridge Forty Creek	brf	93	1999	4975023.00	452950.38	Hard	Coast Range	CO	Central Coast	Component
Sweet Creek	swe	88	2001	4865603.50	432341.28	Soft	Coast Range	CO	Central Coast	Component
EF Millicoma Creek	efm	94	2000	4807899.00	436663.63	Soft	Coast Range	CO	Coos River	Component
Glenn Creek	gle	96	2000	4820370.50	428690.00	Soft	Coast Range	CO	Coos River	Component
Dead Horse Creek	dea	96	2001	4779452.50	436894.16	Soft	Coast Range	CO	Coquille River	Complete
Drowned Out Creek	dro	91	2000	4729015.50	418643.84	Soft	Coast Range	CO	Coquille River	Complete
Rock Creek (Coquille)	roc	82	2001	4766737.50	437381.41	Soft	Coast Range	CO	Coquille River	Component
NF Ecola Creek	eco	96	2001	5076097.00	431525.69	Hard	Coast Range	CO	North Coast	Component
Muletail Creek	mul	95	2000	5007318.00	453145.69	Soft	Coast Range	CO	North Coast	Complete
Tucca Creek	tuc	96	1999	5018858.00	458526.22	Soft	Coast Range	CO	North Coast	Component
Wolf Creek	wol	96	2000	5058416.50	467060.63	Hard	Coast Range	CO	North Coast	Complete
Camp Creek	cam	92	2000	4820829.50	445105.72	Soft	Coast Range	CO	Umpqua River	Complete
Rock Creek (Youngs)	roy	94	2000	5093481.00	442359.16	Soft	Coast Range	SW–CR	North Coast	Component
RF Salt Creek	rfs	86	2001	4722844.00	499061.06	Hard	Klamath Moutains	SO–NC	Rogue River	Component
Salt Creek	sal	83	2001	4727443.00	499260.63	Hard	Klamath Moutains	SO–NC	Rogue River	Component
Little Stratton Creek	str	32	2001	4713908.00	456924.09	Soft	Klamath Moutains	SO–NC	Rogue River	Component

*Evolutionarily significant units: CO, Coastal Oregon; UW, Upper Willamette; SW–CR, Southwest Washington – Columbia River; SO–NC, Southern Oregon – Northern California.

© 2008 NRC Canada

restricted to 1000 ha. Camp Creek (≈ 2000 ha), the focus of an intensive within-watershed genetic study (Wofford et al. 2005), is the only exception to this criterion. For the remaining 26 watersheds, the size was restricted in two ways. First, sampling was initiated immediately above the isolating barrier if the drainage area was 500–1000 ha. This situation will be referred to as the "complete" watershed sampling strategy. Second, if the drainage area above the isolating barrier was >1000 ha, sampling was initiated at the first tributary junction (working progressively upstream) that drained a watershed meeting the size criterion. If the watershed contained two or more subwatersheds between 500 and 1000 ha, one watershed was randomly selected for sampling. The watersheds in the second group were collectively assigned the term "component" watershed sampling strategy (Table 1).

Prior to field surveys, the channel network of each watershed was divided into stream segments (Frissell et al. 1986; Moore et al. 1999) using information from previous surveys, topographic and geologic maps, aerial photographs, and field reconnaissance to identify tributary junctions and barriers to fish movement (Gresswell et al. 2006). In the field, segments were divided into geomorphic reach types based on substrate, gradient, bed morphology, and pool spacing (Montgomery and Buffington 1997), and in each reach, channel-unit types (e.g., pools, riffles, and cascades) were classified using criteria of Bisson et al. (1982). Physical variables that described channel-unit size, substrate size class, valley segment type, channel type, and woody debris accumulations were recorded for each channel unit (Gresswell et al. 2006).

Genetic samples were collected from coastal cutthroat trout in each of the 27 watersheds between 1999 and 2002. Fish were collected using single-pass electrofishing techniques starting in the lowest portion of each watershed and continuing upstream (Bateman et al. 2005). To capture a large portion of the genetic diversity from each sampling location (Banks et al. 2000), fin tissue was taken from up to 96 fish per watershed. In some locations, the upper extent of fish distribution was reached before 96 samples were obtained. In cases with less than 96 samples, we assumed that a large proportion of the genetic variation was captured for two reasons. First, single-pass electrofishing techniques capture the majority of fish in the initial pass (Bateman et al. 2005). Second we took a fin clip from every fish captured from these small isolated populations. To reduce the chances of family sampling (Hansen et al. 1997), tissue collections were restricted to fish >50 mm (fork length). Tissue was collected from up to 10 fish in each 10 mm size class from each geomorphic segment (Frissell et al. 1986; Montgomery and Buffington 1997) until 96 samples were obtained or the upper extent of fish distribution was reached. Captured fish were anesthetized with clove oil to reduce handling stress (Taylor and Roberts 1999). Each fish was weighed and measured, and a small portion of the caudal fin was removed and stored in a desiccant (anhydrous sulfide crystals) or a buffer solution (100 mmol·L^{-1} Tris–HCl (pH 8), 100 mmol·L^{-1} ethylenediaminetetraacetic acid (EDTA, pH 8), 10 mmol·L^{-1} NaCl, 0.5% (*w/v*) sodium dodecyl sulphate (SDS)). Subsequently all fish were released to their source location.

Microsatellite analysis

Seven microsatellite loci in three multiplexed sets were chosen after screening for reliable polymerase chain reaction (PCR) amplification, ease of scoring, and polymorphism (Table 2). Genomic DNA was extracted from fin tissue using Chelex 100 following the procedure of Banks et al. (2000). Each multiplex set was amplified with a MJ Research PTC-225 thermocycler under varying reagent concentrations and PCR conditions (Table 2; Appendix A, Table A1). The PCR products were analyzed on a 5% acrylamide gel using electrophoresis on a MJ Research Basestation DNA fragment analyzer (MJ Bioworks Inc.). Allele sizes were scored using the computer program Cartographer (MJ Geneworks, Inc.), verified visually, and hand-corrected as necessary.

Statistical analysis

Within-population parameters sample size (n), number of alleles per locus (A), expected heterozygosity (H_e), observed heterozygosity (H_o), and allele frequencies were calculated using FSTAT version 2.9.3.2 (Goudet 1995). Pairwise F_{ST} (theta) values (Wier and Cockerham 1984) were compared among locations and ecoregions using a permutation approach in FSTAT. To evaluate results from an ecological basis, F_{ST} values were calculated among ESU population groups (Waples 1991). In addition, pairwise Cavalli-Sforza Edwards chord distance (CSE) was calculated using the GENDIST program (PHYLIP, phylogeny inference package; Felsenstein 2002). To test for differences in allelic frequencies between all population pairs, Fisher's exact test was implemented with default parameters in GENEPOP (Raymond and Rousset 1995). Tests for deviations from Hardy–Weinberg equilibrium for each locus and population combination and for genotypic linkage disequilibrium for all combinations of loci pairs within a population were performed using an exact test based on Markov chain iterations in GENEPOP with default parameters. Statistical significance was evaluated using Bonferroni-adjusted P values where appropriate (Rice 1989). Effective population size (N_e) for each population was estimated using a linkage disequilibrium-point estimation method (Hill 1981) in the program NeEstimator (Peel et al. 2004). The linkage disequilibrium-point estimation method requires only a single sampling visit if the assumptions of neutral alleles, no migration, no subpopulation structure, and a large sample size representative of the entire population are satisfied (Hill 1981). N_e for West Fork Deer could not be calculated because alleles were fixed at all but one locus. Hierarchical partitioning of genetic diversity was assessed as the percentage of variation explained by groupings into ecoregions, ESUs, and major hydrological watersheds (e.g., Willamette River and Umpqua River, Table 1) and between complete and component watersheds using an analysis of molecular variance (AMOVA) procedure in Arlequin version 2.0 (Schneider et al. 1997).

Isolation-by-distance (IBD) was assessed by examining correlation between genetic distance and geographic distance using Mantel tests in GENEPOP with default parameters. Both F_{ST} and CSE pairwise genetic distance values were evaluated separately for all tests. Geographic distances among sampling locations were calculated as stream net-

© 2008 NRC Canada

Table 2. Microsatellite loci with annealing temperatures (°C) in parentheses, number of nucleotide repeats, primer concentration in PCR reaction, total number of alleles, allele size range, average expected heterozygosity (H_e), and original citation for loci in each multiplex used to assess variation in coastal cutthroat trout (*Oncorhynchus clarkii clarkii*).

Multiplex (temp., °C)	Locus	Repeat	Primer (mmol·L^{-1})	No. of alleles	Size range (bp)	Avg. H_e	Reference
Set A (49)	*One102*	Tetra	0.50	20	192–268	0.55	Olsen et al. 1996
	One103	Tetra	0.50	16	106–166	0.55	Olsen et al. 1996
	One108	Tetra	0.50	31	138–266	0.59	Olsen et al. 1996
Set B (56)	*Omy77*	Di	0.50	30	97–169	0.62	Morris et al. 1996
	Ots4	Di	0.08	11	107–129	0.47	Banks et al. 1999
Set C (63)	*Ots209*	Tetra	0.08	11	139–195	0.54	Greig et al. 2003
	Ots212	Tetra	0.50	21	103–223	0.59	Greig et al. 2003

work distances using regional 1 : 100 000 hydrologic stream layers with ArcGIS software (version 8.2, Environmental Systems Research Institute, Redlands, California). To determine the relative importance of drift and gene flow (in this case historical) among isolated watersheds, a second Mantel test was performed independently for complete, component, and all watersheds combined using the residuals from the initial relationship and geographic stream distance. The degree of scatter around the second fitted line allows a comparison of relative contribution by the factors that differentiate (i.e., high scatter factors such as genetic drift, bottlenecks, and founder effects) or homogenize (i.e., low scatter factors such as historic gene flow) the genetic structure of populations (Hutchison and Templeton 1999; Costello et al. 2003; Taylor et al. 2003).

To determine whether grouping populations by ecoregion (large-scale physical habitat data) or by ESUs (previously defined genetic, geographic, and life-history groupings) has a greater correspondence with observed genetic structure among isolated coastal cutthroat trout, IBD tests were repeated for populations partitioned into Coast Range and Cascades ecoregions and Oregon Coast and Upper Willamette River ESUs (Johnson et al. 1999). The degree of "scatter" (Hutchison and Templeton 1999) in the genetic distance metric of IBD plots was compared among ecoregions and ESU groupings to ascertain the relative contribution of differentiating and homogenizing forces in each grouping (Hutchison and Templeton 1999; Costello et al. 2003; Taylor et al. 2003). Populations in the Klamath Mountains ecoregion and in the Southwest Washington – Columbia River and Southern Oregon – California Coast ESUs were not included in these IBD analyses because sample sizes were too low ($n < 3$).

Environmental comparisons

Genetic diversity (i.e., total number of alleles for all loci, raw or corrected for sample size) and physical environmental variables that we assumed to influence genetic structure (i.e., degree of isolation, watershed area, topological stream channel complexity, and within-watershed connectivity) were compared between the Coast Range and Cascades ecoregions using two-sample t tests. Comparisons were conducted for complete, component, and all of the watersheds combined. We compared genetic diversity and barrier height among regions to test for regional biases in samples collected above what were assumed to be substantial barriers (>4 m). In addition, N_e and drainage area above the barrier (km^2) were compared among ecoregions and sampling strategies to detect population size or habitat area bias. An index of topological stream network complexity was developed using the ratio of summed tributary lengths to the longest length (m) of stream (i.e., main stem) per watershed. Network complexity was predicted to support persistence in the stream network following local extirpation related to a catastrophic event in any single tributary. To compare within-watershed connectivity, the total number of vertical falls (i.e., steps > 1 m) was divided by the total number of channel units per watershed (calculated from field surveys). Field survey measurements rather than a GIS-based estimate of stream gradient were used for this analysis because we believed that habitat-level impediments to stream fish movement would not be captured using a lower resolution remote sensing approach. Statistical analyses were conducted using Number Cruncher Statistical Systems Software (NCSS, Kaysville, Utah).

Results

Within-population variation

Genotypes from 2232 individual fish were successfully obtained from 27 sampling locations. Genetic variation was generally high despite the isolation of sampling sites above waterfalls. Number of alleles per locus for all populations ranged from 11 (*Ots4*) to 31 (*One108*), with a mean of 20 per locus. Mean expected heterozygosity was 0.60 (range: 0.47 for *Ots4* to 0.62 for *Omy77*). Tests for Hardy–Weinberg equilibrium at individual loci across populations (7 loci × 27 populations) revealed failures in 21 of 189 cases (11.1%) after Bonferroni corrections ($\alpha = 0.05/27 = 0.0019$). Failures were generally spread among all loci and populations, but a slight concentration was observed in *Omy77*. Failures were reduced to 9.3% with *Omy77* removed, but results from all subsequent analyses were not appreciably different. Therefore, *Omy77* was retained for all analyses. Tests for linkage disequilibrium yielded 10 departures among 567 comparisons (1.8%, $\alpha = 0.05/27 = 0.0019$), and thus, no concentration of departures among locus pairs or within populations was detected.

Among-population variation, effective population size, and genetic structure

Genetic differentiation among populations was substantial.

© 2008 NRC Canada

Allelic frequency distributions from 351 pairwise population comparisons suggested significant population independence ($\alpha = 0.05/27 = 0.0019$), and the majority of comparisons by locus were statistically significant ($\alpha = 0.05/7 = 0.007$; Table 3). Similarly, the mean F_{ST} value (0.33) suggested considerable population genetic structure. Pairwise F_{ST} values ranged from 0.04 to 0.98 ($P < 0.05$) (Table 3). Miller Creek was unique because *Omy77* and *Ots4* did not amplify in PCR reactions despite repeated attempts; apparently, this result was related to priming site mutations. Pairwise F_{ST} comparisons among populations, including Miller Creek, were significant even after *Omy77* and *Ots4* were removed from the data.

Differences in hierarchical genetic variation among populations grouped by ecoregions, ESU, and major hydrological watersheds were statistically significant ($P < 0.05$), but in each comparison, more genetic variation occurred within and among populations than among major groups. Among ecoregion groups (Coast Range, Klamath Mountains, and Cascades), 5% of the variation was among groups, 27% among populations, and 68% within populations ($P < 0.01$). Comparison of populations by ecologically and genetically based ESU groups (Oregon Coast, Upper Willamette River, and Southern Oregon – Northern California) produced similar results. Approximately 7% of the variation was among groups, 27% among populations, and 67% within populations ($P < 0.01$). Less variation was attributable to grouping by major watershed (3% among groups, 28% among populations, and 69% within populations; $P = 0.02$). Differences between sampling strategies (complete or component) were not statistically significant ($P = 0.12$), and <1% of the variation was partitioned among groups, 32% among populations, and 68% within populations.

Isolation-by-distance

Isolated coastal cutthroat trout populations in western Oregon (considered as a group) exhibited migration–drift equilibrium. A positive IBD relationship was detected when all populations were combined ($r = 0.32$, $P < 0.01$; Fig. 2; Table 4), and the subsequent Mantel test comparing residuals from the initial IBD test against stream distance was positive ($r = 0.02$, $P < 0.02$). IBD relationships were also detected when all component watersheds ($r = 0.29$, $P < 0.01$) and complete watersheds ($r = 0.55$, $P < 0.01$) were examined separately. When populations were grouped by ecoregion, IBD was detected for the Cascades ecoregion ($r = 0.09$, $P < 0.05$), but the Mantel test of residuals did not confirm migration–drift equilibrium ($r = -0.06$, $P < 0.82$). None of the IBD assessments for populations in the Coast Range ecoregion or the Oregon Coast and Upper Willamette River ESUs was statistically significant (Fig. 2; Table 4). The degree of scatter in comparisons between the initial IBD residuals and geographic distance was strikingly different between ecoregions. The scatter was consistently lower for the Coast Range ecoregion than for the Cascades ecoregion (Fig. 2), and mean F_{ST} values were higher in the Cascades ecoregion than in the Coast Range ecoregion (Table 4). Although the geographic distance among watersheds is generally greater in the Cascades than in the Coast Range, IBD estimates for watersheds < 500 km apart are more variable in the Cascades ecoregion (Fig. 2). The large gap in the Cascades scatterplot occurred because watersheds located in the lower Willamette and Columbia River watersheds were not included in the sample, and thus, there were no pairwise comparisons among Cascades watersheds separated by a distance of 400–1000 km.

It is important to note, however, that distinguishing between historical associations and ongoing gene flow using F_{ST} can sometimes be problematic (Nielsen and Slatkin 2000). This is particularly relevant for data sets from large, relatively panmictic populations where the effects of genetic drift are weak. In this study, however, F_{ST} can be perceived as a dynamic balance between genetic drift and historical gene flow, because all of these populations were isolated by barriers to upstream fish migration, and drift is predicted to be a major factor in populations with small N_e (Neigel 2002).

Environmental patterns

Comparisons of genetic and environmental characteristics for Coast Range and Cascades ecoregions (component and complete sampling strategies combined) revealed differences in genetic diversity, channel topology, and within-watershed connectivity (Table 5). Differences in mean N_e of populations from Coast Range and Cascades ecoregions were not statistically significant (Table 5) nor were differences in watershed area and barrier heights. The total number of alleles for all loci was higher in the Coast Range when all watersheds ($P = 0.02$) and component watersheds ($P = 0.01$) were compared separately, but the difference in the mean number of alleles in complete watersheds from the two ecoregions was not statistically significant ($P = 0.06$). For component watersheds, the differences in within-watershed connectivity were not significant between the two ecoregions ($P = 0.15$), but differences were statistically significant for complete watersheds ($P = 0.02$) and all watersheds combined ($P = 0.03$).

Discussion

Regionally dependent genetic structuring and IBD scatterplots suggest that differences in regional habitat structure shape genetic diversity. Consistently different F_{ST} and CSE values and IBD plots in the Cascades and Coast Range suggest that habitat variation in ecoregions interacts with the genetic forces that differentiate (drift, founder effects, and bottlenecks) and homogenize (Hutchison and Templeton 1999). Disturbance events (e.g., mass wasting) are very common features in headwater landscapes of western Oregon (Swanson and Lienkaemper 1978; May and Gresswell 2003). Evidence of debris flows over a range of ages was conspicuous throughout all watersheds examined in this study. Debris flow can scour stream channels, potentially extirpating or severely reducing populations of stream fishes, especially in headwater habitats (Lamberti et al. 1991; Ensign et al. 1997; Roghair et al. 2002). In any given isolated population, resistance to extirpation and subsequent recolonization after a stochastic disturbance is dependent upon the degree of watershed complexity (relationship between tributary and mainstem length) and the ability of individuals in the population to move within the watershed (within-watershed connectivity as determined by the number

© 2008 NRC Canada

Table 3. Genetic distance and allelic differentiation results for populations of coastal cutthroat trout (*Oncorhynchus clarkii clarkii*)

	Population												
	gle	roy	hef	dea	efl	wol	cav	luk	eco	tuc	mal	swe	roc
gle	—	0.11	0.10	0.21	0.13	0.33	0.13	0.19	0.05	0.09	0.18	0.08	0.13
roy	7	—	0.14	0.25	0.14	0.36	0.14	0.18	0.11	0.14	0.19	0.14	0.16
hef	7	7	—	0.28	0.13	0.36	0.13	0.18	0.09	0.10	0.17	0.10	0.10
dea	7	7	7	—	0.24	0.39	0.19	0.28	0.21	0.26	0.28	0.26	0.24
efl	7	7	7	7	—	0.29	0.15	0.17	0.12	0.14	0.22	0.13	0.13
wol	7	7	7	6	7	—	0.38	0.36	0.33	0.35	0.40	0.36	0.33
cav	7	7	7	7	7	7	—	0.20	0.12	0.15	0.18	0.13	0.13
luk	7	7	7	7	7	7	7	—	0.17	0.18	0.20	0.18	0.19
eco	7	7	7	7	7	7	7	7	—	0.05	0.15	0.04	0.10
tuc	7	7	7	7	7	7	7	7	3	—	0.18	0.09	0.15
mal	7	7	7	7	7	7	7	7	7	7	—	0.16	0.19
swe	7	7	7	7	7	7	7	7	7	7	7	—	0.11
roc	7	7	5	7	7	7	7	7	7	7	7	7	—
ner	5	6	7	7	7	7	7	7	5	5	7	7	7
mil	5	5	4	5	5	5	5	5	5	5	5	5	5
cam	7	7	7	7	7	7	7	7	7	7	7	7	7
har	7	7	7	7	7	7	7	7	7	7	7	7	7
gra	7	7	7	7	7	7	7	7	7	7	7	7	7
efm	7	7	7	7	7	7	7	7	7	7	7	7	7
sal	7	7	7	7	7	7	7	7	7	7	7	7	7
cof	6	7	7	7	7	7	7	7	7	7	7	7	7
dro	7	7	7	7	7	7	7	7	6	7	7	5	7
rfs	7	7	7	7	7	7	7	7	7	7	7	7	7
sfb	7	7	7	7	7	7	7	7	7	7	7	7	7
wfd	7	7	7	7	7	7	7	7	7	7	7	7	7
nev	6	7	7	7	6	7	7	7	6	6	7	7	7
sen	7	7	7	7	7	7	7	7	7	7	7	7	7

Note: Values above the diagonal represent pairwise F_{ST} values; all estimates were significant at the adjusted nominal level (5%) for multiple comparisons between populations after Bonferroni adjustments ($\alpha = 0.007$). Refer to Table 1 for population code definitions.

Fig. 2 Isolation by distance plots for all watersheds in (*a*) western Oregon ($r = 0.32$, $P < 0.01$), (*b*) Coast Range ecoregion ($r = 0.06$, $P = 0.28$), (*c*) Cascades ecoregion ($r = 0.09$, $P = 0.05$), (*d*) Oregon Coast evolutionarily significant unit (ESU; $r = 0.20$, $P = 0.08$), and (*e*) Upper Willamette River ESU ($r = -0.54$, $P = 0.94$).

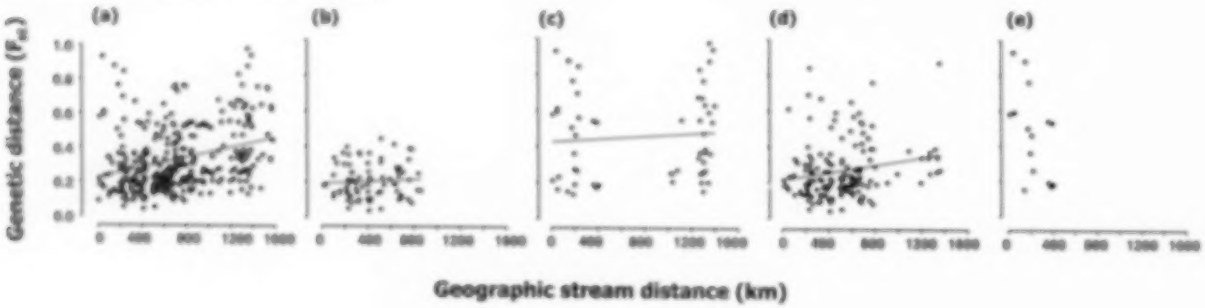

of waterfalls). Coastal cutthroat trout in the Coast Range appear to be buffered from the loss of genetic material primarily because drainage networks are more complex, and there are fewer instream impediments to movement in the watershed after disturbances. Coast Range populations are better able to retain genetic diversity than populations in the steep, predominantly single-channel Cascades watersheds where drift appears to be the principal factor influencing genetic organization. In Cascades watersheds, a single debris flow can cause an immediate decrease in genetic diversity followed by a lasting resistance to upstream recolonization and gene flow.

It appears that environmental factors defined by ecoregions may be more informative than ESU boundaries when describing the observed genetic structuring in isolated populations of coastal cutthroat trout. For example, analysis of IBD scatter revealed greater divergence among populations in the Oregon Coast ESU than among populations in the Coast Range ecoregion. In this comparison, the Oregon Coast ESU and the Coast Range ecoregion groupings funda-

© 2008 NRC Canada

included in this study.

ner	mil	cam	har	gra	efm	sal	cof	dro	rfs	sfb	wfd	nev	srn
0.18	0.13	0.15	0.47	0.27	0.18	0.27	0.19	0.12	0.27	0.55	0.55	0.20	0.20
0.20	0.20	0.22	0.46	0.22	0.26	0.35	0.22	0.15	0.34	0.55	0.53	0.23	0.20
0.23	0.18	0.21	0.53	0.25	0.18	0.33	0.21	0.12	0.33	0.53	0.52	0.20	0.20
0.31	0.22	0.36	0.58	0.39	0.30	0.36	0.29	0.31	0.31	0.65	0.65	0.34	0.31
0.25	0.20	0.21	0.46	0.26	0.21	0.34	0.20	0.17	0.33	0.54	0.50	0.15	0.16
0.48	0.42	0.45	0.73	0.48	0.41	0.54	0.45	0.39	0.53	0.76	0.75	0.42	0.46
0.23	0.16	0.25	0.47	0.27	0.26	0.30	0.19	0.16	0.28	0.56	0.55	0.25	0.16
0.25	0.25	0.31	0.53	0.18	0.27	0.37	0.27	0.22	0.34	0.55	0.54	0.19	0.26
0.19	0.09	0.15	0.45	0.23	0.19	0.27	0.18	0.08	0.28	0.52	0.52	0.21	0.19
0.23	0.19	0.22	0.47	0.22	0.22	0.30	0.22	0.12	0.31	0.54	0.53	0.19	0.21
0.24	0.15	0.31	0.55	0.26	0.31	0.38	0.27	0.23	0.37	0.59	0.53	0.29	0.30
0.21	0.13	0.14	0.51	0.24	0.21	0.33	0.16	0.11	0.33	0.51	0.53	0.25	0.23
0.23	0.17	0.22	0.57	0.27	0.19	0.37	0.18	0.13	0.34	0.49	0.53	0.26	0.21
—	0.21	0.33	0.77	0.37	0.33	0.43	0.27	0.25	0.42	0.84	0.83	0.37	0.37
4	—	0.27	0.67	0.32	0.26	0.35	0.13	0.22	0.33	0.69	0.68	0.34	0.26
6	5	—	0.61	0.41	0.30	0.47	0.28	0.17	0.47	0.67	0.68	0.38	0.36
7	5	7	—	0.58	0.64	0.62	0.59	0.52	0.64	0.94	0.93	0.76	0.65
7	5	7	7	—	0.38	0.44	0.36	0.29	0.45	0.63	0.59	0.36	0.36
7	5	7	7	7	—	0.37	0.30	0.25	0.39	0.59	0.65	0.34	0.31
7	5	7	7	7	7	—	0.34	0.37	0.09	0.76	0.74	0.48	0.34
7	5	7	7	7	7	7	—	0.24	0.29	0.61	0.63	0.39	0.24
5	5	7	7	7	7	7	7	—	0.37	0.57	0.56	0.27	0.25
6	5	7	7	7	7	2	7	7	—	0.76	0.75	0.48	0.34
7	5	7	7	7	7	7	7	7	7	—	0.98	0.87	0.76
7	5	7	6	7	7	7	7	7	7	7	—	0.88	0.76
6	4	7	7	7	7	7	7	6	7	7	7	—	0.33
6	5	7	7	7	7	7	7	7	7	7	7	6	—

(α = 0.000 132). Values below the diagonal represent the number of loci out of 7 (Miller Creek (mil) = 5) that revealed significant differentiation

mentally share nearly all of the same populations. The principal difference is that "up-river" populations in the Umpqua River are placed into the Cascades ecoregion based on habitat similarities; however, they are included in the Oregon Coast ESU group because of presumed ecological and genetic similarities that occur throughout the watershed. Thus, higher divergence in the ESU grouping appears to reflect a strong habitat effect on the genetic structuring of Umpqua River up-river populations.

Geomorphology (connectivity and complexity) within ecoregions was similar because the Coast Range ecoregion is predominantly composed of bedrock materials that are less erosion resistant (sandstone) than the common bedrock in the Cascades ecoregion (basalt). Study watersheds were selected using a probabilistic design based on the proportion of the two bedrock types in each ecoregion, but the geology of an ecoregion can be very complex. For instance, both rock types can be found even in a single watershed. Results from previous studies in the Coast Range suggest that differences in substrate size, channel gradient, predominant channel-unit type, mean summer discharge, and community structure are related to basalt and sandstone rock types. In contrast, if the estimated number of individuals and biomass of coastal cutthroat trout are compared between the two bedrock types, differences are not statistically significant (Connolly and Hall 1999, Hicks and Hall 2003). An important goal of future studies would be to determine if genetic diversity in isolated watersheds was directly related to the dominant bedrock geology of the system.

Because the southernmost lobes of the Cordilleran ice sheet did not cover western Oregon (Bretz 1913), it is likely that coastal cutthroat populations in this study are closer to mutation–drift equilibrium than fishes in more northern regions, and therefore, genetic structure is more likely the result of contemporary extinction–recolonization processes (Wade and McCauley 1988; McCauley 1991). A persistent signature of historical events, such as founder effects from postglacial expansion, may confound contemporary factors in recently colonized habitats where populations have not yet reached mutation–drift equilibrium (Castric et al. 2001). It was not possible to accurately assess the age of each barrier in this study or determine if the population residing above individual barriers resulted from colonization following barrier formation or isolation during the formation period. The geomorphology of watersheds in this study did not reveal evidence of glacial activity, and there is the potential for populations to have existed above each barrier for millennia. Although the persistence and formation history of each barrier may be geologically recent and potentially unique, each appeared to be a formidable barrier to contemporary migration relevant to the scale of microsatellite markers.

Genetic analysis supports these observations. All pairwise population comparisons were statistically significant (mean

© 2008 NRC Canada

Table 4. Regional isolation-by-distance (IBD) results and average genetic distance for coastal cutthroat trout (*Oncorhynchus clarkii clarkii*) populations under varying sampling strategies.

			F_{ST}		Residuals		
Regional grouping	Sampling strategy	Populations (n)	r	P	r	P	Avg. F_{ST}
Combined	All watersheds	27	0.32	**<0.01**	0.02	**0.02**	0.33
	Component	18	0.29	**0.00**	0.01	0.63	0.27
	Complete	9	0.55	**0.01**	0.27	0.44	0.46
Coast Range	All watersheds	13	0.06	0.28	—	—	0.21
	Component	8	0.18	0.10	—	—	0.13
	Complete	5	0.13	0.10	—	—	0.33
Cascades	All watersheds	11	0.09	**0.05**	–0.06	0.82	0.46
	Component	7	0.24	**0.01**	0.12	0.31	0.35
	Complete	3	0.35	0.50	—	—	0.68
Oregon Coast	All watersheds	18	0.20	0.08	—	—	0.27
	Component	10	0.26	0.07	—	—	0.24
	Complete	8	0.26	0.16	—	—	0.30
Upper Willamette	All watersheds	6	–0.54	0.94	—	—	0.47
	Component	4	–0.38	0.54	—	—	0.22
	Complete	2	—	—	—	—	0.92

Note: Correlation coefficients and P values (values significant at the 0.05 level in bold) represent the relationship between genetic distance and geographic distance (r, F_{ST}) or residuals and geographic distance plots (r, residuals) based on Mantel tests using 1000 permutations. The results for all tests were consistent using either F_{ST} or Cavalli-Sforza Edwards chord distance as the genetic distance metric (F_{ST} presented).

Table 5. Results of two-sample t tests comparing mean genetic and environmental variables by sampling strategy and ecoregion.

Sampling strategy	Ecoregion	n	A	N_e	Barrier height (m)	Basin area (1000 km^2)	Trib/MS (Complexity)	Steps/H_t (Connectivity)
Western Oregon	Coast Range	13	47	75	19	23.5	0.54	0.02
	Cascades	11	30	39	7	19.4	0.10	0.04
	P	—	**0.02**	0.12	0.15	0.60	**<0.01**	**0.03**
Component	Coast Range	8	56	97	23	32.0	0.68	0.01
	Cascades	7	38	56	9	26.3	0.11	0.03
	P	—	**0.01**	0.16	0.21	0.44	**0.01**	0.15
Complete	Coast Range	5	32	41	12	10.0	0.31	0.02
	Cascades	4	16	19	3	7.3	0.09	0.04
	P	—	0.06	0.17	0.29	0.50	**0.03**	**0.02**

Note: Means and associated P values (values significant at the 0.05 level in bold) are summarized for total number of alleles for all loci (A), effective population size (N_e), barrier height, basin area, the ratio of summed tributary length to mainstem stream length (Trib/MS), and the number of steps > 1 m divided by the total number of habitat units per watershed (Steps/H_t).

F_{ST} = 0.33, mean alleles for all loci = 5). Populations in this study reflected a higher degree of isolation than has been previously observed among populations of anadromous coastal cutthroat trout (mean F_{ST} = 0.05, mean alleles for 10 loci = 9; Wenburg and Bentzen 2001). Pairwise microsatellite F_{ST} values in this study were comparable to potamodromous westslope cutthroat (*Oncorhynchus clarkii lewisi*) in British Columbia (mean F_{ST} = 0.32, mean alleles for eight loci = 4; Taylor et al. 2003), but over half of the populations in the Canadian study were not located above physical barriers to migration. Our findings are consistent with recent studies showing the importance of barriers to the structuring of genetic diversity among stream fishes on both local (Carlsson and Nilsson 2001) and regional scales (Taylor et al. 2003; Costello et al. 2003). These studies reveal that the inclusion of barrier-isolated populations in genetic analyses can strongly influence patterns of genetic diversity. Isolated populations can be strongly differentiated because of drift, founder effects, or repeated genetic bottlenecks (Nei et al. 1975), all of which can act quickly on small populations existing in isolated habitats (Wofford et al. 2005).

Although N_e tended to be larger among Coast Range populations and in component watersheds, differences were not significant. We believe that the selection of comparably sized watersheds (<1000 ha) above migration barriers allowed the detection of regional genetic differences that may have otherwise been confounded by habitat area-based N_e differences or by gene flow. Recent attempts to use indices of habitat quality and complexity as predictors of genetic diversity have only been marginally successful. For example, a lack of concordance between habitat size and genetic diversity has been reported for lake populations of brook trout (*Salvelinus fontinalis*), presumably because of the difficulty in describing the demographic factors responsible for regulating population size (Hebert et al. 2000; Cas-

© 2008 NRC Canada

tric et al. 2001). Similarly, physical habitat differences (except migration barriers) among populations of bull trout (*Salvelinus confluentus*) were not related to patterns of genetic diversity (Costello et al. 2003). In addition, comparisons among populations with large differences in N_e may obscure the effect of habitat on genetic structuring. Populations with large N_e may be buffered against the stochastic loss or fixation of alleles from the interaction between landscape structure and demographic processes (Costello et al. 2003).

Conservation implications

Findings described here may be applicable to many populations of coastal cutthroat trout. In the steep headwaters of streams, which comprise the majority of the total landscape area in the native range of the subspecies (Shreve 1969), waterfalls are common, and coastal cutthroat trout are often the only fish present. Furthermore, during the process of selecting sampling locations, it was determined that about 10% (269 watersheds out of 2678) of the third-order watersheds in western Oregon contained isolated populations of coastal cutthroat trout (Gresswell et al. 2004). In addition, because 24 of the 27 populations were randomly selected from the larger pool of isolated populations, a scope of inference encompassing all of these isolated populations can be assumed.

Although coastal cutthroat trout exist in relatively abundant assemblages of isolated headwater populations, the effects of downstream gene flow are poorly understood. Small populations encounter strong selection pressures, and heritable differences have been detected between above-barrier and below-barrier populations of rainbow trout and coastal cutthroat trout (Northcote and Hartman 1988). Novel genotypes can develop and occur in high frequency in small isolated populations. In some cases, these novel differences may prove to be adaptive, especially with uncertain future situations (Scudder 1989).

Finally, our findings suggest that headwater populations of coastal cutthroat trout above barriers to migration are genetically differentiated. Hierarchical genetic structuring among populations appears to result more from the effect of regional differences in environmental factors than from genetic dispersal following traditional island (Wright 1969) or stepping-stone models (Kimura and Weiss 1964). Genetic diversity was much higher in the Coast Range than in the Cascades, and this pattern appears to be related to the relative forces of drift and historical gene flow in these different physical environments. Comparisons between landscape structure and genetic diversity suggest that an interaction between stochastic disturbances and physical landscape features may play a substantial role in the structuring of genetic diversity among isolated cutthroat trout populations.

Acknowledgements

The Cooperative Forest Ecosystem Research program, a consortium of Oregon State University, Bureau of Land Management, Oregon Department of Forestry, and the US Geological Survey, financially supported this research. We thank J. Wofford and D. Bateman for many influential discussions throughout this project. We thank D. Jacobson and D. Gomez-Uchida for technical assistance in the lab and for guidance with genetic data analysis. We are also grateful to C. Torgersen and D. Hockman-Wert for assistance with GIS analysis. R. Harrison, D. Markle, J. Nielsen, P. Connolly, A. Zale, and three anonymous reviewers provided comments on earlier versions of this paper. The use of trade, product, or firm names in this publication is for descriptive purposes only and does not imply endorsement by the US Government.

References

Angers, B., Magnan, P., Plante, M., and Bernatchez, L. 1999. Canonical correspondence analysis for estimating spatial and environmental effects on microsatellite gene diversity in brook charr (*Salvelinus fontinalis*). Mol. Ecol. **8**: 1043–1053. doi:10.1046/j.1365-294x.1999.00669.x.

Banks, M.A., Blouin, M.S., Baldwin, B.A., Rashbrook, V.K., Fitzgerald, H.A., Blankenship, S.M., and Hedgecock, D. 1999. Isolation and inheritance of novel microsatellites in Chinook salmon (*Oncorhynchus tshawytscha*). J. Hered. **90**: 281–288. doi:10.1093/jhered/90.2.281.

Banks, M.A., Rashbrook, V.K., Calavetta, M.J., Dean, C.A., and Hedgecock, D. 2000. Analysis of microsatellite DNA resolves genetic structure and diversity of chinook salmon (*Oncorhynchus tshawytscha*) in California's Central Valley. Can. J. Fish. Aquat. Sci. **57**: 915–927. doi:10.1139/cjfas-57-5-915.

Bateman, D.S., Gresswell, R.E., and Torgersen, C.E. 2005. Evaluating single-pass catch as a tool for identifying spatial pattern in fish distribution. Freshwater Ecol. **20**: 335–345.

Behnke, R.J. 1992. Native trout of western North America. American Fisheries Society, Bethesda, Md.

Benda, L., and Dunne, T. 1997. Stochastic forcing of sediment supply to channel networks from landsliding and debris flow. Water Resour. Res. **33**: 2849–2863. doi:10.1029/97WR02388.

Bernatchez, L. 1995. A role for molecular systematics in defining evolutionarily significant units in fishes. *In* Symposium 17: Evolution and the Aquatic Ecosystem: Defining Unique Units in Population Conservation, Monterey, California, May 1994. *Edited by* J.L. Nielsen. American Fisheries Society, Bethesda, Md. pp. 114–132.

Bisson, P.A., Nielsen, J.L., Palmasono, R.A., and Grove, L.E. 1982. A system of naming habitat types in small streams, with examples of habitat utilization by salmonids during low streamflow. *In* Acquisition and utilization of aquatic habitat inventory information. *Edited by* N.B. Armantrout. American Fisheries Society, Western Division, Bethesda, Md. pp 62–73.

Bretz, J.H. 1913. Glaciation of the Puget Sound region. Washington State Geological Survey, Division of Mines and Geology, Olympia, Wash. Wash. St. Geol. Surv. Bull. 8.

Campton, D.E., and Utter, F.M. 1987. Genetic structure of anadromous cutthroat trout *Salmo clarki clarki* populations in the Puget Sound area: evidence for restricted gene flow. Can. J. Fish. Aquat. Sci. **44**: 573–582. doi:10.1139/f87-070.

Carlsson, J., and Nilsson, J. 2001. Effects of geomorphological structures on genetic differentiation among brown trout populations in a northern boreal river drainage. Trans. Am. Fish. Soc. **130**: 36–45. doi:10.1577/1548-8659(2001)130<0036:EOGSOG>2.0.CO;2.

Castric, V., Bonney, F., and Bernatchez, L. 2001. Landscape structure and hierarchical genetic diversity in the brook charr, *Salvelinus fontinalis*. Evolution, **55**: 1016–1028. doi:10.1554/0014-3820(2001)055[1016:LSAHGD]2.0.CO;2. PMID: 11430638.

Castric, V., and Bernatchez, L. 2003. The rise and fall of isolation

© 2008 NRC Canada

by distance in the anadromous brook charr (*Salvelinus fontinalis* Mitchill). Genetics, **163**: 983–996. PMID:12663537.

Connolly, P.J., and Hall, J.D. 1999. Biomass of coastal cutthroat trout in unlogged and previously clear-cut basins in the central Coast Range of Oregon. Trans. Am. Fish. Soc. **128**: 890–899. doi:10.1577/1548-8659(1999)128<0890:BOCCTI>2.0.CO;2.

Costello, A.B., Down, T.E., Pollard, S.M., Pacas, C.J., and Taylor, E.B. 2003. The influence of history and contemporary stream hydrology on the evolution of genetic diversity within species: an examination of microsatellite DNA variation in bull trout, *Salvelinus confluentus* (Pisces: Salmonidae). Evolution, **57**: 328–344. PMID:12683529.

Currens, K.P., Schreck, C.B., and Li, H.W. 1990. Allozyme and morphological divergence of rainbow trout (*Oncorhynchus mykiss*) above and below waterfalls in the Deschutes River, Oregon. Copeia, 1990: 730–746.

Dunham, J.B., Peacock, M., Tracy, C.R., Nielsen, J., and Vinyard, G. 1999. Assessing extinction risk: integrating genetic information. Conservation Ecology [online] **3**(1): 2. Available from www.consecol.org/vol3/iss1/art2 [accessed 8 August 2003].

Ensign, W.E., Leftwich, K.N., Angermeier, P.L., and Dolloff, C.A. 1997. Factors influencing stream fish recovery following a large-scale disturbance. Trans. Am. Fish. Soc. **126**: 895–907. doi:10.1577/1548-8659(1997)126<0895:FISFRF>2.3.CO;2.

Fagan, W.F. 2002. Connectivity, fragmentation, and extinction risk in dendritic metapopulations. Ecology, **83**: 3243–3249.

Felsenstein, J. 2002. PHYLIP: phylogeny inference package. Department of Genetics, University of Washington, Seattle, Wash.

Frissell, C.A., Liss, W.J., Warren, C.E., and Hurley, M.D. 1986. A hierarchical framework for stream classification: viewing streams in a watershed context. Environ. Manage. **10**: 199–214. doi:10.1007/BF01867358.

Goudet, J. 1995. FSTAT version 1.2: a computer program to calculate F-statistics. J. Hered. **86**: 485–486.

Greig, C., Jacobson, D.P., and Banks, M.A. 2003. New tetranucleotide microsatellites for fine-scale discrimination among endangered Chinook salmon (*Oncorhynchus tshawytscha*). Mol. Ecol. Notes, **3**: 376–379. doi:10.1046/j.1471-8286.2003.00455.x.

Gresswell, R.E. 1999. Fire and aquatic ecosystems in forested biomes of North America. Trans. Am. Fish. Soc. **128**: 193–221. doi:10.1577/1548-8659(1999)128<0193:FAAEIF>2.0.CO;2.

Gresswell, R.E., Bateman, D.S., Lienkaemper, G., and Guy, T.J. 2004. Geospatial techniques for developing a sampling frame of watersheds across a region. *In* The Proceedings of the Second International Symposium on GIS in Fisheries Science, University of Sussex, Brighton, UK, 3–6 September 2002. *Edited by* T. Nishida, P.J. Kailola, and C.E. Hollingworth. Fisheries Research Group, Saitama, Japan. pp. 517–530.

Gresswell, R.E., Torgersen, C.E., Bateman, D.S., Guy, T.J., Hendricks, S.R., and Wofford, J.E.B. 2006. A spatially explicit approach for evaluating relationships among coastal cutthroat trout, habitat, and disturbance in headwater streams. *In* Influences of landscapes on stream habitats and biological assemblages. *Edited by* R. Hughes, L. Wang, and P. Seelbach. American Fisheries Society, Bethesda, Md. pp. 457–471.

Griswold, K.E., Currens, K.P., and Reeves, G.H. 1997. Genetic and meristic divergence of coastal cutthroat trout residing above and below barriers in two coastal basins *In* Sea-run cutthroat trout: biology, management, and future conservation. *Edited by* J.D. Hall, P.A. Bisson, and R.E. Gresswell. Oregon Chapter of the American Fisheries Society, Corvallis, Ore. pp. 167–169.

Hansen, M.M., Nielsen, E.E., and Mensberg, K.L.D. 1997. The problem of sampling families rather than populations: relatedness among individuals in samples of juvenile brown trout *Salmo trutta* L. Mol. Ecol. **6**: 469–474. doi:10.1046/j.1365-294X.1997.t01-1-00202.x.

Hanski, I. 1998. Metapopulation dynamics. Nature (London), **396**: 41–49. doi:10.1038/23876.

Hebert, C., Danzman, R.G., Jones, M.W., and Bernatchez, L. 2000. Hydrography and population genetic structure in brook charr (*Salvelinus fontinalis*, Mitchill) from eastern Canada. Mol. Ecol. **9**: 971–982. doi:10.1046/j.1365-294x.2000.00965.x. PMID: 10886659.

Hicks, B.J., and Hall, J.D. 2003. Rock type and channel gradient structure salmonid populations in the Oregon Coast Range. Trans. Am. Fish. Soc. **132**: 468–482. doi:10.1577/1548-8659(2003)132<0468:RTACGS>2.0.CO;2.

Hill, W.G. 1981. Estimation of effective population size from data on linkage disequilibrium. Genet. Res. **38**: 209–216.

Hutchison, D.W., and Templeton, A.R. 1999. Correlation of pairwise genetic and geographic distance measures: inferring the relative influences of gene flow and drift on the distribution of genetic variability. Evolution, **53**: 1898–1914. doi:10.2307/2640449.

Johnson, O.W., Ruckelshaus, M.H., Grant, W.S., Waknitz, F.W., Garret, A.M., Bryant, G.J., Neely, K., and Hard, J.J. 1999. Status review of coastal cutthroat trout from Washington, Oregon, and California. National Oceanic and Atmospheric Administration, Northwest Fisheries Science Center, Seattle, Wash. NMFS Tech. Memo. NMFS-NWFSC 37.

Kimura, M., and Weiss, G.H. 1964. The stepping stone model of population structure and the decrease of genetic correlation with distance. Genetics, **49**: 561–576. PMID:17248204.

Lacy, R.C. 1987. Loss of genetic diversity from managed populations: interacting effects of drift, mutation, immigration, selection, and population subdivision. Conserv. Biol. **1**: 143–157. doi:10.1111/j.1523-1739.1987.tb00023.x.

Lamberti, G.A., Gregory, S.V., Ashkenas, L.R., Wildman, R.C., and Moore, K.M.S. 1991. Stream ecosystem recovery following a catastrophic debris flow. Can. J. Fish. Aquat. Sci. **48**: 196–208. doi:10.1139/f91-027.

Moore, K., Jones, K., and Dambacher, J. 1999. Methods for stream habitat surveys. Oregon Department of Fish and Wildlife, Corvallis, Ore. Aquat. Inventories Proj. Info. Rep. 97-4.

May, C.L., and Gresswell, R.E. 2003. Processes and rates of sediment and wood accumulation in headwater streams of the Oregon Coast Range, USA. Earth Surf. Process. Landforms, **28**: 409–424. doi:10.1002/esp.450.

May, C.L., and Gresswell, R.E. 2004. Spatial and temporal patterns of debris-flow deposition in the Oregon Coast Range, USA. Geomorphology, **57**: 135–149. doi:10.1016/S0169-555X(03)00086-2.

McCauley, D.E. 1991. Genetic consequences of local population extinction and recolonization. Trends Ecol. Evol. **6**: 5–8. doi:10.1016/0169-5347(91)90139-O.

McPhail, J.D. 1967. Distribution of freshwater fishes in western Washington. Northwest Sci. **41**: 1–11.

McPhail, J.D., and Lindsey, C.C. 1986. Zoogeography of the freshwater fishes of Cascadia (the Columbia River and rivers north to the Stikine). *In* The zoogeography of North American freshwater fishes. *Edited by* C.H. Hocutt, and E.O. Wiley. John Wiley and Sons, New York. pp. 615–637.

Montgomery, D.R., and Buffington, J.M. 1997. Channel-reach morphology in mountain drainage basins. Geol. Soc. Am. Bull. **109**: 596–611. doi:10.1130/0016-7606(1997)109<0596:CRMIMD>2.3.CO;2.

Moritz, C. 1994. Defining 'Evolutionarily Significant Units' for

© 2008 NRC Canada

conservation. Trends Ecol. Evol. **9**: 373–375. doi:10.1016/0169-5347(94)90057-4.

Morris, D.B., Richard, K.R., and Wright, J.M. 1996. Polymorphic microsatellites from rainbow trout (*Oncorhynchus mykiss*) and their use for genetic study of salmonids. Can. J. Fish. Aquat. Sci. **53**: 120–126. doi:10.1139/cjfas-53-1-120.

Nehlsen, W., Williams, J.E., and Lichatowich, L.A. 1991. Pacific salmon at the crossroads: stocks at risk from California, Oregon, Idaho, and Washington. Fisheries, **16**: 4–21.

Nei, M., Maruyama, T., and Chakraborty, R. 1975. The bottleneck effect and genetic variability in populations. Evolution, **29**: 1–10. doi:10.2307/2407137.

Neigel, J.E. 2002. Is F_{ST} obsolete? Conserv. Genet. **3**: 167–173. doi:10.1023/A:1015213626922.

Nielsen, J.L., and Sage, G.K. 2002. Population genetic structure in Lahontan cutthroat trout. Trans. Am. Fish. Soc. **131**: 376–388. doi:10.1577/1548-8659(2002)131<0376:PGSILC>2.0.CO;2.

Nielsen, R., and Slatkin, M. 2000. Likelihood analysis of ongoing gene flow and historical association. Evolution, **54**: 44–50. PMID:10937182.

Northcote, T.G., and Hartman, G.F. 1988. The biology and significance of stream trout populations (*Salmo* spp.) living above and below waterfalls. Pol. Arch. Hydrobiol. **35**: 409–442.

Olsen, J.B., Wenburg, J.K., and Bentzen, P. 1996. Semiautomated multilocus genotyping of Pacific salmon (*Oncorhynchus* spp.) using microsatellites. Mol. Mar. Biol. Biotechnol. **5**: 259–272. PMID:8983195.

Omernik, J.M. 1987. Map supplement: ecoregions of the conterminous United States. Ann. Assoc. Am. Geogr. **77**: 118–125. doi:10.1111/j.1467-8306.1987.tb00149.x.

Peel, D., Ovenden, J.R., and Peel, S.L. (2004). NeEstimator: software for estimating effective population size, Version 1.3. Queensland Government, Department of Primary Industries and Fisheries, Queensland, Australia.

Pater, D.E., Bryce, S.A., Thorson, T.D., Kagan, J., Chectaresppell, C., Omernik, J.M., Azevedo, S.H., and Woods, A.J. 1998. Ecoregions of western Washington and Oregon. US Geological Survey, Washington, D.C. Scale 1: 350 000.

Raymond, M., and Rousset, F. 1995. GENEPOP (Version 1.2): population genetics software for exact tests and ecumenicism. J. Hered. **86**: 248–249.

Reeves, G.H., Benda, L.E., Burnett, K.M., Bisson, P.A., and Sedell, J.R. 1995. A disturbance-based ecosystem approach to maintaining and restoring freshwater habitats of evolutionarily significant units of anadromous salmonids in the Pacific Northwest. *In* Symposium 17: Evolution and the Aquatic Ecosystem: Defining Unique Units in Population Conservation, Monterey, California, May 1994. *Edited by* J.L. Nielsen. American Fisheries Society, Bethesda, Md. pp. 334–349.

Reeves, G.H., Bisson, P.A., and Dambacher, J.M. 1998. Fish Communities *In*. River ecology and management. *Edited by* R.J. Naiman and R.E. Bilby. Springer-Verlag, New York. pp. 200–234.

Rice, W.R. 1989. Analyzing tables of statistical tests. Evolution, **43**: 223–225. doi:10.2307/2409177.

Roghair, C.N., Dolloff, C.A., and Underwood, M.K. 2002. Response of a brook trout population and in stream habitat to a catastrophic flood and debris flow. Trans. Am. Fish. Soc. **131**: 718–730. doi:10.1577/1548-8659(2002)131<0718:ROABTP>2.0.CO;2.

Schneider, S., Kueffer, J.-M., Roessli, D., and Excoffier, L. 1997. Arlequin version 1: an exploratory population genetics software environment. Genetics and Biometry Laboratory, University of Geneva, Switzerland.

Scudder, G.G.E. 1989. The adaptive significance of marginal populations: a general perspective. *In* Proceedings of the National Workshop on Effects of Habitat Alteration on Salmonid Stocks, 6–8 May 1987, Nanaimo, B.C. *Edited by* C.D. Levings, L.B. Holtby, and M.A. Henderson. Can. Speci. Publ. Fish. Aquat. Sci. 105. pp 180–185.

Shreve, R.L. 1969. Stream lengths and basin areas in topologically random channel networks. J. Geol. **77**: 397–414.

Southwood, T.R.E. 1977. Habitat, the template for ecological strategies. J. Anim. Ecol. **46**: 337–365.

Swanson, F.J., and Lienkaemper, G.W. 1978. Physical consequences of large organic debris in Pacific Northwest streams. Pacific Northwest Forest and Range Experiment Station, Portland, Ore. USDA For. Serv. Gen. Tech. Rep. PNW-69.

Swanson, F.J., Benda, L.E., Duncan, S.H., Grant, G.E., Megahan, W.F., Reid, L.M., and Ziemer, R.R. 1987. Mass failures and other processes of sediment production in Pacific Northwest forest landscapes. *In* Streamside management: forestry and fishery interactions. *Edited by* E.O. Salo, and T.W. Cundy. University of Washington, Institute of Forest Resources, Seattle, Wash. Contrib. No. 57. pp. 9–38.

Taylor, E.B., Redenbach, Z., Costello, A.B., Pollard, S.M., and Pacas, C.J. 2001. Nested analysis of genetic diversity in northwestern North American char, Dolly Varden (*Salvelinus malma*) and bull trout (*Salvelinus confluentus*). Can. J. Fish. Aquat. Sci. **58**: 406–420. doi:10.1139/cjfas-58-2-406.

Taylor, E.B., Stamford, M.D., and Baxter, J.S. 2003. Population subdivision in westslope cutthroat trout (*Oncorhynchus clarki lewisi*) at the northern periphery of its range: evolutionarily inferences and conservation implications. Mol. Ecol. **12**: 2609–2622. doi:10.1046/j.1365-294X.2003.01937.x. PMID:12969465.

Taylor, P.W., and Roberts, S.D. 1999. Clove oil: an alternative anesthetic for aquaculture. N. Am. J. Aquacult. **61**: 150–155.

Trotter, P.C. 1989. Coastal cutthroat trout: a life history compendium. Trans. Am. Fish. Soc. **118**: 463–473. doi:10.1577/1548-8659(1989)118<0463:CCTALH>2.3.CO;2.

Trotter, P.C., Bisson, P.A., and Fransen, B.R. 1993. Status and plight of the searun cutthroat trout. *In* Genetic conservation of salmonid fishes. *Edited by* J.G. Cloud, and G.H. Thorgaard. Plenum, New York. pp. 203–212.

Wade, M.J., and McCauley, D.E. 1988. The effects of extinction and colonization on the genetic differentiation of populations. Evolution, **42**: 995–1005. doi:10.2307/2408915.

Waples, R.S. 1991. Pacific salmon, *Oncorhynchus* spp., and the definition of a species under the Endangered Species Act. Mar. Fish. Rev. **53**: 11–22.

Waples, R.S. 1995. Evolutionarily significant units and the conservation of biological diversity under the Endangered Species Act. *In* Symposium 17: Evolution and the Aquatic Ecosystem: Defining Unique Units in Population Conservation, Monterey, California, May 1994. *Edited by* J.L. Nielsen. American Fisheries Society, Bethesda, Md. pp. 8–27.

Wenburg, J.K., and Bentzen, P. 2001. Genetic and behavioral evidence for restricted gene flow among coastal cutthroat trout populations. Trans. Am. Fish. Soc. **130**: 1049–1069. doi:10.1577/1548-8659(2001)130<1049:GABEFR>2.0.CO;2.

White, P.S., and Pickett, S.T.A. 1985. Natural disturbance and patch dynamics: an introduction. *In* The ecology of natural disturbance and patch dynamics. *Edited by* S.T.A. Pickett, and P.S. White. Academic Press, Orlando, Fla. pp. 3–13.

Wier, B.S., and Cockerham, C.C. 1984. Estimating F-statistics for the analysis of population structure. Evolution, **38**: 1358–1370.

Wofford, J.E.B., Gresswell, R.E., and Banks, M.A. 2005. Influence of barriers to movement on within-watershed genetic variation

© 2008 NRC Canada

of coastal cutthroat trout. Ecol. Appl. **15**: 628–637. doi:10.1890/04-0095.

Wright, S. 1969. The theory of gene frequencies, Vol 2. University of Chicago Press, Chicago, Ill.

Wydoski, R.S., and Whitney, R.R. 1979. Inland fishes of Washington. University of Washington Press, Seattle, Wash.

Appendix A

Table A1. Thermocycler conditions and reagents used for each multiplex.

		Reagent		
Multiplex[a]	Marker	$MgCl_2$ (mmol·L^{-1})	dNTPs (mmol·L^{-1})	Thermocycler conditions
Set A	*One102*	0.4000	0.1000	94 °C for 180 s
	One103			12 cycles at 94 °C for 60 s + 49 °C for 30 s + 72 °C for 15 s
	One108			15 cycles at 94 °C for 30 s + 49 °C for 30 s + 72 °C for 15 s
				94 °C for 30 s
				49 °C for 30 s
				72 °C for 300 s
Set B	*Omy77*	0.0240	0.1000	92 °C for 300 s
	Ots4			25 cycles at 92 °C for 30 s + 56 °C for 30 s + 72 °C for 30 s
				72 °C for 1800 s
Set C	*Ots209*	0.4000	0.0625	94 °C for 180 s
	Ots212			32 cycles at 94 °C for 30 s + 63 °C for 20 s + 72 °C for 30 s
				72 °C for 120 s

[a]All PCR reactions were conducted in 5 μL volumes using 1 μL DNA template, 0.25 μL enhancer mix (830 μL H_2O, 20 μL Tween, 50 μL bovine serum albumin (BSA) (20 mg·mL^{-1})), 100 μL formamide, and 5 μL Tris–KCl buffer (Set A and B) or Promega 10× buffer (Set C).

© 2008 NRC Canada

PERSPECTIVE / PERSPECTIVE

A preliminary national analysis of some key characteristics of Canadian lakes

Charles K. Minns, James E. Moore, Brian J. Shuter, and Nicholas E. Mandrak

Abstract: Knowledge of Canada's lakes is needed to manage environmental stresses. Lake inventory and lake feature databases were used to build a national impact assessment template and assess regional typology. There are ~910 400 lakes with area ≥ 0.1 km^2 (10 ha), 37% of the Earth's total. Lake features (number of lakes by size class, maximum depth, mean–maximum depth ratio, Secchi depth, pH, and total dissolved solids) were modeled regionally by secondary watershed (SWS) using linear regression models. Lake trout (*Salvelinus namaycush*) occurrence was analyzed as a cofactor to highlight regional links between lake characteristics and aquatic biota. Significant (R^2 from 0.231 to 0.492) regional models were obtained using area or maximum depth, lake trout occurrence, and their cross products as covariates. Analyses of fitted SWS coefficients showed that ecozones were a better predictor of lake characteristics than primary watersheds. The national typology was consistent with previous regional assessments. The regional models were used to estimate the number, area, and volume of lake trout lakes by size class and ecozone. There are ~66 500 lake trout lakes covering ~3 510 000 km^2 primarily on Boreal and Taiga Shield areas. Regional lake resource models will enable national assessment of stresses such as climate change and invasive species.

Résumé : Il est essentiel de connaître les lacs canadiens afin de pouvoir gérer les stress de l'environnement. Nous avons utilisé des banques de données d'inventaire des lacs et des caractéristiques lacustres afin de bâtir une matrice nationale d'évaluation des impacts et d'évaluer la typologie régionale. Il y a ~910 400 lacs à superficie ≥ 0,1 km^2 (10 ha), soit 37 % du total mondial. Nous avons modélisé les caractéristiques lacustres (nombre de lacs par classe de taille, profondeur maximale, rapport des profondeurs moyenne–maximale, profondeur de Secchi, pH et solides dissous totaux) par région en fonction des bassins versants secondaires (SWS) à l'aide de modèles de régression linéaire. Nous avons analysé la présence du touladi (*Salvelinus namaycush*) comme co-facteur pour souligner les liens régionaux entre les caractéristiques lacustres et les organismes. Nous avons obtenu des modèles régionaux significatifs (R^2 de 0,231 à 0,492) en utilisant la superficie, ou la profondeur maximale, la présence du touladi et leurs produits croisés comme covariables. Des analyses des coefficients SWS ajustés montrent que les écozones sont de meilleures variables prédictives des caractéristiques lacustres que les bassins versants primaires. La typologie nationale s'accorde aux évaluations régionales antérieures. Les modèles régionaux ont servi à estimer le nombre, la superficie et le volume des lacs à touladis par classe de taille et par zone. Il y a ~66 500 lacs à touladis couvrant ~3 510 000 km^2, principalement dans les régions boréales et la taïga sur le bouclier canadien. Les modèles régionaux de ressources lacustres permettront une évaluation nationale des stress, tels que le changement climatique et les espèces envahissantes.

[Traduit par la Rédaction]

Received 16 August 2007. Accepted 12 March 2008. Published on the NRC Research Press Web site at cjfas.nrc.ca on 1 August 2008. J20138

C.K. Minns[1,2] **and N.E. Mandrak.** Great Lakes Laboratory for Fisheries and Aquatic Science, Fisheries and Oceans Canada, P.O. Box 5050, 867 Lakeshore Road, Burlington, ON L7R 4A6, Canada.
J.E. Moore. JEMSys Software Systems Inc., 22 Marion Crescent, Dundas, ON L9H 1J1, Canada.
B.J. Shuter. Department of Ecology and Evolutionary Biology, University of Toronto, Toronto, ON M5S 3B2, Canada; Harkness Laboratory of Fisheries Research, Aquatic Ecosystem Science Section, Ontario Ministry of Natural Resources, 300 Water Street, Peterborough, ON K9J 8M5, Canada.

[1]Corresponding author (e-mail: ken@minns.ca).
[2]Present address: Department of Ecology and Evolutionary Biology, University of Toronto, 25 Willcocks St., Room RW417, Toronto, ON M5S 3B2, Canada.

 doi:10.1139/F08-110 © 2008 NRC Canada

Introduction

Canada has a great abundance of lakes, representing the largest national share of the Earth's readily accessible freshwater resources (Minns and Moore 1995; Downing et al. 2006); however, Schindler (2001) has pointed to the growing realization that much of Canada's freshwater resources are under pressure from a multitude of stressors. Chu et al. (2003) presented a national assessment of stressors affecting Canada's freshwater fishes showing a clash of human-driven development pressures and conservation needs mainly along the southern margin of the country, whereas climate change is already impacting the northern regions of Canada (Reist et al. 2006). Minns (2001), reporting on the science of freshwater fish habitat management in Canada, noted the poor state of knowledge of our freshwater ecosystems. Among eight priorities for the future, Minns identified the need for increased efforts on pattern recognition and inventory to "address the longer-term need for documentation of resource properties and change over the vast areas of freshwater habitat in Canada." To expand the scope for assessing the existing and potential cumulative impacts of human stresses on freshwater fishes and their ecosystems, there is a need to deploy all available information to characterize our freshwater ecosystems. Lakes, which account for the majority of freshwater resources and fisheries production, are impacted by many human activities and are the focus of this study. This characterization of lakes must span large regions as the spatial scale of threatening environmental disturbances like climate change and invasive species (Jensen et al. 1996) and of resource management challenges like eutrophication and overfishing (Carpenter et al. 1999; Post et al. 2002; Lester et al. 2003) increases.

Regional, or synoptic, limnology has a long history. Early in the 20th century, Naumann (1929) explored the imprint of landscape on Swedish lakes following ideas laid down earlier (cf. Rawson 1939). Most synoptic studies of lakes have concentrated on small localities, although more recently, larger lake districts have been gaining more attention (Kratz and Frost 2000). Again in Sweden, Hakanson (1996) advanced an approach and techniques for modelling key lake variables from map-based information. Since 2000, several European countries have been working to develop a lake typology in response to a European Union directive on water policy (Moss et al. 2003). In addition to developing a pan-European typology, individual countries have been developing national typologies, e.g., Poland (Kolada et al. 2005) and Finland (Nykänen et al. 2005).

In Canada, localized synoptic limnology might be exemplified by the studies at the Experimental Lakes Area in northwestern Ontario and in the Laurentian region of Quebec (cf. Minns 2001). Contributed papers in Frey (1963) provide much of the history of regional lake typology in Canada. Regional efforts are exemplified by the early classification work of Northcote and Larkin (1956) in British Columbia, by the assessments in the 1980s of the impacts of acidic deposition on lakes east of the Ontario–Manitoba border and south of latitude 52° (Kelso et al. 1990), and more recently, the surveys of lakes by John Smol and his associates across the Taiga and Arctic regions of Canada and elsewhere (cf. Ruhland and Smol 1998). There have been no previous attempts to study synoptic limnology across the whole of Canada.

This study has three components: (*i*) a statistical representation of Canada's lake resources for use as a template in a national-scale impact assessment model; (*ii*) an assessment of regional typology for Canadian lakes; and (*iii*) a pilot demonstration of the potential use of the regional lake characteristic models for assessment and management. Although the lakes were the primary focus, lake trout (*Salvelinus namaycush*) occurrences by region and lake were examined as an example of how biota might be incorporated into models of lake characteristics. The first component addresses the need to characterize Canada's lake resources with approaches advocated by Minns (2001) and outlined by Hakanson (1996). The numerical models will subsequently be used to facilitate national assessments of the likely impacts of climate change on fishery resources. The second component lays the foundation for an aquatic ecological classification system for Canada's freshwater lake resources. The third component provides first-order estimates of the extent of lake trout resources in Canada.

Materials and methods

Canadian secondary watersheds and ecozones

Watershed units are the preferred basis for organizing regional data on freshwater ecosystems as it is through the drainage networks of watersheds that freshwaters are connected and flow and, thereby, energy and nutrients move. Watersheds also helped establish the distributions of many freshwater biota. Canada has a hierarchical scheme of watersheds with 11 primary, 164 secondary, and 953 tertiary units. The primary watersheds are determined by which ocean the largest rivers drain toward, and the secondary and tertiary watersheds represent sub- and sub-sub-drainages of the primary river systems. We chose the secondary watershed (SWS) as the basic unit for aggregation and analysis of lake patterns (Fig. 1*a*). They provide a readily manageable number of units while providing broad representative coverage of watersheds and landscape features, e.g., ecozones, that vary across Canada. Canada has a terrestrial ecological classification system (Ecological Stratification Working Group 1996) that is based on landscape features (geology, soils, terrestrial vegetation, and climate). There are 15 ecozones (Fig. 1*b*), and most SWS lie predominantly within a single ecozone (mean percentage of any SWS in one ecozone is 83.1%, the minimum is 45.7%, and 31.7% of SWS lie wholly in a single ecozone). Most of the SWS with lower dominant percentages straddle the Northern Arctic and Arctic Cordillera ecozones. We examine to what extent a regional lake typology was consistent with the terrestrial ecozonation.

Number of lakes

There are an estimated 90 358 lakes with area ≥ 1 km^2 (100 ha) in Canada in the Global Lakes and Wetlands Database (GLWD; www.wwfus.org/science/data.cfm). Lehner and Doll (2004) showed that lakes with area < 1 km^2 have not been completely inventoried, primarily because of the limited resolution of available maps. Our first objective was to estimate, by secondary watershed (SWS), the numbers of

© 2008 NRC Canada

Fig. 1. Maps of Canada showing (*a*) primary (PWS) and secondary (SWS) watersheds and (*b*) terrestrial ecozones (in *a*, PWS are outlined in black lines and SWS are outlined in shaded lines; in *b*, Taiga and Boreal regions are cross hatched NW–SE and SW–NE, respectively).

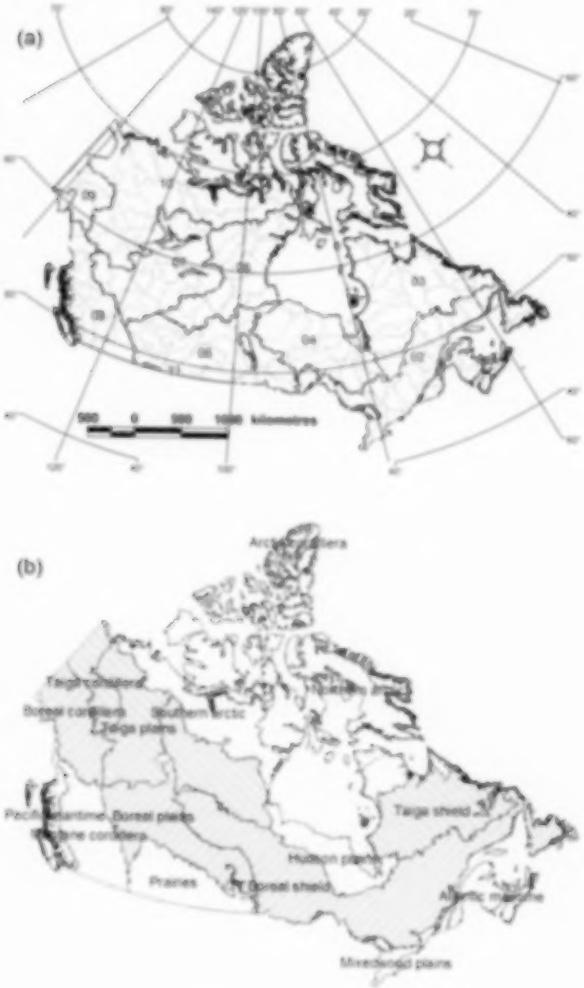

lakes in a semilogarithmic series of size classes starting at 0.1 km^2 and with boundary limits at 0.2, 0.5, 1.0, 2.0, 5.0, 10.0, 20.0, 50.0, and 100.0 km^2.

In their global analysis of aggregated lake size data, Lehner and Döll (2004) showed that observed distributions followed the function, $N_{a\geq A} = aA^{\beta}$, where N is the number of lakes with area (a) greater than or equal to a threshold area (A). This function approximates the Pareto distribution, which has been shown to be useful in many fields (Vidondo et al. 1997). Downing et al. (2006) used the Pareto distribution model to estimate the global abundance and size distribution of lakes. Here, a similar approach is used to estimate, by secondary watershed, the numbers of lakes in the smaller lake size classes that are underassessed in available estimates of the numbers of lakes in Canada.

The GLWD data for Canada were used to estimate the Pareto distribution parameters using the logarithmic version of the equation: $\mathrm{Ln}(N) = \mathrm{Ln}(\alpha) + \beta\mathrm{Ln}(A)$ with a common slope, β, and categorical variables for SWS units. The lake data were attributed with secondary watershed identifiers using ESRI's Arcview 3.3 GIS, and the data were grouped into a semilogarithmic series of lake-area size classes delimited by 1, 2, 5, 10, 20, 50, and 100 km^2. Lehner and Döll showed that counts below 1 km^2 were incomplete.

Estimates of the numbers and size distribution of Canadian lakes by SWS were derived by combination of estimation for smaller lakes and summary for larger lakes. The regression equations obtained with the Pareto distribution analysis were used to estimate numbers of lakes in the area size intervals 0.1–0.2, 0.2–0.5, and 0.5–1.0 km^2 for all secondary watersheds. A bias correction (exp(EMS/2), where EMS is the error mean square from the Ln–Ln regression) was applied to adjust for the data transformation effect (Sprugel 1983). The average lake area in each size class was estimated using eq. 8 in Downing et al. (2006). For the size-class intervals 1.0–2.0, 2.0–5.0, 5.0–10.0, 10.0–20.0, 20.0–50.0, and 50.0–100.0 km^2, the numbers and areas of lakes used were those reported in the GLWD data. By size class and secondary watershed, an average lake area was computed as the ratio of total area and number. For lakes with area ≥ 100.0 km^2, individual lakes with areas reported by S. Wang and A. Davidson (Canada Centre for Remote Sensing, Ottawa, Ontario, Canada, unpublished data) were assigned by secondary watershed.

National lakes database

Data about lakes, including name and identification data, latitude and longitude (or northing and easting), lake area, elevation above sea level, maximum and mean depth, Secchi depth, pH, conductivity, and total dissolved solids (TDS), were gathered from a wide range of government agency sources and supplemented by published material (Appendix A, Table A1 and references therein). These lake characteristics are ones that have been frequently included in models of lake productivity (Hakanson 1996). Records of the presence of lake trout (*S. namaycush*) were also summarized by tertiary watershed from a national fish distribution database (N.E. Mandrak, unpublished data). These sources were supplemented with data from published literature, particularly for larger lakes. Nicholson and Moore's (1988) bibliography of Canadian freshwater limnology and fisheries was especially useful for locating older sources of lake data.

As any single source of data rarely included all parameters of interest, we attempted to use lake name, geographic coordinates, and any identification information to match data from multiple sources by lake. Where multiple values of particular parameters were obtained for a single lake, we established a hierarchy for valuing data sources when choosing a value. Generally, we ranked the larger, more established, data sets more highly that smaller ones and ranked more recent data more highly than older data. The source data sets were assembled in a Microsoft Access database and procedures were written to implement the matching and selection process. This meant that the software remained open-ended, allowing the addition of new data sets and parameters in the future. As a minimum requirement, we specified that every lake selected must have a lake area and

© 2008 NRC Canada

geographic coordinates. Once a composite lake data set had been assembled, the records were attributed with tertiary watershed, ecozone, and province or territory membership. The reduced data set was then screened for inconsistencies such as mean–maximum depth ratios ≥ 1 or Secchi depth that exceeded maximum depth. Such data entries were deleted. Although the record of lake trout occurrences was clearly incomplete, lakes without a recorded occurrence were treated as denoting an absence in the analyses reported here.

As of 30 January 2007, there were 50 262 individual lake data records with one or more selected parameters in the database. After selection and consolidation of that information, there was a reduced data set of 16 950 lake data records with one or more of the selected parameters. The level of matching success was relatively low, reflecting the lack of standardization of lake names, the inconsistent application of identification systems, and inaccuracies and imprecision in geographic coordinates. Existing naming conventions for Canadian topographical features such as lakes do not cover all sizes of lakes. Often different agencies within, and between, levels of government have established independent identification systems that cannot be cross-matched. Much of the data were gathered and recorded before the advent of more recent global positioning system (GPS) and geographic information system (GIS) technologies with the result that locations are often only recorded by degrees and minutes of latitude and longitude, leaving a wide margin for error both in location of the sites and in matching data from multiple sources. Resource limitations meant that not all identifiable data could be included in the current version of the database.

Modelling lake morphometry and water quality characteristics

Regional patterns in lake parameters (maximum depth (Z_{max}), mean to maximum depth ratio (Z_{ratio}), Secchi depth (Secchi), pH, and total dissolved solids (TDS)) were modeled via least-squares regression equations. To reduce the size-related dispersion of points in some lake parameters lake area (Area), Z_{max}, Z_{ratio}, Secchi, and TDS were transformed to natural logarithms (Ln). Z_{ratio} was modeled rather than mean depth, as it is a key parameter in a model of hypsometric curves linking area to depth in lakes (Lester et al. 2004). The approach was to model each dependent lake parameter as a function of Area (or Z_{max}), the presence (1) or absence (0) of lake trout, and the cross product of Area or Z_{max} with lake trout presence or absence as the independent variables. This approach allowed for the possibility that both the intercept and slope might provide information about differences between lakes with, and without, lake trout. Lake size characteristics like Area and Z_{max} are involved in many predictive models for lakes (Leach and Herron 1992). The basic models were then extended to consider regional variation by inclusion of primary (PWS) or secondary (SWS) watershed membership as dummy variables; an overall intercept was included in the regression model along with coefficients for all but one of the dummy variables.

The models were fitted using linear least-squares regression. Final model selection was based on consideration of R^2, the minimization of the EMS and the residual sum-of-squares, the significance of the constituent parameters, and the corrected Akaike information criterion (AIC_c) (Hurvich and Tsai 1989; Burnham and Anderson 2004), with watersheds or ecozones being taken altogether in a single step. The emphasis in model selection was on parsimony, recognizing that regional models must often rely on a minimal number of input parameters as many are rarely available extensively. Posteriori testing of differences among fitted primary or secondary watershed, or ecozone coefficients, was not undertaken as the intent of the modelling was to characterize regional variables in lake characteristics and not to generate a minimal set of regional groups.

As there were a number of SWS with no data for each key parameter, a method of estimating missing SWS values in the lake parameter models was devised. The available estimated SWS coefficients for each parameter were grouped by either PWS or ecozone, and an analysis of variance was performed. In one instance, pH was modeled with the TDS coefficient as a covariate as the pH coverage was much less than that of other parameters. AIC_c was used to choose between the PWS and ecozone models. The selected model was used to estimate the missing SWS values and generate an overall picture of how each parameter varied across Canada.

Lake trout distribution

Lake trout were chosen as a working example of an aquatic species of interest because this study was part of ongoing work to examine the potential impact of climate change and other stressors on key fishery species in Canadian lakes. The occurrence of lake trout in lakes was examined in three ways. First, a national distribution database (N.E. Mandrak, unpublished data) was used to determine the occurrence by tertiary watershed (TWS) using all available records from lakes and rivers. Occurrence was summarized by secondary watershed as the percentage of TWS units with lake trout present (WS%). Second, all lakes within TWS with one or more occurrences of lake trout were selected as a subset of the national lakes database. Using that subset, the percentage of lakes with lake trout present (LK%) was estimate by SWS. Not all SWS had a sample size of lakes (N_{SWS}) sufficient to produce a reliable estimate of LK%. Where WS% was greater than 0.0 and $N_{SWS} < 10$, a composite estimate of LK% was obtained from the available data and used to fill SWS gaps. The product of WS% and LK% provided an overall estimate of the percentage of all lakes with lake trout present by secondary watershed.

Third, as the percent occurrence of lake trout varies with lake size, an independent analysis was performed to derive a means of scaling the overall SWS occurrences (WS%-LK%) by lake size class. There were insufficient data across the species range to support any analysis supporting both location and lake size simultaneously. The analysis here assumed that all the subset of the database could be used to estimate the variation in occurrence by size class as an odds ratio applied to the SWS mean (WS%-LK%). By size class, we estimated the percentage of lakes with lake trout (SZ%) and expressed the SZ% values as odds ratios (SZ_{ratio}) against the overall value obtained. Then adjusted LK% (size class) values were computed as $(LK\%\text{-}SZ_{ratio})/(LK\%\text{-}SZ_{ratio} + (1 - LK\%)1)$. Then WS%-LK% (size class) gives the estimated

© 2008 NRC Canada

proportion of lake trout lakes by SWS and size class. Lakes with area ≥ 100 km^2 were assumed to be completely enumerated with respect to lake trout occurrence.

Lake and lake trout resources

The models obtained in the previous sections were used in combination to estimate the number, area, and for lake trout lakes, volume of lakes by secondary watershed and size class. Bias corrections were applied where the equations involved Ln transformations (Sprugel 1983). These values were summarized across all size classes and across all ecozones. By size class, the extent of lake trout resources was also tallied for Boreal and Taiga Shield ecozones to assess the contribution of the Shield to the total. By ecozone, the extent of lake trout resources was summed both above and below the 100 km^2 area threshold.

Results

Numbers of lakes

Three (8P, 9E, and 9M) of 164 secondary watersheds (SWS) had no lakes according to the GLWD database. The largest portions of these watersheds are outside of Canada. Analysis of covariance of the regression model of Ln(N) with Ln(A) as a covariate and SWS as a categorical variable produced the following results: $F_{\mathrm{Ln}(A)}$ = 13 425.7 (df = 1,880) and F_{SWS} = 59.7 (df = 160,880), both significant at $P < 0.001$. (EMS = 0.17884, giving a bias correction of exp(EMS/2) = 1.094 when detransforming and estimating numbers of lakes.) The slope was –1.032, with SWS intercept values ranging between 1.051 (~34 lakes > 0.1 km^2) and 8.188 (~42 375 lakes > 0.1 km^2), with a mean of 5.245 (~2674 lakes > 0.1 km^2) (Fig. 2). The slope lies above the mean value, –0.89, reported for regional estimates (Downing et al. 2006) but very close to the global value, –1.06, obtained by Lehner and Doll (2004). Applying the resulting equations across all Canadian secondary watershed and summing the results, the numbers of lakes are 910 371 with area ≥ 0.1 km^2 (10 ha) and 84 516 with area > 1.0 km^2. Using Downing et al.'s (2006) global estimate of the number of lakes, Canada holds 36.8% of the Earth's total.

The area with the highest number of lakes is on the Canadian Shield centered on Hudson's Bay (Fig. 2). The lowest number of lakes is mainly found in the Plains region between the Shield and the mountain ranges between Alberta and British Columbia in the west and in the Maritime regions on both coasts.

National lakes database

The number of data values varied from a low of 8741 for pH to 16 949 for Area (Table 1). All parameters had considerable ranges. Depending on the lake parameter, there were data in 106 to 138 of 164 SWS, although there were from 10 to 20 with a single value. All lake parameters spanned considerable ranges, as expected for a national data set covering from the smallest to largest lakes across the regions of Canada. All but one (Ln(Z_{max}) vs. pH) of the pairwise Pearson correlations were highly significant at $P < 0.001$ (Table 2). The highest correlations were between Ln(Z_{max}) and Ln(Z_{mean}) (0.924), followed by pH and Ln(TDS) (0.694), and those of Ln(Z_{max}) and Ln(Z_{mean}) with Ln(Secchi) (>0.57). Correlations of pH and Ln(TDS) with lake dimensions were lower than those among lake metrics.

Fig. 2. Estimated number of lakes, with area >0.1 km^2, by secondary watershed based on the intercept of the Pareto model of lake frequency (Ln($N_{\mathrm{cc}A}$)) versus area (Ln(A)) for Canadian lakes.

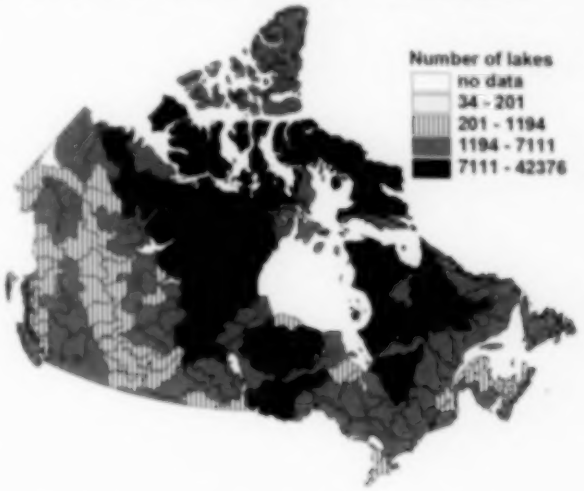

Lake morphometry and water quality models

In many instances, there were obvious variations in the distributions of lake variables both regionally, using primary watersheds to illustrate, and with or without the presence of lake trout (Fig. 3). Lake area, maximum depth, and Secchi depth were consistently greater when lake trout were present (Figs. 3*a*, 3*b*, and 3*d*). There was also much regional variation in some variables, notably pH, Ln(TDS), and mean–maximum depth ratio (Figs. 3*c*, 3*e*, and 3*f*). pH values were markedly lower in primary watersheds 01 and 02 in the southeastern quadrant of Canada, the area most impacted by acidic deposition (Kelso et al. 1990). TDS distributions included much higher values in primary watersheds 05 and 08 in the central Canadian Prairies and Plains where saline lakes are most prevalent.

Predictive models were developed for all lake characteristics (Table 3). AIC$_c$ was used to guide selection of the simplest regional model using covariates. For Z_{max}, Z_{ratio}, and Secchi, the parameters included produced large increases in the R^2 and noticeable reductions in EMS. For pH, addition of parameters beyond Area made little difference to R^2 and EMS. For TDS, all covariate models explained very little of the variance and so no covariate was included. All covariates included and secondary watershed (SWS) factors were significant at $P < 0.001$. In every case, comparison of model fits without watersheds, with primary watersheds (PWS), or with SWS showed that with SWS produced the best fit (R^2, EMS) and improved fit (AIC$_c$) compared with the other choices (Table 4). Not all covariates were included in every model. Lake trout presence or absence (LTPA) was included in the models of Z_{max}, Z_{ratio}, and Secchi; Area was included for Z_{max} and pH; and Z_{max} was used for Z_{ratio} and Secchi. Area was a good predictor of Z_{max}, but Z_{max} was the better predictor for other important depth-related parameters. The

© 2008 NRC Canada

Table 1. Summary statistics for Canadian lake characteristics indicating the number of SWS with data ($n > 0$) and with a single value ($n = 1$).

Parameter	*N*	Minimum	Maximum	Mean	SD	No. of SWS with data ($n > 0$)	No. of SWS with a single value ($n = 1$)
Area (km^2)	16 949	0.001	82 900.000	27.749	909.376		
Z_{max} (m)	16 605	0.200	614.000	18.276	23.045	138	10
Z_{mean} (m)	14 059	0.100	172.000	6.589	8.827		
Z_{ratio}	13 767	0.005	1.000	0.374	0.126	113	13
Ln(Area)	16 949	−11.859	11.325	−0.464	2.022		
Ln(Z_{max})	16 605	−1.609	6.420	2.467	0.957		
Ln(Z_{mean})	14 059	−2.303	5.147	1.482	0.877		
Secchi (m)	14 348	0.100	41.050	3.857	2.348	129	19
Ln(Secchi)	14 348	−2.303	3.715	1.176	0.619		
pH	8 741	3.030	11.000	7.063	0.956	106	20
TDS (mg·L^{-1})	12 858	1.000	84 314.000	100.628	966.395	126	13
Ln(TDS)	12 858	0.000	11.342	3.882	0.926		

Table 2. Pearson correlations among pairs of parameters in Canadian lakes.

Parameter	Ln(Area)	Ln(Z_{max})	Ln(Z_{mean})	Z_{ratio}	Ln(Secchi)	pH	Ln(TDS)
Ln(Area)		**0.458**	**0.405**	**−0.162**	**0.052**	**0.085**	**−0.047**
Ln(Z_{max})	16 605		**0.924**	**−0.334**	**0.576**	0.024	**−0.146**
Ln(Z_{mean})	14 059	13 767		**0.035**	**0.579**	**0.121**	**−0.138**
Z_{ratio}	13 767	13 767	13 767		**−0.098**	**0.067**	**0.091**
Ln(Secchi)	14 348	14 234	12 589	12 480		**0.036**	**−0.118**
pH	8 741	8 729	7 368	7 357	7 646		**0.694**
Ln(TDS)	12 858	12 745	11 788	11 681	12 219	6 350	

Note: Upper right matrix is the correlation; lower left matrix is the number of data pairs; Bonferroni-corrected significance at $P < 0.001$ is presented in bold.

cross-product term Z_{max}-LTPA was only retained in the Secchi model. No covariates were included in the TDS model. The lake size coefficients were positive in the Z_{max}, Secchi, and pH models. The coefficients for LTPA were positive, indicating higher values with lake trout present. In the Secchi model, the cross-product term indicated that although Secchi depths were generally higher in lake trout lakes, the slope of the relationship with Z_{max} was lower. This indicates that Secchi values are higher in shallower lake trout lakes but converge to similar values regardless of lake trout presence in deeper lakes.

The available estimated SWS coefficients were grouped by both primary watershed (PWS) and ecozone. Analysis of variance models examined as a basis for completing the mapped coverage of each lake parameter showed that ecozone was a better predictor than primary watershed membership (Table 5). This was also true for the Pareto intercept coefficients in the model of lake numbers by SWS. The ecozone models were used to estimate missing values for five lake characteristics.

Overall, data for the five lake parameters were most available along the southern parts of Canada (Figs. 4*a*, 4*c*, 5*a*, 5*c*, and 5*e*) with the greatest abundance in Ontario and British Columbia. The areas with the least data were concentrated in northern Quebec and Labrador and in the eastern Arctic. Those areas with the least or no data, and hence with estimated SWS coefficients, will be the most unreliable. However, there are discernible patterns across the country.

The spread of SWS coefficient means across ecozones reveals much of the spatial structure of lake characteristics in Canada (Fig. 6). Allowing for Area via the covariate fitting, there are three main areas of lakes with greater Z_{max}: along the edge of the St. Lawrence drainage (PWS 02), in the west in British Columbia and Yukon (Pacific-Maritime and Montane Cordillera ecozones), and in the northern mainland areas of the western Arctic (Taiga Cordillera and Southern Arctic ecozones) (Fig. 4*b*). Allowing for Z_{max}, the lower Z_{ratio} values are concentrated on the Canadian Shield south of Hudson's Bay and the higher values are concentrated in the west and north of the country, particularly in the Taiga Cordillera and Plains (Fig. 4*b*). Higher Secchi depths are more prominent in the far northern regions, whereas lower values are more common on the Prairies and through Boreal and Taiga Plains (Fig. 5*b*). pH values were generally lower on the Canadian Shield, with the lowest values occurring in those areas most affected by acidic deposition in southern Newfoundland and Nova Scotia and south-central Ontario (Fig. 5*d*). The higher pH values were found in the Prairies and Boreal and Taiga Plains. TDS values were higher on the Prairies and Boreal Plains and lower in eastern parts of Canada, particularly in Quebec and Labrador on the Canadian Shield (Fig. 5*f*).

Lake trout distribution

The distribution records for lake trout, and many other fish species, in Canada were insufficient to allow a definitive mapping of occurrence at this time. In the more remote regions of the country, considerable effort would be required

© 2008 NRC Canada

Fig. 3. Box plots showing the distributions of lake characteristics by primary watershed (PWS) and absence–presence of lake trout: (*a*) Ln(lake area, km²), (*b*) Ln(maximum depth, m), (*c*) mean–maximum depth ratio, (*d*) Ln(Secchi depth, m), (*e*) pH, and (*f*) Ln(TDS, mg·L⁻¹). (Lake trout absence on the left and presence on the right of each PWS marker.)

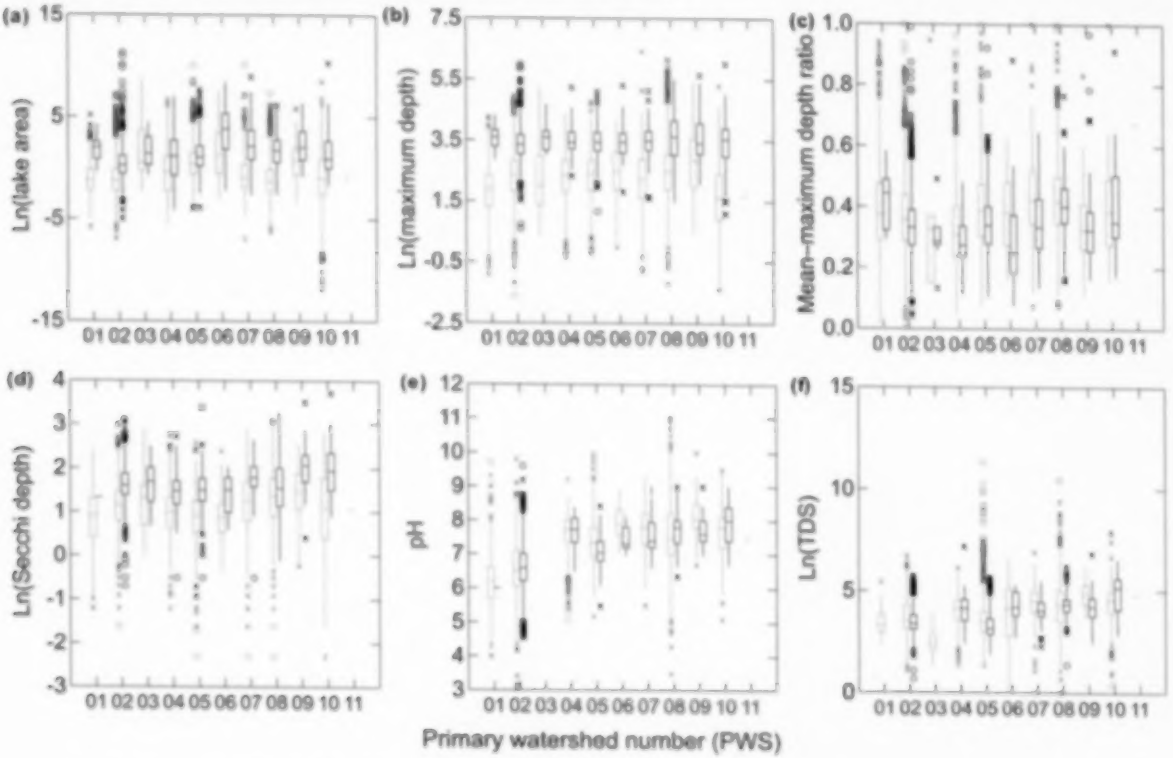

Table 3. Linear regression models of key lake characteristics, maximum depth (Z_{max}), mean to maximum depth ratio (Z_{ratio}), Secchi depth (Secchi), pH, and total dissolved solids (TDS), by secondary watershed (SWS) with covariates (lake area (Area), lake trout presence or absence (LTPA), Z_{max}).

Dependent	Source	Coefficient	*N*	df	Mean-square	*F* ratio	Probability	R^2
Ln(Z_{max})	SWS	*		137	14.438	28.51	<0.001	
	Ln(Area)	0.1949		1	1587.716	3135.23	<0.001	
	LTPA	0.7765		1	1044.438	2061.61	<0.001	
	Error		16 605	16 465	0.506			0.4519
Z_{ratio}	SWS	*		112	0.228	18.63	<0.001	
	Ln(Z_{max})	–0.0570		1	24.532	2005.57	<0.001	
	LTPA	0.0253		1	0.862	70.50	<0.001	
	Error		13 767	13 652	0.012			0.2310
Ln(Secchi)	SWS	*		128	3.509	15.72	<0.001	
	Ln(Z_{max})	0.3617		1	925.188	4145.32	<0.001	
	LTPA	0.5826		1	18.774	84.12	<0.001	
	Cross†	–0.1368		1	11.879	53.23	<0.001	
	Error		14 234	14 102	0.223			0.4215
pH	SWS	*		105	36.943	78.59	<0.001	
	Ln(Area)	0.0528		1	57.989	123.36	<0.001	
	Error		8 741	8 634	0.470			0.4924
Ln(TDS)	SWS	*		125	35.021	67.66	<0.001	
	Error		12 858	12 732	0.523			0.3969

*See Figs. 4 and 5 for maps showing the distributions of fitted SWS coefficients.
†Cross product of Ln(Z_{max}) and LTPA.

© 2008 NRC Canada

Table 4. Comparison of fit statistics for models of lake characteristics without or with primary (PWS) or secondary (SWS) watershed coefficients.

Modeled character	Covariates	Watershed variables*	AIC_c†	Error mean square	R^2
Z_{max}	Area	None	−7 896.1	0.621	0.3219
	LTPA	PWS	−9 183.6	0.575	0.3732
		SWS	−11 154.3	0.506	0.4519
Z_{ratio}	Z_{max}	None	−58 775.5	0.0140	0.1135
	LTPA	PWS	−60 189.2	0.0126	0.2012
		SWS	−60 507.3	0.0122	0.2310
Secchi	Z_{max}	None	−19 571.2	0.253	0.3389
	LTPA	PWS	−20 161.3	0.242	0.3667
	Z_{max}:LTPA	SWS	−21 211.4	0.223	0.4215
pH	Area	None	−836.8	0.908	0.0070
		PWS	−4 754.7	0.580	0.3672
		SWS	−6 487.2	0.470	0.4924
TDS	None	PWS	−3 348.0	0.770	0.1031
		SWS	−8 217.9	0.522	0.3969

*None, model with covariates but no watershed variables.

†$AIC_c = AIC + 2K(K + 1)/(N - K - 1)$ and $AIC = N \cdot Ln(RSS/N) + 2K$, where RSS is residual sum of squares, N is sample size, and K is the number of parameters fitted (Hurvich and Tsai 1989; Burnham and Anderson 2004).

Table 5. Model selection results for estimating missing secondary watershed values for key lake characteristics based on regression models with primary watersheds (PWS) or ecozones as the determining factor.

		PWS			Ecozone		
Lake character	N	R^2	K	AIC_c	R^2	K	AIC_c
Pareto lake numbers	161	0.332	12	56.10	0.591	15	−15.79
Maximum depth (Z_{max})	138	0.330	12	−151.82	0.372	15	−153.43
Mean–maximum depth ratio (Z_{ratio})	113	0.226	12	−522.10	0.280	15	−527.69
Secchi depth (Secchi)	129	0.167	12	−175.81	0.236	15	−179.49
pH	106	0.323	11	−123.27	0.473	15	−139.17
pH (with TDS as a covariate)	96	0.526	12	−137.81	0.584	16	−139.24
TDS	126	0.456	12	−2.71	0.673	15	−59.27

Note: N is number of SWS and K is the number of parameters.

to delimit lake trout distribution by tertiary watershed and to determine the proportion of lakes with the species present. The available occurrence records by TWS indicated that lake trout are widely distributed on the Boreal Shield and Taiga Shield and on the Montane and Boreal Cordillera (Fig. 7*a*). The greatest recorded numbers of lake trout lakes were found on the southern Boreal Shield (Ontario and Quebec) (Fig. 7*b*). The overall proportion of lakes with lake trout in TWS with the species present and with a lake sample of 10 or more was 0.23 (Fig. 7*c*). This proportion was used to fill missing LK% gaps where presence was noted by SWS (WS% > 0). This proportion is probably an underestimate as lake trout are expected to occur more often in the northern parts of their range where lower surface water temperatures should allow it to succeed in a wider range of lakes. Hershey et al. (2006) showed that 44.6% of 158 Arctic Alaskan lakes supported lake trout. The product of WS% and LS% gave an estimate of the proportion of lakes in each SWS with lake trout (Fig. 7*d*). There are three main concentrations of lake trout lakes on the southern Boreal Shield, on the Taiga Shield west of Hudson Bay, and in the Boreal Cordillera. Those areas of highest occurrence are consistent with the patterns of glacial refugia and postglacial dispersal identified via genetic markers by Wilson and Hebert (1998).

The analysis of lake trout occurrence by size class showed that the proportion of lakes with lake trout (SZ%) was 0.210 overall and varied from 0.038 in the 0.1–0.2 km^2 size class to 0.389 in the 10.0–20.0 size class (Table 6). The overall value here differed slightly from the values used to fill LK% gaps in SWS (0.21 vs. 0.23) because of the sample size restriction used for the latter. The SZ% values rose with increasing lake size. The resulting odds ratios, SZ_{ratio}, ranged from 0.179 to 1.853.

Lake and lake trout resources

Combining the results given above, the size of total and lake trout resources in Canada were estimated by lake size class and by ecozone (Table 7). There are an estimated 910 132 lakes with area > 0.1 km^2 in Canada, with an estimated total area of 1 028 151 km^2. Lakes larger than 100 km^2 account for 44.5% of the total area, and other size classes contribute 4.5%–8.5% of the total. The majority of lakes (number, 53.7%; area, 54.7%) are on the Canadian Shield (Boreal and Taiga). The Arctic zone contains the

© 2008 NRC Canada

Fig. 4. The distributions for maximum depth (Z_{max}) and mean–maximum depth ratio (Z_{ratio}), respectively, of (*a*, *c*) sample size and (*b*, *d*) regression-fitted watershed coefficients by secondary watershed.

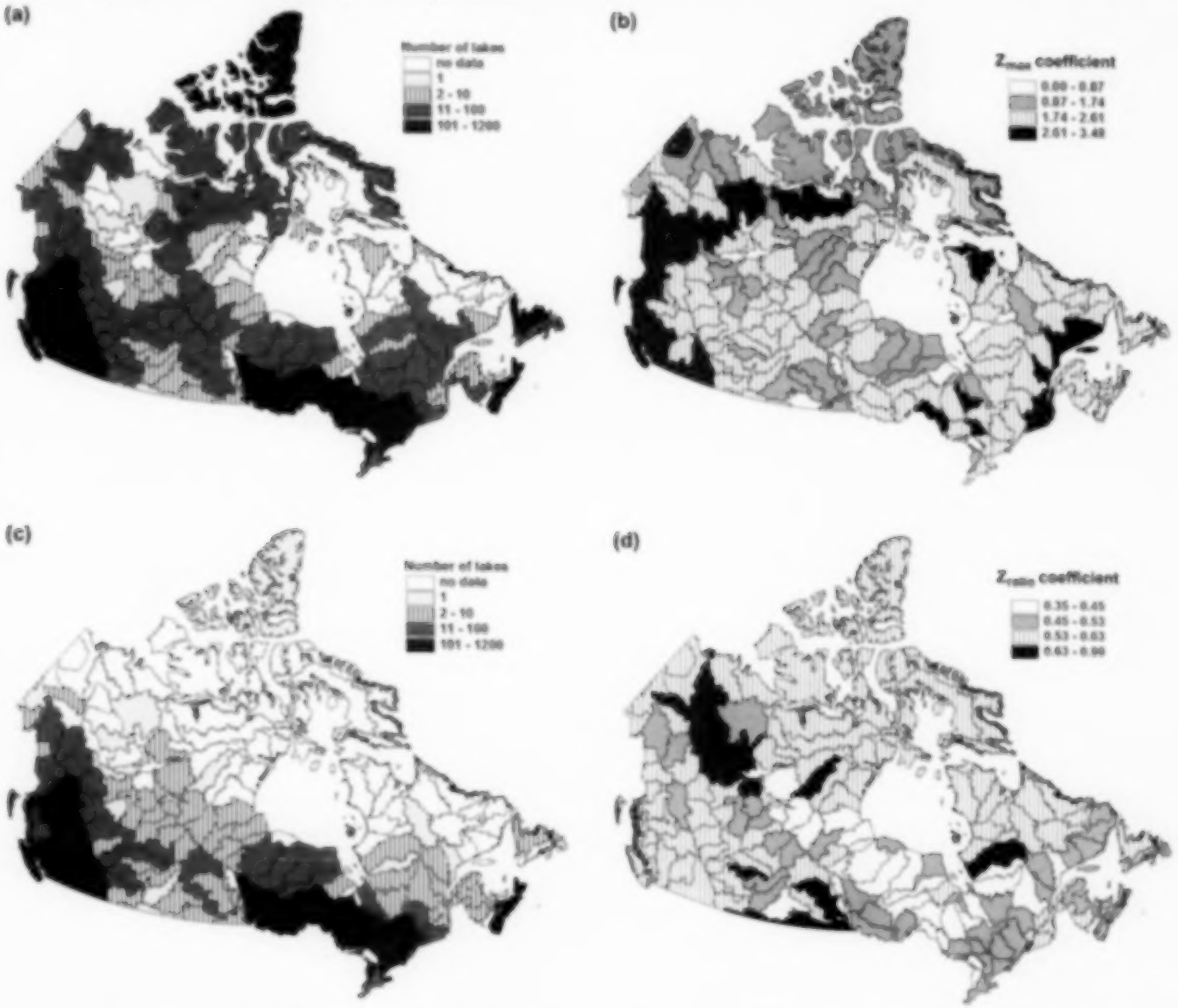

next largest share (number, 29.5%; area, 20.1%). There are an estimated 66 500 lake trout lakes in Canada, with 50% on the Boreal Shield, 29% on the Taiga Shield, and 8% in the Southern Arctic. By number, the largest percentage of lake trout lakes (38%) are estimated to be in the 0.2–0.5 km^2 area size class, with 25% in the 0.1–0.2 size class and 17% in the 0.5–1.0 size class. The lakes larger than 100.0 km^2 dominated by area and volume, 76.6% and 95.6%, respectively. The St. Lawrence – Great Lakes account for much of the area and volume in the >100.0 km^2 size class. The next highest area contribution was in the 2.0–5.0 interval (4.36%), and the next volume contribution was in the 20.0–50.0 interval (0.86%). Most of the lake trout resource is on the Shield (Boreal and Taiga combined), with 79% by number, 65.2% by area, and 74.8% by volume.

Discussion

Although the country-wide lake database described here is undoubtedly incomplete, there were sufficient data to successfully fit predictive models and to discern regional patterns in the characteristics of Canada's lakes. To evaluate the results obtained here, there are four areas to consider: the database; the regional models and typology; the potential uses of these models; and the direction of future studies.

The Canada lakes database analyzed here has several shortcomings. The data collection is incomplete, but moving beyond the more readily accessible assemblages of data would require considerable person power and time. Some areas such as British Columbia, Ontario, Quebec, and Nova Scotia have undertaken extensive inventories of lake resources in the past. Our data coverage was weakest on the Taiga Shield, especially in northern Quebec and Labrador and in the eastern Arctic.

The set of lake characteristics examined here is limited compared with the many identified by Leach and Herron (1992). Chemical parameters such as total phosphorus, chlorophyll *a*, dissolved organic matter, and alkalinity that

© 2008 NRC Canada

Fig. 5. The distributions for Secchi depth (Secchi), pH, and total dissolved solids (TDS), respectively, of (*a*, *c*, *e*) sample size and (*b*, *d*, *f*) regression-fitted watershed coefficients by secondary watershed.

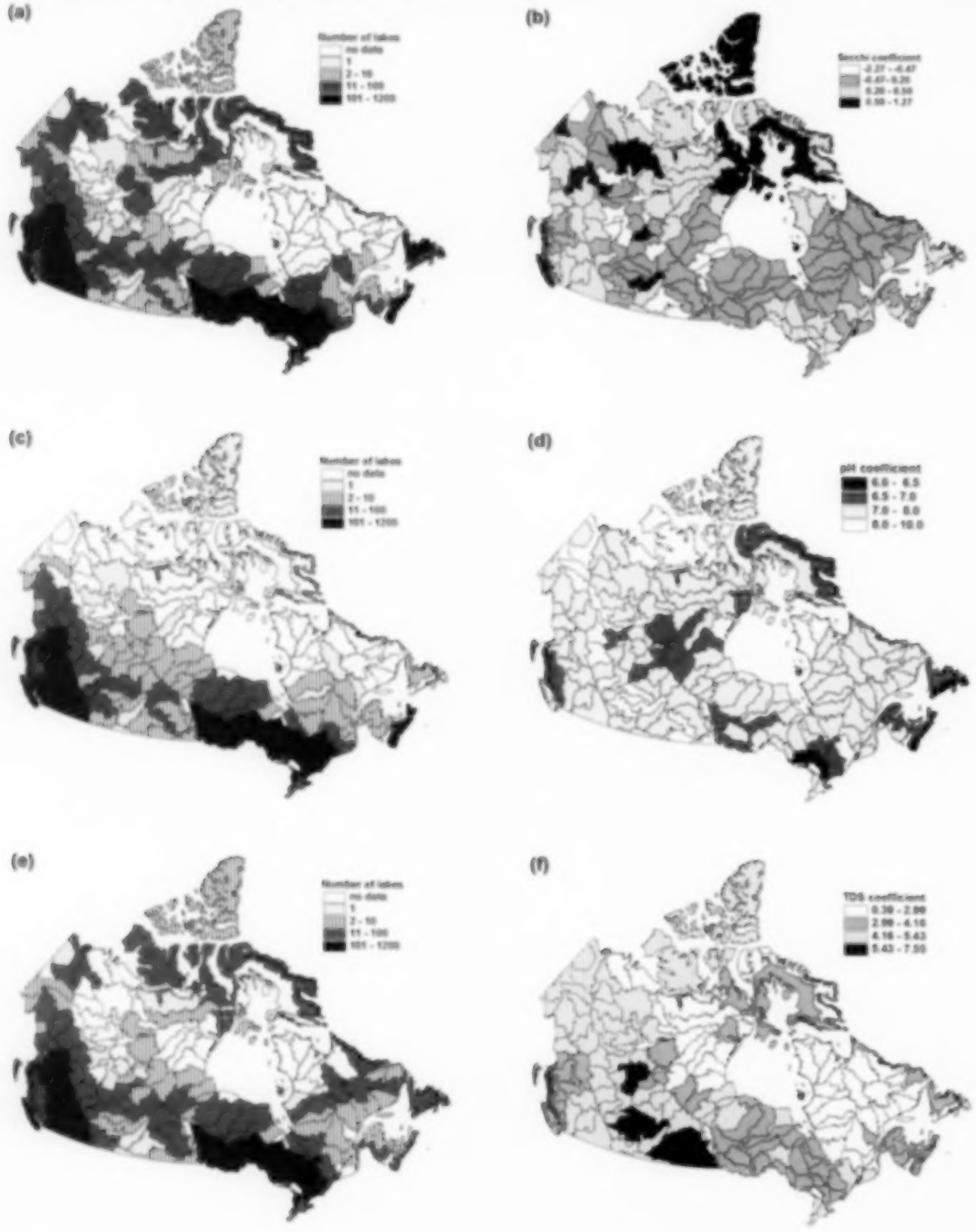

© 2008 NRC Canada

Fig. 6. Mean regression coefficients by ecozone for the lake characteristic SWS coefficients: numbers of lakes, Z_{max}, Z_{ratio}, Secchi, pH, and TDS. (Lakes, pH and TDS on the left *y* axis scale and the rest on the right *y* axis scale).

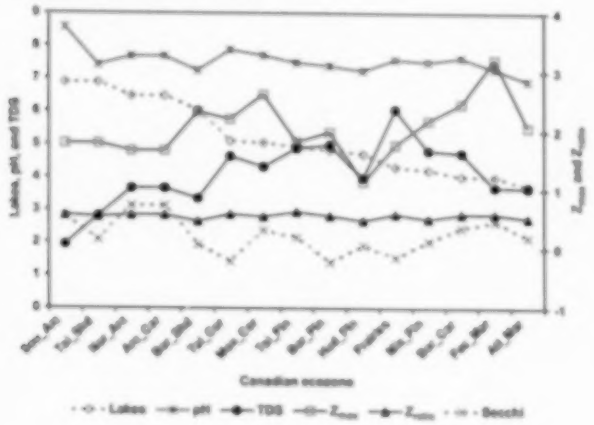

have been shown to be more immediate factors in lake productivity would be valuable additions to a lakes database. However, the current parameters Secchi depth, pH, and TDS are often highly correlated with those potential additions. For example, total phosphorus in lake water is an important predictor of components of biomass and production in lakes (Hakanson 1996), but in earlier studies, TDS was often the parameter cited as a good predictor (Leach and Herron 1992). The regional pattern in Secchi depth is inversely similar to the regional variation in dissolved organic matter (DOM) levels (Molot et al. 2004); DOM is a primary determinant of light attenuation in lakes and hence higher levels lead to lower Secchi values.

The temperature and oxygen regimes are important factors in shaping the levels and forms of productivity in lakes, especially for cold stenotherms like lake trout (Ryan and Marshall 1994), although those regimes are formed through the interaction of morphometric (e.g., area, depth), edaphic (e.g., total phosphorus, TDS), and climatic (e.g., air temperature and precipitation) factors as described by Rawson (1939) and many others (cf. Leach and Herron 1992) during the evolution of limnology. Temperature and oxygen were not added to the present framework as representing the seasonal and spatial dynamics with individual lakes would require much more complexity in the database.

The regional models obtained here have a predictive power greater than we expected a priori. The use of secondary watershed membership as a dummy variable provided a convenient means of bypassing the potential complexities inherent in Canada's terrestrial ecoclassification system with all the detail of soil types, surficial and bedrock geology, permafrost status, landform types, land use, etc. (Ecological Stratification Working Group 1996). The models presented here assumed that the variables operate independently. It is likely that compound variables based on the variables assessed here and additional ones such as light, temperature, and nutrient levels would further improve the performance of the predictive models. Examples include the simple models of lake fishery productivity of Schlesinger and Regier (1982) based on climate and the morphoedaphic index of Ryder (1965) and the more complex multifactor model of lake trout productivity (Shuter et al. 1998) where life history features are linked to lake characters.

Regional lakes studies have shown how landscape factors influence lake attributes (Stendera and Johnson (2006) in Sweden; Martin and Soranno (2006) in Michigan). The post hoc analyses of secondary watershed coefficients by primary watershed and ecozone to find a method for estimating missing values showed that ecozone was a better predictor of regional variation in lake characteristics, which is in line with expectations from landscape studies. The results suggest that there is scope for further investigation of the links between landscape and lake features on a Canada-wide scale. Because the primary objective was to obtain models representing lake attributes for use in large-scale assessment studies, the secondary watersheds provided a convenient and acceptable resolution for capturing regional variation in lake attributes.

The preliminary ecozone typology of Canadian lakes obtained here is consistent with that from earlier regional studies. Northcote and Larkin (1956) indicated that TDS and mean depth were important parameters in lake typology for British Columbia lakes in the Pacific-Maritime and Montane Cordillera ecozones. The Schlesinger and Regier (1982) model of fish yield in lakes brings together the three main elements of regional limnology (morphometric, edaphic, and climatic) as described by Rawson (1939). These elements parallel the features that are overlain in terrestrial ecozone classifications. Therefore, it should not be surprising that ecozones explained much of the regional variation evident in lake attributes assessed by secondary watershed. Those aspects of the lake characteristic models related to lake trout occurrence, taken here as a sample biotic component, are consistent with other efforts that have sought to integrate abiotic and biotic elements in lake typologies. Johnson et al. (1977) presented a typology for Ontario lakes based on similar lake characteristics and the occurrences of several top predators. Hershey et al. (2006) developed a similar typology for Alaskan lakes. The results obtained here indicate that in future, it should be feasible to derive a more sophisticated national lake classification and assessment tool similar to that developed for shallow European lakes (Moss et al. 2003).

Those components of the regional lake feature models tied to lake trout occurrence were consistent with previously reported patterns (Ryan and Marshall 1994; Marshall 1996; Gunn et al. 2003). Lake trout occur more frequently in larger lakes than in smaller ones, in deeper ones, with greater Secchi depths. It was expected that the proportion of lakes with lake trout would be lower in the smaller lake size classes. Smaller lakes are less likely to have sufficient maximum depth to allow either thermal stratification, thereby ensuring suitable thermal habitat is available during summer in the southern reaches of the species range, or winter refuge from freeze-out with greater ice thicknesses during winter in the northern reaches of the range. Depth and Secchi depth, an inverse indicator of productivity, also interact in shaping oxygen levels below the thermocline in the cooler waters preferred by lake trout, thereby affecting the suitability of lakes for lake trout (Ryan and Marshall 1994). The absence

© 2008 NRC Canada

Fig. 7. Lake trout occurrence by secondary watershed (SWS): (*a*) percentage of tertiary watersheds (TWS) with lake trout present (WS%); (*b*) number of lakes with lake trout by SWS; (*c*) percentage with lake trout (LK%) from TWS with lake trout; and (*d*) percentage of lakes (WS%-LK%).

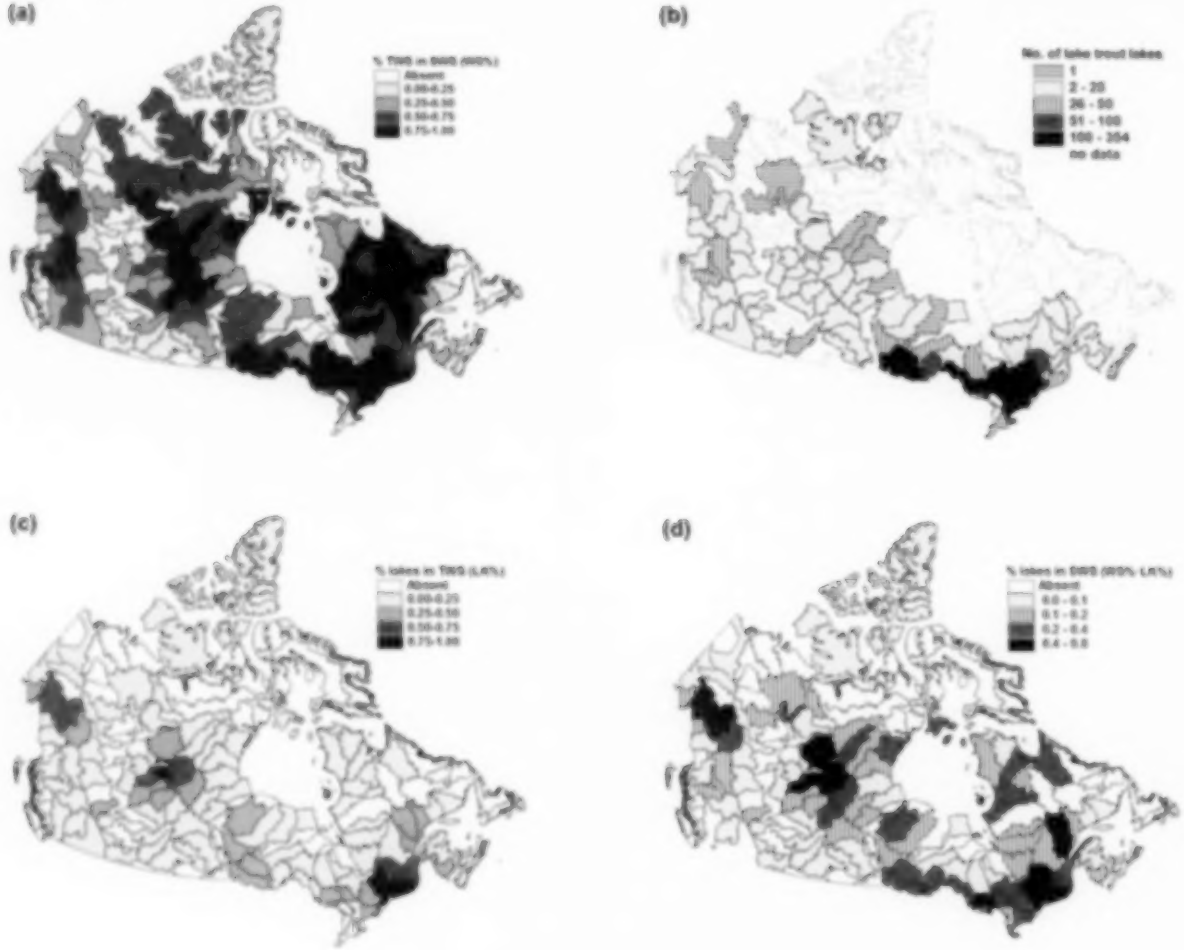

Table 6. Numbers of lakes by size class in the national lakes database and the proportion with lake trout present (SZ_{prev}) and the odds ratio (SZ_{ratio}) by size class to the overall proportion.

Size class (km^2)	No. of lakes	SZ_{prev}	SZ_{ratio}
0.1 to 0.2	2 017	0.038	0.179
0.2 to 0.5	3 011	0.122	0.579
0.5 to 1	2 490	0.198	0.945
1 to 2	2 159	0.258	1.229
2 to 5	1 990	0.305	1.453
5 to 10	863	0.352	1.677
10 to 20	573	0.389	1.853
20 to 50	404	0.366	1.744
50 to 100	192	0.344	1.637
100 plus	282	0.340	1.621
Total	13 981	0.210	

of lake trout effects in the pH and TDS models was consistent with the regional patterns of occurrence of lake trout. Although TDS is an indicator of lake trout carrying capacity (Shuter et al. 1998), lake trout distribution predominantly covers areas with moderate to low TDS levels. The pH levels, although lower in those eastern areas of Canada affected by acidic deposition, are mainly above extirpation thresholds for lake trout (Schindler 1988), and lower values typically occur in smaller lakes that are less suited to lake trout for reasons already given.

The total lake counts and area are derived primarily by direct counts and measures from extensive mapping of Canada's landscape, but the estimates for the lake trout resource are limited by the incomplete coverage of distribution data and the lack of adequate lake inventory data in the more remote regions of the country. Although the more southerly estimates of occurrence by watersheds and lake size draw on relatively large samples of data, the northerly estimates may well be underestimates as limited surveys such as that

© 2008 NRC Canada

Table 7. Total and lake trout lake resources (number, area (km^2), and for lake trout, volume (km^3)) in Canada by (*a*) area size class (km^2) and (*b*) ecozone.

(*a*) Size class.

	All lakes		Lake trout lakes (all ecozones)			Lake trout lakes (Shield)		
Category	Number	Area	Number	Area	Volume	Number	Area	Volume
0.1–<0.2	465 256	64 415.5	16 489	2 282.9	15.2	13 367	1 850.8	11.5
0.2–<0.5	272 256	82 970.2	25 051	7 634.3	58.0	19 866	6 054.2	42.9
0.5–<1.0	88 341	61 154.8	11 573	8 011.3	69.4	9 056	6 269.1	50.4
1.0–<2.0	39 195	54 052.7	5 323	7 339.3	68.8	4 028	5 567.5	48.1
2.0–<5.0	29 094	87 239.8	656	15 305.5	163.5	504	11 860.9	117.9
5.0–<10.0	8 898	60 757.8	5 067	11 382.9	141.4	3 922	8 917.4	103.0
10.0–<20.0	3 855	52 761.4	403	9 006.1	125.4	316	6 928.5	89.6
20.0–<50.0	1 994	60 267.3	1 668	12 196.1	193.1	1 312	9 502.8	140.9
50.0–<100.0	681	46 624.4	132	9 062.3	162.1	100	6 872.8	110.6
≥100.0	562	457 907.2	119	269 056.3	21 443.1	69	165 372.8	16 062.7
Total	910 132	1 028 151.1	66 479	351 277.0	22 440.0	52 540	229 196.7	16 777.5

(*b*) Ecozone.

	All lakes		Lake trout lakes < 100 km^2			Lake trout lakes ≥ 100 km^2		
Category	Number	Area	Number	Area	Volume	Number	Area	Volume
Northern Arctic*	125 433	103 013.3	846	1 296.8	11.0	2	719.0	1.3
Southern Arctic	142 737	114 259.9	5 041	7 237.1	90.3	10	5 175.6	256.6
Taiga Cordillera	4 215	2 590.7	60	74.8	0.6	0	0.0	0.0
Taiga Shield	249 587	246 645.1	19 436	26 386.5	273.9	27	41 033.3	2 131.4
Taiga Plains	42 194	64 024.6	2 051	2 818.6	65.4	12	34 222.5	2 318.3
Boreal Cordillera	11 241	8 580.6	1 824	1 958.2	38.9	5	1 728.0	105.9
Hudson Plains	15 889	12 068.0	120	186.7	0.9	0	0.0	0.0
Boreal Plains	40 266	74 834.6	2 389	2 962.5	39.9	14	8 133.2	111.5
Boreal Shield	238 950	315 375.2	33 036	37 437.3	440.9	42	124 339.5	1 3931.4
Montane Cordillera	13 559	14 010.4	404	536.7	11.1	4	1 220.8	51.3
Prairies	12 464	8 903.3	139	209.8	2.1	0	0.0	0.0
Atlantic Maritime	4 874	3 382.4	165	201.3	2.6	0	0.0	0.0
Pacific Maritime	4 030	2 791.0	0	0.0	0.0	0	0.0	0.0
Mixedwood Plains	4 693	57 672.0	850	914.7	19.2	3	52 484.3	2 535.4
Total	910 132	1 028 151.1	66 360	82 220.8	997.0	119	269 056.3	21 443.1

Note: The lake trout resources on the Boreal Shield and Taiga Shield are shown by size class. The ecozones are ordered by mean annual air temperature (1961–1990 norms), and the lake trout resource by ecozone is divided at the 100 km^2 size boundary.

*Northern Arctic and Arctic Cordillera were combined within secondary watershed units.

of Hershey et al. (2006) suggest that lake trout are more common, especially in smaller lakes in regions with colder climates.

The simple application of a model of species occurrence with regional lake character models to estimate the extent of lake trout lake resources readily demonstrates how such models can be used for large-scale environmental assessments. Similar assessments were made for the impacts of acidic deposition on lake biotic resources in eastern Canada (Jones et al. 1990) and for a national mass balance of contaminants (Woodfine et al. 2002). Such large-scale assessment tools are necessary to gauge long-term and cumulative impacts and to weigh them against social and economic constraints if we are to move beyond limitations that currently render most cumulative effects assessment futile (Duinker and Grieg 2007). Assessing potential large-scale impacts of stressors, such as climate change, land use change, and invasive species, is a critical precursor to identification of vulnerabilities and the formulation of mitigation and adaptation strategies (Metzger and Schröter 2006). These assessments need to be spatially explicit and quantitative to compete with social and economic imperatives that inevitably impact many ecosystems.

The increasing geographic scope of environment stresses requires a broader canvas both for inventory and characterization of lake resources and for the development of management and adaptation strategies. This study has demonstrated that a national synoptic limnology of Canada is within reach and that such a framework can be usefully applied. The next steps should include expanding the spatial coverage by assembling existing information sources, and where gaps still remain, new inventory work will be needed. The range of parameters assessed on a national scale should be expanded, especially with respect to those such as temperature, oxygen, total phosphorus, and DOM where more localized studies have demonstrated their importance to understanding lake processes and productivity. As this national lake assessment capability increases, so the ability to

© 2008 NRC Canada

evaluate large-scale environmental stresses will be enhanced, bringing us closer to a more useful assessment of cumulative impacts.

Acknowledgements

The authors thank all those individuals who aided in the gathering of lake data from across Canada. The authors especially thank Carolyn Bakelaar at Fisheries and Oceans, Burlington, for all her help with GIS data acquisition and manipulations. This work was made possible with funding from the Climate Change Action Fund, Fisheries and Oceans Canada, and the Ontario Ministry of Natural Resources.

References

Burnham, K.P., and Anderson, D.R. 2004. Multimodel inference: understanding AIC and BIC in model selection. Sociol. Methods Res. **33**: 261–304. doi:10.1177/0049124104268644.

Carpenter, S.R., Ludwig, D., and Brock, W.A. 1999. Management of eutrophication for lakes subject to potentially irreversible change. Ecol. Appl. **9**: 751–771. doi:10.1890/1051-0761(1999)009[0751:MOEFLS]2.0.CO;2.

Chu, C., Minns, C.K., and Mandrak, N.E. 2003. Comparative regional assessment of factors impacting freshwater fish biodiversity in Canada. Can. J. Fish. Aquat. Sci. **60**: 624–634. doi:10.1139/f03-048.

Downing, J.A., Prairie, Y.T., Cole, J.J., Duarte, C.M., Tranvik, L.J., Striegl, R.G., McDowell, W.H., Kortelainen, P., Caraco, N.F., Melack, J.M., and Middelburg, J.J. 2006. The global abundance and size distribution of lakes, ponds, and impoundments. Limnol. Oceanogr. **51**: 2388–2397.

Duinker, P.N., and Grieg, L.A. 2007. Scenario analysis in environmental impact assessment: improving explorations of the future. Environ. Impact. Assess. Rev. **27**: 206–219. doi:10.1016/j.eiar.2006.11.001.

Ecological Stratification Working Group. 1996. A national ecological framework for Canada. Agriculture and Agri-Food Canada, Research Branch, Centre for Land and Biological Resources Research, and Environment Canada, State of Environment Directorate, Ottawa. Map at scale 1:7.5 million. Available online at http://www.ec.gc.ca/soer-ree/English/Framework/default.cfm. Pdf copy available from http://res.agr.ca/cansis/publications/ecostrat/intro.html.

Frey, D.G. (*Editor*). 1963. Limnology in North America. University of Wisconsin Press, Madison, Wis.

Gunn, J.M., Steedman, R.J., and Ryder, R.A. (*Editors*). 2003. Boreal shield watersheds: lake trout ecosystems in a changing environment. Lewis Publishers, Boca Raton, Florida.

Håkanson, L. 1996. Predicting important lake habitat variables from maps using modern modelling tools. Can. J. Fish. Aquat. Sci. **53**(Suppl. 1): 364–382. doi:10.1139/cjfas-53-S1-364.

Hershey, A.E., Beaty, S., Fortino, K., Keyse, M., Mou, P.P., O'Brien, W.J., Ulseth, A.J., Gettel, G.A., Lienesch, P.W., Luecke, C., McDonald, M.E., Mayer, C.H., Miller, M.C., Richards, C., Schuldt, J.A., and Whalen, S.C. 2006. Effects of landscape factors on fish distribution in arctic Alaskan lakes. Freshw. Biol. **51**: 39–55. doi:10.1111/j.1365-2427.2005.01474.x.

Hurvich, C.M., and Tsai, C.-L. 1989. Regression and time series model selection in small samples. Biometrika, **76**: 297–307. doi:10.1093/biomet/76.2.297.

Jensen, M.E., Bourgeron, P., Everett, R., and Goodman, I. 1996. Ecosystem management: a landscape ecology perspective. Water Resour. Bull. **32**: 203–215.

Johnson, M.G., Leach, J.H., Minns, C.K., and Olver, C.H. 1977. Limnological characteristics of Ontario lakes in relation to associations of walleye (*Stizostedion vitreum vitreum*), northern pike (*Esox lucius*), lake trout (*Salvelinus namaycush*), and smallmouth bass (*Micropterus dolomieu*). J. Fish. Res. Board Can. **34**: 1592–1601.

Jones, M.L., Minns, C.K., Marmorek, D.M., and Elder, F.C. 1990. Assessing the potential extent of damage to inland lakes in eastern Canada due to acidic deposition: II. Application of the regional model. Can. J. Fish. Aquat. Sci. **47**: 67–80. doi:10.1139/f90-007.

Kelso, J.R.M., Shaw, M.A., Minns, C.K., and Mills, K.H. 1990. An evaluation of the effects of atmospheric acidic deposition on fish and fishery resource of Canada. Can. J. Fish. Aquat. Sci. **47**: 644–655. doi:10.1139/f90-072.

Kolada, A., Soszka, H., Cydzik, D., and Golub, M. 2005. Abiotic typology of Polish lakes. Limnologica, **35**: 145–150.

Kratz, T.K., and Frost, T.M. 2000. The ecological organization of lake districts: general introduction. Freshw. Biol. **43**: 297–299. doi:10.1046/j.1365-2427.2000.00568.x.

Leach, J.H., and Herron, R.C. 1992. A review of lake habitat classification. *In* The development of an aquatic habitat classification system for lakes. *Edited by* W.D.N. Busch and P.G. Sly. CRC Press, Boca Raton, Fla. pp. 27–72.

Lehner, B., and Döll, P. 2004. Development and validation of a global database of lakes, reservoirs, and wetlands. J. Hydrol. (Amst.), **296**: 1–22. doi:10.1016/j.jhydrol.2004.03.028.

Lester, N.P., Marshall, T.R., Armstrong, K., Dunlop, W.I., and Ritchie, B. 2003. A broad-scale approach to management of Ontario's recreational fisheries. N. Am. J. Fish. Manage. **23**: 1312–1328. doi:10.1577/M01-230AM.

Lester, N.P., Dextrase, A.J., Kushneriuk, R.S., Rawson, M.R., and Ryan, P.A. 2004. Light and temperature: key factors affecting walleye abundance and production. Trans. Am. Fish. Soc. **133**: 588–605. doi:10.1577/T02-111.1.

Marshall, T.R. 1996. A hierarchical approach to assessing habitat suitability and yield potential of lake trout. Can. J. Fish. Aquat. Sci. **53**(Suppl. 1): 332–341. doi:10.1139/cjfas-53-S1-332.

Martin, S.L., and Soranno, P.A. 2006. Lake landscape position: relationships to hydrologic connectivity and landscape features. Limnol. Oceanogr. **51**: 801–814.

Metzger, M.J., and Schröter, D. 2006. Towards a spatially explicit and quantitative vulnerability assessment of environmental change in Europe. Reg. Environ. Change, **6**: 201–216. doi:10.1007/s10113-006-0020-2.

Minns, C.K. 2001. Science for freshwater fish habitat management in Canada: current status and future prospects. Aquat. Ecosyst. Health Manage. **4**: 423–436. doi:10.1080/14634980131726099.

Minns, C.K., and Moore, J.E. 1995. Factors limiting the distributions of Ontario's freshwater fishes: the role of climate and other variables, and the potential impacts of climate change. Can. Spec. Publ. Fish. Aquat. Sci. No. 121. pp. 137–160.

Molot, L.A., Keller, W., Leavitt, P.R., Roberts, R.D., Waiser, M.J., Arts, M.T., Clair, T.A., Pienitz, R., Yan, N.D., McNicol, D.K., Prairie, Y.T., Dillon, P.J., Macrae, M., Bello, R., Nordin, R.N., Curtis, P.J., Smol, J.P., and Douglas, M.S.V. 2004. Risk analysis of dissolved organic matter-mediated ultraviolet B exposure in Canadian inland waters. Can. J. Fish. Aquat. Sci. **61**: 2511–2521. doi:10.1139/f04-165.

Mons, B., Stephen, D., Alvarez, C., Becares, E., Van De Bund, W., Collings, S.E., Van Donk, E., De Eyto, E., Feldmann, T., Fernández-Aláez, C., Margarita Fernández-Aláez, M., Franken, R.J.M., García-Criado, F., Gross, E.M., Gyllström, M., Hansson, L.-A., Irvine, K., Järvalt, A., Jensen, J.-P., Jeppesen, E., Kairesalo, T., Kornijów, R., Krause, T., Künnap, H., Laas, A., Lill, E., Lorens,

© 2008 NRC Canada

B., Luup, H., Miracle, M.R., Nõges, P., Nõges, T., Nykänen, M., Ott, I., Peczula, W., Peeters, E.T.H.M., Phillips, G., Romo, S., Russell, V., Salujõe, J., Scheffer, M., Siewertsen, K., Smal, H., Tesch, C., Timm, H., Tuvikene, L., Tonno, I., Virro, T., Vicente, E., and Wilson, D. 2003. The determination of ecological quality in shallow lakes — a tested system (ECOFRAME) for implementation of the European Water Framework Directive. Aquat. Conserv. Mar. Freshwat. Ecosyst. **13**: 507–549. doi:10.1002/aqc.592.

Naumann, E. 1929. The scope and chief problems of regional limnology. Int. Rev. Hydrobiol. **22**: 423–444. doi:10.1002/iroh.19290220128.

Nicholson, H.F., and Moore, J.E. 1988. Bibliography on the limnology and fisheries of Canadian freshwaters. No. 10. (Final cumulative edition.) Vols. 1, 2, and 3. Can. Tech. Rep. Fish. Aquat. Sci. No. 1600.

Northcote, T.G., and Larkin, P.A. 1956. Indices of productivity in British Columbia lakes. J. Fish. Res. Board Can. **13**: 515–540.

Nykänen, M., Kairesalo, T., Mäkelä, S., Huitu, E., Ala-Opas, P., and Mannio, J. 2005. A typology and ecological classification system for Finnish lakes: applicability of the ECOFRAME scheme. Boreal Environ. Res. **10**: 159–179.

Post, J.R., Sullivan, M., Cox, S., Lester, N.P., Walters, C.J., Parkinson, E.A., Paul, A.J., Jackson, L., and Shuter, B.J. 2002. Canada's recreational fisheries: the invisible collapse. Fisheries, **27**: 6–17. doi:10.1577/1548-8446(2002)027<0006:CRF>2.0.CO;2.

Rawson, D.S. 1939. Some physical and chemical factors in the metabolism of lakes. Am. Assoc. Adv. Sci. **10**: 9–26.

Reist, J.D., Wrona, F.J., Prowse, T.D., Power, M., Dempson, J.B., Beamish, R.J., King, J.R., Carmichael, T.J., and Sawatzky, C.D. 2006. General effects of climate change on arctic fishes and fish populations. Ambio, **35**: 370–380. doi:10.1579/0044-7447(2006)35[370:GEOCCO]2.0.CO;2. PMID:17256641.

Ruhland, K., and Smol, J.P. 1998. Limnological characteristics of 70 lakes spanning Arctic treeline from Coronation Gulf to Great Slave Lake in the central Northwest Territories, Canada. Int. Rev. Hydrobiol. **83**: 183–203. doi:10.1002/iroh.19980830302.

Ryan, P.A., and Marshall, T.R. 1994. A niche definition for lake trout (*Salvelinus namaycush*) and its use to identify populations at risk. Can. J. Fish. Aquat. Sci. **51**: 2513–2519. doi:10.1139/f94-250.

Ryder, R.A. 1965. A method for estimating the potential fish production of north-temperate lakes. Trans. Am. Fish. Soc. **94**: 214–218. doi:10.1577/1548-8659(1965)94[214:AMFETP]2.0.CO;2.

Schindler, D.W. 1988. Effects of acid rain on freshwater ecosystems. Science (Washington, D.C.), **239**: 149–157. doi:10.1126/science.239.4836.149.

Schindler, D.W. 2001. The cumulative effects of climate warming and other human stresses on Canadian freshwaters in the new millennium. Can. J. Fish. Aquat. Sci. **58**: 18–29. doi:10.1139/cjfas-58-1-18.

Schlesinger, D.A., and Regier, H.A. 1982. Climatic and morphoedaphic indices of fish yields from natural lakes. Trans. Am. Fish. Soc. **111**: 141–150. doi:10.1577/1548-8659(1982)111<141:CAMIOF>2.0.CO;2.

Shuter, B.J., Jones, M.L., Korver, R.M., and Lester, N.P. 1998. A general, life history based model of regional management of fish stocks: the inland lake trout (*Salvelinus namaycush*) fisheries of Ontario. Can. J. Fish. Aquat. Sci. **55**: 2161–2177. doi:10.1139/cjfas-55-9-2161.

Sprugel, D.G. 1983. Correcting for bias in log-transformed allometric equations. Ecology, **64**: 209–210. doi:10.2307/1937343.

Stendera, S., and Johnson, R.K. 2006. Multiscale drivers of water chemistry of boreal lakes and streams. Environ. Manage. **38**: 760–770. doi:10.1007/s00267-005-0180-8. PMID:16955233.

Vidondo, B., Prairie, Y.T., Blanco, J.M., and Duarte, C.M. 1997. Some aspects of the analysis of size spectra in aquatic ecology. Limnol. Oceanogr. **42**: 184–192.

Wilson, C.C., and Hebert, P.D.N. 1998. Phylogeography and postglacial dispersal of lake trout (*Salvelinus namaycush*) in North America. Can. J. Fish. Aquat. Sci. **55**: 1010–1024. doi:10.1139/cjfas-55-4-1010.

Woodfine, D., MacLeod, M., and Mackay, D. 2002. A regionally segmented national scale multimedia contaminant fate model for Canada with GIS data input and display. Environ. Pollut. **119**: 341–355. doi:10.1016/S0269-7491(01)00344-X. PMID:12166668.

Appendix A

Table A1 appears on the next page.

© 2008 NRC Canada

Table A1. List of main lake data sources and contacts by province or territory.

	Source	Contact
Canada	Evans 2000[1]	
Newfoundland and Labrador	Van Zyll De Jong and Cows 2005[2]	Michael van Zyll De Jong
	LRTAP NIS Lake Database	
Nova Scotia	Lake Inventory Database	John MacMillan
	Alexander et al. 1986[3]	
Prince Edward Island	No data	
New Brunswick	Environment Canada	Tom Clair, Ian Dennis
	Pilgrim et al. 2003[4]	
Quebec	Ministère du Développement Durable de l'Environnement et des Parcs	Diane Morin, Daniel Blais, Mario Bérubé, Marc Simmoneau, Pierre Levasseur, Jacques Dupont
	Hydro-Québec	Richard Verdon, Jean-Louis Fréchette
	Fallu et al. 2000[5]	Marie-Andrée Fallu
Ontario	Lake Inventory Database, Ontario Ministry of Natural Resources	Brian Shuter, Nigel Lester
	Ontario Environment Water Quality Database	
Manitoba	DFO Fish Habitat Management GIS	William Franzin, DFO Winnipeg
	Manitoba Conservation/Water Stewardship	Walt Lysack
Saskatchewan	DFO Fish Habitat Management GIS	William Franzin, DFO Winnipeg
	Saskatchewan Environment	Kevin Murphy, Mark Duffy, Ken Scott
Alberta	Alberta Environment	Bridgette Helbig, Ron Tchir, Thai Nguyen Huu
	Sustainable Resource Development	Ken Crutchfield, Stuart Nadeau
	Atlas of Alberta Lakes	http://alberta-lakes.sunsite.ualberta.ca/
British Columbia	BC Ministry of Sustainable Resource Development online databases	http://srmapps.gov.bc.ca/apps/fidq/
		Rick Nordin
Yukon, NWT, and Nunavut	Hamilton et al. 2001[6]	P.K. Hamilton, Kathleen Ruhland, Darlene Lim, John Smol, Dermot Antoniades
	Antoniades et al. 2003*a*,[7] 2003*b*[8]	
	Bouchard et al. 2004[9]	
	Falk 1979[10]	
	Lindsey et al. 1981[11]	
	Pienitz et al. 1997*a*, [12]1997*b*[13]	
	Ruhland et al. 2003[14]	
	Shortreed and Stockner 1986[15]	
	Wilson and Gajewski 2002[16]	

[1]Evans, M.S. 2000. The large lake ecosystems of northern Canada. Aquat. Ecosyst. Health Manage. **3**: 65–79. doi:10.1016/S1463-4988(99)00071-8.

[2]Van Zyll De Jong, M.C., and Cows, I.G. 2005. Association between biogeographical factors and boreal lake fish assemblages. Fish. Manag. Ecol. **12**: 189–199. doi:10.1111/j.1365-2400.2005.00442.x.

[3]Alexander, D.R., Kerekes, J.J., and Sabean, B.C. 1986. Description of selected lake characteristics and occurrence of fish species in 781 Nova Scotia lakes. Proc. N.S. Inst. Sci. **36**: 63–106.

[4]Pilgrim, W., Clair, T.A., Choate, J., Hughes, R. 2003. Changes in acid precipitation-related water chemistry of lakes from southwestern New Brunswick, Canada, 1986–2001. Environ. Monit. Assess. **88**: 39–52. doi:10.1023/A:1025592202153. PMID:14570410.

[5]Fallu, M.-A., Allaire, N., and Pienitz, R. 2000. Freshwater diatoms from northern Québec and Labrador (Canada): species–environment relationships in lakes of boreal forest, forest–tundra and tundra regions. Bibliotheca Diatomologica, Vol. 45. J. Cramer, Berlin/Stuttgart.

[6]Hamilton, P., Gajewski, K., Atkinson, D., and Lean, D. 2001. Physical and chemical limnology of lakes from the Canadian Arctic Archipelago. Hydrobiologia, **457**: 133–148. doi:10.1023/A:1012275316543.

[7]Antoniades, D., Douglas, M.S.V., and Smol, J.P. 2003*a*. The physical and chemical limnology of 24 ponds and one lake from Isachsen, Ellef Ringnes Island, Canadian High Arctic. Int. Rev. Hydrobiol. **88**: 519–538. doi:10.1002/iroh.200310665.

[8]Antoniades, D., Douglas, M.S.V., and Smol, J.P. 2003*b*. Comparative physical and chemical limnology of two Canadian High Arctic regions: Alert (Ellesmere Island, NU) and Mould Bay (Prince Patrick Island, NWT). Arch. Hydrobiol. **158**: 485–516. doi:10.1127/0003-9136/2003/0158-0485.

[9]Bouchard, G., Gajewski, K., and Hamilton, P. 2004. Biogeography of diatoms from the Canadian Arctic Archipelago. J. Biogeogr. **31**: 1955–1973. doi:10.1111/j.1365-2699.2004.01143.x.

[10]Falk, M.R. 1979. Biological and limnological data on ten lakes surveyed in the Northwest Territories, 1971–72. Environ. Can. Fish. Mar. Serv. Data Rep. No. 129.

[11]Lindsey, C.C., Patalas, K., Bodaly, R.A., and Archibald, C.P. 1981. Glaciation and the physical, chemical and biological limnology of Yukon lakes. Can. Tech. Rep. Fish. Aquat. Sci. No. 966.

[12]Pienitz, R., Smol, J.P., and Lean, D.R.S. 1997*a*. Physical and chemical limnology of 59 lakes located between southern Yukon and the Tuktoyaktuk Peninsula, Northwest Territories (Canada). Can. J. Fish. Aquat. Sci. **54**: 330–346. doi:10.1139/cjfas-54-2-330.

[13]Pienitz, R., Smol, J.P., and Lean, D.R.S. 1997*b*. Physical and chemical limnology of 24 lakes located between Yellowknife and Contwoyto Lake, Northwest Territories (Canada). Can. J. Fish. Aquat. Sci. **54**: 347–358. doi:10.1139/cjfas-54-2-347.

[14]Ruhland, K.M., Smol, J.P., Wang, X., and Muir, D.C.G. 2003. Limnological characteristics of 56 lakes in the central Canadian Arctic treeline region. J. Limnol. **62**: 9–27.

[15]Shortreed, K.S., and Stockner, J.G. 1986. Trophic status of 19 subarctic lakes in the Yukon Territory. Can. J. Fish. Aquat. Sci. **43**: 797–805. doi:10.1139/f86-098.

[16]Wilson, S.E., and Gajewski, K. 2002. Surface-sediment diatom assemblages and water chemistry from 42 subarctic lakes in the southwestern Yukon and northern British Columbia, Canada. Ecoscience, **9**: 256–270.

© 2008 NRC Canada

PERSPECTIVE / PERSPECTIVE

Taste and odour and cyanobacterial toxins: impairment, prediction, and management in the Great Lakes

Susan B. Watson, Jeff Ridal, and Gregory L. Boyer

Abstract: This paper reviews the issues associated with algal–cyanobacterial taste–odour (T&O) compounds and toxins in the Great Lakes. As with other remediated water bodies, the Great Lakes have undergone significant shifts in nutrient and food-web regimes and are exhibiting erratic blooms and noxious algal metabolite (NAM) outbreaks, despite reduced offshore nutrient levels. We appraise the chemistry, biota, and distribution of NAM impairments and conclude that management strategies based on lakewide monitoring and remedial action plans are often unsuccessful because they attempt NAM control through an unsustainable reliance on water treatment and broad-scale nutrient–biomass models. This approach is undermined by several factors: (*i*) only some species produce NAMs; (*ii*) different taxa show disparate patterns across nutrient and mixing regimes; (*iii*) nuisance species may be planktonic or benthic and located outside remedial boundaries; and (*iv*) species differ significantly in NAM biochemistry and release. Thus, there are no robust relationships between total plankton biomass, toxins, and T&O compounds in these and other source waters. Given the potential ecological and socioeconomic threats posed by NAM outbreaks, there is a critical need to develop a multistep management framework based on more stringent restoration targets, combining broad-scale screening and nutrient management with system and taxa-specific approaches.

Résumé : Notre travail passe en revue les problèmes associés aux composés et aux toxines reliés aux goûts et aux odeurs (T&O) chez les algues et les cyanobactéries dans les Grands Lacs. Comme d'autres masses d'eau ayant subi un traitement curatif, les Grands Lacs ont connu des changements significatifs de leurs régimes de nutriments et de leurs réseaux alimentaires et ils produisent des floraisons erratiques et des proliférations de métabolites algaux nocifs (NAM), malgré les niveaux réduits de nutriments dans les eaux du large. Nous évaluons la chimie, les organismes et la répartition des dégradations dues aux NAM et concluons que les stratégies de gestion basées sur les plans de surveillance à l'échelle du lac entier et les plans d'action correctifs sont infructueuses, car elles tentent de contrôler les NAM au moyen d'une utilisation insoutenable à long terme du traitement des eaux et des modèles nutriments–biomasse à grande échelle. Cette approche est rendue moins efficace par divers facteurs : (*i*) seules certaines espèces produisent des NAM, (*ii*) les divers taxons suivent des patrons disparates en fonction des divers régimes de nutriments et de brassage, (*iii*) les espèces nuisibles peuvent être planctoniques ou benthiques et se trouver hors de portée du traitement curatif et (*iv*) les espèces diffèrent dans leur biochimie et leur libération des NAM. C'est pourquoi, il n'y a pas de relations robustes entre la biomasse planctonique totale, les toxines et les composés T&O dans ces eaux productrices de NAM et dans les autres masses d'eau. Étant donné les menaces potentielles écologiques et socioéconomiques posées par les éruptions de NAM, il y a un besoin urgent de mettre au point un cadre de gestion en plusieurs étapes basé sur des cibles plus rigoureuses de restauration qui combinent un dépistage à grande échelle et une gestion des nutriments, d'une part, et des approches à l'échelle des systèmes et des espèces, d'autre part.

[Traduit par la Rédaction]

Received 3 May 2007. Accepted 25 February 2008. Published on the NRC Research Press Web site at cjfas.nrc.ca on 1 August 2008. 19982

S.B. Watson.[1,2] Ecosystems Management Research, Environment Canada, Canada Centre for Inland Waters, Burlington, ON L7R 4A6, Canada.
J. Ridal. Saint Lawrence River Institute of Environmental Sciences, Cornwall, ON K6J 4Z1, Canada.
G.L. Boyer. State University of New York, College of Environmental Science and Forestry, Syracuse, NY 13210, USA.

[1]Corresponding author (e-mail: sue.watson@ec.gc.ca).
[2]Present address: Aquatic Ecosystem Management Research Division, National Water Research Institute, Canada Centre for Inland Waters, Burlington, ON L7R 4A6, Canada.

 doi:10.1139/F08-084 © 2008 NRC Canada

Introduction

The biomass produced by excessive algal growth has long been a major source of impairment in many culturally eutrophied surface waters (for simplicity, "algae" is used to denote both eukaryotic algal taxa and cyanobacteria). Because of their high visibility and ecological and socioeconomic impacts, this biomass has been the target of extensive research and remediation efforts for some time. Recently, there has been increasing concern with the more insidious impairment by compounds synthesized, stored, and released during the growth and decay of these blooms, in particular, those compounds that are toxic or harmful to humans and other organisms or cause taste and odour (T&O). Research continues to add to the list of these noxious algal–cyanobacterial metabolites (NAMs), which include terpenoids, sulphides, lipid and pigment derivatives, aromatics, long-chain hydrocarbons, amines, alkaloids, lipopolysaccharides (LPS), and peptides (e.g., Watson 2003; Codd et al. 2005). Many NAMs are far less conspicuous than the algal cells that produce them; nevertheless, they can have pervasive ecological and socioeconomic effects, with important implications for the integrity, aesthetics, and safety of surface waters used for drinking and recreation. The most problematic of these compounds are generally highly stable. As a result, they are not removed by boiling or conventional water treatment and can persist in surface waters and bioaccumulate in aquatic food webs, leaving beach and recreational areas, small water users, and fisheries industries particularly vulnerable.

Considerable scientific effort has made progress towards understanding the major causes and ecological and socioeconomic effects of these blooms, but far less is known about the noxious metabolites they produce, many of which have been recognized and (or) chemically identified only recently. Nevertheless, source-water impairment by these compounds (e.g., as T&O) has been a long-standing issue for managers, and with little or no scientific information at hand, attempts to mitigate these metabolites have often been unsuccessful. Prediction and management has been greatly hindered by a general lack of understanding of the identity, causes, and controls of these metabolites; thus the majority of episodes are not anticipated or formally recorded (Watson 2004). Management has traditionally considered NAMs as degradation products that are generated as a direct function of phytoplankton standing stock and thereby controllable through nutrient–biomass management, based on models developed by the Organisation for Economic Cooperation and Development (OECD) and others (cf. Janus and Vollenweider 1981; OECD 1982; Brett and Benjamin 2008). These empirical models have provided valuable and practical first-step management goals that can be addressed at regional and local levels, an approach which has been used to reduce planktonic algal blooms in the Great Lakes and other surface waters with some degree of success (Cullen and Forsberg 1988; Sas 1989; Johengen et al. 1994).

However, this broad-scale approach has been applied less successfully to NAM outbreaks, which often show little relationship to total phytoplankton biomass. There are several reasons for the apparent disconnect. Not all bloom-forming taxa produce these compounds, planktonic taxa are not the only producers, and the compounds themselves show different patterns of synthesis, storage, and (or) release. These are governed by their roles in cell signalling and metabolism, the intrinsic production capacity of the producers, and external agents. Ironically, in some cases, remedial biomass reduction may result in species shifts towards taxa with a high potential for NAM production (Cronberg et al. 1999; Watson et al. 2001*a*, 2005).

This paper evaluates these biochemical source-water impairments in the Great Lakes and examines why their sustainable management has been generally unsuccessful. We will focus on two major metabolite groups, algal volatile organic compounds (VOCs) that cause T&O and the more recently recognized cyanobacterial toxins. We briefly review their chemical characteristics, the species that produce them, the factors that modify their production, and why these are important considerations for successful management. We assess current management approaches via traditional broad-scale models and why these may be ineffective in reducing biomass and metabolite outbreaks, particularly in remediated surface waters. We then will evaluate this biochemical impairment in the Great Lakes, which collectively provide drinking water to over 24 million consumers and support many other human-related activities. The severe eutrophication and degradation of these major ecosystems during the last century led to the establishment of one of the world's largest and longest-standing restoration initiatives, which has operated since 1987 under the binational Great Lakes Water Quality Agreement (GLWQA) (Environment Canada Green Lane (EC-GL) 2004). This programme integrates lake-wide management with local remedial action plans (RAPs) in designated areas of concern (AOCs) and initially served as a successful working model for this and other restoration efforts (e.g., Charlton 1997; Millard et al. 1996). Drinking water T&O is one of the 14 "beneficial use impairments" (BUIs) specifically targeted for remediation under the GLWQA in the 1980s (e.g., International Joint Commission (IJC) 1991; Keene 2002). Yet despite this specific recognition, T&O and other NAM-related impairments have been inadequately characterized and addressed by most RAPS, which are largely managed by local restoration councils and community committees. Faced with limited resources, these remedial programmes have focussed on AOC delisting by attaining defined BUI target levels, in many cases, using surrogate measures (below), and have not addressed newly emerging threats arising from the major shifts in the ecology of these lakes.

Current management approaches: algal biomass

The compliance of aquatic systems to the OECD and similar nutrient–biomass management models is generally good (Reynolds 2003). Nevertheless the limitations of these models are often disregarded, which can undermine their successful application (Sas 1989). As statistical fits of empirical means, they were not designed to imply the mechanisms or dynamic ranges behind these averages (e.g., Janus and Vollenweider 1981). Numerous nutrient–biomass models, which vary in their predictive ability (e.g., Brett and Benjamin 2008), have been derived. Many of these models are linear fits of log-transformed data, despite the fact

© 2008 NRC Canada

phytoplankton biomass follows a sigmoid increase and varies in taxonomic structure and biochemistry with enrichment (Watson et al. 1997; Brown et al. 2000; Watson 2004). There can be significant differences in the relationships between nutrients and biomass when derived from small data sets, which are influenced by local factors such as catchment geology, development, and size, morphometry, flushing, water chemistry, latitude, and climate. These small data sets cannot predict changes over broad nutrient ranges with a high level of confidence (e.g., White 1989; Mazumder 1994; Brown et al. 2000). Many such models are based on seasonal averages, which incorporate bias from sampling protocols, biomass maxima and minima, surface scums, deep-layer maxima, and other biomass aggregations (France et al. 1995; Chorus and Bartram 1999). Depth-segregated maxima are a particular consideration with cyanobacteria, many of which are buoyancy-regulating or mat-forming taxa. Again, these sources of bias can be particularly problematic with small data sets. Although planktonic biomass is the most visible and frequently measured autotrophic compartment, benthic and littoral communities can also be major sources of noxious metabolites, particularly in clear, shallow, or lotic systems (Izaguirre et al. 1983; Baker et al. 2001, Watson and Ridal 2004). Properly constructed nonlinear models, especially when based on large data sets with nutrient ranges spanning several orders of magnitude (e.g., Smith et al. 1987), can be used with more confidence, provided that these bias errors are recognized.

The residual variance about broad-scale nutrient–biomass models thus is often considerable. Janus and Vollenweider (1981) observed maximum chlorophyll *a* (chl *a*) levels of up to three times the predicted mean, whereas later authors report a range of ~30%–300% around the predicted value over a 10-fold total phosphorus (TP) span (e.g., Brown et al. 2000). Total phytoplankton biovolume shows a similar variance, as does that of two of the three major taxa that most frequently produce noxious metabolites, cyanobacteria and diatoms (Fig. 1; Watson et al. 1997). In contrast, a third problematic group, chrysophytes (i.e., Chrysophyceae and Synurophyceae), show no predictable biomass pattern with TP (Watson et al. 1997). Mixing regime and other factors can further modify the response of these three taxonomic groups to nutrient levels (Fig. 1; Nicholls 1995; Annadotter et al. 1999; Tessier and Woodruff 2002). These are important considerations because each major taxon shows a significant shift in relative and absolute biomass with eutrophication, potentially with very different metabolite-related impacts (Seip et al. 1992).

Above all, simple measures of nutrients and algal biomass are pragmatic estimates of highly complex variables. TP includes refractive, particle-bound, and biologically available fractions; mean seasonal TP measures the average net result of external and internal loading minus sedimentation and flushing. This estimate of TP provides no insight into the relative importance of external vs. internal supplies or the short-term dynamics of particulate and dissolved and (or) bioavailable fractions that accompany many algal (and NAM) outbreaks (e.g., Hudson et al. 2000; Reynolds 2003; Baldwin et al. 2003).

Similarly, average total algal standing stock integrates a seasonal succession of diverse taxonomic assemblages.

Fig. 1. LOWESS (locally weighted scatterplot smoothing) fits of log-transformed growing season average biomass for three major noxious metabolite producing phytoplankton groups vs. total phosphorus (TP): (*a*) cyanobacteria, (*b*) diatoms, and (*c*) chrysophytes in polymictic lakes (shaded line, open symbols) and stratified lakes (solid line, solid symbols). (Data adapted from Watson et al. (1997).)

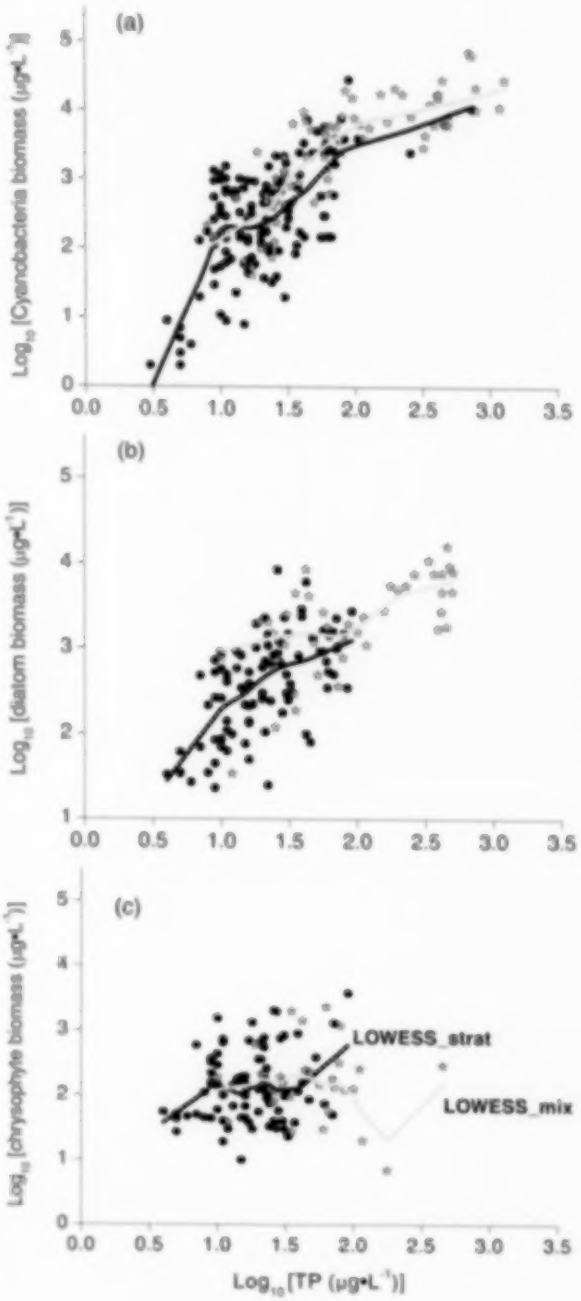

© 2008 NRC Canada

Fig. 2. Relationship between concurrent seasonal mean values of algal standing stock estimated as chl *a* or biomass taken from a range of north-temperate lakes. Linear fit of log-transformed data shown together with 95% upper and lower limits of prediction. (Data adapted from Watson et al. (1997).)

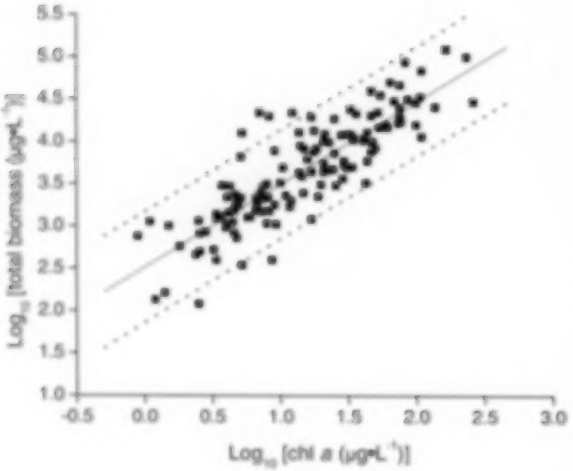

Although often used interchangeably, the two most common measures of standing stock, chl *a* and biomass (biovolume), are correlated poorly (Fig. 2; Nicholls and Dillon 1978; Felip and Catalan 2000), and neither is a robust measure of the risk or nature of noxious algal metabolites. Chl *a*:biomass varies with protocol, environmental factors, and algal size and taxonomic groups (Tolstoy 1979; Nicholls and Dillon 1978; Masson et al. 2000) and shows the most variability in mesotrophic systems, where, for example, ~15 μg chl *a*·L^{-1} can translate to 2500, 9000, or 22 000 μg algal biomass·L^{-1} in different lakes (Fig. 2). At this level of enrichment, algal communities tend to be most taxonomically diverse (e.g., Lazerte and Watson 1981) and exhibit major shifts between edible and inedible algal size fractions (i.e., ingestible by grazers), pointing to the significant and highly variable roles of both bottom-up and top-down processes (Pace 1984; Watson and McCauley 1988; Carpenter et al. 2001).

Similarly, NAM outbreaks are also highly unpredictable in the meso-eutrophic region of the TP–biomass curve. This is particularly evident in remediated systems, where algal biomass often does not follow the decrease with nutrient reduction projected by management models (e.g., Sas 1989). Instead, biomass exhibits nonlinear changes, species shifts, and erratic interannual resurgences (e.g., Peters 1990; Carpenter 2003). Depending on the length and intensity of eutrophication, many systems undergo major shifts in dynamic regime, reflected by changes in food-web structure, water quality and transparency, and internal nutrient pools (e.g., Johannsson et al. 1998; Carpenter 2003; Mayer and Rietkerk 2004). This can delay their restoration response, particularly in such spatially complex systems as the Great Lakes where there are numerous other local and system-wide impacts such as species invasions and widespread agricultural, industrial, and urban development (cf. Van Nes and Scheffer 2005). The extensive invasion of dreissenid mussels in some areas of the Great Lakes has modified light and nutrient regimes, increased littoral productivity, and effectively decoupled inshore–offshore exchange processes implied by steady-state "mixed reactor" management models (Johengen et al. 1995; Hecky et al. 2004). Thus, although long-term remediation has dramatically reduced offshore TP levels across the Great Lakes, this has not achieved a consistent reduction in algal biomass, and some areas are experiencing noxious or toxic algal outbreaks. For example, long-term remedial efforts have reduced nutrients and chl *a* to meso-eutrophic levels in Hamilton Harbour, a historically eutrophic AOC in western Lake Ontario (Charlton 1997). Nevertheless, increases in transparency and phytoplankton diversity in the Harbour have been accompanied by erratic outbreaks of noxious and sometimes toxin-producing cyanobacteria (Fig. 3; Watson et al. 2003). Similarly, severe outbreaks of toxic cyanobacteria have been reported recently in other AOCs undergoing remediation. The Bay of Quinte in northwestern Lake Ontario has also seen a major phytoplankton species shift in the last decade towards a greater predominance of the hepatotoxin-producing cyanobacteria *Microcystis aeruginosa*. Mid- to late-summer levels of hepatotoxic microcystins (MCs) in the open water, recreational areas, and water treatment plant (WTP) intakes in the Bay can range from 2 to 15 times the Health Canada guideline for treated drinking water (1.5 μg total MC·L^{-1}), leaving non-municipal domestic supplies, livestock, and other animals potentially vulnerable (Watson et al. 2005). Although Canada has no recreational guidelines, the observed MC maxima exceed recreational advisory levels adopted in other countries (10–20 μg MC·L^{-1}; cf. Chorus 2001). Outbreaks of toxin-producing cyanobacteria have been reported from other inshore areas of the Great Lakes, some not listed as AOCs, such as Saginaw Bay (Lake Huron), Maumee River and Sandusky Bay (eastern Lake Erie), and southern Lake Ontario embayments (e.g., Brittain et al. 2001; Ouellette et al. 2006; Hotto et al. 2007).

These recent outbreaks have led to a general perception that cyanobacterial impairments are increasing across the Great Lakes. This phenomenon has been attributed by some authors to the invasion of filter-feeding dreissenids and associated shifts in transparency, nutrient recycling, and food-web structure (e.g., Baker et al. 1998; Nicholls 2001; Vanderploeg et al. 2001), although the mechanism is unresolved (Bailey et al. 1999; Sarnelle et al. 2005). Most documented cyanobacterial outbreaks have occurred in areas with high urban shoreline and basin development such as western and southeastern Lake Ontario, western Lake Erie, and Lake Huron's Saginaw Bay. Overall, however, there are too few data to statistically evaluate the apparent increase in the frequency of these blooms in the Great Lakes and other water bodies, an increase that may reflect, in part, greater public and scientific awareness and vigilance of this issue (e.g., Hallegraeff 1993; Smith 2003).

Predicting noxious metabolite outbreaks

Broad-scale nutrient–biomass relationships provide the first step towards a management strategy at the ecosystem level, but alone, they cannot provide the basis for a sustainable and proactive approach for several reasons. Most

© 2008 NRC Canada

Fig. 3. Chlorophyll *a* (chl *a*) levels in Hamilton Harbour, Lake Ontario. Mean (shaded squares), standard deviation (solid capped bars), maximum (solid diamonds), minimum (open diamonds), and range (broken line) calculated from weekly or biweekly 1 m samples collected between May and September of 1986–2006.

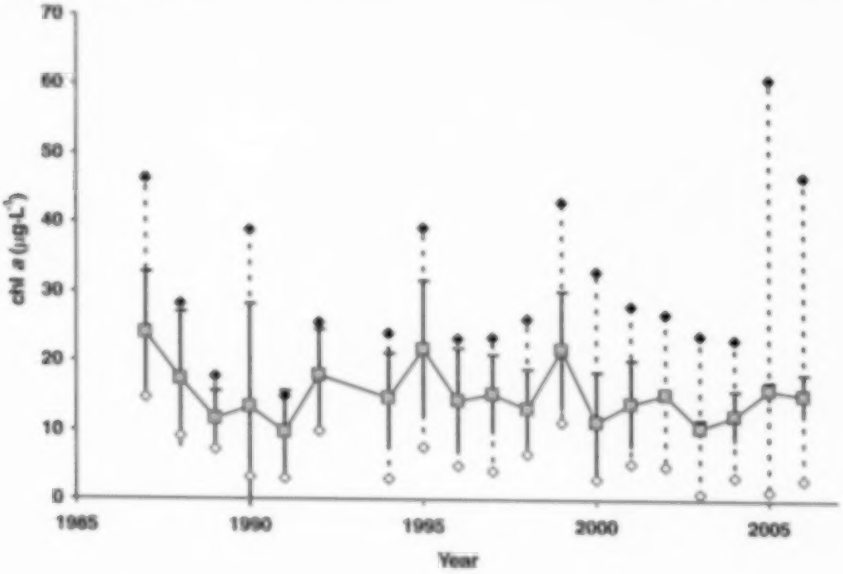

among-lake models do not predict the biomass maxima for a given system, when NAM outbreaks are potentially of most concern. Individual surface waters may show little interannual change in average nutrient levels, but marked differences in mean and maximum biomass and algal taxa. For example, Hamilton Harbour has "meso-eutrophic" annual average levels of chl *a* but high seasonal maxima and erratic and sometimes toxin-containing blooms (Fig. 3). Broad-scale models do not resolve the underlying range in structure and biomass of algal communities, which determine the risk, concentration, and nature of problematic metabolites. These are governed by small- and large-scale processes: (*i*) the capacity of cells for production; (*ii*) their growth and spatial–temporal dynamics; (*iii*) triggers and feedback that modify production; and (*iv*) the properties of the compounds and their fate once released into the environment. Surface waters can contain a mix of noxious and "benign" metabolites and algal species. Research continues to add to the list of NAMs that impair water resources, which include terpenoids, sulphides, lipid and pigment derivatives, aromatics, long-chain hydrocarbons, amines, alkaloids, lipopolysaccharides (LPS), and peptides (Jüttner 1995; Carmichael 1997; Singh et al. 2005). At least some of these compounds are known to act as toxins, deterrents, or attractants, but their importance in intracellular processes and food-web signalling is still largely unresolved but may be key to understanding some of their production dynamics (Watson 2003; Gouvea et al. 2008).

Individual species produce NAMs that differ in chemistry, potency, toxicity, and stability. Cell production (chemistry, timing, internal–external release) varies among and within species and with growth and environment (Orr and Jones 1998; Chorus 2001; Watson and Satchwill 2003). This means that NAM outbreaks may show little direct relationship to measures of ambient nutrients or algal biomass, as seen in Lake Ontario where recent erratic episodes of T&O and toxins have increased despite the remedial P reduction in offshore waters and frequent lack of visible surface blooms. Hydrological and physical vectors may transport metabolites away from cells attached to surfaces, or move planktonic, metabolite-containing cells over considerable distances; for example, downwelling plays a key role in the timing and severity of the odour events detected by northwestern Lake Ontario municipalities (Rao et al. 2003; Watson et al. 2007).

Taste and odour: volatile organic compounds

As noted above, the taxonomic composition of blooms affects both the nature and the magnitude of their metabolite-related impacts on water quality. Fishy–rancid–"cucumber" smelling polyunsaturated fatty acid (PUFA) derivatives (mainly unsaturated aldehydes) show erratic outbreaks that cannot be predicted or managed using conventional nutrient-based models. Chrysophytes, which are common sources of these VOCs, show little apparent relationship to nutrients on a broad scale (Watson et al. 1997). Erratic rancid- or fishy-smelling blooms can occur in oligotrophic surface waters in response to small or undetectable changes in nutrient levels (<5–10 $\mu g \cdot L^{-1}$) or bacteria (Watson et al. 2001*b*) and may develop as deep-layer or under-ice populations that are not usually monitored or included in growing season average planktonic biomass estimates. Chrysophytes also produce major outbreaks in eutrophic systems, and remedial nutrient reduction may actually increase these episodes (e.g., Jüttner et al. 1986; Yano et al. 1988; Nicholls 1995). PUFA derivatives are produced only at cell disruption or death (e.g., via grazing, treatment), are short-lived, and range in the odour threshold

© 2008 NRC Canada

concentrations (OTCs) at which they are detectable to humans (from ng·L^{-1} to µg·L^{-1} levels). Even closely related species may produce different VOCs, and therefore equivalent biomasses can have different effects on final odour (Watson and Satchwill 2003); differences in the reactivity of the aldehydes mean that they respond differently to treatment (Satchwill et al. 2007).

In more eutrophic systems, cyanobacteria are a frequent source of VOCs such as terpenoids, thiols, and pigment derivatives, which differ markedly from the PUFA derivatives in biochemistry, production, and release dynamics. Cyanobacteria are also the major group of freshwater photoautotrophs to produce toxins that can affect human health and well-being (below). In many cases, toxin and odour production by these taxa are neither concurrent nor well predicted by traditional models. Cyanobacteria differ among species and strains in their metabolite chemistry, habitat, and production dynamics (Mikalsen et al. 2003; Jüttner and Watson 2007), and surface scums, deep-layer maxima, biofilms, and benthic mats all can be a source of these compounds. Thus, producers and metabolites can become spatially and temporally decoupled.

Two earthy–muddy–musty smelling terpenoids, geosmin and 2-methylisoborneol (2-MIB), account for the global majority of drinking water odour outbreaks and are widespread in the Great Lakes. These VOCs are highly potent (detectable to humans at <10 ng·L^{-1}), stable, and resist conventional water treatment. They are synthesized by a select number of planktonic bloom-forming and benthic–littoral cyanobacteria (also by some Actinomyces, myxobacteria, and fungi and other soil microbiota). There is a tremendous range in intrinsic production capacity among even closely related taxa (e.g., Watson 2003). Most production is retained within the cells (tightly bound to thylakoids) with minimal external release during growth; the bulk production occurs at senescence, death, or during grazing or treatment (Durrer et al. 1999; Jüttner and Watson 2007). Isopropylthiols, by contrast, are continuously excreted over the growth cycle by select strains of *Microcystis aeruginosa* (also a potent toxin-producing species), whereas large amounts of the musty-tobacco-smelling pigment derivative β-cyclocitral are generated at cell damage or death by all *Microcystis* spp. via enzyme-mediated catalysis (Jüttner 1984). Both isopropylthiols and β-cyclocitral are short-lived in the water and rapidly lost by volatilization and chemical–photooxidative breakdown. As a result, *Microcystis* rarely causes significant off flavour in treated drinking water supplies because it does not produce either of the more resilient T&O compounds geosmin and 2-MIB.

Toxins

Algal toxins, on the other hand, are colourless and tasteless. Ingestion or inhalation can cause a range of symptoms (gastroenteritis, vomiting, fever, flu-like symptoms, ear–eye–throat–mouth irritation, rashes, abdominal pain, blurred vision, kidney and liver damage or haemorrhage). Long-term chronic exposure has been linked with increased incidence of liver cancer (Fleming et al. 2002; Falconer 1996; Codd et al. 2005). Potential exposure pathways for humans include contaminated drinking water, recreational exposure, toxin residue on crops irrigated with contaminated water, ingestion of contaminated animal tissue, and dietary supplements. There is growing evidence that cyanobacterial toxins can have differential and severe impacts on food-web structure and function and lead to degradation or impairment of phytoplankton, zooplankton, zoobenthos, or fish populations (Wiegand and Pflugmacher 2005). For example, the common hepatotoxic microcystin peptides are toxic to some algae and many primary consumers (e.g., cladocerans, copepods, larval invertebrates, and microzooplankton), although some consumers (e.g., copepods) may have developed avoidance mechanisms to limit intoxication (Reinikainen et al. 2002). These toxins can be accumulated and (or) bound in tissues of bivalves such as dreissenids, or passed through their guts in pseudofaeces, which may facilitate their release in the dissolved form. Microcystins are also readily accumulated (but not concentrated) in fish tissue (Ibelings et al. 2005), and this may represent another important pathway for human exposure.

Cyanotoxins vary in their response to treatment, and removal effectiveness is greatly influenced by the levels of dissolved vs. cell-bound toxin and dissolved organic material in the water (see, e.g., review by Svrcek and Smith 2004). Chlorination at levels generally employed by water supply facilities has little effect on the levels of many cyanobacterial toxins; however, they can be removed by activated carbon filtration, ozonation, or other advanced methods, suggesting that major water supplies represent only a minor risk for human intoxication if these treatments are employed effectively. However, treatment can be compromised during peak water-use periods (e.g., in the summer) and as a result of high background levels of organic material, as is often associated with blooms. Of particular concern are minor water treatment or distribution facilities, home filters, or individual exposure (e.g., via contact with, or ingestion of, concentrated surface scums) where preventative measures may not have been employed.

Similar to odour events, we presently cannot predict when toxic blooms will occur in most water bodies, particularly large and spatially complex systems such as the Great Lakes. For example, the production of freshwater cyanobacterial toxins affecting humans, domestic animals, or wildlife has only been linked to some species of bloom-forming (or benthic mat forming) cyanobacteria; thus models predicting the abundance of cyanobacteria as a whole cannot resolve among these taxa (e.g., Smith 1983; Dokulil and Teubner 2000; Downing et al. 2001). Microcystins, the most common cyanobacterial toxins, are known to be produced by species of *Microcystis*, *Anabaena*, *Planktothrix*, and *Oscillatoria*, and it is likely that other yet unidentified species are also sources (for reviews of these and other toxins, see, e.g., Falconer 1996; Chorus 2001; Codd et al. 2005). Each of the genera also has nontoxic representatives, making microscopic identification of the responsible organism(s) difficult. For example, recent molecular evidence from the western basin of Lake Erie showed that the fraction of *Microcystis* present in a toxic bloom that actually carry the genetic potential for toxin production ranges from 5% to 100% (Rinta-Kanto et al. 2005); thus it is extremely difficult to predict toxin levels from cyanobacteria biomass or cell counts. Work in the Sandusky Harbour region has shown

© 2008 NRC Canada

that *Planktothrix* species may be the major toxin-producing genera in that system, despite the widespread occurrence of *Microcystis* spp. (Rinta-Kanto and Wilhelm 2006). Similar work in the embayments of Lake Ontario has shown that the genetic potential for toxin production is widespread, even though the actual levels of microcystin toxin production are generally low (Boyer 2007*a*; Hotto et al. 2007). Furthermore, we still have a very poor understanding of the physiological and ecological basis for toxin production. Most effort has focused on microcystins, as these toxins have been the major focus of the water industry, government, and health agencies; however the neurotoxin anatoxin-*a* has also been detected throughout the western basin of Lake Erie and the embayments of Lake Ontario (Yang 2007).

As seen with VOCs, the risk of these toxins cannot be assessed by simple visual inspection of a water body; furthermore, there is no consistent relationship between odour and toxin production as noted above. The potential for toxicity increases with eutrophication and (or) the presence of bloom scums or detached benthic mats; for example, some 60% of blooms surveyed in Europe were found to be toxic (Willén 1999; Kotak et al. 2000; Codd et al. 2005) and up to 40% of the subsurface (1 m) samples collected in Lake Erie and 20% of the samples from less eutrophic Lake Ontario from different surveys carried out July–September of 2000–2004 through the NOAA Monitoring and Event Response in the Lower Great Lakes (MERHAB-LGL) program had detectable levels of microcystins (Boyer 2007*a*, 2007*b*; Fig. 4). Interestingly, however, in those samples that showed detectable levels of toxin, there was no significant difference between these two Great Lakes in the range of MC production per unit chl *a*, indicating that nutrient levels (i.e., P, N) do not have a major influence on per capita toxin production. This is consistent with laboratory studies that generally show that per capita toxin production varies less than fivefold with changing nutrient conditions (Sivonen and Jones 1999). On the other hand, toxin levels can show rapid spatial and temporal variation as a result of diurnal vertical cell migration or wind action; for example, Kotak et al. (1995) observed a sixfold change in raw water MC levels over a 24 h period, demonstrating the critical importance of frequent monitoring during high risk periods. As with many VOCs, most toxin is retained within the cyanobacterial cells and released upon death or cell damage (e.g., by grazers). Some toxins (e.g., microcystins) can remain in the open water after the collapse of a bloom and (or) bioaccumulate in the aquatic food web (e.g., macrophytes and primary consumers such as zooplankton, benthos, filter feeders), even persisting in dried shoreline cyanobacterial mats (Kotak et al. 1996; Chorus et al. 2000; Yin et al. 2004). Open-water MC levels have been found to be most closely allied with the predominance of certain species such as *Microcystis aeruginosa* (e.g., Kotak et al. 1996; Willén 1999; Brittain et al. 2001); however, the presence of these species is not always indicative of toxicity, which not only varies among strains, but also under different growth-modifying conditions (Chorus and Bartram 1999; Mikalsen et al. 2003). For example, *Microcystis* blooms in the Sandusky Basin of Lake Erie appear to be low-level or nontoxin producers, with most of the MC toxin in this ecosystem produced by *Planktothrix*

Fig. 4. Occurrence by concentration range of microcystins (total particulate) in samples collected from 1 m at offshore and inshore sites in Lakes Ontario and Erie between 2000 and 2004. Toxicity was determined by the protein phosphatase inhibition assay. Samples were collected from both the area of concern (AOC) and offshore stations (MERHAB-LGL data adapted from Boyer 2007*a*).

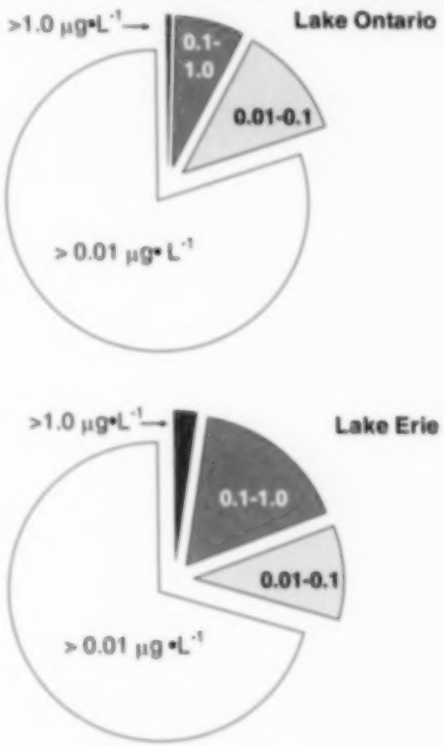

species (Rinta-Kanto and Wilhelm 2006). The determination of toxin producers within a genus is even more difficult. Thus, although *M. aeruginosa* is the most widely reported *Microcystis* species across the Great Lakes, considerable expertise is often needed to distinguish among different growth stages of some nine species of *Microcystis* that have been identified in these water bodies (Watson et al. 2003). Molecular techniques hold considerable promise in this regard (Rinta-Kanto et al. 2005; Hotto et al. 2007); however, we are only now starting to understand how variations in the microcystin biosynthetic pathway translates to occurrences of toxins in the water body (Mikalsen et al. 2003). This remains an area in need of further research.

Metabolite impairments in the Great Lakes: status and management approaches

Taste and odour

Many areas of the Great Lakes are prone to outbreaks of noxious metabolites including, but not restricted to, AOCs (Fig. 5; Table 1). Most of the available T&O data are based on nonquantitative measures such as informal records of customer complaints and treatment plant operator notes, although some include odour descriptors (fishy, earthy–muddy, sewage, chlorine) and timing (i.e., seasonality).

© 2008 NRC Canada

Fig. 5. (*a*) Location of Great Lakes Areas of Concern (AOCs; shown as triangles) and those AOCs with eutrophication as a listed impairment (crosses); (*b*) taste–odour (T&O) and toxin impairment in AOCs and other areas (data from published papers cited in text, AOC reports, published and unpublished water treatment plant records, and MERHAB-LGL). Stars, the occurrence of harmful algal blooms for which production of toxins has been confirmed by chemical means; circles, reported taste and odour impairment.

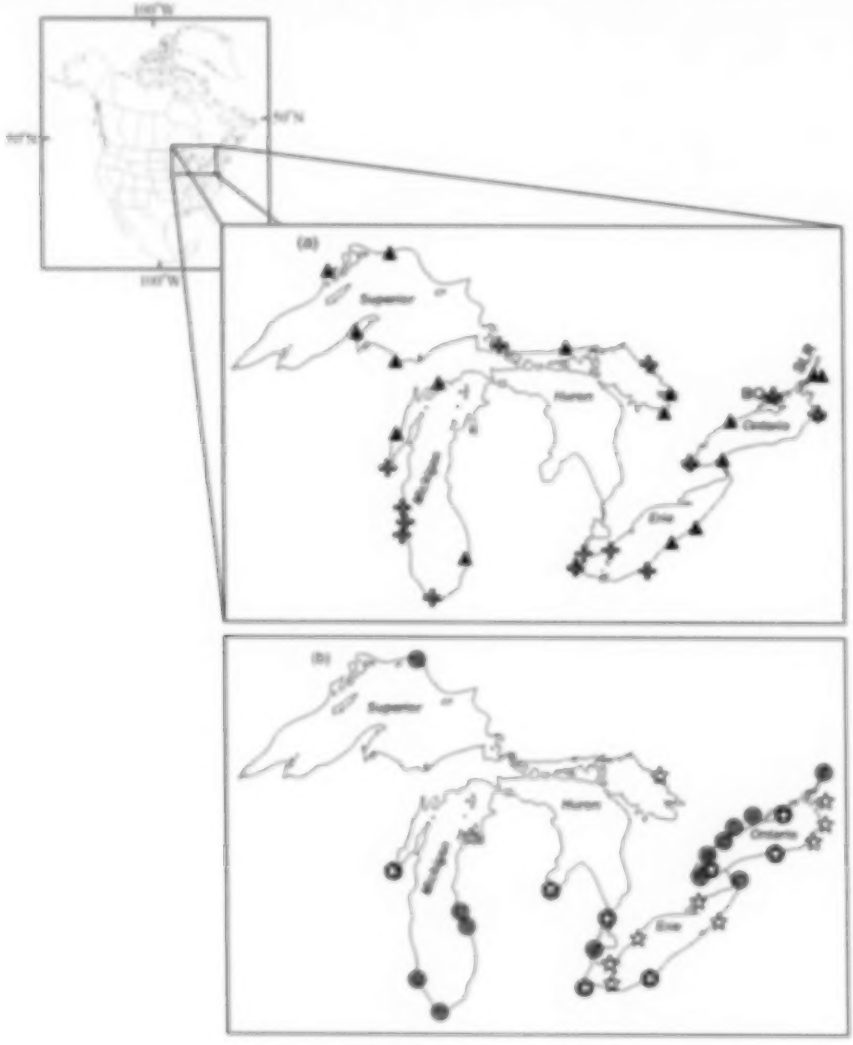

Nevertheless, even these qualitative data indicate a significant level of T&O impairment across the Lakes, with over one-third of the AOCs known to be affected (Table 1). In fact, the level and spatial extent of this problem is likely underestimated. For example, a recent survey of 59 Great Lakes drinking water treatment plants (most of these not within AOCs) reported that ~20% of these utilities are affected by annual T&O and a further 27% experience erratic episodes. Not surprisingly, most of the affected utilities draw water from the Lakes in areas near more densely populated regions, with the majority of T&O outbreaks occurring in the summer or fall during peak biological activity.

A more quantitative assessment measured concentrations of several VOCs (trichloroanisoles, methoxypyrazines, geosmin, and 2-MIB) in raw and treated water of Ontario municipal drinking water supplies (Ontario Ministry of the Environment 2000). Samples collected at individual treatment plants during a 2-year observation period often did not include the high risk summer–fall period, but nevertheless, a significant number showed VOC levels in treated water that exceeded odour threshold levels. In this survey, it is likely that the limited sampling regime (~2–3 times per year over 2 years) underrepresented the impairment, as T&O outbreaks are often episodic, vary among years, and can be missed by infrequent sampling. For example, between 1999 and 2006, the annual episodic late-summer geosmin peaks in both offshore surface waters and treatment plant intakes in western Lake Ontario have shown a ~100-fold interannual

© 2008 NRC Canada

Table 1. Great Lakes Areas of Concern (AOCs) and incidence of selected beneficial use impairments (BUIs)[a] related to algal–cyanobacterial growth.

AOC	Beneficial use impairment					
	No. 8	No. 13	No. 9	No. 11	No. 12	Tox
Lake Superior						
Peninsula Harbour	—	—	+	—	—	—
Jackfish Bay	—	—	—	+	—	—
Nipigon Bay	+	—	—	+	—	—
Thunder Bay	—	+	—	+	+	—
St. Louis Bay – River	—	—	—	+	—	—
Torch Lake	—	—	—	—	—	—
Deer Lake – Carp Creek.	—	—	—	—	—	—
Total[b]	1	1	1	4	1	0
% AOCs impaired	14	14	14	57	14	0
Lake Michigan						
Manistique River	—	—	—	+	—	—
Menominee River	—	—	—	—	—	—
Fox River – Green Bay	+	+	(+)	+	—	P
Sheboygan River	+	+	—	—	—	—
Milwaukee Estuary	+	+	—	+	—	—
Waukegan Harbour	—	—	—	—	—	—
Grand Calumet River – Indiana Harbour	+	+	+	+	+	—
Kalamazoo River	—	—	—	—	—	—
Muskegon Lake	+	(+)	+	+	—	—
White Lake	+	(+)	+	+	—	—
Total[b]	6	7	4	6	1	(1)
% AOCs impaired	60	70	40	60	10	10
Lake Huron						
Saginaw River – Bay	+	+	+	+	—	+
Collingwood	—	—	—	—	—	—
Severn Sound	+	—	—	+	—	—
Spanish Harbour	—	P	—	—	+	—
Total[b]	2	2	1	2	1	1
% AOCs impaired	50	29	14	29	14	14
Lake Erie						
Clinton River	+	+	—	+	—	—
Rouge River	+	—	—	+	—	—
River Raisin	—	—	—	—	—	—
Maumee River	+	—	+	+	—	+
Black River	+	(+)	—	+	—	—
Cuyahoga River	+	(+)	(+)	+	—	—
Ashtabula River	—	—	—	—	—	—
Presque Isle Bay	—	—	—	—	—	—
Wheatley Harbour	P	+	—	—	—	—
Total[b]	6	3	2	5	0	1
% AOCs impaired	67	33	22	56	0	11
Lake Ontario						
Buffalo River	—	—	—	—	—	—
Eighteen Mile Creek	—	—	—	—	—	—
Rochester Embayment	+	+	+	+	+	—
Oswego River	+	(+)	(+)	P	—	+
Bay of Quinte	+	+	+	+	—	+
Port Hope	—	—	—	—	—	
Metro Toronto	+	(+)	—	+	—	
Hamilton Harbour	+	—	—	+	—	+
Total[b]	5	4	3	5	1	3
% AOCs impaired	63	50	25	63	13	25

© 2008 NRC Canada

Table 1 (*concluded*).

AOC	Beneficial use impairment					
	No. 8	No. 13	No. 9	No. 11	No. 12	Tox
Connecting channels						
St. Mary's River	+	—	—	+	—	—
St. Clair River	—	—	+	+	+	—
Detroit River	—	—	+	+	—	—
Niagara River (Ont.)	+	(+)	—	—	—	—
Niagara River (N.Y.)	—	—	—	—	—	—
St. Lawrence River (Cornwall)	+	(+)	(+)	+	+	—
St. Lawrence River (Massena)	—	—	+	—	—	—
Total[b]	3	2	4	4	2	0
% AOCs impaired	43	29	57	57	29	0
All						
Total[b]	23	19	15	25	6	6
% AOCs impaired	51	42	33	56	13	13

Note: Abbreviation and BUI listing numbers (1–14): No. 8, undesirable algae – eutrophication; No. 13, degradation of phytoplankton and zooplankton; No. 9, taste and odour – drinking water restrictions; No. 11, degradation of aesthetics; No. 12, increased costs for agriculture–industry; "+" indicates BUI formally listed by RAP; "(+)" indicates BUI under RAP investigation; (P) indicates BUI not listed but highly probable. Recorded occurrence of toxic cyanobacteria also included (Tox), although not a listed BUI.

[a]For listing of BUIs 1–14, see, e.g., http://www.on.ec.gc.ca/greatlakes/default.asp?lang=En&n=FD65DFE5-1.

[b]Totals include probable impairment (P).

range, although there were no similarly significant changes in ambient nutrient or chlorophyll levels among years (Watson et al. 2007).

Overall, however, there are too few quantitative data to evaluate T&O in the Great Lakes formally. Most importantly, few of the recorded T&O events have been traced to their chemical and biological origin(s), in contrast to a number of the reported toxic outbreaks (below). Qualitative (sensory) T&O measures and incidental reports indicate greater impairment in the lower Great Lakes near major urban centres (Fig. 5), but the few quantitative studies to date (e.g., above) report a range of spatial and temporal variability that cannot be effectively evaluated or traced using such qualitative measures.

An early study of T&O impairment in Saginaw Bay by Bierman et al. (1984) provides further insight into this issue. This AOC has a history of eutrophication and industrial contaminants, and T&O has long been an issue, especially before the 1980s when raw and treated water repeatedly exceeded the sensory threshold odour number (TON; Table 2), and WTPs were faced with high treatment costs. Investigators attributed summer odour during 1970–1980 to cyanobacteria and actinomycete bacteria, although in fact, VOC production by either of these taxa was not verified directly. Actinomycetes are primarily terrestrial aerobes and common in spring and storm runoff but are difficult to monitor even with current advanced techniques and, in fact, are not a predominant cause of aquatic T&O (e.g., Zaitlin and Watson 2006; Jüttner and Watson 2007). Odours generated by rotting organic debris (algae, macrophytes, invertebrates) in beach areas was also highly problematic in the Saginaw Bay area and, currently, again a major (nonquantified) issue with the recent widespread resurgence of dense beds of attached algae (e.g., *Cladophora glomerulata*) in inshore areas in the Great Lakes (Brownlee et al. 1984; Painter and Kamaitis, 1987; Higgins et al. 2005).

As noted above, not all cyanobacterial taxa produce problematic VOCs. Bierman et al. (1984) clearly highlighted this important point in their study and, furthermore, demonstrated the importance of using relevant time scales and measures of algal standing stock to resolve relevant dynamics in water quality, T&O, and taxonomic assemblages. These authors analyzed seasonal changes in threshold odour numbers at the Saginaw–Midland WTP in relationship to three different measures of algal biomass in the Bay (numerical abundance, biomass, and chl *a*). They showed that T&O was strongly correlated to the total cyanobacteria biomass but not to cyanobacterial abundance (cell counts) and not to any of the three measures of total algal biomass. The relationship between odour and cyanobacteria was strongest in the fall when total algal biomass was much reduced, but the proportion (percentage) of cyanobacteria had increased. This suggested that the main VOC producers were cyanobacteria and, furthermore, that the species involved were not the most numerically abundant cyanobacterial taxa (typically small-celled nano- or pico-plankton) but were large colonial taxa, which contributed disproportionately to the biomass. Numerous other studies have also implicated large colonial or filamentous cyanobacteria as primary sources of aquatic T&O in the Great Lakes and elsewhere (e.g., Jüttner et al. 1986; Jones and Korth 1995, Watson et al. 2007).

The study by Bierman et al. (1984) also highlights the need for continued vigilance after T&O impairment has been initially moderated. Even though the analysis and identification of T&O compounds has been greatly improved since this work was carried out, most RAPs do not collect quantitative data but rely instead on infrequent measures of treated municipal drinking water, customer complaints (if

© 2008 NRC Canada

Table 2. Listing of US EPA non-mandatory secondary maximum contaminant level (SMCL) adopted by some state health agencies and public water systems for drinking water contaminants that have undesirable effects on aesthetics, cosmetics (i.e., no harmful effects on body), and equipment or treatment effectiveness.

Contaminant	SMCL	SMCL exceedence effects
Chloride (a)	250 mg·L^{-1}	Salty taste
Copper (a,c)	1.0 mg·L^{-1}	Metallic taste; blue-green staining
Iron (a,c)	0.3 mg·L^{-1}	Rusty colour, staining; sediment; metallic taste
Manganese (a,c)	0.05 mg·L^{-1}	Black-brown colour, staining; bitter metallic taste
Sulfate (a)	250 mg·L^{-1}	Salty taste
Zinc (a)	5 mg·L^{-1}	Metallic taste
Odour (a)	3 TON*	Rotten-egg, musty, or chemical smell
pH (a,c)	6.5–8.5	Low pH: bitter metallic taste; corrosion High pH: slippery; soda taste; deposits
Corrosivity (a,c)	Noncorrosive	Metallic taste; corroded pipes and (or) fixtures
Foaming agents (a,c)	0.5 mg·L^{-1}	Frothy, cloudy; bitter taste; odour
Total dissolved solids (a,c)	500 mg·L^{-1}	Deposits; colour; staining; salty taste
Aluminium (a)	0.05–0.2 mg·L^{-1}	Colour
Colour (a)	15 units	Colour
Fluoride (b)	2.0 mg·L^{-1}	Tooth discoloration
Silver (b)	0.1 mg·L^{-1}	Skin and eye discoloration

Note: Contaminants followed by the letter "a" have undesirable effects on aesthetics, contaminants followed by the letter "b" have undesirable cosmetic effects (i.e., no harmful effects on body), and contaminants followed by the letter "c" have undesirable effects on equipment or treatment effectiveness.

*TON is defined as the greatest dilution of sample with odour-free water yielding a perceptible odour, or how much dilution it takes to "dilute away" the odour. TON = 0 if the neat solution has no odour. TON is subject to the variability in individual testers and depends on the starting concentration; thus, the same compound in different waters at different starting concentrations would have different TON.

recorded), and incidental reports. In some cases, proxy measures are still used (e.g., total P and algal biomass anticipated from measures of TP, chemical treatment doses, disinfection by-products), with the questionable assumption that these are correlated with VOC levels (e.g., Keene 2002). For example, the most recent Saginaw Bay RAP report relied on incidental testimony and interviews to conclude that T&O impairment is no longer problematic (Public Sector Consultants Inc. 2002). Yet the same report also indicates that data are "inconsistent, often haphazard and subject to fiscal restraints". T&O was assessed by this RAP using periodic measures of the ratio of TN to TP in the Bay close to WTP intakes, based on the premise that when TN:TP < 30 (by weight), there is a high risk of cyanobacterial dominance (and therefore T&O) (cf. Smith 1983). This broad and indirect approach overlooks the fact that total cyanobacteria biomass, in fact, is far more strongly related to total P (Downing et al. 2001) and also disregards the major differences in NAM production (and N requirements) among and within different algal taxonomic and size fractions. Importantly, the recent increase in nonodourous toxic cyanobacteria (*Microcystis*) in this AOC is not addressed under the RAP programme (cf. Budd et al. 2002). It is of note that several recent empirical studies have described significant relationships between inorganic N fractions (NO_3, NH_4) or N–P ratios and both microcystins and specific cyanobacterial genera (*Microcystis*, *Anabaena* spp.) (Kotak et al. 2000; Giani et al. 2005), again demonstrating the importance of a more fine-grained approach to these impairments (cf. Mayer and Rietkerk 2004).

As noted above, as with all other ecological indicators, there is a critical need for long-term data. Thus, 6 years of multidisciplinary research by the Ontario Waterworks Research Consortium (OWWRC) were required to characterize complex mechanisms behind the sources, timing, and severity of erratic geosmin outbreaks in western Lake Ontario (Watson et al. 2007; Moore and Watson 2007). This study demonstrated how climate and large-scale water movement play a key role in these annual episodes by transporting patchy distributions of offshore pelagic cyanobacteria (*Anabaena lemmermanii*) and geosmin to deep inshore treatment plant intakes (Rao et al. 2003). The OWWRC study also has provided valuable climate-related predictors of these outbreaks for use by the water industry and a revised delineation of the potential zone of influence around drinking water intakes, central to the development of relevant source water protection programmes. In the St. Lawrence River (SLR) – Cornwall AOC, a similar long-term research effort was required to trace annual geosmin and MIB events to shoreline algal biofilms in the extensive and complex littoral zone that generate severe T&O along a 200 km stretch of shoreline (Ridal et al. 2007). Nevertheless, because the source of the odour in the SLR is considered "natural" (as opposed to anthropogenically induced) and to originate outside AOC boundaries, this impairment is not addressed by the Cornwall RAP, although it is listed on the US side of the river by the partnered Massena RAP. This example again highlights the need for flexible remedial programmes that balance practical constraints against ecologically meaningful remedial criteria and boundaries.

The working definition of taste and odour as a beneficial impaired use places a disturbing onus on the drinking water industry to "fix" this problem at individual treatment plants. This approach is inherently unsustainable and also beyond

© 2008 NRC Canada

Table 3. Current regulatory and advisory limits for cyanobacterial toxins in drinking and recreational waters (from Chorus 2001).

	Current regulatory and advisory limits	
	Drinking water	Recreation
Australia	6500 cells·mL^{-1}	20 000 cells·mL^{-1}
Microcystins	1.3 μg·L^{-1}	10–20.0 μg·L^{-1}
Cylindrospermopsin	1.0·L^{-1}	Australia also has a livestock consumption value
PSTs (saxitoxin)	3.0·L^{-1}	—
Anatoxin-a	12.0 μg·L^{-1}	—
Brazil (MAV)	10 000 cells·mL^{-1}	—
Microcystins	1.0 μg·L^{-1}	—
Cylindrospermopsin	15.0 μg·L^{-1}	—
PSTs (saxitoxin)	3.0 μg·L^{-1}	—
Canada	—	—
Microcystins	1.5 μg·L^{-1}	—
New Zealand (MAV)	—	—
Microcystins	1.0 μg·L^{-1}	—
Cylindrospermopsin	1.0 μg·L^{-1}	—
PSTs (saxitoxin)	3.0 μg·L^{-1}	—
Anatoxin-*a*	6.0 μg·L^{-1}	—
Anatoxin-*a*(S)	1.0 μg·L^{-1}	—
World Health Organization	—	20–100 000 cells·mL^{-1}
Microcystins	1.0 μg·L^{-1}	20.0 μg·L^{-1}
	Czech Republic, France, Japan, Norway, Poland, Spain	Australia, France, Germany, Netherlands

the resources of many municipalities. It requires that utilities maintain or upgrade treatment technology to stay ahead of this impairment, along with many other chemical threats, and to constantly monitor raw and treated water for changes in their levels. Yet unlike many other recognized contaminants, there are no uniform standards or guidelines defining acceptable T&O levels that can be targeted by treatment plants or remedial programmes. In Canada, there are only subjective T&O guidelines set by different provinces; for example, Ontario has an "aesthetic" guideline for treated drinking water as "inoffensive". In the US, agencies have adopted the US EPA nonmandatory secondary maximum contaminant level (SMCL) for T&O, which recommends "odour" levels below a TON of 3.0, an ambiguous and inadequate measure of odour (Table 2). As shown above, many Great Lakes utilities (and RAPs) use proxy measures or customer complaints as an indication of exceedences, a reactive and haphazard approach that can be biased by media coverage of T&O episodes ("snowball effect").

The criteria and methods used to define and evaluate T&O have generally underrepresented the scope and severity of this impairment across the AOCs and Great Lakes (and still do), as demonstrated above. The RAP definition considers only treated drinking water from municipal supplies drawn from within the boundaries of the AOCs. It does not include the often-significant T&O impairment of water drawn by small or remote communities, or individual users who are not served by municipal supplies. The definition considers only those episodes that are not removed using "standard treatment" (i.e., coagulation, settling, disinfection). And finally, it does not recognize other sectors that are severely affected by this impairment, e.g., beaches, recreational waters, and tourist and fishing industries (IJC 1991; Thorstenberg and L'Italien 1998).

Toxins

Cyanobacterial toxins, on the other hand, were identified far more recently as a potential threat in freshwaters, although human and animal poisonings from bloom-laden waters have been reported for many centuries (Carmichael 1997). Because little was known about these toxins when the RAPs were first developed, they were not recognized as a threat or considered as delisting criterion and thus have not been monitored or assessed in most AOCs or other areas across the Great Lakes. However, recent studies indicate moderate to severe impairment in several areas, including AOCs such as the Bay of Quinte and Hamilton Harbour. As noted above, in many cases, outbreaks of T&O are not concurrent with (or caused by) recorded toxic biota, although there is some overlap (Fig. 5). Even though cyanobacterial toxins are a more "recent" concern, guidelines have already been established in many European, South American, and other countries such as New Zealand and Australia, indicative of their importance as an impairment and potential health threat (e.g., Codd et al. 2005; Chorus 2001; Table 3). Canada has a (non-mandatory) Health Canada drinking water guideline of 1.5 μg MC-LR·L^{-1}, one of the most toxic microcystin congeners and also one of the more common forms reported in the Great Lakes (e.g., Brittain et al. 2001). Ontario has adopted this level as the maximum acceptable concentration (MAC) and furthermore advocates visual monitoring of drinking and recreational water bodies with a history of algal blooms during the high-risk (summer)

© 2008 NRC Canada

season for bloom formation hence toxin production; in the event of a potential threat, follow-up is urged according to a protocol similar to that developed in Europe and Australia and by the World Health Organization. A few larger Ontario municipalities recently began to monitor total MC in drinking water (Ontario Ministry of the Environment (OME) 2003); however, some have now discontinued this practice because of exacting provincial licensing requirements for the analysis. Nevertheless, the vast majority of Ontario water supplies are not monitored for toxins. The US currently has no standards or monitoring or sampling protocols for these or other algal toxins, although microcystins cylindrospermopsin and anatoxin-*a* have been listed on the US EPA Contaminant Candidate List (CCL) for further research since 1992, and the recent reauthorization of the Harmful Algal Bloom and Hypoxia Research and Control Act (HABHRCA) in 2004 required US Federal agencies to assess the presence and risk from harmful cyanobacteria blooms in freshwater and estuarine environments and develop plans to reduce the likelihood of their formation and to mitigate their damage (Fristachi and Sinclair 2008). It is anticipated that in response to this requirement, the US EPA may issue guidelines for cyanobacterial toxins in the near future.

Although reports of toxic cyanobacteria blooms in the Great Lakes appear to have increased significantly over the past decade and (similar to T&O) are more prevalent in the lower, more heavily populated Great Lakes (Fig. 5), the short- and long-tem risks to humans, wildlife, and domestic animals and aquatic food webs are still unknown. An increasing numbers of studies point to an unpredictable but potentially serious level of risk to human health. Sporadic, episode-based outbreaks of high toxin levels have been reported in studies of toxin-producing *Microcystis* blooms in inshore areas where exposure to humans is increased (Lakes Huron, Michigan, Erie, and Ontario; e.g., Brittain et al. 2001; Vanderploeg et al. 2001; Rinta-Kanto et al. 2005). Lake-wide late-summer spatial surveys have indicated that there may be a higher potential risk in the lower lakes than previously thought (e.g., Ouellette et al. 2006; Hotto et al. 2007). In the past few years, data collected by larger Ontario municipalities (e.g., Toronto, Hamilton, Deseronto, etc.) show periods of elevated MC in raw water but adequate removal by municipal treatment plants (Watson et al. 2005; S.B. Watson, D. Fellowes, and C. Dunn, unpublished data). We have characterized spatial and temporal levels of these toxins in specific AOCs such as the Bay of Quinte, Hamilton Harbour, and the Rochester embayments; these indicate periods of severe impairment of inshore sites by windblown accumulations of toxic material, where MC levels can reach levels in excess of 300 $\mu g \cdot L^{-1}$. These elevated concentrations represent a potential exposure hazard to human recreational users, domestic animals, and wildlife. To date, there are little published data on other cyanobacterial toxins, notably the neurotoxic anatoxins or the paralytic shellfish toxins (PSTs) saxitoxin and neosaxitoxin. Many of the blooms in these lakes are dominated by potential neurotoxin-producing cyanobacteria species (e.g., Barbiero and Tuchman 2001; Watson et al. 2003, 2005), and recent surveys have indicated the widespread occurrence of low concentrations of anatoxin-*a* in both nearshore and offshore sites of Lakes Erie and Ontario (Boyer 2007*a*, 2007*b*; Yang 2007). The other toxins (PSTs and the hepatotoxin cylindrospermopsin) appear to be quite rare in these systems.

An integrated management approach: summary and conclusions

Algal metabolite impairment is the net result of (*i*) the growth and dynamics of individual algal species, (*ii*) the production rate and physical, chemical, and biological properties of their metabolites, and (*iii*) the triggers and feedback that modify production. None of these processes is easy to predict or measure, and many are overlooked because they occur at different spatial and temporal scales. Noxious metabolite sources and controls cannot be assumed, and each case requires a systematic multiyear investigation, as with other impairments. At the same time, NAM studies can provide valuable insight into the major factors that affect broader issues of source-water function and integrity. For example, VOC outbreaks in oligotrophic and mesotrophic systems have served to trace sources of variability in aquatic systems that contribute to their divergence from classic nutrient management models, such as large- and small-scale physical processes (Rao et al. 2003), elevated bacterial levels (Watson et al. 2001*b*), chemical food-web signalling (Wendel and Jüttner 1996), contaminants (Jüttner 1992), and "hidden" and nonpelagic algal development (Sabater et al. 2003; Vilalta and Sabater 2005; Ridal et al. 2007). As shown above, there is no consistent relationship between toxins and T&O; nevertheless, VOC outbreaks may diagnose the presence of potentially toxic biota present as conspicuous blooms or hidden mats (Henatsch and Jüttner 1985; Baker et al. 2001).

Above all, effective NAM abatement requires a multilevel approach for immediate and long-term management. As a first measure, broad-scale nutrient–biomass management models can be applied to reduce the overall risk of metabolite-producing blooms (e.g., Bierman et al. 1984; Smith et al. 2002; Smith 2003). Such models may provide a better gauge of the risk if designed to predict maximum, rather than mean, biomass and can be applied to specific algal groups (e.g., cyanobacteria) or species (e.g., Smith et al. 1987; Watson et al. 1997; Downing et al. 2001). This approach has been used to predict levels of more stable toxins (microcystins) among comparable water bodies in Alberta and Quebec, where inorganic N and N:P were identified as significant driving factors (Kotak et al. 2000; Giani et al. 2005). Similarly, Davies et al. (2004) reported some degree of correlation between geosmin occurrence and eutrophic status (total algal biomass) in drinking water sources (British Columbia).

However, successful restoration requires ecological understanding at a finer scale (cf. Bradshaw 1996) and a more system-specific approach is also necessary, particularly in recovering systems such as the Great Lakes, where other attributes can obscure nutrient–biomass relationships (e.g., significant spatial heterogeneity, species invasions, nonplanktonic NAMs sources). Initial characterization of the problem can be facilitated using simple flow charts (cf. Oliver and Ganf 2000) and screening methods to assess

© 2008 NRC Canada

nonspecific levels of NAMs impairment (e.g., sensory VOC assessment, enzyme-linked or toxicity assays; Smith et al. 2002; Boyer 2007*b*). These methods can also facilitate the identification of the key factors that influence the dominance and growth of nuisance taxa, their innate capacity for NAMs production, and the chemistry, timing, and level of this production. Such information can then be combined with knowledge of other major factors (e.g., climate, hydrological, top-down) that influence the distribution and fate of NAMs and associated producers within the water body to develop more specific predictive models and management approaches.

The Great Lakes remedial programme requires that identified impairments are monitored and assessed against targets using specific measures in a "scientifically defensible process" (IJC 1991; Hartig et al. 1997). However, with the exception of a few recent studies, noxious metabolites remain an uncharacterized impairment in these and many other source waters. This highlights one of the limitations of the RAP program framework, that BUIs have an inherent time bias. Their status was assessed in the late 1980s and early 1990s and reflects the conditions and the ecological science of the day. Even now, current methods of assessing impairment by algal metabolites are ambiguous and difficult to evaluate, largely because of the lack of standards and defined, measurable targets. For T&O, more effective criteria would include regular measures of the most problematic VOCs (e.g., geosmin, MIB, isopropylthiol, β-cyclocitral, aldehydes) in source waters and municipal supplies and comparison against OTCs. Where resources are lacking, sensory techniques can provide a less diagnostic but practical means of monitoring and anticipating T&O outbreaks (Rashash et al. 1997; Smith et al. 2002). The occurrence of toxins and species containing the genes for toxin production should be systematically investigated using regular monitoring at recreational areas and intake zones. Mid- to late-summer spatial surveys during high-risk periods and application of an alert-level framework such as developed by the World Health Organization (Watzin et al. 2006) are a good first step but may not be sufficient to detect toxin production by genera not normally associated with cyanobacteria toxin production (e.g., *Gloeotrichia*; Carey et al. 2007) or by those species that bloom early in the growing season. The use of emerging molecular techniques for the detection of potentially toxic species needs to be coupled with rapid field- or laboratory-based analytical techniques for the detection of the chemical toxins themselves. Combined with nutrient and biomass controls, this approach offers the greatest potential for safeguarding users against outbreaks of toxin-producing cyanobacteria (Boyer 2007*b*).

In the Great Lakes, considerable progress has been made in many areas towards RAP goals, not the least of which has been an increased public awareness and participation in this initiative (e.g., Krantzberg et al. 1999). However, current remedial efforts are addressing a moving target, and a more integrated watershed-based approach is required. The Great Lakes ecosystems are under constant assault by an expanding human population and emerging threats. Rapid increases in nutrients and subsequent remediation have been followed closely with increased demand for clean water resources, the spread of invasive species, shoreline development, climate change, and new pollutants, leaving these lakes in a constant state of flux. Advances in our understanding of these and other impacted systems have not kept pace with these changes, and it is clear that management must adopt a more adaptable long-term approach.

Above all, as scientific and technical advances add to the list of pathogenic, toxic, or noxious organisms that threaten aquatic resources, it is essential that remedial and management programmes frequently revaluate the list of target criteria, their acceptable levels, and the progress towards these. Restoration goals and expectations need to be realistic, success needs to be defined and measured with tangible parameters (i.e., longevity, indicators, levels, scales; Bradshaw 1996; Lewis et al. 1996), and attention needs to be given to potential impacts on aquatic food webs. The widespread concern with NAMs outbreaks in the Great Lakes and other water bodies underlines the significant need for a formal recognition of the potential threat of these and other HABs-related impairments. Traditional Great Lakes management models cannot successfully address the significant shift in nutrient sources and sinks and decoupling of inshore–offshore exchange, and a multistep management framework is required that would combine broad-scale screening and nutrient management with system and taxa-specific approaches. This may require more stringent remedial goals to address the dynamic regime shift that has occurred in these ecosystems (cf. Carpenter 2003; Mayer and Rietkerk 2004). As one of the world's largest collective body of freshwater, the Great Lakes represent major resources for over 24 million people. Given the rising demands on these systems and the continued human impacts, a lake-wide initiative to develop effective and vigilant restoration programmes is long overdue.

Acknowledgements

We thank the Ontario Waterworks Research Consortium, Environment Canada, and NOAA's COP through their MERHAB – Lower Great Lakes Program for funding and support.

References

Annadotter, H., Cronberg, G., Aagren, R., Lundstedt, B., Nilsson, P.A., and Strobeck, S. 1999. Multiple techniques for lake restoration. Hydrobiologia, **396**: 77–85. doi:10.1023/A:1017011132649.

Bailey, R., Grapentine, L., Stewart, T., Schaner, T., Chase, M.E., Mitchell, J., and Coulas, R. 1999. Dreissenidae in Lake Ontario: impact assessment at the whole lake and Bay of Quinte spatial scales. J. Great Lakes Res. **25**: 482–491.

Baker, P.D., Steffensen, D.A., Humpage, A.R., Nicholson, B.C., Falconer, I.R., Lanthois, B., Fergusson, K.M., and Saint, C.P. 2001. Preliminary evidence of toxicity associated with the benthic cyanobacterium *Phormidium* in South Australia. Environ. Toxicol. **16**: 506–511. doi:10.1002/tox.10009. PMID:11769248.

Baker, S.M., Levinton, J.S., Kurdziel, J.P., and Shumway, S.E. 1998. Selective feeding and biodeposition by zebra mussels and their relation to changes in phytoplankton composition and seston load. J. Shellfish Res. **17**: 1207–1213.

Baldwin, D.S., Whittington, J., and Oliver, R.A. 2003. Temporal variability of dissolved P speciation in a eutrophic reservoir — implications for predicating algal growth. Water Res. **37**: 4595–4598. doi:10.1016/S0043-1354(03)00403-2. PMID:14568044.

© 2008 NRC Canada

Barbiero, R., and Tuchman, M. 2001. Results from the U.S. EPA's biological open water surveillance program of the Laurentian Great Lakes: I. Introduction and phytoplankton results. J. Great Lakes Res. **27**: 134–154.

Bierman, V.J., Jr., Dolan, D.M., Kasprzyk, R., and Clark, J.L. 1984. Retrospective analysis of the response of Saginaw Bay, Lake Huron, to reductions in phosphorus loadings. Environ. Sci. Technol. **18**: 23–31. doi:10.1021/es00119a007.

Boyer, G.L. 2007*a*. Cyanobacterial toxins in New York and the lower Great Lakes ecosystems. Adv. Exp. Med. Biol. **619**: 151–163.

Boyer, G.L. 2007*b*. The occurrence of cyanobacterial toxins in New York lakes: lessons from the MERHAB – Lower Great Lakes Program. Lake Reservior Manage. **23**: 153–160.

Bradshaw, A.D. 1996. Underlying principles of restoration. Can. J. Fish. Aquat. Sci. **53**(Suppl. 1): 3–9. doi:10.1139/cjfas-53-S1-3.

Brett, M.T., and Benjamin, M. 2008. A review and reassessment of lake phosphorus retention and the nutrient loading concept. Freshw. Biol. **53**: 194–211.

Brittain, S., Wang, S., Babcock-Jackson, L., Carmichael, W., Rinehart, K., and Culver, D. 2001. Isolation and characterization of microcystins, cyclic heptapeptide hepatotoxins from a Lake Erie strain of *Microcystis aeruginosa*. J. Great Lakes Res. **26**: 241–249.

Brown, C., Hoyer, M., Bachmann, R., and Canfield, D., Jr. 2000. Nutrient–chlorophyll relationships: an evaluation of empirical nutrient–chlorophyll models using Florida and north-temperate lake data. Can. J. Fish. Aquat. Sci. **57**: 1574–1583. doi:10.1139/cjfas-57-8-1574.

Brownlee, B.G., Painter, D.S., and Boone, R.J. 1984. Identification of taste and odour compounds from western Lake Ontario. Water Pollut. Res. J. Can. **19**: 111–118.

Budd, J., Beeton, A., Stumpf, R., Culver, D., and Kerfoot, W. 2002. Satellite observations of *Microcystis* blooms in western Lake Erie. Verh. Internat. Verein. Limnol. **27**: 3787–3793.

Carey, C.C., Haney, J.F., and Cottingham, K.L. 2007. First report of microcystin-LR in the cyanobacterium *Gloeotrichia echinulata*. Environ. Toxicol. **22**: 337–339. doi:10.1002/tox.20245. PMID:17497639.

Carmichael, W. 1997. The Cyanotoxins. *In* Advances in botanical research. *Edited by* J.A. Callow. Academic Press, London, UK. pp. 211–240.

Carpenter, S.R. 2003. Regime shifts in lake ecosystems: pattern and variation. Excellence in Ecology Series No. 15, International Ecology Institute, Oldendorf/Luhe, Germany.

Carpenter, S.R., Cole, J.J., Hodgson, J.R., Kitchell, J.F., Pace, M.L., Bade, D., Cottingham, K., Essington, T., Houser, J., and Schindler, D.E. 2001. Trophic cascades, nutrients, and lake productivity: whole-lake experiments. Ecol. Monogr. **71**: 163–186.

Charlton, M. 1997. The sewage issue in Hamilton Harbour: implications of population growth for the Remedial Action Plan. Water Qual. Res. J. Can. **32**: 407–420.

Chorus, I. 2001. Cyanotoxins. Occurrence, causes, consequences. Springer, Berlin, Germany.

Chorus, I., and Bartram, J. 1999. Toxic cyanobacteria in water. E&FN Spon, London, UK.

Chorus, I., Falconer, I., Salas, H., and Bartram, J. 2000. Health risks caused by freshwater cyanobacteria in recreational waters. J. Toxicol. Environ. Health B, **3**: 323–347. doi:10.1080/109374000436364.

Codd, G.A., Morrison, L., and Metcalfe, J. 2005. Cyanobacterial toxins: risk management for health protection. Toxicol. Appl. Pharmacol. **203**: 264–272. doi:10.1016/j.taap.2004.02.016. PMID:15737680.

Cronberg, G., Annadotter, H., and Lawton, L. 1999. The occurrence of toxic blue-green algae in Lake Ringsjon, southern Sweden, despite nutrient reduction and fish biomanipulation. Hydrobiologia, **404**: 123–131. doi:10.1023/A:1003780731471.

Cullen, P., and Forsberg, C. 1988. Experiences with reducing point sources of phosphorus to lakes. Hydrobiologia, **170**: 321–336.

Davies, J.M., Roxborough, M., and Mazumder, A. 2004. Origins and implications of drinking water odours in lakes and reservoirs of British Columbia, Canada. Water Res. **38**: 1900–1910. doi:10.1016/j.watres.2004.01.008. PMID:15026245.

Dokulil, M.T., and Teubner, K. 2000. Cyanobacterial dominance in lakes. Hydrobiologia, **438**: 1–3. doi:10.1023/A:1004155810302.

Downing, J.A., Watson, S.B., and McCauley, E. 2001. Predicting cyanobacteria dominance in lakes. Can. J. Fish. Aquat. Sci. **58**: 1905–1908. doi:10.1139/cjfas-58-10-1905.

Durrer, M., Zimmermann, U., and Jüttner, F. 1999. Dissolved and particle-bound geosmin in a mesotrophic lake (Lake Zurich): spatial and seasonal distribution and the effect of grazers. Water Res. **33**: 3628–3636. doi:10.1016/S0043-1354(99)00069-X.

Environment Canada Green Lane. 2004. Environment Canada Green Lane. Available online at http://www.on.ec.gc.ca/greatlakes/default.asp?lang=En&n=FD65DFE5-1.

Falconer, I.R. 1996. Potential impact on human health of toxic cyanobacteria. Phycologia, **35**: 6–11.

Felip, M., and Catalan, J. 2000. The relationship between phytoplankton biovolume and chlorophyll in a deep oligotrophic lake: decoupling in their spatial and temporal maxima. J. Plankton Res. **22**: 91–105. doi:10.1093/plankt/22.1.91.

Fleming, L.E., Rivero, C., Burns, J., Williams, C., Bean, J.A., Shea, K.A., and Stinn, J.A. 2002. Blue-green algal (cyanobacterial) toxins, surface drinking water, and liver cancer in Florida. Harmful Algae, **1**: 157–168. doi:10.1016/S1568-9883(02)00026-4.

France, R., Peters, R., and Rishikof, R. 1995. Optimal sampling period for predicting phosphorus and chlorophyll concentrations in north-temperate lakes. Can. J. Fish. Aquat. Sci. **52**: 1812–1815. doi:10.1139/f95-173.

Fristachi, A., and Sinclair, J.L. 2008. Occurrence of harmful cyanobacterial blooms. *In* Cyanobacterial harmful algal blooms: state of the science and research needs. *Edited by* H. Kenneth Hudnell. Adv. Exp. Med. Biol. **619**: 45–104.

Giani, A., Bird, D.F., Prairie, Y.T., and Lawrence, J.F. 2005. Empirical study of cyanobacterial toxicity along a trophic gradient of lakes. Can. J. Fish. Aquat. Sci. **62**: 2100–2109. doi:10.1139/f05-124.

Gouvea, S.P., Boyer, G.L., and Twiss, M.R. 2008. Influence of ultraviolet radiation, copper, and zinc on microcystin content in *Microcystis aeruginosa* (cyanobacteria). Harmful Algae, **7**: 194–205. doi:10.1016/j.hal.2007.07.003.

Hallegraeff, G.M. 1993. A review of harmful algal blooms and their apparent global increase. Phycologia, **32**: 79–99.

Hartig, J.H., Zarull, M.A., Reynoldson, T.B., Mikol, G., Harris, V.A., Randall, R.G., and Cairns, V.W. 1997. Quantifying targets for rehabilitating degraded areas of the Great Lakes. Environ. Manage. **21**: 713–723. doi:10.1007/s002679900061. PMID:9236285.

Hecky, R.E., Smith, R.E., Barton, D.R., Guildford, S.J., Taylor, W.D., Charlton, M., and Howell, T.E. 2004. The nearshore phosphorus shunt: a consequence of ecosystem engineering by dreissenids in the Laurentian Great Lakes. Can. J. Fish. Aquat. Sci. **61**: 1285–1293. doi:10.1139/f04-065.

Hertsch, J., and Jüttner, F. 1985. Evidence of beta carotene 7,8,7′,8′-oxygenase beta cyclocitral cyvectindial generating in *Microcystis*. Arch. Microbiol. **141**: 337–343.

© 2008 NRC Canada

Higgins, S.N., Howell, E.T., Hecky, R.E., Guildford, S.J., and Smith, R.E. 2005. The wall of green: the status of *Cladophora glomerata* on the northern shores of Lake Erie's eastern basin, 1995–2002. J. Great Lakes Res. **31**: 547–563.

Hotto, A.M., Satchwell, M.F., and Boyer, G.L. 2007. Molecular characterization of potential microcystin-producing cyanobacteria in Lake Ontario embayments and nearshore waters. Appl. Environ. Microbiol. **73**: 4570–4578. doi:10.1128/AEM.00318-07. PMID:17526791.

Hudson, J.J., Taylor, W., and Schindler, D. 2000. Phosphate concentration in lakes. Nature (London), **406**: 54–56. doi:10.1038/35017531. PMID:10894537.

Ibelings, B.W., Bruning, K., de Jonge, J., Wolfstein, K., Pires, L., Postma, J., and Burger, T. 2005. Distribution of microcystins in a lake foodweb: no evidence for biomagnification. Microb. Ecol. **49**: 487–500. doi:10.1007/s00248-004-0014-x. PMID:16052377.

International Joint Commission. 1991. List/delist criteria for Great Lakes areas of concern, International Joint Commission, March–April 1991, Windsor, Ont. – Detroit, Michigan. Available online at http://www.ijc.org/rel/focus/listdelist/.

Izaguirre, G., Hwang, C.J., Krasner, S.W., and McGuire, M.J. 1983. Production of 2-methyl-isoborneol by two benthic cyanobacteria. Water Sci. Technol. **15**: 211–220.

James, L., and Vollenweider, R.A. 1981. The OECD cooperative programme on eutrophication. Canadian contribution. Environ. Can. NWRI Tech. Rep. No. 131.

Johannsson, O.E., Millard, E.S., Ralph, K.M., Myles, D.D., Graham, D.M., Taylor, W.D., Giles, B.G., and Allen, R.E. 1998. The changing pelagia of Lake Ontario (1981 to 1995): a report of the DFO Long-Term Biomonitoring (Bioindex) Program. Can. Tech. Rep. Fish. Aquat. Sci. No. 2243.

Johengen, T.H., Johannsson, O.E., Pernie, G.L., and Millard, E.S. 1994. Temporal and seasonal trends in nutrient dynamics and biomass measures in Lakes Michigan and Ontario in response to phosphorus control. Can. J. Fish. Aquat. Sci. **51**: 2570–2578. doi:10.1139/f94-257.

Johengen, T.H., Nalepa, T.F., Fahnenstiel, G.L., and Goudy, G. 1995. Nutrient changes in Saginaw Bay, Lake Huron, after the establishment of the zebra mussel (*Dreissena polymorpha*). J. Great Lakes Res. **21**: 449–464.

Jones, G.J., and Korth, W. 1995. In situ production of volatile odour compounds by river and reservoir phytoplankton populations in Australia. Water Sci. Technol. **31**: 145–151. doi:10.1016/0273-1223(95)00469-4.

Juttner, F. 1984. Characterization of *Microcystis* strains by alkyl sulfides and beta cyclocitral. Z. Naturforsch. Sect. C J. Biosci. **39**: 867–871.

Juttner, F. 1992. Flavour compounds in weakly polluted rivers as a means to differentiate pollution sources. Water Sci. Technol. **25**: 155–164.

Juttner, F. 1995. Physiology and biochemistry of odorous compounds from freshwater cyanobacteria and algae. Water Sci. Technol. **31**: 69–78. doi:10.1016/0273-1223(95)00458-Y.

Juttner, F., and Watson, S.B. 2007. Biochemical and ecological control of geosmin and 2-methylisoborneol in source waters. Appl. Environ. Microbiol. **73**: 4395–4406. doi:10.1128/AEM.02250-06. PMID:17400777.

Juttner, F., Hoflacher, B., and Wurster, K. 1986. Seasonal analysis of volatile organic biogenic substances (VOBS) in freshwater phytoplankton populations dominated by *Dinobryon*, *Microcystis*, and *Aphanizomenon*. J. Phycol. **22**: 169–175. doi:10.1111/j.1529-8817.1986.tb04160.x.

Keene, B. 2002. Bay of Quinte Remedial Action Plan Update on Impaired Beneficial Use No. 9: restrictions on drinking water consumption, taste and odour. Quinte Conservation Authority, Belleville, Ontario, Canada.

Kotak, B., Lam, A., Prepas, E., Kenefick, S., and Hrudey, S. 1995. Variability of the hepatotoxin microcystin-LR in hypereutrophic drinking water lakes. J. Phycol. **31**: 248–263. doi:10.1111/j.0022-3646.1995.00248.x.

Kotak, B., Zurawell, R., Prepas, E., and Holmes, C. 1996. Microcystin-LR concentration in aquatic food web compartments from lakes of varying trophic status. Can. J. Fish. Aquat. Sci. **53**: 1974–1985. doi:10.1139/cjfas-53-9-1974.

Kotak, B., Lam, A., Prepas, E., and Hrudey, S. 2000. Role of chemical and physical variables in regulating microcystin-LR concentration in phytoplankton of eutrophic lakes. Can. J. Fish. Aquat. Sci. **57**: 1584–1593. doi:10.1139/cjfas-57-8-1584.

Krantzberg, G., Ali, H., and Barnes, J. 1999. What progress has been made in the Remedial Action Plan Program after ten years of effort? *In* Aquatic restoration in Canada. *Edited by* T. Murphy and M. Munawar. Backhuys Publishers BV, Leiden, the Netherlands. pp. 1–13

Lazerte, B., and Watson, S. 1981. The prediction of lacustrine phytoplankton diversity. Can. J. Fish. Aquat. Sci. **38**: 524–534. doi:10.1139/f81-074.

Lewis, C.A., Lester, N.P., Bradshaw, A.D., Fitzgibbon, J.E., Fueller, K., Hakanson, L., and Richards, C. 1996. Considerations of scale in habitat conservation and restoration. Can. J. Fish. Aquat. Sci. **53**(Suppl. 1): 440–445. doi:10.1139/cjfas-53-S1-440.

Masson, S., Pinel, A.B., and Smith, V.H. 2000. Total phosphorus–chlorophyll *a* size fraction relationships in southern Quebec lakes. Limnol. Oceanogr. **45**: 732–740.

Mayer, A., and Rietkerk, M. 2004. The dynamic regime concept for ecosystem management and restoration. Bioscience, **54**: 1013–1019. doi:10.1641/0006-3568(2004)054[1013:TDRCFE]2.0.CO;2.

Mazumder, A. 1994. Phosphorus–chlorophyll relationships under contrasting herbivory and thermal stratification: predictions and patterns. Can. J. Fish. Aquat. Sci. **51**: 390–400. doi:10.1139/f94-040.

Mikalsen, B., Boison, G., Skulberg, O.M., Fastner, J., Davies, W., Gabrielsen, T.M., Rudi, K., and Jakobsen, K.S. 2003. Natural variation in the microcystin synthetase operon mcyABC and impact on microcystin production in *Microcystis* strains. J. Bacteriol. **185**: 2774–2785. doi:10.1128/JB.185.9.2774-2785.2003. PMID:12700256.

Millard, E.S., Myles, D., Johannsson, O., and Ralph, K. 1996. Phytoplankton photosynthesis at two index stations in Lake Ontario 1987–1992: assessment of the long-term response to phosphorus control. Can. J. Fish. Aquat. Sci. **53**: 1092–1111. doi:10.1139/cjfas-53-5-1092.

Moore, L., and Watson, S.B. 2007. The Ontario Waterworks Consortium: a functional model of source water management/understanding. Water Sci. Technol. **55**: 195–201.

Nicholls, K.H. 1995. Chrysophyte blooms in the plankton and neuston. *In* Chrysophyte algae: ecology, phylogeny and development. *Edited by* C. Sandgren, J. Smol, and J. Kristiansen. Cambridge University Press, Cambridge, UK. pp. 181–215.

Nicholls, K.H. 2001. CUSUM phytoplankton and chlorophyll functions illustrate the apparent onset of dreissenid mussel impacts in Lake Ontario. J. Great Lakes Res. **27**: 393–401.

Nicholls, K.H., and Dillon, P.J. 1978. An evaluation of phosphorus–chlorophyll phytoplankton relationships for lakes. Int. Rev. Gesamten Hydrobiol. **63**: 141–154. doi:10.1002/iroh.19780630203.

Oliver, R.L., and Ganf, G.G. 2000. Freshwater blooms. *In* The ecology of cyanobacteria. Their diversity in time and space. *Edi-*

© 2008 NRC Canada

ted by B.A. Whitton and M. Potts. Kluwer Academic Publishers, Dordrecht, Netherlands. pp.149–194.

Ontario Ministry of the Environment. 2000. Drinking Water Surveillance Program 2000–2002. Available online at http://www.ene.gov.on.ca/envision/water/dwsp/0002/.

Ontario Ministry of the Environment. 2003. Ontario Ministry of the Environment Technical Support Document for Ontario Drinking Water Quality Standards, Objectives and Guidelines, PIBS 4449e01. Available online at http://www.ene.gov.on.ca/envision/gp/4449e01.pdf.

Organisation for Economic Cooperation and Development. 1982. Eutrophication of waters: monitoring, assessment and control. Organization for Economic and Cooperative Development, Paris, France.

Orr, P.T., and Jones, G.J. 1998. Relationship between microcystin production and cell division rates in nitrogen-limited *Microcystis aeruginosa* cultures. Limnol. Oceanogr. **43**: 1604–1614.

Ouellette, A.J.A., Handy, S.M., and Wilhelm, S.W. 2006. Toxic *Microcystis* is widespread in Lake Erie: PCR detection of toxin genes and molecular characterization of associated cyanobacterial communities. Microb. Ecol. **51**: 154–165. doi:10.1007/s00248-004-0146-z. PMID:16435169.

Pace, M. 1984. Zooplankton community structure, but not biomass, influences the phosphorus–chlorophyll *a* relationship. Can. J. Fish. Aquat. Sci. **41**: 1089–1096. doi:10.1139/f84-128.

Painter, D.S., and Kamaitis, G. 1987. Reduction of *Cladophora* biomass and tissue phosphorus in Lake Ontario, 1972–83. Can. J. Fish. Aquat. Sci. **44**: 2212–2215. doi:10.1139/f87-271.

Peters, R.H. 1990. Pathologies in limnology. Mem. Ist. Ital. Idrobiol. **47**: 181–217.

Public Sector Consultants Inc. 2002. Targeting environmental restoration in the Saginaw River/Bay Area of Concern. 2001 Remedial plan update. Available online at http://www.pscinc.com/Documents/Saginaw_Bay/2002_RAP/RAPupdatereport_2002.pdf.

Rao, Y.R., Skafel, M.G., Howell, T., and Murthy, R.C. 2003. Physical processes controlling taste and odor episodes in Lake Ontario drinking water. J. Great Lakes Res. **29**: 70–78.

Rashash, D., Dietrich, A., and Hoehn, R. 1997. FPA of selected odorous compounds. J. AWWA, **89**: 131–141.

Reinikainen, M., Lindvall, F., Merukyiti, J.A.O., Repka, S., Sivonen, K., Spoof, L., and Wahlsten, M. 2002. Effects of dissolved cyanobacterial toxins on the survival and egg hatching of estuarine calanoid copepods. Mar. Biol. (Berl.), **140**: 577–583. doi:10.1007/s00227-001-0720-6.

Reynolds, C.S. 2003. The development of perceptions of aquatic eutrophication and its control. Ecohydrol. Hydrobiol. **3**: 149–163.

Ridal, J.J., Watson, S.B., and Hickey, M. 2007. Macrophytes: key substrates for taste and odour producers in the St. Lawrence River. Water Sci. Technol. **55**: 15–21. PMID:17489389.

Rinta-Kanto, J.M., and Wilhelm, S.W. 2006. Diversity of microcystin-producing cyanobacteria in spatially isolated regions of Lake Erie. Appl. Environ. Microbiol. **72**: 5083–5085. doi:10.1128/AEM.00312-06. PMID:16820510.

Rinta-Kanto, J.M., Ouellette, A.J.A., Twiss, M.R., Boyer, G.L., Bridgeman, T., and Wilhelm, S.W. 2005. Quantification of toxic *Microcystis* spp. during the 2003 and 2004 blooms in western Lake Erie using quantitative real-time PCR. Environ. Sci. Technol. **39**: 4198–4205. doi:10.1021/es048249u. PMID:15984800.

Sabater, S., Vilalta, E., Guasch, A., Guasch, H., Munuz, I., and Romani, A. 2003. Ecological implications of mass growth of benthic cyanobacteria in rivers. Aquat. Microb. Ecol. **32**: 175–184. doi:10.3354/ame032175.

Sarnelle, O., Wilson, A.E., Hamilton, S.K., Knoll, L.B., and Raikow, D.F. 2005. Complex interactions between the zebra mussel, *Dreissena polymorpha*, and the harmful phytoplankter, *Microcystis aeruginosa*. Limnol. Oceanogr. **50**: 896–904.

Sas, H. 1989. Lake restoration by reduction of nutrient loading: expectations, experiences, extrapolations. Academia Verlag Richarz, St. Augustin, Germany.

Satchwill, T., Watson, S.B., and Dixon, E. 2007. Odourous algal-derived alkenes: differences in stability and treatment responses in drinking water. Water Sci. Technol. **55**: 95–102. PMID:17489398.

Seip, K.L., Sas, H., and Vermij, S. 1992. Nutrient–chlorophyll trajectories across trophic gradients. Aquat. Sci. **54**: 58–76. doi:10.1007/BF00877264.

Singh, S., Kate, B.N., and Banerjee, U.C. 2005. Bioactive compounds from cyanobacteria and microalgae: an overview. Crit. Rev. Biotechnol. **25**: 73–96. doi:10.1080/07388550500248498. PMID:16294828.

Sivonen, K., and Jones, G. 1999. Cyanobacterial toxins. *In* Toxic cyanobacteria in water. *Edited by* I. Chorus and J. Bartram. World Health Organization, London, UK. pp. 41–112.

Smith, V.H. 1983. Low nitrogen to phosphorus ratios favor dominance by blue-green algae in lake phytoplankton. Science (Washington, D.C.), **221**: 669–671. doi:10.1126/science.221.4611.669. PMID:17787737.

Smith, V. 2003. Eutrophication of freshwater and coastal marine ecosystems: a global problem. Environ. Sci. Pollut. Res. **10**: 1–14.

Smith, V.H., Willén, E., and Karlsson, B. 1987. Predicting the summer peak biomass of four species of blue-green algae (Cyanophyta/Cyanobacteria) in Swedish lakes. Water Resour. Bull. **23**: 397–402.

Smith, V.H., Sieber, D.J., deNoyelles, F., Campbell, S., Pan, S., Randtke, S.J., Blain, G.T., and Strasser, V.A. 2002. Managing taste and odor problems in a eutrophic drinking water reservoir. Lake Reservior Manage. **18**: 319–323.

Svrcek, C., and Smith, D.W.A. 2004. Cyanobacteria toxins and the current state of knowledge on water treatment options: a review. J. Environ. Eng. Sci. **3**: 155–185. doi:10.1139/s04-010.

Tessier, A.J., and Woodruff, P. 2002. Cryptic trophic cascade along a gradient of lake size. Ecology, **83**: 1263–1270.

Thorstenberg, L., and L'Italien, S. 1998. Impairment assessment of beneficial uses: drinking water consumption restrictions or taste and odor problems. Environment Canada – US EPA, Lake Erie LaMP Tech. Rep. No. 11. Available online at http://epa.gov/lakeerie/buia/lamp11.pdf.

Tolstoy, A. 1979. Chlorophyll *a* in relation to phytoplankton volume in some Swedish lakes. Arch. Hydrobiol. **85**: 133–151.

Vanderploeg, H., Liebig, J., Carmichael, W., Agy, M., Johengen, T., Fahnenstiel, G., and Nalepa, T. 2001. Zebra mussel (*Dreissena polymorpha*) selective filtration promoted toxic *Microcystis* blooms in Saginaw Bay (Lake Huron) and Lake Erie. Can. J. Fish. Aquat. Sci. **58**: 1208–1221. doi:10.1139/cjfas-58-6-1208.

Van Nes, E.H., and Scheffer, M.A. 2005. Implications of spatial heterogeneity for catastrophic regime shifts in ecosystems. Ecology, **86**: 1797–1807. doi:10.1890/04-0550.

Vilalta, E., and Sabater, S. 2005. Structural heterogeneity in cyanobacterial mats is associated with geosmin production in rivers. Phycologia, **44**: 678–684. doi:10.2216/0031-8884(2005)44[678:SHICMI]2.0.CO;2.

Watson, S.B. 2003. Chemical communication or chemical waste? A review of the chemical ecology of algal odour. Phycologia, **42**: 333–350.

Watson, S.B. 2004. Aquatic taste and odour: a primary signal of drinking water integrity. J. Toxicol. Environ. Health A, **67**: 1779–1795. doi:10.1080/15287390490492377. PMID:15371216.

© 2008 NRC Canada

Watson, S., and McCauley, E. 1988. Contrasting patterns of net- and nanoplankton production and biomass among lakes. Can. J. Fish. Aquat. Sci. **45**: 915–920. doi:10.1139/f88-112.

Watson, S.B., and Ridal, J.J. 2004. Periphyton: a primary source of widespread and severe taste and odour. Water Sci. Technol. **49**: 33–39. PMID:15237604.

Watson, S.B., and Satchwill, T. 2003. Chrysophyte odour production: the impact of resources at the cell and population levels. Phycologia, **42**: 393–405.

Watson, S.B., McCauley, E., and Downing, J.A. 1997. Patterns in phytoplankton taxonomic composition across temperate lakes of differing nutrient status. Limnol. Oceanogr. **42**: 486–495.

Watson, S.B., Satchwill, T., and McCauley, E. 2001*a*. Drinking water taste and odour: a chrysophyte perspective. Nova Hedwigia, **122**: 119–146.

Watson, S.B., Satchwill, T., and McCauley, E. 2001*b*. Under-ice blooms and source-water odour in a nutrient-poor reservoir: biological, ecological and applied perspectives. Freshw. Biol. **46**: 1–15. doi:10.1046/j.1365-2427.2001.00769.x.

Watson, S.B., Charlton, M.N., Murphy, T., Mamone, T., and Parr, T. 2003. Hamilton Harbour: phytoplankton and algal toxins. *In* Hamilton Harbour Remedial Action Plan Report 2002 Season, Burlington, Ontario. ISSN 1703–4043. pp. 67–80

Watson, S.B., Millard, S., and Burley, M. 2005. Taste–odour and toxins in the Bay of Quinte. Project Quinte Monitoring Report No. 16, Bay of Quinte RAP Restoration Council – Project Quinte, Trenton, Ontario.

Watson, S.B., Charlton, M., Yerubandi, R., Howell, T., Brownlee, B., Marvin, C., Ridal, J., and Millard, S. 2007. Off-flavour issues in large waterbodies: physics, chemistry and biology in concert. Water Sci. Technol. **55**: 1–8. PMID:17489387.

Watzin, M.C., Brines Miller, E., Shambaugh, A.D., and Kreider, M.A. 2006. Application of the WHO alert level framework to cyanobacteria monitoring on Lake Champlain, Vermont. Environ. Toxicol. **21**: 278–288. doi:10.1002/tox.20181. PMID:16646001.

Wendel, T., and Jüttner, F. 1996. Lipoxygenase-mediated formation of hydrocarbons and unsaturated aldehydes in freshwater diatoms. Phytochem. **41**: 1445–1449. doi:10.1016/0031-9422(95)00828-4.

White, E. 1989. Utility of relationships between lake phosphorus and chlorophyll *a* as predictive tools in eutrophication control studies. N.Z. J. Mar. Freshw. Res. **23**: 35–41.

Wiegand, C., and Pflugmacher, S. 2005. Ecological effects of selected cyanobacterial secondary metabolites: a short review. Toxicol. Appl. Pharmacol. **203**: 201–218. doi:10.1016/j.taap.2004.11.002. PMID:15737675.

Willén, E. 1999. Phytoplankton in water quality assessment — an indicator concept. *In* Hydrological and limnological aspects of lake monitoring. *Edited by* P. Heinonen, G. Ziglio, and A. van der Beken. John Wiley and Sons, Chichester, Sussex, UK. pp. 57–81.

Yang, X. 2007. Occurrence of a cyanobacterial neurotoxin, anatoxin-*a*, in New York State waters. Ph.D. thesis, State University of New York, College of Environmental Science and Forestry, Syracuse, N.Y.

Yano, H., Nakahara, M., and Ito, H. 1988. Water blooms of *Uroglena americana* and the identification of odorous compounds. Water Sci. Technol. **20**: 75–80.

Yin, L.Y., Huang, J.Q., Shen, Q., Li, D.H., and Liu, Y. 2004. Uptake of the cyanobacterial hepatotoxin microcystin-RR by submergent macrophyte *Vallisneria natans* (Lour.). Acta Hydrobiol. Sin. **28**: 151–154.

Zaitlin, B., and Watson, S.B. 2006. Actinomycetes in relation to taste and odour in drinking water: myths, tenets and truths. Water Res. **40**: 1741–1753. doi:10.1016/j.watres.2006.02.024. PMID:16600325.

© 2008 NRC Canada

Benjamin H. Letcher and Gregg E. Horton	**1649–1666**	Seasonal variation in size-dependent survival of juvenile Atlantic salmon (*Salmo salar*): performance of multistate capture–mark–recapture models
A. Jamie F. Gibson, Heather D. Bowlby, and Peter G. Amiro	**1667–1680**	Are wild populations ideally distributed? Variations in density-dependent habitat use by age class in juvenile Atlantic salmon (*Salmo salar*)
Momoko Ichinokawa, Atilio L. Coan, Jr., and Yukio Takeuchi	**1681–1691**	Transoceanic migration rates of young North Pacific albacore, *Thunnus alalunga*, from conventional tagging data
Meghan Elizabeth Brown	**1692–1704**	Nature and nurture in dormancy: dissolved oxygen, pH, and maternal investment impact *Bythotrephes longimanus* resting egg emergence and neonate condition
Guillaume Guénard, Daniel Boisclair, Ola Ugedal, Torbjørn Forseth, and Bror Jonsson	**1705–1720**	Comparison between activity estimates obtained using bioenergetic and behavioural analyses
Suzanne Roy, Frédérick Blouin, André Jacques, and Jean-Claude Therriault	**1721–1737**	Absorption properties of phytoplankton in the Lower Estuary and Gulf of St. Lawrence (Canada)
Stefan Palm, Johan Dannewitz, Torbjörn Järvi, Marja-Liisa Koljonen, Tore Prestegaard, and K. Håkan Olsén	**1738–1748**	No indications of Atlantic salmon (*Salmo salar*) shoaling with kin in the Baltic Sea
Troy J. Guy, Robert E. Gresswell, and Michael A. Banks	**1749–1762**	Landscape-scale evaluation of genetic structure among barrier-isolated populations of coastal cutthroat trout, *Oncorhynchus clarkii clarkii*
PERSPECTIVES	PERSPECTIVES	
Charles K. Minns, James E. Moore, Brian J. Shuter, and Nicholas E. Mandrak	**1763–1778**	A preliminary national analysis of some key characteristics of Canadian lakes
Susan B. Watson, Jeff Ridal, and Gregory L. Boyer	**1779–1796**	Taste and odour and cyanobacterial toxins: impairment, prediction, and management in the Great Lakes

National Research Council Canada
Ottawa, Canada K1A 0R6

Conseil national de recherches Canada
Ottawa, Canada K1A 0R6

Postage paid at Ottawa
Publications mail
Registration No. 40062581

Port payé à Ottawa
Poste-publication
Enregistrement n° 40062581

USPS periodical postage paid at Plattsburgh, NY 12901, USA

Canadian Journal of FISHERIES AND AQUATIC SCIENCES

Volume 65, Number 8, August 2008

Journal canadien des SCIENCES HALIEUTIQUES ET AQUATIQUES

Volume 65, numéro 8, août 2008

RAPID COMMUNICATIONS		COMMUNICATIONS RAPIDES
John D. Neilson and Steven E. Campana	**1523–1527**	A validated description of age and growth of western Atlantic bluefin tuna (*Thunnus thynnus*)
Martin Castonguay, Stéphane Plourde, Dominique Robert, Jeffrey A. Runge, and Louis Fortier	**1528–1531**	Copepod production drives recruitment in a marine fish
ARTICLES		ARTICLES
Thibault Datry and Scott T. Larned	**1532–1544**	River flow controls ecological processes and invertebrate assemblages in subsurface flowpaths of an ephemeral river reach
Simon Blanchet, Géraldine Loot, Louis Bernatchez, and Julian J. Dodson	**1545–1553**	The effects of abiotic factors and intraspecific versus interspecific competition on the diel activity patterns of Atlantic salmon (*Salmo salar*) fry
Roderick R.O. Hazewinkel, Alexander P. Wolfe, Sergi Pla, Chris Curtis, and Kris Hadley	**1554–1567**	Have atmospheric emissions from the Athabasca Oil Sands impacted lakes in northeastern Alberta, Canada?
John W. Ferguson, Gene R. Ploskey, Kjell Leonardsson, Richard W. Zabel, and Hans Lundqvist	**1568–1585**	Combining turbine blade-strike and life cycle models to assess mitigation strategies for fish passing dams
Steven J.D. Martell, William E. Pine III, and Carl J. Walters	**1586–1600**	Parameterizing age-structured models from a fisheries management perspective
Steven J.D. Martell and Carl J. Walters	**1601–1609**	Experimental policies for rebuilding depleted stocks
Julie A. Thayer, Douglas F. Bertram, Scott A. Hatch, Mark J. Hipfner, Leslie Slater, William J. Sydeman, and Yutaka Watanuki	**1610–1622**	Forage fish of the Pacific Rim as revealed by diet of a piscivorous seabird: synchrony and relationships with sea surface temperature
Lisa D. Kraemer, Peter G.C. Campbell, and Landis Hare	**1623–1634**	Modeling cadmium accumulation in indigenous yellow perch (*Perca flavescens*)
Tadayasu Uchiyama, Bruce P. Finney, and Milo D. Adkison	**1635–1648**	Effects of marine-derived nutrients on population dynamics of sockeye salmon (*Oncorhynchus nerka*)

Continued on inside back cover / Suite au verso

Front cover: Ihoko Saito/Toshiyuki Tajima/Dex Image/Getty Images.

Page couverture : Ihoko Saito/Toshiyuki Tajima/Dex Image/Getty Images.

Canada

Printed in Canada by / Imprimé au Canada par
NRC Reprographic Services / Service de reprographie CNRC
Page production by / Mise en page par
NRC Research Press / Presses scientifiques du CNRC

0706-652X(200808)65:8;1-G